Australian Government

Natural hazard risk *in* PERTH

Western Australia

COMPREHENSIVE REPORT

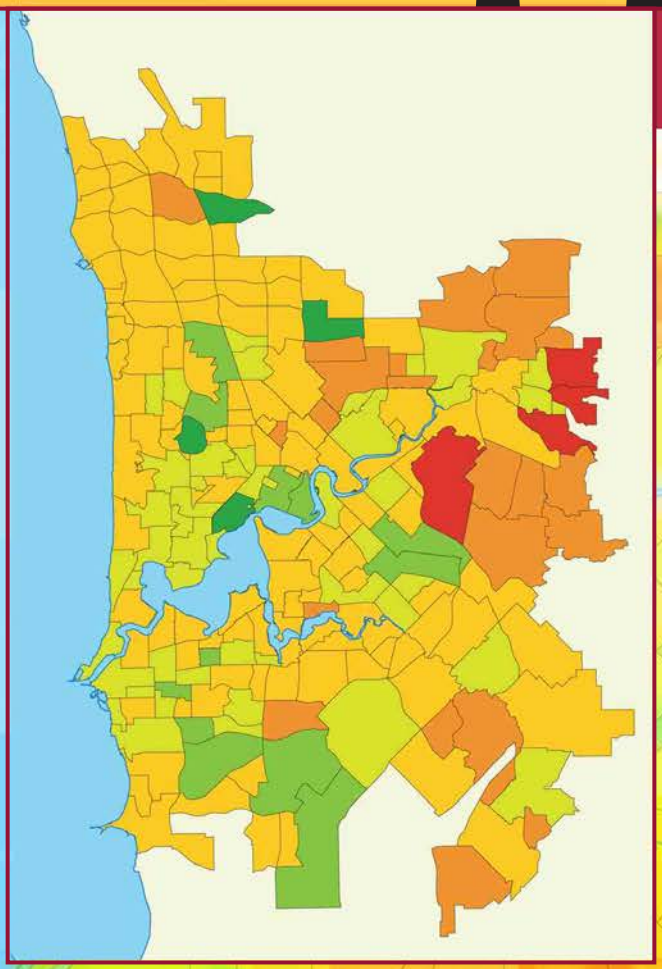

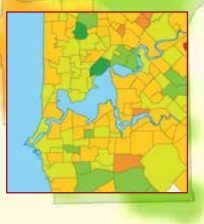

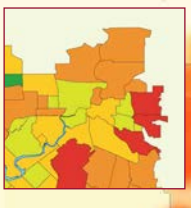

Compiled by
T. Jones, M. Middelmann and N. Corby
Geoscience Australia

Natural Hazard Risk in Perth, Western Australia

Comprehensive Report

Compiled by Trevor Jones, Miriam Middelmann and Neil Corby

Geoscience Australia

Department of Industry, Tourism and Resources
Minister for Industry, Tourism and Resources: The Hon Ian Macfarlane MP
Parliamentary Secretary: The Hon Warren Entsch MP
Secretary: Mr Mark Paterson

Geoscience Australia
Chief Executive Officer: Dr Neil Williams

ISBN: 1 920871 41 1

GeoCat No. 63527

Australian Government
Geoscience Australia
Bureau of Meteorology

Department for Planning and Infrastructure
Department of Environment
Western Australian Land Information System
Department of Land Information

Cities Project Perth

Main report

Table of Contents

Acknowledgements

We wish to thank Cities Project Perth partners who were the leaders and mainstay of the project from its inception to its completion.

Full partners in Cities Project Perth are the WA Fire and Emergency Services Authority (FESA), the WA Department for Planning and Infrastructure (DPI, formerly the WA Ministry for Planning), the Bureau of Meteorology (BOM) through its WA Regional Office, and Geoscience Australia (GA). A Project Agreement was signed by these agencies in June and July 2001. The WA Department of Environment (DOE, formerly the Water and Rivers Commission) also participated fully in this study throughout its duration although the department was not a signatory to the agreement.

We extend our warm thanks to Lisa Buckleton, who was Project Leader for Cities Project Perth from September 2000 to September 2003. Lisa was a GA employee based in FESA House in Perth. We are grateful for Lisa's skills and dedication in establishing the project in its early stages and forming excellent relationships with a wide stakeholder base including Local Governments and the media.

We would also like to thank the members of the Cities Project Perth Steering Committee who offered their time and expertise to guide the project and review its progress. Over time, members included: Jo Harrison-Ward and James Butterworth (FESA), Joe Courtney (BOM), Mike Allen (DPI), Richard Bretnall (DOE), Mark Taylor (WA Land Information System, WALIS), Lisa Buckleton and Trevor Jones (GA).

We would like to thank FESA, who provided the WA 'home base' for the project and extended encouragement and support throughout the duration of the study through the provision of data and information. We are especially grateful to Bob Mitchell, FESA CEO, and Jo Harrison-Ward (formerly Executive Director, Emergency Management Services), James Butterworth, Brendan Power and Barry Hamilton, the latter of whom was the original project representative from FESA. GA is especially grateful to FESA for providing office facilities for Lisa Buckleton for three years in the project.

Our thanks are extended to the Bureau of Meteorology's WA Regional Office (BOM). In particular we would like to acknowledge the support of project representatives Joe Courtney and Andrew Burton. Thank you for your excellent contribution to the meteorological chapter and your ongoing advice and ideas. We also thank Gary Foley, Regional Director, and Graham Ezzy.

We are grateful to Richard Bretnall from DOE for his excellent guidance and leadership on flood hazard assessment and floodplain management towards this project.

We thank DPI for contribution through the life of the project. Also, we thank DPI for their positive and pro-active approach to making provision for the reduction of natural hazard risk through State Planning Policies and Guidelines, based in part on the activities and outcomes of this project. In particular we would like to acknowledge Mike Allen, as well as Howard Drabsch and Matt Devlin for their enthusiastic support of the project.

The Department of Land Information (DLI) supplied the project with many datasets including building footprint data that were integral for the earthquake risk assessments and development of building databases in the project. We thank Graham Searle, CEO, and members of his team including Ron Vincent, Marty Stamatis and Paul Duncan, for their contribution. We would also like to extend our gratitude to Valuer-General Gary Fenner for providing access to their data.

Thank you to Jim Rhoads, Marnie Leybourne and especially Mark Taylor of WALIS for sourcing key spatial datasets used within this study. WALIS has played a key role in acting as a coordinator to

distribute the spatial databases developed in Cities Project Perth to WA agencies who will be custodians and users of the databases in the future.

We thank those at the Department of Industry and Resources, particularly Stephen Bandy, Richard Langford, Mike Freeman, Tim Griffin (CEO of the Geological Survey) and others for their guidance with regard to environmental geology and earthquake hazard.

We would like to acknowledge the enthusiasm and effectiveness of Phil Calley (City of Wanneroo) Noelene Jennings (City of Perth), Tex McPherson (City of Swan) and Denis Cluning (City of Joondalup) for their time and role in promoting this study to emergency managers.

We thank the WA State Emergency Management Committee (SEMC) and the WA State Mitigation Committee (SMC) for playing an advisory and guiding role throughout the duration of the project. We would also like to acknowledge the SEMC infrastructure committees. In particular we thank the Lifelines Services Group, chaired by Albert Koenig, from the WA Office of Energy, and the Lifeline Services Operational Group, chaired by Mark Fitzhardinge, from the WA Water Corporation. We thank you for your encouragement, cooperation and excellent advice.

Thank you Laurie Curro of Western Power for your friendship and willingness to cooperate with regard to provision of data on electric power supply network assets.

We are grateful to Daryl Cameron, Group Manager for Western Australia and the Northern Territory (Insurance Council of Australia) for his ongoing interest and support in the project. We also thank Daryl for providing information on the impact of the May 1994 cool season storm and advice on other insurance losses in southwest WA.

Chapter One (introduction) and Chapter Eight (conclusions) were prepared by Trevor Jones. We thank Joe Courtney, Richard Bretnall, Mike Allen, James Butterworth and Marnie Weybourne for comments that improved the historical disaster database.

Chapter Two (meteorological) was compiled primarily by Joe Courtney. Thankyou to the external reviewers Bill Wright from the Bureau of Meteorology (Melbourne office) and Ian Foster from the Western Australian Department of Agriculture. Thanks also go to Andrew Burton and Glenn Cook from BOM for their comments on the chapter.

Chapter Three (wind) was prepared by Xun Guo Lin and Krishna Nadimpalli. Thank you to Joe Courtney of BOM for supplying meteorological data, providing technical expertise and collaboration. Thank you also to Geoff Robinson of CSIRO Mathematics & Information Sciences for his advice and chapter review. Appreciation is extended to Mark Edwards, Ingo Hartig and Neil Corby for their assistance.

Chapter Four (flood) was compiled by Miriam Middelmann. Much appreciation is extended to Richard Bretnall (DOE), Simon Rodgers (DOE), Chris Zoppou (GA), Justin White (formerly GA), Lisa Cornish (GA), Soori Sooriyakumaran (BOM) and Mark Bailey (BOM) for their assistance, guidance and review. Thanks also to the organisations who provided data, in particular DOE, DPI, and the Water Corporation. Photos were reproduced with the courtesy of the Battye Library. Particular thanks go to Richard Bretnall from the Department of Environment for his local experience and good humour.

Chapter Five (earthquake) was prepared by Mark Edwards (with contributions by many other authors). Thank you to Marion Leiba for the technical edits. We are grateful to many geophysicists and geologists from many organisations who contributed to the preparation of the seismicity model for southwest WA.

Chapter Six (community recovery) and Chapter Seven (coastal erosion) were prepared by Anita Dwyer and Andrew Jones respectively.

We thank WA reviewers of all parts of this report from FESA, DPI, DOE, BOM, WALIS and DLI.

We also thank all GA reviewers of chapters and appendices and those who provided quality assurance checks on databases. These people included John Schneider, Clive Collins, Bob Cechet, David Burbidge, Chris Zoppou, Ken Dale, David Robinson, Mary Milne, Kane Orr, Matt Hayne, Dan Clark, Mark Edwards, Justin White, Tony Hunter, Donald Gordon, Duncan Moore and Lisa Cornish. We thank Stephen Roberts of ANU for his advice on the floods chapter.

We thank the editor of this report, Karen McVicker, for her valuable and careful work in editing, correcting and formatting the whole report.

We thank GA's Judy Huxley, Monica Osuchowski, Felicity Edge, Anita Dwyer and Ken Dale for their roles in preparing the summary booklet and the main report for this report. We thank the GA Communications team including Len Hatch, Felicity Edge and Chris Thompson for their role in promoting this report.

The figures throughout this report were produced by Ingo Hartig, Lisa Cornish, Krishna Nadimpalli and Neil Corby from Geoscience Australia to an excellent standard over several years. We thank you. We also thank the GA graphic designers of this report Lindy Gratton, Leanne McMahon and Jim Mason for their contributions.

We thank the field survey team who collected microtremor (ambient or 'background' seismic noise) data to assist in determining the response of the Perth and Northam shallow geology to future earthquakes. These were Ingo Hartig, David Pownall, Ray deGraaf, Jim Whatman, Andrew Hislop and Brian Gaull. We particularly thank Brian Gaull from Guria Consulting for preparing a report on this work.

Many thanks to the GA field survey teams who collected field building data for this project. We are grateful to Donald Gordon and Andrew Hislop who collected information on the building database for the CBD in June 2002. We thank Neil Corby, Ingo Hartig and Justin White who collected building information in the vicinity of the Swan and Canning Rivers (December 2003) to assist with flood risk assessments.

Wally Johnson, Geoscience Australia's former Chief of Geohazards Division, provided outstanding support and inspiration to the Cities Project. Wally, along with Ken Granger and John Schneider, were instrumental in GA's role in establishing Cities Project Perth.

We would also like to thank all the WA and local government agencies who are now playing a key role in the custodianship of models and data developed in the project, and are implementing policy and practice based on the results of this report.

Finally, we thank other people involved in provision of data and advice for this project, its coordination, research and analysis, promotion and dissemination of the findings and outcomes of the project, whom we may have overlooked in our thanks above.

To all these people we extend our appreciation and thanks.

ABBREVIATIONS AND ACRONYMS

ABS	Australian Bureau of Statistics
ACRES	Australian Centre for Remote Sensing
AEP	annual exceedance probability
AHD	Australian height datum
ARI	average recurrence interval
AWS	automatic weather stations
BOM	Bureau of Meteorology
BTE	Bureau of Transport Economics
CD	census district
CDF	cumulative distribution function
COAG	Council of Australian Governments
DEM	digital elevation model
DLI	Department of Land Information
DCLM	Department of Conservation and Land Management
DMAP	Disaster Mitigation Australia Package
DPI	Department for Planning and Infrastructure (WA)
EMA	Emergency Management Australia
FCB	functional classification of buildings
FDI	fire danger index
FESA	Fire and Emergency Services Authority (WA)
GA	Geoscience Australia
GIS	geographic information system
GSS	General Social Survey
HAT	highest astronomical tide
HEC-RAS	Hydraulic Engineering Center – river analysis system (US Army Corps of Engineers)
IDRO	Insurance Disaster Response Organisation
IFD	intensity–frequency–duration (rainfall curves)
IOCI	Indian Ocean climate initiative
IPCC	Intergovernmental Panel on Climate Change
LAT	lowest astronomical tide
LGA	local government areas
MSLP	mean sea level pressure
PMF	probable maximum flood
PMP	probable maximum precipitation
PML	probable maximum loss
POT	peaks over threshold
SCPT	seismic cone penetrometer test
SEIFA	Socioeconomic Index For Areas (ABS)
SEMC	State Emergency Management Committee (WA)
SLIP	Shared Land Information Platform
SLWS	severe local wind storms
SWSZ	southwest seismic zone
TIN	triangulated irregular network
UTM	Universal Transverse Mercator
WALIS	Western Australian Land Information System
WAPC	Western Australian Planning Commission
WMO	World Meteorological Organization
WRC	Water and Rivers Commission (WA), now part of the Department of the Environment

EXECUTIVE SUMMARY

Cities Project Perth is a natural hazard risk assessment study of a major Australian capital city by Geoscience Australia (GA) and its Federal, State and Local collaborators. Cities Project Perth has produced authoritative knowledge on the risks from sudden-onset natural hazards in Australia's fourth largest city and the capital of the state of Western Australia (WA).

Cities Project Perth is the most recent multi-hazard risk assessment undertaken by GA and collaborating agencies (notably the Bureau of Meteorology (BOM) and local governments), following earlier studies of the Queensland cities of Cairns (Granger et al., 1999), Mackay (Middelmann and Granger, editors, 2000), Gladstone (Granger and Michael-Leiba, editors, 2001) and South-East Queensland (Granger and Hayne, editors, 2001). GA also published the single-hazard report *Earthquake Risk in Newcastle and Lake Macquarie*, New South Wales (Dhu and Jones, editors, 2002).

This study is aimed at estimating the impact on the Perth community of several sudden-onset natural hazards. The natural hazards considered are both meteorological and terrestrial in origin. The hazards investigated most comprehensively are riverine floods in the Swan and Canning Rivers, severe winds in metropolitan Perth, and earthquakes in the Perth region. Some socio-economic factors affecting the capacity of the citizens of Perth to recover from natural disaster events have been analysed and the WA data compared with data from other Australian states. Additionally, new estimates of earthquake hazard have been made in a zone of radius around 200 km from Perth, extending east into the central Wheatbelt. The susceptibility of the southwest WA coastline to sea level rise from climate change has also been investigated. A commentary on the tsunami risk to WA coastline communities is also included.

This report aims to improve our understanding of the future costs to Perth for earthquakes through direct calculation of earthquake risk. The report also provides estimates of hazard for floods and severe winds that, with additional work on loss estimation, would provide quantitative information on the costs of these two hazards also.

Such new information on natural hazard risk to Perth provides input into the decision making processes by WA and local government community, planning and emergency management agencies with regard to setting priorities in:

- prevention, planning response and recovery (PPRR);
- risk management of the natural hazards against each other, for example floods against severe winds;
- applying resources in the most cost effective way in Perth to reduce the impacts of natural hazards, prioritised against other parts of WA; and
- applying resources to risk management of natural hazards, against applying resources to other 'all hazard' events that affect communities.

The key findings and recommendations are summarised below.

Severe wind hazard

- The severe wind hazard calculated in this report for Perth Airport is in close agreement with the wind hazard for Perth in the Australian wind loadings standard (Standards Australia, 2002). The standard places Perth in Region A, the lowest hazard region of four in Australia. However, the historical record from the automatic weather station (AWS) at Perth Airport was the sole dataset used in calculations for the wind loadings standard. This airport is some 20 km inland. Winds from the western quadrant, the strongest in Perth, are reduced in intensity in

their path from the coast inland, and return period wind speeds in the standard are most applicable to Perth sites some kilometres inland.

- In this report, the data from eight stations in the Perth region were used, along with spatial modelling of the effects of topography, terrain roughness and shielding on the incoming winds, thus producing a much more comprehensive and broad-based knowledge of wind hazard across the metropolitan area. Our statistical analysis of the AWS data, the model of decrease in wind speed from the coast, and the modelling of terrain, shielding and topographic factors across Perth have revealed a richness in wind hazard across Perth.
- Across metropolitan Perth, severe wind hazard varies considerably. Localised areas of Perth with measurably higher hazard than the wind loadings standard lie:
  - in a band several kilometres wide along the coastline, with a near-shore coastal strip a few hundred metres wide having the greatest hazard;
  - in a north–south band several kilometres wide running along the top of the Darling Scarp; and
  - on exposed shores of the lower reaches of the Swan River, extending inland approximately as far as the Kwinana Freeway.
- The reader needs to be aware that variability in wind speed, wind turbulence, incoming wind direction, and the ability of the models themselves to describe accurately the physical characteristics of the wind, all add variability to the wind hazard at any place and for any particular wind event. The variability in the behaviour of buildings and other structures, due to variability in construction strength and orientation to the wind, will also add variability to damage for any specific event.

Recommendations

Use the wind hazard maps:

- **to review, improve and complement the design and construction guidelines for severe winds set by state and local governments;**
- **as a source of information for response planning and response;**
- **as a basis for further research on severe wind risk in Perth; and**
- **as an aid to bushfire risk assessment at the Perth urban/rural interface.**

Use the wind hazard multipliers for topography, terrain roughness and shielding:

- **to review, improve and complement the design and construction guidelines for severe winds set by state and local governments;**
- **as a reference for design engineers and the construction industry;**
- **as a basis for further research on severe wind risk in Perth; and**
- **as an aid to bushfire risk assessment at the Perth urban/rural interface.**

Flood hazard

The key results follow.

- There are six major catchments in the study area that contribute flow to the Swan River, of which the Avon catchment is by far the largest. Not surprisingly, the hydrologic estimation of flows showed that the Avon River was by far the most dominant flow contributor to the Swan River. Simulations showed that another significant source of flow is from the tributaries, particularly the Canning and Southern Rivers.
- The season of the tidal cycle was found to influence flood flows marginally, with water levels slightly higher in winter. As expected, the variation in water levels decreased with distance upstream from the Port of Fremantle.
- Eight flood scenarios were modelled for the Swan River and its tributaries ranging from AEPs of 10% to 0.05% (return periods of approximately 10 years to 2,000 years). Previously, only

the 1% AEP scenario had been mapped using a less complex steady flow model. The new model provides emergency managers and planners with important new hazard information for scenarios with a large range of return periods. The unsteady flow model and the stream levels predicted by the modelled events are now held by government agencies in WA, including the DOE and BOM.

- Perth has experienced a lengthy dry period in the past 40 years. Only two major flows have occurred, in 1983 and 1987, since all the streamflow gauging stations at the outer boundaries of the model became operational. Therefore, when more data become available, the unsteady flow model should be recalibrated as far as possible.
- Water levels in this study were found to be lower than those modelled previously for the 1% AEP flood event. The variation in water levels can be explained by the differing methodology of this model and the earlier DOE model. The model differences are best explained by the inclusion of the tributaries, followed by the use of an unsteady flow model rather than a steady flow model, in the Cities Project Perth model. The current lack of data has resulted in the model results being inconclusive and, therefore, the availability of the new model, on its own, does not warrant a complete replacement of current procedures on 1% floodplain mapping. This report provides recommendations that will help reconcile the two models and reduce uncertainties in flood hazard estimates.

Recommendations

- **Further data are acquired and applied to refine, revise and recalibrate the unsteady flow model for flooding in the Swan and Canning Rivers.**
- **Systematic data are collected during future major flood events.**
- **The model for river flooding in the Swan and Canning Rivers is reviewed after each major event.**
- **Until adequate data are available to further refine and calibrate the unsteady flow model, the Department of Environment's 1% AEP floodplain mapping should continue to be used as the basis for ensuring that future development has adequate flood protection.**

Earthquake risk

The earthquake risk to Perth discussed in Chapter 5 can be summarised by the following results.

- Overall, the estimates of earthquake hazard on rock foundation in Perth and in southwest WA are similar to those in the current and draft Australian earthquake loading standards. These results have come from a comprehensive update of the earthquake hazard in Perth and in southwest WA. The reader is referred to Chapter 5 for a comparison of the earthquake hazard calculated in this report and the hazard described in the current and draft earthquake loadings standards.
- The earthquake risk to Perth has been aggregated across the metropolitan area and illustrated by a risk curve or probable maximum loss (PML) curve in Chapter 5. Loss is expressed as a percentage of the total value of all buildings and their contents in the study region.
- The results of this study suggest that, on average, greater metropolitan Perth will suffer an estimated economic loss of around 0.04% per year.
- About three-quarters of the earthquake risk in the study region is from events that have annual probabilities of occurrence of 0.004 or less (return periods of 250 years or more). This suggests that about three-quarters of the risk to metropolitan Perth is from rare events with major or, in extreme cases, catastrophic impacts. The long-term nature of earthquake risk to Perth and regional communities to the east indicates that the risk is likely to be realised very rarely. These earthquake events will have relatively high consequences. This provides a motivational challenge for emergency managers to remain vigilant and for appropriate risk treatments such as adequate insurance to remain in place.

- The earthquake risk to Perth varies spatially across the study region. A gradual reduction in risk occurs across metropolitan Perth in a southwesterly direction as distance from the southwest seismic zone (SWSZ) increases. The effect of the higher earthquake hazard in the Wheatbelt region can thereby be discerned.
- Most of the annualised risk for building usage type is for the residential types (almost 90%) with the next most common being commercial. This is mainly because residential buildings make up the overwhelming majority of buildings in the study area, and comprise the majority of the total estimated value of all buildings in the study area.
- The unique capital city profile of Perth has also influenced the results in that the residential building stock is predominantly unreinforced double brick construction with a much smaller proportion of framed timber construction. Unreinforced masonry is significantly more vulnerable than framed timber construction.
- The locations of earthquakes that create most of the risk to metropolitan Perth show a split distribution. About half of the earthquake risk in metropolitan Perth is due to moderate to strong earthquakes (magnitudes in the range about 5 to 6.5) that could occur with epicentres at distances of less than 30 km from Perth. Estimates of earthquake risk in Perth are sensitive to model assumptions of the rate of occurrence of earthquakes for these close-in earthquakes, because historic seismicity has been low in and around Perth.

  The second significant contribution to earthquake risk in Perth comes from large earthquakes that could occur at the western margin of the SWSZ (60–90 km from Perth), where the earthquake activity is higher than it is in Perth.
- The area of elevated hazard in the Wheatbelt is considerably more extensive than identified in the current earthquake loadings standard. This area is wider in an east-west direction, extends further northward and is generally located closer to Perth.

Recommendations

Use the earthquake hazard maps for metropolitan Perth and the Perth region:
- **to review, improve and complement the design and construction guidelines for earthquakes set by state and local governments;**
- **as a source of information for response planning and response.**

Enforce the compliance with current earthquake loading standards for all new structures.

Promote the importance of adequate insurance against earthquakes for householders, small business operators and corporations.

Protect facilities such as police, SES, fire and ambulance stations and hospitals, which provide essential services following any earthquake event. These facilities could be examined by suitably qualified engineers on a site-by-site basis to assess their performance under earthquake loadings. This recommendation is pertinent for SWSZ communities.

Indicators of social resilience for recovery

The indicators ‘household financial capacity’, ‘community and social networks’ and ‘distance to services’, explored in Chapter 6, show that Perth households and the broader community have many characteristics that will favourably influence the recovery process following a natural hazard event. However, these indicators are only three of many influencing recovery.

- The majority of households in metropolitan Perth have good economic resources, relative to the rest of Australia. Twenty-nine of 30 Local Government Areas (LGA) in the Perth Statistical Division rank in the top 50% of Australian LGAs in the ABS Index for Economic Resources (ABS, 2004a). Of these 29 LGAs, 22 rank in the top 25% nationally. Therefore, in the event of any natural disaster that has direct and widespread effects on residences, the community has

many households that can draw on their economic resources to assist their recovery. However, it must be noted that there are some areas, or clusters, of households within suburbs that may experience difficulties in the recovery process due to limited financial capacity.

- The strong community network in WA is indicated by results from the General Social Survey (GSS) (ABS, 2004b). This strong network suggests that, for many in Perth, recovery may involve a strong utilisation of friends, family, neighbours and informal organisations, such as community groups or sporting clubs. Almost all WA participants in the GSS indicated that they could ask someone outside of their home for assistance in times of need, including a health, legal or financial professional, charity or religious organisation. This information may assist recovery managers in tailoring programs and services for people in the Perth community.
- People in some outer suburban areas may have further to travel to access major services than those living more centrally. These major services, whether they are medical, welfare, social or cultural, can be important factors in influencing the recovery of these outer communities. This information may assist recovery managers in understanding some access/transport issues for people living in this part of the Perth metropolitan community.

Recommendations

We recommend that relevant WA government agencies and local governments participate in national research in social vulnerability models as they apply to all sudden-onset hazards.

Potential impact on the southwest WA coast from sea level rise due to climate change

Key findings follow.

- It is highly likely that coastal erosion will have a significant impact on coasts around the globe, including Australian coasts, over the next century.
- Three sections of the Fremantle to Hillarys coastline appear to be susceptible to coastal erosion: Port/South Beach; Swanbourne to Floreat Beach; and the Pinaroo Point area. The hazard decreases from south to north, primarily due to the northward net longshore drift.
- Given a sea level rise of 18 cm over the next 50 years, and 48 cm over the next 100 years, Swanbourne beach is likely to erode approximately 40–50 m and 100–130 m respectively.
- The impact of modelled recession at Swanbourne Beach is not significant due to a lack of overlying infrastructure. Similar erosion at the other vulnerable localities would have a much greater impact.
- The majority of the Mandurah to Fremantle coastline does not appear to be susceptible to coastal erosion over the next century, despite the fact that the Tamala Limestone is preserved below sea level across the majority of the area. This is due to the fact that this sector has been the primary depositional province for the Swan coast over the last 8,000 years.
- The Bunbury to Mandurah coastline is the section of Swan coast that appears to be most susceptible to coastal erosion over the next century. This is because the Tamala Limestone is preserved below sea level, this sector is not well sheltered from offshore swell, and this location is at the southern end of the net northward littoral conveyor that operates along the Swan Coast.
- The Hillarys to Yanchep coastline does not appear to be susceptible to erosion over the next century as Tamala Limestone is preserved above sea level along the majority of the coast, and the beaches are well sheltered by three lines of offshore reefs.
- The Cape Naturaliste to Bunbury area may be impacted by coastal erosion associated with long-term sea level rise. With increasing development of coastal urban infrastructure, this sector is an important focus for quantitative coastal erosion modelling in southern Western Australia.

Recommendations

To improve decision making and reduce uncertainties about the potential for future coastal erosion due to sea level rise:

- **Undertake a Bruun Rule calculation as a preliminary methodology in planning for coastal recession due to sea level rise.**
- **Focus future research on the Bunbury to Mandurah coastline, the Cape Naturaliste to Bunbury coastline, and the Port/South beach area of Fremantle.**
- **Improve data availability, particularly sector specific wave data and more detailed subsurface data.**
- **Improve the sophistication of current models to allow for calculation in areas where the nearshore/offshore includes competent substrate.**

Bushfire risk assessment

- Historic records indicate that bushfires have caused major impacts in southwest WA. Climate change may also modify the frequency and intensity of these events in future decades. A bushfire threat analysis is currently being undertaken by government agencies such as FESA and the WA Department of Conservation and Land Management. Bushfire risk at the Perth urban/rural interface could be compared more systematically with other natural hazard risks assessed in Cities Project Perth if similar methods and measurables are developed across all of the risk assessments.

Recommendations

Align the bushfire threat analysis currently being undertaken by WA government agencies with the hazard, exposure, vulnerability and loss assessment methodologies and databases of Cities Project Perth in order to develop a systematic and consistent set of information on the risks from the major sudden-onset natural hazards in Perth.

Spatial databases and risk assessment models

- More than a dozen major spatial databases and risk assessment models, including the flood hazard model and comprehensive building and building footprint databases, digital elevation models and GIS hazard maps, were developed in Cities Project Perth. The Western Australian Land Information System (WALIS) and the Department of Land Information (DLI) have played leading coordination roles in ensuring that the Cities Project Perth databases will be added to, maintained and made available by the appropriate WA Government agencies. These databases will be reviewed for possible inclusion in the WA Shared Land Information Platform (SLIP).

Recommendations

WALIS and DLI have played leading coordination roles in ensuring that the Cities Project Perth databases will be added to, maintained and made available by the appropriate WA government agencies. These databases will be reviewed for possible inclusion in the WA Shared Land Information Platform (SLIP).

Where to from here?

In this chapter we have suggested risk management options that could reduce natural hazard risks in Perth based on the results of the research in Cities Project Perth. Most of the suggested options are aimed at the key public and private sector agencies who are responsible for emergency management, land use planning and information management in WA. Some of these risk management options include recommendations for additional research and additional data gathering.

It is now largely the task of the WA partners in Cities Project Perth, and the people and organisations with whom they work, to implement decisions based on the new information made available.

References

Australian Bureau of Statistics (2004a) *SEIFA 2001 Standalone (CD-ROM)*, Release 2 2004, Australian Bureau of Statistics, Canberra.

Australian Bureau of Statistics (2004b) *2002 General Social Survey (CD-ROM)*, Australian Bureau of Statistics, Canberra.

Standards Australia (2004) *DR 04303 : Structural design actions – Part 4 : Earthquake actions in Australia*, Standards Australia, Homebush, Sydney.

Standards Australia (2002) *Structural Design Actions, Part 2: Wind actions*, AS/NZS 1170.2:2002.

Standards Australia (1993) *Minimum Design Loads on Structures, Part 4: Earthquake loads*, AS 1170.4-1993.

Chapter 1: INTRODUCTION

Trevor Jones

Geoscience Australia

1.1 Cities Project Perth

Cities Project Perth is a natural hazard risk assessment study of the city of Perth by Geoscience Australia (GA) and its Federal, State and Local collaborators. Cities Project Perth has produced authoritative knowledge on the risks from sudden-onset natural hazards in Australia's fourth largest city and the capital of the state of Western Australia (WA).

Cities Project Perth is the most recent multi-hazard risk assessment undertaken by GA and collaborating agencies (notably the Bureau of Meteorology (BOM) and local governments), following earlier studies of the Queensland cities of Cairns (Granger et al., 1999), Mackay (Middelmann and Granger, editors, 2000), Gladstone (Granger and Michael-Leiba, editors, 2001) and South-East Queensland (Granger and Hayne, editors, 2001). GA also published the single-hazard report *Earthquake Risk in Newcastle and Lake Macquarie*, New South Wales (Dhu and Jones, editors, 2002).

This study is aimed at estimating the impact on the Perth community of several sudden-onset natural hazards. The natural hazards considered are both meteorological and terrestrial in origin. The hazards investigated most comprehensively are riverine floods in the Swan and Canning Rivers, severe winds in metropolitan Perth, and earthquakes in the Perth region. Some socioeconomic factors affecting the capacity of the citizens of Perth to recover from natural disaster events have been analysed and the WA data compared with data from other Australian states. Additionally, new estimates of earthquake hazard have been made in a zone of radius around 200 km from Perth, extending east into the central Wheatbelt. The susceptibility of the southwest WA coastline to sea level rise from climate change has also been investigated. A commentary on the tsunami risk to WA coastline communities is also included.

1.2 Aims of Cities Project Perth

The aims of Cities Project Perth were stated in the Project Agreement in 2001:

> *The goal of [the] Cities Project is to ascertain the vulnerability of Australian urban communities to the effects of geological and meteorological hazards (collectively referred to as geohazards), thereby providing emergency managers and planners with information and decision support tools that will aid in the mitigation of geohazards. The objective of the WA Cities Project is to improve the methodology, develop decision support tools and generate information to assist in the mitigation of geohazards.*

This statement of aims has remained relevant throughout the project. However, we can be more specific about these aims, and also broaden our original expectations from the project, reflecting the development of the project over time and developments in natural disaster risk assessment and mitigation nationally.

The historic cost of natural hazard events in WA has been approximately $62 million per year, according to the Bureau of Transport Economics (BTE, 2001). See Table 1.1. These estimates of

cost by BTE are based on an analysis of historical data largely in the period 1967-1999, with prices in 1999 dollars.

Table 1.1: Average annual cost of natural disasters (drawn from Table 3.1, BTE, 2001)

	Average annual cost ($ million)						
	Flood	**Severe storms**	**Cyclones**	**Earthquakes**	**Bushfires**	**Landslide**	**Total**
WA	2.6	11.1	41.6	3.0	4.5	0.0	62.7
Australia	314.0	284.4	266.2	144.5	77.2	1.2	1087.5

The question arises as to how well the costs in Table 1.1 represent the true costs of natural disasters for WA. BTE (2001) described at length the limitations of the data that were available to estimate the cost of natural disasters across Australia. It is thought that the costs of natural hazards in WA have not been fully recorded, for example through the Natural Disaster Relief Arrangements and preceding arrangements, and therefore the costs to WA have been underestimated (Jo Harrison-Ward, verbal communication, 2004).

This report aims to improve our understanding of the future costs to Perth for earthquakes through direct calculation of earthquake risk. The report also provides estimates of hazard for floods and severe winds that, with additional work on loss estimation, would provide quantitative information on the costs of these two hazards also.

Such new information on natural hazard risk to Perth provides input into the decision making processes by WA and local government community, planning and emergency management agencies with regard to setting priorities in:

- prevention, planning response and recovery (PPRR);
- risk management of the natural hazards against each other, for example floods against severe winds;
- applying resources in the most cost effective way in Perth to reduce the impacts of natural hazards, prioritised against other parts of WA; and
- applying resources to risk management of natural hazards, against applying resources to other ‘all hazard’ events that affect communities.

One of the difficulties of estimating accurate costs from a short history is that only a small sample of all of the events that could possibly occur have in fact been observed. BTE’s estimates of the costs of natural disasters are largely based on the events that occurred in a short, historic ‘snapshot’ of time (1967–1999). Few rare disaster events (those with long return periods and major consequences) are likely to have occurred in this 33-year period. Some rare events did occur in the period considered by BTE, such as cyclone *Tracy*, the 1989 Newcastle earthquake, and the 1999 Sydney hailstorm. These three events dominated the costs of disasters considered by BTE, contributing 31% of the total costs of all events in Australia in that period.

We illustrate the limitations of a short historical catalogue with a couple of examples. Consider a natural hazard event that has an annual probability of occurrence of 1% (that is, a return period of 100 years). The probability that this event would occur at least once in any 33-year period is about

28%, under certain assumptions[1]. An event with an annual probability of 0.2% (that is, a return period of 500 years), has only a 6% probability of occurring at least once in any 33-year period.

This report aims to overcome some of the limitations of the relatively short historic record by predicting, through computational modelling, the intensity, likelihood and variability of rare earthquakes, floods and severe winds that could impact on Perth, thus extending our understanding of possible future events.

Nationally, after the commencement of Cities Project Perth, a High Level Group reporting to the Council of Australian Governments (COAG) identified a 'lack of independent and comprehensive and systematic natural disaster risk assessments' and made recommendations to COAG to improve this situation, including 'develop and implement a five-year national programme of systematic and rigorous disaster risk assessments' (Reform Commitment 1, High Level Group, 2002). Cities Project Perth partners are active in pursuing this goal. The needs of government and non-government emergency managers and planners for improved information on natural hazard risk to Perth have much in common with these needs expressed at a national level.

More pointedly then, the aims of Cities Project Perth are to:

- produce authoritative information on the risk to greater metropolitan Perth from important sudden-onset natural hazards;
- improve the evidence base for implementation of emergency management and planning policy and practice for the benefit of government and non-government sectors;
- provide databases and datasets on hazard, exposure and vulnerability to be incorporated in databases for emergency management and planning policy and practice in WA;
- produce foundation information on flood, coastal erosion and wind hazard for further risk assessment studies by the WA, local or federal governments;
- develop methodologies, databases and models that can be applied to estimating hazard, vulnerability or risk from other types of hazards in Perth, for example human-caused hazards, or that can be applied elsewhere in Australia to estimate hazard, vulnerability or risk from any natural or human-caused hazard;
- produce estimates of hazard and risk that add to systematic and rigorous knowledge of natural hazard risk from a national perspective.

1.3 Participating Agencies

Full partners in Cities Project Perth are the WA Fire and Emergency Services Authority (FESA), the WA Department for Planning and Infrastructure (DPI, formerly the WA Ministry for Planning), the BOM through its WA Regional Office, and GA. A Project Agreement was signed by these agencies in June and July 2001. The WA Department of Environment (DOE, formerly the Water and Rivers Commission) also participated fully in this study throughout its duration although the department was not a signatory to the agreement.

The Local Governments that are partly or wholly contained in Greater Metropolitan Perth comprise a key client group for the project outputs. Their participation in the project was largely coordinated by FESA. Several Local Governments directly contributed data or advice on hazards and community vulnerability. These included the Cities of Perth, Wanneroo, Joondalup and Swan.

[1] The stated probability of exceedance applies for events that follow a Poisson distribution. That is, events occur randomly, with no 'memory' of the time, size or location of any preceding events (Kramer, 1996).

The WA State Emergency Management Committee (SEMC) and the WA State Mitigation Committee also played an advisory and guiding role through the duration of the project. The Lifelines Services Group and the Lifeline Services Operational Group, both subcommittees of the SEMC, also provided expert advice to the project.

The valuable contributions of many other agencies and individuals are accredited in the Acknowledgements section.

1.4 Historical Events in Southwest WA

Natural hazard events in WA have caused much economic impact, personal hardship and loss of life. Dominant among these events has been a long succession of tropical cyclones that in early years caused many deaths.

> *There have been several historical Western Australian cyclones causing a significant loss of lives at sea. In March 1912 over 150 lives were claimed at sea. The coastal passenger vessel the* Koombana *was lost after setting out from Port Hedland to Broome with about 140 people on board. At least another 15 people died as other vessels went down in the same event…*
>
> *There have been two events in WA when about 140 men perished in pearling fleet disasters:*
> *- 22 April 1887 off Ninety Mile Beach*
> *- 26-27 March 1935 near the Lacepede Islands off Broome*
>
> (BOM, 2005).

Cyclones causing major economic losses in WA since around 1970 have included *Madge* (1973), *Joan* (1975), *Alby* (1978), *Hazel* (1979) and *Vance* (1999). Their cost in WA in the years 1967-1999 was estimated by BTE to be almost two-thirds of the total costs of natural disasters in WA (Table 1.1). Other natural hazards have had significant impacts on WA including severe storms, bushfires, earthquakes and floods.

Perth's natural hazard history includes damaging earthquakes, tropical cyclones, cool season storms, thunderstorms, bushfires, riverine and flash floods, often accompanied by related phenomena such as storm surge, tornadoes, hail, lightning, and dust storms. The most significant historical events in the Perth region are listed in Table 1.2. Most of the events in the table, and many others, are described more fully in the following chapters.

The criteria for including events in Table 1.2 were:

- events caused impacts on communities within about 200 km of Perth, and may also have had a significant impact on metropolitan Perth; and
- the estimated losses from individual events totalled more than $5 million in 1998 prices; or
- the estimated number of deaths from individual events totalled five or more.

Table 1.2: Significant natural disaster events in Perth region WA

Local Date Start	Event	Location	Original loss ($M)	Loss (1998 $M)	Deaths
1862 Jul	The 1862 Swan River flood, estimated to have an ARI of 60 years, was said to be unprecedented by some sources. The *Perth Gazette* reported that much property was destroyed, with gardens backing onto the river between the Causeway and Mt Eliza largely underwater. [1] [2] [3]	Perth	£30,000		5
1872 Jul	Largest Swan River flood on record with an estimated ARI of 100 years. The flood reportedly caused considerable property damage along the Swan-Avon River. [4]	Perth	NA	NA	
1878 Jul 20	Cool season storm. *James Service* shipwrecked offshore from Rockingham–Mandurah with loss of all crew and passengers. [5]	Perth region			20
1899 Jul 12	Cool season storm. *Carlisle Castle* shipwrecked off Rockingham with loss of all hands (est. 24–26 persons) and cargo (est. £40,000–£50,000). *City of York* wrecked off Rottnest Island with loss of 11 crew. [5]	Perth region	> £40,000	NA	35
1926 Jul	The 1926 Swan River flood, although having an estimated ARI of only 30 years, resulted in the collapse of the Fremantle Railway Bridge and the Upper Swan Bridge. It also caused significant flooding of property in South Perth and in the Upper Swan–Guildford areas.	Perth	NA	NA	
1937 Feb 9	Cyclone and bushfire. A 'cyclone lashed the lower west coast on the 9th and 10th' Widespread property damage occurred, particularly south of Perth. Many boats damaged at Rockingham and further south. Severe bushfires in Denmark and Walpole. Hundreds of acres of forest, pasture and fruit trees were destroyed by the fires and stock losses were great. Widespread severe duststorms over the Wheatbelt. [6] [7]	Southwest WA	NA	NA	
1961 Jan 19	'Dwellingup' bushfires. Several fires ignited by extreme fire weather, and more by lightning on 20 January, from Mundaring to Manjimup. On 24 January, the fires flared, driven by hot, gusty northwesterly winds influenced by a tropical cyclone in the Pilbara. Over 40,000 ha of forest burnt. Dwellingup destroyed, with 132 homes, 74 motor vehicles and other buildings lost, including the hospital. [8] [9]	Southwest WA		35	
1968 Oct 14	Earthquake magnitude 6.8 Ms wrecked Meckering, damaged central Wheatbelt towns including York and Northam, and ruptured the Goldfields water supply pipeline. More than 6,400 insurance claims received for damage in metropolitan Perth. [10] [11] [12]	Meckering	1.5	12	
1978 Apr 4	Tropical cyclone *Alby*. Gale-force winds and widespread damage to property. Storm surge and large waves caused coastal inundation and erosion. Widespread fires and severe dust storms. [8] [13] [14]	Southwest WA (Perth to Albany)	13	39	5
1979 Jun 2	Earthquake magnitude 6.0 Ms wrecked buildings and infrastructure centred on Cadoux township 180 km northeast of Perth. More than 2,800 insurance claims for minor damage in Perth. [15] [16]	Cadoux	3.5	12	

Local Date Start	Event	Location	Original loss ($M)	Loss (1998 $M)	Deaths
1988 Sep 22	Cool season storm. The storm caused extensive damage from Perth to Albany. Hundreds of roofs were damaged and several ripped off entirely, trees were downed, and power was lost to over 100,000 homes in the metropolitan area. [17]	Southwest WA (Perth to Albany)	8	12	1
1994 May 23	Cool season storm. Windstorm was one of the most destructive weather events to affect Perth. Majority of property damage minor, most claims being for fence damage. Downed powerlines, mostly due to fallen trees and branches, caused widespread blackouts, leaving up to one-third of Perth without power at the height of the storm. [8 17]	Perth	37		2
1997 Jan 8	Bushfires at Wooroloo and Wundowie (believed deliberately lit) destroyed 16 homes, part of the Wooroloo Prison Farm, sheds, fencing, livestock, vehicles and stored fodder. Total losses in excess of $12 million. [8 18]	Perth region	12		
2005 Jan 15	Largest bushfire in Perth Hills in 40 years. The fire was believed deliberately lit and burnt 27,000 ha of state forest, national park and bushland in Mundaring, Pickering Brook, Karagullen and Barton's Mill. [19]	Perth rural interface	NA	NA	

Notes: Estimated contemporary losses and losses in 1998 dollars are insured losses from Insurance Disaster Response Organisation unless otherwise stated.

[1] Loss estimate in 1862 pounds from the *West Australian*, March 12, 1934.
[2] *Perth Gazette*, 11 July, 1862, including estimate of 5 deaths.
[3] EMA Disaster Database cites 12 deaths.
[4] BOM, 1995.
[5] Western Australian Museum, 2005.
[6] BOM, 2005.
[7] Hanstrum, 1992.
[8] EMA Disaster Database.
[9] *West Australian*, 24 January, 1981.
[10] Everingham and Gregson, 1970.
[11] Gordon and Lewis, 1980
[12] Everingham *et al*., 1982.
[13] Estimate of deaths from Hanstrum, 1992.
[14] EMA Disaster Database estimates $50 million damage to property alone in 1978 prices.
[15] Lewis *et al*., 1981.
[16] Gregson, 1980, estimated costs at $3.8 million in 1979 dollars.
[17] Estimate of deaths from EMA Disaster Database.
[18] Loss estimate from Bushfires Board of Western Australia, 1997.
[19] FESA, 2005.

The radius from Perth of exposed communities was extended to about 200 km in Table 1.2 to ensure that many significant events that have had widespread impacts, such as cyclone *Alby* in 1978, the 1968 Meckering earthquake, thunderstorms in southwest WA, and cool season storms, would be included in the table. Events such as these had significant aggregated losses, even though their maximum impact may not have been in Perth itself.

The estimated losses in Table 1.2 are, with only three exceptions, estimates of insured losses published by the Insurance Disaster Response Organisation (IDRO, 2005) post-dating 1967. IDRO has maintained a Major Disaster Event List for events from June 1967. Events included in their list had disaster costs likely to have cost $10 million or more or, alternatively, had been declared a disaster by an appropriate government authority.

For all events, total losses must at least equal the insured losses and, therefore, the estimated cost of the events in Table 1.2 must be considered a minimum. Total losses include direct losses due to building and infrastructure damage and business disruption, tangible indirect losses due to impacts on businesses not directly impacted by the event and additional costs of post-disaster services, and intangible, indirect losses from death and injury, loss of personal effects, psychological, social and environmental effects. Total costs are probably several times higher than aggregated insured losses but are not known currently.

The proportion of total losses to insured losses has been estimated by Joy (1991), and BTE (2001) used factors derived from these proportions to estimate the costs of natural disasters nationally (Table 1.3). However, BTE (2001) more thoroughly costed a small sample of natural hazard events and produced ratios of uninsured to insured losses quite different from those of Joy. Their limited analysis indicated wide variability in these proportions and therefore, while we need to employ some scheme such as that of Joy, better means of estimating non-insured losses are essential to improve our understanding of the total costs of disasters and therefore improve decision-making for allocating resources to reduce these costs.

Table 1.3: Proportion of insured loss to total loss (Joy, 1991; after BTE, Table 2.2, 2001)

	Proportion of insured loss to total loss	**Factor**
Severe storm	35%	3
Tropical cyclone	20%	5
Flood	10%	10
Earthquake	25%	4
Bushfire (Wildfire)	35%	3

An analysis of the limited data on insured losses since 1967 in Table 1.2 indicates that tropical cyclones, combined with bushfires associated with them, have been the most costly natural hazards in southwest WA in recent times. Cool season storms rank second, earthquakes third, and there are no data in the table for floods. These rankings are similar to those of BTE (2001) for WA as a whole (Table 1.1), except that BTE estimated that annualised losses from floods in WA were similar to those from earthquakes.

Using the insured losses in Table 1.2 and the proportions of insured losses to uninsured losses of Joy (Table 1.3), we obtain annualised losses of approximately $15 million per year from the most costly natural hazard events in southwest WA in the period 1967 to 2004. These annualised losses are approximately one-quarter of those listed by BTE (2001) for WA as a whole (Table 1.1).

Floods

The author has included several historic events in Table 1.2 for which no estimate of cost was available. For example, the 1926 floods brought down the Fremantle Railway Bridge and the Upper

Swan Bridge and, as a consequence of the collapse of the Fremantle Railway Bridge, freight costs rose because goods traffic between Perth and Fremantle had to be diverted through Armadale. The costs from this event would probably have exceeded the criterion for Table 1.2.

The 1862 flood is also considered to meet the cost criterion for Table 1.2, even though Perth and the surrounding communities were then much smaller. Considerable infrastructure and buildings have been constructed on the floodplain and we estimate that, if a similar major event were to occur at the present time, significant losses would ensue. Chapter 4 presents graphic accounts of the impacts of the 1862 floods.

In other cases, significant floods have been excluded from the table because no evidence of damage or loss could be located in contemporary accounts or in the EMA or IDRO databases. Flood events been omitted from the table for this reason include events in August 1945 ('Approached 1926 flooding'), February 1955, and August 1963 (in which Guildford/Bassendean area flooding was 'almost as bad as 1926') (comments in parentheses by Richard Bretnall, WA DOE, written comm., 2005).

Tropical Cyclones

Although most WA tropical cyclones have wreaked their major havoc in the northwest of the state, a significant number also have made rapid, damaging transitions to the southwest. Cyclone *Alby* in 1978 (Table 1.2) is probably the most damaging of these events in the Perth region in terms of financial and economic impact, if not in loss of life. Chapter 2 of this report provides descriptions of the cyclones since 1830 that have made this transition to affect Perth and southwest WA.

Earthquakes

Perhaps surprisingly, Wheatbelt earthquakes, with epicentres more than 100 km distant from Perth, have caused significant losses to Perth. A total of 3,668 insurance claims arose from the 1979 Cadoux earthquake and, of these, 2,850 claims comprising 46% of the total value were from the metropolitan area (Lewis et al., 1981). The epicentre of this earthquake was approximately 180 km from Perth.

For the 1968 Meckering earthquake, with an epicentre 130 km distant from Perth, the ratio of the value of claims in metropolitan Perth to the total value of claims was much higher. Of a total of 7,706 insurance claims for both Houseowners and Fire (Commercial), 6,483 were received from metropolitan Perth (defined as within a radius of 48 km from Perth GPO). Total value of claims from the metropolitan area was $907,848, or 67% of the total value of $1,346,763 for all claims (1968 dollars; Gordon and Lewis, 1980). Claims for dwellings comprised about 78% of the total value of claims.

Other Hazards

Other types of natural hazard events have caused damage, financial and economic losses, deaths and other effects. These events include severe local wind storms (SLWS). SLWS can be divided into tornadoes and downbursts. The winds generated from tornadoes are the strongest that have occurred in Perth and southwest WA, and tornadoes have caused localised intense damage. For example, a tornado through Kings Park and South Perth on 15 July 1996 led to 35 insurance claims totalling $447,963 (Joe Courtney, written communication, 2005). A severe wind squall likely to have been a tornado destroyed 40 caravans and extensively damaged 24 cottages at Naval Base, south of Fremantle on 8 June 1968.

Because tornadoes and downbursts are very localised and frequently short lived, individually and collectively they have not contributed significantly to total historical economic losses and casualties, so none are listed in Table 1.2. Chapter 2 provides further accounts of these events and their historical occurrence.

Numerous other natural hazard events that did not cause at least $5 million dollars in damage losses, or did not cause five fatalities or more, have occurred in southwest WA including Perth. It is notable

that these events appear more often in event listings since about 1990. This increase in the numbers of events is probably due to two factors. First, reporting through the EMA Disaster Database and through the IDRO Disaster Event List has probably improved since that time. Also, like most major cities around the world, Perth is probably increasingly vulnerable to the impacts of natural disaster events because of its increasing population, urban expansion and its sensitivity to the availability of effective transport, communications and energy supply.

Several recent examples taken from the EMA Disaster Database illustrate the apparent increase in frequency of 'significant' albeit second-order events. It is noteworthy that all of these examples occurred in the summer months and nearly all were related to thunderstorm activity. Examples of recent events include:

- 8 February 1992, thunderstorm. Slow-moving storms caused Perth's wettest day on record, with falls over 100 mm. Strong winds and golf-ball sized hail damaged apartment blocks in Glendalough in the morning. Estimated $5 million losses in 1998 dollars;
- 23 February 1995, warm season thunderstorm downburst. Caused damage of over $4 million in the eastern suburbs of Perth;
- 15 January 2000, severe storms. Thousands of people were caught up in lightning, rain and hail which sparked fires and floods, jammed traffic and cut power to about 4,000 homes and businesses. Crop losses in Swan Valley. Estimated $5 million losses;
- 22 January 2000, flash flood. Second-highest Perth rainfall. While the event did not cause a major flood of the Swan River, it did considerable damage and disrupted activities in the city;
- 14 January 2002, thunderstorm. A supercell formed north of Perth causing hail at Regans Ford, before moving offshore and striking Kwinana, shifting an oil tanker from its moorings, and causing millions of dollars damage to the refinery. Estimated $5 million losses.

In preparing Table 1.2, discrepancies, omissions and inconsistencies for cost data and other information were noted among sources such as the IDRO database and the EMA Disasters Database. We do not underestimate the difficulty of obtaining accurate information, or in preparing and maintaining databases of rigorous and systematic information on costs of natural disasters. The estimates of loss that are available are almost exclusively estimates of total insurance claims. Almost any estimates of other losses, apart from casualty estimates, are rare and have not been systematically presented. BTE (2001) also described the many difficulties in obtaining cost information including, but not confined to, the relationship between insured and uninsured losses, cost of intangibles and indirect costs.

The costs of natural hazards in Perth must be considered against the costs of other, human caused hazards in priority setting for whole of government expenditure on risk reduction. Transport accidents are one source of comparison. Transport accidents feature strongly in the catalogue of disasters that have occurred in the Perth region, apart from natural disasters. In the 19th Century, scores of shipwrecks occurred in the shallow waters off the southwest WA coastline, many caused by navigation errors. Some of the most disastrous, however, were brought about by winter gales, and these wind events are described in Table 1.2. In the 20th Century, aircraft crashes have caused significant loss of life. In July 1949, a DC-3 aircraft crashed near Guildford Airport, metropolitan Perth, with the loss of 18 lives. In June 1950, an Australian National Airlines DC-4 aircraft crashed near York, approximately 90 km east of Perth, killing all 29 people aboard (EMA, 2005). BTE (2000) estimated the cost of road crashes in Australia in 1996 as $15 billion.

The types of impacts on the community from historic disaster events in southwest WA reflect the changing nature over time of community vulnerability. In early events, loss of life was significant. Improved warning systems, emergency management response capability, land management planning and building codes have reduced the risk of loss of life from natural and technological hazards. Nonetheless, we cannot dismiss the threat of multiple loss of life from bushfires, gales, floods,

earthquakes (and transport accidents) in southwest WA. In future events, however, losses may be highest from environmental impacts and economic losses apart from casualties.

The reader will note from Table 1.2 that, despite the wide range of natural hazards that have occurred in Perth and southwest WA, no event has been truly catastrophic. No event for more than 100 years has caused more than five fatalities, and no event has caused more than $100 million insured losses, for example. This is a fortunate position indeed when Perth is compared with other cities and regions such as Brisbane (1985 storms), Newcastle (1989 earthquake), Sydney (1999 hailstorm), Canberra (2003 fires), Hobart (1967 fires), South Australia and Victoria (1983 Ash Wednesday fires), Darwin (1974 cyclone *Tracy*), and so on.

Are the citizens of Perth and its hinterland fortunate to live in a benign natural environment? What is the likelihood of future natural disaster events of a ferocity not experienced in Perth's relatively short continuous written history (since 1829)? This report provides answers to many key questions that lay the foundation for addressing current risk to Perth. Cities Project Perth has also developed many databases on hazard, exposure and vulnerability that will facilitate further investigations on natural hazard risk in Perth in the future.

1.5 Key Questions for this Report

There are a number of key questions regarding natural hazards and natural hazard risk that this report addresses. The answers to these key questions form the basis of the research work for this report. The key questions are listed below.

What is the severe wind hazard to Perth?

- How does the wind hazard, calculated in this report, compare with the hazard that is defined for Perth in the Australian/New Zealand wind loadings standard?

What is the flood hazard to Perth in the Swan River and its tributaries?

- What do improvements to the flood hazard model of the DOE add to our understanding of flood hazard for these rivers?

What is the earthquake risk to Perth?

To analyse the earthquake risk to Perth, we seek solutions to the following questions in Chapter 5:

- What is the earthquake risk to Perth when aggregated across the metropolitan area?
- What is the estimated annualised loss to Perth, expressed for example as a percentage of the total value of the building stock?
- Is the earthquake risk to Perth significantly higher in some local areas than others, and are particular building types at higher risk than other types?
- Where do the earthquakes occur that generate most risk to Perth, and how often are they likely to occur?
- What is the earthquake hazard in Perth?
- What is the earthquake hazard in the Perth region, that is, in a radius of about 200 km from Perth CBD? How does the earthquake hazard in Wheatbelt areas compare with the hazard in metropolitan Perth?
- How does the earthquake hazard, calculated in this report for Perth and southwest WA, compare with that defined in the Australia/New Zealand earthquake loadings standard?

How can socio-economic models and information improve our understanding of how well the Perth community will cope with recovery following significant natural hazard events?

What is the potential impact on the southwest WA coast from sea level rise due to climate change?

- Which areas of coastline near Perth are the most susceptible to coastal erosion due to sea level rise?

For each of the hazards considered, what are the most important risk management actions to reduce the risks from these hazards?

1.6 Study Area

The study area covers the places of work, sleep and play for most of the population of greater metropolitan Perth at the current time. The study area for social vulnerability research is identical to the ABS Perth Statistical Division that had a population of approximately 1.3 million people in 2001[2]. The study area for wind hazard contains a total of approximately 544,000 rateable buildings of all types[3], compared to approximately 550,000 residences in the broader ABS Perth Statistical Division. The study area for earthquake risk contains a building stock of approximately 355,000 buildings of all rateable types (Figure 1.1).

In general, the borders of the study area for Cities Project Perth are those of greater metropolitan Perth. However, the study area differs somewhat for the various investigations of hazard, vulnerability and risk in the report. For example, our investigations into factors that affect community recovery span the entire metropolitan area, whereas our assessment of flood hazard focuses on the floodplains of the Swan River and tributaries. Our choices in study area for the various hazard and risk assessments were driven by the need to cover as much area as possible, in two ways: first, to include those areas of the Perth community that could be affected by the individual hazards, and second to consider the region in which hazard events are generated, or traverse on their path towards Perth. On the other hand, the study area was restricted by the availability of data, usually hazard-related data such as Automatic Weather Station (AWS) data, or to where we could generate new data, using methods such as such as Seismic Cone Penetrometer Testing.

A core area covering the greater part of metropolitan Perth was used for the most of the hazard and risk assessments in this report, enabling us to report across a range of hazard events that could strike common areas of the city. This core area extends about 25 km east from the Perth CBD to the Darling Range, and to the Indian Ocean in the west. In the south, the core area extends about 60 km north–south, from Wanneroo and Joondalup in the northwest to Kwinana and Armadale. (See Figure 1.1.)

Our study area extends far beyond Perth for our assessment of the potential coastal erosion due to long-term sea level rise from climate change and for earthquake hazard. (See Figure 1.2.) For coastal erosion due to long-term sea level rise, we have considered a 300 km-long coastal strip from Cape Naturaliste, in the state's southwest, to Yanchep, at the northwest margin of greater metropolitan Perth. However, the area of greatest attention is along the coast of greater Perth.

[2] ABS figures from 2001 Census.
[3] Rateable building data from WA Valuer-General's Office building database, 2002.

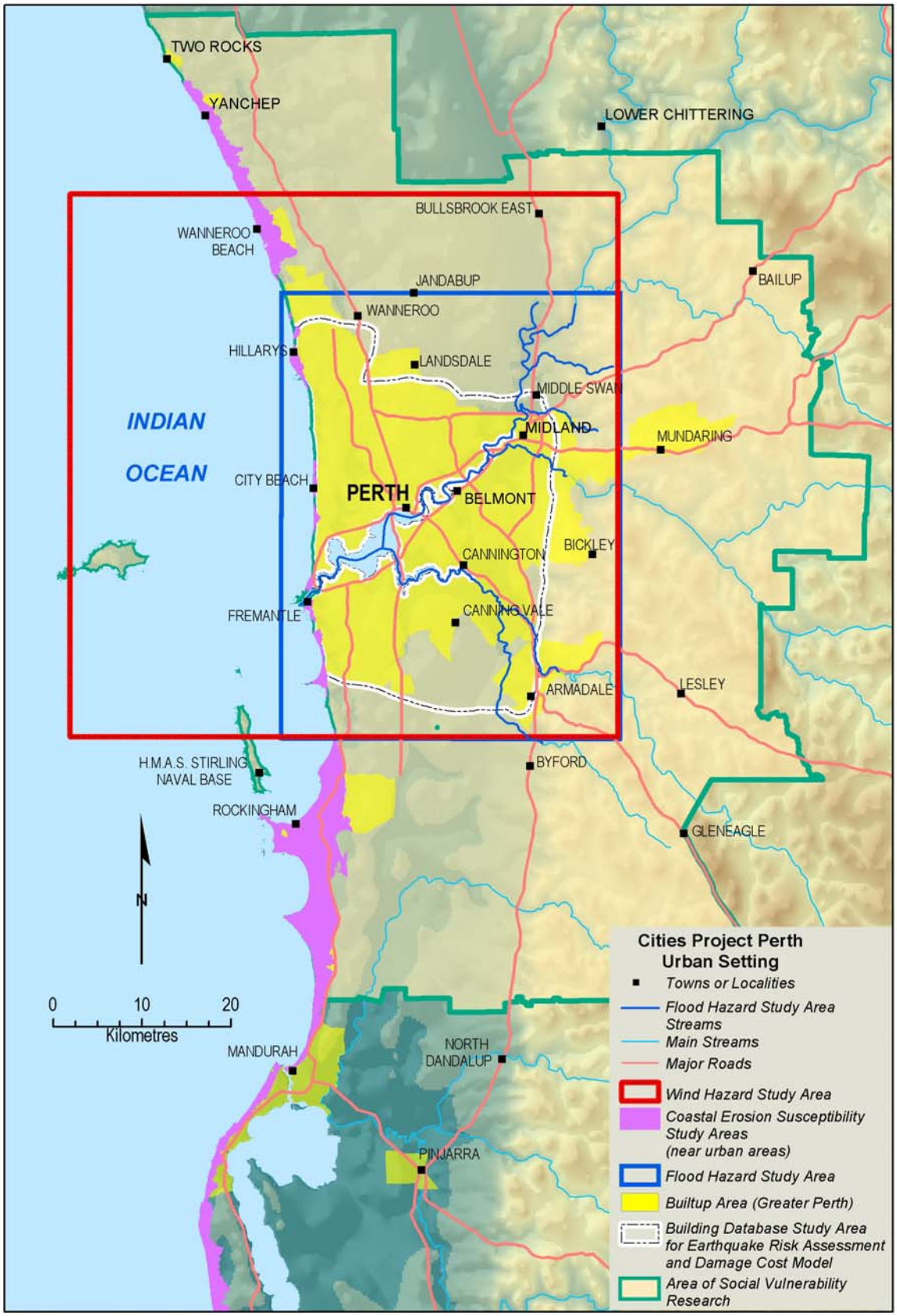

Figure 1.1: Study area – greater metropolitan Perth

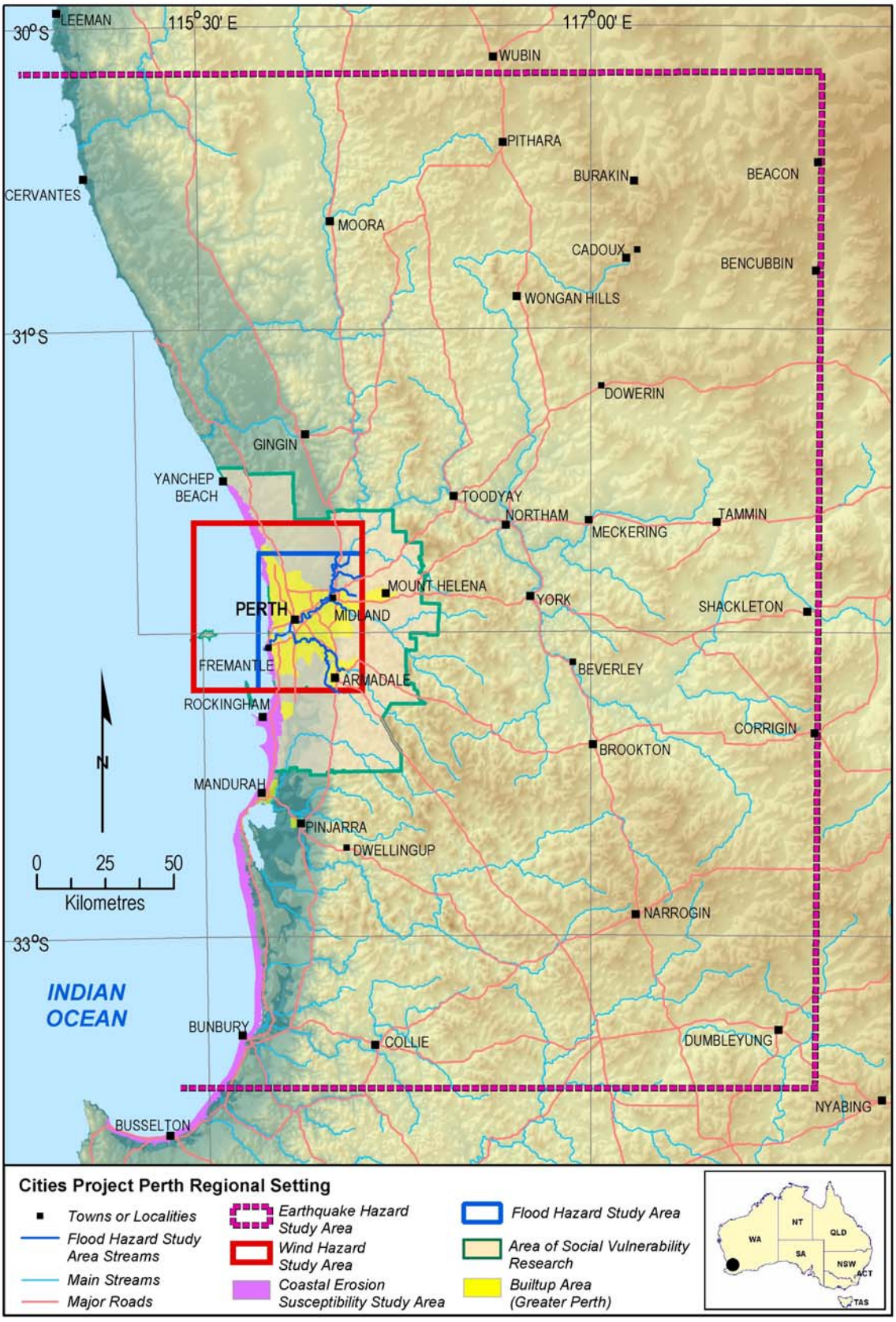

Figure 1.2: Study area in southwest WA

For assessing earthquake hazard, we chose a zone with a radius of around 200 km from Perth CBD. Earthquakes occurring within this radius, such as strong earthquakes originating at the western margin of the Wheatbelt, have the potential to cause widespread damage and disruption across metropolitan Perth. Also, in the Wheatbelt itself the earthquake hazard is significantly higher than in metropolitan Perth and WA emergency risk managers have a direct interest in managing the earthquake threat to their communities. For earthquake *risk* assessments, as against earthquake *hazard* assessments, the study area comprises the major part of metropolitan Perth (Figure 1.2).

The study area for severe wind hazard was influenced by the locations of the AWS operated by the BOM in the Perth region (Chapter 3).

1.7 Study Area and Future Growth in Perth

Cities Project Perth focuses on assessing hazard, vulnerability and risk to the current population of Perth and its built infrastructure. However, the databases and assessment methods developed for this report provide an excellent foundation for assessing hazard and risk to the city in its future form. The study area in this report extends across much of the city in its planned expansion to 2030. Also, the most comprehensive assessments of hazard and risk have been conducted on the central core of the city that is planned to undergo major urban infill in future decades.

The WA Planning Commission's (WAPC) community consultation document *Network City* contains a comprehensive and well-defined set of strategies, options and objectives for the future development of Perth and Peel to the year 2030 (WAPC, 2004). The study area of Cities Project Perth is largely consistent with the WAPC area, except that we have excluded Mandurah City and Murray Shire, collectively called Peel, immediately south of metropolitan Perth, from our investigations.

Perth is one of the fastest growing capital cities in Australia, in both population and area. Urban spread and population growth was consistently high through the 20th Century (see Table 1.4).

Table 1.4: Population change in selected capital cities, 1921–2001 (adapted from Troy, Table 1(i), 1995)

		1 Metropolitan/urban population (000)	2 Ratio of population to 1921 population	3[1] Population in 1921, metro boundary (000)	4 % of total living in 1921 boundary
Perth	1921	155		127	82
	1971	731	4.7	228	31
	1991	1019	6.5	205	20
Sydney	1921	899		899	100
	1971	2725	3.0	1513	56
	1991	3098	3.4	1351	44
Melbourne	1921	718		718	100
	1971	2408	3.3	1199	50
	1991	2762	3.8	977	35
Adelaide	1921	255		249	98
	1971	809	3.1	575	71
	1991	957	3.7	544	57

Note: *1* 'The metropolitan area boundary was used for column [3] except where it could not be traced in later years because of boundary changes. In the case of Perth some additional areas were omitted because the 1921 boundary was very wide. In all cases the area used for column [4] is constant… Source: Australian Census of Population and Housing 1921, 1971, 1991.
(Troy, 1995, p.3).

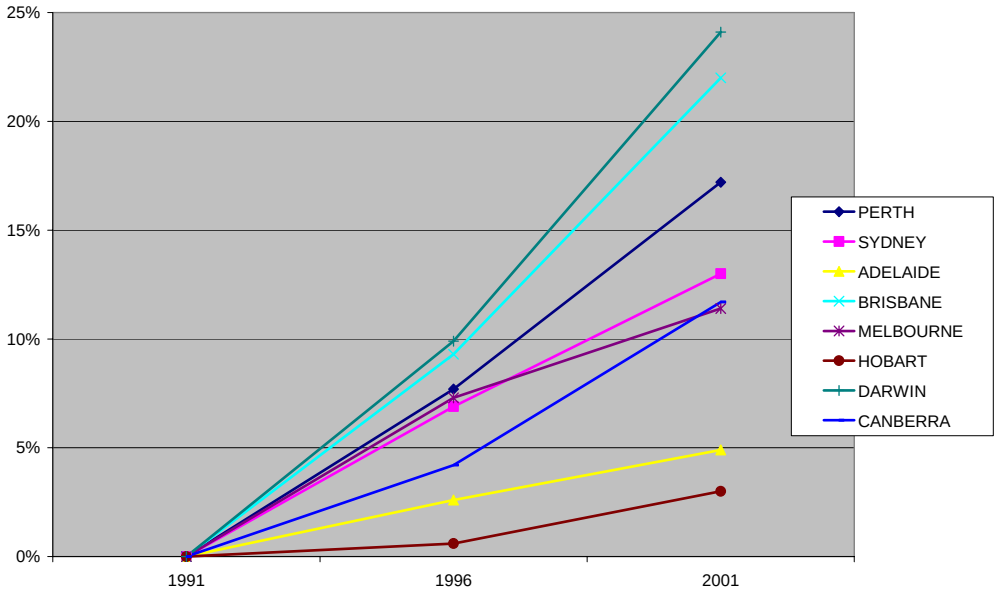

Figure 1.3. Population growth for Australian capital cities in the 1996 and 2001 Census as a percentage of population in the 1991 Census (source of data: ABS, 2005)

Recent population growth in metropolitan Perth has continued strongly (Figure 1.3).

It is worth quoting in part from the WAPC strategy because it sets out priority areas for growth in population, dwellings and employment to 2030. Growth in these areas indicate areas where community exposure to natural hazard risk will increase in future, and indicate increases in the aggregated risk for the future city (Figure 1.4).

> *'WAPC has developed a comprehensive planning strategy through extensive public consultation leading, to several well defined options for future growth. Faced with a population that will grow by about 760,000t in the next 25 years, Perth and Peel require an additional 375,000 homes and 350,000 new jobs.*

One of the priority strategies proposed in Network City is to achieve 60% of future dwelling growth within already developed urban areas, with only 40% being provided in "greenfield" sites on the fringe of the city. This represents a significant change from previous patterns of growth, where the majority of dwellings have usually been provided in fringe locations.

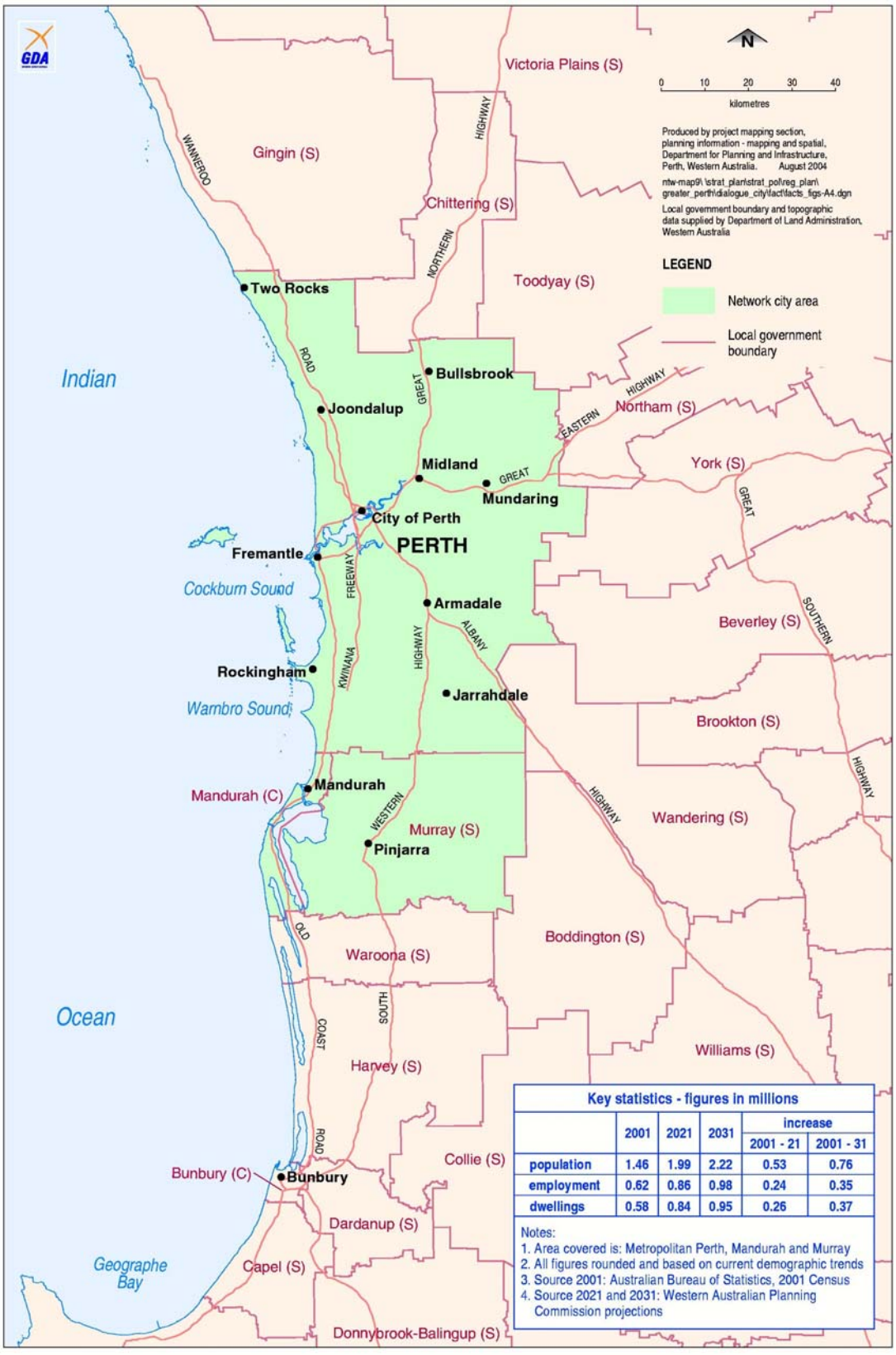

Figure 1.4: Network City – key facts and figures (from *Network City: Community planning strategy for Perth and Peel, for public comment*, September 2004. Figure reproduced courtesy WAPC)

1.8 Overview of this Report

Chapter 2: Meteorological Hazards, provides an overview of meteorological phenomena in the southwest of WA that affect Perth. The chapter was prepared primarily by Joe Courtney from the BOM, WA Regional Office, as a part of the contribution by the Bureau to the Cities Project Perth. The chapter provides descriptions of the origins and physical development of cool season storms including severe local wind storms, thunderstorms, heavy rain and flooding, tropical cyclones, heatwaves and bushfires. The chapter also provides a record of major historical events and their impacts in Perth and in southwest WA.

Chapters 3, 4 and 5 report the essential findings of hazard and risk assessments for severe winds, floods and earthquakes respectively. They are the core of the risk assessment in Cities Project Perth. They report the results of major computational investigations into these hazards by researchers from GA, the WA DOE, BOM, the Commonwealth Scientific and Industrial Research Organisation (CSIRO) and other institutions.

Chapter 3 investigates the wind hazard across metropolitan Perth. The estimates of wind hazard are based on an innovative extreme value analysis of data from AWS operated by BOM in and around metropolitan Perth. The AWS data have captured wind gusts from tropical cyclones, cool season storms, thunderstorm downdraughts and airflow from the east over the Darling Scarp. Estimates for wind speeds were calculated for return periods in the range 50 years to 1,000 years.

Ground surface topography, terrain roughness and shielding of buildings by other buildings all affect the incoming windfield upon its interaction with the urban environment. We have calculated terrain multipliers that take these three effects into account. These multipliers have been calculated at each point across metropolitan Perth at intervals of 25 m, with different multipliers for eight cardinal directions of the compass calculated at each point. These multipliers have been calculated in a GIS environment using a method consistent with the Australian/New Zealand wind loadings standard (Standards Australia, 2002).

We have developed a model that attenuates the windspeeds of westerly winds on their travel inland from the coastline. This model was developed to improve our interpretation of expected future wind speeds in Perth, because winds from the western and northern quadrants have historically been the strongest and are expected to be in the future. This model matches well with the historical data collected from the AWS.

The return period wind speeds calculated using these methods provide a guide to engineers and planners of return period wind speeds that can be expected in relation to design considerations, extending across metropolitan Perth.

In Chapter 4, we estimate flood hazard on the Swan and Canning Rivers. An unsteady state flow model has been developed that estimates flood levels for annual exceedance probabilities (AEPs) in the range 5% to 0.02% (corresponding to return periods approximately in the range 20 years to 500 years). This model updates earlier models developed by the WA DOE and will be incorporated in the Department's hydraulic modelling program. A comprehensive field survey was also conducted to capture attributes of all buildings in the floodplains in metropolitan Perth, extending from the streams up to levels approximating those of flood events with AEP 0.02% (return periods of approximately 500 years). The attribute information collected in the field estimates of ground floor height for each building. The floor height and other building attribute information such as building age, construction type and occupancy type, will assist risk assessments that examine potential losses in the future, and also response plans in relation to the scale and location of potentially affected structures and their occupants.

Chapter 5 is a comprehensive study on earthquake risk in metropolitan Perth. A broad-based assessment of earthquake hazard was conducted for this part of the continent under Cities Project

Perth, and this assessment is considered to be the best available at the time of publication, significantly improving and refining the estimates of earthquake hazard in the Australian earthquake loading standard AS1170.4:1993 and the new version of the standard, currently in draft form and due for publication in 2005. The earthquake hazard assessment has also included the collection of 'microtremor' field information (ambient seismic noise) at Northam, in the Wheatbelt, to assist the assessment of earthquake site response and earthquake hazard there.

The earthquake hazard assessment thus provides new and important information, not only for Perth but also for regional communities from Burakin in the north to Collie in the south, including Northam, York, Meckering and Cadoux, where the earthquake hazard on rock foundation is higher than that of rock sites in Perth. The earthquake hazard in these Wheatbelt communities is a significant planning and emergency risk management consideration for protection of residents and for continuity of critical infrastructure such as electric power supply, water supply and emergency services.

Chapter 6: Community Recovery, expands the scope of this report beyond estimates of the likelihood of various hazard events and, in the case of earthquakes and floods, estimates of the impacts on the Perth community of a range of return period events. Chapter 6 provides insights into how Perth as a whole, and Perth citizens in local areas as small as Census Collectors Districts, may cope with future disaster events. A recovery framework with three factors of recovery – household financial capacity, community and social networks and distance to services – is established, and measures of these three attributes are analysed in the chapter utilising published data from the Australian Bureau of Statistics (ABS).

Chapter 7 investigates the potential coastal erosion of the Swan Coastal Plain due to long-term sea level rise. It is highly likely that coastal erosion due to long-term sea level rise associated with global warming will have a significant impact on Australia's coastal systems and any associated infrastructure over the next century. Therefore, attempting to quantify this natural hazard is critical to future development and management of these localities. The potential impact of coastal erosion on the Western Australian built environment between Cape Naturaliste and Yanchep is assessed in this chapter.

Local wind-generated ocean waves are the dominant mechanism controlling net northward sand transport and determining the nearshore structure of sandy beaches. The subsurface distribution of the erosion-resistant limestone has been determined in order to assess the erosion potential of the coastline. An evaluation of potential erosion rates over the next century using a conventional two-dimensional coastal behaviour model is presented for one site within the Fremantle to Hillarys sector.

The final chapter, Chapter 8: Conclusions, draws together the major results from this study. It comments on the implications for the residents of Perth of the flood hazard, wind hazard, coastal erosion susceptibility earthquake risk, and community attributes of recovery. The chapter also integrates the recommendations for future work that were set out in individual chapters.

Five appendices also accompany the main body of the report. These appendices provide additional detail on models that were developed for the risk assessments. Appendix A provides details of the computational wind hazard assessment methodology.

Appendix B provides metadata for spatial databases that were developed in this project. These databases include GIS datasets for the Perth building database, approximately 600,000 building footprints, and other, smaller building databases developed from field surveys in the CBD area of Perth and in the Swan and Canning floodplains.

Appendix C describes the cost model that was developed for remediation or replacement of buildings and replacement of building contents. This cost model was used in the earthquake risk assessment and could be readily applied to risk assessments for flood and severe wind, among other possibilities.

Appendix D is a description of the Perth Basin that underlies Perth. The appendix features a comprehensive analysis of the Cainozoic geology and the development of geological Site Classes for earthquake hazard assessment. Ultimately, in this report, the site classification described in Appendix D was not used for the earthquake risk assessment because the original geophysical model of the Perth Basin did not describe adequately the damping of seismic wave energy travelling through the many kilometres of sediments. Instead, in this report, a simplified, empirically-based Perth Basin model was employed that did reflect the reduction in energy of seismic waves travelling through the Perth Basin (see Chapter 5). Nonetheless, the site class description in Appendix D is a robust work based on empirical data gathered from agencies such as DOE, and also collected by GA in the field. This classification is a valuable reference for design engineers and planners who employ the earthquake loading standard. The site class model could be incorporated in earthquake hazard assessment models for Perth in future with improved model parameters for the underlying Perth Basin sediments.

Appendix E is a commentary on the potential for tsunamis, generated by Indonesian earthquakes, to impact on southwest WA. The appendix is particularly timely, following the appalling Boxing Day 2004 Indonesian earthquake and tsunami which killed more than 200,000 people in southern Asia. The appendix refers to remarkably premonitory research by the author on the tsunamigenic effects of previous great Sumatran earthquakes in 1833 and 1861, and the potential for future great earthquakes to generate tsunami in the region.

1.9 References

Australian Bureau of Statistics (2005) Website: *Capital city statistical division counts for ABS 2001 Census.* Accessed February 2005.

Bureau of Transport Economics (2000) *Road crash costs in Australia*, Report 102, Bureau of Transport Economics, Commonwealth of Australia, Canberra.

Bureau of Transport Economics (2001) *Economic costs of natural disasters in Australia*, Report 103, Bureau of Transport Economics, Commonwealth of Australia, Canberra.

Bureau of Meteorology (2005) Website: http://www.bom.gov.au/weather/wa/cyclone/about/extremes.shtml. Accessed February 2005.

Bureau of Meteorology (1995) *Climate of Western Australia,* Bureau of Meteorology, Commonwealth of Australia, Melbourne.

Bushfires Board of Western Australia, (1997), Annual Report (?).

Dhu, T. and Jones, T.D. (editors) (2002) *Earthquake Risk in Newcastle and Lake Macquarie, New South Wales*, Geoscience Australia, Canberra.

EMA Disaster Database (2005) Website: http://www.ema.gov.au/ema/emaDisasters.nsf. Accessed January 2005.

Everingham, I.B.E., McEwin, A.J. and Denham, D. (compilers) (1982) *Atlas of isoseismal maps of Australian earthquakes*, BMR Bulletin 214, Canberra.

Everingham, I.B.E. and Gregson, P.J. (1970) *Meckering earthquake intensities and notes on earthquake risk for Western Australia*, Bureau of Mineral Resources, Geology and Geophysics Record 1970/97, Canberra, 1970.

FESA (2005) 'Deliberate Hills inferno sparks mammoth response' in *24seven, Official magazine of the Fire & Emergency Services Authority of Western Australia*, April, pp. 12–15.

Gordon, F.R. and Lewis, J.D. (1980) *The Meckering and Calingiri earthquakes: October 1968 and March 1970*, Geological Survey of Western Australia Bulletin 126.

Granger, K., Jones, T., Leiba, M. and Scott, G. (1999) *Community Risk in Cairns: A multi-hazard risk assessment*, Australian Geological Survey Organisation, Department of Industry Science and Resources, Canberra.

Granger, K. and Hayne, M. (editors) (2001) *Natural Hazards and the Risks They Pose to South-East Queensland*, Australian Geological Survey Organisation, Department of Industry Science and Resources, Canberra.

Granger, K. and Michael-Leiba, M.O. (editors) (2001) *Community Risk in Gladstone: A multi-hazard risk assessment*, Australian Geological Survey Organisation, Department of Industry Science and Resources, Canberra.

Gregson, P.J. (1980) *Mundaring Geophysical Observatory annual report, 1979*, Bureau of Mineral Resources, Australia, Record 1980/51.

Hanstrum, B.N. (1992) *A history of tropical cyclones in the southwest of Western Australia 1830–1992*, Journal and proceedings of the Royal WA Historical Society (Inc), 10:397–407.

High Level Group (2002) *Natural Disasters in Australia: Reforming mitigation, relief and recovery arrangements, a report to the Council of Australian Governments*, Australian Department of Transport and Regional Services, Canberra.

Insurance Disaster Response Organisation (2005) Website: www.idro.com.au. Accessed January 2005.

Joy, C.S. (1991) *The cost of natural disasters in Australia*, paper presented at Climate Change Impacts Workshop, Climatic Impacts Centre, Macquarie University, New South Wales, Australia, 13–15 May.

Kramer, S.L. (1996) *Geotechnical earthquake engineering*, Prentice Hall, New Jersey.

Lewis, J.D. *et al.* (1981) *The Cadoux earthquake*, Geological Survey of Western Australia Report 11.

McCready, L.A. and Hanstrum, B.N. (1996) 'Two ordinary cell severe downburst cases at Perth, Western Australia', *Proceedings of 5th Australian Severe Thunderstorm Conference, Avoca Beach, New South Wales*, pp. 65–76.

Middelmann, M. and Granger, K. (editors) (2000) *Community risk in Mackay: A multi-hazard risk assessment*, Australian Geological Survey Organisation, Department of Industry, Science and Resources, Canberra.

Perth Gazette, 11 July 1862.

Standards Australia (2002) *Wind loading standard* AS/NZS 1170.2: 2002.

Troy, P. (editor) (1995) *Australian Cities: Issues, strategies and policies for urban Australia in the 1990s*, Cambridge University Press, Cambridge.

West Australian, March 12, 1934 and 24 January 1981.

Western Australian Museum (2005) Website: www.museum.wa.gov.au. Accessed February 2005.

Western Australian Planning Commission and WA Department for Planning and Infrastructure (2004) *Network City: Community planning strategy for Perth and Peel, for public comment, September 2004*.

Chapter 2: METEOROLOGICAL HAZARDS

Joe Courtney[1] and Miriam Middelmann[2]

[1] Bureau of Meteorology, WA Regional Office
[2] Geoscience Australia

2.1 Introduction

This chapter provides an introduction to meteorological hazards. It is divided into the different meteorological phenomena that affect the Perth region, including cool season storms, warm season thunderstorms, heavy rain and flooding, tropical cyclones, heatwaves and bushfires. A number of hazards such as hail, flooding or wind can occur as a result of more than one of these meteorological phenomena. The modelling of severe wind and riverine flooding is described for Perth in Chapters 3 and 4 respectively.

Cost of meteorological hazards

Table 2.1 shows the average annual cost of the four most costly meteorological hazards between 1967 and 1999 in Western Australia and Australia as a whole. The unpublished Emergency Management Australia database (EMA Track) has been used for the analysis and is biased by large events, such as the Sydney hailstorm (Bureau of Transport Economics (BTE), 2001). In Western Australia cyclones produce the largest average annual cost, with cyclonic activity focused in northern Western Australia. The damage from cyclones may be from flooding, severe winds or storm surge. However, the values shown in Table 2.1 considerably underestimate the damage, with a major cost of cyclones to the industry, which has not been included. The average annual cost from severe storms ranks it as the second most costly meteorological hazard in the state. Accounts of historical events illustrate the prevalence of severe storms in the Perth area, with severe winds in particular resulting in damage to buildings and infrastructure. Bushfires have also impacted the region, and have an average annual cost in Western Australia of $4–5 million, followed by flooding at a cost of about $3 million. Heatwaves, though not ranking in the top four meteorological hazards in terms of cost, can result in loss of life, particularly among the elderly.

Table 2.1: Average annual cost of meteorological hazards (Extracted from BTE, 2001)

	Average annual cost ($ million)			
Location	**Flood**	**Severe storm**	**Cyclones**	**Bushfires**
WA	2.6	11.1	41.6	4.5
Australia	314	284.4	266.2	77.2

2.2. Cool Season Storms

The storm threat

During the cooler months of the year the southwest of Western Australia experiences moist westerly winds that generally produce over 80% of the region's annual rainfall Cold fronts embedded in the westerly flow bring the rain and strong winds on an irregular cycle every few days. Each front is unique, varying with the strength of wind, and amount and distribution of rainfall.

Some of the more vigorous fronts produce severe wind gusts in excess of 90 km/h, or may spawn tornadoes. The level of threat to life and property may also be described in terms of wind strength. Damaging winds refer to wind gusts between 90 and 125 km/h, and destructive winds refer to wind

gusts in excess of 125 km/h. These events are not necessarily accompanied by lightning, but they are still referred to as ‘storms’.

It is possible to distinguish two general types of storm threats that cause severe winds during the cooler months:

- Strong fronts and intense lows that cause sustained gale-force winds and severe gusts over a widespread area, and
- Fronts that cause localised severe winds, including tornadoes.

Widespread severe winds

Although fronts frequently move over southwest Western Australia in the cooler months, only a few times each year do very strong cold fronts associated with deep low-pressure systems affect the region. These can cause gale-force winds and heavy rain over the southwest, including Perth. The more significant events also produce an increase in tidal levels known as a storm surge, and also large waves that can result in coastal erosion. Wind damage, such as fallen power lines, typically occurs over a wide area, with the potential to cause significant power outages and traffic disruption. Often fallen trees and branches cause much of the property damage. More severe damage, likely to be caused by destructive winds exceeding 125 km/h, is usually localised.

The wind event is more significant if the strong westerlies remain for extended periods. Usually this occurs when a low or series of deep lows moves slowly south of the state and generates multiple fronts maintaining a strong westerly airstream over the southwest. On 7–8 June 1981, for example, winds at Fremantle (recorded at a height of 60 m) exceeded 55 km/h for 36 hours.

A characteristic of major westerly events is the strong winds associated with downdrafts accompanying showers and thunderstorms. These winds are transported from higher levels to the surface, causing severe squalls of at least 90 km/h, but usually less than 125 km/h. Gusts may be quite localised, becoming more widespread if associated with showers on a front or pre-frontal line.

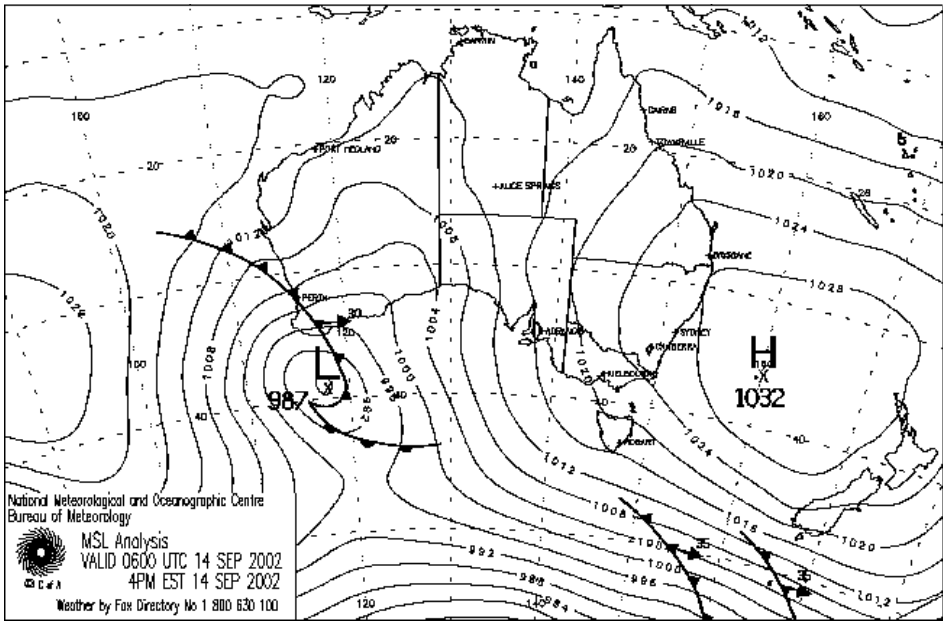

Figure 2.1: Mean Sea Level Pressure analysis showing a strong front extending through Perth to a deep low south of Albany, 14 September 2002

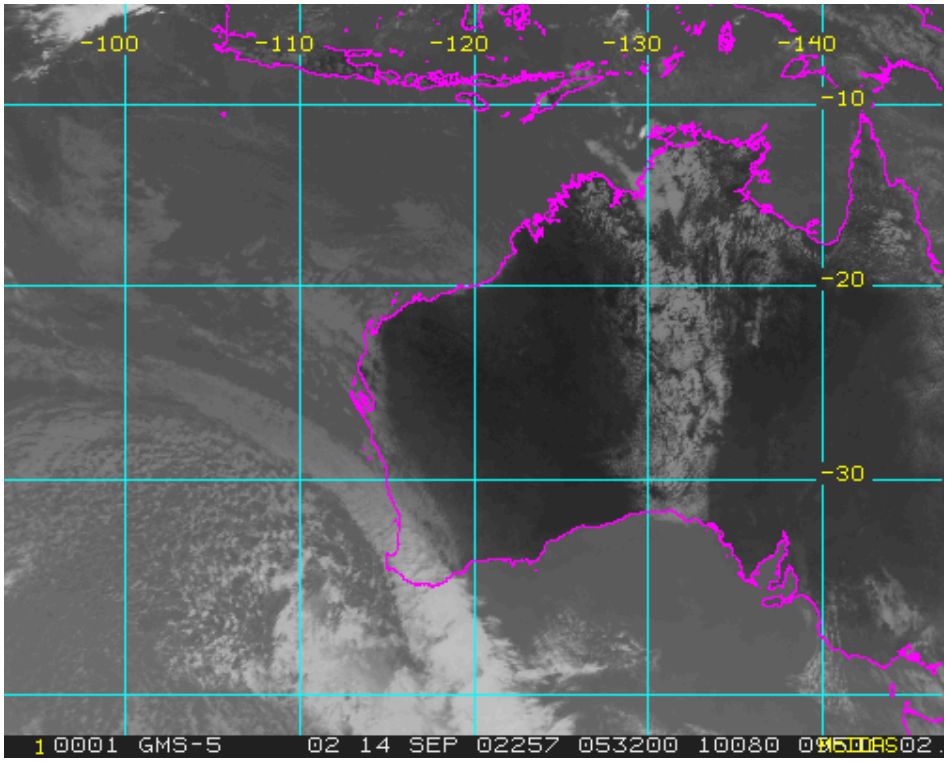

Figure 2.2: Satellite image of a strong front near Perth, 14 September 2002 (Courtesy of the Japan Meteorological Agency)

An example of a deep low and associated strong pressure gradient over the southwest is shown in the mean sea level pressure analysis of 14 September 2002 in Figure 2.1. The accompanying satellite image in Figure 2.2 shows the distinctive cloud band along the frontal boundary followed by the speckled cloud indicative of the cold airmass to the west.

Historical events

Winter storms have long been recognised as a major hazard of the area. The indigenous Nyungar people in the Perth region tended to move inland during the cooler months, partly to avoid the westerly gales. In June 1801, the French explorer Nicholas Baudin felt the full force of a winter gale as he rounded Cape Leeuwin *en route* to Rottnest Island. The early settlers were quickly made aware of the dangers of winter gales. The loss of the *Marquess of Anglesea* and damage to other vessels during a gale in 1830 threatened the existence of the colony, being described at the time as almost a 'death blow to the infant colony' (Bureau of Meteorology (BOM), 1929, p. 164). Winter gales posed a frequent threat to shipping, not only disrupting services but occasionally sending ships aground and sometimes wrecking ships completely. A list of some of the major winter storms of the last fifty years and their impact is shown in Table 2.2.

In more recent times, the event of 23 May 1994 ranks as one of the most significant wind storms experienced in Perth, causing an estimated $37 million damage (1998 dollars). Apart from two houses that were unroofed, most of the damage was of a minor nature such as damage to fences, with the average insurance claim only $700 (McCready and Hanstrum, 1995). The *Australian* (25 May 1994) reported that at least 600 homes in Perth had sustained some form of damage. Power outages were so widespread with more than 250,000 buildings affected, that it took almost a week to fully restore power to Perth homes. In addition to affecting businesses and homes, the loss of power affected pumping stations resulting in minor spills of raw sewage into the Swan and Canning Rivers from 29 pumping stations (*West Australian*, 25 May 1994). Two people on board a yacht were lost at sea off Jurien, north of Perth. Huge seas and above normal tides caused significant erosion to beaches, while

parts of the Perth river foreshore were inundated. Fremantle recorded 25 wind gusts of at least 129 km/h, more than three times the number recorded for any other event since the 1960s.

Table 2.2: Notable deep winter lows causing gales during the cooler months

Date	Description
14 August 1955	Several westerly gale events caused massive coastal erosion on Perth's beaches. At Cottesloe not a vestige of sand was left anywhere along the seaward side of the main 120 m promenade, leaving exposed the underlying limestone.
19–20 August 1963	A strong front caused a wind gust of 156 km/h in Perth, the highest ever recorded in the Perth area. A suspected tornado demolished a factory in Scarborough just before midnight and the trail of damage extended through Doubleview and Innaloo.
8 June 1981	Strong, squally winds, accompanied by heavy rain, produced widespread damage about the southwest coast. Perth metropolitan area was littered with fallen trees and power lines and the debris from damaged buildings. Damage extended north to Geraldton, inland to Northam, and south to Harvey.
28–29 June 1983	This storm was responsible for widespread damage in the southwest, including the loss of two lives. Bad weather was blamed for a road crash fatality and an American sailor was crushed behind a ship's door in high winds. The storm downed trees and power poles, with blackouts lasting up to three days after the event. Roads were cut due to heavy rain. The damage bill for this storm was estimated to be greater than $1 million (1983 dollars).
22 September 1988	The storm caused extensive damage from Perth to Albany. Hundreds of roofs were damaged and several ripped off entirely, trees were downed, and power was lost to over 100,000 homes in the metropolitan area. Damage was sustained to about twenty boats in the Perth area after breaking their moorings. Severe damage was also done to Perth market gardens and vineyards. The cost was estimated (in 1991 dollars), to be $8 million (McCready and Hanstrum, 1995).
23–24 May 1994	The windstorm was one of the most destructive weather events to affect Perth, with a total damage bill of $37 million (1998 dollars). Several houses were completely unroofed but the majority of property damage was minor, most claims being for fence damage. Downed powerlines, mostly due to fallen trees and branches, caused widespread blackouts, leaving up to one-third of Perth without power at the height of the storm. Two people on a yacht off the coast from Jurien Bay were lost at sea. Huge seas and above normal tides caused significant erosion to beaches. Parts of the Perth river foreshore were also inundated. Swanbourne recorded a maximum gust of 143 km/h, while winds at Fremantle averaged 107 km/h over a 30-minute period.
16 May 2003	A deep low moved over the coast near Cape Naturaliste where the pressure fell to 982 hPa, one of the lowest pressures ever recorded in southern Western Australia. A storm surge of 0.8 m caused the highest tide ever recorded at Fremantle, about 0.5 m above the highest astronomical tide. The resulting flooding in low-lying parts disrupted traffic and undermined the foundations of a canal property near Mandurah. The high tides and heavy surf caused widespread beach erosion. Wind damage was general, although mostly minor. Rottnest Island recorded a gust of 117 km/h and Ocean Reef 115 km/h.

Frequency

A simple indicator of the intensity of fronts affecting the lower west coast is the pressure gradient from Geraldton to Albany. A 'storm event' can be defined when the pressure gradient exceeds 15 hPa. Although this does not always reflect the intensity of every system, it does provide an objective comparison between events since 1965, when three hourly pressure data was available from both Geraldton and Albany. This threshold generally correlates to gale-force winds on the coast and wind gusts exceeding 90 km/h. There have been exactly 100 such events over a 39-year period from 1965 to 2003, equating to about 2.6 per year. There have been eight major events when the pressure gradient has reached at least 20 hPa such as in May 1994. On average this equates to one major event every five years. The monthly frequency of storm events is shown in Figure 2.3. Seventy percent of events are relatively evenly distributed between the months of June and September, though storm events have been recorded as early as April and as late as November.

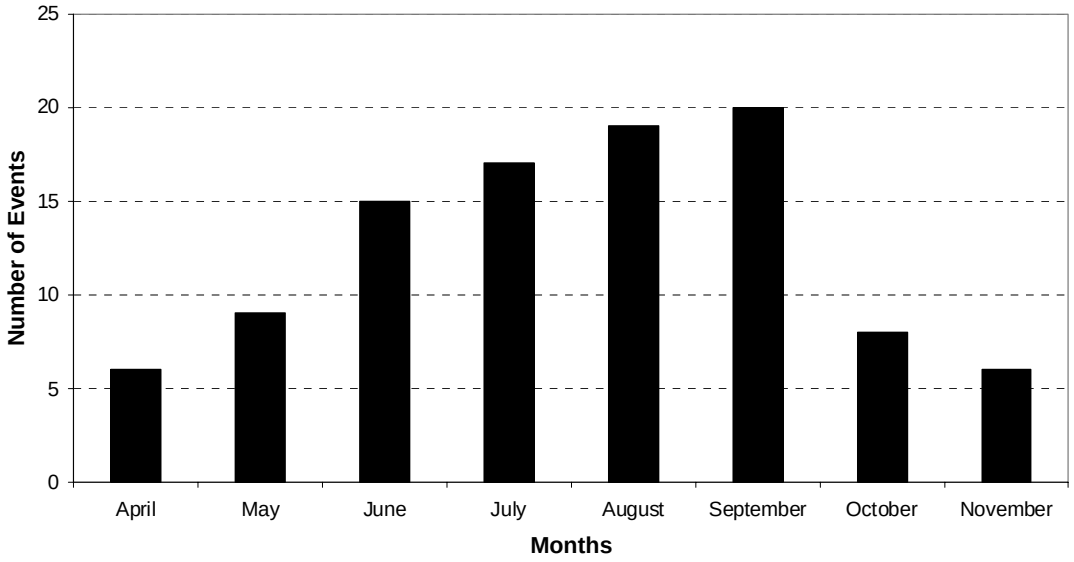

Figure 2.3: Monthly frequency of major winter storm events, 1965 – 2003. An event is defined by the occurrence of the Geraldton to Albany pressure gradient exceeding 15 hPa

Severe local wind storms

The most severe winds that occur in Perth are very localised, typically causing a narrow swathe of damage just tens of metres in width. Severe local wind storms (SLWS) can be divided into tornadoes and downbursts. It is often difficult to determine the exact cause of damage, particularly for weaker storm events. Where significant damage has occurred, indicating destructive winds in excess of 125 km/h, it can be easier to attribute the cause of damage to a tornado, colloquially called a 'cock-eyed bob' in Western Australia. Apart from the strong fronts, more moderate systems can also produce a SLWS, making these events particularly difficult to forecast. They typically occur with deep convective clouds on the frontal boundary, but may also occur on convergent lines ahead of the front, or in the cold air following the front.

SLWS are typically short-lived and move at speeds of up to 80 km/h with the associated front. Their narrow width and short path lengths, typically less than 5 km, means that they affect only small areas. They are relatively weak, usually only rating F0 (62–117 km/h) or F1 (118–178 km/h) on the Fujita tornado scale, based on extent and severity of damage. Damage reports and eyewitness accounts of these events indicate that damage varies considerably along the track. Some houses may be significantly damaged, while others of a similar construction nearby can escape any impact at all. Some reach F2 category (179–250 km/h), such as the Collie tornado in 1960.

Damage is often discontinuous along the track, suggesting that severe winds do not move evenly over the ground, especially when the terrain varies. Exposed elevated areas are more vulnerable to severe winds than sheltered parts on the leeward side of hills. Trees are often affected at different heights. Larger trees snapped off near the base indicate a much stronger wind than those with higher branches only broken off. A farmer described a tornado at Williams in 1959 passing over a flock of sheep without disturbing them. Fronts may spawn more than one tornado at a time. On 17 October 2002, a front of what appeared to be moderate intensity caused widespread localised damage across the South West Land Division with four tornadoes in the metropolitan area and several other confirmed tornadoes. It is likely that many more went unreported.

Cool season tornadoes are very different from those associated with severe thunderstorms in the warmer months, including those on the Great Plains in the USA. It is quite rare to have a report of a

funnel cloud extending from the base of a cloud. Visibility is typically very low as it is usually raining heavily and they move at typical speeds of 60–80 km/h. Many people have reported hearing a sound like an approaching freight train or similar, which is a common description of tornadoes elsewhere.

Historical events

The earliest recorded probable tornado occurred during the early morning of 18 June 1842 at Australind, north of Bunbury. The *Perth Enquirer* reported a 'wind storm' that moved across the narrow strip of land between the sea and the Leschenault Estuary, creating a lane through the forest 300–400 yards wide and extending from the northwest to southeast across the Collie and Preston Rivers. In the centre of the path nothing was left standing but bare trunks of trees. The storm was accompanied by rain, hail and lightning and the wind turned from northerly on the 17th to the west southwest on the 18th.

The first observation of a probable tornado in the Perth area was reported by a Captain Wray on 4 June 1856. He described a 'whirlwind' that moved over Fremantle prison from northwest to southeast, accompanied by a loud hissing noise. The whole north boundary prison wall was laid flat, 'turning over its foundations like a hinge' (BOM, 1929).

One of the most intense tornadoes to affect southwest Western Australia swept through dense Jarrah forest at Lyall's Mill near Collie on 6 April 1960. The tornado cut a path averaging 240 m wide along a continuous 30 km track. Forestry officers estimated that the volume of felled timber was enough to provide a year's work at a local mill. On 11 July 1964, a teenager was killed and several others injured when a tornado pushed a moving car off the road at Busselton (*Sunday Times*, 12 July 1964).

Closer to Perth, on 8 June 1968 a severe wind squall likely to have been a tornado destroyed 40 caravans and extensively damaged 24 cottages at Naval Base, south of Fremantle. The damage trail is shown in Plate 2.1. Plate 2.2 shows one of eight homes in Mandurah destroyed by storms which damaged more than 100 dwellings on 22 September 1993 (Hanstrum, 1994). The damage to an apartment building in Fremantle on 13 August 1999 is shown in Plate 2.3. The remains of a house after a reported tornado at Rockingham on 13 June 2001 are shown in Plate 2.4. The experience of a man who narrowly escaped death from the 12 August 1987 tornado in Mandurah is described in the *West Australian* (13 August 1987):

> *He heard the terrifying scream of ripping steel. He looked up and saw guttering, tiles and branches flying across the street. At one stage, a shed flew about 20 m over a house on the other side of the street. A flash of white rebounded off the side of one house and on to the roof of another. It was an aluminium boat…A 135 kg waste disposal bin from next door was picked up by the wind and smashed into the side of their house. It took several men to lift it back into place. The Bairds' water tank was carried about 70 m, smashing through fences and a sign before coming to rest in bushland.*

Frequency

The occurrence of severe localised winds (including tornadoes) is much greater than is commonly thought. While most events occur in coastal parts between Perth and Albany, they have been recorded across the South West Land Division from Geraldton, Southern Cross and near Esperance. It is not coincidental that the highest number of reports comes from the most heavily populated parts of the coastal strip between Perth and Busselton. The highly localised nature of these events mean that those in remote bushland are likely to go unreported, making it very difficult to give meaningful statistics on frequency, especially in an area of low population density.

Coastal suburbs are more likely to experience a SLWS than those further inland, probably due to frictional discontinuity at the coast. A particularly high proportion of reports are from the Mandurah and Rockingham areas south of Perth. It has been conjectured that the change in coastline orientation makes these locations more susceptible to SLWS events than other parts of the Perth metropolitan area. The extra lifting and frictional effects of the Darling Escarpment suggest that the frequency of

events should be higher near the escarpment than on the adjacent coastal plain but the extent of bushland near the escarpment makes this claim difficult to confirm.

Plate 2.1: Damage from the tornado at Naval Base, 8 June 1968 (Courtesy of the *West Australian*)

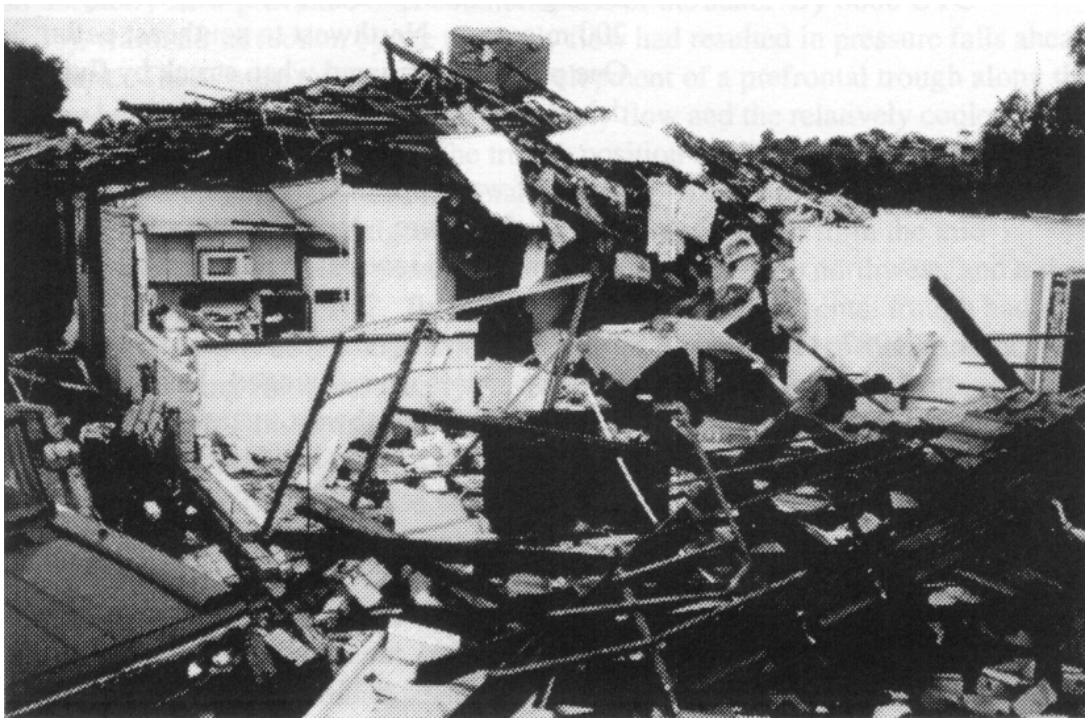

Plate 2.2: A house destroyed in Mandurah, 22 September 1993 (Courtesy of the *West Australian*)

Plate 2.3: Damage to apartments in Fremantle, 25 August 1999 (Courtesy of BOM)

Plate 2.4: A house destroyed by a suspected tornado in Rockingham, 13 June 2001 (Courtesy of the BOM)

SLWS have been reported between April and October. The earliest in any year that a storm has occurred has been on the 6 April (1960) and the latest on 31 October (2002). They occur most commonly in June. They can occur at any time of the day and there appears to be no higher concentration of occurrence at any particular time of the day.

Foley and Hanstrum (1990) analysed SLWS during the cooler months in the southwest of the State from 1958 to 1988. They identified 51 cases on 47 days in the 31-year period using newspaper

clippings, averaging 1.6 per year. This included 33 cases in the Perth metropolitan area. However, they concluded the frequency of events along the Lower West coastal strip to be higher at 5.6 per year, after accounting for variations in reports due to population density. From 1993 to 2003 there has been an average of 5.5 reports per year in the region, a considerable increase in reports over the 1958 to 1988 study. In Perth there were 31 suspected tornado cases on 26 days in the eleven years to 2003, almost the same number as in the 31 years in the previous study. However, this increase is likely to be more attributable to an improved detection rate rather than an actual increase in frequency. Additionally there were many more SLWS when wind gusts exceeded 90 km/h but did not cause any known damage.

An alternative method of assessing the frequency of SLWS is to identify the atmospheric environmental features in which they occurred. In a study of 20 tornadoes in Western Australia and South Australia from 1994–96, Hanstrum *et al.* (1998) identified the critical environmental features for tornado development. This study has not only improved the ability to forecast such events but also assists in more objectively assessing the frequency of occurrence.

An unpublished study of observational records from 1967 to 2003 showed the frequency of potential tornado days to be about nine per year for Perth. Experience suggests that this is probably an overestimate of actual tornado days, especially when considering the incidence in just the Perth metropolitan area. Based on reports from 1993 to 2003, the average number of tornadoes in the Perth area seems to be in the order of three per year. However, the theoretical number of nine potential tornado days may more closely match the number of frontal events that cause severe wind gusts in Perth. An unpublished study of cold fronts from 1995 to 2003 showed that there were an average 9.5 events per year causing severe wind gusts in Perth. Of these, two to three were considered major fronts accounting for widespread minor damage, four caused local damage, and three events had no known damage although severe wind gusts were recorded. A description of some significant severe local wind squalls in Perth and the Southwest region is given in Table 2.3.

Rainfall

Although the aforementioned events causing severe winds can also cause periods of heavy rain, they do not represent the strongest rainfall-producing events. Cold fronts that generate slow-moving cloudbands extending into the tropics typically cause the heaviest cumulative rainfall. These are discussed in more detail in section 2.4.

Storm surge and coastal erosion

One of the consequences of sustained gale-force winds about the lower west coast is storm surge. Storm surge is a rise in the normal water level caused by strong onshore winds and reduced air pressure. The impact is greatest if the storm surge peaks near the time of high tide. This can result in the inundation of the river foreshore such as Riverside Drive near the Perth city centre and on the freeway just south of the Narrows Bridge. Low-lying coastal areas such as at Mandurah, Bunbury and Busselton are particularly vulnerable to inundation. Flooding is exacerbated when river levels are high because of heavy rains. More details on storm surge are provided below.

Coastal erosion results when the pounding of large waves generated by significant wind speeds combine with a storm surge. Every winter Perth's beaches are temporarily modified due to the scouring of beach sand by strong winter storms. A strong westerly gale on 20 July 1910 caused damage to the Fremantle North Mole and the foundation of the Jandakot railway line (BOM, 1929). During the May 1994 event, significant coastal erosion occurred because of wave action, despite the storm surge peaking near the time of the normal low tide. The open water swell was estimated at 8–9 m. Storms in August 1955 badly damaged many of the beaches between South Beach and Sorrento. South of the jetty at Cottesloe Beach, 150m of foreshore were eroded back about 25 m during the storms. An extract from the *West Australian* (18 August 1955) describes some of the damage.

At Cottesloe not a vestige of sand is now left anywhere along the seaward side of the main 400 ft. promenade. The whole of the area is rugged dangerous limestone. The 12 ft. high wall of the promenade is firmly embedded in the limestone reef, but yesterday morning heavy seas were dashing high against it. A certain amount of undermining was going on. At the foot of the former jetty where the waves were heaviest a 4 ft. wide hole had been made in the promenade bitumen surface…The main damage at North Cottesloe has been the undermining of an 50 ton wartime beach observation post of concrete and steel and the collapse of the 30 ft. steel shark alarm tower… In Sunday's storm hundreds of tons of sand and big slabs of concrete were carried away from in front of the Swanbourne Nedlands Surf Club pavilion.

Table 2.3: Notable severe local wind squalls, including tornadoes

Date	Description
16 June 1954	Damage through Jarrah forest near Dwellingup to 200 m wide along 10 km track.
6 April 1960	Tornado through Jarrah forest near Collie, 240 m wide for 30 km. The estimated volume of timber useful for milling was enough for a year's work at the local mill.
15 June 1964	Tornado through the northeastern part of Mandurah caused extensive damage to houses and vegetation along a narrow track about 30–50 m wide. One person was injured by flying debris.
8 June 1968	A severe wind squall destroyed 40 caravans and extensively damaged 24 cottages at Naval Base. Eye-witness accounts do not describe a tornado, although damaging winds came from several directions.
9 September 1968	Thirty houses were unroofed at Kewdale.
21 June 1980	A tornado in Shoalwater Bay caused major damage to 38 homes and minor damage to another 60 in a 100 m wide strip along a 3 km path.
22 August 1983	In Fremantle a tornado damaged several hotels, 40 houses and two storage buildings. Eye-witnesses reported a 'whirlwind of sand and stones' in places and a 'spray of water' as it crossed the Swan River.
3 September 1983	About 50 houses damaged, some almost totally destroyed, along a path from Scarborough to Mt Lawley. Damage was worst on higher ground.
12 August 1987	A tornado, first observed as a waterspout at sea, damaged 70 houses along a 3 km path in Mandurah. One man was injured when his car was rolled over.
22 September 1993	Two tornadoes swept through Mandurah at 5 pm. The stronger one passed through Halls Head, destroying 8 houses and damaging a further 100.
15 July 1996	Tornado through Kings Park and South Perth. One house badly damaged and insurance claims, mostly for minor damage such as fences and ridge capping, totalled approximately $447,000.
25 August 1999	One person was injured in Fremantle when the roof blew off a block of flats
23 August 2001	Two separate lines of damage, up to 100 m wide, occurred in Kelmscott and Como. About ninety homes sustained damage, most because of roof damage done by fallen trees. Up to 10,000 homes were without power as lines were brought down.
13 June 2002	A tornado on a pre-frontal squall line moved through Rockingham at 2:40 am. The SES was called to 28 homes in the tornado's 50 m wide and 2 km long path.

Hail

During the winter months hail can occur in the cold airmass following the passage of a front. However, the growth of hail is much less than in summer thunderstorm clouds and the size is generally on the order of one centimetre or less, and not large enough to cause damage. Nevertheless, a large amount of small hail can block drains that can lead to water inundation to properties. Larger hail is more common in spring and the warmer months, and is discussed in more detail in section 2.3.

Thunderstorms and lightning

Despite cool season events being described as storms, only a minority of them actually cause thunderstorms and lightning. In Perth there are an average of two thunderstorms per month from May to July and one per month for the remainder of the year. One such lightning event cut all computers and telephones in the Royal Perth Hospital and subsequently put human life at risk (*West Australian*, 1 July 1996). The electrification process is weaker in cool season thunderstorms than those of the

warmer months, so the number of lightning strikes is considerably lower between May and July than in the months of January to March.

2.3 Warm Season Thunderstorms

The thunderstorm threat

Compared to eastern and northern Australia, thunderstorms are infrequent in Perth during the warm season between October and April, occurring on average five to six times. Only a small number of these storms become severe enough to pose a serious threat to the community. The number of warm season thunderstorm days varies considerably from year to year, ranging from 14 in 1991–92, to just one in the 1990–91 and 1993–94 seasons.

Most storms develop in the afternoon when surface heating is greatest. A typical feature of the weather pattern in the warmer months is a low-pressure trough that extends from the Pilbara to southern parts of the state. Surface heating combined with convergence near this trough in the low levels of the atmosphere can trigger convection providing there is sufficient moisture. Figure 2.4 is a satellite image showing storms developing along the trough near the west coast.

Storms are more frequent to the north and east of Perth. Typically, a trough forms inland of the city, or moves inland during the day with the seabreeze prior to storms developing along it. On such days storm clouds can be clearly seen to the east of the city over the ranges. When the trough is near the coast they are more likely to form in the warmer air to the north and be steered to the southeast by mid-level winds. For these reasons the eastern hills areas such as Chittering and Gidgegannup have a higher incidence of warm season storms than other areas.

About 30–40% of Perth's warm season storms occur in the early morning. They usually result from uplift forced by strong easterly winds near the surface rather than from surface heating. These storms are more difficult to forecast. They are not usually associated with severe weather phenomena, but when combined with other forcing mechanisms or tropical moisture, as happened on 8 February 1992, strong winds, hail and heavy rain can be produced.

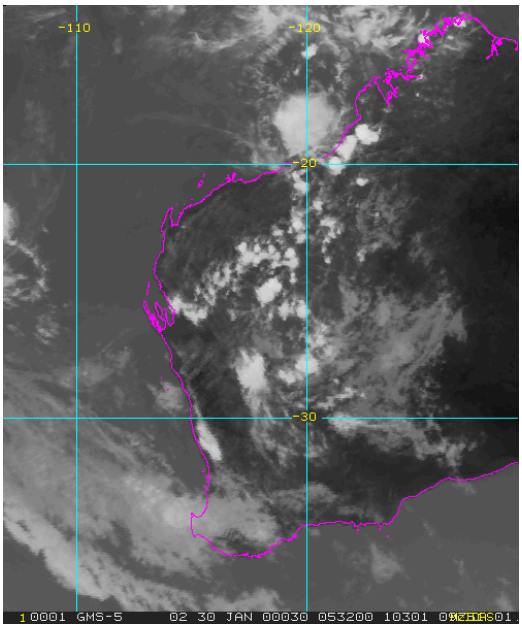

Figure 2.4: Satellite image showing thunderstorms developing near the west coast trough just to the north of Perth on 30 January 2000 (Courtesy of the Japan Meteorological Agency)

Most storm events are highly localised and do not affect large areas, in contrast to tropical cyclones and winter fronts. Individual thunderstorms typically extend over an area less than 10 km^2, move at

20-40 km/h, and last only a few hours. Multiple thunderstorm cells commonly form in any given situation so the overall area affected may be considerably greater. Figure 2.5 shows composite tracks of thunderstorm cells over 4 hours on 27 March 1995. Storms developing over a widespread area usually require abundant moisture inland, possibly associated with a tropical low or cyclone to the north. The satellite image in Figure 2.6 shows widespread storms over the southwest associated with a low off the Pilbara coast during the 22 January 2000 rain event. Some types of severe storms can last for several hours. Plate 2.5 shows low-level cloud indicating the approach of storms on 30 March 2003. On this day, 29 mm of rain was recorded in just 30 minutes at Perth Airport.

Although all thunderstorms pose a danger to life and property through lightning strikes, very few of Perth's thunderstorms reach 'severe' status. A severe thunderstorm is defined as producing one or more of the following:

- hailstones with a diameter of 2 cm or more;
- wind gusts of 90 km/h or greater;
- flash flooding; and/or
- tornadoes.

Table 2.4 is a list of notable warm season thunderstorms in the Perth region. There are several different types of severe warm season thunderstorms that affect Perth. Although quite infrequent, the supercell type storm can maintain an intense state for several hours. It has an organised structure of co-existing updraught and downdraught and can move in different directions to normal thunderstorms. Of particular concern to Perth are those that form to the north of Perth and move to the right of the typical southeasterly track. Therefore, rather than moving inland they move to the south or even southwest near the coast as shown in Figure 2.5. On 27 March 1995 and 14 January 2002, supercells caused large hail just north of Perth before moving offshore. These storms are capable of producing large hail, heavy rain severe wind gusts and even tornadoes. In January 1960, a tornado caused a swathe of damage in the Byford area. However, such events are rare in the metropolitan area.

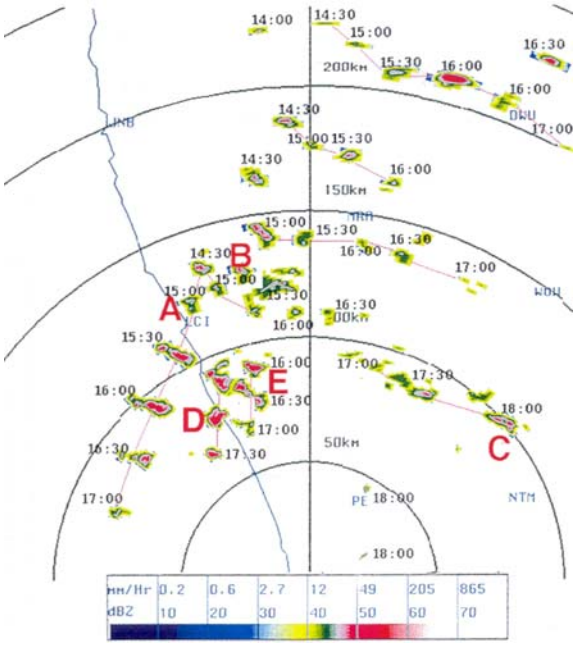

Figure 2.5: Composite tracks of thunderstorm cells over four hours (4–8 pm, 27 March 1995). Most cells move to the southeast but severe cells A and D split away and move to the south-southwest. Fortunately these were most severe after moving off the coast but cell D caused hail to 5 cm diameter near the coast

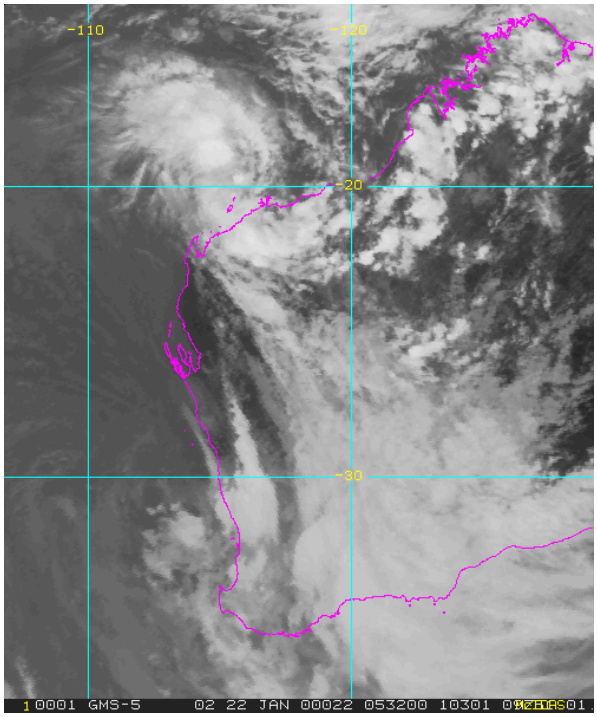

Figure 2.6: Satellite image showing thunderstorm area over the southwest during the 22 January 2000 rain event. A tropical depression off the Pilbara coast provided the moisture while an upper-level low off the west coast combined with a surface trough near the coast to cause widespread heavy rain (Courtesy of the Japan Meteorological Agency)

Plate 2.5: Photo of low-level cloud indicating the approach of storms on 30 March 2003 (Courtesy of Radek Doleki)

Severe wind gusts can also be caused by downbursts – a strong downdraught that reaches the surface. These are sometimes accompanied by heavy rain, but may also occur in the absence of rain when they are referred to as dry downbursts. For most of these cases the extent of the severe gusts is highly localised, so the term microburst is often used. In December 1991 a dry microburst was able to move a parked passenger aircraft at Perth Airport, while others have been known to unroof houses.

Table 2.4: Some notable warm season thunderstorms affecting the Perth region

Date	Description
1 January 1960	An afternoon storm that initially brought heavy rain and hail to the western suburbs produced a tornado at Byford, cutting a swathe of damage, mostly through bushland. Damage was minor, apart from one house unroofed.
20 February 1977	An afternoon storm caused severe winds, recorded to 113 km/h in the city. The winds created havoc on the Swan River, with one person drowning when a yacht capsized. In adjacent eastern and southern suburbs buildings were unroofed, caravans overturned and trees and power lines brought down.
2 January 1982	Golf-ball sized hail occurred in the northern suburbs.
7–8 November 1986	Overnight storms lasted for ten hours and caused some isolated strong gusts.
16 January 1991	A dry microburst, measured to 108 km/h, moved a parked passenger jet at Perth Airport, resulting in structural damage in excess of $1 million.
8 February 1992	Slow-moving storms caused Perth's wettest day on record, with falls over 100 mm (Medina 231 mm). Strong winds and golf-ball sized hail damaged apartment blocks in Glendalough in the morning.
23 February 1995	An afternoon severe thunderstorm downburst caused damage amounting to over four million dollars in the eastern suburbs of Perth. A five-tonne demountable home was flipped onto the roof of another building and 30 one-tonne swimming pools were picked up by the winds and scattered about. Perth Airport recorded a gust of 115 km/h.
27 March 1995	A severe storm caused hail measured to 5 cm diameter at Woodbridge, north of Perth.
14 December 1998	Lightning killed a jockey at Ascot racecourse. Wind damage affected tens of properties in the southern suburbs while hail damaged vegetable crops.
22 January 2000	Slow-moving widespread storms caused heavy rain resulting in flooding. Perth registered 104 mm, its second highest daily fall.
18 November 2001	Overnight storms caused severe localised winds that damaged more than 25 houses in the northern suburb of Ridgewood (Wanneroo).
14 January 2002	A supercell formed north of Perth causing hail at Regans Ford, before moving offshore and striking Kwinana, shifting an oil tanker from its moorings and causing millions of dollars damage to the refinery.
29–30 March 2003	Storms overnight on the 29th and during the 30th caused power outages to 70,000 Perth homes at its peak and the SES received over 100 callouts for flood-related damage. Karragullen registered 40 mm of rain in 45 minutes.

Rainfall

While most thunderstorms are capable of producing heavy rain for a period during their mature phase, the amount of moisture in the lower levels of the atmosphere is usually a constraining factor for storms near the west coast. The continental airmass is usually significantly drier than that over the tropics or near the eastern Australian coast. Perth residents usually welcome rain from thunderstorms during the dry season, particularly if it brings some respite from the heat.

Although the natural environment of the coastal plain is not particularly prone to flash flooding, heavy summer rains have a major impact on a population unaccustomed to rain during the warm season. Sufficiently heavy rain that may cause flash flooding is rare and usually requires a moisture source from tropical origins or an unusual combination of features such as a slow moving low-level convergence zone and deep upper-level trough. On 8 February 1992 such a combination led to sustained heavy rainfall in the Perth region and flooding, particularly near the Darling Ranges. Perth registered its highest daily fall of 121 mm while Medina recorded 230 mm (see section 2.4).

Hail

Large hailstones (in excess of 2 cm diameter) are infrequent and are usually associated with supercell-type storms. Although hail size reports are often quite subjective there have been confirmed reports of

hail greater than 3 cm in diameter in Perth. The largest reported hail was 5 cm, and fell at Woodridge, just north of Perth, on 27 March 1995.

Lightning

A significant consequence of summer thunderstorms is lightning. In Australia, lightning accounts for five to ten deaths and well over 100 injuries annually. In Perth, lightning-caused deaths are infrequent, with only one over the last decade. A roof tiler who narrowly escaped death after being hit by lightning described his ordeal to the *West Australian* (28 March 1995):

> *"I heard a crack, saw a big blue flash, then time just stood still", he said from his bed at Sir Charles Gairdner Hospital. "I was still on my feet but the top half of my body just folded over"…He told doctors he felt a sharp pain in his neck and ankle – the suspected entry and exit points of the lightning.*

Significant damage to electrical and communications equipment and appliances is common. Following lightning strikes in January 1999, for example, 900 fault calls were received by Telstra, amounting to almost $1 million in costs (*West Australian*, 25 January 1999). Lightning-ignited bushfires are a frequent problem, particularly if little rain occurs. On 22–23 December 2002, lightning ignited dozens of fires in the metropolitan area, creating havoc for fire agencies. Plate 2.6 illustrates the spectacular show that can be created by lightning. Lightning illuminates the 'shelf' cloud of the severe thunderstorm that caused damage in the northern suburbs.

Plate 2.6: A spectacular lightning show on the night of 18 November 2001 (Courtesy of Radek Doleki)

2.4. Heavy Rain and Flooding

Frequency of heavy rainfall

Perth is not commonly associated with heavy rain and flood events particularly in recent decades. Nevertheless, there is sufficient historical evidence to suggest that the flood risk in Perth is real and serious and the potential impact made worse by the lack of events in recent memory.

Table 2.5 shows the frequency distribution of daily rainfall by month using composite data from the official Perth site from 1880 to May 2004. The heaviest rainfall occurs in June and July. Of the 78 events when daily rainfall has exceeded 50 mm, half occurred in June and July, and only 15%

occurred in the months from September to March. However the two highest rainfall amounts occurred in February (121 mm on 9/2/1992) and January (104 mm on 22/01/2000).

Table 2.6 shows the peak daily rainfall for the ten highest rainfall events in the Lower West District. This district is approximately centred on Perth, extending for about 150 km in a north-south direction and 50 km inland. While most of these rainfall events occurred from May to July, the top three events occurred in either February or March. The number of sites recording more than 100 mm during the same event is also shown. However, it should be noted that the number of sites recording rainfall has gradually increased over time.

Table 2.5: Frequency analysis of daily rainfall at Perth, 1880–2003

Rainfall	Jan	Feb	Mar	Apr	May	Jun	Jul	Aug	Sep	Oct	Nov	Dec	Total
0	3518	3223	3377	2827	2169	1590	1577	1721	1975	2490	2923	3326	30716
0.1 to 5	305	259	427	624	905	966	1023	1095	1088	931	638	419	8680
5.1 to 10	27	37	58	157	324	398	506	457	370	233	95	59	2721
10.1 to 15	12	14	36	77	181	258	276	256	143	91	33	19	1396
15.1 to 20	5	11	15	40	119	186	183	136	93	51	11	13	863
20.1 to25	3	7	7	23	73	117	127	85	35	23	15	4	519
25.1 to 30	0	2	8	12	42	72	75	63	26	9	2	2	313
30.1 to 35	0	1	3	8	30	65	51	26	10	9	1	0	204
35.1 to 40	1	0	2	3	26	43	18	14	3	3	2	0	115
40.1 to 45	1	1	2	2	12	13	18	9	3	1	0	1	63
45.1 to 50	1	0	0	2	11	22	4	5	2	1	0	1	49
50.1 to 55	1	1	1	1	7	7	3	3	2	0	0	0	26
55.1 to 60	0	0	0	1	3	5	5	1	0	1	0	0	16
60.1 to 65	0	1	0	1	1	2	3	2	0	0	0	0	10
65.1 to 70	0	0	0	2	2	3	3	0	0	1	0	0	11
70.1 to 75	0	0	0	0	0	1	0	2	0	0	0	0	3
75.1 to 80	0	0	1	0	1	2	1	0	0	0	0	0	5
80.1 to 85	0	0	0	0	0	0	0	0	0	0	0	0	0
85.1 to 90	0	1	0	0	0	1	1	0	0	0	0	0	3
90.1 to 95	0	0	0	0	0	0	1	0	0	0	0	0	1
95.1 to 100	0	0	0	0	0	1	0	0	0	0	0	0	1
100.1 to 105	1	0	0	0	0	0	0	0	0	0	0	0	1
105.1 to110	0	0	0	0	0	0	0	0	0	0	0	0	0
110.1 to 115	0	0	0	0	0	0	0	0	0	0	0	0	0
115.1 to 120	0	0	0	0	0	0	0	0	0	0	0	0	0
120.1 to 125	0	1	0	0	0	0	0	0	0	0	0	0	1
No. of days	3875	3559	3937	3780	3906	3752	3875	3875	3750	3844	3720	3844	45717
No. of years	125	126	127	126	126	125	125	125	125	124	124	124	125.17
Rainfall > 25 mm	5	8	17	32	135	237	183	125	46	25	5	4	822
Rainfall > 50 mm	2	4	2	5	14	22	17	8	2	2	0	0	78

Table 2.6: Highest ten daily rainfall events in the Lower West District

Peak rainfall for the event (mm)	Site of peak rainfall	Date of event	No. other sites recording > 100 mm for the same event
230.0	Medina	9/2/1992	20
196.3	Bindoon	9/3/1934	17
190.5	Wannamal	16/02/1955	15
164.8	Rockingham	11/06/1945	8
159.2	Serpentine	29/7/1987	22
155.8	Mundaring	30/07/2001	13
154.7	Rottnest Is	21/06/1984	2
145.8	Karnet	26/06/1967	7
138.9	Highgate	10/06/1920	8
137.0	Lupin Valley	2/05/1953	6

Heavy rainfall events are not confined to a 24-hour period. Intense rainfall of short duration can result in flash flooding; causing gutters and drains to overflow in five to ten minutes. Perth's sandy soils on the coastal plain and relative lack of topography diminish the impact of heavy rain. Also, Perth's infrastructure is not designed to cope with very heavy rainfall, especially when compared to tropical locations. Every year there are reports of properties becoming inundated due to short-term heavy rain. On 30 March 2003, for example, the State Emergency Service responded to over 100 requests for flood-related damage when a thunderstorm caused 29 mm of rain in half an hour at Perth Airport.

To assist in hydrological design procedures the frequency analysis of rainfall data can be indicated by derived intensity–frequency–duration (IFD) design rainfall curves. IFD curves for Perth are shown in Figure 2.7. These show the rainfall rate for periods ranging from 5 minutes to 72 hours, which correspond to average recurrence intervals (ARI) ranging from 1 year to 100 years. The ARI of 2 years, for example, corresponds with 20 mm of rainfall in one hour, and an ARI of 50 years corresponds with the occurrence of 40 mm of rainfall in one hour.

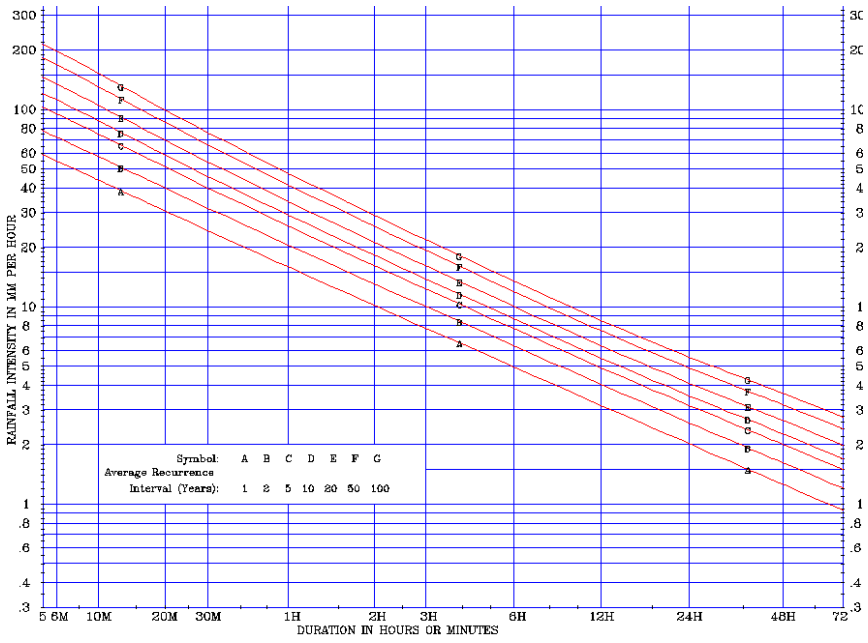

Figure 2.7: IFD curves for Perth

Mechanisms

Heavy rainfall in the Perth region can be caused by a range of meteorological mechanisms, but are usually associated in some way with one of the following patterns.

- A mid-latitude low and cold front embedded in the westerlies (see winter storms).
- The most typical pattern for heavy rain is for a front to interact with a tropical moisture source to produce a band of cloud stretching from the northwest to southeast as shown in Figure 2.8 (July 2001). A slow-moving low to the south or southwest can result in this rainband causing extensive heavy rain or even a succession of rainbands as several fronts sweep across southern Western Australia. These rainbands have the potential to cause widespread rain although it is common for particularly heavy rain to occur in a strip owing to strong convergence in a northwest to southeast orientation.
- A tropical low or cyclone off the west coast and moving south (see section 2.5).
- Thunderstorms (see section 2.3).

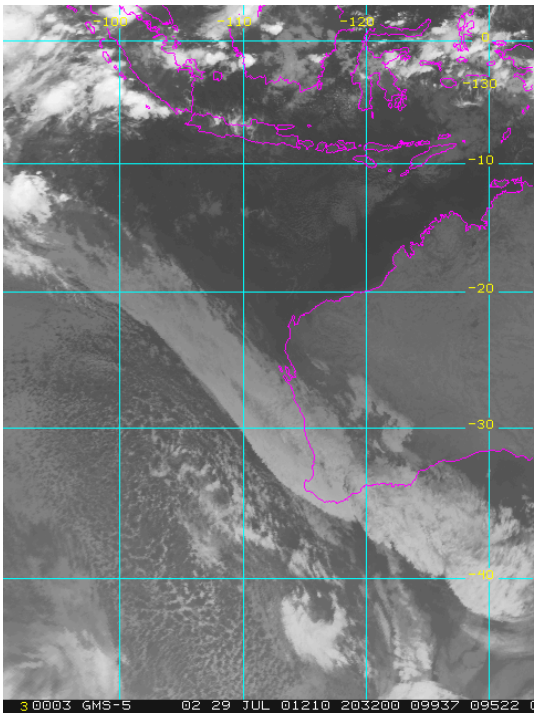

Figure 2.8: Satellite image of a rainband responsible for heavy rain in Perth in July 2001 (Courtesy of the Japan Meteorological Agency)

Flooding

Typically, flooding occurs in one of these forms.

- Localised flash flooding as a result of heavy rain over a short period.
- Inundation of low-lying land after prolonged rain. Improved drainage has reduced the risk of flooding in these areas that were once prone to seasonal flooding.
- Flooding caused by a rise in river height on the Swan and Canning Rivers. Although uncommon, major river floods have the most significant impact on Perth.
- Inundation of low-lying coastal areas by high tides caused by storm surge.

A heavy rain event does not automatically result in a sufficient rise in river levels to flood surrounding areas. While properties may be affected by flash-flooding, more significant flooding on the Swan and Canning Rivers is associated with heavy rainfall over prolonged periods. This is demonstrated in Figure 2.9 which shows rainfall over a 70-day period for four different rain and flood events in 1926, 1945, 1963 and 2001. The rainfall event in July 2001 recorded the heaviest daily rainfall at 99 mm. However, this event did not produce a major flood in Perth as just 184 mm fell in the previous seven weeks. Major floods did occur in 1926, 1945 and 1963 as heavy rain over the proceeding period had already raised river levels. In 1945 a total of 842 mm of rainfall fell over a 70-day period compared to just 184 mm prior to the 2001 event.

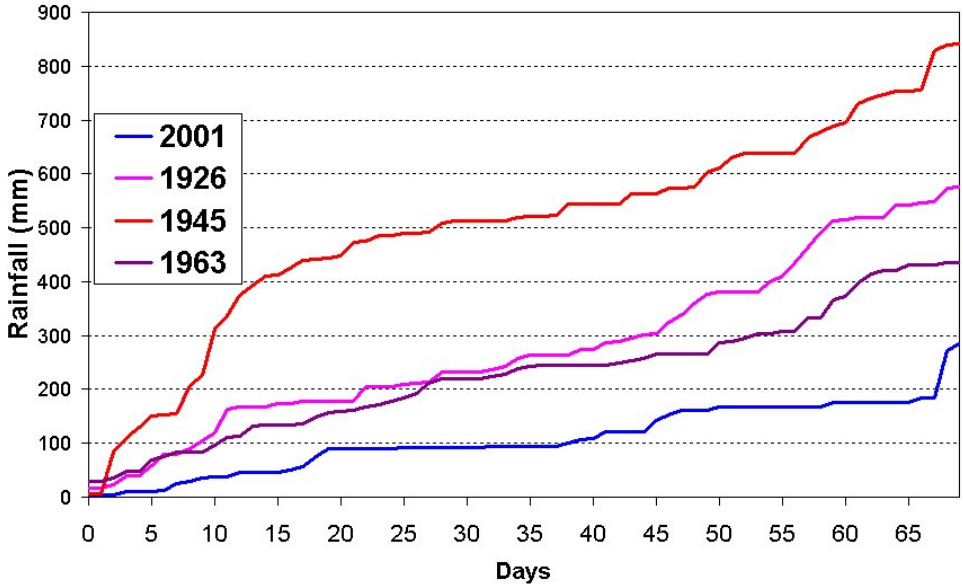

Figure 2.9: Rainfall over 70 days for the major floods in 1926, 1945 and 1963, and the rainfall event of July 2001 showing the importance of accumulated rainfall

Indeed rainfall can be important as much as 12 months prior to the event. The 1963 flood, for example, influenced the consequences of rain the following year. The Collie flood in 1964 (see Plate 2.7a and b) was rated as a one in 80 year event, yet the rainfall that fell was only rated as a one in 20 year event.

The requirement for preceding rain events to saturate the catchment and raise river levels provides an explanation as to why flooding on the Swan River is primarily a winter-time phenomenon. Those uncommon warm-season rainfall events generally do not cause major floods on the Swan River because of the river's capacity to discharge large volumes of water when existing river levels are low. This is not the case for some other towns such as Moora and Greenough that are located on smaller river catchments more susceptible to short-term heavy rain. Rainfall associated with tropical cyclone *Elaine,* for example, flooded the town of Moora in March 1999.

Very exceptional rainfall events can however cause flooding on large river catchments such as the Swan River. In March 1934, the Swan River reportedly rose 5.8 m in less than eight hours at Guildford in response to heavy rain (134 mm in just four hours at Clackline) associated with a tropical cyclone. In January 1982, 250 mm of rain fell in association with tropical cyclone *Bruno,* resulting in a flood with a 100 year ARI on the Blackwood River in the Southwest.

Plate 2.7 (a): Medic St, Collie, August 1964 flood (Courtesy of the Collie Camera Club)

Plate 2.7 (b): Medic St, Collie, not in flood (Courtesy of the Collie Camera Club)

Even if summer rain events do not cause a major flood on the Swan River, they can still cause considerable damage and disrupt activities in the city. The impact of one such event is illustrated by the newspaper headlines relating to rainfall on 22 January 2000 (Figure 2.10).

Figure 2.10: The heavy rainfall event of 22 January 2000. While not causing a major flood on the Swan River, the event did considerable damage and disrupted activities in the city

Historical trends

Historical rainfall patterns in the southwest have been the subject of intense study in recent times owing to a sustained reduction of annual rainfall in the last 40 years. Studies associated with the Indian Ocean Climate Initiative (IOCI) showed that heavy rainfall events decreased both in frequency (the number of events) and intensity (the amount of rainfall in each event), particularly since the 1960s (Haylock and Nicholls, 2000). Using the Manjimup site south of Perth, the ARI for daily rainfall of 50 mm increased from 1.5 years (0.0018 AEP) in the 1930–65 period, to 7.5 years (0.0004 AEP) in the 1966–2001 period (IOCI, 2002). Such changes are less dramatic in Perth, but nevertheless the number of heavy rain events has decreased noticeably. Figure 2.11 shows the frequency at 15 year intervals of daily rainfall exceeding 50 mm for Perth since 1883. This highlights the sudden decrease in heavy rainfall events in the 1960s.

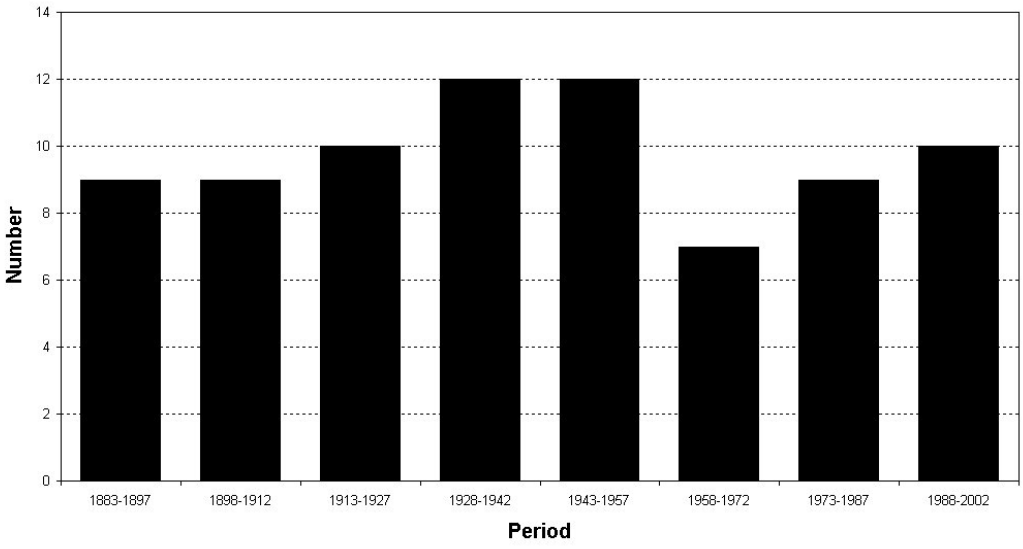

Figure 2.11: Frequency of daily rainfall exceeding 50 mm at Perth in 15 year intervals 1883–2002

This drier period agrees with the flood record on the Swan River where the last major floods occurred in 1963 and 1964. Although there have been significant individual rain events in the last forty years they have not caused major floods. The most serious of these was in July 1983, when heavy rain over the Swan-Avon catchment flooded the upper Swan Valley and threatened some properties in Bassendean and Guildford.

Storm surge

Sustained strong westerly or northwesterly winds can cause a build up of water on the coast that is referred to as storm surge. This enhances the water level above the normal tidal variation. This includes water levels on the Swan River subject to tidal variation so that parts of the river foreshore may be inundated near high tide. A storm surge also exacerbates flooding on the coastal plain by not allowing the river water to escape out to sea. The extent of flooding in Perth is dependent upon:

- the intensity of the surge itself which relates to the strength and duration of onshore winds;
- the timing of the peak surge in relation to the predicted high tide; and
- existing river levels from rainfall in the catchment area.

Most storm surge events are associated with sustained westerly gales caused by intense lows and cold fronts in the cool season (refer section 2.2). During the 23 May 1994 storm, the tidal elevation measured at Fremantle showed a storm surge of 0.98 m. Fortunately the potential for more serious and extensive flooding was not realised, as the peak surge occurred near low tide. A strong westerly gale on 20 July 1910 caused damage along the west coast to as far north as Geraldton. The Fremantle North Mole was damaged while on the Swan River all the surrounding low-lying lands and many of the jetties were submerged. More recently, gales associated with a low passing near Busselton on 16 May 2003 caused a storm surge of 0.8 m at Fremantle at close to the time of high tide as shown in Figure 2.12. The actual tide was 0.5 m above the highest astronomical tide and significant coastal erosion occurred. Plate 2.8 shows water overflowing onto Riverside Drive near the city centre. Fortunately existing river levels were low owing to dry conditions in the previous months, otherwise flooding would have been significantly worse.

Wave action adds to coastal erosion. Intense winter lows to the south generate significant swells. During the May 1994 storm the open-water swell was estimated at 8–9 m.

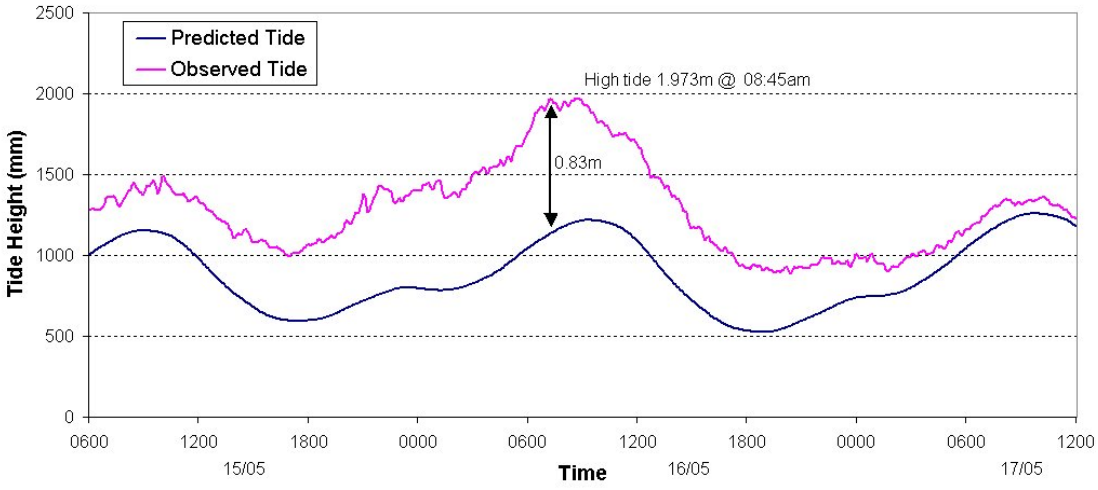

Figure 2.12: Actual tide above the predicted tide at Fremantle, 15–16 May 2003, showing the impact of a storm surge during a cool season westerly storm (Data courtesy of DPI)

Plate 2.8: The effects of the storm surge on Riverside Drive, 16 May 2003 (Courtesy of Lee Evelegh)

In addition to cool season events tropical cyclones can also cause storm surges in Perth. Cyclone *Alby* (refer to section 2.5) in April 1978 generated northerly gales responsible for large waves and a storm surge, which caused substantial coastal erosion along the Lower West coast. At Fremantle the surge was about 0.6 m, causing a high tide of 1.8 m, about 0.5 m above the highest astronomical tide. Very dry conditions and northerly, rather than westerly winds negated the flood potential on the Swan River. Low-lying areas further south on the coast at Bunbury and Busselton, more prone to a northerly surge, were flooded.

2.5 Tropical Cyclones

Tropical cyclone threat

Although an infrequent occurrence in the Perth region, tropical cyclones have historically been the most significant weather hazard in the southwest. In April 1978 cyclone *Alby* resulted in five deaths and caused coastal erosion, destructive winds the equivalent of the strongest of winter fronts, and conditions conducive to the spread of devastating wildfires.

The region off the northwest Australian coast is a prolific breeding area for tropical cyclones, producing about four to five cyclones each year on average. The vast majority of these storms dissipate well to the north of Perth, but a small number maintain considerable intensity as they travel south, despite moving over cooler water and into a generally less favourable environment.

Media and public interest usually diminishes when a cyclone begins to lose its tropical cyclone characteristics and the intensity is downgraded as it moves south. However, occasionally a decaying tropical cyclone interacts with a cold front and evolves into an intense, fast-moving system. These systems can produce a range of destructive phenomena: from intense rainfall, storm surges and large waves resulting in coastal erosion and inundation, to damaging winds and hot, dry conditions conducive to the spread of bushfires. The sudden onset of these phenomena tends to intensify their impact on a population more accustomed to benign weather conditions through the warmer months. The infrequency of these cyclones, combined with the accompanying changes in structure and motion as they move south, makes them a difficult forecasting problem.

Cyclones in the southwest can move at speeds greater than 70 km/h, in contrast to their average speed of 10–15 km/h in the north. The structure of the cyclone changes as it accelerates so that the regions of dense cloud and heavy rainfall are displaced towards the right quadrants of the system (when looking along the direction of the track), leaving the left quadrants largely free of significant cloud. As a result, the heaviest rainfall, for example, would occur when a cyclone crosses the coast near, and to the north of Perth, as in March 1934.

The strongest winds associated with these fast-moving systems occur in the left quadrants where the clockwise rotating winds are augmented by the system's translational speed. The cloud-free squally winds from the north or northeast are a recipe for severe dust storms and an extremely dangerous environment in which fires can engulf the countryside with frightening speed. The wildfires associated with cyclones in February 1937 and April 1978 typify this potentially devastating weather scenario.

The change in structure described above is known as 'extra-tropical transition'. This process is observed in other tropical cyclone basins around the world and can result in a re-intensification of the system even though it loses tropical cyclone characteristics. A study by Foley and Hanstrum (1994) showed that accelerating tropical lows were associated with intensifying cold fronts that moved to the northeast towards the tropical low. This 'capture' process and the resulting weather is shown schematically in Figure 2.13 and described in the section on cyclone *Alby* (see below).

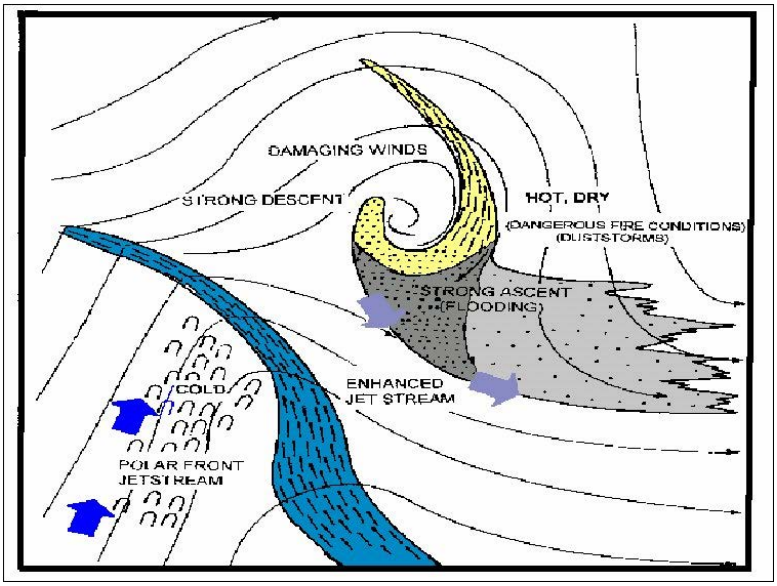

Figure 2.13: Schematic diagram showing features of a tropical cyclone undergoing extra-tropical transition (Foley and Hanstrum, 1994)

Climatology

During the 95-year period from 1910 to 2004 there were a total of 14 tropical cyclones that either caused gales or wind-related property damage in the Perth region. Decaying cyclones that caused heavy rain but not gales are not included in this number. The annual frequency of occurrence is 0.15: about equivalent to one every 6–7 years. Interestingly, there have been no cyclone events between 1992 and 2004. This has probably increased the level of complacency in the population regarding the risk of a cyclone impact. There is considerable variation in decadal occurrence within the 95 year data period. Given the small number of events, a much longer data set is required before meaningful conclusions can be made in trends of occurrence.

Cyclones affecting the lower west coast have occurred between the months of January and May and tend to occur later in the cyclone season than those in the tropics, peaking in March. Indeed, over 70% of the cyclones affecting Perth have occurred in March and April.

Figure 2.14 shows the tracks of significant cyclones affecting the Perth region. The majority originate from north of the Pilbara coast. They initially move to the southwest, and then move to the south, then to the southeast. Some of these cyclones have affected large parts of the west coast. The 1956 cyclone moved down the west coast causing considerable damage along the way. On rare occasions, cyclones such as *Marcelle* (1973, not shown) have originated from further west in the Indian Ocean and affected the west coast. The tracks of cyclones prior to the introduction of weather satellites in the 1960s should be treated with caution. A common factor between the cyclones is the increase in speed as they move southwards. By the time they reach Perth they can be moving at speeds in excess of 70 km/h.

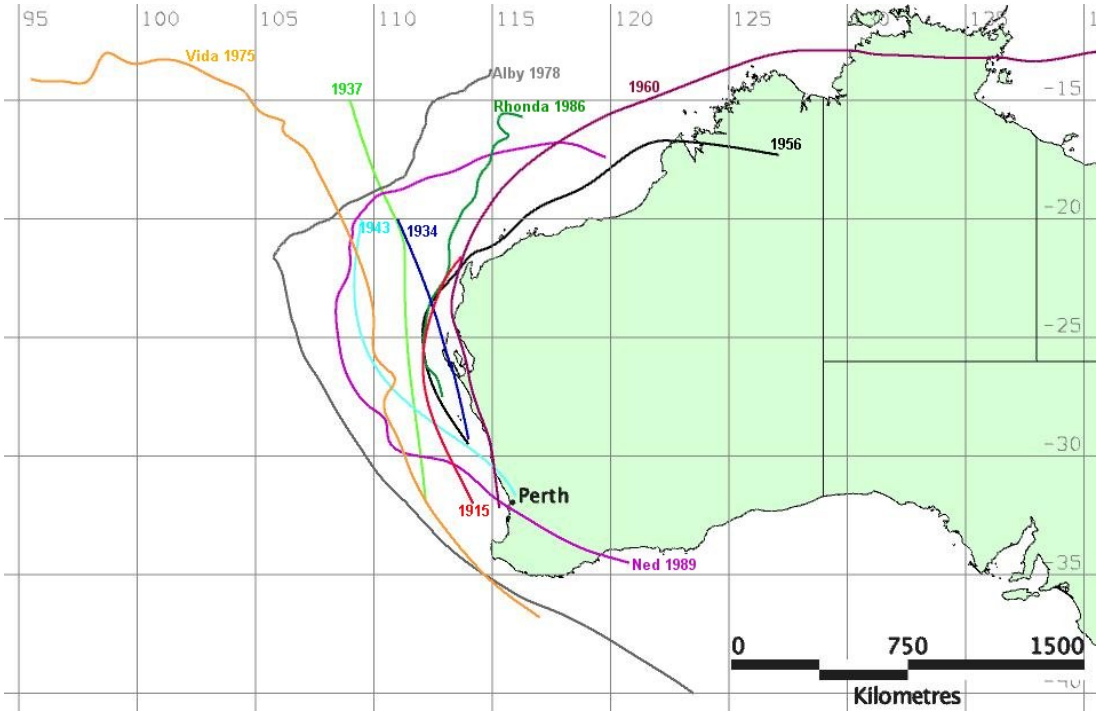

Figure 2.14: Tracks of cyclones causing gale-force winds in Perth

Historical events

Table 2.7 shows the list of major cyclones that have affected Perth since 1830. While it is difficult to compare the severity and impact of these events, cyclone *Alby* in 1978 is arguably the strongest in terms of winds in Perth (see below). The convention of giving names to cyclones only began in 1964.

One of the early accounts of strong winds in Perth and in Western Australia was believed to be the result of a tropical cyclone which occurred on 11 April 1843. This is the first cyclone event recorded for the fledgling Perth colony which transcended all experience of previous weather during the warmer months. The following account of the event is taken from *Results of Rainfall Observations made in Western Australia* (BOM, 1929):

> *Perth was visited by a most terrific gale from the northwest, amounting to a full hurricane. Strong gales from this quarter have frequently occurred during the winter months; but this gale was unusually severe, although it lasted for such a short time. It set in about 6 p.m., and lasted until nearly 10 p.m., when it gradually lulled. The gale was so sudden and tremendous as to force the 'Success' to drift ashore with two anchors down.*

Table 2.7: Description of significant tropical cyclone events near Perth

Date	Description of impact
11 April 1843	A 'terrific' northwest gale lasting four hours struck the Perth area, then moved southwards to Bunbury, where the tidal surge in excess of 4 feet drove two large vessels aground.
10 March 1872	A storm described as being of 'unprecedented severity' occurred. The destruction of property in Perth was considerable and many trees were levelled.
27 February1893	A fierce gale blew at Geraldton and Fremantle. Several boats, including the *Alastar* and *Flinders*, broke their moorings and were damaged.
26 February 1915	A storm moved southwards on the 25th from Onslow towards Perth at a speed estimated at 50 mph. There was extensive damage to property along the track. At Midland Junction, near Perth, a child was killed and several others were injured when the Swan Mission dormitory collapsed.
9-10 March 1934	Perth recorded 77 mm and Toodyay 191 mm of rain as flooding caused damage across Perth and the Wheatbelt. The Swan River at Guildford rose 5.8 m in less than 8 hours, causing considerable damage to unharvested grapes.
10 February 1937	Widespread property damage occurred across the southwest of the state, particularly south of Perth. Many boats were damaged at Rockingham but many more were damaged further south, and the Busselton jetty was extensively damaged. The storm surge forced people to evacuate in parts of Mandurah and Bunbury. Severe bushfires were reported from the forest areas, most notably from Denmark and Walpole. Hundreds of acres of forest, pasture and fruit trees were destroyed by fires and stock losses were great. Widespread severe duststorms over the Wheatbelt reduced visibility to just a few metres in parts.
15 March 1943	A cyclone crossed the coast near Lancelin causing extensive damage along a narrow band from Lancelin to the southeast wheatbelt. Buildings were unroofed, telegraph poles were blown down and roads were blocked by falling trees.
4 March 1956	Buildings and property were damaged in parts of the southwest including Geraldton and Perth. Shipping was battered in Geraldton Harbour and the Perth to Geraldton highway was blocked by numerous fallen trees.
27 March 1960	Many small boats were blown ashore and damaged. Perth recorded winds to 113 km/h. Many centres in the Wheatbelt reported damage to outbuildings, wheat silos and homestead roofs.
20 March 1975	During cyclone *Vida*, winds of 128 km/h and 109 km/h were recorded in Fremantle and Perth respectively Many properties were damaged including St George's Cathedral and the Perry Lakes Stadium. At Rockingham a 7 m yacht sank, a 6 m cabin cruiser was destroyed and many other craft were damaged.
4 April 1978	Cyclone *Alby* passed close to Cape Leeuwin causing a period of gale-force north to northwest winds. Five lives were lost. Damage to property was widespread and most severe in the region between Mandurah and Albany. Widespread fires and severe duststorms reduced visibility to less than 100 m over a large area.
21-22 February 1986	The remains of cyclone *Rhonda* crossed the coast near Perth causing heavy rain (131 mm at Greenmount). Flooding, albeit minor, was widespread across Perth. Over 100 traffic crashes were attributed to the wet conditions.
1 April 1989	Cyclone *Ned* crossed the coast near Rockingham. Rottnest and Fremantle reported wind gusts of more than 100 km/h between 6 and 7 am. Only minor damage was reported on land.

While further cyclones affected Perth in 1845, 1867 and 1871, possibly the next most severe summer storm experienced occurred on 10 March 1872.

> *In Perth a storm of unprecedented severity occurred on the 10th March. About 7 am heavy rain fell, and from then for about five hours the gale raged with unabated fury. At noon the barometer read 29.20 inches, and the wind blew from east northeast. The destruction of property within the city was considerable, chimneys having been blown down and trees levelled to the ground. Telegraph*

> *communication was cut off between Perth and Fremantle, also beyond Guildford, and between Pinjarra and Bunbury. The town hall of Perth and the Colonist's Hospital were greatly damaged. Several cottages were blown down but no lives were lost.*
>
> *At Fremantle the port was visited by the most extraordinary weather that had been witnessed for some considerable time at that period of the year. The wind was so terrific that huge stones were lifted a distance of several feet from the ground.*
>
> (BOM, 1929)

A storm in February 1915 broke in the early hours of the morning. Strong winds, heavy rain, lightning and thunder continued for approximately an hour resulting in building and roof collapse, trees being felled, and the death of a young girl. The following account in the *West Australian* (27 February 1915) describes some of the impact:

> *A two storey brick building near the corner of Aberdeen and Lake streets, tenanted by Mr Thompson, sewing machine merchant, collapsed like a pack of cards when the full force of the elements caught it… St Patrick's Mission hall, a wood and iron structure, capable of accommodating 200 persons, was reduced to a shapeless heap of wood and iron…*
>
> *A remarkable happening occurred at the Boonomic Stores, Hay Street. At a certain moment during the disturbance the air pressure about the shop windows must have been so intense that two or three of the great panes of glass moved a fractional part of an inch from their brass fames. Through the tiny cracks so caused the force of air setting like a powerful suction pump, drew the edges of a number of feather boas and pieces of silk and satin. When the air pressure ceased the panes resumed something like their former position. Yesterday curious crowds gathered to view the sight of feathers and satin protruding through and wedged tightly in the window cracks…*
>
> *The most serious damage was occasioned at the Native and Half Caste Mission in Middle Swan. The new dormitory about 50 ft. x 18 ft., built of brick, and erected only about two years ago at a cost of something like 500 pounds, collapsed like a pack of cards, and a number of inmates were pinned down by the fallen masonry and timber… Of the girls who were still in bed when the structure fell, one about nine years of age, was found to be beyond all human aid. She had been struck on the head and shoulder by a heavy jarrah beam and the skull was fractured… Seven of the inmates are now confined to their beds as a result of the injuries received. In three cases, the injuries are serious, but in none are they considered dangerous.*

Tropical cyclone *Alby*

Tropical Cyclone *Alby* passed close to the southwest corner of Western Australia on 4 April 1978, killing five people and causing widespread but mostly minor damage to the southwest. The damage bill was estimated to be $39 million (2003 dollars). One man was blown from the roof of a shed and a woman was killed by a falling pine tree. Another man was killed when a tree fell on the bulldozer he was operating and two men drowned at Albany when their dinghy overturned. Storm surge and large waves caused coastal inundation and erosion from Perth to Busselton. Fires fanned by the very strong winds burned an estimated 114,000 ha of forest and farming land.

Track and intensity

A low developed on 27 March well north of the state, some 800 km north-northwest of Karratha. It moved slowly to the southwest and steadily intensified, peaking on 2 April with an estimated central pressure of 930 hPa (category 4 intensity) about 850 km west northwest of Carnarvon (refer to the track shown in Figure 2.16). The satellite image at 6 pm (Figure 2.17 (a)) shows a well-developed eye and banding structure – distinctive features of a strong tropical cyclone. *Alby* subsequently turned to the south-southeast and accelerated from about 10 to 25 km/h by midnight on the 3 April at a distance 750 km west northwest of Geraldton. At about this time the satellite image (Figure 2.17b) showed a weakening in the eye and banding structure around the centre and a broad mass of cloud to the south ahead of a cold front approaching from the southwest. This pattern indicates that *Alby* was changing into an extra-tropical system.

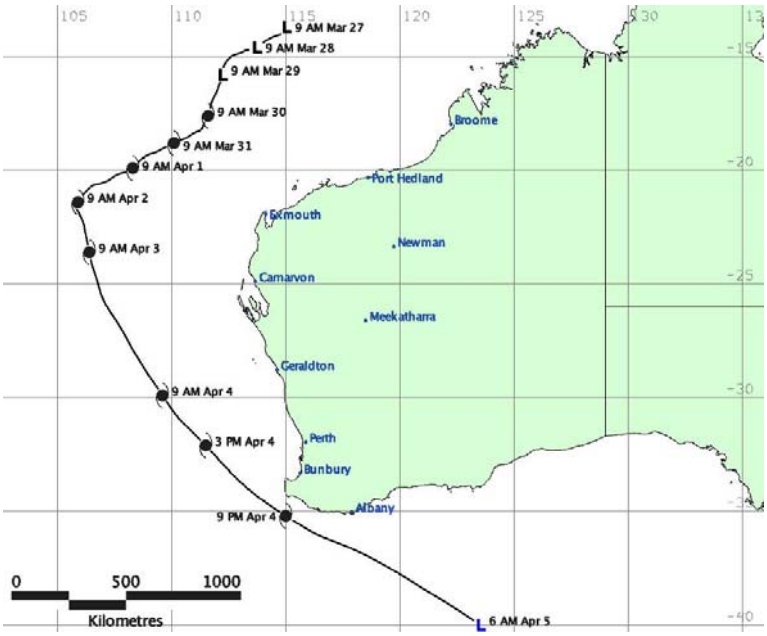

Figure 2.16: Track of cyclone *Alby*

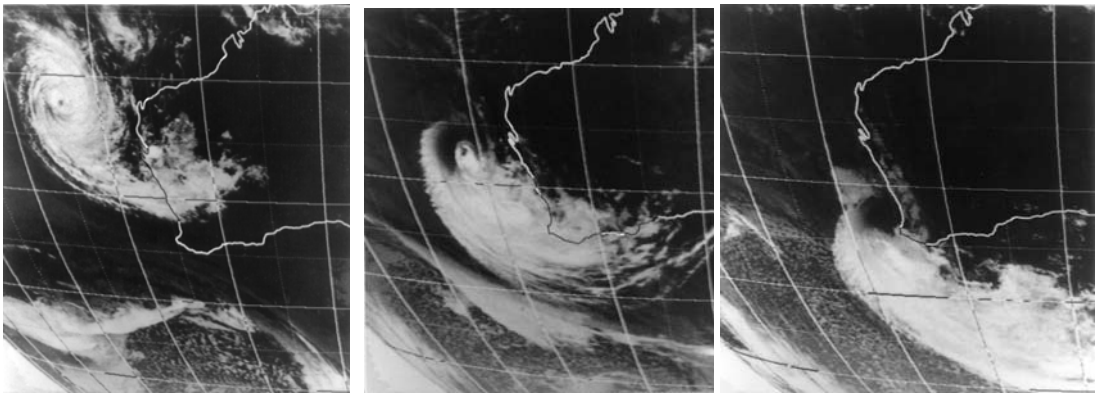

Figure 2.17a–c: Infra-red satellite imagery showing cyclone *Alby* as it moved from the tropics to the mid-latitudes; (a) 6 pm, 2 April; (b) 2 am, 4 April; and (c) 5 pm, 4 April 1978 (Courtesy of the Japan Meteorological Agency)

On 4 April *Alby* continued to accelerate, captured by strong upper-level northwest winds. The satellite image at 5 pm (Figure 2.17c) showed a complete absence of storms near the centre and the eastern half of the cyclone virtually devoid of cloud. The front had merged with the broad mass of cloud south of the centre. This pattern is very different from that associated with a mature tropical cyclone, yet it was still estimated as a category 3 system with a central pressure of 960 hPa. By 9pm *Alby* reached its closest approach to the mainland, about 60 km south of Cape Leeuwin, and was moving at a speed of 80 km/h to the southeast. The centre of the system was 250 km southwest of Perth at its closest. The centre became difficult to locate on the 5 April as it moved south of 40°S.

Table 2.8 shows the maximum gusts recorded around Perth on 4 April. The Fremantle gauge recorded the highest gust at 143 km/h. Winds increased abruptly on the 4th as *Alby* accelerated closer. Gales commenced in Perth City at 2:30 pm, and the maximum gust of 130 km/h was the third highest gust recorded at a city site in the record from 1942 to 2003. At Fremantle gales lasted for almost seven hours, while winds exceeded storm force (90 km/h) for four hours.

Table 2.8: Maximum wind gusts recorded around Perth, 4 April, 1978

Location	Highest gust (km/h)	Time (WST)
Pearce	113	16:50
Perth Airport	98	16:53
Perth City	130	16:50
Fremantle	143	15:55

Impact

Wind damage was extensive, with the greatest damage occurring in the coastal area south of Perth between Bunbury and Albany. There were no reports of houses being completely destroyed but partial roof damage occurred in Perth as described in *The West Australian* (5 and 6 April, 1978):

> *A car showroom in Queen Victoria Street, Fremantle, was partly demolished during the storm… Roofing iron from the sheds was blown several hundred metres to Leach Highway and walls of the unroofed sections caved in. Part of Henry Street Fremantle, was closed off after glass windows of a disused warehouse blew into the street. Parts of an iron and timber warehouse opposite were blown into the street below.*
>
> *An aluminium roof was whipped off the home of Mr and Mrs W R Hyams of Riverview Place, Mosman Park, and continued on an upward destructive path to damage a further six houses. Pieces of the roof were scattered over a wide area in Saunders Street, which is about seven metres above the wind damaged house. A piece of the roof was found 400 m away. Most of the roof fell on the property of Mr and Mrs D Robinson of Saunders Street, cutting off a chimney part of their roof, falling across Mr Robinson's car and slicing through several trees.*

Existing fires (normal end-of-harvest burn-off) combined with fires started on that day, and exploded into wildfires with measured rates of spread of between 5– 10 km/h. This resulted in an estimated 114,000 ha of forest and farming land being burned. The strong winds and dry conditions produced extensive dust storms that reduced visibility over a large area of the southwest on the afternoon of the 4th. The deposition on power lines of dust and, in coastal areas, of salt, eventually caused a failure of the electricity distribution system. Perth and all the area between Geraldton and Albany and east to Southern Cross were without power. The *West Australian* (6 April 1978) described the results:

> *Power supplies are still disrupted and more than 2000 fire fighters last night were still battling at least 70 fires… Insurance companies say the destruction caused by Tuesday's storm could cost many times the $20 million damage inflicted on Port Hedland by cyclone Trixie in 1975. The metropolitan area and nearly every town from Geraldton to Albany has suffered extensive damage… some Perth people had been without power for 30 hours last night… At one stage all five power stations supplying the grid system were out. There were problems when water and sewage treatment plants and pumping stations went out of action with the power failures. Liquid disposal tankers were called to sewerage pumping stations. The general manager of the Metropolitan Water Board, Mr F Armstrong, said that service reservoirs had met the demand for water but some people in high level areas had been temporarily inconvenienced.*

Large waves and a storm surge generated by the northerly winds caused substantial coastal erosion between along the Lower West coast, particularly in the Geographe Bay area. Low-lying areas at Bunbury and Busselton were flooded, forcing the evacuation of many homes including the Bunbury Nursing Home. Plate 2.9 shows floodwaters through the streets of Bunbury.

Plate 2.9: Flooding in Bunbury (Courtesy of *West Australian*)

An approximate 1.3 m surge at Busselton caused the tide to peak at 2.5 m, about 1 m above the highest astronomical tide. The Busselton Jetty was severely damaged. At Fremantle there was a storm surge of about 0.6 m, causing a high tide of 1.8 m, about 0.5 m above the highest astronomical tide. While this was not sufficient to cause flooding in Perth it did combine with large waves to scour beaches, as shown in Plate 2.10. A large number of small craft were also damaged. By contrast there was little rainfall during the event. Perth did not record any rainfall and the heaviest rainfall in the southwest was less than 40 mm. An extract from the *West Australian* (6 April 1978) describes some of the damage from cyclone *Alby*:

> *Heavy damage along metropolitan beaches became evident yesterday as Perth began clearing up after the storm. Local councils' surf clubs and individuals face many thousands of dollars worth of damage. Long time residents described the damage as the worst in living memory. The metropolitan coastline was altered dramatically by the storm. The Floreat Surf Life Saving Club was left teetering on the brink of a seven metre drop to the beach. The sea had swept in as darkness fell on Tuesday night taking a four metre bitumen road and five metres of beach approach with it. Further south along the coast which was littered with roof tiles and smashed boats, the storm completely destroyed the Cottesloe Surf Life Saving Club's boat house and ambulance room. The Vice-President of the club, Mr R Redfern, said that at least $30,000 worth of boats, skis, boards and reels had been swept out to sea and dumped in splinters on the beach… Councils with ocean or river frontages will face the highest repair bills because of erosion. Most ocean groynes from City Beach south were damaged and the PCC has already tentatively estimated the cost of repairs on its beachfront at $10,000.*

Plate 2.10: Coastal erosion on Perth's beaches (Courtesy of *West Australian*)

2.6 Heatwaves

The heatwave threat

Heatwaves are probably the most under-rated weather hazard in Australia, essentially because they are viewed as a 'passive' hazard in contrast to the more widely studied catastrophic hazards such as tropical cyclones and earthquakes. According to Coates (1996), heatwaves kill more people than any other natural hazard experienced in Australia. In a study on the consequences of heatwaves, Andrews (1994) reported that in the period between 1803 and 1992, at least 4,287 people died as a direct result of heatwaves. This was almost twice the number of fatalities attributed to either tropical cyclones or floods over much the same time frame. In the United States, heatwaves are the second greatest cause of human mortality resulting from a natural hazard, killing more people than hurricanes, tornadoes, lightning and floods combined. Only low winter temperatures have killed more people. Recent heatwaves that caused a large number of deaths include Brisbane in January 2000, when 22 people died, and New York City in 1980, when 1,600 deaths were attributed to a heatwave and economic losses totalled 15 billion dollars.

In Western Australia a total of 392 deaths have been caused by excessive heat between 1807 and 1994, compared to 1,250 in New South Wales. This equates to a death rate per 100,000 of 0.68 in Western Australia, ranking second to South Australia (1.14) and above New South Wales (0.41). Heat-related fatalities in Australia are decreasing. Between 1973 and 1992 the heat-related fatality rate per 100,000 has declined to just 0.06 in Western Australia.

In addition to the official statistics, there are many more heatwave-associated deaths that are caused mainly by heart disease and strokes, particularly in the elderly. Not all heat-related deaths occur on days of extremely high temperatures, however, suggesting that other factors in addition to maximum temperature are significant in influencing mortality.

The impact of heatwaves extends further than just mortality rates. High temperatures are linked to:

- increased hospital admissions relating to heat stress, dehydration, or as a result of heat exacerbating existing conditions;
- increased rates of certain crimes, particularly those related to aggressive behaviour such as homicide;
- increased number of work-related accidents and reduced work productivity; and
- decreased sports performance.

An extract from the *West Australian* (21 February 1995) illustrates the effect of a heat wave in Perth:

> *Perth's heatwave caused record power consumption and overstretched the ambulance service yesterday… A spokesman said the demand was caused by elderly people collapsing and having heart problems in the stifling heat. There were also many more assaults and brawls than normal in the early hours of Sunday when Perth sweltered through the hottest February night for ten years. Ambulances were called out 70 times, compared with an average of 30… Royal Perth and Sir Charles Gairdner hospitals reported treating people for dehydration, severe sunburn and heat exhaustion. Many people who came in with other illnesses also complained that the heat was making their problems worse.*

High temperatures can also cause significant economic losses through livestock/crop losses and damage to roads, railways, bridges, power reticulation infrastructure and electrical equipment (EMA, 1998). Heatwave conditions also significantly increase demand for electricity to power domestic air conditioners, water consumption and retail sales of cold drinks. During a heatwave in February 2004, the power supply was unable to cope with demand, resulting in power outages across Perth.

In assessing heatwaves as a natural hazard, consideration should also be given to the interaction of high temperatures and population vulnerability, which is a result of both the social and physiological systems. The distribution of heat-deaths is complex, the most vulnerable being the elderly, the sick and infants living in low socioeconomic urban areas during early summer heatwaves. Physiological adjustments primarily include acclimatisation to high temperatures, which is an issue for the increasing number of tourists arriving from the northern hemisphere winter.

The vulnerability of the population has decreased through the development and use of air-conditioners, better housing design, more suitable clothing, a trend towards more people working indoors, education and temperature forecasts for seven days in advance. Offsetting this, the percentage of elderly people in the population has increased, with those aged 65 and over comprising 11.2% of the population in Western Australia in 2001.

Defining heatwaves

There is no universal definition of a heatwave although in a general sense it is a prolonged period of excessive heat. The difficulty in defining a heat wave in Australia has been in establishing an appropriate heat index with an acceptable event threshold and duration, and relating it to the climatology of the area under investigation. Various heat or thermal comfort indices have been developed to evaluate heat-related stress combining air temperature and humidity, and in some cases, wind and direct sunlight. Two of the most widely used indices are the apparent temperature work of Steadman (1984) and the Relative Strain Index, RSI, derived by Belding and Hatch (1955) and discussed in the Goldfields–Eucla climatic survey (BOM, 2000).

High temperatures in the Perth area typically correspond to low humidity values because the prevailing east to northeasterly winds originate from the dry inland parts of the state. A study of temperatures at Perth Airport at 3 pm indicates that for temperatures exceeding 35ºC, the relative humidity exceeds thirty per cent on about 10% of occasions. Also, for the same air temperatures, the apparent temperature exceeds the air temperature on only 12% of occasions. While more humid conditions can exist when the air temperature is closer to 30ºC and can provoke some degree of discomfort, such days are not generally associated with heatwave conditions. As a result, for Perth the air temperature alone can provide a reasonable measure of heat stress.

Heatwave risks

The level of heat discomfort is determined by a combination of factors:

- meteorological: air temperature, humidity, wind and direct sunshine;
- cultural: clothing, occupation and accommodation; and
- physiological: health, fitness, age and the level of acclimatisation.

Heat stress makes us feel uncomfortable not so much because we feel hot, but rather because we sense how difficult it has become to lose body heat at the rate necessary to keep our inner body temperature close to 37ºC. The body responds to this stress progressively through three stages.

- **Heat cramps**: muscular pains and spasms caused by heavy exertion. Although heat cramps are the least severe stage they are an early signal that the body is having trouble with the heat.
- **Heat exhaustion**: typically occurs when people exercise heavily or work in a hot, humid place where body fluids are lost through heavy sweating. Blood flow to the skin increases, causing a decrease of flow to the vital organs. This results in mild shock with symptoms of cold, clammy and pale skin, together with fainting and vomiting. If not treated the victim may suffer heat stroke.
- **Heat stroke**: this stage is life threatening. The victim's temperature control system, which produces sweating to cool the body, stops working. Body temperature may exceed 40.6ºC, potentially causing brain damage and death if the body is not cooled quickly.

(Information from American Red Cross: http://www.redcross.org/)

Heatwaves in the Perth area

Perth's summer patterns follow a typical sequence. A ridge of high pressure south of the state combines with a deepening trough off the west coast to direct east to northeasterly winds over the Perth region. This pattern causes rising temperatures over successive days. The trough then moves inland, allowing early seabreezes along the coast resulting in a cool change. A new ridge then develops to the south producing southeasterly then easterly winds and the sequence begins again. Prolonged spells of hot days occur when this pattern is slow moving, the high being maintained south of the state and the west coast trough remaining off the coast. On such occasions, the east to northeasterly winds prevent the early arrival of the seabreeze and cause temperatures well above the average. Figure 2.18 shows a typical heatwave weather chart from March 2003. Tropical cyclones off the west or northwest coast can also help to maintain the trough offshore resulting in high temperatures in southern Western Australia (see section 2.5). These days are usually associated with hazardous fire weather conditions (refer to section 2.7).

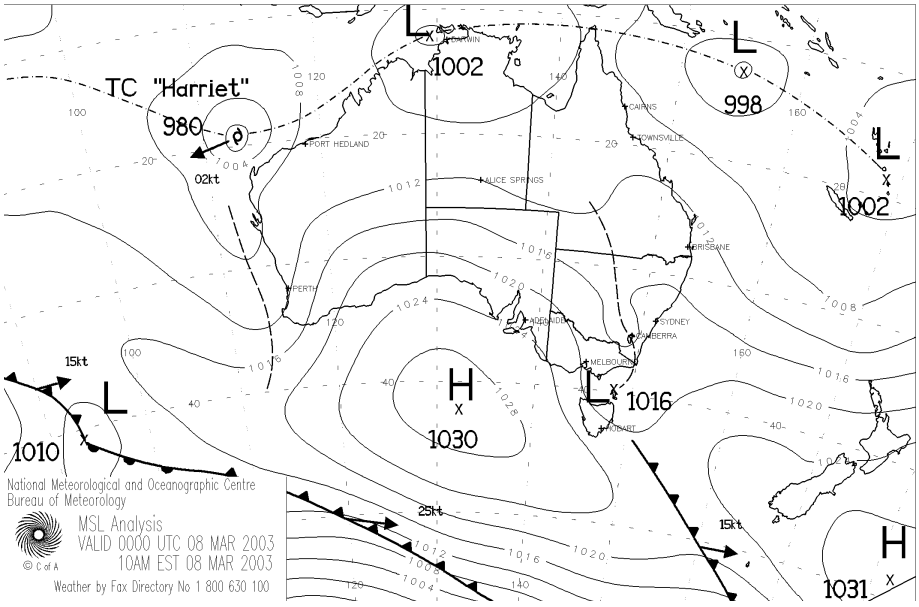

Figure 2.18: Mean Sea Level Pressure analysis of a typical heatwave pattern in Perth. A large and slow-moving high south of Australia combining with a tropical cyclone off the Pilbara coast maintains hot northeast winds in Perth

The occurrence of sequences of maximum temperatures of 35ºC or greater and 40ºC or greater at Perth Airport over 59 summers (1944–45 to 2003–04) is shown in Table 2.9. There have been 185 occasions where maximum temperatures of 35ºC or greater were recorded on at least three successive days, about three times per summer on average; and 15 occasions when at least three successive days have occurred on which maxima reached 40ºC or more, about once every four years on average.

Table 2.10 lists notable heatwaves showing data from Perth and Perth Airport. One of the greatest heatwaves occurred from 20 January to 6 February 1956, when for 17 consecutive days the maximum temperature at Perth Airport remained above 32ºC and averaged 38.8ºC. For five consecutive days maxima remained above 40ºC. The hottest summer on record was in 1978 when the temperature averaged 34ºC over 64 days from January to March.

Sequences of three successive days with maxima of 35ºC or greater have begun in all months between November and March, inclusive. Longer sequences of days with maxima of 35ºC or greater have been largely confined to the period from late December to mid-March.

Table 2.9: The occurrence of sequences of heatwaves at Perth Airport (1944–45 to 2003–04)

Duration of Sequence (days)	Maximum Temperature	
	35ºC or greater	40ºC or greater
3	91	11
4	39	2
5	23	1
6	18	1
7	4	
8	3	
9	2	
10	3	
11	1	
12	0	
13	1	
Total	**185**	**15**

Table 2.10: Notable heatwaves in Perth

Date	No. of days	Perth[1]		Perth Airport		Comments
		Average Temp. (°C)	Highest Temp. (°C)	Average Temp. (°C)	Highest Temp. (°C)	
16–27 January 1920	12	36.6	41.6			
3–11 February 1933	9	40.2	44.6			
20 January – 5 February 1956	17	37.1	43.7	38.8	43.7	Eight days over 40ºC at airport
29 December 1961 – 13 January 1962	16	36.0	40.5	37.1	41.6	
29 December 1964 – 5 January 1965	8	39.1	41.2	39.9	42.1	Six consecutive days over 40ºC at airport
29 January – 5 February 1975	8	36.9	40.4	38.5	42.4	
11–23 February 1975	13	37.1	40.9	36.4	40.9	
3 January – 7 March 1978	64	33.2	44.7	34.0	44.2	Perth's hottest summer ever
5–17 February 1985	23	36.5	43.7	37.5	43.4	
6–22 February 1988	17	35.8	39.0	36.6	40.8	
27–31 January 1991	5	39.1	45.8	40.5	46.0	
19–23 February 1991	5	39.1	46.2	40.5	46.7	Perth's highest temperature on record.
1–16 February 1996	16	36.5	42.4	37.5	43.2	
24 December 1999 – 7 January 2000	15	35.8	39.3	36.2	40.4	
21 February - 6 March 2001	14	34.7	39.7	35.3	40.1	

Note: [1] The station of Perth has undergone many changes throughout the observational record. The Perth station was moved from West Perth to East Perth in 1967, and then to Mt Lawley in 1993.

The primary environmental influences on day-time temperature variations across the greater Perth area are the ocean, the Darling Scarp, the Swan River estuary, and the nature and extent of urban development. The greatest single factor is proximity to the coast, because of the impact of the seabreeze on temperatures. Perth's reliable afternoon seabreeze, commonly referred to as the 'Fremantle Doctor', provides cooling relief from the east to northeast winds on hot summer days. The breeze initially arrives on the coast then progressively extends inland, often decreasing the temperature on hot days to below 30ºC within a few hours from onset. The degree of cooling varies according to the initial temperature, the time of onset and the strength of the seabreeze. Seabreezes typically take several hours to extend from the coast to the foothills, although there is significant variability in its movement inland. During very hot periods the seabreeze is delayed until at least mid-afternoon, and may not reach the coast at all on some days. On those days coastal suburbs may experience higher temperatures than elsewhere.

Figure 2.19 shows temperatures from a number of Perth sites during the heatwave from 1–16 February 1996. In general the temperatures follow the same behaviour day to day, however on any one day temperatures vary between sites. The highest temperatures tend to occur at Pearce and Gosnells. On most days, the coastal site of Swanbourne has the lowest temperature reflecting the influence of the earlier seabreeze. The difference in temperature between Pearce and Swanbourne can be up to 9ºC on some days. On other days (e.g. 2nd, 7–9th, 11th and 13th February), when the seabreeze is very late or does not reach the coast at all, Bickley, located in the hills, has the lowest recorded temperature, reflecting the influence of altitude on temperature.

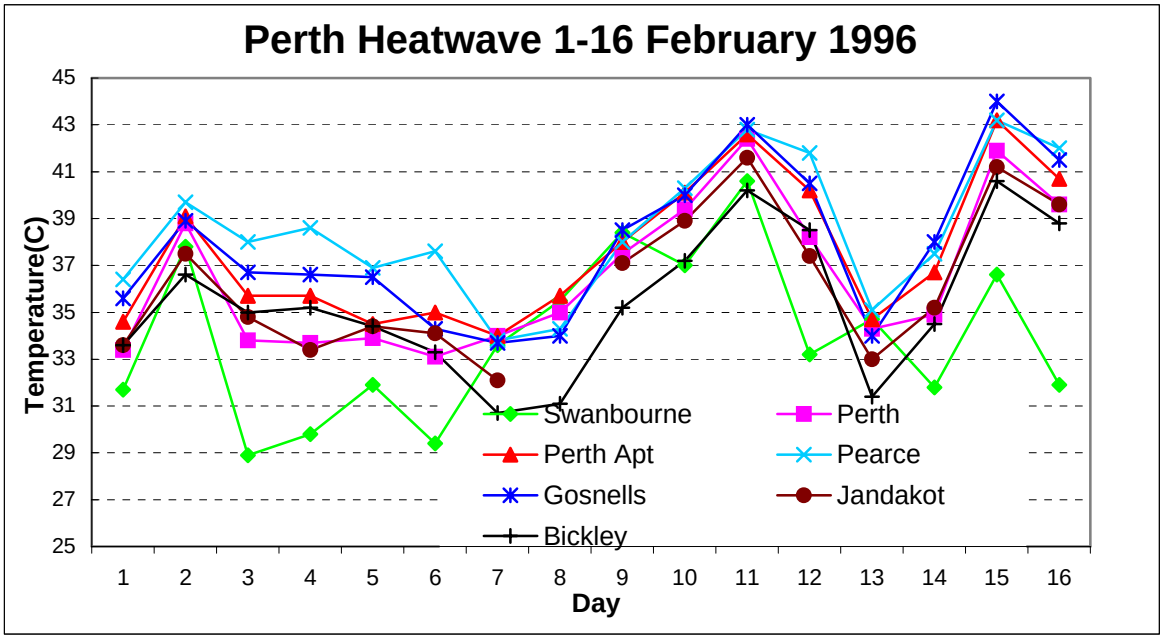

Figure 2.19: Maximum temperatures at Perth sites during the February 1996 heatwave

Trends and future projections

In contrast to the decline in the number of heat-related fatalities, the temperature record suggests an increase in the number of hot days in the Perth area. Summer maximum temperatures are estimated to have increased at the rate of over one degree per 100 years using data between 1950–1998. Collins *et al.* (2000) determined a slight increase in the frequency of heatwave events (at least three successive days of temperatures 35ºC or greater) at Perth Airport of 0.4 events per decade from 1957 to 1996.

Concern has been expressed at the possibility of temperature rises as a result of human-induced changes to the climate system. Current computer modelling by the CSIRO of the effect of an enhanced greenhouse effect on temperatures in the summer months suggests an increase in the number of days

of 35ºC or greater at Perth from 15 to between 16 and 22 by 2030 and 18 to 39 by 2070. It is likely that the number of successive days of high temperatures would also increase.

2.7 Bushfires – a meteorological perspective

The bushfire risk

The rate of spread of fires is strongly associated with the weather conditions at the time. In Perth and about the lower west coast the fire risk is greatest from summer through autumn, when the moisture content in vegetation is low. Summer and autumn days of high temperatures, low humidity and strong winds are particularly conducive to the spread of fires. Indeed temperature, relative humidity, wind speed, and the curing rate of vegetation can be combined into a fire danger index (FDI) that is the basis for the fire danger rating (Low, Moderate, High, Very High and Extreme) included on forecasts. In Western Australia the FDI used is the Revised Grasslands Fire Behaviour Meter which is based on the CSIRO-modified McArthur Mk IV Grassland Meter.

Perth's most susceptible area to bushfires is the forest areas in the hills suburbs. These are prone to strong morning easterlies that can fan existing fires. These easterlies can also be enhanced by topographical variations such as the Helena Valley. Other areas of bushland in Perth are also vulnerable to wildfires and can threaten neighbouring residential areas if they catch fire. On one afternoon in January 1989 a wildfire burned 45% (120 ha) of Kings Park.

The fire threat is increased when thunderstorms develop; producing lightning that causes ignition for fires. This is particularly the case when thunderstorms cause little or no rain, as is sometimes the case on hot days.

Fire weather climatology

Table 2.11(a and b) shows the monthly frequency of the five fire danger ratings for Perth Airport (1993–2004) and Bickley (19972004). These ratings are based on the highest FDI calculated each day and assumes a curing rate of 100%. The maximum number of Very High and Extreme days occurs in January. The calculated FDI values are higher than actual values in December because the curing rate early in the season is less than 100%. The annual number of such Very High to Extreme days is considerably higher at Perth Airport (31) than at Bickley (3) because the summer temperatures on the coastal plain away from the coast are higher than in the hills. The frequency of Very High to Extreme days decreases towards the coast on the coastal plain because of the seabreeze effect. Despite the curing rate being 100% in autumn, the fire danger rate declines because of lower temperatures and lower wind speeds on average.

Table 2.11(a): Perth Airport Fire Danger Ratings (1993–2004)

Month	Low	Moderate	High	Very High	Extreme
January	0.1	0.2	24.3	4.7	1.6
February	0.0	0.4	21.9	5.2	0.8
March	0.1	0.6	26.5	3.3	0.6
April	0.3	3.8	24.9	1.0	0.1
May	0.1	11.1	19.1	0.6	0.1
June	0.9	12.7	16.1	0.3	0.0
July	0.7	13.5	16.3	0.4	0.1
August	0.1	11.9	18.5	0.5	0.0
September	0.1	8.1	21.0	0.4	0.4
October	0.2	1.5	27.7	1.4	0.1
November	0.3	0.3	26.2	2.3	0.9
December	0.0	0.3	23.8	5.1	1.9
Year	**2.8**	**64.3**	**266.3**	**25.3**	**6.6**

Table 2.11(b): Bickley Fire Danger Ratings (1997 –004)

Month	Low	Moderate	High	Very High	Extreme
January	0.7	2.0	27.8	0.3	
February	0.4	1.3	26.1	0.4	0.0
March	1.4	5.3	23.1	0.4	0.7
April	0.6	14.7	14.6	0.1	0.0
May	3.0	19.6	8.4	0.0	0.0
June	4.9	19.6	5.5	0.0	0.0
July	5.7	18.8	6.5	0.0	0.0
August	2.5	22.0	6.5	0.0	0.0
September	0.8	19.3	9.7	0.2	0.0
October	2.6	16.2	12.1	0.0	0.2
November	0.0	7.6	22.4	0.0	0.0
December	1.1	2.9	26.3	0.6	0.1
Year	**23.8**	**149.2**	**189.0**	**2.0**	**1.2**

Extreme fire weather conditions in the Perth region typically occur with strong easterly or northeasterly winds associated with a strong high to the south of the state and a trough offshore as shown in Figure 2.20(a). Easterly winds represent about 60% of extreme fire weather days (events) compared to less than 5% associated with southerly winds. This is in contrast to Geraldton where winds on 40% of extreme events are southerly and at Albany and Esperance where winds on over 75% on extreme events are northerly. About 15% of Perth events occurred in a westerly flow following the passage of a trough. This number increases inland from the west coast where the westerly or northwesterly winds can be strong and gusty while temperatures initially remain high with the trough change. The eastward movement of the trough is shown in the sequential mean sea level pressure charts in Figure 2.20(a–b).

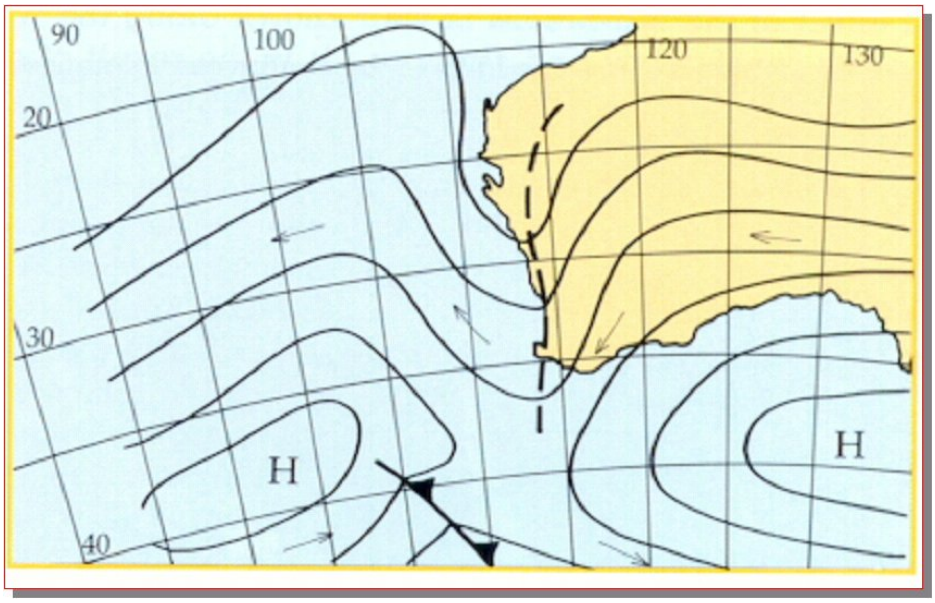

Figure 2.20(a): Mean Sea Level Pressure chart showing a typical day of hazardous fire weather. A high south of the continent directs east to northeasterly winds towards a trough near the west coast. Such days in Perth are typically very hot and dry

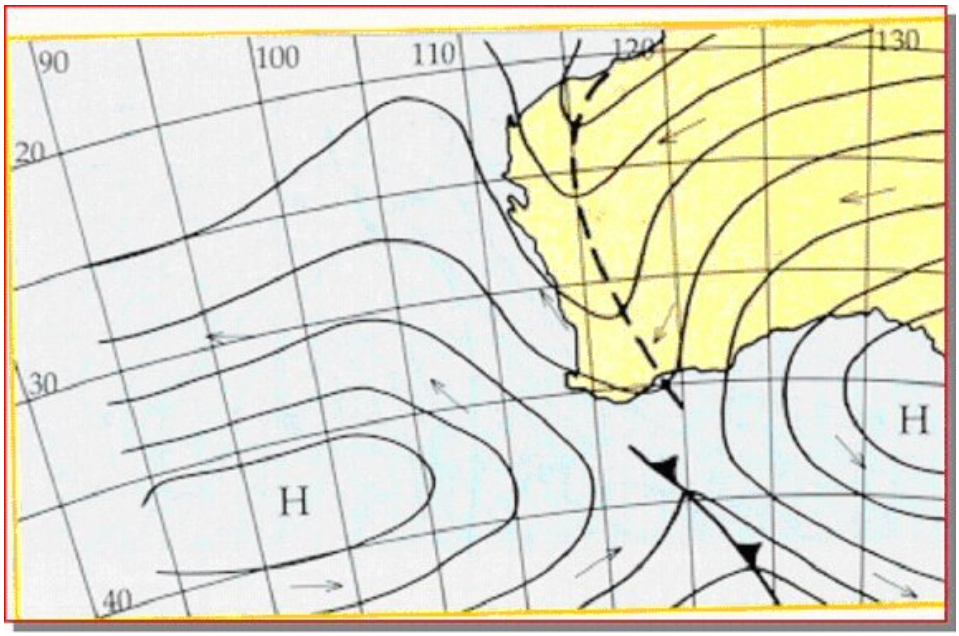

Figure 2.20(b): Mean Sea Level Pressure chart representative of the following day. The eastward mobility of the highs to the south helps to move the trough inland of the west coast resulting in significantly cooler conditions about the west coast

Very dangerous fire weather conditions often follow a sequence of hot days and easterly winds that culminate in the deepening of the trough near the coast and movement inland. The presence of a tropical cyclone off the Pilbara coast often helps maintain the trough offshore for longer than is normal. Such conditions occurred in January 1961 when the temperature at Wandering exceeded 40ºC on eight of the ten days from the 15th to the 24th. Strong winds associated with the trough passage on the 24th also coincided with thunderstorms that ignited fires east of the city and a major fire completely engulfed Dwellingup (Plate 2.11 and below).

Plate 2.11: The charred remains of Dwellingup after the devastating January 1961 bushfire (Courtesy of *West Australian*)

Tropical cyclones can cause a major fire threat in the southwest as demonstrated in February 1937 and again in April 1978 (cyclone *Alby*). Although tropical cyclones are normally associated with driving rain, destructive winds and storm surges, ones that accelerate into the mid-latitudes off the west coast can cause strong winds without rainfall over land (to the east of its track). The co-location of very strong winds and dry conditions creates a dangerous environment for wildfires to spread rapidly.

Some significant historical events in the Perth region

On 24 January 1961, a prolonged hot spell culminated in a very hot day and strong, gusty northwesterly winds associated with a trough change. Many fires that had been ignited by lightning in the previous week flared during the day and one fire front burned through Dwellingup, destroying 132 homes and a number of other buildings (Plate 2.14). Fortunately there were no serious human casualties. The situation was described by the *West Australian* (24 January 1981) as follows:

> *About 8.30 pm on Tuesday January 24, 1961, hundreds of terrified people watched helplessly as fire engulfed and destroyed most of Dwellingup, a timber milling town 100 km south of Perth. A short time before they had hurriedly abandoned their homes with only the clothes they wore. They watched a petrol station blow up, houses and motor vehicles explode into flames seconds after being abandoned and flames jump hundreds of metres ahead of the main front, fanned by 120 km/h winds. Some people jumped into a well to escape the inferno and workers trapped at a forestry mill lay face down on the ground and took turns spraying water on each other…*
>
> *Miraculously no one was killed or seriously injured. But about 800 people were left homeless and scores of people were treated for smoke inhalation and eye complaints. When the damage had been tallied up, 132 houses had been destroyed, as well as the hospital, two saw mills, two service stations, three general stores, offices, outbuildings and 74 motor vehicles. The value of the damage was estimated to be about $10 million - $50 million on today's [1981] values.*

Smoke from fires burning in the hills near Keysbrook and in the hills near Perth blanketed the city. Due to the poor visibility, Perth Airport was closed to light aircraft and at Fremantle shipping traffic had to be tracked by radar (*West Australian*, 24 January 1961).

On 4 April 1978, pre-existing fires were fanned by gale-force winds as cyclone *Alby* accelerated down the west coast. The Bushfires Board reported 78 fires in the area south of Eneabba to Lake Grace. These burnt over 31,000 ha and had a total perimeter of 470 km. Falling trees killed two people during fire fighting operations.

On 1 December 1979, a large bushfire near Mandurah cut power lines resulting in a power blackout. Perth lost one-third of its power, causing residents to swelter in 37° heat. The havoc it caused is described by the *Sunday Times* (2 December 1979):

> *A major power failure plunged Perth and the South West into chaos for several hours yesterday. The blackout, caused by a bushfire near Mandurah, cut both transmission lines between Perth and Bunbury, as most of the State sweltered in near century heat. At one stage, the entire metropolitan area and the South West were blacked out. State Energy Commission (SEC) officials worked for several hours to restore power and boost output from Kwinana and South Fremantle power stations. Late yesterday the two Bunbury transmission lines were still out as a huge bushfire raged out of control 8 km east of Mandurah. SEC engineers took to the air in an attempt to determine the point of the failure. They were flying along the transmission lines from the southern terminal at Cannington to Bunbury. The blackout hit Perth and the South West at about 12.30 pm bringing disruption to thousands of homes, hospitals, emergency services and sporting fixtures. It caused havoc in the racing world as the Ascot races were forced on to emergency power and 37 TAB shops were closed down. The SEC shifted the power load around the metropolitan area in a bid to ease the disruption. It was 3 pm before power was restored to most areas. The SEC's marketing manager, Mr Don Saunders, said the two transmission lines from Bunbury were cut suddenly at 12.30 pm. At that point Perth lost a third of its power. The total load for Perth is 600 megawatts and we lost 200 megawatts, he said.*

On 8 January 1997, bush fires at Wooroloo and Wundowie destroyed 16 homes and part of the Wooroloo Prison Farm. Other losses, including sheds, fencing, livestock, vehicles and stored fodder, contributed to a total cost well in excess of $12 million (Bushfires Board of Western Australia, 1997).

More recently, a bushfire burnt through 2,000 ha of scrub and damaged six homes in Perth's northern suburbs in early February 2001. Less than two weeks later this was followed by a bushfire which burnt through 1,000 ha of scrub in Perth's northeastern suburbs and threatened several homes and the Perth International Telecommunications Centre (*West Australian*, 15 February 2001).

2.8 Summary

The Perth region is subject to a range of meteorologically related hazards: winter storms, summer storms, floods, tropical cyclones, heatwaves and bushfires. Of these, cool season storms are the most frequent hazard and on average have the greatest economic impact. Strong fronts cause winds of gale-force intensity near the coastal fringe of the southwest producing mostly minor damage over a wide area. Damage is typically associated with roof damage and to power lines. These fronts may also spawn severe localised winds, including tornadoes. Winds may be strong enough to unroof houses although such damage is fortunately confined to small areas.

The meteorological hazards that have individually had the greatest impact on Perth have been floods and tropical cyclones. If Perth was to experience floods of the magnitude of those in 1862, 1872, 1917, 1926 or 1945, then the economic impact would be on the order of many tens of millions of dollars. However, Perth's average annual rainfall has decreased in the last 40 years, lessening the risk of a flood of such magnitude. Possibly Perth's single greatest meteorological event was cyclone *Alby* in 1978, when damage was estimated at $39 million (2003 dollars). Strong winds damaged properties and fanned bushfires, while a storm surge and large waves caused massive coastal erosion and flooding in low-lying areas.

Although summer thunderstorms storms are much less common in Perth than in most other Australian cities, there is the potential for them to be as severe as the Sydney hailstorm in 1999 that caused over $2 billion damage. Fortunately such a storm has not impacted Perth. Heatwaves, although viewed as a 'passive' hazard, kill more people than any other meteorological phenomenon. However, the impact of heatwaves has been reduced by factors such as increased use of air-conditioners, better housing design and greater awareness of the risk.

2.9 References

Andrews, K. (1994) *The consequences of heatwaves in Australia,* Master of Science thesis, Macquarie University, NSW.

Belding, H.S. and Hatch, T. F. (1955) 'Index for evaluating heat stress in terms of resulting physiological strain', *Heating, Piping, and Air Conditioning*, 27:129–36.

Brewster, A.K. (1970) *Tornadic squall at Naval Base, Western Australia on 8 June 1968*, Meteorological Note 43, Bureau of Meteorology, Australia.

Brook, R. R. (1965) 'Tornado at Mandurah, 15th June 1964', *Australian Meteorological Magazine*, 50:26–34.

Bureau of Transport Economics (2001) *Economic costs of natural disasters in Australia*, Report 103, Bureau of Transport Economics, Commonwealth of Australia, Canberra.

Bureau of Meteorology (2000) *Goldfields–Eucla Western Australia: climatic survey*, Department of the Environment and Heritage.

Bureau of Meteorology (1995) *Climate of Western Australia*, Bureau of Meteorology, Commonwealth Australia, Melbourne.

Bureau of Meteorology (1929) *Results of Rainfall Observations made in Western Australia*, Bureau of Meteorology, Commonwealth Australia, Melbourne.

Bushfires Board of Western Australia, (1997), Annual Report (?).
Coates, L. (1996) 'An overview of fatalities from some natural hazards in Australia', in R.L. Heathcoote, C. Cuttler, and J. Koetz, (editors*), Natural Disaster Reduction (NDR96): Conference proceedings*, Institute of Engineers Australia, Canberra, pp 49–54.
Collins, D.A., Della-Marta, P.M., Plummer, N. and Trewin, B.C. (2000) 'Trends in annual frequencies of extreme temperature events in Australia', *Australian Meteorological Magazine*, 49:277–92.
Emergency Management Australia (1998) *Heatwave Action Guide*, Emergency Management Australia, Disaster Awareness Program, Canberra.
Foley, G. R. and Hanstrum, B. N. (1994) 'The capture of tropical cyclones by cold fronts off the west coast of Australia', *Weather and Forecasting*, 9(4):577–92.
Foley, G.R. and Hanstrum, B.N. (1990) 'Severe local wind storms over southwestern Australian during the cooler months', *Proceedings 2nd Australian Severe Thunderstorm Conference*, Melbourne, Victoria. Appendix 2.
Frich P., Alexander L.V., Della-Marta P., Gleason B., Haylock M., Klein Tank A.M.G., and Peterson, T. (2002) 'Observed coherent changes in climatic extremes during second half of the 20th century', *Climate Research*, 19:193–212. CSIRO.
Hanstrum, B.N., Mills, G.A. and Watson, A. (1998) 'Cool season tornadoes in Australia, Part 1: Synoptic climatology', *Proceedings 6th Australian Severe Thunderstorm Conference*, Brisbane, Queensland, pp. 75–8.
Hanstrum, B.N. (1994) 'The Mandurah tornado of 22 September 1993', *Proceedings 4th Australian Severe Thunderstorm Conference*, Mt Macedon, Victoria.
Hanstrum, B.N., Holland, G.J. and Sobott. S.K. (1998) 'A simple objective technique for estimating the strength of convective wind gusts during the cooler months', *Proceedings 6th Australian Severe Thunderstorm Conference*, Brisbane, Queensland, pp. 120–3.
Hanstrum, B.N. and Foley, G.R. (1990) 'A diagnostic case study of the thunderstorm event of 8 November 1986 at Perth, Western Australia', *Australian Meteorological Magazine*, 38:271–79.
Haylock, M. and Nicholls, N. (2000) 'Trends in extreme rainfall indices for an updated high quality data set for Australia, 1910–1998', *International Journal of Climatology*, 20:1533–41.
Indian Ocean Climate Initiative (2002) *Climate Variability and Change in south west Western Australia*, Indian Ocean Climate Initiative Panel, Perth.
Kingwell, J. and Watson, A.S. (1982) 'A study of the Shoalwater Western Australia tornado 21 June 1980 and comparison with ten other Australian tornadoes', Meteorological Note 136, Bureau of Meteorology, Australia.
McCready L. and Hanstrum, B.N. (1996) 'Two ordinary cell severe downburst cases at Perth, Western Australia', *Proceedings 5th Australian Severe Thunderstorm Conference*, Avoca Beach, New South Wales, pp. 65–76.
McCready, L. and Hanstrum, B.N. (1995) *The severe storm of 23/24 May 1994 over southwest Western Australia*, Meteorological Note 208, Bureau of Meteorology, Australia.
Newspapers – Daily News, Perth Gazette newspaper, The Australian, The West Australian, Sunday Times, Perth Enquirer. Various dates.
Southern, R.L. (1960a) 'A tornado at Byford, Western Australia – January 1960', *Australian Meteorological Magazine*, 31:29, 49–67.
Southern, R.L. (1960b) 'Study of a tornado situation in southwest Australia', *Australian Meteorological Magazine*, 31:1–12.
Steadman, R.G. (1984) 'A universal scale of apparent temperature', *Journal of Climate and Applied Meteorology*, 23:1674–87.
Water and Rivers Commission (2000) *Water Facts 13*, Water and Rivers Commission, July.
Watson, A. (1994) 'Cool season tornadoes in South Australia, Some recent examples and a suggested mechanism', *Proceedings 4th Australian Severe Thunderstorm Conference*, Mt Macedon, Victoria.
Watson, A. (1985) *An examination of three winter tornadoes in southwest Western Australia*, Meteorological Note 162, Bureau of Meteorology, Melbourne.
Vivers, P.M. and Hanstrum, B.N. (1996) 'Severe splitting thunderstorms near Perth, Western Australia on 27 March 1995', *Proceedings of the 5th Australian Severe Thunderstorm Conference*, Avoca Beach, New South Wales, pp. 162–77.

Volprecht, R. (1955) ‘The Dwellingup storm—June 1954’, *Australian Meteorological Magazine*, 9:61–66.

Chapter 3: SEVERE WIND HAZARD ASSESSMENT IN METROPOLITAN PERTH

Xun Guo Lin[1] and Krishna Nadimpalli[2]

1. CSIRO, Mathematical and Information Sciences
2. Geoscience Australia

3.1 Introduction

In this chapter a severe wind hazard assessment for metropolitan Perth is described. There were three stages to this wind hazard assessment.

- The wind data description provides information about the location of weather stations, the service periods of these stations and the maximum historical wind gust recorded at each site.
- The section on local wind effects estimates the local effect of terrain for the structure height concerned; the shielding effect provided by upwind structures and the topographic effect. These effects were numerically estimated using remote sensing techniques, digital elevation data and by using formulas given in the Australian wind loading design standard.
- The last stage was the estimation of likely severe wind speeds within a given time period. These wind speeds are commonly called return period wind speeds or return levels. The wind speed estimation for various return periods includes a sensitivity analysis. The final adopted return period wind speeds were a combination of statistical analysis, expert judgement and the satisfaction of internal consistency.

The output of this assessment is the combined (terrain/height, shielding and topographic) local wind multipliers for eight cardinal directions on a 25 m by 25 m grid across metropolitan Perth and the local return period wind speeds (called the wind hazard maps) at the same grid locations. These local wind multipliers and the wind hazard maps may be used in decision-making processes by local and state governments in disaster planning, mitigation and emergency management. They may also be useful for city and suburb planning processes.

3.2 Wind Study Area

Extreme wind is one of the major natural hazards experienced in Perth. These extreme winds are generally produced by cold fronts and not by cyclones (see for example Lin and Courtney, 2004) or thunderstorm-related downbursts. The wind study area covers Perth City and its surroundings, including Rottnest Island. The geographic extent of the area in the Universal Transverse Mercator (UTM) coordinate system lies between 354500 to 416475 longitude and 6437995 to 6498970 latitude covering an area of about 3,767 km^2. The red box in **Figure 3.1** shows the study area.

3.3 Wind Data from Weather Stations in Metropolitan Perth

Historical wind-gust datasets from ten weather stations, were provided by the Bureau of Meteorology's (BOM) Perth Office. Eight of these are current automatic weather station (AWS) sites. Their geographic locations are shown in Figure 3.1

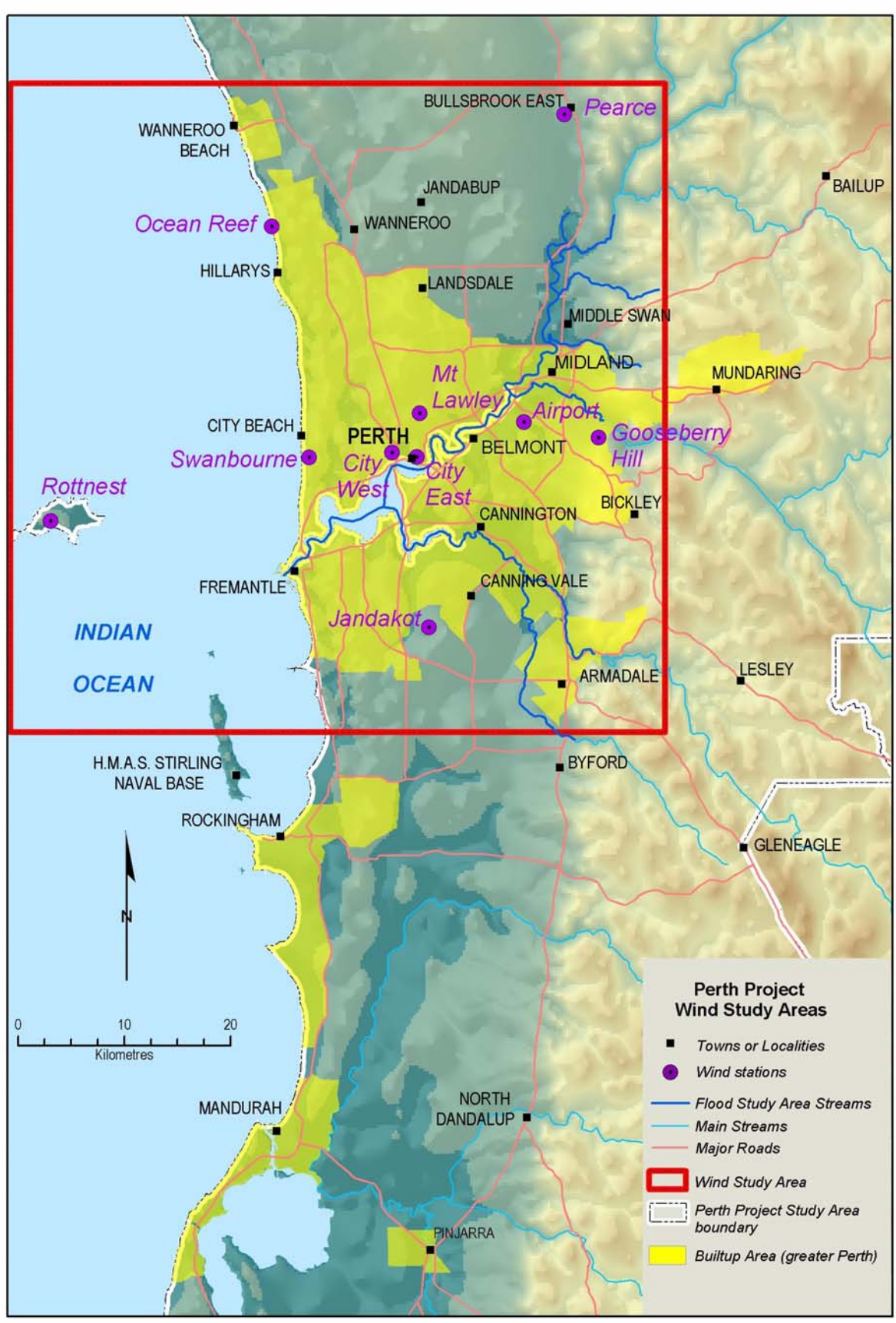

Figure 3.1: The setting of the wind study area in metropolitan Perth

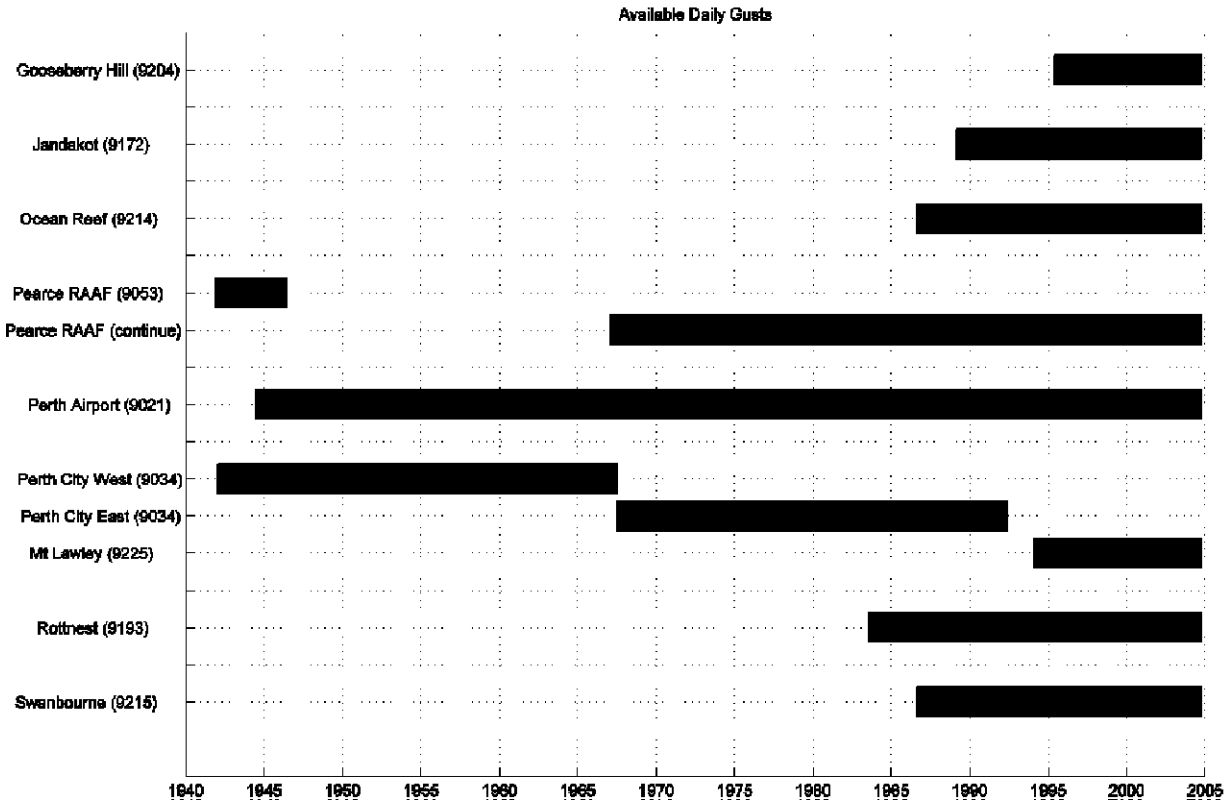

Figure 3.2: The timeline of historical and current weather stations in metropolitan Perth

Table 3.1: Weather station statistics and the historical largest gusts

Station site	Latitude	Longitude	Station height	Mast height	Data length (years)	Calendar period	Hist max (m/s)	Hist max (km/h)	Hist max date
City East	115.8667	-31.95	19	40	24.6	1967–1992	36	130	4/4/1978
Rottnest Is.	115.5	-32.0086	43.1	10	18.2	1983–2004	39.1	141	22/9/1988
Jandakot	115.8794	-32.1011	30.2	10	12.3	1989-2004	31.4	113	7/6/1990
Swanbourne	115.7619	-31.9558	40.96	10	17.9	1986-2004	39.6	143	23/5/1994
Mt Lawley	115.8728	-31.9192	24.9	10	10.6	1994–2004	26.2	94	17/7/1996
Perth Airport	115.9764	-31.9275	15.4	10	60.2	1944-2004	34.5	124	22/7/1990
Gooseberry Hill	116.0506	-31.9414	220	20	8.8	1995-2004	37.6	135	8/6/1995
Ocean Reef	115.7278	-31.7594	10	10	17.8	1986-2004	35	126	19/7/1989
Pearce	116.0189	-31.6669	40	10	35.0	1941-2004	36	130	28/7/1975
City West	115.8453	-31.9508	58	22	25.5	1942-1967	43.2	156	20/8/1963

The period of each station's observations is shown in Table 3.1. The latest wind data from the eight current sites was for 1 October 2004. The average wind speed over a 3-second period is referred to as a 'gust'. The majority of the wind data are daily maximum gusts. The rest of them are 1-minute maxima and 10-minute maxima which have been used to calculate daily maximum gusts for this study. As a by-product of this study, a complete set of daily maximum gusts covering the whole historical period at ten weather stations in Perth has been provided to the BOM for future research and study.

Details of the locations of weather stations and the largest wind gust at each site are listed in Table 3.1. The strongest gust recorded was 43.2 m/s (or 156 km/h) at the City West site in 1963. The longest

continuous recording period was over 60 years at Perth Airport. This record was the basis for the wind hazard published in AS/NZS 1170.2 (2002). The shortest continuous recording period was only about 8 years at the Gooseberry Hill site. The current City site at Mt Lawley has also had a relatively short history (about 10 years). The strongest gust recorded at Mt Lawley was 26.2 m/s (or 94 km/h) which was the weakest amongst the ten sites in metropolitan Perth with their various operating time periods.

3.4 Local Wind Effects

The impact of severe wind varies considerably between structures at various locations because of the geographic terrain, the height of the structures concerned, the surrounding structures and topographic factors. These site wind, exposure and speed modifications can be numerically described by so-called wind multipliers. These multipliers give quantitative measures of local wind conditions relative to the regional wind speed (defined as open terrain at 10 m height) at each location. There are three wind multipliers: the terrain/height multiplier (M_z), the shielding multiplier (M_s) and the topographic (or hill-shape) multiplier (M_h). The local site wind speed at a reference height (V_{site}) is estimated by multiplying the regional wind speed (V_R) by the local wind multipliers:

$$V_{site} = V_R \, M_z \, M_s \, M_h \qquad \textbf{Equation 3.1}$$

The local site wind speed is determined separately for each of the eight cardinal directions.

Formulas to estimate these wind multipliers for a given location are given in AS/NZS 1170.2 (2002). However, efficient and effective computational methods to estimate these wind multipliers across a larger area with higher resolution need to be developed. Satellite remote-sensing techniques, geographic information systems (GIS), image analysis software and a digital elevation dataset have been used to apply these formulas to calculate the three wind multipliers. In Figure 3.3 an overview is given of the methodology to develop terrain/height, shielding and hill-shape multipliers for eight cardinal wind directions. The process is described under separate headings below.

Terrain classification mapping

In order to estimate the terrain/height multiplier and the shielding multiplier, a terrain classification map needed to be developed. Terrain classes from AS/NZS 1170.2 Supp 1 (2002) were used to classify the Perth metropolitan area. The following classes were relevant to our wind hazard assessment.

- City buildings
- Forests
- Centres of small towns and industrial areas
- Suburban and wooded country
- Long grass with few trees
- Air fields and uncut grass
- Water
- Sandy beaches
- Cut grass

To map the terrain of the study area, Landsat Thematic Mapper data was used as input. It has 25 m spatial resolution and 6 frequency bands. (Further information about the data specifications can be obtained from the Australian Centre for Remote Sensing (ACRES) website: http://www.ga.gov.au/acres/prod_ser/landdata.htm). The satellite database of bands 432 is depicted in Figure 3.4. The terrain map development process is described in the top left hand corner of Figure 3.3 and the estimated terrain classification map using image software is shown in Figure 3.5.

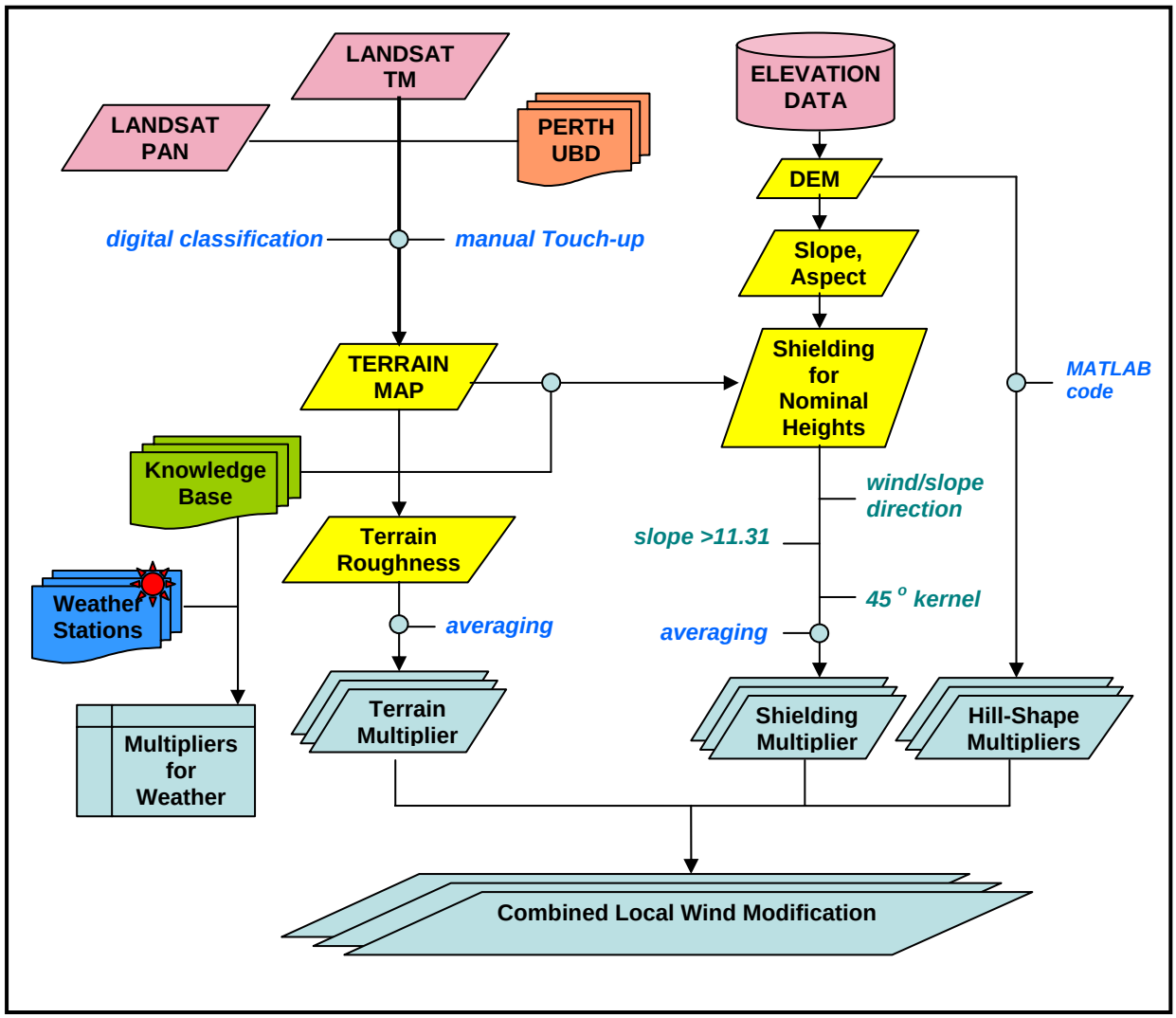

Figure 3.3: Diagram of methodology used in estimation of local wind modification multipliers

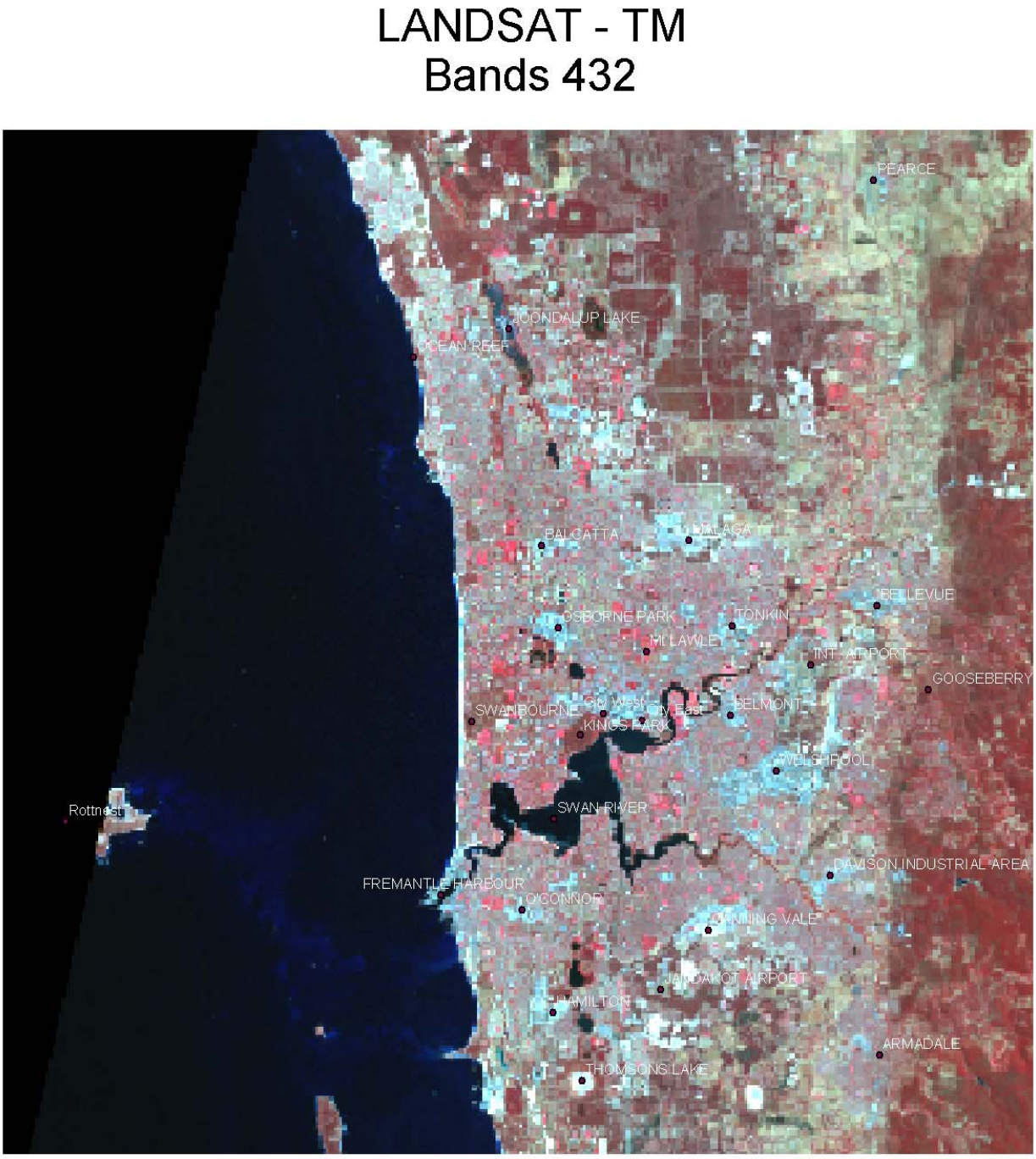

Figure 3.4: LANDSAT satellite database of Bands 432 of metropolitan Perth

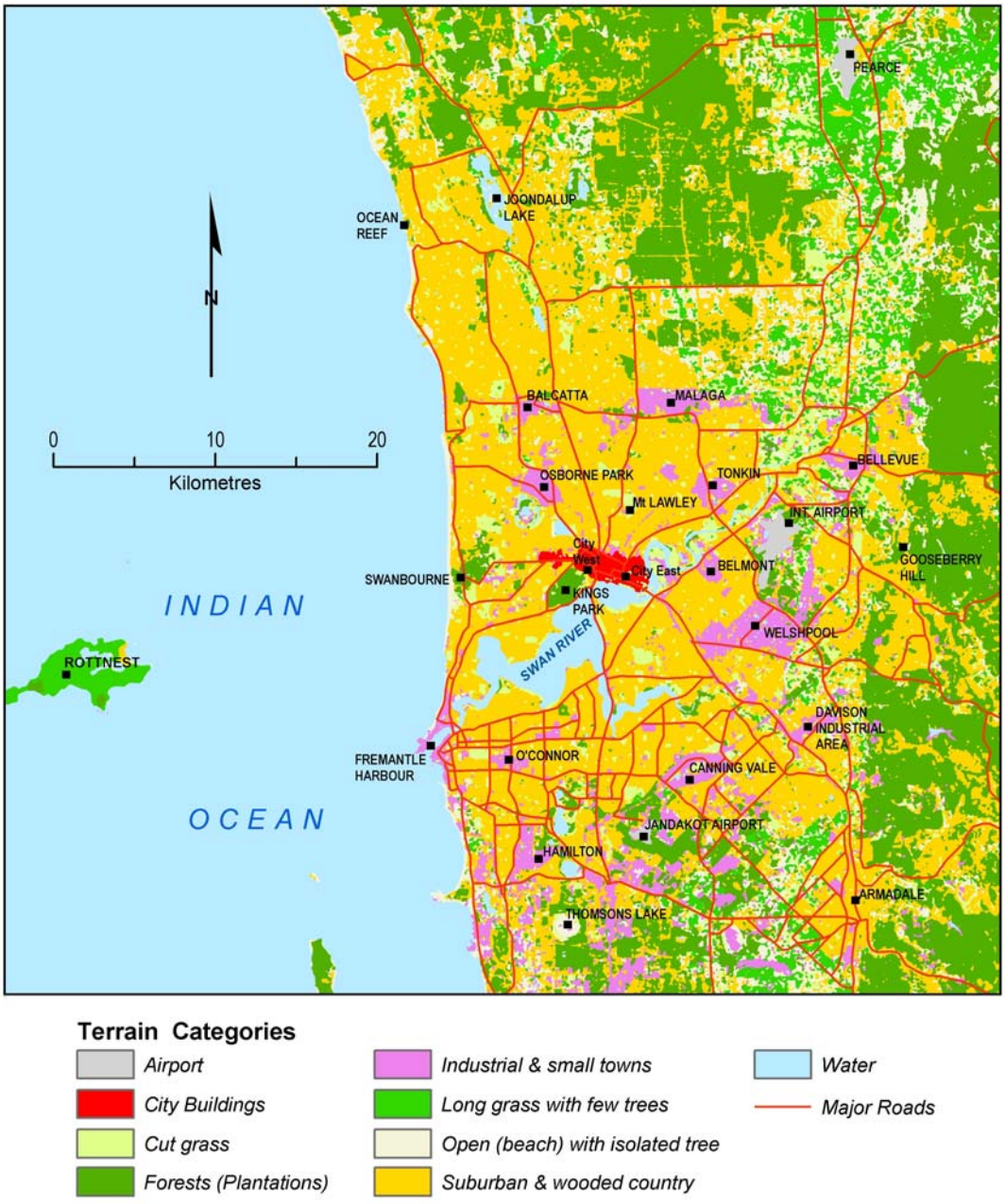

Figure 3.5: Terrain map of Perth wind study area

Table 3.2: The nominated height in each terrain category

Terrain category	Terrain classification	Nominated height (m)	M_z
4	City	50	0.9
	Forest	20	0.794
	Town centre/Industrial	20	0.92
3	Suburb buildings	3–10	0.83
	Trees	<5	0.89
2	Water/Airport	<3	0.91
	Cut grass	<3	0.92

When there are different terrain classifications upwind of a structure of primary interest, the method of averaging described in AS/NZS 1170.2 (2002) was applied. The distance for averaging depends on the

height of the structure. However, since the nominated heights for various terrain classifications in the Perth wind study area are all less than 50 m, an averaging distance of 1 km was adopted, following Table 4.2(A) of AS/NZS 1170.2 (2002). Using the averaging method, the terrain/height multipliers were estimated. The process is shown in the bottom left hand side of Figure 3.3 and Figure 3.6 shows the study region M_z values for the wind direction from west to east.

The M_z for AWS sites are listed in Table 3.3. Note that, since we know the exact mast heights of the AWS, these heights were used in the calculation of M_z rather than using the nominated building height for the terrain categories in which they are situated. Also, note that as the City West site was (and is) surrounded by town-centre-like buildings rather than urban city high-rises, the M_z estimated using the current city terrain classification may overestimate the actual terrain effect. After consulting with meteorologists in the BOM Perth Office, a 15% reduction of the M_z derived using the current terrain was adopted for adjusting wind speeds to appropriate terrain category. The M_z values for the City West AWS listed in the last row of Table 3.3 are the adjusted values.

Table 3.3: Terrain/height multipliers M_z for AWS locations

Name	North	NE	East	SE	South	SW	West	NW
City East	0.85	0.94	0.85	0.85	1.02	0.99	0.85	0.85
Rottnest Is.	0.96	0.97	0.96	0.96	0.97	0.96	0.96	0.96
Jandakot	0.93	1.00	0.91	0.92	0.87	0.86	0.95	0.91
Swanbourne	0.80	0.80	0.82	0.86	0.80	0.89	0.89	0.84
Mt Lawley	1.03	0.92	0.88	0.88	0.91	0.84	0.83	0.91
Perth Airport	0.82	0.82	0.94	0.97	0.97	1.00	1.00	0.93
Gooseberry Hill	0.93	0.87	0.91	0.92	0.90	0.86	0.89	0.88
Ocean Reef	0.90	0.84	0.87	0.84	1.00	1.00	1.00	1.00
Pearce	1.00	0.88	0.90	0.96	1.00	1.00	0.99	1.00
City West	0.92	0.87	0.91	0.93	1.06	0.98	0.94	0.87

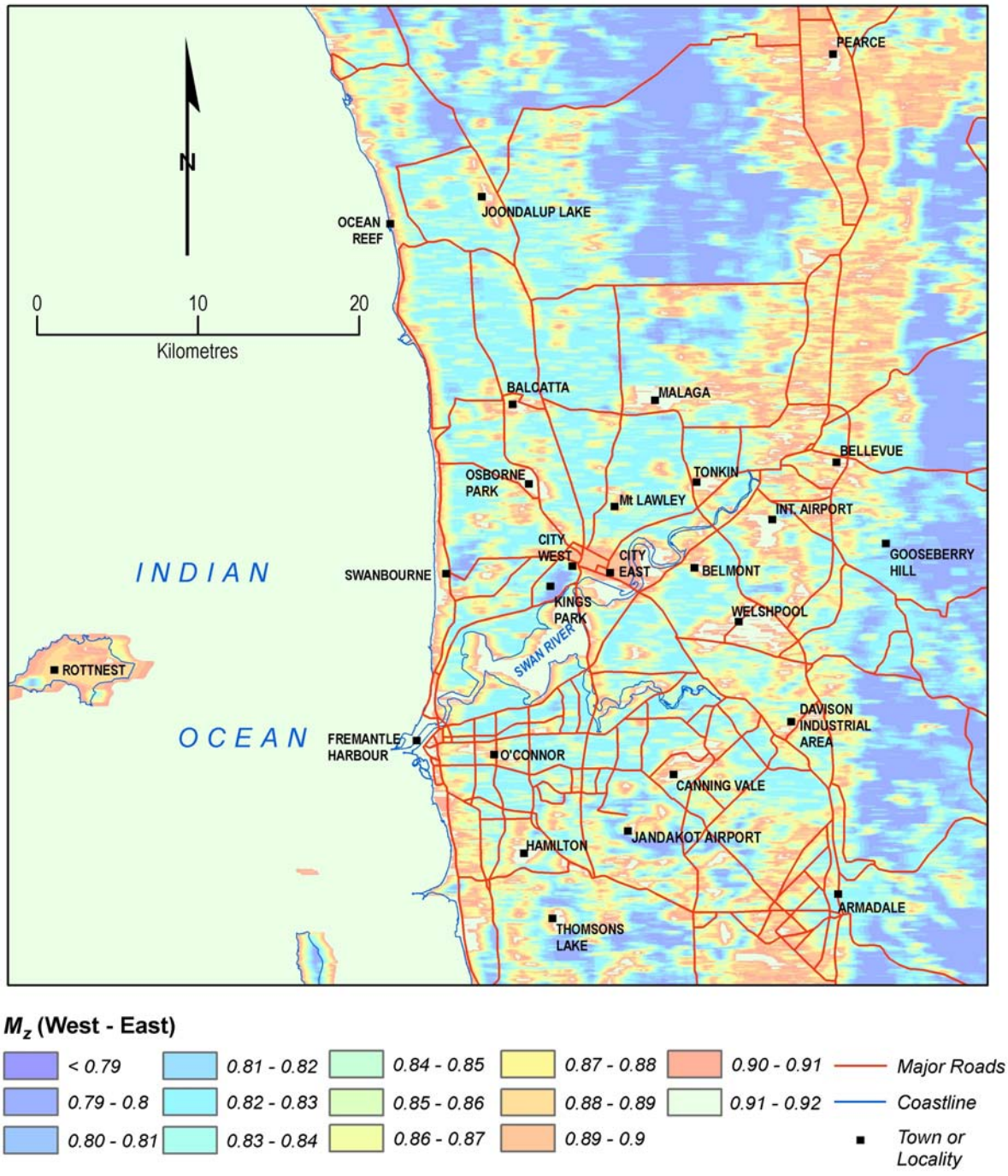

Figure 3.6: Terrain/height multipliers M_z for the wind direction from west to east

Shielding multipliers

The shielding multiplier (M_s) of a structure depends on the number of buildings upwind in a shielding zone with at least the same height as the structure concerned. The shielding zone is defined as a 45 degrees upwind sector area with a radius of 20 times the building height and centred on the building concerned. A formula is provided in AS/NZS 1170.2 (2002) to calculate the shielding multiplier, given the average building height, the number of buildings in the shielding zone and the width of those buildings. Figure 3.7 shows the estimated shielding multipliers for winds from west to east in the study area. For each of the ten weather station sites, manual study of aerial photographs has been carried out for all directions within its shielding zone. It was found that the only shielding

multipliers less than unity are for the City East site in several wind directions. Using the formula given in AS/NZS 1170.2 (2002), these M_s have been calculated and checked with meteorologists in the BOM's Perth Office. Table 3.4 lists the M_s for AWS locations.

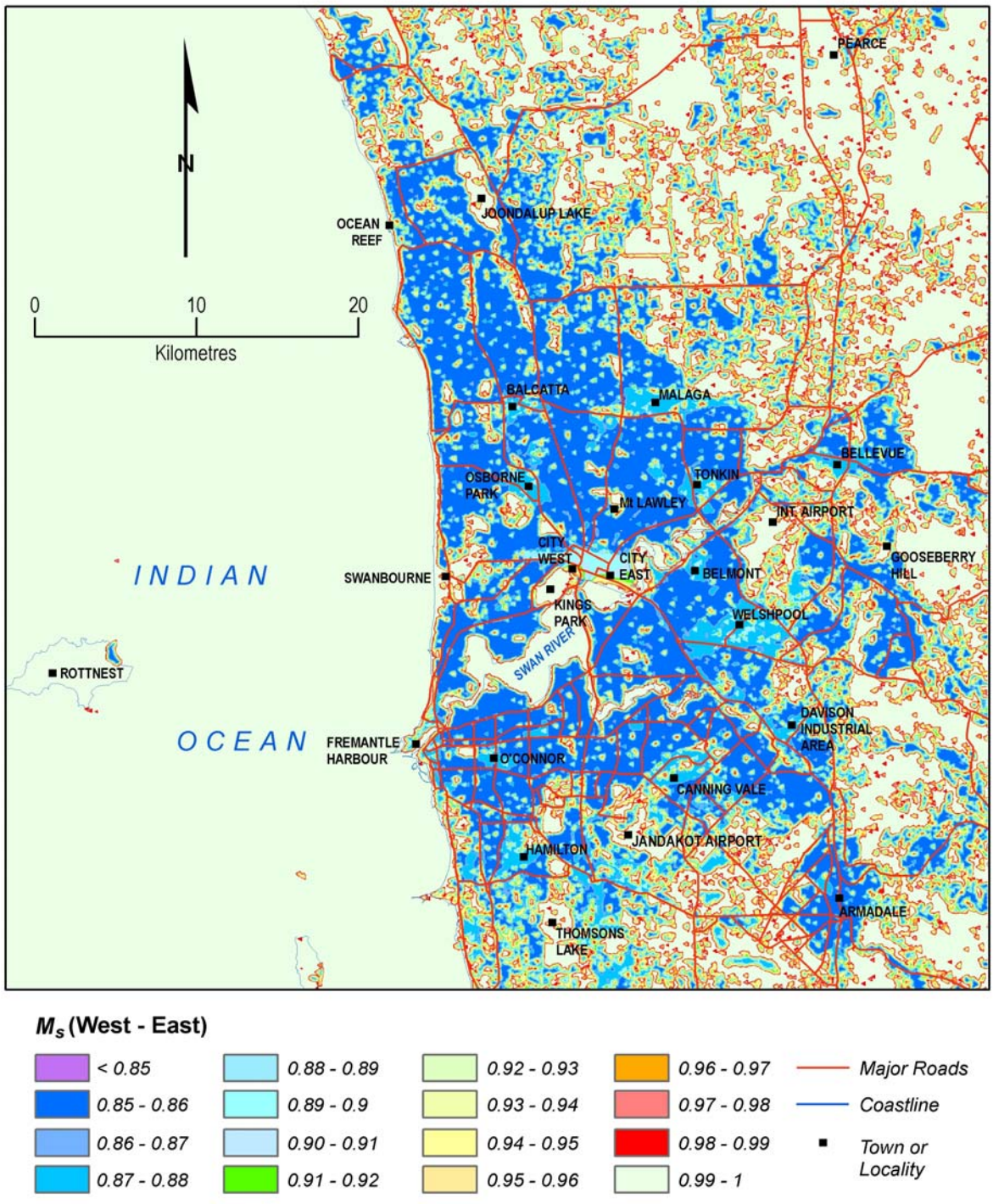

Figure 3.7: Shielding multipliers M_s for the study area

Table 3.4: Shielding multipliers M_s for AWS locations

Name	North	NE	East	SE	South	SW	West	NW
City East	1	1	1	0.91	1	0.86	0.84	0.93
Rottnest Is.	1	1	1	1	1	1	1	1
Jandakot	1	1	1	1	1	1	1	1
Swanbourne	1	1	1	1	1	1	1	1
Mt Lawley	1	1	1	1	1	1	1	1
Perth Airport	1	1	1	1	1	1	1	1
Gooseberry Hill	1	1	1	1	1	1	1	1
Ocean Reef	1	1	1	1	1	1	1	1
Pearce	1	1	1	1	1	1	1	1
City West	1	1	1	1	1	1	1	1

Topographic features of metropolitan Perth

The topographic features of metropolitan Perth have been captured by a digital elevation model (DEM) generated from spot height data at a spacing of 1 minute UTM. The DEM of metropolitan Perth in a 25 m by 25 m grid is shown in Figure 3.8. It can be seen that the majority of metropolitan Perth is gently undulating, except the Darling Range Scarp which is more than 200 m above mean sea level. Note that the Gooseberry Hill weather station was built on the Darling Range Scarp with the purpose of catching the easterly winds.

Topographic wind multipliers

Standing on an uphill slope will normally feel windy comparing to standing on a flat area. This is called the topographic (or hill-shape) wind effect. In wind engineering, it is calculated by multiplying the regional wind speed, V_R, by the topographic (or hill-shape) multiplier M_h. The methodology that uses a DEM to produce the M_h multiplier is shown on the far right of Figure 3.3.

AS/NZS 1170.2:2002 specifies that slopes below 5% are assigned a M_h of 1 and slopes of 45% and above are assigned a M_h of 1.71 within the local topographic zone defined in the Standard. For the slopes between 5% and 45%, the formula in AS/NZS 1170.2:2002 will provide values for M_h. Table 3.5 gives M_h values for some different slopes. It can be seen that the hill-shape multiplier has a minimum value of 1 but a maximum value of 1.71 when the slope is equal or greater than 45% (or 24.2 degrees).

Table 3.5: Hill-shape multiplier at crest ($|x| = 0$) when $z = 0$, from Table 4.4 of AS/NZS 1170.2 (2002)

Hill slope (%)	Hill slope (degrees)	M_h
< 0.05	< 2.9	1.0
0.05	2.9	1.08
0.10	5.7	1.16
0.20	11.3	1.32
0.30	16.7	1.48
≥ 0.45	≥ 24.2	1.71

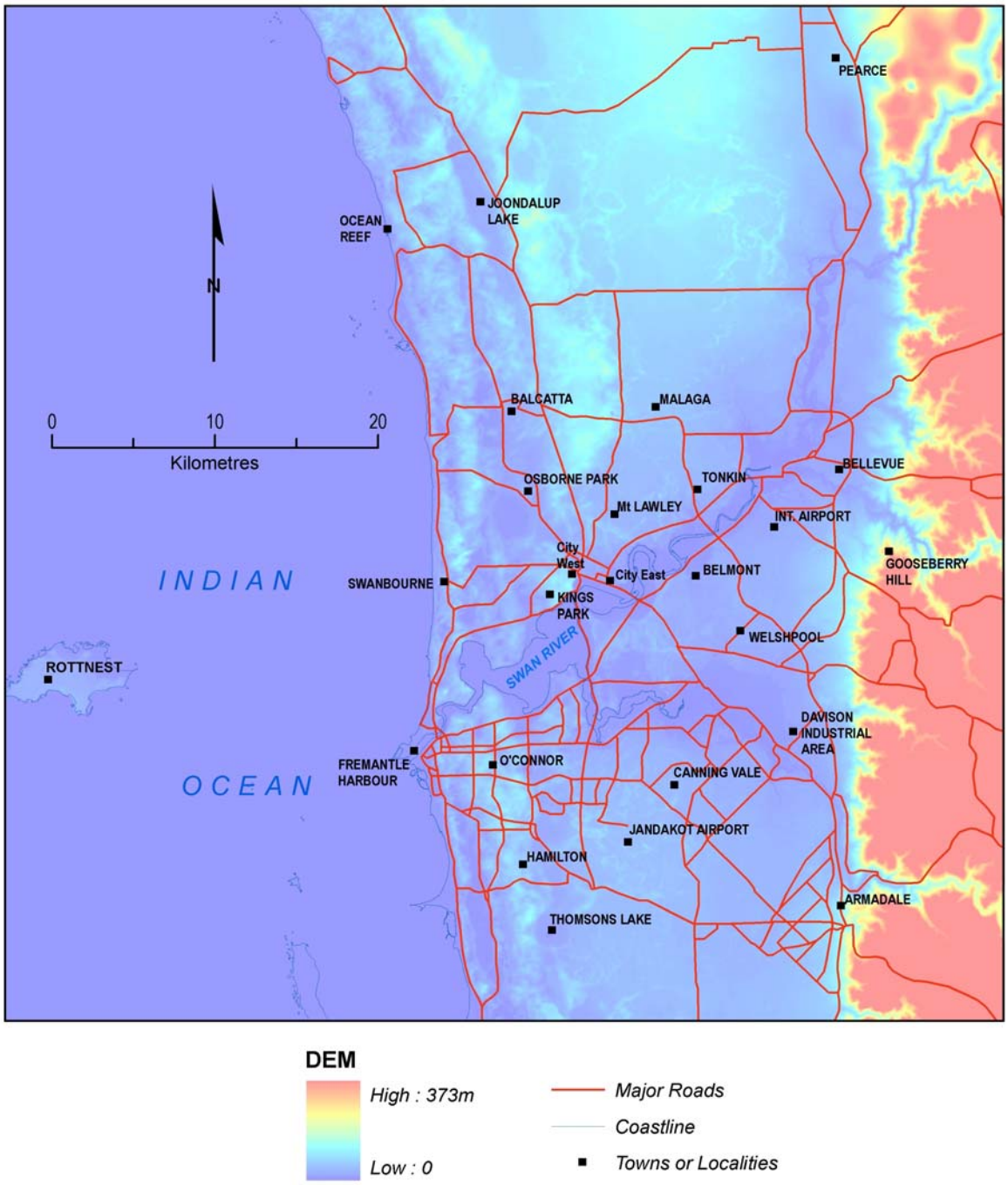

Figure 3.8: The elevation (m) of metropolitan Perth in a 25 m by 25 m grid

In calculating M_h for metropolitan Perth, the height of the structure above the local ground level was set to zero. There were three reasons to do this. First, the estimate of a hill-shape multiplier is required for every point within the study area of metropolitan Perth, whether it currently has a building on it or not. So a building height may not currently exist. Secondly, even in the case of an existing building, in general we do not know the height of the building without a physical building survey having been done. Thirdly, the M_h value has been found to be insensitive to the height of the building.

The 8-directional topographic wind multipliers for metropolitan Perth on a 25 m by 25 m grid have been estimated. Among them, the M_h for west to east is shown in Figure 3.9. The M_h values of AWS sites have been estimated using the DEM on grids. Note that for each site, the nearest grid point has

been used to represent the true AWS location. Table 3.6 shows the values of M_h for each AWS site in each direction.

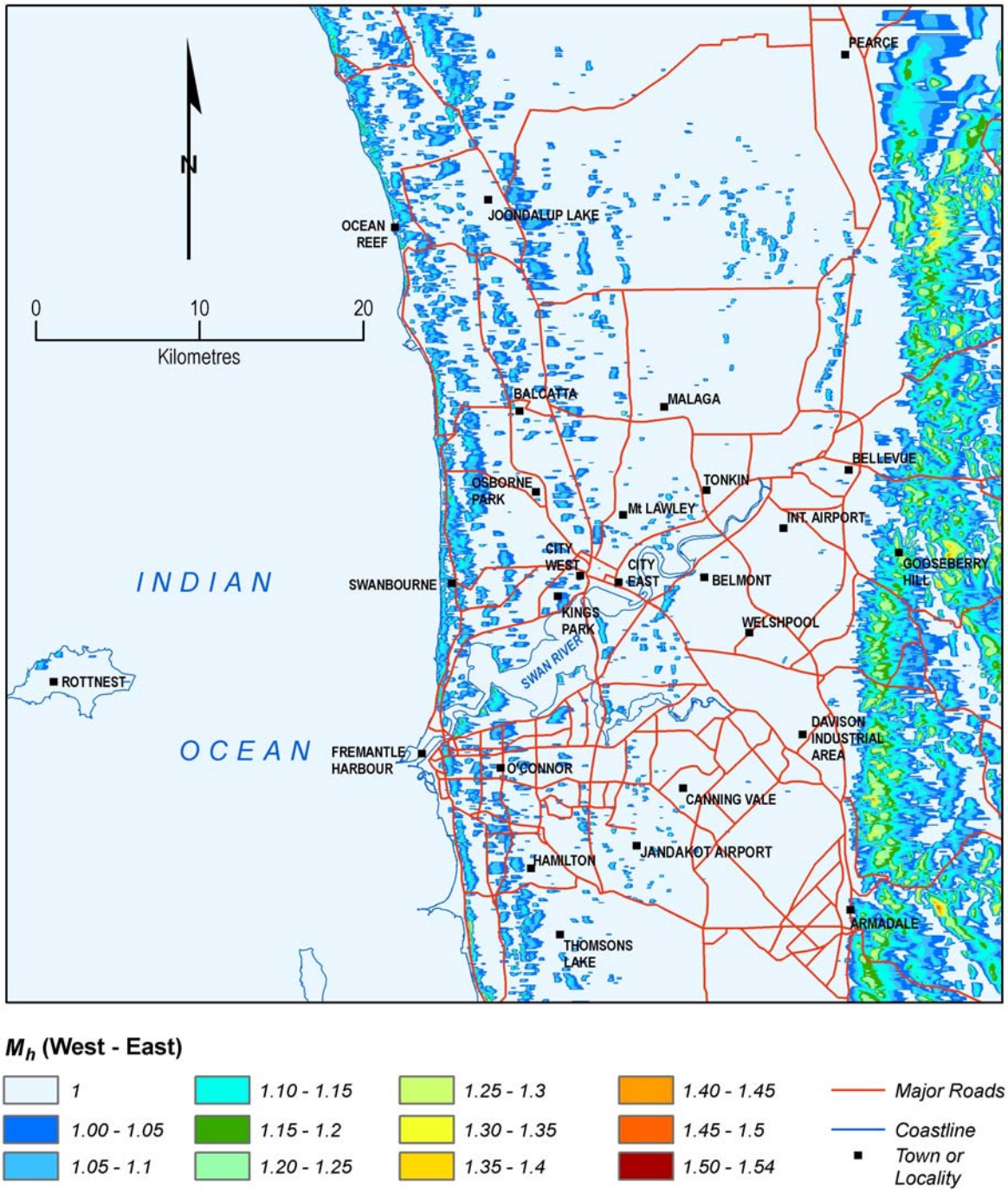

Figure 3.9: the M_h of metropolitan Perth from west to east

Table 3.6: Hill-shape multiplier M_h for AWS locations

Name	North	NE	East	SE	South	SW	West	NW
City East	1.00	1.00	1.04	1.00	1.00	1.00	1.00	1.00
Rottnest Is.	1.11	1.14	1.13	1.10	1.09	1.11	1.09	1.07
Jandakot	1.00	1.00	1.00	1.00	1.00	1.00	1.00	1.00
Swanbourne	1.06	1.08	1.09	1.08	1.00	1.09	1.12	1.14
Mt Lawley	1.00	1.00	1.00	1.00	1.00	1.00	1.00	1.00
Perth Airport	1.00	1.00	1.00	1.00	1.00	1.00	1.00	1.00
Gooseberry Hill	1.25	1.35	1.30	1.03	1.31	1.42	1.27	1.29
Ocean Reef	1.00	1.00	1.00	1.00	1.00	1.08	1.01	1.02
Pearce	1.00	1.00	1.00	1.00	1.00	1.00	1.00	1.00
City West	1.09	1.12	1.17	1.18	1.00	1.00	1.00	1.00

Combined local wind effects

The combined local wind effect multiplier (named *M3*) was obtained by multiplying the three individual multipliers M_z, M_s and M_h together for each wind direction. Figure 3.10 displays the *M3* of the study area with the wind direction from west to east.

Table 3.7 lists *M3* for all AWS sites for each wind direction. Using this table, the speed of each recorded gust has been adjusted by dividing by the corresponding *M3* according to the wind direction the gust was coming from. Equation 3.1 has been solved for V_R using the observed weather station wind speed V_{site}. This converts historically recorded wind speeds to the standard condition of open level terrain and a 10 m observation height. When the station mast height (see Table 3.1) was not at the standard height of 10 m, a speed–height conversion was also made using the following relationship (Whittingham, 1964):

$$V_{10m} = V_h \left(\frac{10}{h} \right)^{\frac{1}{8}} \qquad \textbf{Equation 3.2}$$

By using Equations 3.1 and 3.2, a new set of adjusted daily gusts has been generated for each AWS site. It was used for the return period analysis discussed in the next section.

It should be pointed out that the gust that was strongest before adjustment may differ from the gust that was strongest after adjustment. For instance, at Pearce, a 20 m/s gust from the north would give an adjusted speed of 20 m/s, because *M3*=1.00, but an 18 m/s gust from the NE would give an adjusted speed of 18/0.88 = 20.45 m/s.

Table 3.7: Combined local wind multipliers (*M3*) for AWS locations for eight wind directions

Name	North	NE	East	SE	South	SW	West	NW
City East	0.85	0.94	0.88	0.77	1.02	0.86	0.71	0.79
Rottnest Is.	1.07	1.11	1.09	1.06	1.06	1.07	1.05	1.03
Jandakot	0.93	1.00	0.91	0.92	0.87	0.86	0.95	0.91
Swanbourne	0.85	0.86	0.89	0.93	0.80	0.98	1.00	0.95
Mt Lawley	1.03	0.92	0.88	0.88	0.91	0.84	0.83	0.91
Perth Airport	0.82	0.82	0.94	0.97	0.97	1.00	1.00	0.93
Gooseberry Hill	1.16	1.17	1.18	0.95	1.17	1.22	1.13	1.13
Ocean Reef	0.90	0.84	0.87	0.84	1.00	1.08	1.01	1.02
Pearce	1.00	0.88	0.90	0.96	1.00	1.00	0.99	1.00
City West	1.00	0.98	1.06	1.10	1.06	0.98	0.94	0.87

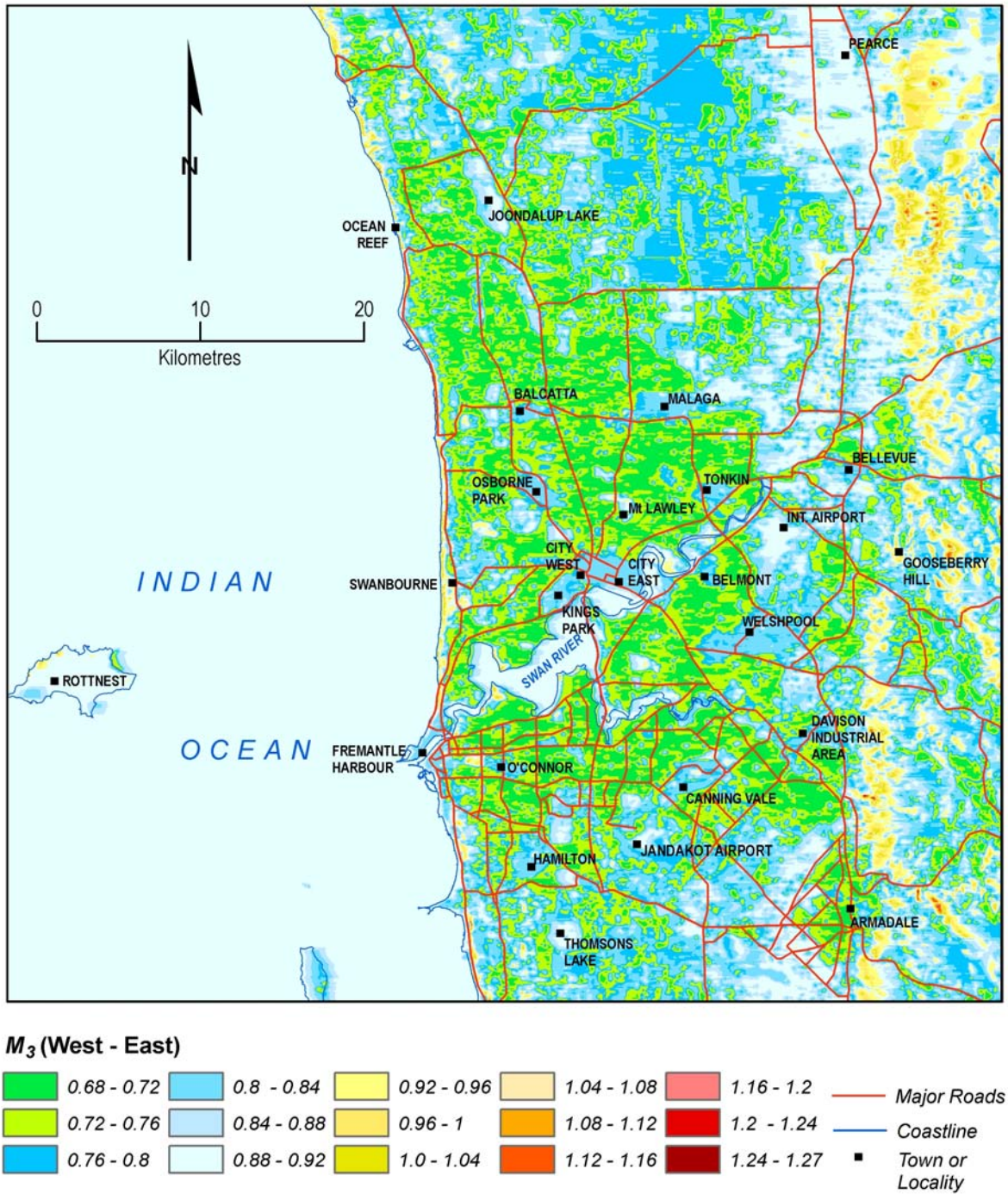

Figure 3.10: Multiplier *M3* for wind from west to east for the study area

3.5 Return Period Wind Speed Estimation

Extreme value theory is a statistical technique for describing one tail of the distribution of unusual (extreme) events rather than the usual events. It includes data fitting (or model parameter estimation) and quantile estimation. Sensitivity analysis is also carried out to examine the uncertainty of these speed estimates.

Extreme value analysis

Classical extreme value theory is based on the analysis of the largest (or smallest) value in an epoch. In wind engineering, an epoch is assumed to be a calendar year. The yearly maximum wind gust is usually used as data input for classical extreme value analysis. However, if the amount of data recorded is too small, monthly maxima may also be used.

Classical extreme value theory is based on three asymptotic extreme value distributions identified by Fisher and Tippett (1928). The generalized extreme value (GEV) distribution introduced by Jenkinson (1955) combines the three distributions into a single mathematical form. A brief description of GEV is given in the appendix.

In the past 20 years a new body of extreme value theory has been developed, called ‘peaks over threshold’ (POT) modelling. This theory allows for the use of all available data exceeding a sufficiently high threshold. A brief introduction to POT is given in Lin (2003).

An attempt was made to apply the POT method to the Perth wind dataset, but the results were not satisfactory. Return period wind speeds seemed to be underestimated by about 10–20%. There are two possible reasons for this. First, the POT method assumed independent events. However, a storm may continue for up to two or three days at a time, generating 2–3 large daily maximum gusts. Such data are not independent of each other. A technique called ‘de-clustering’ was developed to extract the largest gust within a given time window (e.g. three days). However, after this was done, return period wind speeds still seemed to be underestimated.

The second reason is the difficulty in choosing the threshold value. Using a smaller threshold value might allow the model to fit normal events well, but fail to fit the extreme ones. However, using a higher threshold value might leave insufficient data points to fit the model. Available techniques such as the sample mean excess function have been applied to the dataset, but it did not show a clear linear trend. This suggests that the dataset is not suitable for the POT method. This may need further investigation.

The technique of GEV has therefore been adopted in this study to estimate the return period wind speeds.

An introduction to extreme value theory can be found in Embrechts *et al.* (2001) and Colse (2001). A review of methods for calculating extreme wind speeds using extreme value techniques can be found in Palutikof *et al.* (1999).

Fitting Perth wind dataset to a GEV

Yearly and monthly maximum gusts have been recalculated from the adjusted daily gusts. When the lengths of datasets were shorter than ten years, only the monthly maximum gusts were fitted since there were too few points in the yearly data to compute a reliable estimate. These maxima were then fitted to a GEV and its parameters estimated. (See Appendix A for information on data fitting methods and the general function of GEV.)

After a GEV distribution has been fitted, the return period wind speeds were then calculated for given time periods with the results given in the next section.

There are a few issues that require discussion here. Firstly, there are three city weather station sites in Perth City: City West, City East and Mt Lawley. The first two sites have about 25 years of data each, while Mt Lawley has only about 10 years. Also, the strongest daily gust in Mt Lawley was only 94 km/h comparing to 156 km/h in City West and 130 km/h in City East. If we fit these three sites separately, they will have quite different return period wind speeds but they are physically located close to each other. Another important point about these three sites is that they were never operated in parallel. Rather, they have been used one after another, because one replaced another. One logical way to handle this issue is to combine the adjusted daily gusts for these three sites together to form a 'super city' site with about 60 years of data. This approach was adopted with the 'super city' weather station site nominally placed at the geometric centre of these three sites. Extreme value analysis was then performed on adjusted data contributed from three cities sites.

Secondly, it should be pointed out that return period wind speed estimation is based on fitting historical wind gusts with extreme value distributions. Hence, it is subject to uncertainties within the data and the nature of wind gusts. The recorded daily maximum gusts at each site represent a very localised phenomenon. Each one only indicates an instantaneous wind speed at a particular location at a particular time. It may only be used with some uncertainty to represent other locations (even locations nearby) or other time periods (either before or afterwards). For example, the largest historical gust was 156 km/h at the City West site recorded in 1963. It was under the historical terrain condition prevailing more than 40 years ago. The current wind environment characteristics, including surrounding buildings and terrain (vegetation), may be quite different to those of 40 years ago.

Thirdly, the estimates are subject to data fitting errors. Particularly, when the data periods are smaller than 20 years, the fitting error and uncertainty can be quite large. A number of techniques have been applied to reduce/contain the fitting error and to estimate the uncertainty. Several fitting methods have been used and the maximum value of return period wind speed derived from different methods has been adopted. Furthermore, statistical hypothesis tests have been performed to make certain the statistical basis of choosing the underline extreme value distribution is statistically sound. Finally, sensitivity analysis has been carried out at selected sites by removing/replacing the historical largest gusts, by adding artificial large gusts and by halving the datasets.

Fourthly, predictions based on historical data are somewhat uncertain because of the effect of long-term weather variation and global warming. In particular, recent research (Li *et al.*, 2005) has shown a change point in weather patterns around 1965 in southwest Western Australia, including metropolitan Perth. It claims that the mean sea level pressure (MSLP) had increased in the mid-latitudes while rainfall had decreased after 1965. With the increased MSLP, the westerly winds are expected to have decreased.

Estimated return period wind speeds

The 50, 100, 500 and 1000-year return period regional wind speeds (in m/s) are listed in Table 3.8, together with the historical largest gusts at each site for comparison.

Return period wind speeds are also given in Australian wind loading standard (AS/NZS 1170.2, 2002). In the standard, Perth is located in Region A which has the return period wind speeds listed in Table 3.9. We understand that the wind data used in the analysis were from Perth Airport. We have therefore included our estimates for the airport in Table 3.9 for comparison purposes. It can be seen that they are very similar. However, looking at Table 3.8, the return period speeds at coastal sites and the city site (which is closer to the coast than the airport site) are much greater than those for the airport. This suggests that return period speeds may be underestimated if the speeds estimated for the airport are applied to the whole of metropolitan Perth.

Table 3.8: Historical largest gusts and return period wind speed estimations (m/s) for open terrain at 10 m height

AWS site	Data length (years)	Record period	Hist max (m/s)	Hist max (km/h)	50y V	100y V	500y V	1000y V	50y V (90–04)
Super City	60.7	1942–2004	43.2	156	44	47	53	56	
Rottnest Is.	18.2	1983–2004	39.1	141	39	40	41	42	38
Jandakot	12.3	1989–2004	31.4	113	36	37	39	40	36
Swanbourne	17.9	1986–2004	39.6	143	45	47	54	56	45
Perth Airport	60.2	1944–2004	34.5	124	38	40	45	47	42
Gooseberry Hill	8.8	1995–2004	37.6	135	31	32	33	33	
Ocean Reef	17.8	1986–2004	35	126	44	46	53	55	44
Pearce	35.0	1941–2004	36	130	38	40	45	47	34

The last column in Table 3.8 shows the regional 50-year return speeds estimated using the data for 1990–2004. There are two uses for these figures. First, they show the estimated return speeds for a consistent time period. The fact that they are quite different indicates that the windfield does differ from location to location. Secondly, comparison may be made to the 50-year return speeds (as shown in the sixth column of Table 3.8) using all available data. Two locations show differences; the airport site (38 m/s vs 42 m/s) and Pearce (38 m/s vs 34 m/s).

Table 3.9: Comparison of estimated return period wind speeds with those given in the Australian Wind Standard

Estimated return period wind speed	50y V (m/s)	100y V (m/s)	500y V (m/s)	1000y V (m/s)
Region A, Australian Wind Standard	39	41	45	46
Perth Airport	38	40	45	47

Model validation

An important question when considering any numerical model of a complex physical process is the reliability and appropriateness of the chosen model. Graphical methods are commonly used in model validation. Two popular methods involve plotting cumulative distribution functions (CDF) and quantile–quantile plot (QQ-plot). Both of these methods have been used to validate the statistical models generated.

Sensitivity analysis

Sensitivity analysis is a way of quantifying the uncertainty in the estimates. The form of sensitivity analysis conducted was to investigate the effects of omitting the largest gusts and of changing the length of the data period. To simplify this task, the sensitivity analysis was done using the original gust dataset rather than the adjusted dataset.

It was suspected that the single data record of 156 km/h at City West has played a significant role in the return period wind speed estimation at the site. To test the effect of this large gust record, it was removed from the City West dataset and the extreme value analysis was conducted again. The resulting estimates are listed as the second row in Table 3.10. It can be seen that the 50-year and 100-year return wind speeds have been reduced from 46 m/s and 49 m/s to 45 m/s and 48 m/s, respectively. The effect of a single large data point is not as significant as was expected.

Next, instead of removing this data point, it was added into the dataset for the City East, Mt Lawley and Perth Airport sites. Table 3.10 shows that the effect of adding this larger gust is about 2–5 m/s (or 7.2–18 km/h) speed difference. A 5 m/s effect was obtained at Mt Lawley site, where the original largest wind gust was only 26.2 m/s (94 km/h), much smaller than the 156 km/h point added. The

short data period at Mt Lawley has probably also contributed to a larger difference (with and without the 156 km/h gust) than at the other two sites (City East and Perth Airport).

The second series of sensitivity analysis has been done in order to examine the effects of the length of datasets. The longest dataset (the airport site) has been divided into 2 subsets of about 30 years each. From Table 3.10, it can been seen that the earlier 30-year period gives estimates of 35 m/s and 36 m/s as the 50-year and 100-year return winds, about 2 m/s smaller than the original estimates arrived at using the full 60 years of data. The second 30 years of data gives the same result as the whole dataset for 50-year return speed: a slightly larger estimated 100-year return period speed (40 m/s versus 38 m/s). This is not surprising since the strongest gust (124 km/h) is in this second 30-year period.

Finally, the airport dataset has been divided into four smaller sets, each of about 15 years of wind gust records. The results from this sensitivity analysis can be seen in Table 3.10 and are not particularly surprising. Two datasets have 50-year and 100-year return period estimates of 35 and 36 m/s each, the same as the for first 30 years of data but 2 m/s slower than the original dataset. The other two datasets have higher value of estimates (39 and 41 m/s), possibly due to the occurrences of a larger wind gust in the relatively short period (15 years).

Table 3.10: Results from the sensitivity analysis

Based on original data	Sensitivity analysis	50y V (m/s)	100y V (m/s)
City West		46	49
	City West (remove 156 km/h)	45	48
City East		42	45
	City East (add 156 km/h)	44	47
Mt Lawley		27	29
	Mt Lawley (add 156 km/h)	32	34
Perth Airport		37	38
	Airport (add 156 km/h)	39	40
	Airport (earlier 30 years)	35	36
	Airport (later 30 years)	37	40
	Airport (1st 15 years)	35	36
	Airport (2nd 15 years)	39	41
	Airport (3rd 15 years)	35	36
	Airport (4th 15 years)	39	41

Some general conclusions from the sensitivity analysis are as follows:

- Single large data points have some influence on the estimated return period speeds, but such influence is not excessive. In other words, higher estimates of return period speeds come from a number of large events, not just one.
- Estimating return period speeds from a short dataset are highly sensitive to its largest gusts. If the largest gusts were not very much bigger in value, it may lead to a smaller (underestimated) return period speed. Mt Lawley may be such a case: it only has about 10 years of records with the largest gust only 26.2 m/s. Hence, its estimated 50-year and 100-year return wind speeds are only 27 and 29 m/s, and are quite possibly underestimated. On the other hand, if there are several bigger gusts in a relative short period, the estimates tend to give larger (overestimated) return wind speeds. Swanbourne may be an example of this.
- This may partially answer the question of why these three coastal sites (Swanbourne, Ocean Reef and Rottnest Island) have similar wind conditions and similar operating periods, but their estimates were quite different. Swanbourne's estimates are higher than the other two coastal sites (see Table 3.8). This was probably due to the concentration of bigger gusts in a short period. This is also reflecting the uncertainty (or estimate errors) associated with a short time period. These three coastal sites may warrant further investigation.

Interpolation of estimated return period wind speeds to all of metropolitan Perth

Using the return period wind speeds at the eight AWS sites (Table 3.8), several interpolation methods were used to estimate return period wind speeds at grid points. However, the results were not consistent with accepted meteorological knowledge. After consulting with meteorologists in BOM Perth office, a wind spatial profile suitable for metropolitan Perth was developed. It includes a series of north–south strips starting from the coastline and stepping down towards the interior. This follows the principle of gradually decreasing wind energy as wind travels further away from the water with surface/terrain friction having a significant effect. The estimated return speed values at the eight AWS sites (see Table 3.8) have been used in setting up the heights (speed values) of these strips. Minor speed adjustments have also been made to satisfy the principle that wind speed decreases with distance from the coast. Figure 3.11 shows the interpolation of 50-year return period speeds in open terrain at 10 m height. The speeds in brackets are the AWS estimates given in Table 3.8 for comparison with the colour strips (indicating the interpolated return speeds) in which they are located.

Directional return period wind speeds

The return period wind speeds estimated in the previous section are not directional. The available data were not adequate to support estimation of directional return period wind speeds, essentially because the available daily maximum gusts are one record per day, not one direction per day.

A practical way of estimating directional return period wind speeds is to use the direction multipliers M_d published in Table 3.2 of the Australian wind loading standard (AS/NZS 1170.2, 2002). The column for Region A1, which includes Perth, is reproduced in Table 3.11.

Table 3.11: Wind direction multiplier (M_d) from AS/NZS 1170.2 (2002)

	North	**NE**	**East**	**SE**	**South**	**SW**	**West**	**NW**
***M*$_d$ for Region A1**	0.90	0.80	0.80	0.80	0.85	0.95	1.00	0.95

These may then be multiplied by the combined local wind multipliers (*M3*) which were calculated earlier. Hence the overall procedure for finding local directional return period wind speeds is to multiply the grid return period speed (from interpolation) by the wind direction multiplier and the combined local wind multiplier:

$$V_{site,d} = V_{10m}\ M_d\ M3 \qquad \textbf{Equation 3.3}$$

Using this equation, the return period speed at each grid in each direction can be estimated. Figure 3.12 displays the grid 50-year return speeds for westerly winds.

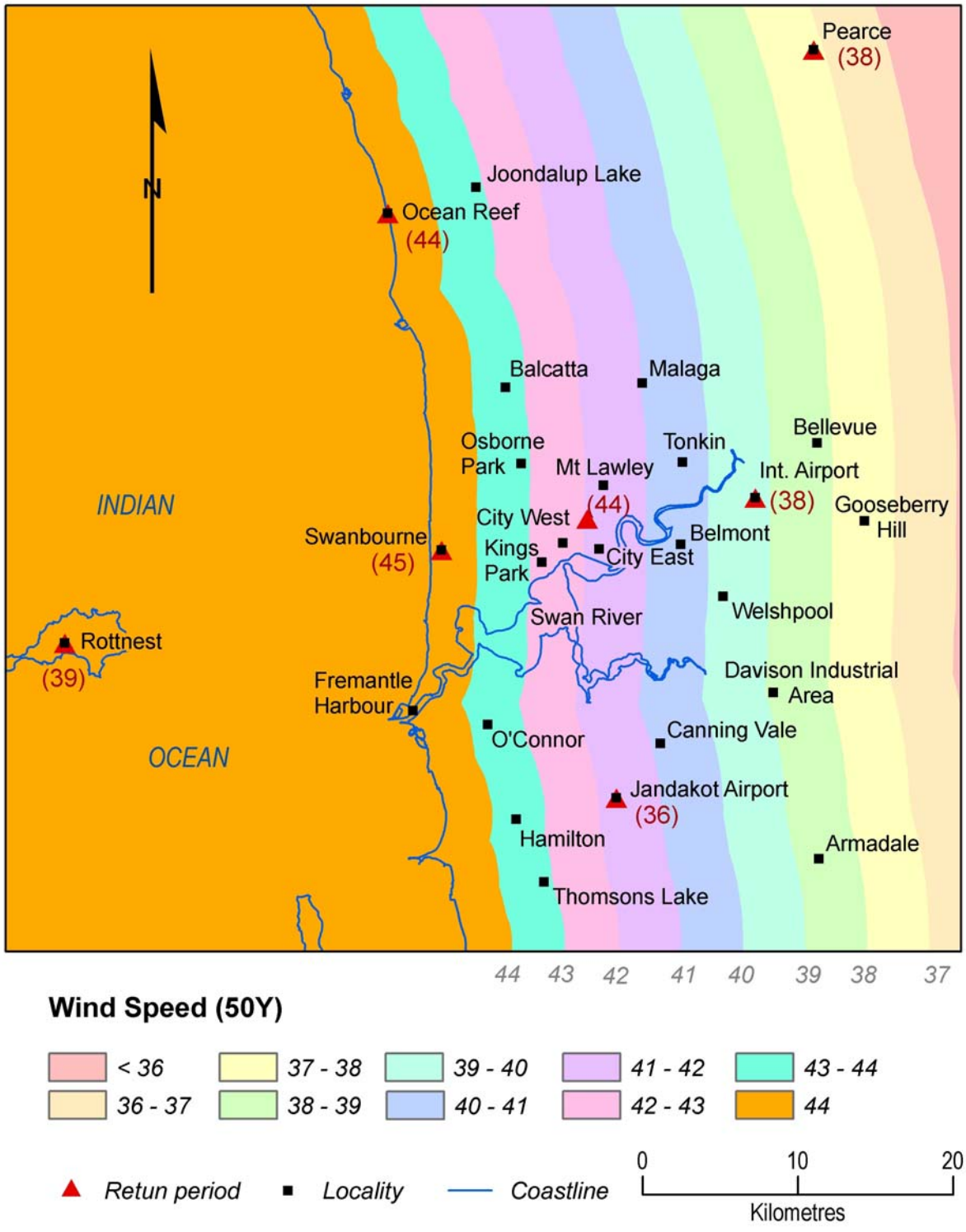

Figure 3.11: The interpolation of 50-year return period speeds for open terrain at 10 m height

Maximum non-directional return period speeds

Since we do not know the orientation of buildings other than those surveyed, directional return period speeds will be difficult to use quantitatively. The purpose of wind risk assessment is to quantitatively estimate the cost of replacing and repairing structures after a return period wind has blown. A maximum non-directional speed may be used to assess possible building damage within a return period. This maximum return period wind speed in every direction at each grid point was calculated using the following equation:

$$V_{site,\max} = \max_{d} V_{site,d} \qquad \textbf{Equation 3.4}$$

Figures 3.13 – 3.16 show the calculated maximum non-directional 50, 100, 500 and 1,000-year return period speeds, respectively. These are the estimated wind hazard maps for metropolitan Perth. They provide valuable wind hazard information for city planning, risk management, emergency management and the like. When building damage models appropriate for Perth construction become available and combined with the building cost models, a quantitative wind risk assessment can be achieved.

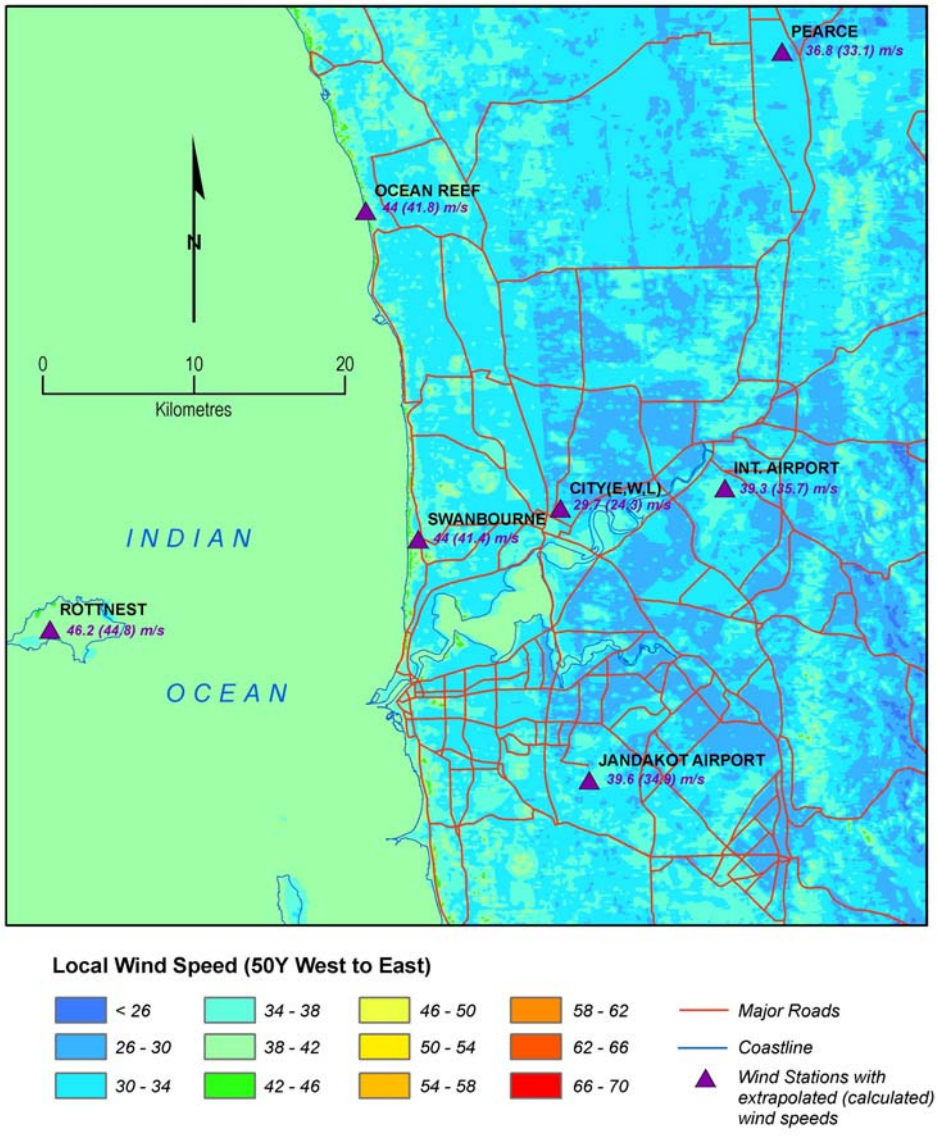

Figure 3.12: Estimated local 50-year return period speed for wind from west to east

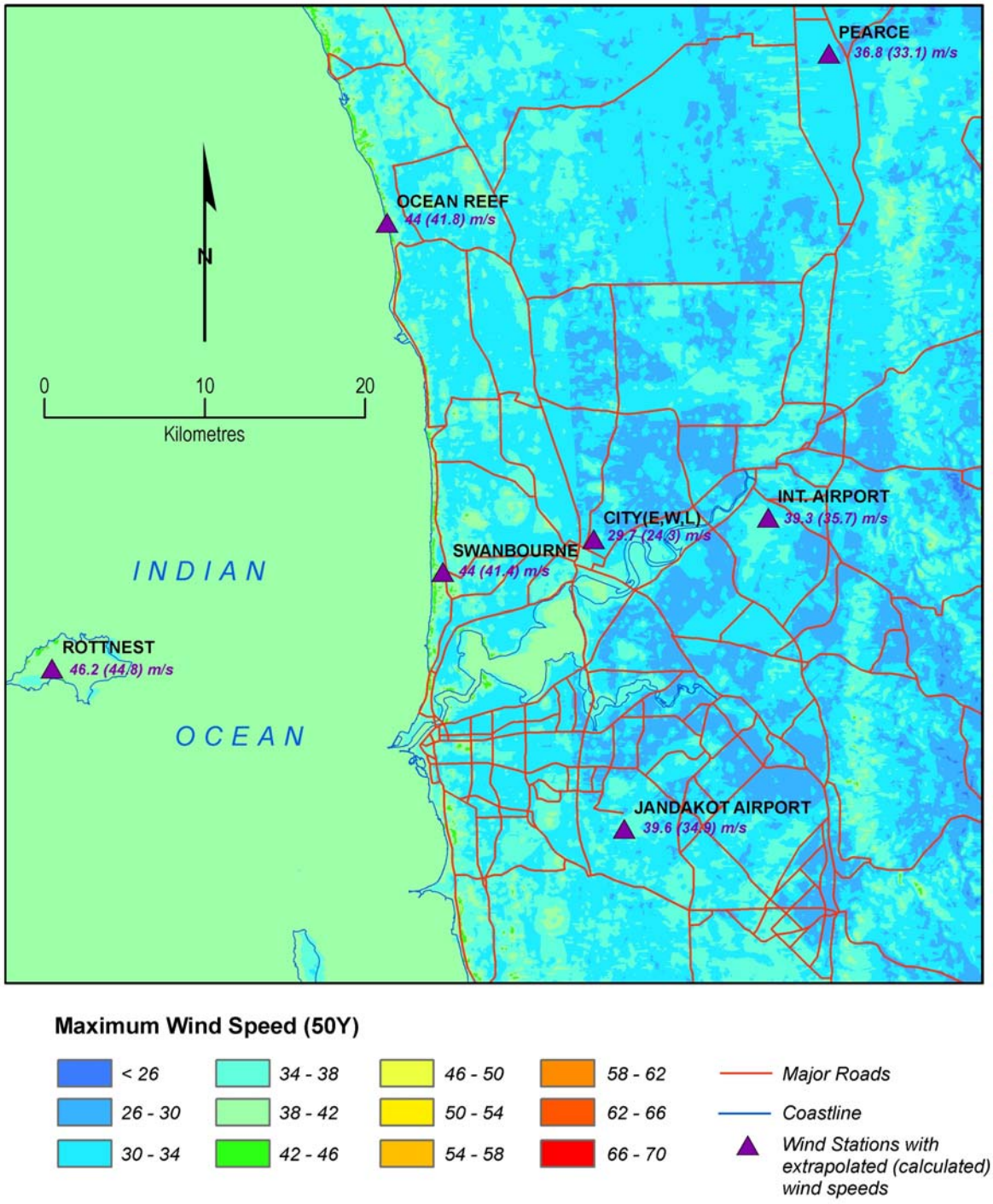

Figure 3.13: Maximum non-directional 50-year return period speeds

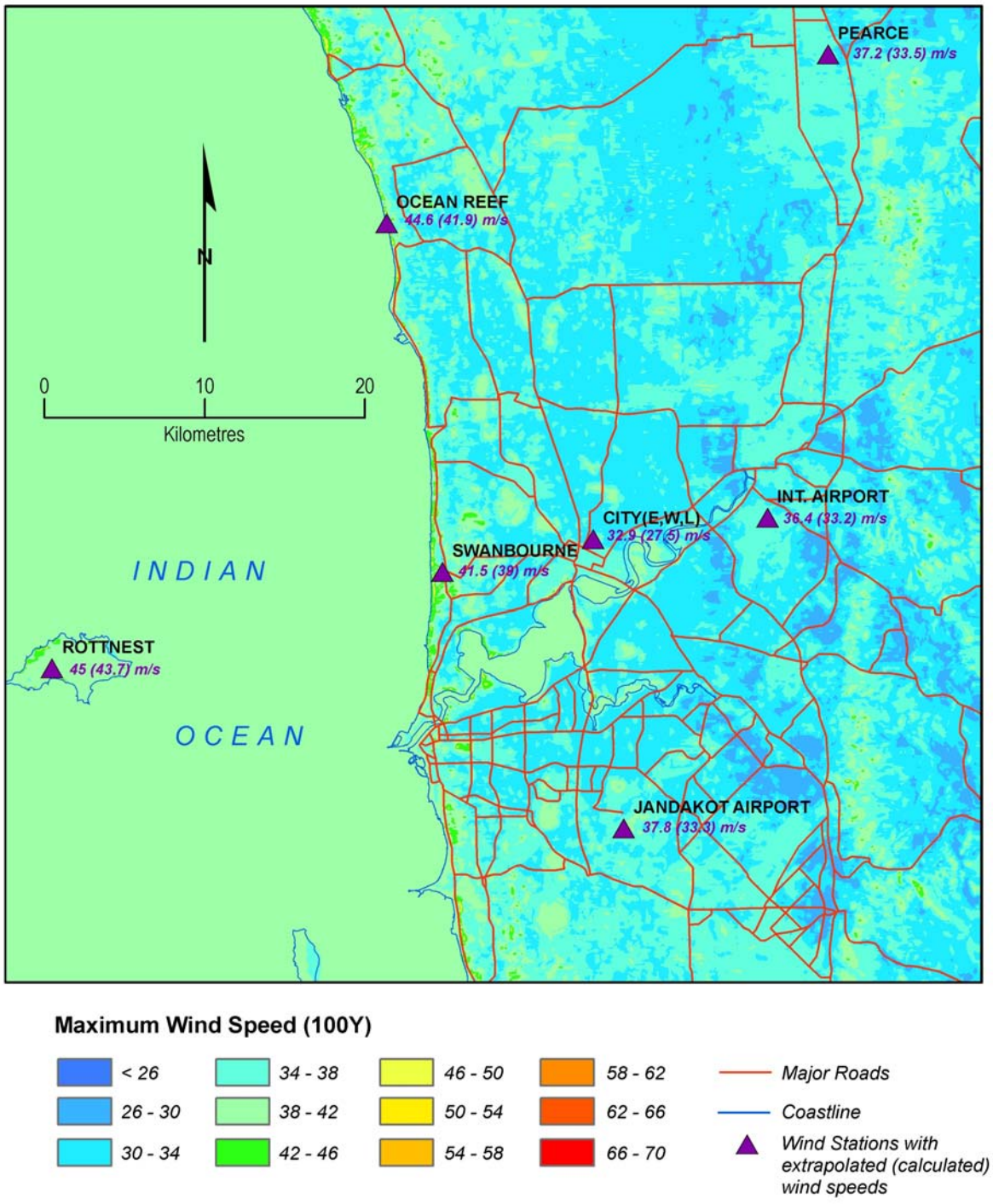

Figure 3.14: Maximum non-directional 100-year return period speeds

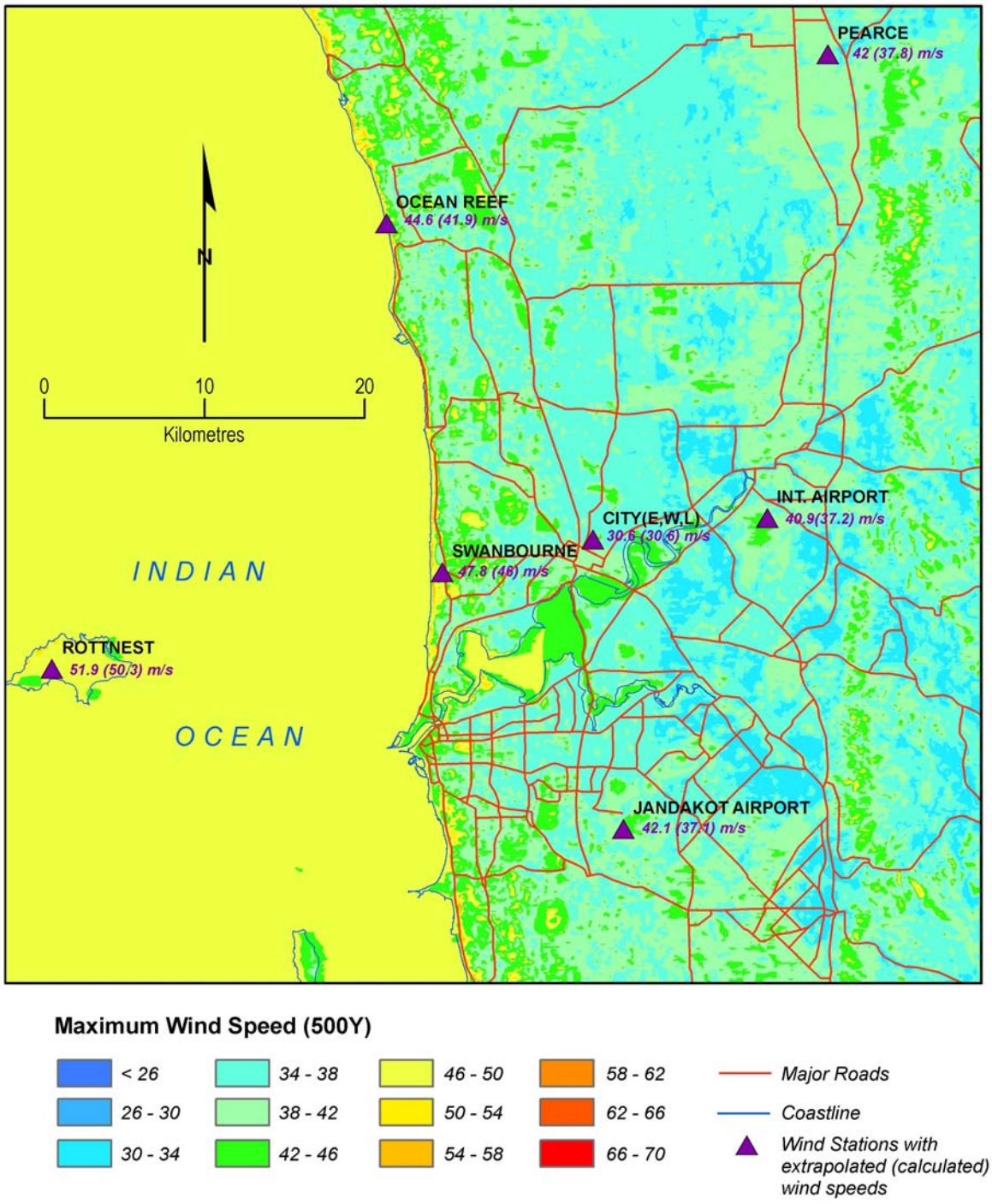

Figure 3.15: Maximum non-directional 500-year return period speeds

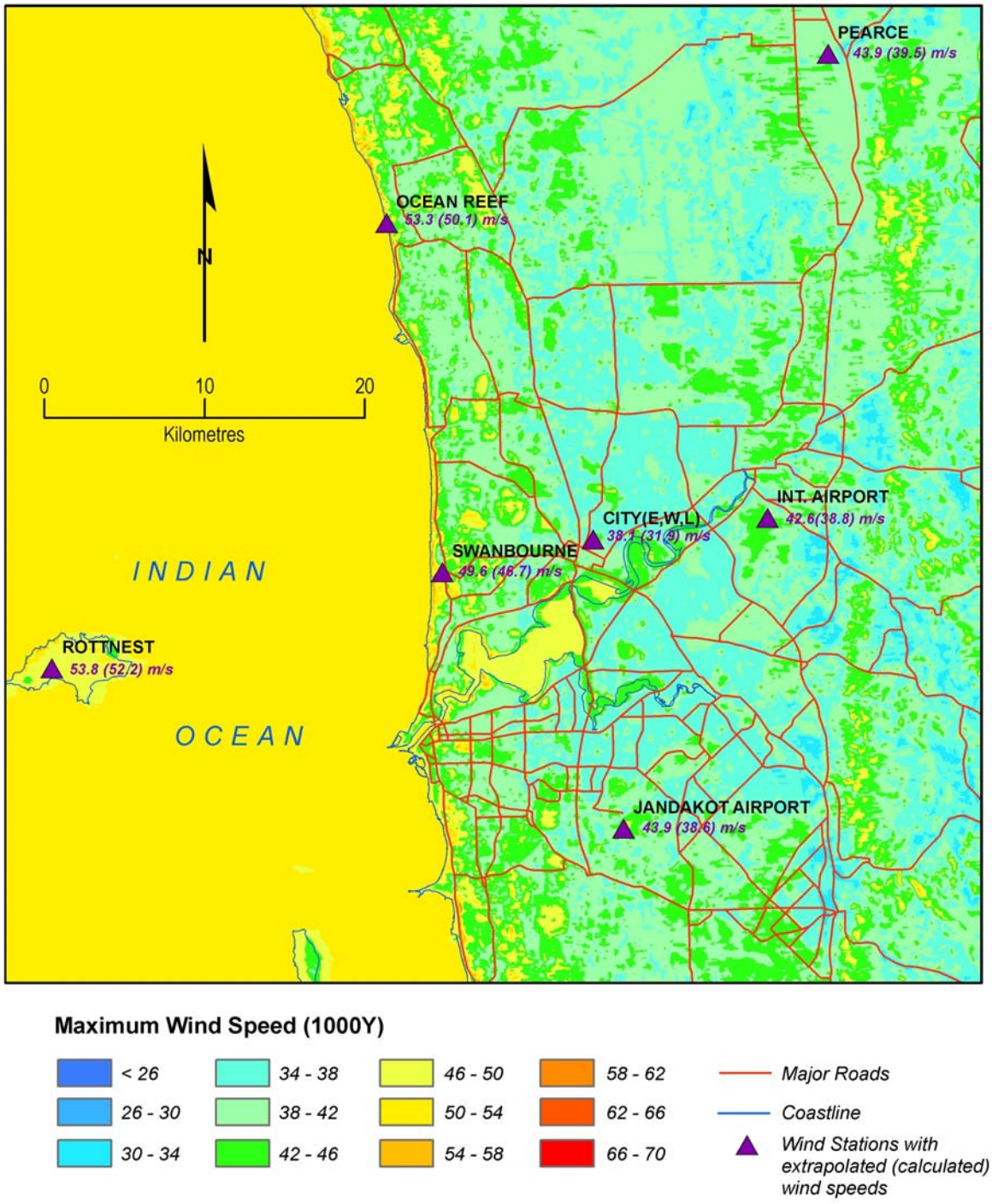

Figure 3.16: Maximum non-directional 1000-year return period speeds

3.6 Conclusions

Assessment of severe wind hazard for metropolitan Perth has been carried out using statistical data analysis, remote sensing and GIS techniques. Return period wind speeds for 50-, 100-, 500- and 1000-year return periods have been estimated for weather station sites using extreme value analysis. These point estimates have been interpolated to the entire study area of metropolitan Perth on a 25 by 25 m grid using a simplified windfield decay model. Finally, wind hazard maps of the study area have been generated. They are in the form of maximum non-directional return period speeds. These maps

provide valuable wind hazard information for city planning, risk management, emergency management and the like. Combined with building damage models and building cost models, these maps can be used for quantitative wind risk assessment.

3.7 Acknowledgments

The author wishes to thank many people who made this project possible, particularly:

- Joe Courtney of the Australian Bureau of Meteorology, WA Regional Office, for supplying meteorological data, providing technical expertise and collaboration,
- Mark Edwards of Geoscience Australia for his engineering judgement and advice,
- Ingo Hartig and Neil Corby of Geoscience Australia for their excellent GIS support, and
- Dr Geoff Robinson of CSIRO Mathematics and Information Sciences for his advice and review of this report.

3.8 References

Colse, S. (2001) *An Introduction to Statistical Modelling of Extreme Values*, Springer, London, 2001.

Embrechts, P., Kluppelberg, C. and Mikosch, T. (2001) *Modelling Extreme Events for Insurance and Finance*, Springer, New York, 3rd printing.

Fisher, R.A. and Tippett, L.H.C. (1928) 'Limiting forms of the frequency distribution of the largest or smallest member of a sample', *Proceedings of the Cambridge Philosophical Society*, 24:180–90.

Jenkinson, A.F. (1955) 'The frequency distribution of the annual maximum (or minimum) values of meteorological elements', *Quarterly Journal of the Royal Meteorological Society*, 81:158–71.

Li**,** Y., Cai, W. and Campbell, E. P. (2005) 'Statistical modelling of extreme rainfall in southwest Western Australia', *Journal of Climate*, 18(6):852–63.

Lin, X. (2003) 'Statistical modelling of severe wind gust', *International Congress on Modelling and Simulation*, MODSIM, Townsville, 14–17 July 2003, Vol. 2, pp. 620–25.

Lin, X. and Courtney, J. (2004) 'Statistical spatial analysis of severe wind gusts in Perth', *International Conference on Storms: Storm science to disaster mitigation*, Brisbane, 5–9 July 2004, pp. 118-119.

Palutikof, J.P., Brabson, B.B., Lister, D.H. and Adcock, S.T. (1999) 'A review of methods to calculate extreme wind speeds', *Meteorological Applications*, 6(1):119–32.

Standards Australia (2002a) *Structural design actions, Part 2: Wind actions*, AS/NZS 1170.2, Australian/New Zealand Standard.

Standards Australia (2002b) *Structural design actions – Wind actions– Commentary*, AS/NZS 1170.2 Supp. 1, Australian/ New Zealand Standard.

Whittingham, H.E. (1964) *Extreme Wind Gusts in Australia*, Bureau of Meteorology Bulletin No. 46, Bureau of Meteorology, place?.

Chapter 4: RIVERINE FLOOD HAZARD

Miriam Middelmann[1], Simon Rodgers[2], Justin White[1], Lisa Cornish[1] and Christopher Zoppou[1]
[1] Geoscience Australia
[2] Department of Environment, Western Australia

4.1 Introduction

This chapter examines flood estimation associated with heavy rainfall, resulting in the overbank flows from rivers or streams onto the floodplain. In general, the factors that influence whether or not a flood will occur include:

- volume, spatial distribution, intensity and duration of rainfall over the catchment;
- catchment and weather conditions prior to the rainfall event;
- ground cover;
- topography;
- the capacity of the watercourse or stream network to convey the runoff; and
- tidal influence.

The Department of Environment (DOE) is Western Australia's lead agency responsible for floodplain mapping and floodplain management. The Department provides advice on development of floodplains to promote wise use of floodplains while minimising flood risk and damage. Previous to this study, the Department undertook floodplain mapping for the 1% annual exceedence probability (AEP) event for the Swan River and other rivers. Though the DOE have only mapped the 1% AEP flood event, flood levels for the 10%, 4% and 2% AEP events have also been determined.

The work undertaken in this study significantly increases the number and range of scenarios modelled and mapped. Eight scenarios are modelled, ranging from the 10% AEP to the 0.05% AEP. This study updates the floodplain geometry to account for changes to the floodplain. It also models the effect of tributaries on flooding in the Swan River and flooding in the tributaries themselves. Through the use of the dynamic hydraulic model HEC-RAS, this study also adds on the information available for the 1% AEP flood through introducing the temporal aspects of inundation. Put simply, it enables changes of flood inundation extent, depth and velocity to be modelled over the period of the flood event. The results shown in this chapter will, however, focus on the maximum depth of inundation. Future work will incorporate the temporal aspects of inundation available from the model with a building database in order to model flood damages and estimate losses.

This chapter focusses on flood estimation. The physical setting of the study area is described and an overview given of historical riverine flooding. The development of the design hydrographs for flood estimation is then described and the reader is referred to previous reports where appropriate. The report then focusses on the hydraulic modelling of the Swan and Canning Rivers and tributaries. Model development is described, followed by the calibration and validation of the model. The impact of the tributaries, simulated inflow hydrographs and tidal cycle variation are covered. Finally, floodplain maps are presented showing maximum water-depth contours.

Flood estimation

Flood estimation for planning purposes aims to estimate the long-term probability of flood impacts so that appropriate planning decisions can be made to minimise that impact. As a complex set of factors

influences whether or not flooding occurs in a catchment, it is difficult to define the causes or the effects of an 'average' flood. Put simply, no two floods in the same catchment are ever identical. To overcome this problem, floodplain managers and hydraulic engineers rely on a series of design flood events and historical rainfall and flood level information. It is upon these that this chapter is based.

Six data sets are important in predicting floods:

- historical rainfall and runoff data across a catchment;
- historical river height and discharge information;
- catchment topography and land use;
- surveys of river and floodplain levels and cross sections;
- models of the hydrologic processes (rainfall, runoff, infiltration, concentration etc.);
- models of the hydraulic processes (propagation, attenuation etc.).

Typically, these analyses are undertaken by hydrologists and specialist engineers skilled in the physical understanding of rainfall patterns and the behaviour of floods. The results of such studies are often used to set freeboards for proposed development (such as housing) or public works like roads, bridges and levee systems.

Items (1) and (2) are essential for describing the statistical nature of the flood hazard. Using this data the various models derived in (3), (4), (5) and (6) can be calibrated and validated. Using statistical analyses of the historical rainfall data, a well-calibrated model is then capable of predicting the impact of floods unlike those experienced in the past. It can also be used test potential flood mitigation strategies, such as the construction of new channels, levees and detention basins. The model may be used to establish planning zones, with regulations that may stipulate that a property be built to a minimum property floor level. The limit of infilling in a floodplain to prevent the raising of flood levels can also be determined by the model.

The data collection and modelling process leads to a statistical description of flooding for a specific community. Planning regulations must then be adopted which aim to limit the social, economic and environmental impact of flooding on a community. Typically, the 1% AEP level is used as the 'designated flood' level for planning purposes. A freeboard allowance, typically 0.5 m, is then applied above the designated level to provide a measure of safety and to allow for wind and wave set-up and the tidal effect caused by vehicles and vessels. The AEP is a statistical benchmark used for flood comparison. Average recurrence interval (ARI) is another commonly used statistical benchmark, and is often referred to interchangeably with AEP. The 1% AEP, for example, is often referred to being the same as the 100 year ARI., Technically, the two terms are not interchangeable. ARI is the average interval in years which would be expected to occur between exceedances of flood events of a given magnitude. AEP is the probability of a flood event of a given magnitude being equalled or exceeded in any one year (Institute of Engineers, 1987).

The definition given for the probable maximum precipitation (PMP) by the World Meteorological Organisation (WMO, 1986) is

> *the greatest depth of precipitation for a given duration meteorologically possible for a given size storm area at a particular location at a particular time of the year, with no allowance made for long-term climatic trends.*

The PMP is used for estimating the probable maximum flood (PMF). The PMF is the limiting-value flood which can reasonably be expected to occur. It is usually perceived as having an AEP of between 0.01% and 0.00001% (Nathan and Weinmann 1999, Laurenson 1994 cited in SCARM, 2000). This report however does not examine the effects of the PMF.

4.2 Physical Setting

Catchment description

The major tributaries of the Swan–Canning estuary are the Swan/Avon River, Ellen Brook, Susannah Brook, Helena River, Jane Brook, Canning River and the Southern River–Wungong Brook (Figure 4.1). The Swan River is tidal to its confluence with Ellen Brook, which is approximately 60 km from the mouth of the Swan River at Fremantle. The Kent St weir (Plate 4.1) on the Canning River in the suburb of Wilson limits the extent of the tidal excursion in all but the most extreme storm surge situations.

Plate 4.1: Kent St weir on the Canning River generally looking upstream (Photo: Middelmann, 2003)

Avon River

The Avon River, with a catchment area of more than 120,000 km^2, is by far the largest catchment that drains into the Swan–Canning estuary (Figure 4.2). Two major systems of inter-connected lakes (Lockhart and Yilgarn systems) account for approximately 75% of the entire catchment area and combine within the Yenyenning Lakes subcatchment to overflow into the Avon River upstream of Beverley during major flood events. The Walyunga gauging station on the Avon River has been operational since 1970. Officially the Avon River changes into the Swan River at the confluence of Wooroloo Brook; but in reality, both the Avon River and Wooroloo Brook flow into a pool which overflows into the Swan. Of the tributaries, the Avon River carries by far the greatest volume of water to the Swan–Canning estuary.

Ellen Brook

Ellen Brook is located west of the Darling Scarp between the town of Gingin, some 70 km north of Perth, and the outlet to the Swan River at Upper Swan (Figure 4.3). Ellen Brook has a catchment area of approximately 640 km^2. More than 70% of the diverse, low-forest native vegetation has been cleared since the 1950s for sheep and cattle grazing, vineyards and orchards. The streamflow gauging station, Railway Parade, is located 7.5 km upstream of the confluence with the Swan River.

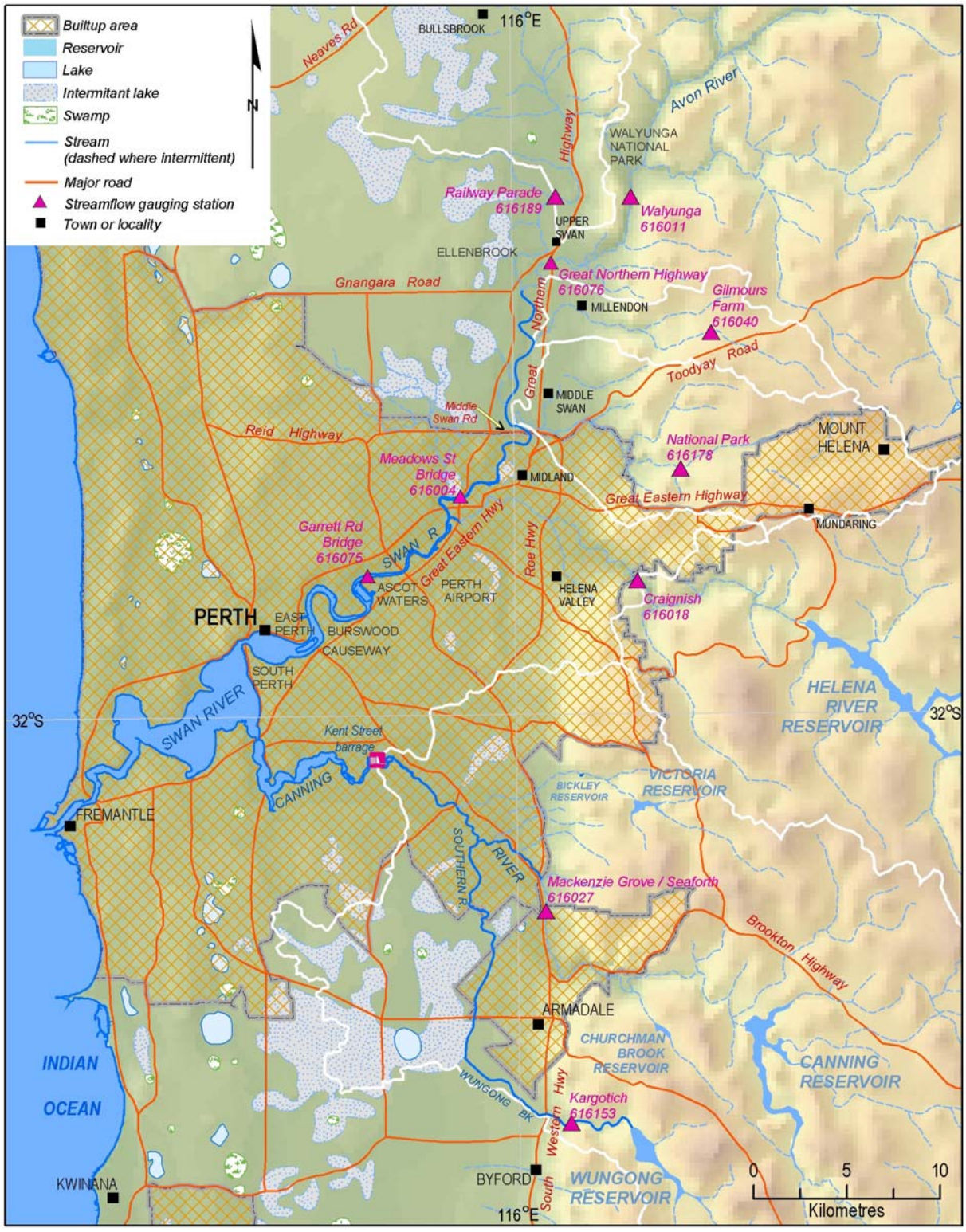

Figure 4.1: The Swan–Canning catchment

Susannah Brook

Susannah Brook has a catchment area of approximately 55 km^2, and is located west of the Darling Scarp about 25 km northeast of Perth (Figure 4.4). Over than 70% of the native vegetation has been cleared since European settlement and is currently used as pasture, orchards and hobby farms. Portions of the catchment have been taken up by suburban developments, particularly in the lower reaches. A streamflow gauging station at Gilmours Farm has monitored the flow from the upper half of the catchment since 1981.

Jane Brook

Jane Brook has a catchment area of approximately 131 km^2, and is located west of the Darling Scarp, about 30 km northeast of Perth (Figure 4.5). Roughly half of the native Jarrah forest vegetation has been cleared since European settlement and is now mainly used for pasture, orchards and hobby farms. Portions of the catchment have been taken up by suburban developments, particularly in the lower reaches. The streamflow gauging station at National Park has been operational since 1962.

Helena River

The Helena River has a catchment area of approximately 1,860 km^2 (Figure 4.6). Almost 75% of the catchment (1476 km^2) is above Mundaring Weir which has a capacity of around 64 GL. Located about 20 km northeast of Perth, the weir supplies water for metropolitan domestic use and also by pipeline to the goldfields, some 600 km east of Perth. The Helena River catchment above Mundaring Weir is completely within the Darling Plateau and has no significant clearing of the natural vegetation. Below Mundaring Weir, about 50% of the catchment has been cleared for pasture and orchards. The streamflow gauging station of Craignish is located 15.5 km upstream from the Swan River confluence and has been operational since the mid-1970s.

Canning River

The Canning River has a catchment area of approximately 1,300 km^2, extending about 70 km southeast of Perth into the Darling Scarp (Figure 4.7). The lower foothills and flat plains west of the Scarp have largely been cleared for agriculture and urbanisation. In the section of the catchment within the Scarp, the majority of the native vegetation is still present.

Three-quarters of the catchment is regulated, largely by the Canning Reservoir, though Wungong and Churchman Brooks, and the Victoria and Bickley Reservoirs also have some influence. Approximately 6 km downstream of Wungong Reservoir, 40% of flow is diverted into the Birrega Drain within the adjacent Serpentine River catchment (Waugh, 1986). Kangaroo Gully diversion weir and contour channel diverts flow from Kangaroo Gully into the Canning Reservoir. Any flow in excess of 2.2 m^3/s spills over the weir and continues down Kangaroo Gully, which joins the Canning River just downstream of the Canning Reservoir.

A number of streamflow gauging stations monitor the flow in the Canning River and its tributaries, the earliest of which commenced operation in the 1950s. Streamflow records from the Mackenzie Grove gauging station, which were used in this study for model calibration, began in 1974. In April 1997, Mackenzie Grove was replaced as the primary gauging station by Seaforth, 520 m downstream.

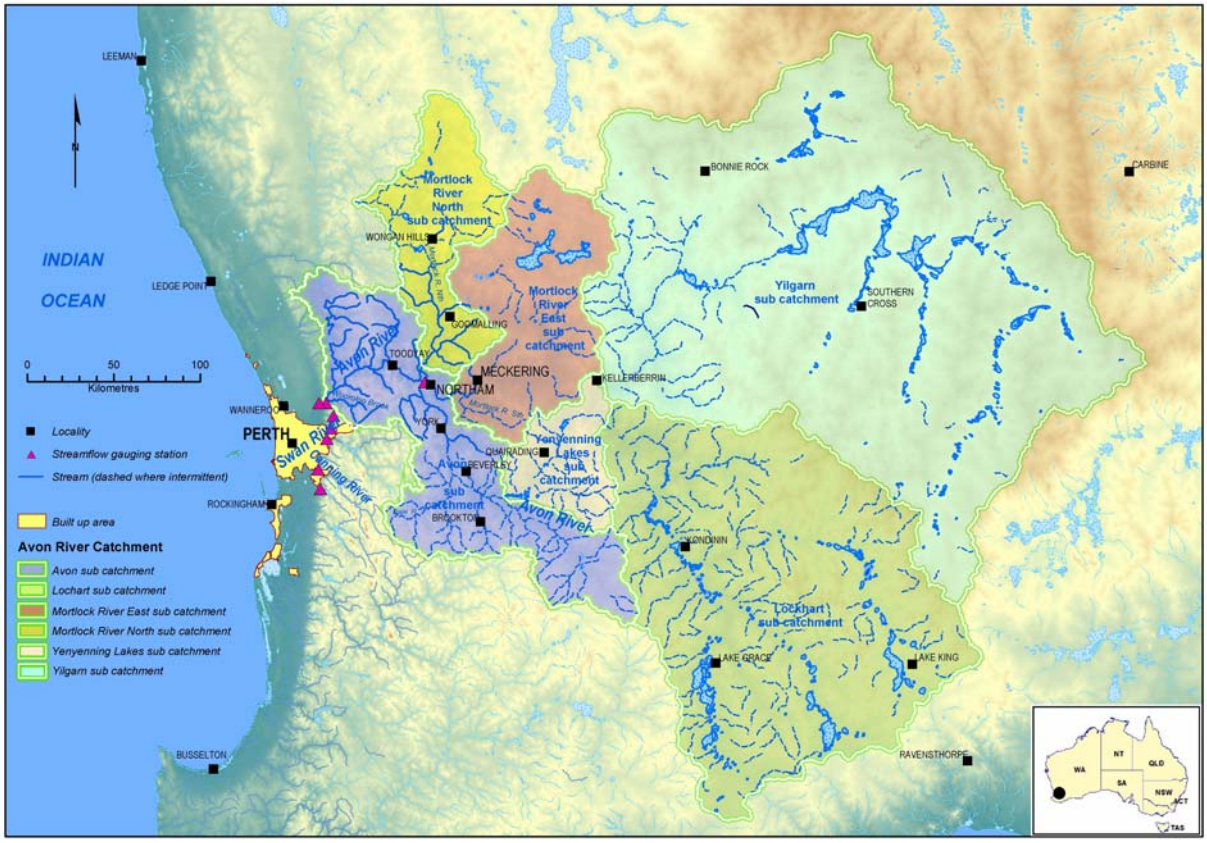

Figure 4.2: The Avon River catchment

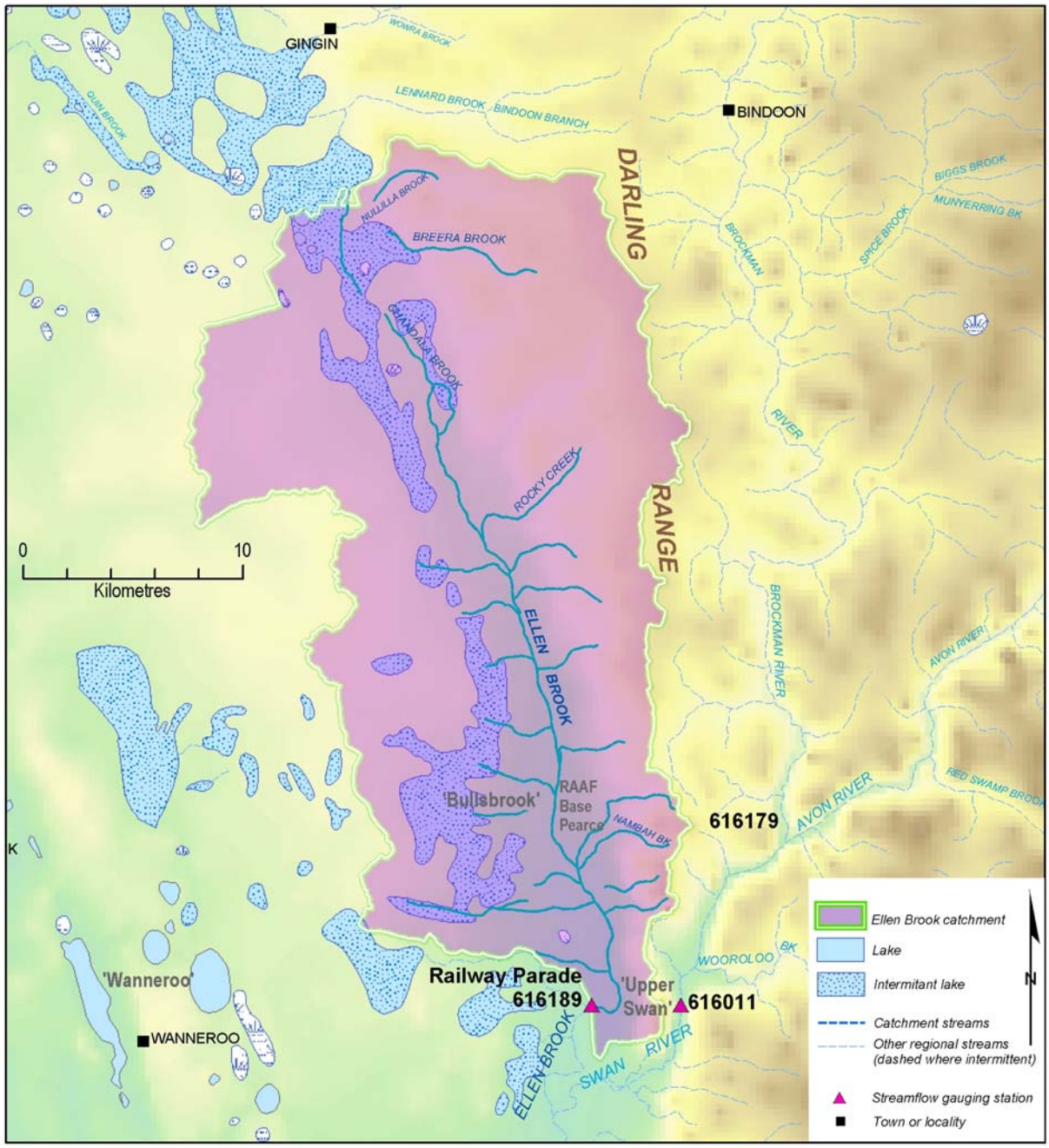

Figure 4.3: The Ellen Brook catchment

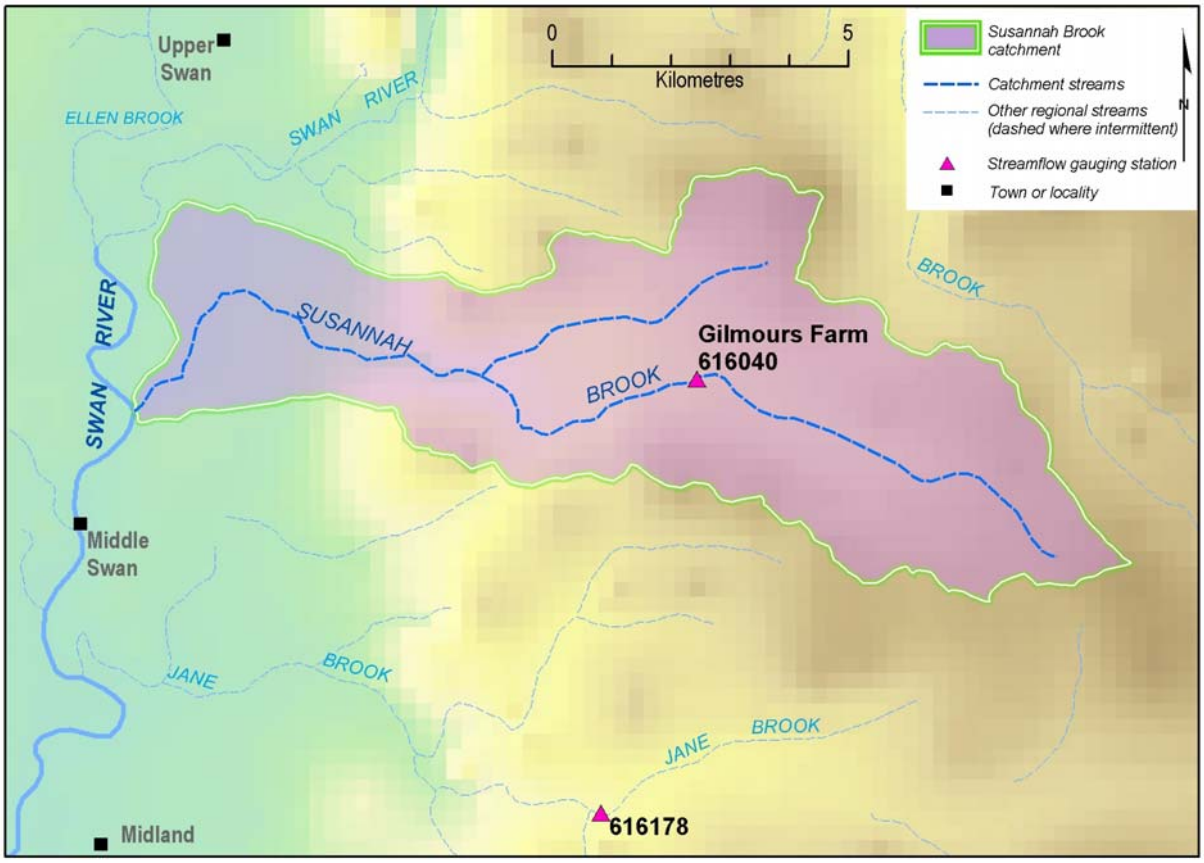

Figure 4.4: The Susannah Brook catchment

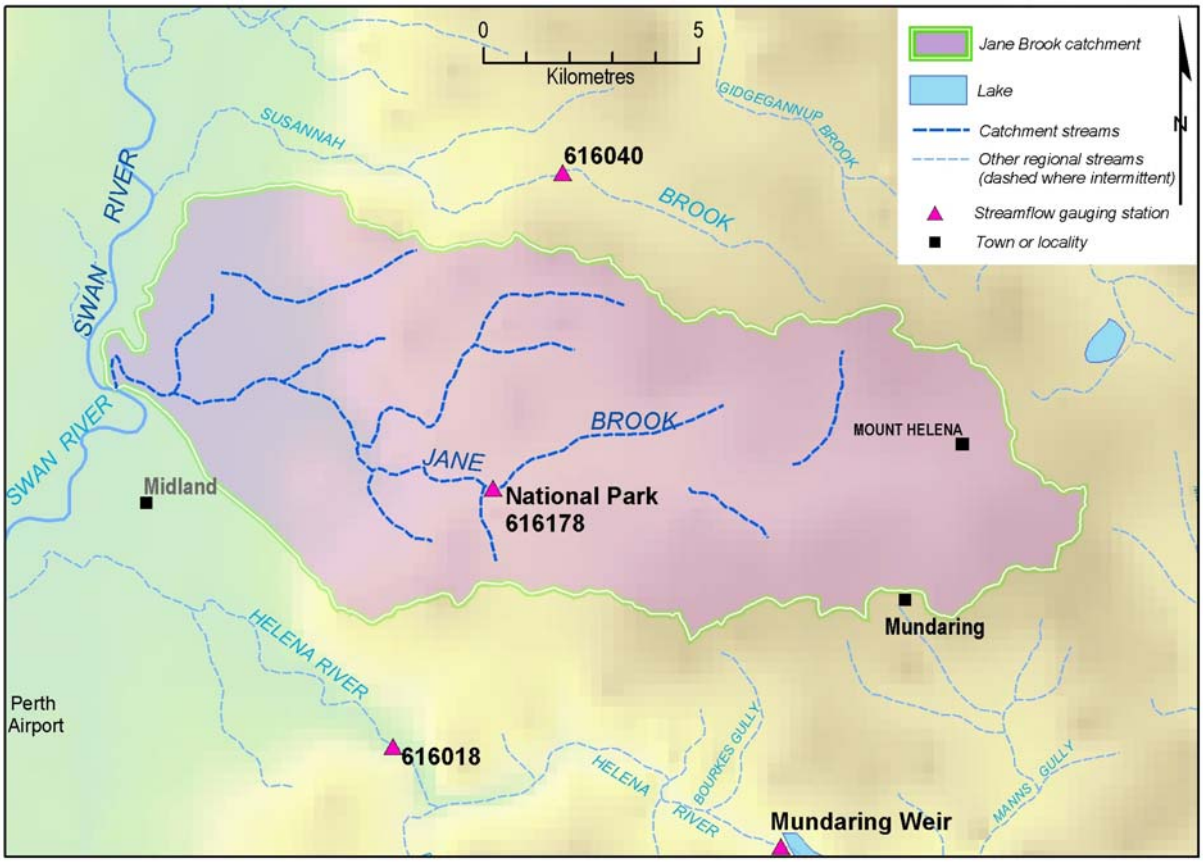

Figure 4.5: The Jane Brook catchment

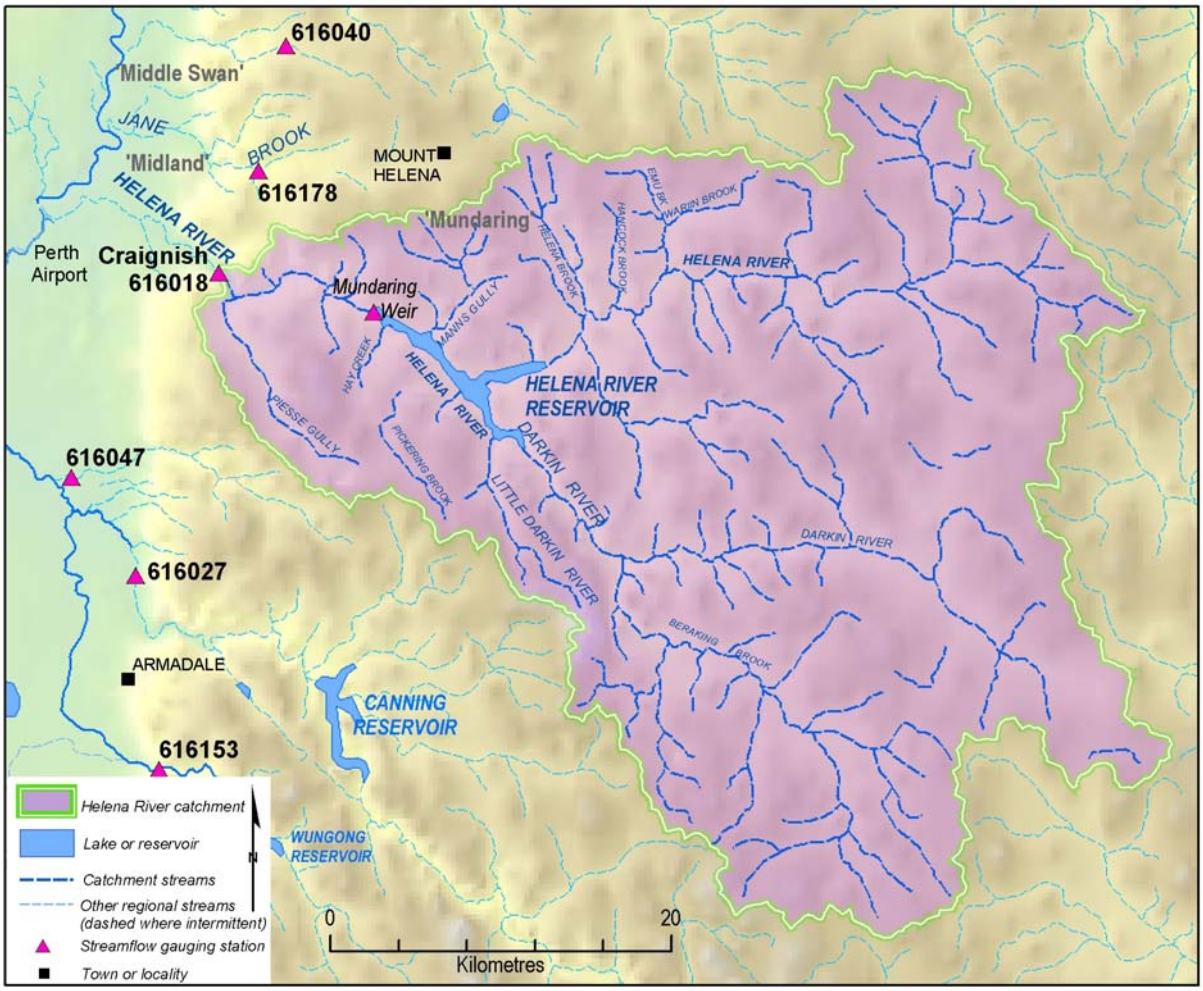

Figure 4.6: The Helena River catchment

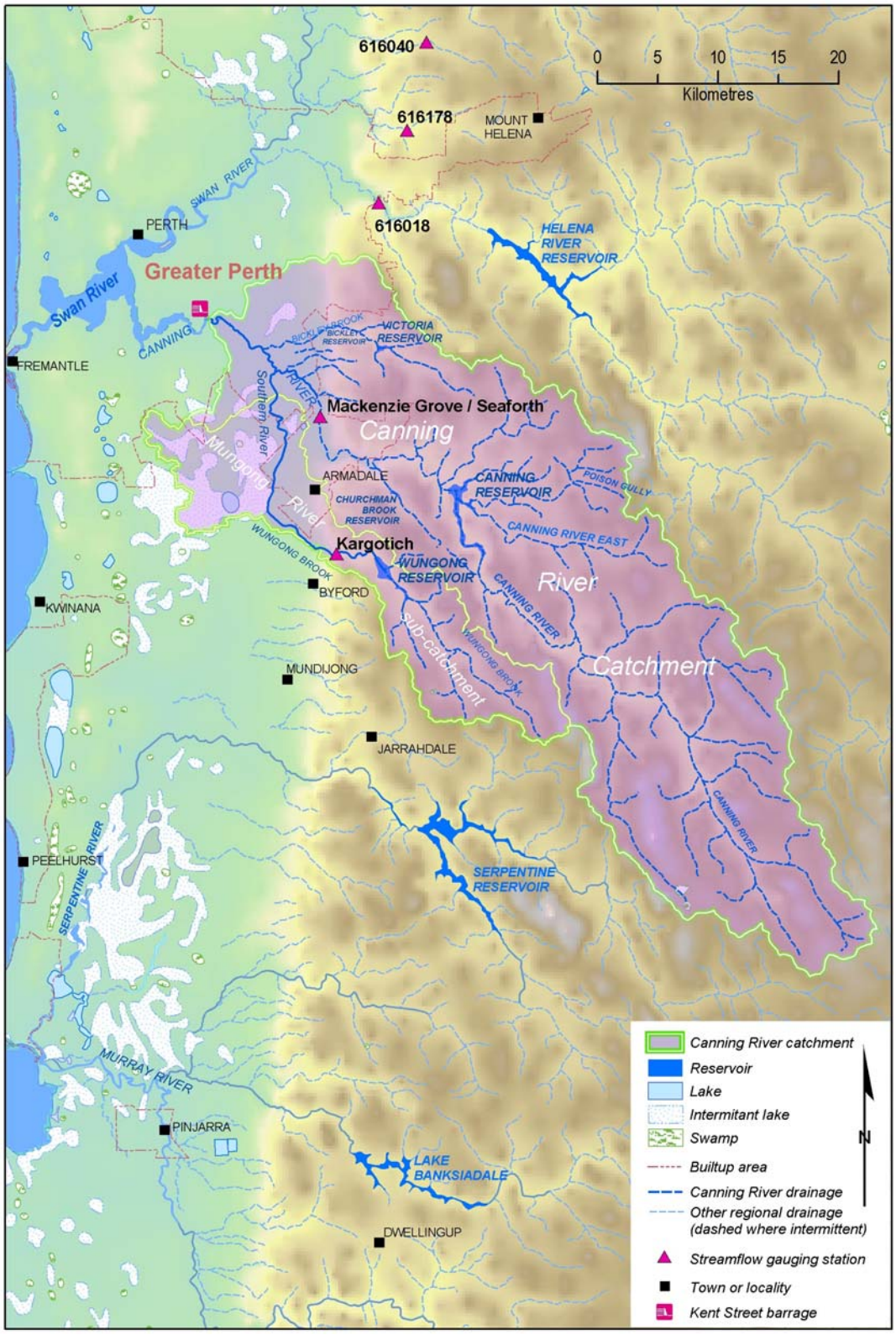

Figure 4.7: The Canning River catchment

4.3 Historical Flooding

Historical flood records and information for the Swan River extend back as far as July 1830.

In July 1830, the Swan River rose more than 6 m above its usual level, doing considerable damage (Bureau of Meteorology (BOM), 1995). In July–August 1847, flooding of the low-lying areas around Perth forced some residents to evacuate their homes (BOM, 1929). On 24 August 1860, the *Perth Gazette* reported extensive flooding along the Avon and Swan Rivers, following a very wet period during the preceding three months. On the Canning River, a flood with a 4% AEP was recorded in July 1987.

Table 4.1 gives the years of major floods from 1862 to 2004 and their estimated return period. The absence of major river flooding since the early 1960s has kept flood damage costs low in Perth.

Table 4.1: Floods in the Swan River, Perth, and their estimated ARI (PWD, 1986)

Year	1862	1872	1910	1917	1926	1930	1945	1946	1955	1958	1963	1964	1983
ARI	60	100	20	20	30	15	20	10	20	20	15	10	10

Losses from the flood in July 1862 were reported on 12 March 1934 in the *West Australian* at an estimated 30,000 pounds (1862 values), a considerable sum at the time. Since then, considerable infrastructure and buildings have been constructed on the floodplain. The 1862 flood, estimated to have an ARI of 60 years, was said by some sources to be unprecedented. The *Perth Gazette* (11 July 1862) reported that much property was destroyed, with gardens backing onto the river between the Causeway and Mt Eliza largely underwater. A contemporary account of the flood, describing the extent, depth and duration of flooding follows:

> *To show the enormous accumulation of water in the Estuary, we may state that the area occupied by Perth and Melville Waters, as laid down in the maps of the Survey Office, is given as 7,100 acres, over all of which the rise of seven feet took place; but in addition, we have to take into consideration the large extent of lowland (but lying above the usual water level) which was also covered to a depth of several feet. The flood maintained its highest level until about 10 pm on 7th (Sunday), when a slight ebb commenced and continued until Wednesday morning, the fall being about one foot. A reaction then commenced (probably owing to spring tides having set in outside) and on the 10th at North Fremantle the whole of the Pensioners Cottages and allotments were under water… The flats on the Swan were flooded for some time, the bridge over the Helena was covered above its top rails, and the Causeway had between seven and eight feet of water upon it. In places the only means of communication was a small boat. Two of the police force, when trying to get across the river on horseback, were swept by the current among the trees on the flat and had a narrow escape from drowning. At Strelly an entire farm and its contents were swept away… the flood maintained its height for fourteen days, and reached two feet above that of 1830… Several losses of life through the floods were reported: - Lieutenant Oliver, 12th Regiment, at Perth; a shepherd at York; one person at Toodyay and two on the Greenough Flats… In the southern districts parts of the bridge over the Canning River disappeared, leaving the centre standing.*

The largest flood in the known record occurred ten years later in July 1872 and has an estimated AEP of 1%. The flood reportedly caused considerable property damage along the Swan–Avon River (BOM, 1995). A contemporary account of the flood from the *Perth Gazette and WA Times* (26 July 1872) follows:

> *In and about Perth, the water owing to the force of the incoming seas at the mouth of the river presented a scene of a great lake, all the jetties were submerged, the high roads to Fremantle covered, and passage traffic rendered impossible, quantities of sandalwood lying along the banks of river were washed away, and the inhabitants of the suburban villas on the slopes of Mt Eliza obliged to scramble up the hill sides to get into Perth. In some of them, especially Mr C Watson's, the water*

> *rose two feet inside, that gentleman getting in and out only by means of his boat. From Guildford and the Swan we hear of serious injury, the Helena Bridge causeway has been much damaged – a large extent of land remains unsown and fortunately as compared with those that have been sown will give no returns… Much live stock has been lost, and but for the noble exertions of police, constable James McCourt a loss of human life also had been incurred. The rise in the Helena was two feet three inches higher than in the great flood of 1862.*

Between 1910 and 1963 there were ten floods ranging between 15–30 years ARI, after which, the area has experienced a much drier period. The flood of July 1926 is perhaps the best-documented case of flooding of the Swan River, though its estimated ARI is only 30 years. The Fremantle Railway Bridge (Plate 4.2) and the Upper Swan Bridge collapsed. Significant flooding of property occurred in South Perth (Plates 4.3 and 4.4) and in the Upper Swan–Guildford areas. Freight costs rose as a consequence of the collapse of the Fremantle Railway Bridge because goods traffic between Perth and Fremantle had to be diverted through Armadale (*Western Mail*, 29 July 1926). A description of the flood follows from the *West Australian* (July 23 1926):

> *The North Fremantle railway bridge was sagging yesterday as a train passed over it. Shortly afterwards, when it was only by a miraculous piece of good fortune that there was no passenger train on it, the structure began to collapse, and the effect of the swirling flood waters soon put it hopelessly out of commission. This is by far the most serious result of the recent floods, as it means that the ordinary Fremantle train service will be disorganised for at least a month…..the disaster will have far reaching effects on the shipping and commerce of the Port… the southern side of the harbour was practically isolated as far as cargoes coming from Perth were concerned, at any rate, until the railways in the country districts were reorganised and goods trains could be frequently sent to Fremantle via Armadale.*

Plate 4.2: Fremantle Railway Bridge destroyed by the July 1926 floods (Courtesy of the Battye Library 54902P)

Plate 4.3: Mill Point, South Perth, in the July 1926 flood (Courtesy of the Battye Library 225145P)

Plate 4.4: View of South Perth showing Point Belches under water during the July 1926 floods (Courtesy of the Battye Library 225147P)

The estimated ARI for the flood of 1917 is less than the 1926 flood (see Table 4.1), and the following extract indicates that at many locations the water levels in the 1926 flood may have been higher than the 1917 flood. This extract from the *Western Mail* (29 July 1926) shows the significant impact of the 1926 flood in the South Perth and Guildford areas:

> *At the foot of Barrack Street the river had burst its banks, and the water was swirling over the garden plots and roadways on the foreshore to a distance of 150 yards from the jetties and ferry offices. The jetties were completely submerged, and the flood had burst into the offices, driving the officials out and causing a certain amount of damage... …an expanse of water varying from a few inches to a foot in depth.*
>
> *… The people of the Mill Point area [South Perth] were in dire need of practical assistance… During the night no fewer than fourteen houses situated in Suburban Road between Scott Street and the Point, were invaded by the rising waters. Two houses in Stone Street and one in Melville Terrace were also flooded… Along the whole road to Mill Point, from the Scott Street intersection as far as eye could see, water flowed – flowed not dully and placidly, but actively, in high surging currents flecked with foam and breaking here and there into actual waves. A yacht in full sail went up Suburban road…*
>
> *Several dwellings in the vicinity of the bridge over the Helena River at South Guildford were submerged to within three or four feet of their roofs. Half a window pane peeped over the flood surface… A dead dog and a couple of dead cats floated nearby. The abomination of desolation marked the whole locality. At Barkers Bridge, on Caversham road just out of Guildford, to the northeast a rowing boat was seen arriving with some Caversham residents who had come in for provisions…*
>
> *The playing field* [at Guildford] *was eleven feet below the surface of the waters. Floodwaters prevailed on Wednesday throughout the whole district of Guildford. Almost as much land was under water as was above it. From some points extraordinary panoramic views were obtained, vistas of enormous sheets of water, extending for three or four miles, the surface of the floods broken by tree tops which emerged disconsolately and the roofs of sheds, and much floating debris of all kinds…*
>
> *When the flood was at its top most crest the Helena River at East Guildford had risen three feet six inches higher than its level during the deluge of 1917, while the Swan River in the flats below the Guildford Grammar School, and in the vicinity of Barkers Bridge on Caversham road had actually reached a level seven feet higher than the 1917 maximum.*
>
> *That the recent floods, however, at all events so far as the Guildford district is concerned, did not reach the height of the flood waters of 1862, was a fact pointed out to the Government Meteorologist (Mr Curlewis). One of the oldest Guildford residents affirmed that while on this occasion the ancient and well known Preston farmhouse had been surrounded by the deluge, in 1862 the waters were right up to the windows. There is little doubt said Mr Curlewis that the 1917 floods have been everywhere eclipsed, but we have every reason to believe that in 1862 the waters were considerably higher generally speaking than the levels of last week.*

Washaways on the railway line between Northam and Perth and on the Great Southern Line reduced supplies to the Midland Junction market on 21 July, increasing prices as reported in the *Western Mail* (29 July 1926):

> *The effect on the sheep market was a rise from 2s to 4s per head, all lambs were 1s to 5s per head dearer but [the price of] pigs remained firm at the preceding weeks rate… Among the sufferers through the torrential rains are the Chinese gardeners who cultivate vegetables along the river at Mount Bay's road South Perth, Belmont and Maylands. All these gardens are flooded, in some cases three or four feet deep.*

Flash floods in Perth have also resulted in large losses, though they are not modelled here. In July 1987, for example, the WA state government declared Perth's southeastern suburbs a natural disaster zone. The *West Australian* (4–5 August 1987) estimated flood damages to local government public facilities at $500,000 – $1 million. Flood damage to roads in the Armadale City Council district was estimated at nearly $500,000. More than 140 houses were damaged by flooding in the suburbs of Westfield, Armadale, Kelmscott, Forrestfield and Kardinya. The *Daily News* (29 July 1987) describes cars being abandoned, and a tow truck which had been responding to the calls for assistance due to the

flash floods also breaking down. The following two extracts from the *West Australian* (30–31 July 1987), illustrate the loss sustained to home and contents:

> *Families lose homes… Kim Daykin, awoke about 5am yesterday to find knee-deep water swirling around her bed. The roof had also partly caved in… Another house in the next street had three walls washed away and a teenage boy was almost crushed as he tried to rescue family possessions.*
> *Once a lake – now dozens of homes… Those families in Excalibur Close, and nearby Lancelot Close, Camelot Place and Ivanhoe Way, were yesterday attempting to clear mud and water from their homes after Tuesday night's deluge… Their home in Excalibur Close had 20 cm deep water flowing through it… "The carpets, lounge suites and beds are ruined – they will go straight to the tip. When I open a cupboard, water gushes out"… The home of Geraint Griffiths, in Ivanhoe Way, escaped the flood waters by centimetres, but the family car floated away.*

Another flash flood occurred on 6 December 1987, severely affecting the Armadale and Kelmscott areas again, causing flooding up to 30 cm deep from a 45-minute downpour. One of the Hill residents described this as the second time that he had lost his back fence to flashflooding in just over four months, with the earlier fence destroyed by a wall of water a metre high (*West Australian*, 7 December 1987).

4.4 Hydrology of the Swan and Canning Rivers Catchments

The hydrologic component of the flood study involved hydrographs being determined for floods of a range of frequencies. Hydrographs were developed in order to run an unsteady flow model, in which changes in area of inundation, depth of inundation and velocity with time could be estimated in the hydraulic component of the study. Peak design flows of varying probability were developed and used to predict floods of the same magnitude. An estimate for the 1% AEP design flow, for example, was used to estimate the 1% AEP design flood. The main focus of the report, however, is on the hydraulic modelling. While we acknowledge that there are uncertainties associated with the hydrology component which is the input to the hydraulic model, they are not discussed in detail here. The interested reader can refer to the original reports which are referenced in the following section, to establish the associated uncertainties for each individual hydrologic model. This section describes the development of the design hydrographs for each catchment.

Design hydrograph development for flood estimation

Where available, the design flows and hydrograph shape used in this study were based on the results of the previous studies undertaken by/for the DOE or its predecessors. In most cases these studies involved running design catchment rainfall through a calibrated RORB (Laurenson and Mein, 1985) runoff routing model of the catchment. For flood events between 10% and 1% AEP, a flood frequency approach, coupled with runoff routing models, was used to estimate peak design flood estimates and hydrograph shape.

Floods between the 1% AEP and the PMP design floods were estimated by interpolating from a flood frequency curve. The flood peak between the 1% AEP and the PMP design flood was determined by calculating the magnitude of two events at designated AEPs based on the methods described in Institution of Engineers (1987, 1999). This method provides estimates of magnitudes ranging from 0.5% to 0.0005% AEP events. The peak estimates produced for all the catchments are for AEPs = 10%, 4%, 2%, 1%, 0.5%, 0.2%, 0.1% and 0.05%, and the PMP. As the probability of the PMP for a catchment is directly related to the catchment area over which it is applied (Institution of Engineers, 1999), the approximate AEP of the PMP design flood varies between the catchments as is shown in Table 4.2.

Hydrograph shape for design flows equal to or less than the 1% AEP was derived using the RORB (Laurenson and Mein, 1985) or URBS (Carroll, 1995) models for each catchment. Hydrograph shape for peak estimates ranging between the 0.5% and 0.05% AEPs were determined based on the shape of

the 1% AEP hydrograph for each respective catchment. The shapes of the hydrographs were scaled by standardising discharges in the 1% AEP flood hydrograph to 1.

Table 4.2: AEP estimates for the PMP design flood at selected locations

Catchment	Location	AEP estimate	ARI estimate[1]
Avon below Yenyenning Lakes	Swan River at Gt Nthrn Hwy	3.3×10^{-5}	30,300 year
Ellen Brook	Swan River confluence	6.4×10^{-7}	1,562,500 year
Susannah Brook	Swan River confluence	1.0×10^{-7}	10,000,000 year
Jane Brook	Swan River confluence	1.3×10^{-7}	7,692,300 year
Helena River	Swan River confluence	1.9×10^{-6}	537,600 year
Canning River	Swan River confluence	1.3×10^{-6}	769,200 year

Note: [1] Please note that technically AEP and ARI are not interchangeable (see Introduction to this chapter). However, in the interests of being understood by the majority of people, both are included.

The PMP for all catchments for the Swan–Canning estuary is of tropical origin, most likely occurring between October and April. In the southwest of Western Australia the rainfall during this period is typically infrequent and evaporation rates are high. As a result, the PMP for each of the streams is likely to coincide with relatively dry antecedent catchment conditions. Therefore, a high initial loss (100 mm) and moderate proportional runoff (45%) was adopted for application of the PMP event to the URBS model of the Avon River catchment and calibrated RORB runoff routing models for the Ellen, Susannah, Jane, Helena and Canning streams. The output from the URBS and RORB models provided an estimate of both the peak discharge and the hydrographs for the PMP design flood.

Table 4.3 shows the design flood estimates for the common AEPs modelled across all catchments. There is a sharp increase in the design flood estimates for the PMP, with an average eleven-fold increase in peak discharge over the modelled 1% AEP.

Table 4.3: Summary of peak design flow estimates (m^3/s) at selected locations

	Location on Stream						
AEP	Avon River	Ellen Brook	Susannah Brook	Jane Brook	Helena River	Canning River	Wungong Brook
Gauging station	616011	616189	616040	616178	616018	Brookton Hwy	616153
10%	640	68	10	19	90	38	10
4%	990	75	15	25	140	49	12
2%	1,300	83	19	27	185	53	13
1%	1,700	97	23	34	225	61	15
0.5%	2,200	125	29	44	300	80	19
0.2%	3,000	170	38	61	420	115	25
0.1%	3,750	200	46	76	530	145	30
0.05%	4,550	250	55	95	635	180	37
PMP design flood*	11,750	2,220	240	510	6950	2740	310

* **Note**: The AEP for the PMP design flood varies, as shown in Table 4.2.

In addition to developing design hydrographs for each of the gauging stations, additional hydrographs were developed in order to capture changes in hydrograph shape and discharge downstream of the gauging stations to account for additional flow from the urban area. The location of these additional simulated inflow hydrographs can be seen in Figure 4.8. The total change (%) in peak flow between the gauging station and the outlet for each tributary is shown in Table 4.4. The peak flow estimate at the most upstream locations were shown in Table 4.3. The one exception is on the Canning River where the upstream boundary is 7.4 km upstream of the gauging station. Table 4.4 shows that the simulated inflow hydrographs can contribute significantly to the predicted peak flow at the outlet of a

tributary. As distance increases away from the gauging stations at the upstream boundaries of the model, the time to peak also increases. Table 4.5 shows the percentage change in peak discharge between the upstream boundary hydrograph H_1 and the nearest downstream modelled lateral inflow hydrograph H_2. The change (%) between hydrograph H_2 and the next most downstream hydrograph H_3 is then shown. While there is significant increase in inflow between some locations, there is minimal change at others.

Table 4.4: Change (%) in peak flow over the stream within the study area for various AEPs

	Annual Exceedance Probability (%)							
Stream	**10**	**4**	**2**	**1**	**0.5**	**0.2**	**0.1**	**0.05**
Ellen Brk	3	1	6	2	4	3	5	4
Susannah Brk	60	53	42	43	45	47	48	51
Jane Brk	53	48	59	47	43	36	32	26
Helena R	0	0	0	0	0	0	0	0
Canning R	182	192	202	192	175	173	134	139
Southern R–Wungong Brk	350	400	377	340	300	260	233	197

In some locations the peak discharge between some of the modelled hydrographs for the tributaries appears to decrease rather than increase downstream. This is an artefact of the model. The flow has been routed relatively long distances without the addition of sufficient tributary inflow to counteract the attenuation resulting from the flow routing. The differences estimated may or may not exist in a real-life situation and will depend on the magnitude and timing of the actual inflows from the small tributaries along the reaches in question.

The generic aspects in the design hydrograph development have been covered. The unique aspects in the development of the hydrographs for each of the major catchments of the Swan–Canning estuary are described in the following sections.

Table 4.5: Change (%) in peak flow between modelled inflow hydrographs for the tributaries to the Swan River for various AEPs

	Inflow Hydrograph		Annual Exceedance Probability (%)							
Stream	**Upstream**	**Downstream**	**10**	**4**	**2**	**1**	**0.5**	**0.2**	**0.1**	**0.05**
Ellen Brk	Railway Parade GS[1] (616189)	Swan confluence	3	1	6	2	4	3	5	4
Susannah Brk	Gilmours Farm GS[1] (616040)	Moore Rd	60	53	47	52	55	61	65	69
	Moore Rd	Railway Line	0	4	4	3	2	2	1	1
	Railway Line	Gt Northern Hwy	0	0	-3	-6	-7	-6	-9	-10
	Great Northern Hwy	Swan confluence	0	-4	-4	-3	-2	-3	-3	-2
Jane Brk	National Park GS[1] (616178)	Toodyay Rd	32	28	33	26	25	20	18	16
	Toodyay Rd	Swan confluence	16	16	19	16	15	14	11	9
Canning R	Brookton Hwy	Mackenzie Grove GS[1] (616027)	11	10	13	13	13	9	7	8
	Mackenzie Grove GS[1] (616027)	Canning U/S Southern R	5	6	7	7	-6	-8	-6	-8
	Canning U/S Southern R	Canning D/S Southern R	73	75	72	64	81	74	69	64
	Canning D/S Southern R	Canning at Nicholson Rd	41	43	45	47	43	40	39	46
Southern R–Wungong Brk	Kargotich GS[1] (616153)	Southern River D/S of Neerigen Bk Sth confluence	150	194	198	195	168	148	137	116
	Southern River D/S of Neerigen Bk Sth confluence	Southern River outlet	80	70	60	49	49	45	41	38

Note: [1] GS = Streamflow gauging station

Avon River

Studies by the Public Works Department (PWD, 1986) and Waugh (1985) employed a flood frequency analysis approach to estimate the design peak flows for AEPs between 50% and 1% at the streamflow gauging station at Walyunga. The observed peak flow data set (1970–1983) was extended using catchment rainfall in conjunction with a Sacramento (Burnash, Ferral and McGuire, 1973) model of the catchment. The Sacramento model was calibrated using the gauged Walyunga streamflow data from 1970 to 1983.

As a result of the flood frequency method employed in these studies, hydrographs for the design flood events were unavailable. To produce hydrographs for these events design catchment rainfall was applied to the flood forecasting model developed by Rodgers (1998). The URBS runoff routing model of the Swan–Avon catchment was used to estimate hydrographs at the towns of Beverley, York, Northam and Toodyay, and at the Walyunga gauging station.

During the runoff routing modelling three design rainfalls were applied to groups of sub-catchments depending on their location. The eastern sub-catchments of Yenyenning Lakes, Yilgarn, Lockhart and Mortlock River East above Meckering, have been grouped together and assigned relatively low design rainfalls. The more centrally located sub-catchments on the eastern part of the Scarp, from Beverley through to Toodyay in the Avon subcatchment and all of Mortlock River North and Mortlock River East below Meckering, make up the second group. The sub-catchments below Toodyay were the final grouping and were assigned slightly higher design rainfalls than the central group. The design rainfall estimates applied to each of these three areas corresponded to the design rainfall estimates for a representative location within each, namely Kellerberrin (East), Northam (Central) and Walyunga (Lower).

An initial loss of 10 mm was adopted for the entire catchment. The proportional runoff coefficients suggested in Rodgers (1998) ranged between 0.5% and 30%. In this study the model was simplified by using only three runoff coefficients across the entire Avon catchment. A runoff coefficient of 1% was adopted for the Yilgarn and Lockhart systems and the flat areas at the top of both the Mortlock River East and North Branches. A runoff coefficient of 15% was adopted for the downstream Mortlock River East and Mortlock River North sub-catchments. For the remaining sub-catchments, a runoff coefficient of 20% was adopted. The design peak flows for AEPs between 10% and 1% obtained from the runoff routing modelling were within 2% of the flood frequency analysis results quoted PWD (1986) and Waugh (1985).

The Lockhart and Yilgarn systems account for approximately 75% of the Avon River catchment area. However, these systems are likely to be only a small contributor to the peak flow discharging from the Avon River at Walyunga because the Lockhart and Yilgarn systems lie within a lower rainfall zone. The catchment is a relatively flat, low relief region with a series of lake formations distributed evenly throughout. These lakes trap a large proportion of the runoff, with runoff averaging <0.3 mm/year. The large flood storage provided by the lake formations also results in significant attenuation of flows during major events when the lake formations interconnect. By comparison the runoff generation in the areas downstream is significantly larger (>20 mm for catchments west of Yenyenning).

The passage of storms within the catchment generally ranges between south-southeast (for summer, ex-tropical events) to northeast (for winter frontal systems). The passage of the storms combined with the sheer size of the Lockhart and Yilgarn systems and the flood storage available within them suggest that it is unlikely that peaks from these sub-areas will coincide with the peak from the smaller catchment downstream of Yenyenning. For catchments the size of the Swan–Avon this temporal variation in the design rainfall should be considered.

The PMP for the entire catchment (~120 000 km^2 to Walyunga) is significantly smaller than the PMP estimate for the ~ 30 000 km^2 catchment below Yenyenning, which is the junction of these two systems (see Figure 4.2). Due to the high losses, low runoff rates, flood storage and attenuation in the

Lockhart and Yilgarn systems, the resulting PMP for the area downstream of Yenyenning has been assumed to be higher than simply applying a PMP to the entire catchment. Therefore, rather than applying a PMP event to the entire Avon catchment which would produce a smaller PMP design flood, a PMP event was applied to the remaining 25% of the catchment (ie, Avon catchment below Yenyenning Lakes). A large flood event (1% AEP) in the Yilgarn and Lockhart systems was then assumed to occur concurrently.

A crude estimate of the PMP for the reduced catchment area downstream of Yenyenning Lakes (approximately 33,000 km^2) was determined based on estimates provided by the BOM for the Ord River Dam (BOM, 1999) and Wellington Dam (BOM, 1996) catchments. The PMP for these two catchments was used because they are the two largest catchments for which estimates of PMP were available at the time that the hydrology for this report was undertaken, with areas of approximately 45,000 km^2 (BOM, 1999) and 2,850 km^2 (BOM, 1996) respectively.

Improved estimates of the PMP are now available following the release of the BOM's generalised tropical storm method revision (GTSMr). A comparison between the original estimates and the estimates based on the GTSMr have not been undertaken, however, the difference is likely to be relatively small in comparison to adopting a different loss model to the simple method applied within this study (initial loss = 100 mm proportional runoff = 0.45). The release of the CRC FORGE database for WA will enable improved estimates of rare event floods (between 1% and 0.05% AEP). It is not yet clear what impact these recent advances will have on the rare and extreme design flood estimates for Swan River and tributaries.

Ellen Brook

The most recent study was undertaken by Waugh and Ng (1987) and employed two runoff routing models (Flout and RORB) to determine design peak flows for AEPs between 4% and 1% at a number of locations along Ellen Brook.

The RORB model of the catchment from Waugh and Ng's (1987) study was adapted to enable estimates to be obtained for a number of additional locations within the catchment. The calibrated model parameters from the study were applied, including an initial loss of 0 and a runoff coefficient of 12.1%. The adapted RORB model successfully reproduced the hydrographs for the 4%, 2% and 1% AEP events at the locations common between the two models. An estimate of the 10% AEP rainfall for the catchment at the critical duration of 48 hours was applied to the RORB model to determine design flows for an event of this probability.

The PMP estimates for Ellen Brook catchment were derived using a relationship between catchment area and the unadjusted January PMP estimates for 15 catchments in southwestern Western Australia provided by the BOM. The estimates were based on a generalised method incorporating depth–area–duration (DAD) curves that had been derived directly from the Australian tropical storm data. The final PMP estimates were estimated by applying adjustment factors for moisture, barrier height, topography and distance from the coast. PMP estimates for Susannah Brook, Jane Brook and the Canning River catchments were derived using the same method.

Susannah Brook

The most recent study was undertaken in August 1992 (McLaughlin, 1992). It employed the RORB model and flood frequency analysis on the gauged data to determine design peak flows for AEPs between 10% and 1% at locations along Susannah Brook.

The RORB model of the catchment from McLaughlin's (1992) study was adapted to allow for estimates at additional locations within the catchment. The calibrated model parameters determined in the previous study were applied and resulted in the successful reproduction of the hydrographs for the 10%, 4% and 1% AEP events. An estimate of the 2% AEP rainfall for the catchment at the critical

duration of 18 hours was applied to the RORB model to determine design flows for an event of this probability.

Jane Brook

The most recent study was carried out in January 1988 by Davies (1988). It employed a RORB runoff routing model to reproduce design peak flows determined by flood frequency analysis for AEPs between 10% and 1% at the Jane Brook National Park streamflow gauging station.

The RORB model of the catchment from Davies (1988) study was adapted to allow for estimates at additional locations within the catchment. The calibrated model parameters determined in the previous study were applied, including an initial loss of 0 and runoff coefficients varying from 12.5% to 17%. The calibrated RORB model successfully reproduced the hydrographs for the 10%, 4% and 1% AEP events at the locations common between the two models. An estimate of the 2% AEP rainfall for the catchment at the critical duration of 24 hours was applied to the RORB model to determine design flows for an event of this probability.

Helena River

The most recent flood study for the Helena River downstream of Mundaring Weir was undertaken in October 1984 (Waugh, 1984). It involved a flood frequency analysis on estimated peak annual flows at Fyfe Road to determine design peak flows at the site for AEPs ranging between 10% and 1%. The estimated flows were based on overflow data for Mundaring Weir and gauged data below the dam.

A study on extreme flood estimation for the Helena River is currently underway as part of Dam Safety Reviews for Mundaring Weir and at the Lower Helena pumpback site. This study involved calibrating the RORB runoff routing model and soil water loss model of the Helena River catchment. Design rainfall information has then been applied to determine the appropriate design peak flows for the 2% AEP to the PMP. Estimates of the PMP were supplied by the BOM.

The design outflow peaks from Mundaring Weir obtained during the recent modelling of the 2% and 1% AEP events were slightly different to the earlier flood frequency results. The flood frequency results from the earlier study were preferentially adopted during this study because they are based on observed data (1905–1983) and the runoff routing results are still only preliminary. Despite the preliminary nature of the runoff routing results, the shape of the design hydrographs have been adopted as the Waugh (1984) study produced peak design flows only.

Canning River

The most recent study was undertaken in April 1989 by Davies (1989). It employed a RORB runoff routing model and a flood frequency analysis to determine design peak flows for AEPs between 10% and 1% at a number of locations along the Canning and Southern Rivers.

The RORB model of the catchment from Davies (1989) study was adapted to allow for estimates at additional locations within the catchment. The calibrated model parameters and median reservoir starting dam levels determined in Davies (1989) were applied. The calibrated RORB model successfully reproduced hydrographs for the 10%, 4% and 1% AEP events. An estimate of the 2% AEP rainfall for the catchment at the critical duration of 48 hours was applied to the RORB model to determine design flows for an event of this probability.

Though estimates of the PMP had previously been supplied by the BOM for the Canning, Wungong and Churchmans' Brook catchments, and for the Victoria and Bickley Reservoir catchments, no PMP was available for the entire Canning River catchment. Therefore, an estimate for the PMP was derived using the same method as used for the Ellen, Susannah and Jane Brook catchments.

4.5 Hydraulic Modelling of the Swan and Canning Rivers and Tributaries

Model development

Hydraulic models are used for predicting the impact of floods. The hydraulic model used in this study is the US Army Corps of Engineers Hydraulic Engineering Center's (2003) River Analysis System (HEC-RAS). HEC-RAS is a one-dimensional steady and unsteady flow water surface model, publicly available from the US Army Corps of Engineers Hydrologic Engineering website. HEC-RAS version 3.1.1 was used for modelling unsteady flows through the river network to estimate the duration and extent of inundation, and changes in water surface elevation and velocity through time at any location. HEC-RAS was interfaced closely with geographical information systems (GIS) for developing additional cross-sections and for visualising the flooding scenarios. Two-dimensional models were not considered as the area modelled is too large. However, the results of the one-dimensional model could be used to identify areas where a two-dimensional model may produce more detailed results.

The key data required for developing the unsteady flow model included geometric data, streamflow hydrographs and tidal data, and are described below. A representation of the model for the Swan River system is shown in Figure 4.8.

Cross-section data

Spatially located cross-section information is required throughout the stream network to capture the geometry of the stream channel and floodplain. Surveyed cross-section data was supplemented with cross-sections derived using GIS.

Surveyed

The surveyed cross-sectional information came from nine separate studies undertaken by the DOE and its predecessors between 1981 and 1990. The studies include:

- Swan River Flood Study, Causeway to Middle Swan Road, Review 1985
- Swan River Flood Study, Middle Swan Road to Walyunga National Park, Review 1985
- Susannah Brook Flood Study, Swan River to Millendon, 1995
- Jane Brook Flood Study, Swan River to Wexcombe, 1989
- Helena River Flood Study, Swan River to Helena Valley, 1987
- Ellen Brook Flood Study, Swan River to Bullsbrook, 1989
- Canning River Flood Study, Canning Bridge to Nicholson Road Bridge, 1981
- Canning River Flood Study, Nicholson Road Bridge to Brookton Highway, 1990; and
- Southern River – Wungong Brook Flood Study, Canning River to South Western Highway, 1988.

Several hundred cross-sections were transformed from hardcopy format into the same spatially referenced digital format (AGD66). The locations of the cross-sections were digitised as northings and eastings from the DOE's flood study survey plans. The spatial location of the cross-sections and the elevation data for each cross-section was entered into HEC-RAS.

The spatial extent of the survey data is limited to the area extending from the Causeway on the Swan River upstream to Walyunga National Park (Figure 4.8). On the tributaries the survey data falls short of the gauging stations used in the model by 1.5 km on the Southern River – Wungong Brook, 6.4 km on Susannah Brook, 3.3 km on Jane Brook and 2.9 km on the Helena River.

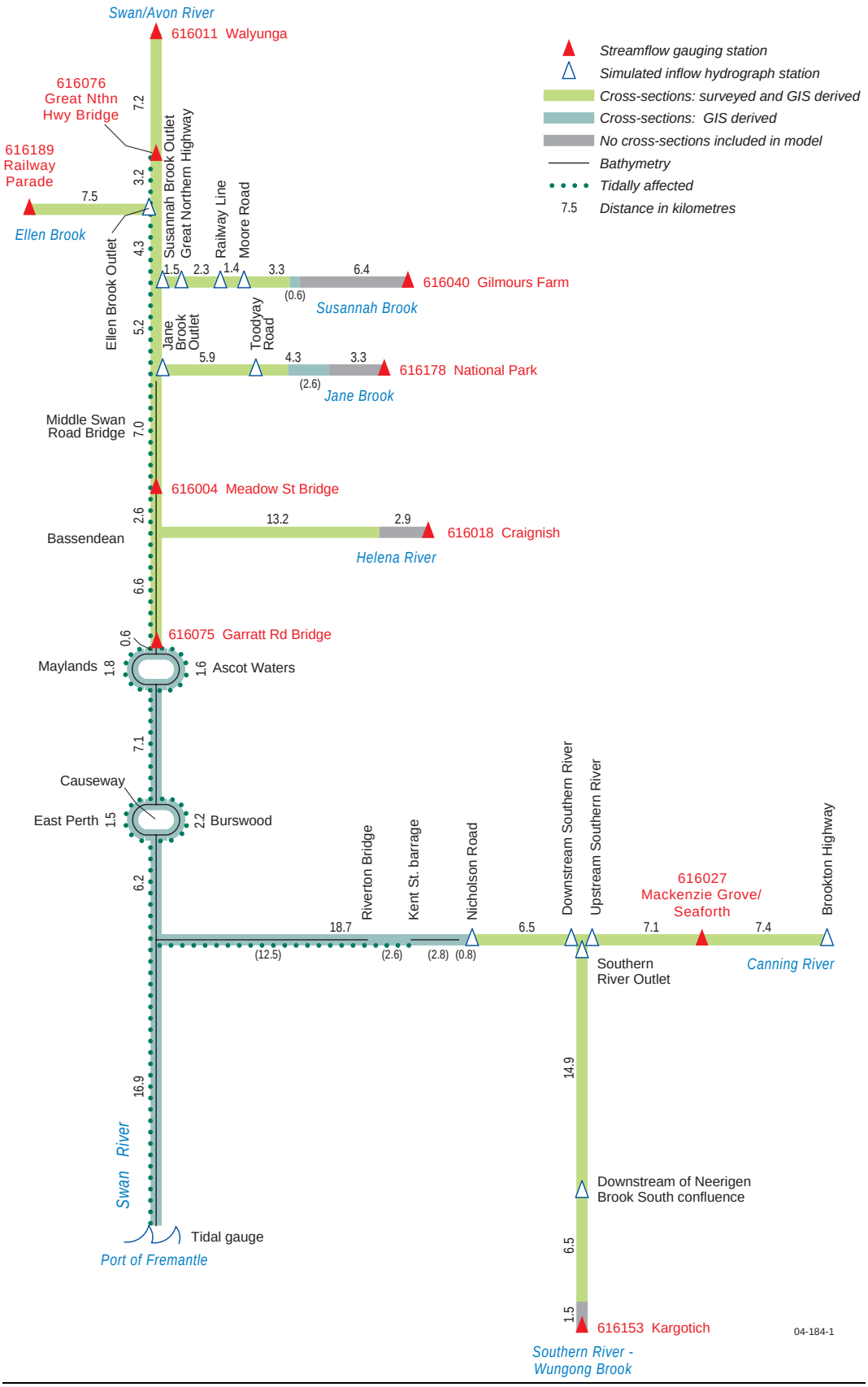

Figure 4.8: A representation of the hydraulic model

Bridges

Detailed modelling of the bridges was not undertaken because the amount of data required to input into the HEC-RAS bridge function was not available for many of the bridges. Where bridges were included, the bridge was treated as a simple surveyed cross-section. Previous studies (Water Authority of Western Australia, 1985a, 1985b, 1986) have also shown that the affluxes for the bridges on the Swan River in a 1% AEP flow are low (i.e. ~0.1 m – 0.2 m), and are considered insignificant when considering the accuracies/sensitivities of the modelling work.

GIS derived

GIS was used as a tool for supplementing and extending the surveyed cross-sections. Additional cross-sections were needed to extend the area modelled over previous studies, to reduce the distance between the surveyed cross-sections and to lengthen the surveyed cross-sections to cover the width of the floodplain for flows greater than the 1% AEP event. Extension of the cross-sections was necessary as the model assumes a vertical wall where a cross-section does not fully extend across the flooded area, underestimating the aerial extent of flooding and overestimating the depth of flooding. The extension of surveyed cross-sections and cross-section supplementation increased the accuracy of water levels and velocities, improved floodplain visualisation (particularly where streams are winding), and increased model stability.

Cross-sections derived solely in GIS were used between the Causeway and the mouth of the Swan River at the Port of Fremantle, a distance of some 23.1 km (Figure 4.8). Although surveyed cross-sectional data was available for the Canning River, the spatial orientations of the cross-sections below the Nicholson Road Bridge at Langford were unknown. Where bathymetry data was available, these cross-sections were not used and cross-sections derived in GIS were used. Where bathymetry data was unavailable, the orientation of these surveyed cross-sections was estimated in GIS.

The floodplain geometry was also updated where there had been substantial changes in topography since the original surveys had been undertaken. Only one major area was identified: the section of the Swan River flowing between the suburbs of Ascot Waters and Maylands. At this location a second channel has been formed, and the adjoining area has been raised for the new residential development of Ascot Waters.

HEC-RAS's companion package, HEC-GeoRAS for ArcView was used for processing geospatial data for use with HEC-RAS. HEC-GeoRAS requires data in TIN format (triangulated irregular network). However, it was found that the cross-sections produced using the TIN did not adequately reflect the channel geometry, largely because of insufficient data sampling points extracted by the program. In order to improve the representation of the channel geometry, an Arc Macro Language (AML) script was written to extract elevations at 5 m intervals along each cross-section from a 5 m Arc-Info grid of the digital elevation model (DEM). Where there was no bathymetry available, channel width was estimated using the orthophotos and channel depth was estimated by interpolating between the surveyed cross-sections. These cross-sections were then incorporated back into the DEM for the damage analysis.

River and channel delineation

The spatial location of the river reaches were derived using a combination of water course data available from the Department of Land Information in Western Australia, the othophotos, the TIN and the survey data. The stream channel was differentiated from the floodplain by manually locating the left and right channel banks for each cross-section. Where the location of the left and right channel banks of the GIS derived cross-sections were unclear from the channel geometry, they were estimated in conjunction with the 2001 orthophotos. However, the location of the stream channel was still sometimes difficult to determine because of dense tree coverage in the orthophotos. On the Swan River around the suburbs of Maylands and Ascot Waters, and the Causeway, the flow in the channel

was split around each island. The levee on Wungong Brook, a tributary of the Canning River, was also added.

Floodplain roughness

Manning's 'n' was used to estimate channel and floodplain roughness for each of the cross-sections, which is used as a measure of the resistance of the channel to the flow. One Manning's 'n' value was used for the combined channel and overbank areas in earlier flood studies, which were calibrated to match actual flood levels. In this research, three roughness values were assigned for each cross-section, namely the left and right overbank areas and the main channel. Roughness was initially estimated using Chow's (1959) book on *Open Channel Hydraulics*, which describes numerous channel and floodplain types and gives a range of recommended values of 'n' for each. These channel and floodplain types were estimated using 2001 orthophotos. However, Manning's 'n' was then calibrated against 47 recorded flood levels from the 1983 and 1987 flood events, to establish the Manning's 'n' values used in the modelling of the design floods.

Digital elevation model

The 5 m DEM and digital terrain model in Arc-Info TIN format was developed for the whole study area using a combination of bathymetry point data in the stream channels, and detailed contour and/or dense spot height data for the remaining floodplain area. This provided significant improvements in resolution over the 10 m DEM initially developed. Availability of computer memory (influenced by the detail of the data used and computational capacity), limit the resolution of the DEM, as the memory required for processing the DEM is thirteen times the size of the final product. The resolution used in the model was more than adequate for the purposes of the flood assessment undertaken.

The bathymetry data used in the DEM was provided by the DPI. The contour and spot height data was obtained from the Department of Land Information in Western Australia. The contours ranged from 1 m in the built-up areas to 10 m in the country. Non-terrestrial artefacts (e.g. tall buildings and trees) were filtered from the input contour and spot height data by comparing cross-sections in HEC-RAS with the DEM and othophotos. Limited fieldwork was also undertaken. As Figure 4.8 shows, the bathymetry data extends from the Indian Ocean, up the Swan River to Middle Swan Road Bridge, Middle Swan, with a small gap in the data in Perth Waters, near South Perth. Up the Canning River the bathymetry data extends to Fern Road at Riverton Bridge, Riverton where there is a gap for 2.6 km until the Kent St barrage. From the barrage the bathymetry data extends for a further 2.8 km upstream. The concentration of points varies on the Swan–Canning, it is typically higher in areas around bridges, where dredging has occurred, or where there has been a history of flooding.

Where no bathymetry data were available, the geometry of the stream channel was estimated by interpolating manually between the nearest surveyed cross-sections. There were only two areas where this was difficult: in the upper Jane and Susannah tributaries, where cross-sections derived in GIS were used to extend the cross-sections beyond the surveyed cross-sections for a further 2.6 km and 0.6 km respectively (Figure 4.8).

The surveyed cross-section data were incorporated into the DEM to reduce anomalies in the floodplain mapping. The anomalies are caused by slight differences in elevation between the DEM and the surveyed data at the same location, resulting in inaccuracies in the modelled spatial extent of flooding and water depths.

Streamflow hydrographs and tidal data

Streamflow and tidal data are used at all external boundaries of the model and establish the flows in the system. The tidal cycle is used as the lower boundary condition at the outlet of the model. Streamflow data is used for the upstream boundary conditions and at a number of locations downstream. Streamflow data can either be historical or can be estimated during the hydrologic component of the model. Boundary conditions can be input in a variety of ways, including flow and/or stage hydrographs, or rating curves.

Initial conditions

Initial conditions establish the starting water surface at the upstream ends of the river system and at the beginning of each reach. These are necessary for the program to begin its calculations. Where the flow is divided, such as around an island, initial conditions were based on the volume of flow estimated to flow on either side of the island, with the main channel (Maylands and Burswood sides) having higher initial conditions (Figure 4.8).

Model stability and uncertainties

Initially a lot of problems were encountered with model stability because of the complexities of the model geometry and rapid changes in discharge in the tributaries. One of the first steps in reducing the instabilities was to adopt a 5 minute time step for all the flow hydrographs, reducing the change in discharge between individual time steps.

Rapid changes in elevation between cross-sections, particularly in the steep upper reaches of the tributaries, also caused instabilities. To reduce the sharp changes in elevation, additional cross-sections were interpolated using the surveyed and GIS derived cross-sections. In the upper reaches of the Susannah and Jane Brooks, the changes in elevation were so rapid (an average drop in elevation of 30 m per kilometre), that the model remained unstable even when the number of interpolated cross-sections was significantly increased. A stable model was attained only when the very steep upper reaches of the Susannah and Jane tributaries, which flow through native bush and farmland, were not included in the model. The discharges recorded at the Gilmours Farm and National Park gauging stations were still used, but were applied 6.4 km and 3.4 km respectively downstream from the gauging stations where the gradients were not as steep. Therefore, though these gauging stations have been tied into AHD, the historical stage hydrographs could not be used.

Although the addition of interpolated cross-sections can improve model stability, the interpolated channel may not necessarily reflect the actual channel geometry. The model assumes a straight line between the two measured cross-sections; therefore, the interpolated channel may not be in the same location as the real channel. The problems become particularly evident when visualising the flooding spatially in GIS, using the othophotos as a backdrop, and when calculating water depths using a DEM. The appropriateness of the interpolated cross-sections was therefore checked using the DEM and othophotos to see if these cross-sections were realistic. Where necessary, additional cross-sections were derived from the DEM at strategic locations to reduce the number of interpolated cross-sections and associated inaccuracies.

A flow minimum of 1 m^3/s was assigned to hydrographs on the Helena, Susannah and Wungong tributaries where the initial flow was lower to help avoid instability problems. This was necessary as the model becomes unstable where there is no flow but made no difference to the impact of flooding. During the 1987 event, a minimum flow of 40 m^3/s was adopted for the Avon River at Walyunga, because the model became unstable for lower initial flows.

A restart file was used to establish initial conditions to keep model from going unstable at the beginning of the simulation. All the inflow hydrographs were set at a constant flow (which was base flow). The stage hydrograph downstream boundary was set up with high tailwater, which was then decreased gradually to the water level of the tidal cycle over a period of 36 hours. A high initial tailwater condition for the restart file was not needed for all the scenarios, though a restart file was.

Model calibration

The primary purpose of model calibration is to replicate the historical water level and/or discharge and volume, the time to peak and hydrograph shape. A properly calibrated model may then be used to estimate the impact of flood events beyond the period of record. In order to calibrate an unsteady flow model, historical streamflow and/or historical stage hydrographs are required for the upstream boundaries of the model, and preferably for at least one location downstream. The historical tidal cycle

is used as the downstream boundary of the model. For calibrating the model along the stream network, historical peak water levels at a number of locations along the Swan and Canning Rivers are necessary.

Streamflow gauging stations in the study area were identified and examined to determine the availability of data for model calibration. The gauging stations in the study area, their length of record, data format available and other associated information is shown in Table 4.6.

The location of the gauging stations (616011, 616189, 616040, 616178, 616018, 616153) shown in Figure 4.8 and included in Table 4.6 delimit the upstream boundaries of the model for calibration purposes with the exception of the gauging stations on the Swan River (ie, Meadow St Bridge, 616004; Garratt Road Bridge, 616075 and the Great Northern Highway, 616076). The lower boundary of the model is delineated by a tidal cycle for the Port of Fremantle. The spatial extent of the model for calibration was slightly smaller than for the design flood events as no historical data was available upstream of Mackenzie Grove gauging station (616027). The design flood events however were modelled as far as the Brookton Highway on the Canning River, another 7.4 km upstream (see Figure 4.8).

A major limiting factor in the calibration of the model is that the streamflow data for the larger flood events was not recorded. Of the six gauging stations at the upstream boundaries of the model, historical streamflow data is only available since 1981. The period since then has been relatively dry, with only two flood events estimated to be equal to or greater than a 10% AEP as shown in Table 4.1. The 1983 flood was estimated to have a 10% AEP on the Avon River at Walyunga (616011). The 1987 flood event was estimated to have a 4% AEP on the Canning River at MacKenzie Grove (616027). The estimated peak discharge for these events is given in Table 4.7.

Table 4.7: Peak discharge and estimated AEP for the July 1983 and 1987 floods

Stream	Gauging station	Peak discharge (m^3/s)		AEP (%)	
		1983	1987	1983	1987
Avon	616011	650	158	10	60
Canning	616027	9	55	40	4

Only the Meadow St Bridge site (616004) can be used for calibration as the Garratt St Bridge (616075) and Great Northern Highway (616076) gauging stations on the Swan River became operational in the 1990s. At the Meadow St Bridge (616004) gauging station only stage hydrograph may be calibrated as this site is tidally affected, which excludes discharge or volume measurements. Unfortunately, due to equipment problems at the Meadow St (616004) gauging station during the 1987 flood event, water levels were not recorded. Historical tidal fluctuations were also not available at the Port of Fremantle during the 1987 flood event. Tidal levels were calculated using tidal modelling software developed by the DPI. This software employs basic astronomical factors, and does not consider the prevailing meteorological factors.

The calibration of the model to the 1983 and 1987 events is described in the following two sections. These two flood events have been previously used in the calibration of earlier flood studies of the Avon River (Waugh, 1985) and Canning River (Water Authority of Western Australia, 1990).

Table 4.6: Streamflow gauging stations within the Swan River catchment study area

Gauging station	Stream	Station name	Managing authority	Longitude	Latitude	Catchment area (km^2)	Discharge	Stage (m AHD)	Site commenced	Site ceased
616004	Swan River	Meadow St Bridge	DOE[2]	115.972	-31.895			√	17/07/1978	29/10/2002
616011	Avon River	Walyunga[1]	DOE[2]	116.067	-31.756	119,000.0	√	√	01/04/1970	
616018	Helena River	Craignish[1]	WC[3]	116.068	-31.937	1600.0	√		c1975	
616027	Canning River	Mackenzie Grove[1]	DOE[2]	116.014	-32.097	920.0	√		01/04/1974	10/11/1999
616027[4]	Canning River	Seaforth[1]	DOE[2]	116.021	-32.097		√	√	22/04/1997	
616040	Susannah Brk	Gilmours Farm[1]	DOE[2]	116.110	-31.818	24.8	√	√	22/05/1981	20/6/2001
616075	Swan River	Garratt Rd Bridge	DOE[2]	115.917	-31.933			√	12/07/1995	28/09/1999
616076	Swan River	Great Northern Highway	DOE[2]	116.018	-31.787		√	√	01/01/1994	
616189	Ellen Brk	Railway Parade[1]	DOE[2]	116.023	-31.752	590.0	√		3/10/1959	
616178	Jane Brk	National Park[1]	DOE[2]	116.091	-34.882	73.0	√	√	17/08/1962	
616153	Wungong Brk	Kargotich[1]	WC[3]	116.028	-32.199	146.0	√		c1980 (post dam)	

Notes:
[1] These gauging stations form the upstream boundaries of the model for calibration purposes.
[2] DOE = Department of Environment, formerly the Water and Rivers Commission.
[3] WC = Water Corporation
[4] The gauging station at Seaforth replaced Mackenzie Grove as the primary gauging station when it became operational in 1997, and adopted the same gauging station number as had been used at Mackenzie Grove.

1983 flood event

Two flood events were recorded in the winter of 1983 on the Swan River, though the West Australian (28 July 1983) reported that there was little property damage. The second and larger of the floods is used for model calibration, peaking at the Walyunga gauging station (616011) on the Avon River on 27 July 1983 at 06:00. This event was approximately a 10% AEP at Walyunga and a 40% AEP on the Canning River at MacKenzie Grove (616027). The same event at the Gilmours Farm (616040) and National Park (616178) gauging stations on the Susannah and Jane tributaries was estimated to be about a 20% AEP event. However, as these gauging stations are well up in the Susannah and Jane catchments (~50% of the catchment), the AEP at the gauging stations may not be indicative of the AEP of the flood event on the tributaries near the confluence with the Swan River. The AEP estimates for the Craignish gauge (616018) on the Helena River is complicated by the presence of Mundaring Weir further upstream, however flow for this flood event would also be well below a 10% AEP event.

Figure 4.9 depicts the flood hydrograph at Walyunga (616011) over the time period 23 July 1983, 24:00 – 7 August 1983, 08:00. The tidal data at the downstream boundary of the model over the corresponding time period is shown in Figure 4.10. Figure 4.11 depicts the historical hydrographs over the equivalent time period on the tributaries. Rather than experiencing a single hydrograph as at Walyunga, the tributaries experienced a series of smaller, peaky hydrographs during the corresponding period.

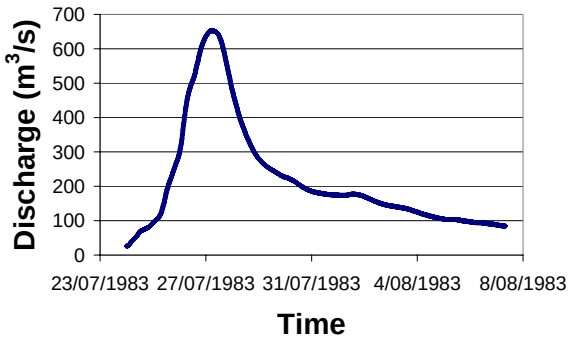

Figure 4.9: Flood hydrograph on the Swan–Avon River at Walyunga gauging station (616011), 23 July 1983, 24:00 – 7 August 1983, 08:00

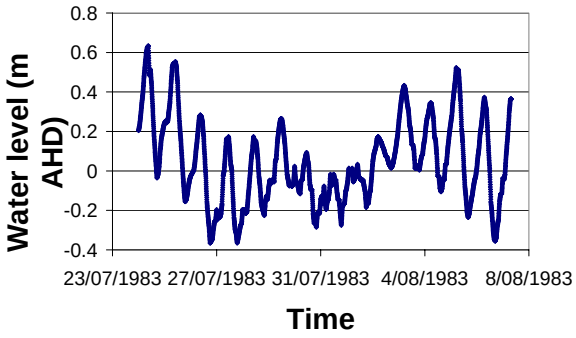

Figure 4.10: Tidal cycle at the Port of Fremantle, 23 July 1983, 24:00 – 7 August 1983, 08:00 (Data courtesy of DPI)

a) Ellen Brook (616189)

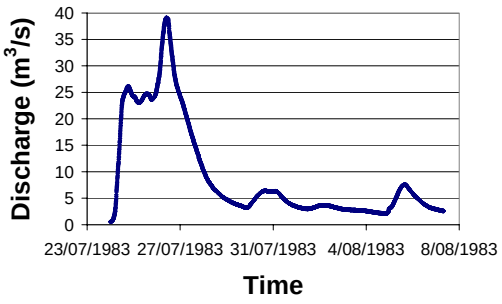

b) Susannah Brook (616040)

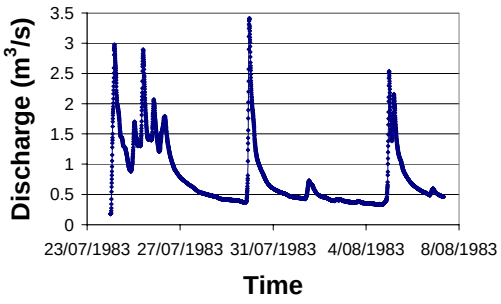

c) Jane Brook (616178)

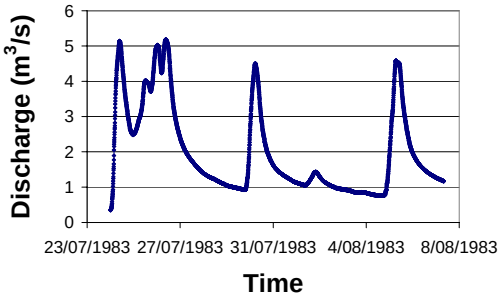

d) Helena River at Craignish (616018)

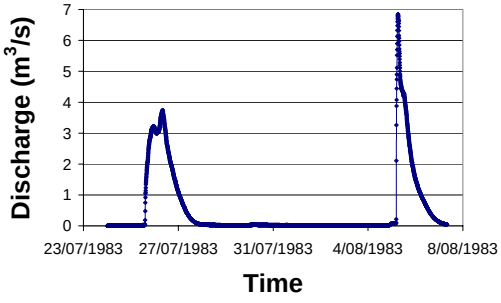

e) Canning River (616027)

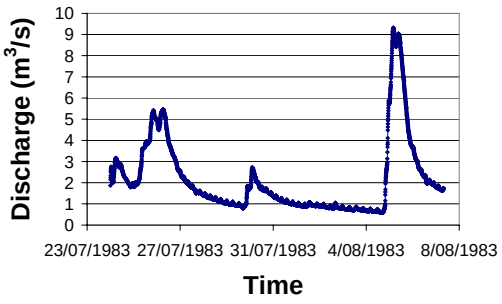

f) Wungong Brook (616153)

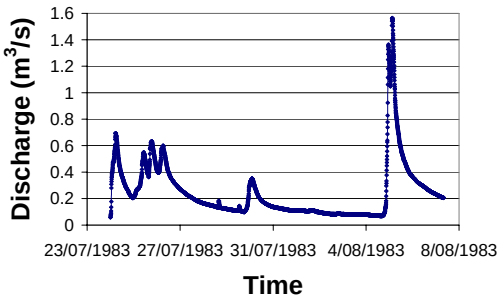

Figure 4.11(a–f): Hydrographs for the streamflow gauging stations on the major tributaries to the Swan River for the period 23 July 1983, 24:00 – 7 August 1983, 08:00

Before the model was calibrated at the Meadow St gauging station (616004) on the Swan River, the peak flow was too low and the time to peak too short. In order to increase the modelled flood peak a trial and error approach was adopted. Small amounts of lateral inflow were added, however, the resulting peak stage was vastly overestimated. Manning's 'n' was then calibrated to 39 peak recorded water levels on the Swan River between the Causeway and the Great Northern Highway Bridge, a distance of 40.1 km. The observed and modelled (after calibration) stage hydrograph at Meadow St (616004) gauging station is shown in Figure 4.12. The calibrated model reduced the difference between the observed and modelled peak water level at the Meadow St (616004) gauging station by 0.4 m and a time of 1.5 hours. Figure 4.13 is a longitudinal profile of the Swan River upstream of the Causeway showing modelled peak flood levels after calibration and the observed peak flood levels.

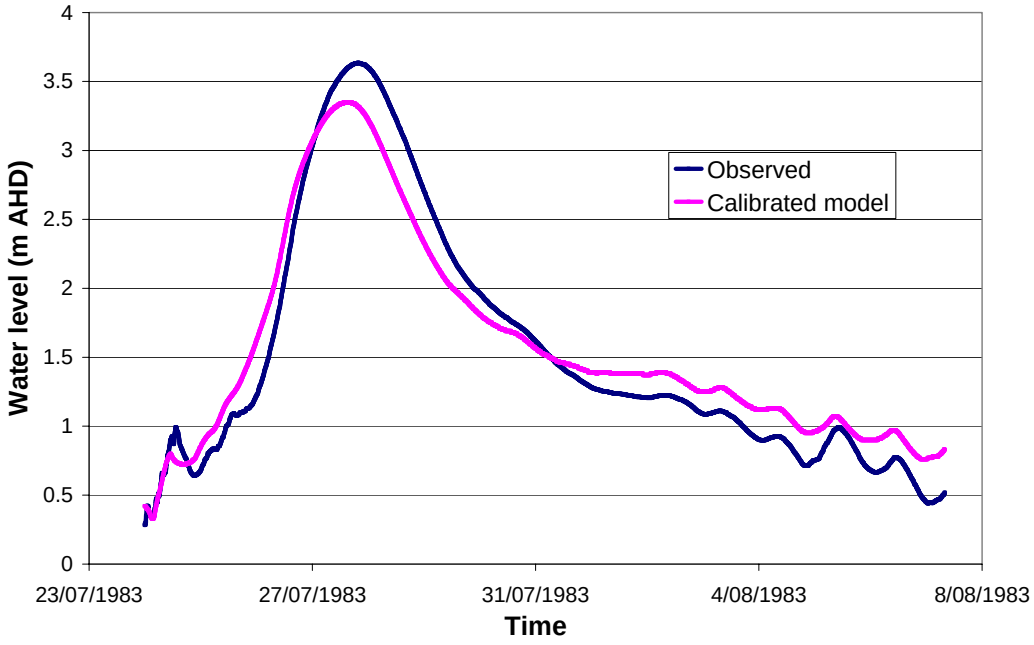

Figure 4.12: Hydrographs at Meadow St gauging station (616004) on the Swan River between 23 July 1983, 24:00 – 7 August 1983, 08:00 (Observed versus modelled)

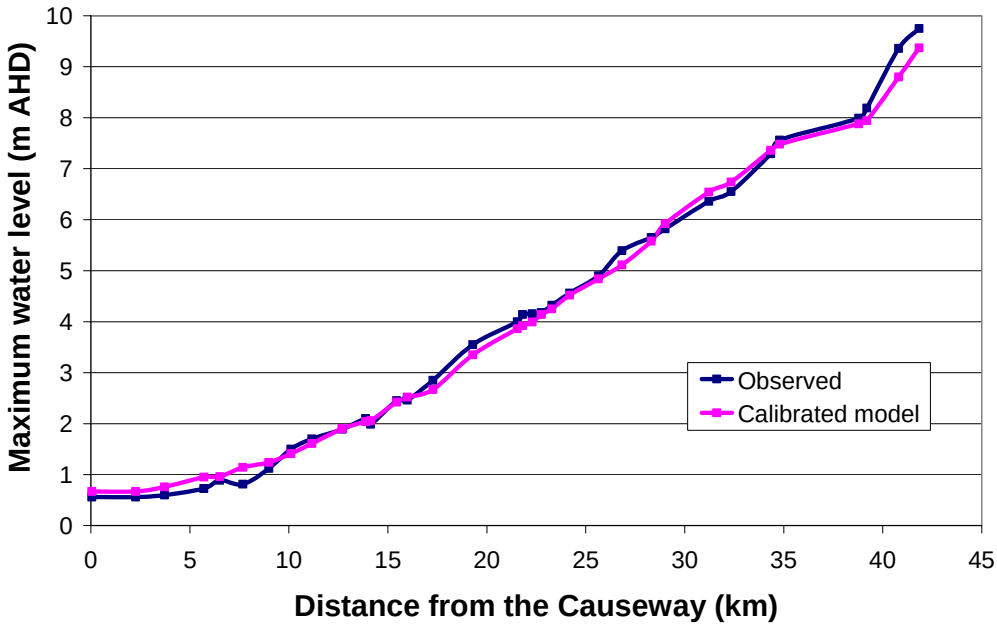

Figure 4.13: Maximum water levels on the Swan River during the July–August 1983 flood event (Observed versus modelled at the corresponding locations)

1987 flood event

The 1987 flood on the Canning River has an estimated AEP of 4%, peaking at the MacKenzie Grove (616027) gauging station on 29/07/1987 at 10:00. The equivalent event on the Avon River is estimated to be roughly a 60% AEP at Walyunga gauging station.

The geometric data which were calibrated to the 1983 flood event on the Swan River were used as the basis for calibrating the geometric data for the Canning River using the 1987 flood event. A longitudinal profile for the Canning River showing modelled peak flood levels after calibration and observed peak flood levels is shown in Figure 4.14. Peak flood values were recorded on the Canning River from Old Nicholson Road, 17.7 km upstream of the junction with the Swan River, for a distance upstream of 16.7 km. No flood levels were available for the Swan River or the other tributaries.

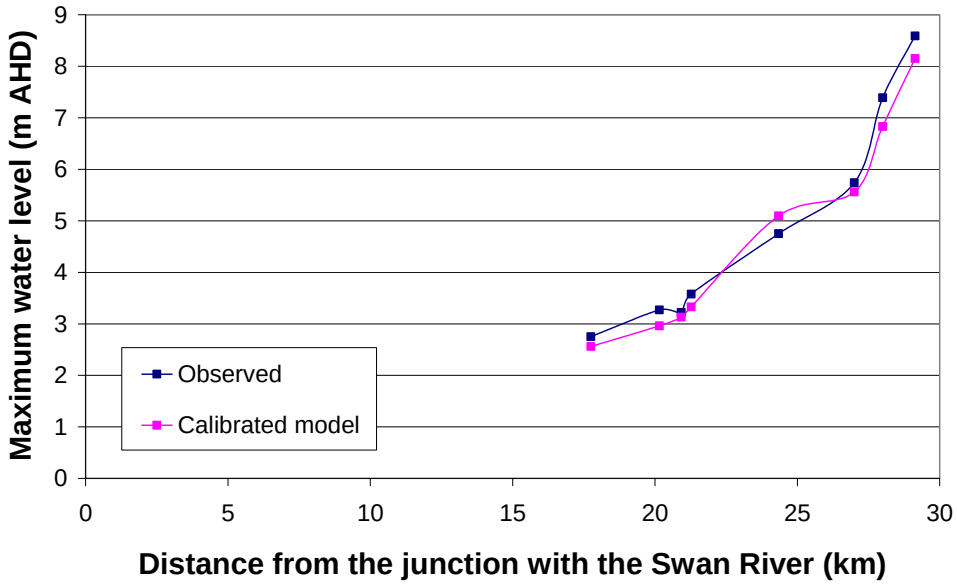

Figure 4.14: Maximum water levels on the Canning River during the 1987 flood event (Observed versus modelled at the corresponding locations)

After calibration the difference between the modelled and historical water levels was reduced by between 0.18–1.08 m. To increase modelled peak flows simulated inflow hydrographs were added to account for increased flows through the urban area. As the 1987 event was equivalent to a 4% AEP event on the Canning River at MacKenzie Grove (616027), the modelled simulated inflow hydrographs for the 4% AEP event were used to calibrate the model. As Table 4.5 shows, lateral inflow has a major effect on flows between the junction with the Southern River and the Nicholson Road Bridge. Adding the simulated design inflow hydrographs increased peak flow and delayed the hydrograph peak, resulting in a calibrated modelled hydrograph much closer in shape, peak and timing to the observed. Minor adjustments to Manning's 'n' further improved calibration.

Model validation

There have been no large historical flood events on the Swan and Canning Rivers since gauging stations in the Swan River system have been operational. Therefore, model validation was difficult because major floods have not been recorded in the system. An alternative approach to model validation is to compare the results from different models. Floodplain modelling carried out by the DOE for the Swan River (Water Authority of Western Australia, 1985) was used to compare the results of the unsteady flow model.

Comparison against the DOE flood model

The 1% AEP floodplain of the Swan River has been mapped by the DOE, and is used as the basis for the provision of floodplain management advice. A comparison of peak water levels for the 1% AEP flood for the Swan River upstream of the Causeway between the two models is shown in Figure 4.16. The locations used for the comparison are the same as those used for calibration (see Figure 4.13).

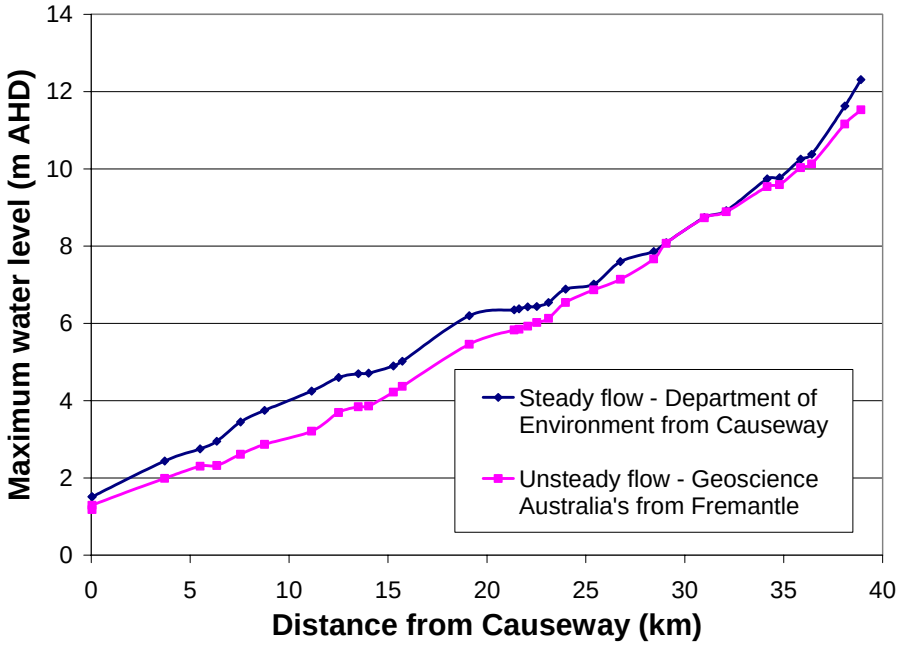

Figure 4.16: Modelled maximum water levels on the Swan River for the 1% AEP event. DOE's results using a steady flow model versus GA's results using an unsteady flow model at the corresponding locations

Flood levels in this study are generally lower than those predicted by the DOE's model at the same location. The greatest difference in water levels is just upstream of the Garrett Road Bridge at the Ascot Racecourse, where peak flood levels are predicted to be 1 m lower than that modelled by the DOE (Figure 4.16). It is important to note that significant differences exist between the two models as shown in Table 4.8, and when these differences are removed, then the results from both studies are similar as shown in Figure 4.17. The inclusion of the tributaries in this study, in particular, played a significant role. The use of the whole flood hydrograph, rather than just peak flow, also played a role in lowering the water levels in places in this study.

As both models have not been validated against high flow events it is difficult to assess the accuracy of the results. There are now sufficient gauging stations operational on the Swan and Canning Rivers and their tributaries to enable proper validation of the models using the flood levels and hydrographs recorded during a future major flood event. However, it is recommended that major river flooding in the Swan and Canning Rivers is reviewed following the next major flood event.

Impact of Tidal Cycle Variation on Flood Flows

Examination of the 19 years of predicted tidal record between 1 January 1992 and 31 December 2010 from the Tides and Waves Section of the DPI, shows seasonal variation in the tidal cycle. As seen in Figure 4.18, the highest astronomical tide (HAT) at the Port of Fremantle tidal gauge (62230) occurs in the winter months and the lowest astronomical tide (LAT) occurs during the summer months, though there is no seasonal variation in the range of water heights. Similar seasonal variations in the tidal cycle are seen at the Barrack St and Guildford tidal gauges on the Swan River as shown in Figure 4.19. During the winter months, flood flows coming down the Swan River can push the tidal cycle up even higher than would be seasonally typical at Guildford. No station numbers are available for Barrack St and Guildford as they are minor tidal gauges.

Table 4.8: Differences between the model employed in this study and the model used by DOE

This study	Earlier study: DOE
Modelled the Swan, Canning and Helena Rivers, and the Ellen, Susannah, Jane and Southern River–Wungong Brooks.	Swan River flood modelling included inflow from Ellen Brook, Jane Brook and the Helena River
Unsteady flow model, hydrographs	Steady flow model, peak discharge
Extended model geometry to Fremantle	Model geometry commenced at the Causeway
Used tidal cycle as lower boundary condition at the Port of Fremantle	Constant 1.5 m AHD was used for downstream boundary condition at the Causeway
Total number of cross-sections used was 2,786 for the Swan River and tributaries; of which 424 were surveyed, 784 were supplementary cross-sections derived in GIS, and 1977 were interpolated cross-sections derived in HEC-RAS	Used 1985 Swan River survey data comprising 128 cross-sections
Treated bridges as surveyed cross-sections	Affluxes through bridges were calculated
Updated floodplain and channel geometry where significant changes	Used 1985 Swan River survey data
Lengthened surveyed cross-sections to extend across the floodplain	Used 1985 Swan River survey data
Manning's values for channel, and left and right overbank areas. Calibrated against 39 recorded flood levels on Swan River for the 1983 flood event and 8 recorded flood levels on Canning River for the 1987 flood event	Average Manning's value for channel and overbank areas were calibrated using 39 recorded 1983 peak Swan River flood levels
Verified against DOE model	Other historical recorded peak flood levels (1872,1926, 1945, 1955, 1963, 1974) were used to verify predicted flood levels

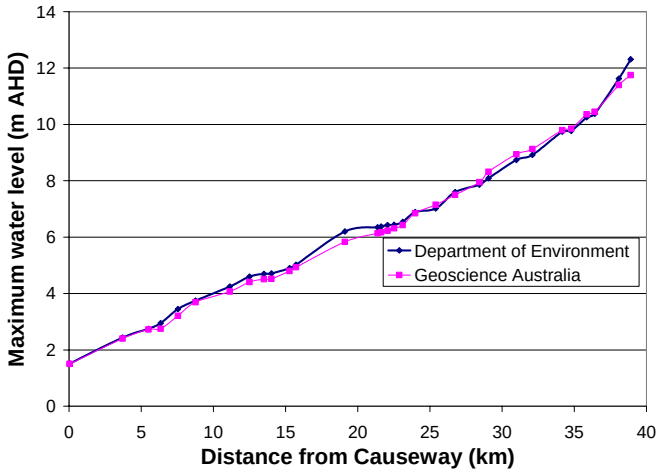

Figure 4.17: Modelled maximum water levels on the Swan River for the 1% AEP event. DOE's results are compared with those of GA's model using the same parameters. In order for GA's model to cover the same geographical location as the DOE's model, the tributaries have been excluded and the Causeway is used as the lower boundary condition rather than Fremantle. In this comparison, GA's model was also run under steady flow conditions

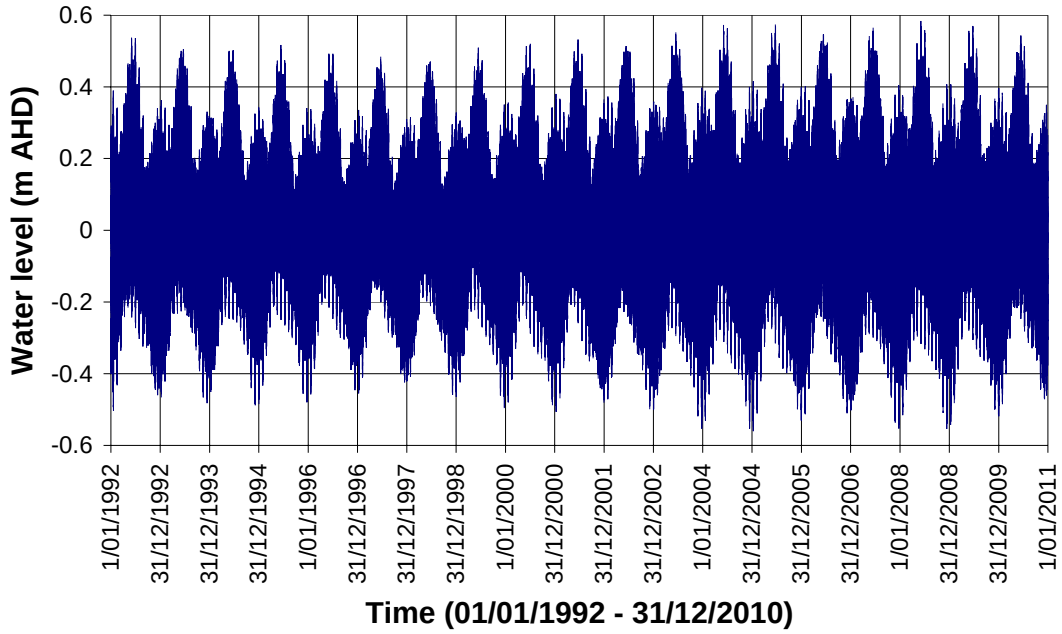

Figure 4.18: Nineteen years of tide predictions for the Port of Fremantle (62230), 1 January 1992 – 31 December 2010 (Data courtesy of DPI)

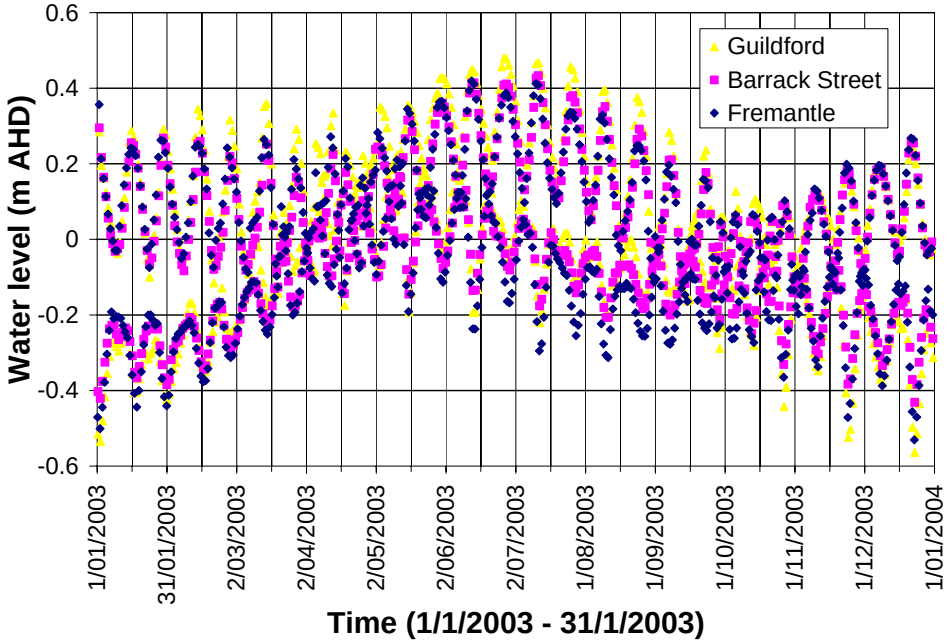

Figure 4.19: Tide predictions for the Port of Fremantle (62230), Barrack St and Guildford for 2003 (Data courtesy of DPI)

In order to assess what impact, if any, the tidal cycle has on water levels in the Swan–Canning River system, the HAT and LAT were assumed to occur simultaneously with the peak of the 1% AEP flood. In 2003, the HAT was predicted to occur on 15 June, 09:10 – 09:30 and the LAT on 24 December, 07:00 – 07:15 (Figure 4.20). The 1% AEP flood was chosen to compare the affect of the tidal cycle as the 1% AEP flood is used as the basis for floodplain management planning in Perth.

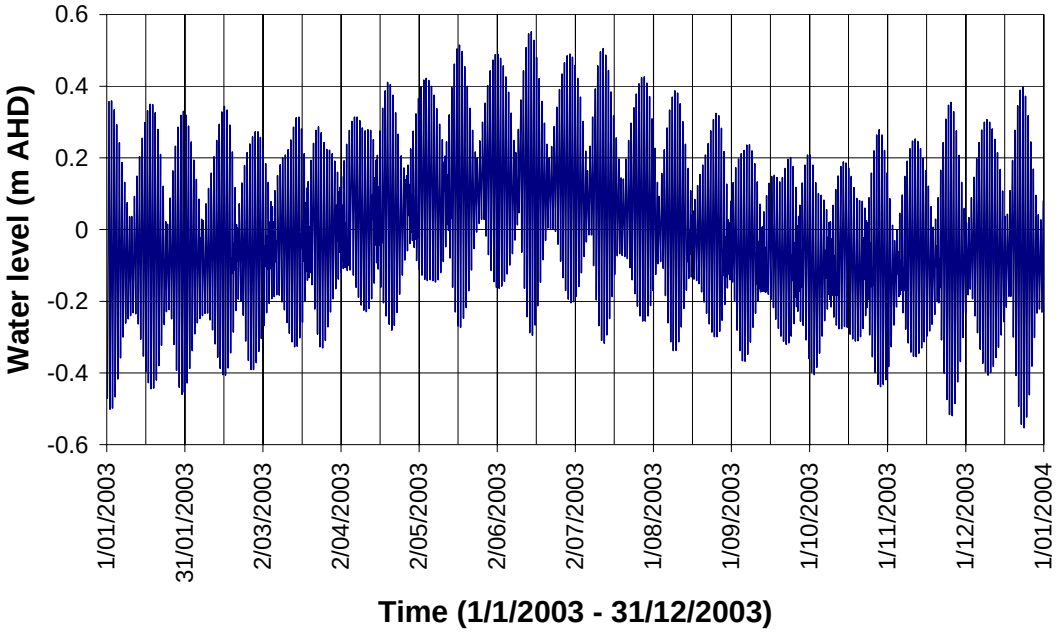

Figure 4.20: Tide predictions for the Port of Fremantle (62230) for 2003 (Data courtesy of DPI)

Figures 4.21 and 4.22 show that varying the tidal cycle has a slight impact on maximum water surface elevations, with maximum differences of 0.16 m and 0.2 m on the Swan and Canning Rivers respectively. The results modelled using the winter tide are slightly higher than those modelled using the summer tide. Upstream of the Causeway, located 25 km from the mouth of the Swan River, the variation in the maximum water surface elevation is less than 0.1 m. Approximately 45 km upstream of the mouth of the Swan River there is no variation in maximum water surface levels. On the Canning River the variation in maximum water surface levels decreased to less than 0.1 m within 12 km from the junction with the Swan River, with no variation 14 km from the junction.

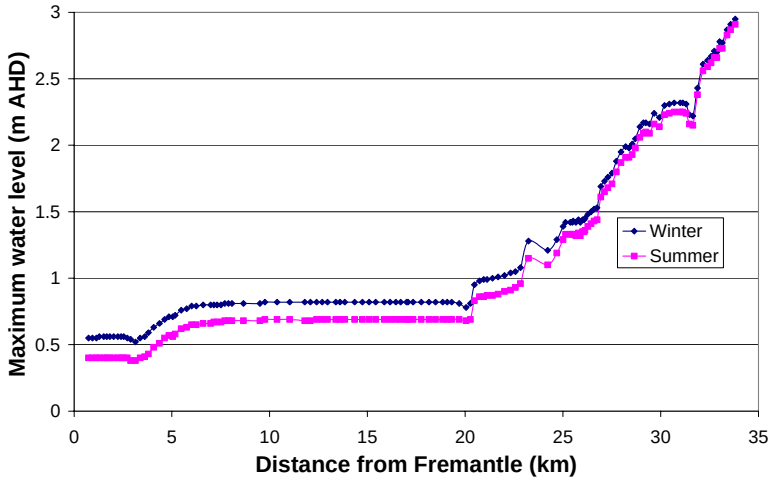

Figure 4.21: Comparison in maximum water surface elevation using the winter and summer tides, from the mouth of the Swan River to Ascot Waters

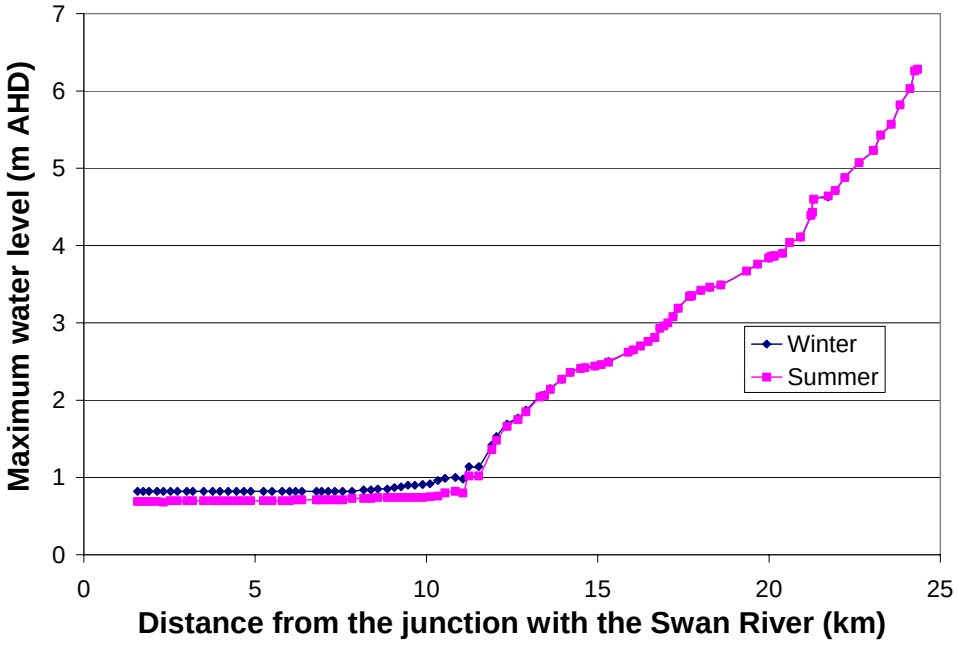

Figure 4.22: Comparison in maximum water surface elevation using the winter and summer tides on the Canning River, between the junctions with the Swan and Southern Rivers

Figure 4.23 shows the impact of varying the tidal cycle on water surface elevation over the simulation period on the Swan River. The impact of tidal cycle variation is greatest downstream of the Causeway, where the peaks and troughs in water surface elevation are reversed between the use of the HAT and the LAT (Figure 4.23). The affect decreases upstream, becoming insignificant just downstream of the Swan and Helena river junction, 40 km upstream from the mouth of the Swan River. On the Canning River there is a noticeable difference in water surface levels only on the falling limb of the hydrograph, 12.7 km upstream of the Swan and Canning river junction (Figure 4.24). As with the maximum water surface levels, the results modelled using the winter tide are only marginally higher than those modelled using the summer tide.

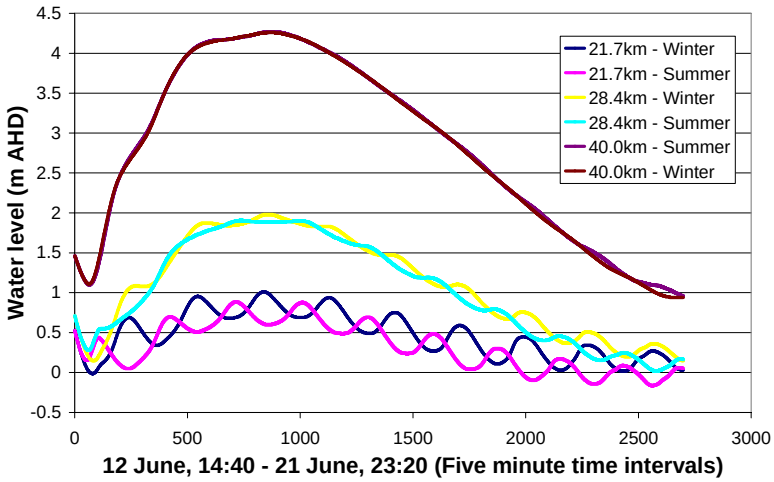

Figure 4.23: Comparison in water surface elevation over time (12 June 2003, 14:40 – 21 June 2003, 23:20) using the winter and summer tides, at distances of 21.7 km, 28.4 km and 40.0 km upstream of the mouth of the Swan River

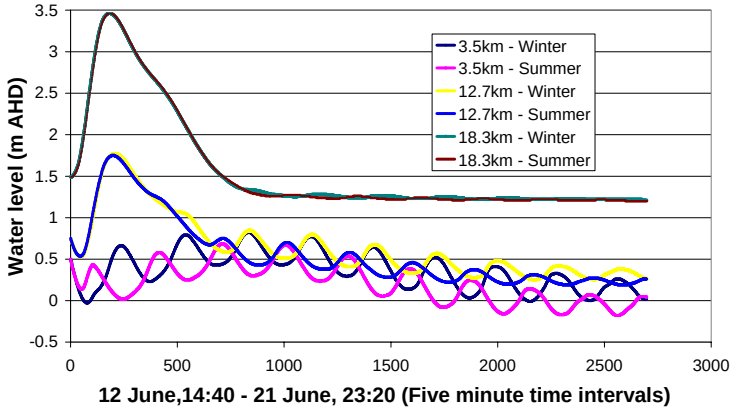

Figure 4.24: Comparison in water surface elevation over time (12 June 2003, 14:40 – 21 June 2003, 23:20) using the winter and summer tides, at distances of 3.5 km, 12.7 km and 18.3 km along the Canning River upstream of the junction with the Swan River

The areas where the variation in maximum water surface levels are the greatest on both the Swan and Canning rivers, coincides with the suburbs which are not affected by flooding during the 1% AEP event.

Impact of a storm surge

High ocean storm surges and large riverine floods generally occur as a result of low-pressure systems crossing the coast. Where the riverine flood and storm surge occur as a result of the same low pressure system, peak riverine flood levels would not occur at the mouth of the Swan River until 3–5 days after the peak ocean storm surge, due to the size of the Swan–Avon catchment. However, a storm surge of any magnitude associated with a later low pressure system than one which has caused flooding has the effect of reducing the discharge capacity of the river mouth, causing flow to back up and raise water levels beyond those identified through the modelling. This has not been studied due to the lack of data on coincident occurrence of both phenomenon. The frequency of storm surge occurrence and the probability of it happening jointly with riverine flooding need separate study.

Modelling of design floods

This section presents the flood inundation mapping for eight scenarios ranging from 10% AEP to the 0.05% AEP for the Swan and Canning Rivers and their tributaries. The modelling used the inflow hydrographs at each of the seven gauging stations, and additional simulated inflow hydrographs at 13 other locations. As floods in Perth occur most commonly during winter, the winter tidal cycle was adopted as the lower boundary condition. The winter tide was also used in the comparison of flood modelling shown in Figure 4.16 earlier.

Each AEP simulation was done with the tributaries experiencing the same event magnitude as the Swan–Avon River at Walyunga (616011), for example, the 1% AEP flow. The flood hydrographs at Walyunga (616011) typically lasted for nine days, with the peak occurring on the third day. The flood hydrographs on the tributaries typically reach base flow on the third day, peaking on either the first or second day. Base flow was assumed on the tributaries for the rest of the simulation. The peak design flow estimates for the hydrographs at the upstream boundaries of the model were shown in Table 4.3, and the difference in flow (%) between the different locations on a single stream in Table 4.5. The PMF was not modelled because of the huge uncertainties involved in modelling the extreme event.

Figures 4.25 to 4.32 show maximum water depth contours for the 10% AEP to 0.05% AEP scenarios.

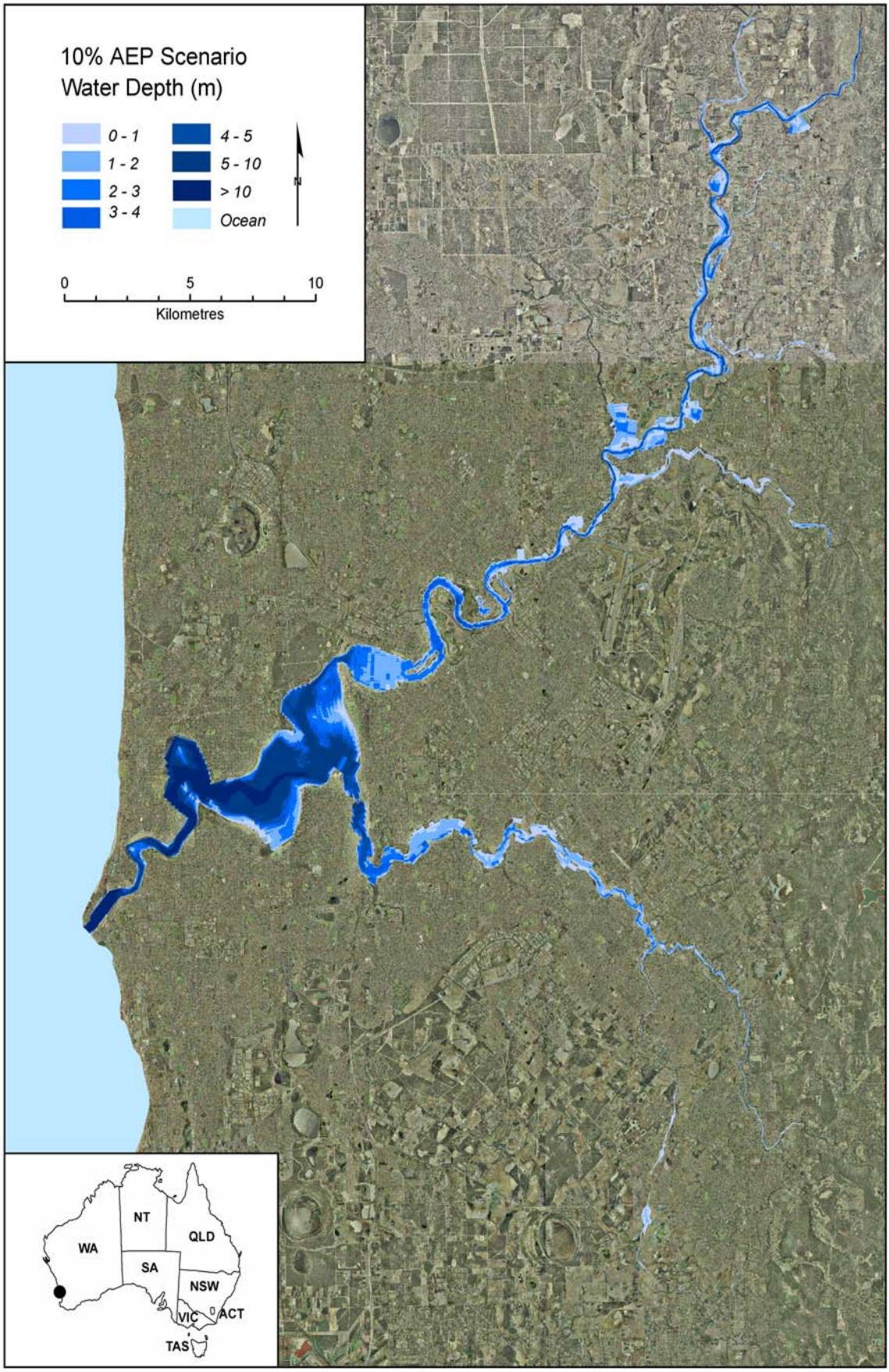

Figure 4.25: Flood inundation mapping for the 10% AEP scenario showing maximum water depth contours

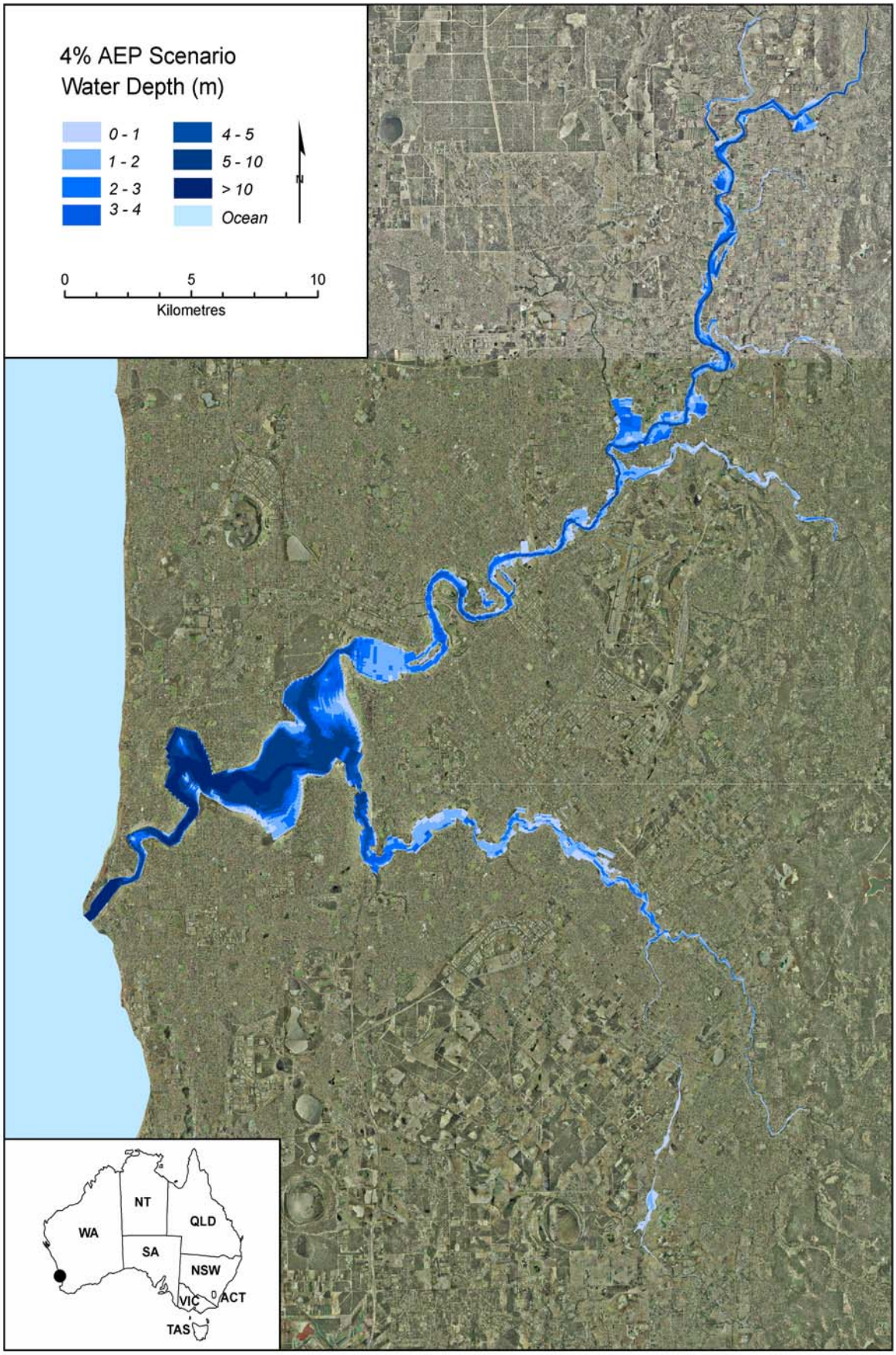

Figure 4.26: Flood inundation mapping for the 4% AEP scenario showing maximum water depth contours

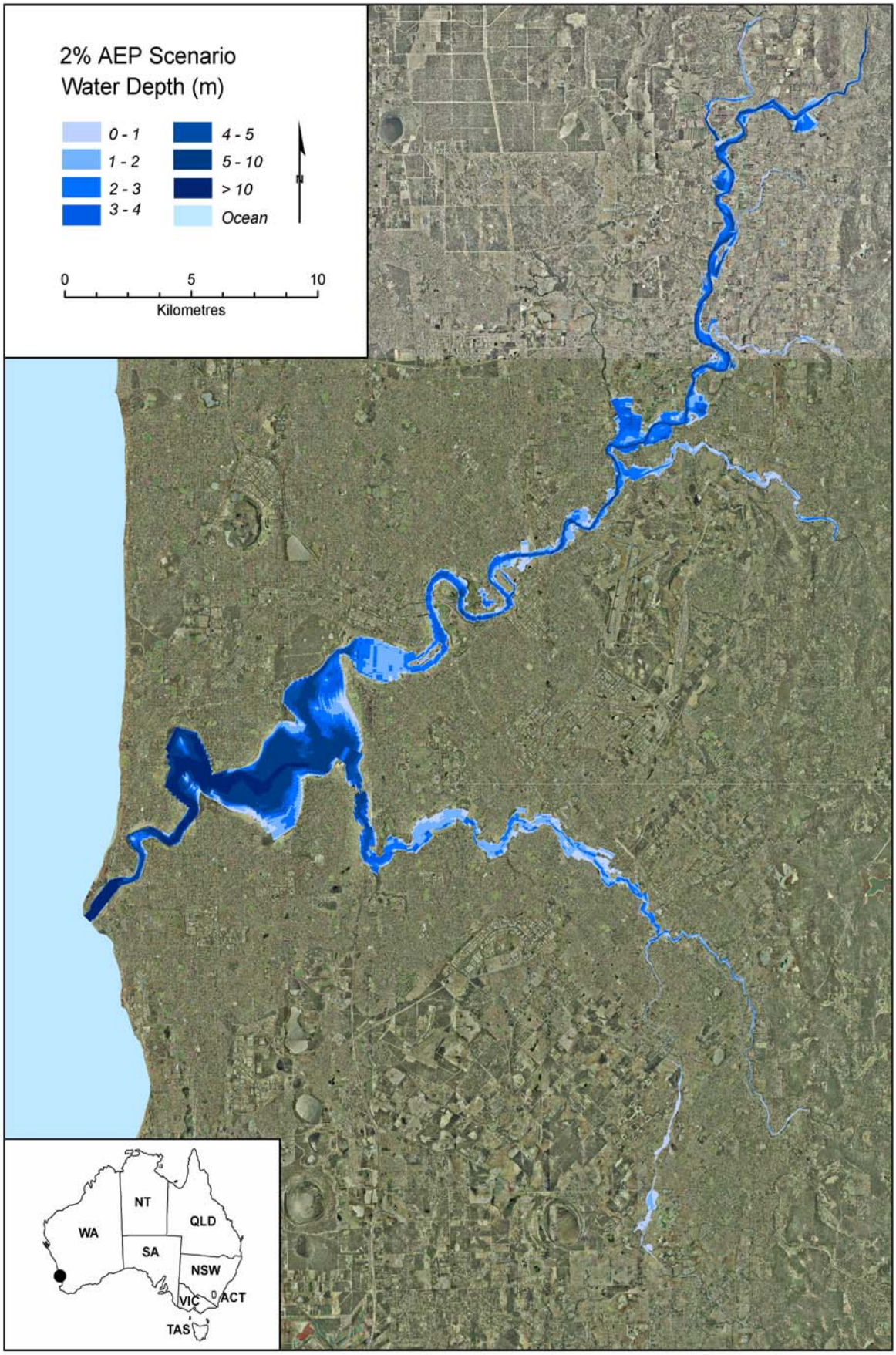

Figure 4.27: Flood inundation mapping for the 2% AEP scenario showing maximum water depth contours

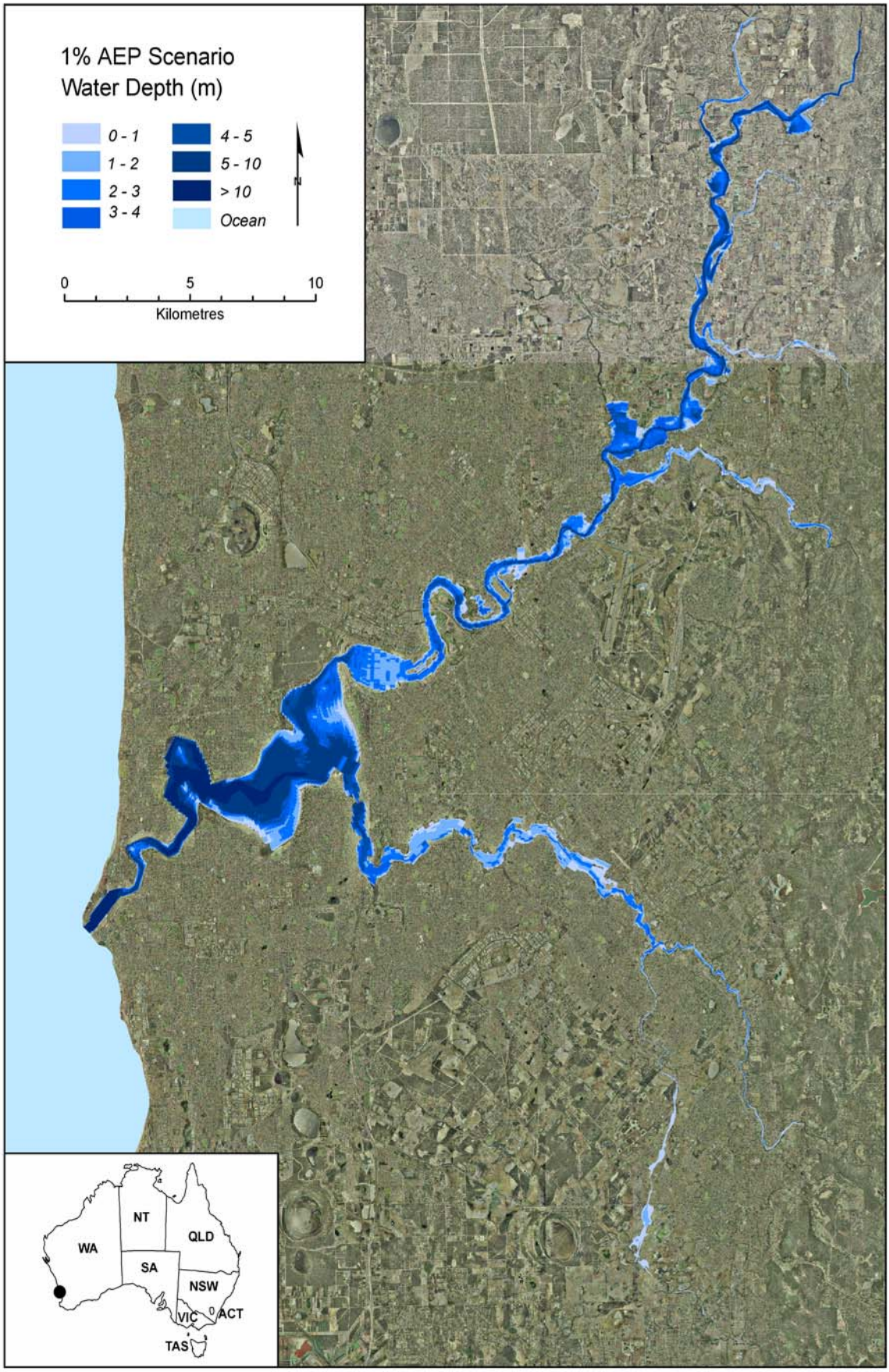

Figure 4.28: Flood inundation mapping for the 1% AEP scenario showing maximum water depth contours

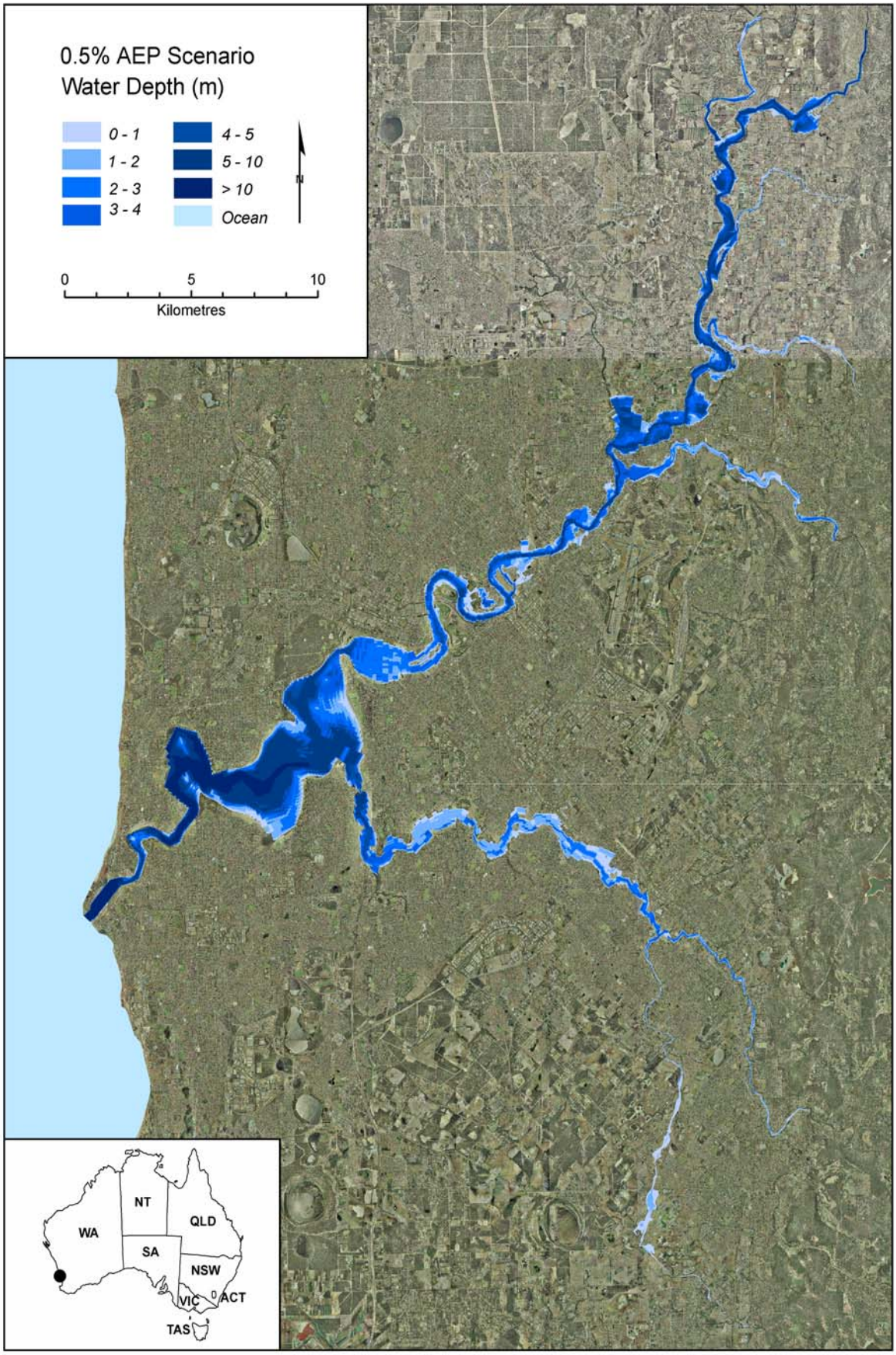

Figure 4.29: Flood inundation mapping for the 0.5% AEP scenario showing maximum water depth contours

Figure 4.30: Flood inundation mapping for the 0.2% AEP scenario showing maximum water depth contours

Figure 4.31: Flood inundation mapping for the 0.1% AEP scenario showing maximum water depth contours

Figure 4.32: Flood inundation mapping for the 0.05% AEP scenario showing maximum water depth contours

4.6 Conclusions

This chapter covered both the hydrologic and hydraulic aspects of flood estimation for the Swan River and its tributaries in Perth, Western Australia. It has incorporated hydrologic estimates and surveyed cross-sections used in previous individual studies into a single study and modelled the interactions of the tributaries with the Swan River. The geometry of the model was significantly enhanced by the addition of many cross-sections derived using a detailed DEM, which was developed specifically for the modelling of flood flows.

There are six major catchments in the study area that contribute flow to the Swan River, of which the Avon catchment is by far the largest. Unsurprisingly, the hydrologic estimation of flows showed that the Avon River at Walyunga (616011) was by far the most dominant flow contributor to the Swan River. Simulated inflow hydrographs (accounting for urban runoff), on the whole provided a significant source of additional flow to the tributaries, particularly on the Canning and Southern Rivers.

HEC-RAS was the hydraulic model used for the modelling of unsteady flows through the Swan River and its tributaries. The season of the tidal cycle was found to marginally influence flood flows, with water levels slightly higher in winter, when peak flood levels at Walyunga were made to coincide with the HAT. As expected, the influence of the tidal cycle decreases with distance upstream from the Port of Fremantle.

Perth has experienced a lengthy dry period. Only two major flows have occurred since all the streamflow gauging stations at the outer boundaries of the model became operational. These events, the 1983 flood on the Swan River and the 1987 flood on the Canning River, were used for model calibration, having estimated AEPs of 10% and 4% respectively. The dry conditions have made validation of the model even more difficult. Therefore, the results of the model were verified against the results of the DOE and found to produce similar results when the differences between the models were removed.

Water levels in this study were found to be up to a metre lower than those modelled previously for the 1% AEP flood event. The variation in water levels can be explained by the significant differences between the two models. Of these, the inclusion of the tributaries, followed by the use of an unsteady flow model rather than a steady flow model provide the best explanation for the differences.

Eight flood scenarios have been modelled for the Swan River and its tributaries ranging from AEPs of 10% to 0.05%. It is recommended that the DOE's 1% AEP floodplain mapping is continued to be used as the basis for ensuring that future development has adequate flood protection. However, it is recommended that major river flooding in the Swan and Canning Rivers is reviewed following the next major flood event.

4.7 References

Bureau of Meteorology (1999) *Generalised Probable Maximum Precipitation Estimates for the Catchments of the A) Ord River to the Ord Main Dam, B) Ord River Between the Ord Main Dam and Kununurra Diversion Dam, C) Dunham River to the Ord River Confluence*, HAS Report No: GPMP/22, Hydrometeorological Advisory Service, Bureau of Meteorology.

Bureau of Meteorology (1999) *Generalised Probable Maximum Precipitation Estimates for the Mundaring Weir, Lower Helena Pumpback Site and Churchmans Brook Dam Catchments*, HAS Report No: GPMP/21, Hydrometeorological Advisory Service, Bureau of Meteorology.

Bureau of Meteorology (1996) *Generalised Probable Maximum Precipitation Estimates for the Wellington Dam Catchment*, HAS Report No: GPMP/11, Hydrometeorological Advisory Service, Bureau of Meteorology.

Bureau of Meteorology (1995) *Climate of Western Australia*, Bureau of Meteorology, Melbourne.

Bureau of Meteorology (1986) *Estimation of Probable Maximum Precipitation for 13 Water Authority Catchments in the South West of Western Australia*, Report prepared for the Water Authority of Western Australia.

Bureau of Meteorology (1929) *Results of Rainfall Observations Made in Western Australia*, Bureau of Meteorology, Melbourne.

Bureau of Transport Economics (2001) *Economic Costs of Natural Disasters in Australia*, Report 103, Bureau of Transport Economics, Canberra.

Burnash, R.J.C., Ferral, R.L. and McGuire R.A. (1973) *A generalized streamflow simulation system: Conceptual modelling for digital computers*, Technical Report, Joint federal and State River Forecast Center, US National Weather Service, Sacramento.

Carroll, D.G. (1995) *URBS-CM Version 3.5i: A Catchment management and flood forecasting model: User Manual*, Gutteridge, Haskins and Davies, Brisbane, Australia.

Chow, V.T. (1959) *Open Chanel Hydraulics*, McGraw Hill, New York.

Davies P. (1989) *Canning River Flood Study – Hydrology*, Report No. WS 49, Water Authority of Western Australia, Water Resources Directorate, Perth.

Davies, P.K. (1988) *Jane Brook Flood Study – Hydrology*, Report No. WS 8, Water Authority of Western Australia, Water Resources Directorate, Perth.

Department of Primary Industry and Energy (1992) *Floodplain Management in Australia*, 2 vols, Australian Water Resources Council, Water Management Series No. 21, Department of Primary Industry and Energy, AGPS, Canberra.

Granger, K., Jones, T., Leiba, M. and Scott, G. (1999) *Community Risk in Cairns: A multi-hazard risk assessment*, Australian Geological Survey Organisation, Department of Industry, Science and Resources, Canberra.

Institution of Engineers (1999) *Australian Rainfall and Runoff: A guide to flood estimation*, Chapter 6, Institution of Engineers, Australia.

Institution of Engineers (1987) *Australian Rainfall and Runoff: A guide to flood estimation*, Volumes 1 and 2, Institution of Engineers, Australia.

Laurenson, E.M. (1994) 'The probability of extreme floods in Australia' in *Acceptable Risks for Extreme Events in the Planning and Design of Major Infrastructure*, Australian National Committee on Large Dams seminar, Sydney, April, 1994.

Laurenson E.M. and Mein, R.G. (1985) *RORB – Version 3, Runoff routing program: User Manual*, Second Edition, Department of Civil Engineering, Monash University, Melbourne.

Lawrence, G. and Harvey, R.A. (1978) *Swan–Avon Rivers Flood Study*, Water Resources Technical Report No. 77, Planning and Design Branch, Public Works Department, Perth.

McLaughlin A. (1992) *Susannah Brook Flood Study – Hydrology*, Report No. WS 108, Water Authority of Western Australia, Water Resources Directorate, Perth.

Middelmann, M., Harper, B. and Lacey, R. (2001) 'Flood risks' in Granger, K. and Hayne, M. (editors) *Natural Hazards and the Risks They Pose to South-East Queensland*, Geoscience Australia, Department of Industry, Tourism and Resources, Canberra, pp.9.1–9.79.

Middelmann, M., Granger, K., Harper, B., Baddiley, P. and Malone, T. (2000) 'Flood Risks', In M. Middelmann and K. Granger (Eds.) Community Risk in Mackay. A Multi-Hazard Risk Assessment. Australian Geological Survey Organisation, Department of Industry, Science and Resources, Canberra. CD-Rom, pp.69-87.

Nathan, R.J and Weinmann, P.E. (1999) *Australian Rainfall and Runoff – A guide to flood estimation*, Volume 1, Book VI, 'Estimation of large to extreme floods', Institution of Engineers, Australia.

New South Wales Government (2001) *Floodplain Management Manual: The management of flood liable land*, NSW Government, ISBN 07313 0370 9.

Public Works Department (1986) *Avon River Flood Study: Revision A*, prepared by Binnie and Partners Pty Ltd, Perth.

Public Works Department (1981) *Canning River Flood Study, Canning Bridge to Nicholson Road Brid*ge, Public Works Department, Perth.

Rodgers S.J. (1998) Swan–Avon Flood Forecasting Study – Model calibration, Unpublished Report No. SWH 16, Water and Rivers Commission, Perth

SCARM (2000) *Floodplain Management in Australia – best practice principles and guidelines*, Agriculture and Resource Management Council of Australia and New Zealand, Standing Committee on Agriculture and Resource Management, Report No. 73, CSIRO Publishing, Collingwood, Victoria.

Scatena, M.C., Jeeveraj, C.G. and Fanayan F. (1995) *Canning Dam PMF Review*, Report No. WS 146, Water Authority of Western Australia, Water Resources Directorate, Perth.

Smith, D.I. (1998) *Urban Flooding in Queensland – a review*, prepared for the Department of Natural Resources, Queensland by Centre for Resource and Environmental Studies, Australian National University, Canberra.

United States Army Corps of Engineers (2003) *HEC-GeoRAS River Analysis System*, Version 3.1, Hydrologic Engineering Centre, United States Army Corps of Engineers, California, United States.

United States Army Corps of Engineers (2003) *HEC-RAS River Analysis System, Hydraulic Reference Manual*, Version 3.1, Hydrologic Engineering Centre, United States Army Corps of Engineers, California, United States.

United States Army Corps of Engineers (2003) *HEC-RAS River Analysis System, User Manual*, Version 3.1, Hydrologic Engineering Centre, United States Army Corps of Engineers, California, United States.

Water and Rivers Commission (2000) 'Water Facts 13', Water and Rivers Commission, Perth.

Water Authority of Western Australia (1985) *Swan River Flood Study – Causeway to Middle Swan Road Review 1985*, WAWA Drawings AF04-4-1 to AF04-4-9, Water Authority of Western Australia, Perth.

Water Authority of Western Australia (1995) *Susannah Brook Flood Study, Swan River to Millendon, Perth, Western Australia*, Water Authority of Western Australia, Perth.

Water Authority of Western Australia (1990) *Canning River Flood Study, Nicholson Road Bridge to Brookton Highway*, Water Authority of Western Australia, Perth.

Water Authority of Western Australia (1989) *Ellen Brook Flood Study, Swan River to Bullsbrook*, Water Authority of Western Australia, Perth.

Water Authority of Western Australia (1989) *Jane Brook Flood Study, Swan River to Wexcombe*, Water Authority of Western Australia, Perth.

Water Authority of Western Australia (1988) *Southern River – Wungong Brook Flood Study. Canning River to South Western Highway*, Water Authority of Western Australia, Perth.

Water Authority of Western Australia (1987) *Helena River Flood Study, Swan River to Helena Valley*, Water Authority of Western Australia, Perth.

Water Authority of Western Australia (1985a) *Swan River Flood Study, Causeway to Middle Swan Road Review 1985*, Water Authority of Western Australia, Perth.

Water Authority of Western Australia (1985b) *Swan River Flood Study, Middle Swan Road to Walyunga National Park*, Review 1985, Water Authority of Western Australia, Perth.

Water Authority of Western Australia (1986) *Swan River Flood Study, Middle Swan Road to Walyunga National Park,* WAWA Drawings AF05-4-1 to AF05-4-7, Water Authority of Western Australia, Perth.

Waugh, A.S and Ng Y.H. (1987) *Ellen Brook Flood Study – Hydrology*, Report No. WS 6, Water Authority of Western Australia, Water Resources Directorate, Perth.

Waugh, A.S. (1986) *Southern River Flood Study*, Hydrology Branch, Water Authority of Western Australia, Perth.

Waugh, A.S. (1985) *Avon River Flood Study – 1985 Flood Hydrology*, Report No. WRB 119, Water Resources Branch, Public Works Department, Western Australia.

Waugh, A.S. (1984) *Helena River Flood Study – Hydrologic Investigations*, Water Resources Branch, Public Works Department, Perth.

World Meteorological Organization (1986) *Manual for Estimation of Probable Maximum Precipitation*, 2nd edition, Operational Hydrology Report No. 1, WMO No. 332, Geneva.

Chapter 5: EARTHQUAKE RISK

Cvetan Sinadinovski, Mark Edwards, Neil Corby, Mary Milne, Ken Dale, Trevor Dhu, Andrew Jones, Andrew McPherson, Trevor Jones, Duncan Gray, David Robinson and Justin White

Geoscience Australia, Canberra

5.1 Introduction

Risk assessment and its associated management is a most effective approach to addressing the impact of natural hazards on a region. It combines the hazard level with the vulnerability of the local infrastructure to give a picture of the aggregated financial consequences of a region's hazard and how this can be reduced through mitigation strategies. While the Perth metropolitan area is situated above a crustal region that exhibits low seismicity, it is located relatively close to adjacent regions that have experienced significant seismic activity during the settled history of Western Australia (WA). In this chapter the earthquake risk posed to the Perth metropolitan area is quantified by considering the seismic context of the city that contributes to its hazard and the vulnerability of its building stock. While the chapter focuses primarily on earthquake risk identification and assessment, the findings provide some basis for local government and Western Australian government agencies to review their susceptibility and preparedness.

Early attempts to quantify earthquake hazard in the southwest of Western Australia are summarised in Gaull and Michael-Leiba (1987). The first significant study was the determination of earthquake frequency in the southwest by Everingham (1968). This was followed by the estimation of ground intensity return periods for ten major centres in WA by Everingham and Gregson (1970). In 1973, McCue carried out an earthquake hazard assessment of southwest WA. Subsequently, McEwin *et al.*, (1976) made the first attempt at zoning the whole of Australia, and Denham (1976) published a preliminary Australian earthquake hazard zoning map. In 1987, Gaull and Michael-Leiba produced probabilistic earthquake hazard maps of southwest WA which were subsequently incorporated into the probabilistic earthquake hazard maps of Australia (Gaull *et al.*, 1990). It was from these maps that the earthquake hazard maps in the current earthquake loadings standard AS1170.4-1993 (Standards Australia, 1993) were derived.

The current Geoscience Australia (GA) study presents the most comprehensive and advanced earthquake risk assessment undertaken for any Australian city to date. It has focused on the economic losses associated with the building and contents damage caused by earthquake ground shaking, excluding the impacts from other secondary hazards such as soil liquefaction, fire, landslides and surface faulting. The study has adopted a probabilistic approach that makes allowances for the variability that is inherent in natural processes as well as the uncertainty in our knowledge. The study also includes an updated hazard assessment of a wider seismic region of southwestern WA which includes the more active Wheatbelt region west of Perth.

The results from this project will assist decision-makers involved in local and state government, policy development, the insurance industry, engineers, architects, and the building and finance industries to manage potential damage and loss of life from earthquakes in the Perth metropolitan region. The results also have implications for the earthquake risk facing other large Australian cities such as Sydney, Melbourne and Adelaide. This is due to a number of factors, including similarities between the earthquake hazard in Perth and that of these other state capital cities. While the Perth residential building stock is somewhat atypical due to the predominance of a single constructional form, other building types are similar to those commonly found in the other cities.

We emphasise that this report should be regarded as the best and most recent assessment of earthquake risk in Perth. However, we acknowledge that there are limitations in the models and data we have used, and that we have an incomplete understanding of the natural variability inherent in ground shaking and building response. The results, interpretations and conclusions could change with the incorporation of new data and with different model assumptions. Therefore, the reader should not take action based on information in this report alone.

In this chapter the risk methodology adopted is described. The historical seismicity of the greater region is examined and the seismic hazard quantified for both the Perth metropolitan area and the greater region. The development of an extensive building database is described, with the associated occupancy types, replacement cost models, and structural behaviour models that have been assigned to each. The risk posed by the earthquake hazard is also presented in financial terms, along with the extent of physical damage that will affect the population. Finally the implications of the results are discussed and possible mitigation strategies that could be investigated in greater detail are outlined.

5.2 Earthquake Risk Methodology

The general risk assessment philosophy adopted by the Cities Project Perth has been developed from the joint Australia/New Zealand Risk Management Standard, AS/NZS4360, (Standards Australia, 1999e). It can be expressed conceptually as follows:

Risk = Hazard × Elements at Risk × Vulnerability of the Elements at Risk

The multiplication sign does not mean a simple product but rather the convolution of the three components. For the specific case of earthquake risk assessments, this process can be described by the flowchart in Figure 5.1. A brief overview of the key risk methodology components shown in the figure is presented under separate headings below.

Earthquake hazard

The earthquake hazard in a region can be described in terms of *the level of ground shaking that has a certain chance of being exceeded in a given period of time*. It is common to describe earthquake hazard in terms of the level of ground shaking that has a 10% chance of being exceeded in 50 years. In order to calculate the earthquake hazard, three key models are needed, specifically:

- a *regional seismicity model*, which describes the chance of an earthquake of a given magnitude occurring in a year in various parts of the region;
- an *attenuation model*, which describes generally how earthquake ground shaking or intensity decreases with distance away from the earthquake source, and;
- a *site response model*, which describes how local regolith (soils, sediments and weathered rock) will affect the ground shaking experienced during an earthquake.

The regional seismicity model defines the regions that generate earthquakes. These regions are called ‘earthquake source zones’. Generally several earthquake source zones are defined with their level of activity determined from both historical seismicity and an understanding of the underlying geological structures. The level of earthquake activity is assumed uniform throughout each source zone, but differs from one zone to the next.

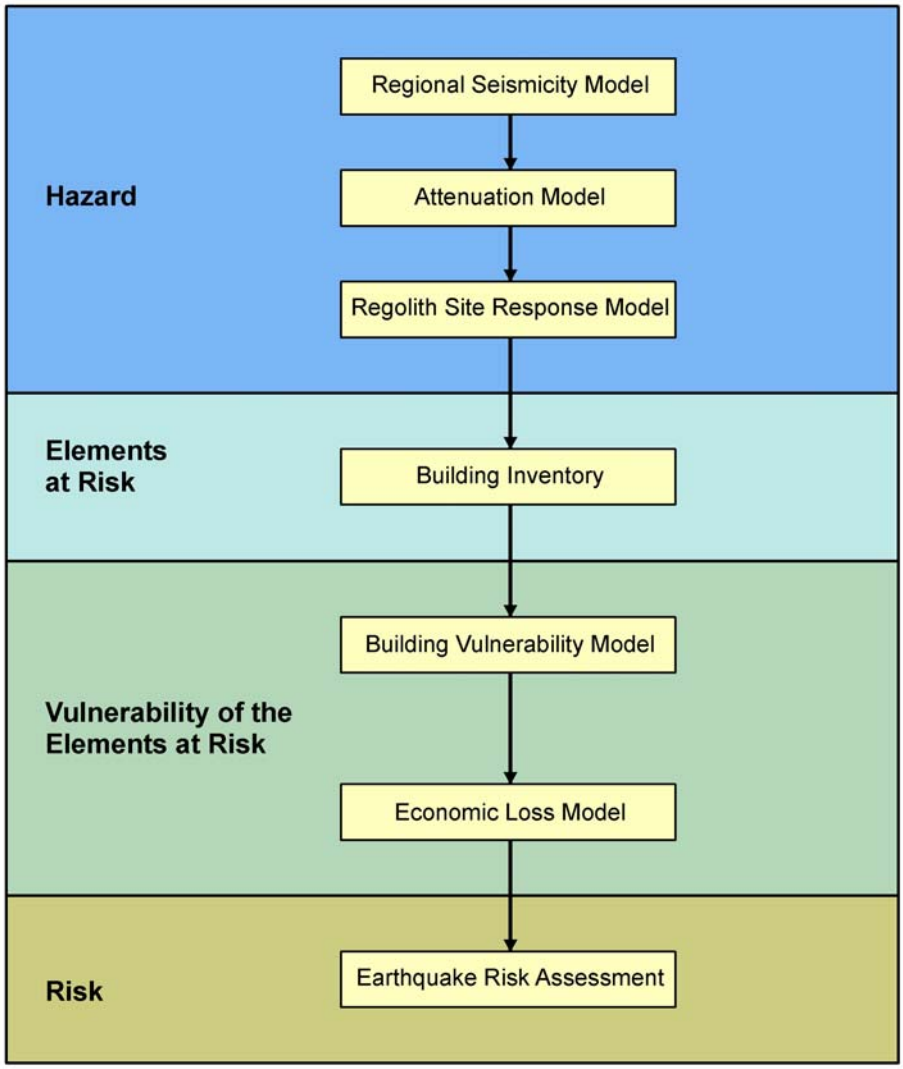

Figure 5.1: Flowchart describing the earthquake risk assessment process as applied to Perth

Attenuation models modify the earthquake waves with distance from the earthquake epicentre to give the characteristics of the earthquake vibrations below a site at bedrock level. Two attenuation models have been used in this study. The first was the model developed by Toro *et al.*, (1997) for central and eastern North America, a region of the world that is thought to have similar attenuation characteristics to Australia. The second attenuation model was that proposed by Atkinson and Boore (1995), developed for eastern North America. However, it must be emphasised that no explicit study has been conducted on the suitability of either model for Australian conditions.

The site response model adjusts the earthquake ground shaking at a site for the influence of weathered rock and overlying soils (regolith) on the propagating seismic waves. These typically amplify the vibrations, thereby causing a greatly accentuated impact upon certain building types. The Perth study region has the added complexity of an underlying sedimentary basin that attenuates components of earthquake motion in a manner not captured by the attenuation models used. The regolith model was separately developed from detailed geotechnical data, acquired primarily in Perth, which served to classify the study region into four different site classes. Subsequently these classes were incorporated into a single combined Perth sedimentary basin and regolith (soils, geological sediments and weathered rock) model that captures the influence of both on ground shaking.

Elements at risk

Risk is directly related to the *elements* exposed to the earthquake hazard. For the Perth study the range of building stock has been primarily determined using metropolitan building data held by the Perth Valuer-General's Office. This data has been supplemented with footprint data, a GA survey of 2,600 buildings using aerial photography, and a Perth flood plain field survey by GA of 2,080 buildings. Assessments of the size and associated full replacement values of the buildings and their contents were also made incorporating cost models developed through a quantity surveying consultancy (Reed Construction Data, 2003).

Vulnerability of elements at risk

Earthquake vulnerability models are used to estimate the level of damage caused by a given level of ground shaking for a wide range of building types. For the purposes of this study, building damage due to earthquake ground shaking was calculated using the method described in Kircher *et al.* (1997). This approach allows the calculation of damage on the basis of building type. For example, given a certain level of ground shaking, the damage to an unreinforced masonry structure would be different from the damage to a timber-framed structure.

Work from the Federal Emergency Management Agency (FEMA) in the United States was used to create models to convert estimates of building damage into estimates of economic loss. These models have gone through a process of modification to better represent the vulnerability of the common Australian building types. In this study, economic loss is defined in terms of the restoration cost of local buildings and their contents. In the modification process the FEMA models were calibrated, in part, using the restoration costs for Australian building types.

Earthquake risk

The earthquake risk to the study region was assessed by taking into account the earthquake hazard, the elements at risk and the vulnerability of those elements to earthquake ground shaking. In this study, these three components have been used to calculate earthquake risk by:

- conducting double computer simulations of approximately 9,400 earthquakes across the study region, each with its own magnitude and probability of occurrence based upon the regional seismicity model;
- using the attenuation and site response models to determine the level of ground shaking from every simulated earthquake at each of the surveyed buildings;
- using the vulnerability models to calculate the damage and economic loss to every building from each earthquake;
- aggregating the losses across all the buildings in the study region to produce an estimate of loss for each of the 18,800 event simulations, and;
- determining the study region earthquake risk by combining all earthquake event losses in accordance with their respective probabilities of occurrence.

The earthquake risk calculations were performed using the GA software EQRM (Robinson and Fulford, 2003) which incorporates all the computational steps described above.

5.3 Earthquake Bedrock Hazard

Introduction

An earthquake hazard model was developed for the Perth metropolitan area as a part of the Cities Project Perth. The earthquake hazard in Perth is influenced by the seismicity of the southwestern seismic zone (SWSZ) to the east of Perth, the site of some of Australia's highest historic earthquake activity. Three large earthquakes have caused considerable destruction and surface ruptures in that zone. The highest incidences of earthquake epicentres are centred on Meckering and Cadoux, where an 's'-shaped zone extends from 180 km northeast to 110 km southeast of Perth. The epicentres south

of Meckering correlate strongly with structural trends inferred from aeromagnetic data and a more general north-northwest trend of the major gravity gradient.

Development of the hazard model requires knowledge of the historical earthquakes and potentially active faults over a broad region centred on Perth. A workshop was held at Geoscience Australia on the 2nd December 2002 with the purpose of defining an appropriate model of seismicity for southwestern WA. It was attended by expert Australian seismologists and structural geologists and was followed by later rounds of discussion and determination of results. The workshop participants proposed a seismicity model with the following earthquake source zones (shown in Figure 5.8):

- Zone 1, the SWSZ, modified from Gaull *et al.* (1990) to include the Burakin events;
- Zone 2, east of the Darling Fault, with boundaries modified from Gaull *et al.* (1990) to align with the Darling Fault and regional structural trends;
- Yilgarn Zone, extending across the remainder of the Yilgarn Craton;
- Zone 3, an offshore zone extending to the continental margin, modified from Gaull *et al.* (1990); and
- Background Zone, including the Perth Basin.

Seismicity parameters were determined for each of the source zones from statistical analyses of historic earthquakes. Alternate source zone models had maximum magnitudes ranging from 7.0 to 8.0 (seismic moment magnitude). The earthquakes were assumed to occur in the top 20 km of the crust, while their mechanisms were assumed to be predominantly reverse faulting with the principal stress axis normal to the regional north-northwest structural trend.

The seismicity models were used to generate earthquake hazard estimates and hazard maps for metropolitan Perth and later combined with models of soil site amplification. Subsequently, earthquake risk was estimated through considerations of likely damage and replacement costs.

Principal results indicate that the new seismicity model produces higher estimates of the Perth earthquake hazard in terms of peak ground acceleration for than those in the current Australian earthquake loadings standard (Standards Australia 1993). However, estimated spectral accelerations were found to be similar suggesting that the current design standard hazard is adequate and, in some instances, conservative. The most significant factor in the hazard calculations was the choice of an attenuation function for earthquake ground shaking. The earthquake strong motion recorded from the Burakin 2001 sequence helped in the preliminary selection of the appropriate regional attenuation relations.

Geology and geophysics

The characteristics of the SWSZ were addressed in the context of Western Australian geology. The exact boundaries of the zone are not precisely defined, but it lies within the Yilgarn Craton, which is part of the Archaean Shield structure – an area of very ancient rocks. (Figure 5.2). The southwest Yilgarn Craton was previously subdivided by Gee *et al.* (1981) into the Western Gneiss Terrane (WGT), and two granite greenstone provinces to the east, the Murchison and Southern Cross Provinces. Boundaries between the provinces were only approximately located but inferred to separate crust with contrasting geological attributes: particularly the relative abundance of older gneissic belts in the WGT, and the structural orientation and lithological content of greenstone belts in the Murchison and Southern Cross Provinces.

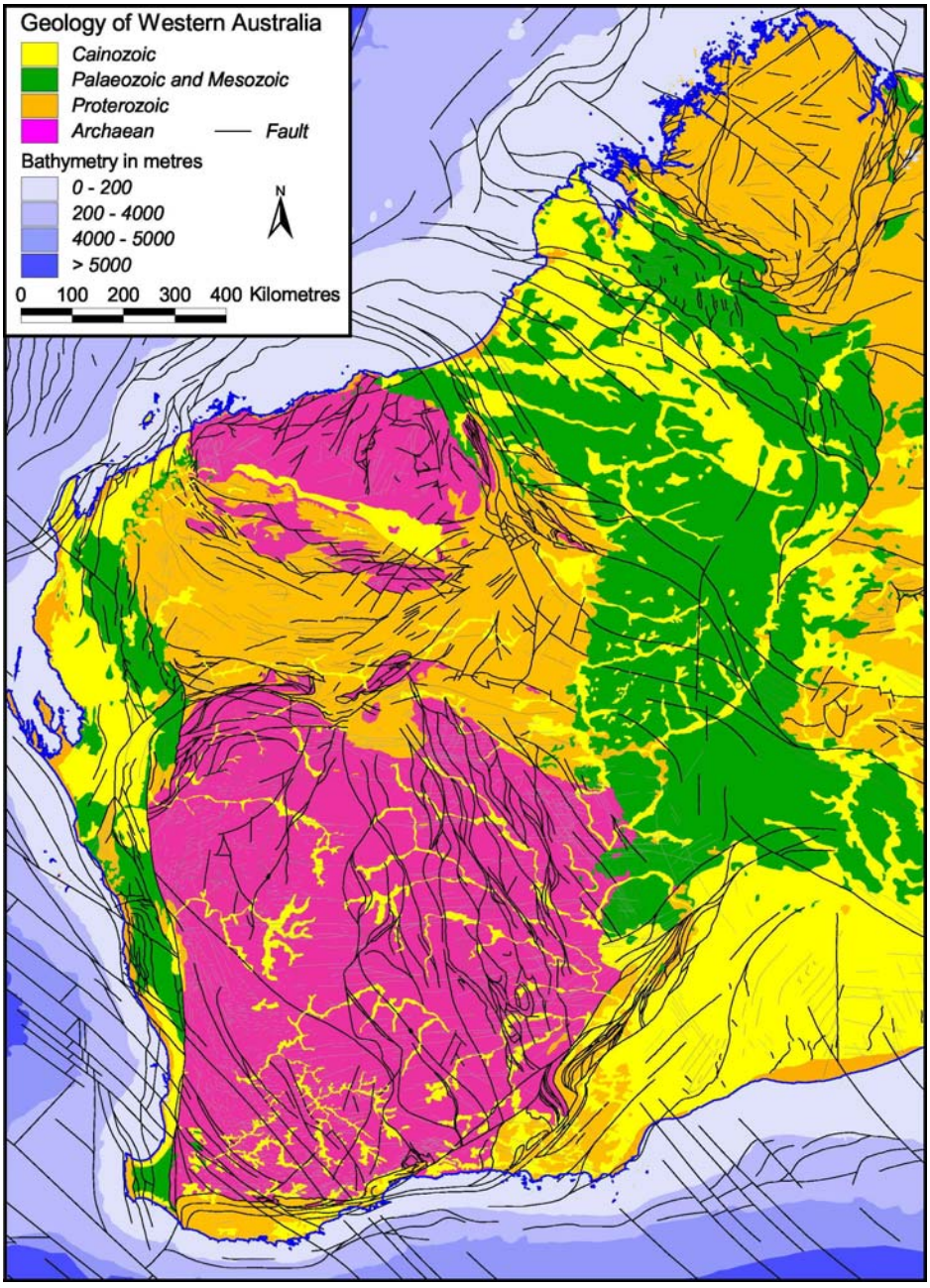

Figure 5.2: Geology of Western Australia. The Cainozoic rocks and sediments are the youngest. The Archaean rocks are some of the oldest on Earth

The absence of outcrop suggests the use of regional geophysical datasets for mapping large scale units and structures in the area (Figure 5.3). These data have also been supplemented by higher resolution surveys undertaken for mineral exploration.

The region has been subdivided a little differently on the basis of more recent aeromagnetic interpretation (Whitaker, 1992; Whitaker and Bastrakova, 2002). In this model the Murchison domain in the north extends westward to the Darling Fault, the western boundary of the Yilgarn Craton, and is separated from the South West domain to the south by the north-northwest-trending Toodyay–Lake Grace domain. The Southern Cross domain bounds the Murchison and Toodyay–Lake Grace domains to the east.

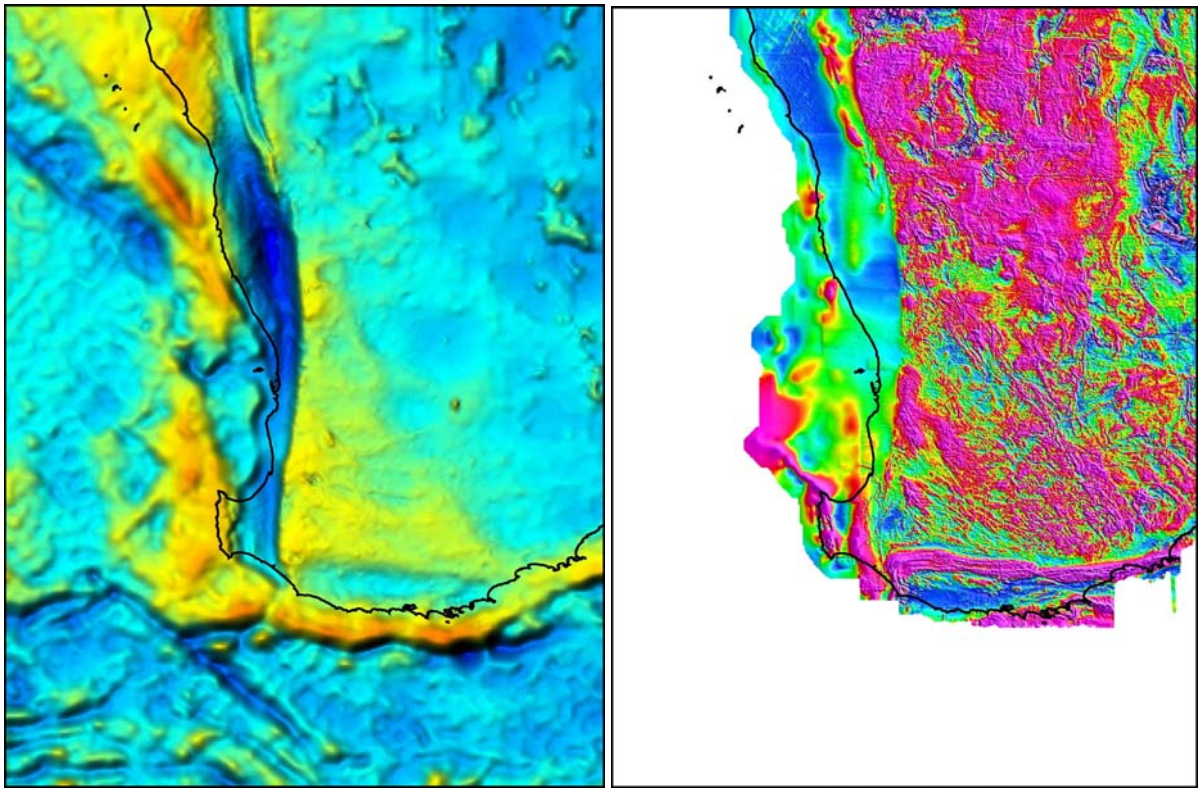

(a) **(b)**

Figure 5.3: Gravity (a) and magnetic (b) anomaly maps of southwest WA

The gravity data of southwestern Australia consist of the national 11 km grid in-filled by government and industry surveys, to about a 5 km average spacing, in a 200 km wide corridor abutting/paralleling the western coast line. These data provide complementary but significantly lower resolution information than the regional aeromagnetic coverage. The combined gravity and magnetics anomaly images are given in Figures 5.4 and 5.5.

Much of the Murchison and Southern Cross domains have an average Bouguer gravity anomaly in the order of –450 μm/sec^2. Local gravity highs to –100 μm/sec^2 in this region correlate with greenstone belts. A major north-northwest trending gravity gradient (the Yandanooka–Cape Riche Lineament of Everingham, 1968) with high values to the southwest transects the South West domain and the northwest of the Toodyay–Lake Grace domain. The high gravity to the south west of the gradient has been linked with crust of higher average thickness and a thick, high seismic velocity, high density basal layer relative to crust to the east (Mathur, 1976). Certainly there is no inferred change in surface geology across the position of this lineament as inferred from interpretation of aeromagnetic data. However, Wilde *et al.* (1996) have interpreted/mapped a zone with abundant migmatite immediately east of the gravity lineament.

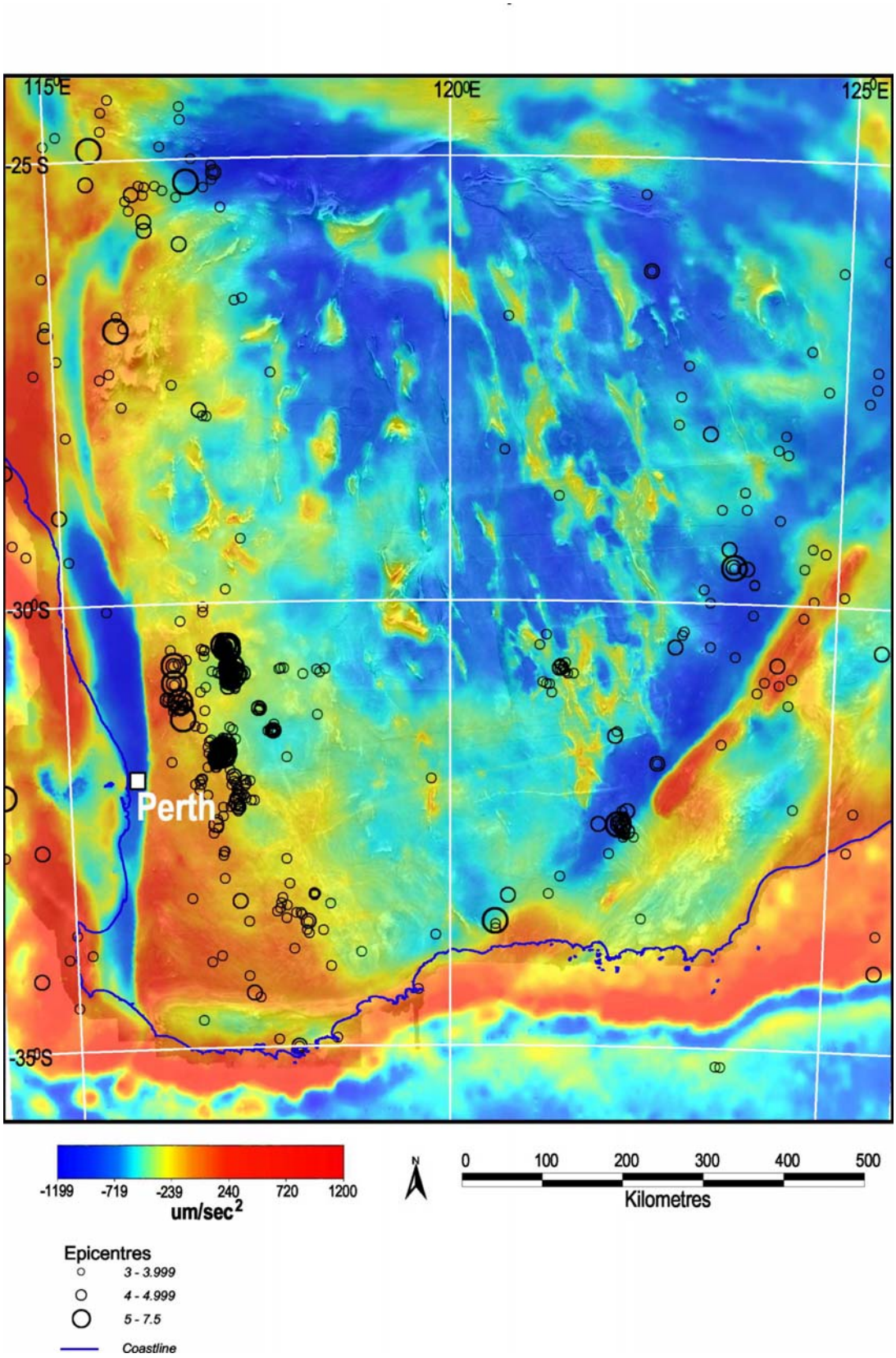

Figure 5.4: Combined gravity/magnetics image with seismicity (earthquake epicentres) for southwest WA. The Richter magnitudes of the earthquakes are indicated by the circle size as shown in the key.

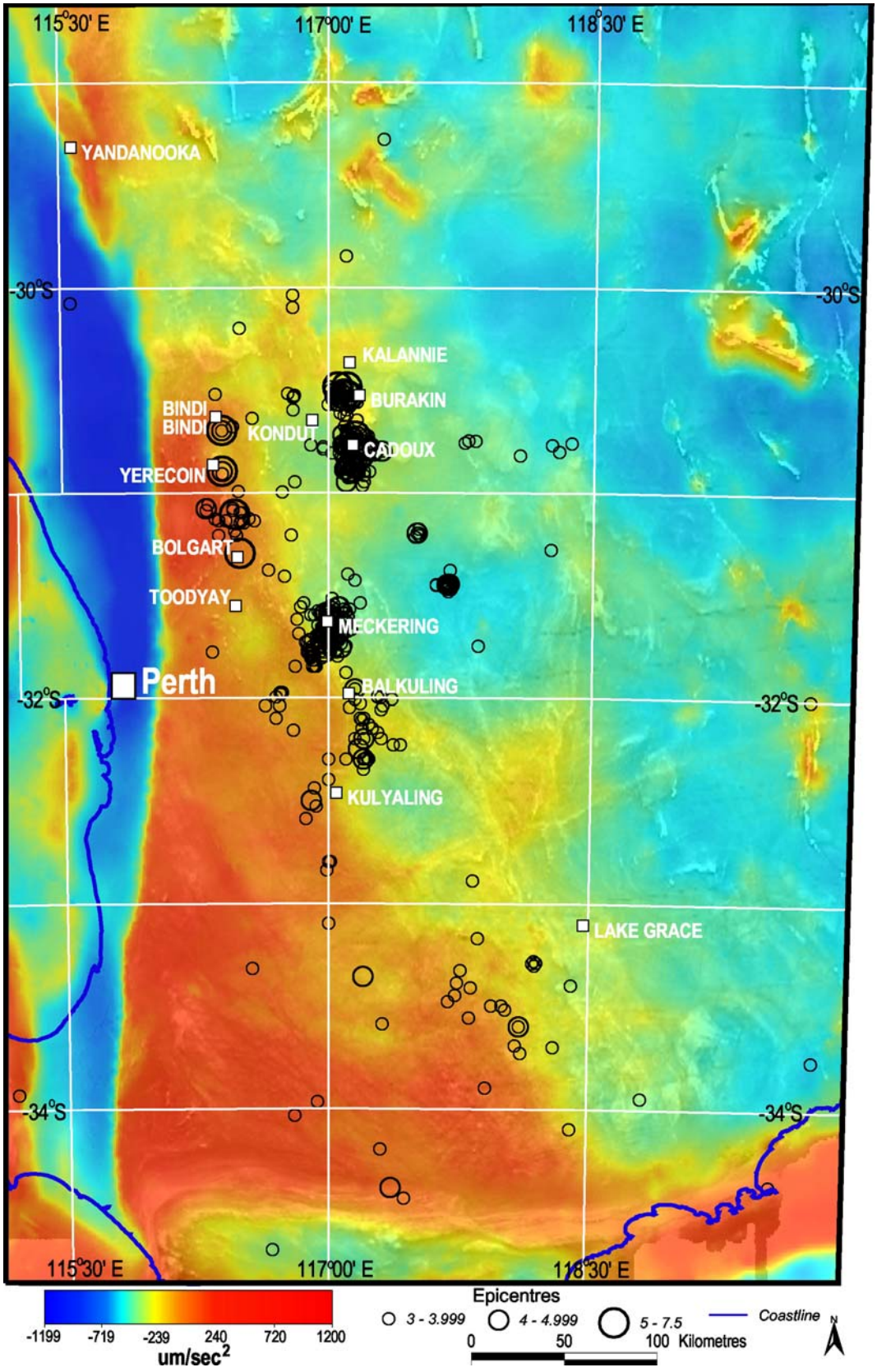

Figure 5.5: Combined gravity/magnetics image with seismicity (earthquake epicentres) around Perth. The Richter magnitudes of the earthquakes are indicated by the circle size as shown in the key.

The highest incidences of earthquake epicentres in the region are centred on Meckering, within the Toodyay–Lake Grace domain, and Cadoux in the southern Murchison domain, as shown in more detail in Figure 5.5. A zone of relatively high epicentre incidence, which includes these two areas of highest incidence, describes an 's'-shaped form (Cadoux–Kondut–Yerecoin–Bolgart–Meckering–Balkuling–Kulyaling) from 180 km northeast to 110 km southeast of Perth. The epicentres from Meckering to Kulyaling correlate strongly with structural trends of the Toodyay–Lake Grace domain as inferred from interpretation of aeromagnetic data. This area also correlates very well with a local curve and more general north-northwest trend of the major gravity gradient (Yandanooka–Cape Riche Lineament) through the area. Further south, earthquake epicentre incidence is relatively abundant across the South West domain but particularly so between the Yandanooka–Cape Riche Lineament and the southwestern boundary of the Toodyay–Lake Grace domain.

More generally, the incidence of epicentres in the southern Murchison and South West/Toodyay–Lake Grace domains drops off extensively east of the western boundary of the Southern Cross domain. Epicentre abundance also drops significantly north of an east-northeast-trending gravity lineament that passes through the central Murchison domain near the towns of Bindi Bindi, Damboring, and Kalannie. Figure 5.6 represents the southwest of WA in more detail where epicentres are superimposed on the fault structures as defined by the geological map of the Geological Survey of Western Australia (Myers and Hocking, 1998).

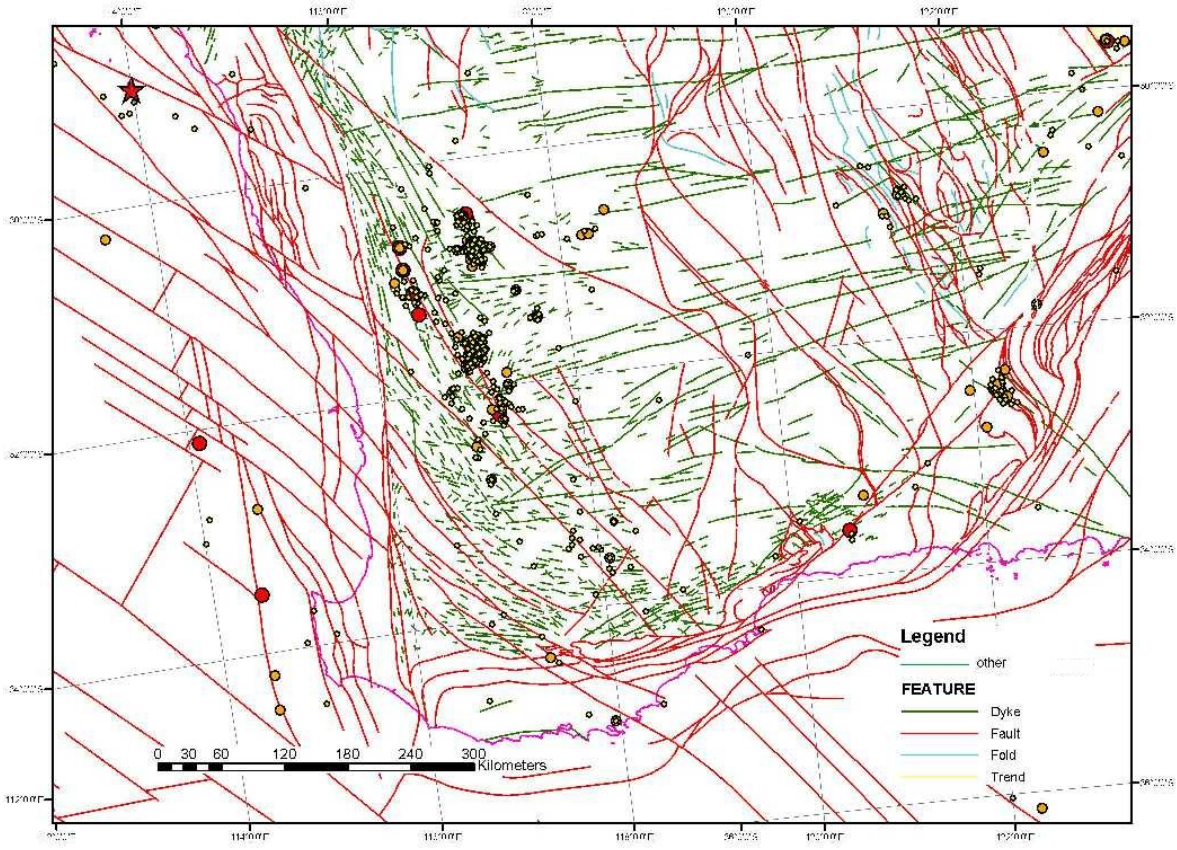

Figure 5.6: Seismicity and faults in southwestern WA

Regional seismology

The seismological data comprised subsets of Geoscience Australia's QUAKE Earthquake Database for Australia for the region around Perth (Figure 5.7), isoseismal maps for the larger events and their fault plane solutions.

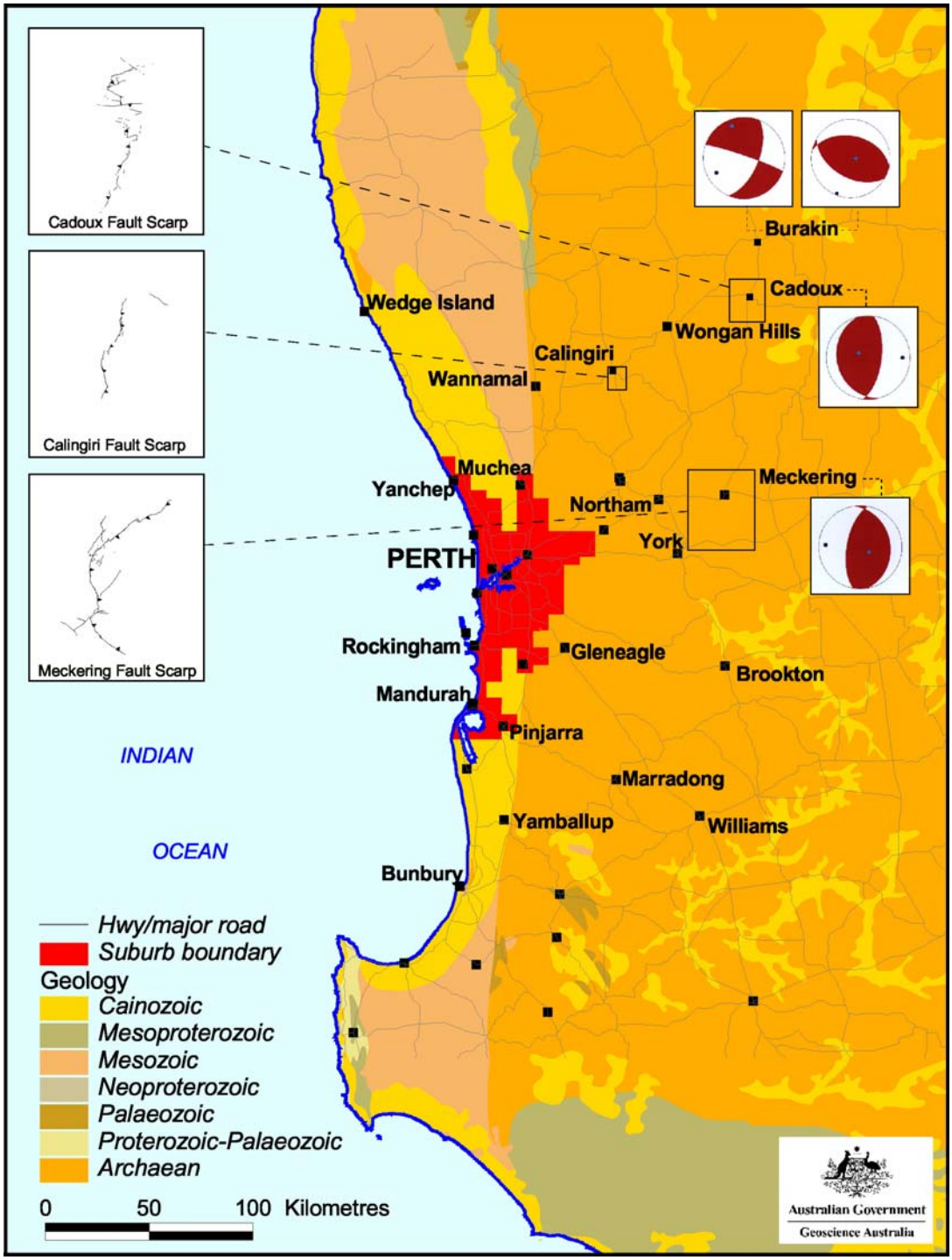

Figure 5.7: Geology of the wider Perth region showing fault scarps for the three largest earthquakes, Meckering, Cadoux and Calingiri. Fault plane solutions are shown for Meckering, Cadoux and the two Burakin 2001 earthquakes.

Seismicity parameters have been estimated only for those times in which the seismic network has been able to consistently record all earthquakes above the specified magnitude threshold (Sinadinovski, 2000) on the Australian continent. In the preliminary analysis for this study the numbers of earthquakes were counted for the declustered dataset of various magnitude ranges in magnitude intervals of 0.2 which is about the uncertainty. The declustered data set has the same magnitude ranges but the identifiable foreshocks or aftershocks are removed. A quake was considered to be a foreshock

or an aftershock if it was within a certain distance of the main shock in a procedure described by Sinadinovski (2000).

Three large earthquakes have caused considerable destruction and surface ruptures in the SWSZ. They are the Meckering 1968 earthquake, magnitude 6.9, the Calingiri event of 1970, magnitude 5.9 and the Cadoux earthquake of 1979, magnitude 6.2.

The original formation of the earthquake source zones was based on the work of Gaull *et al.* in 1990. The epicentral data in the current GA catalogue appear to fit the source zones chosen by Gaull *et al.* (1990) reasonably well, even though an estimated 50% of the events have occurred since they were originally defined. Some modifications were done to the original source zone boundaries, namely the northern border of the Cadoux–Meckering zone, to include the most recent activity in the Burakin area.

The adopted model is presented in Figure 5.8 and is comprised of:

- Zone 1, the SWSZ, modified from Gaull *et al.* (1990) to include the latest Burakin events;
- Zone 2, the larger zone east of Darling Fault, with modified borders from Gaull *et al.* (1990) to follow closely the Darling Fault and the orientation of the main geological structures;
- Yilgarn Zone, covering the remainder of the Yilgarn craton;
- Zone 3, an offshore zone, extending to the continental margin, modified from Gaull *et al.* (1990); and
- Background Zone, or Perth Basin, as part of the continental shelf, modified from the EPRI 1994 report and Gibson and Brown's model (AUS5) discussed at the Australian Earthquake Engineering Society conference in 2002.

The other recommendations for the seismic parameters to be used in the hazard calculation program are summarised below:

- ***Maximum magnitude:*** Two options were anticipated
  - Option-I where maximum moment magnitude of M_W 7.5 was assigned to all of the zones, including the background;
  - Option-II where maximum moment magnitude of M_W 7.0 was assigned to Zones 1 and 2, and M_W 8.0 to Zone 3 and the background (Perth) zone.
- ***Event depth:*** Two distributions of earthquakes were anticipated
  - Distribution-I depths between 0 and 20 km for areas east of the Darling Fault;
  - Distribution-II depths between 0 and 15 km for areas west of the Darling Fault.
  - The probabilistic distribution for the depth dependencies were not defined more specifically by the group of experts. GA is considering using a distribution with maxima in the top 5 km and decreasing with depth.
- ***Fault type:*** Two types of faults were anticipated
  - Reverse faults - 80% of the earthquakes will occur on reverse faults aligned with the structural trend NNW-SSE; and
  - Strike slip - 20% of the earthquakes will occur on strike slip faults.
  - Variation of +/- 30° around these principal fault orientations was allowed.
- ***Fault dip:*** Two positions of fault dips were anticipated
  - Position-I - 50% of the earthquakes occur on faults dipping 35^o East; and
  - Position-II - 50% of the earthquakes occur on faults dipping 35^o West.

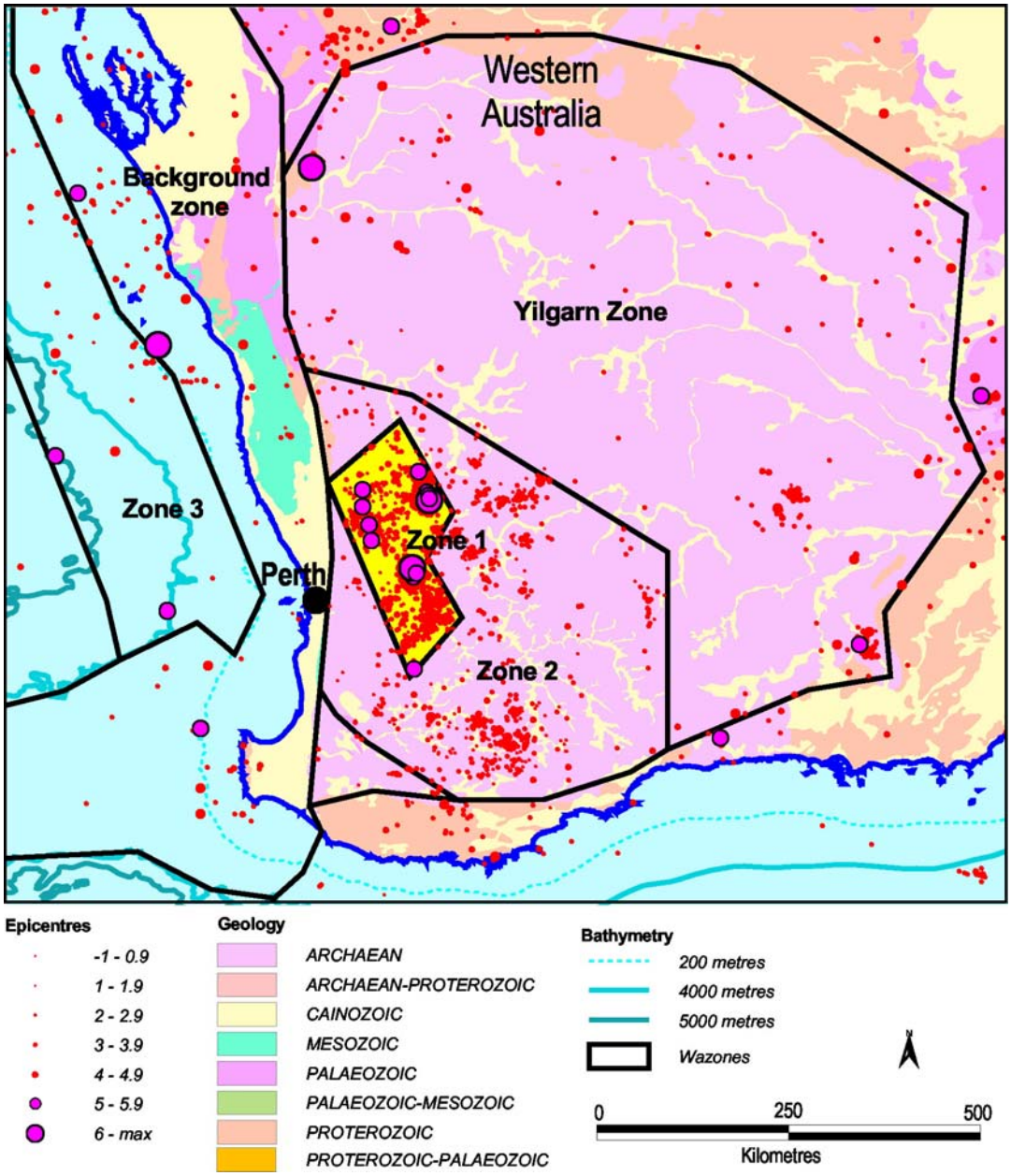

Figure 5.8: Seismic source zones of southwest WA. The Richter magnitudes of historical earthquakes are indicated by the range of circle sizes shown in the key.

Earthquake hazard

Recurrence relationship

The relationship between the number of earthquakes and their magnitude is routinely approximated by the Gutenberg–Richter (GR) empirical formula (1949), represented by a single straight line in log-linear coordinates

$$\log N = a - bM \qquad \textbf{Equation 5.1}$$

where N is usually the cumulative number of earthquakes, greater than or equal to magnitude M, per year, M is the local or Richter magnitude and a, b are constants related to the total number of earthquakes above a certain size and the frequency relation between small and large earthquakes. Data are treated by grouping of N according to the magnitude range.

Because earthquake size is characterised by seismic moment, a relationship between the Richter and moment magnitudes is required. This relationship may be developed empirically, but in the absence of quality data from large Australian earthquakes, a curvilinear relationship was adopted (Electric Power Research Institute (EPRI), 1993) which converts local magnitude M_{Lg} to moment magnitude M_W for earthquakes of magnitude greater than 5.25:

$$M_W = 3.45 - 0.473M_{Lg} + 0.145M_{Lg}^2 \qquad \textbf{Equation 5.2}$$

The local magnitudes measured in Australia, M_L, are mainly derived from earthquake body waves. The more sophisticated local magnitude measure, M_{Lg} as used in Equation 5.2, is based on a combination of earthquake wave types. For the purposes of this research the M_L values available to this study have been substituted in Equation 5.2, thereby assuming both magnitude parameters are equivalent.

The coefficient *b* usually takes a value around 1. In general this relationship fits the data well on a global scale, but not for particular tectonic regions. Various authors have discussed the spatial variation in *b*. In his work Kárník (1971) mentioned that in some cases for the weakest and the strongest earthquakes, the (log *N*, M) distribution deviated significantly from linearity. Recently, some other approximation formulae for that deviation have been applied (for example Utsu, 1999).

For use in prediction and comparative mechanism studies, standard errors of *b* must be supplied for statistical tests. Because earthquakes follow stochastic processes and the *b* value is a random variable, the probability distribution and the variance of *b* are essential in studying its temporal and spatial variation. The *b* value can be calculated by the least-squares method (LSM), but the presence of even a few large earthquakes influences the resulting *b* value significantly. As an alternative, the maximum likelihood estimate (MLE) can be used to calculate *b* because it yields a more robust value when the number of infrequent large earthquakes is considered. Weichert (1980) discusses in detail the advantages and disadvantages of the various methods.

The data used for this study comprised a subset of GA's earthquake database for Australia. Analysis was restricted to only those time intervals in which the seismic network was able to consistently record all earthquakes of the specified magnitude. On our assessment, the periods of completeness were: 1901–2003 for $M \geq 6.0$, 1959–2003 for $M \geq 5.0$, 1965–2003 for $M \geq 4.0$, and 1980–2003 for $M \geq 3.2$ (Sinadinovski, 2000). Principal values of *a* and *b* coefficients for our preferred model with maximum magnitude M_W 7.5 in Western Australia using seismic data up to the end of 2002, are presented in Table 5.1.

Table 5.1: Seismic parameter values for zones closest to Perth

Source zone	Area (km^2)	M_{min}	M_{max}	b	A_{min}
Zone 1	25 365	3.9	7.5	1.00	3.266
Zone 2	134 344	3.9	7.5	1.00	0.252
Zone 3	330 916	3.9	7.5	1.00	3.617
Background	373 291	3.9	7.5	1.00	1.649
Yilgarn	460 465	3.9	7.5	1.00	1.970

M_{min} is the minimum moment magnitude, M_{max} is the upper bound magnitude, and A_{min} is the number of earthquakes per year with $M \geq M_{min}$ (intercept of Equation 5.1 at $M = M_{min}$)

The level of seismicity normalised to 10,000 km^2 for the areal zones is shown in Figure 5.9. This new configuration increases seismicity in the Zone 1 at the expense of decrease of seismicity in Zone 2, when compared with the earlier model of Gaull *et al.* 1990.

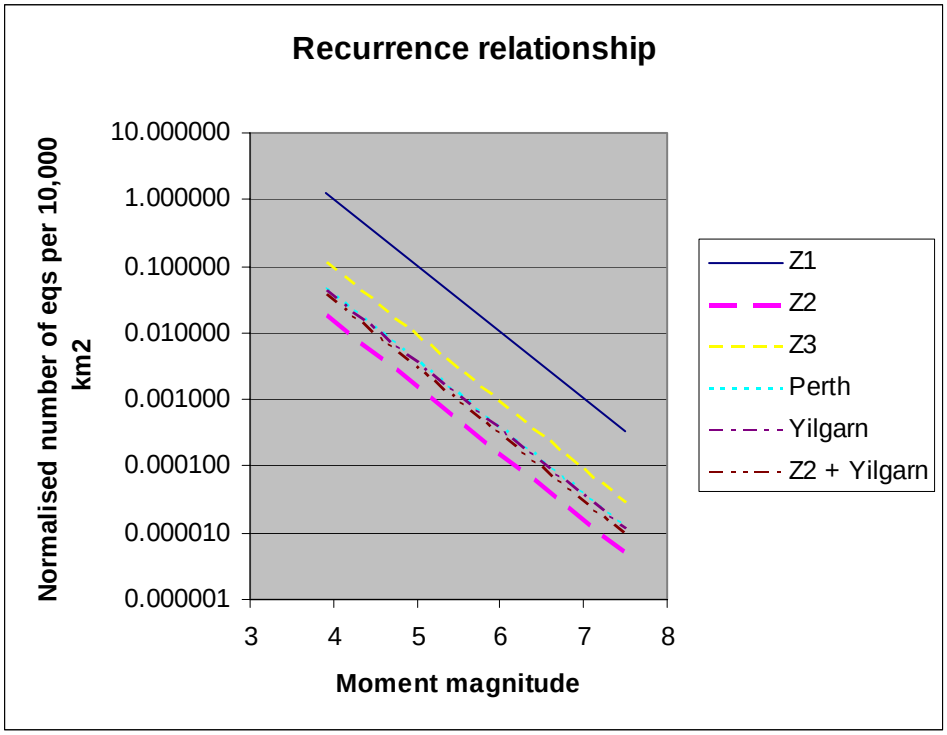

Figure 5.9: Recurrence relationship for the areal seismic zones

Simulation of earthquakes

The computation of hazard relies on the simulation of earthquake events within each of the source zones. The earthquakes are modelled to occur on 'virtual' rupture planes within the Earth. A brief outline of the process used to simulate the events is given below.

1. *Define the number of desired events in each zone.* The number of desired events within a zone depends on the influence of that zone on the overall hazard in the study region. The desired number of events for each of the zones was defined to be the minimum value which, when increased, does not significantly change the hazard. These values were determined through a separate sensitivity analysis and are 10,000 in the zone immediately below Perth and 2,000 in every other zone.
2. *Define a characteristic dip angle for the seismic zone*. A characteristic dip angle of 35 degrees was used for the source zones as recommended by the workshop participants in 2002.
3. *Randomly assign a rupture location for each of the desired events*. The location represents a latitude and longitude for the start of the rupture trace (see Figure 5.10).
4. *Assign a moment magnitude for each event*. The software adopts an approach that forces uniform sampling across the range of magnitudes. In other words, the number of simulated magnitude 5.2 earthquakes in each zone is roughly similar to the number of simulated magnitude 4.6 earthquakes. This ensures that earthquake events with a range of moment magnitudes contribute to the estimated hazard without requiring excessive computation of small events.

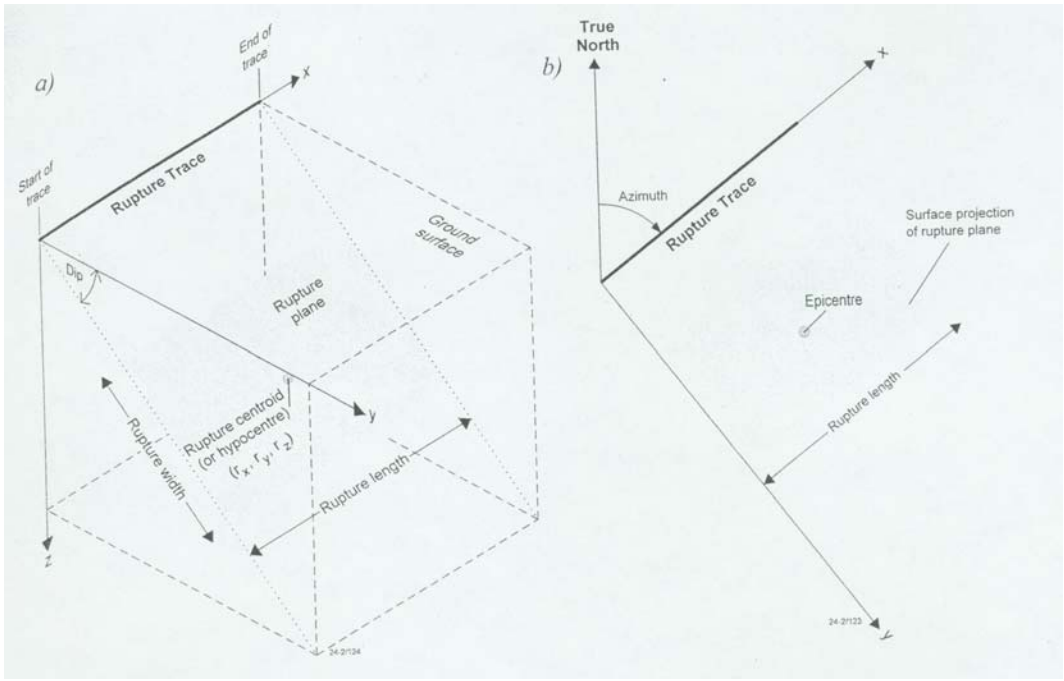

a **b**

Figure 5.10: The orientation and dimensions of the rupture plane in (a) 3D space, and (b) plan view

5. *Compute a likelihood (or probability) of occurrence for the magnitude of each simulated event*. The likelihood of occurrence accounts for the uniform sampling mentioned above, i.e., the number of actual magnitude 5.2 events in each zone is not the same as the number of magnitude 4.6 events. The probabilities are computed using the bounded Gutenberg–Richter probability density function (BGR–PDF), defined by the Gutenberg–Richter parameters in each zone (Kramer, 1996). Note that the BGR–PDF is closely related to the BGR relationship.
6. *Randomly assign an azimuth for each of the events.* These are selected uniformly in the range from 0 to 360 degrees from true north.
7. *Compute the geometry (or dimensions) and location (including depth) of each event*. The motion experienced at a point on the Earth's surface depends on the distance to the rupture plane, not the distance to the plane's centre (hypocentre). Therefore it was important that the position of the rupture plane was modelled as accurately as possible. The important rupture parameters are its dimensions (i.e., area, length and width) and the location of the hypocentre. These are computed using empirical relationships based on magnitude.
8. *Compute the end point of each rupture trace.* The end point is computed using the start of the rupture trace, the azimuth and the rupture dimensions. This information is useful for diagnostics such as Figure 5.11, which gives an overview of the geographical distribution of the simulated events. The location of the rupture trace is also required for Step 9.
9. *Adjust the azimuth of each event* to force, where possible, the rupture trace to lie within the source zone. Zone 1 is defined to favour north-northwest–south-southeast orientation as recommended by the workshop participants in 2002.

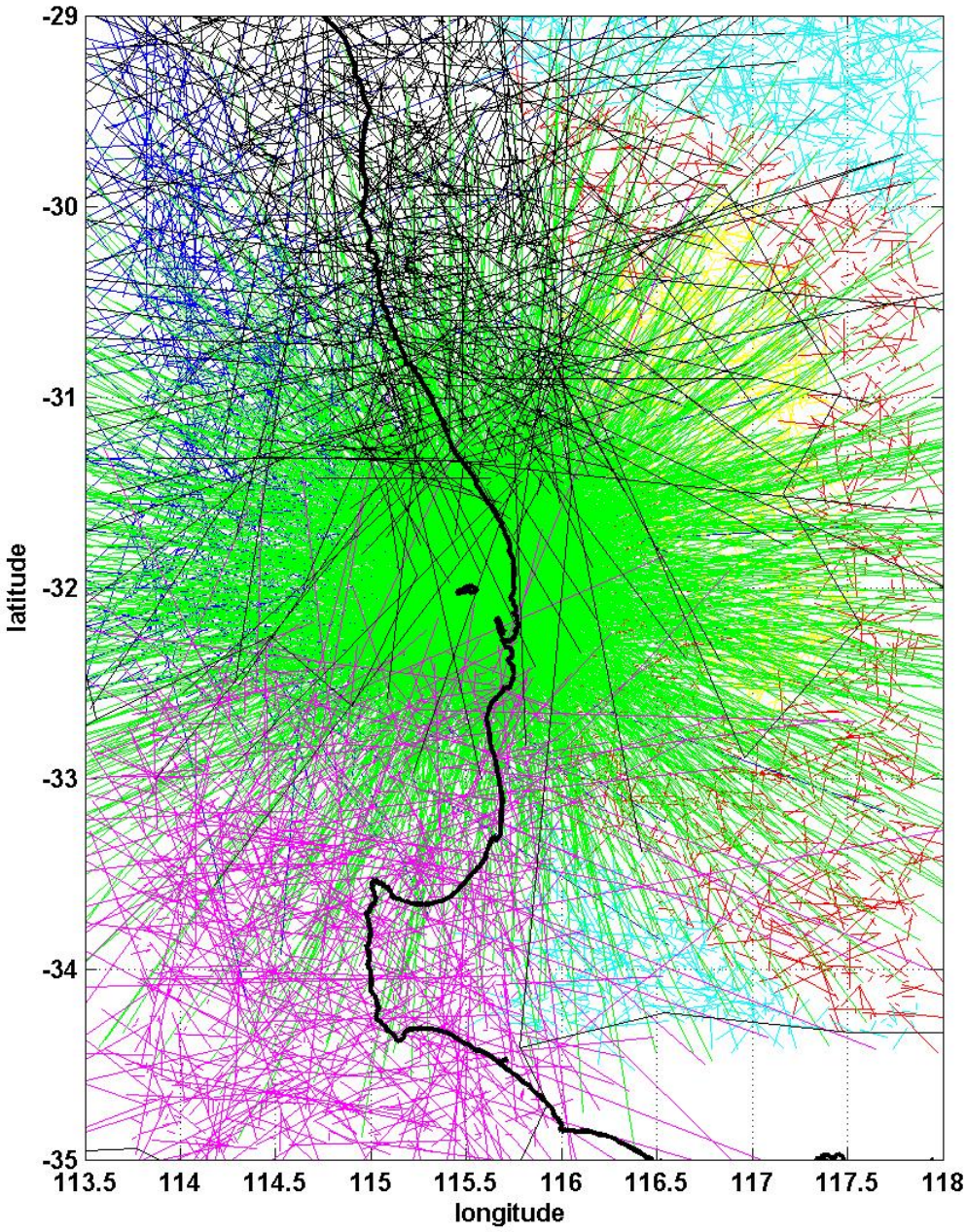

Figure 5.11: The fault traces of simulated events. The colours identify the different origin zones (see Figure 5.8 for seismic zone boundaries)

Attenuation model

Attenuation models describe how the intensity of ground shaking decreases with increasing distance from an earthquake. When few data exist, attenuation relations for Modified Mercalli Intensity can be developed and then converted by empirical formulae to equivalent peak ground accelerations (PGAs, which are expressed as a fraction of the gravity constant g). This approach was employed in the

development of the Australian earthquake hazard maps (Gaull *et al.*, 1990), which were largely adopted in the 1993 Australian earthquake loadings standard (AS1170.4, Standards Australia, 1993).

GA's research of the Burakin data has provided some quantitative support for the use of attenuation models from central and eastern North America (CENA) over models developed for western North America (Dhu *et al.*, 2004). The CENA attenuation models were adopted because the 'intraplate' tectonic environment in central and eastern North America is thought to be generally similar to the environment in southeast Australia. They describe the attenuation of response spectral acceleration (RSA) as well as PGA, and they include both a median attenuation model and a measure of the model variability due to the randomness inherent in natural processes.

In this report we incorporated two different CENA attenuation functions into the estimates of earthquake hazard, namely Atkinson and Boore (1995) and Toro *et al*. (1997). These functions were all derived using similar crustal velocity structures, and they may contain different assumptions about source and path effects. At this stage CENA models are equally weighted when used for Australian conditions.

A comparison of the CENA and the Gaull *et al.* (1990) attenuation models for PGA is presented in Figure 5.12. The Atkinson and Boore model has the highest PGA values and the Toro *et al.* model attenuates the fastest. The Gaull *et al.* model gives the lowest PGA values out to epicentral distances of 100 km but has the lowest rate of attenuation. It should be emphasised that this model used source depths of 10 km and is based on local magnitudes. We calculated our moment magnitudes from the local magnitudes using the Johnston relationship (G. Gibson, personal communication) for all events larger than 5.25.

These assumptions result in different predicted RSAs for any given magnitude-distance combination. The various predicted RSAs for a magnitude 5.5 event at 100 km distance are shown in Figure 5.13 in order to demonstrate the differences in these functions for an earthquake typical of the SWSZ that would be expected to affect Perth.

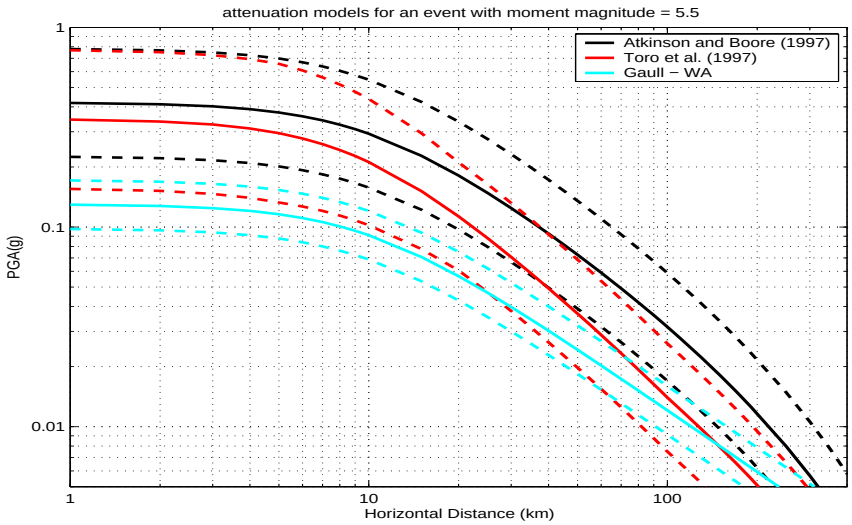

Figure 5.12: Comparison of attenuation models for M_w = 5.5 event at 100 km. Mean model predictions shown along with plus and minus one standard deviation.

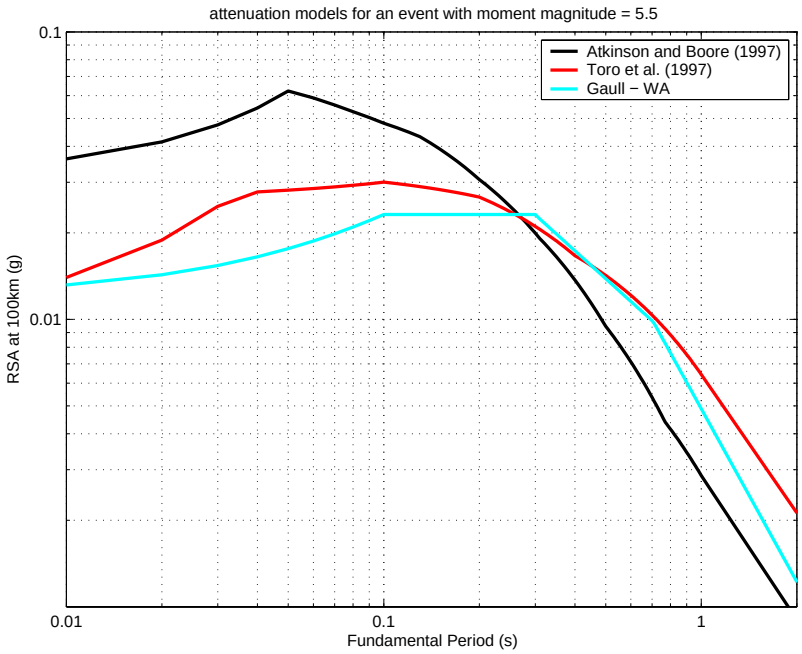

Figure 5.13: Predicted RSA for a magnitude 5.5 event at 100 km for the attenuation functions considered in this report

The Toro *et al.* predictions are approximately half of the values predicted by the Atkinson and Boore model for periods less than 0.2 s, and the Gaull *et al.* values are lower still. The models predict similar RSAs for periods between 0.2 s and 0.4 s. However, the Toro *et al.* model predicts the largest RSAs for periods of 0.5 s or greater.

The models used in this study have two different approaches for incorporating uncertainties. Toro *et al.* (1997) incorporates two distinct types of variability; that associated with the randomness in the natural process (aleatory) and the variability associated with the attenuation relationship in modelling the process (epistemic). In comparison, the Atkinson and Boore (1995) relationship only captures aleatory uncertainties. As mentioned previously, this study has used the two selected attenuation functions independently and then averaged their respective hazard estimates. Consequently, only the aleatory component of uncertainty has been used when combining the two models.

Calculated earthquake hazard on rock

For depicting earthquake ground motion severity, the predictive empirical relationships for intensity, PGA and spectral amplitudes at typical periods (between 0.3 and 1.0 seconds) and for different site classes need to be considered. For this report the PGA and spectral accelerations on rock corresponding to 10% and 2% probability of exceedence in 50 years are presented.

In the previous sections the source and attenuation models developed for the Perth region were described. In order to calculate the earthquake hazard it is necessary to amalgamate these models. The approach taken in this study is outlined below.

- A spacing of 500 m was used to create a uniformly spaced grid of sample points at which the hazard was calculated.
- Earthquakes were generated using the method described in the ‘Simulation of earthquakes’ section.
- For each earthquake – sample point combination, an attenuation function was selected by choosing a random variation from the median attenuation model.

- For a given level of hazard the maximum RSA that has at least that chance of being exceeded in the given time frame was stored. For example, given a hazard level of 10% probability of exceedence in 50 years, the hazard at a sample point is defined as the maximum RSA that has at least a 10% chance of being exceeded in 50 years

The Australian earthquake loadings standard, AS1170.4-1993, presents earthquake hazard in terms of an 'acceleration coefficient' that has a 10% chance of being exceeded in 50 years. This acceleration coefficient shown in Figure 5.14 is considered to be equivalent to the PGA.

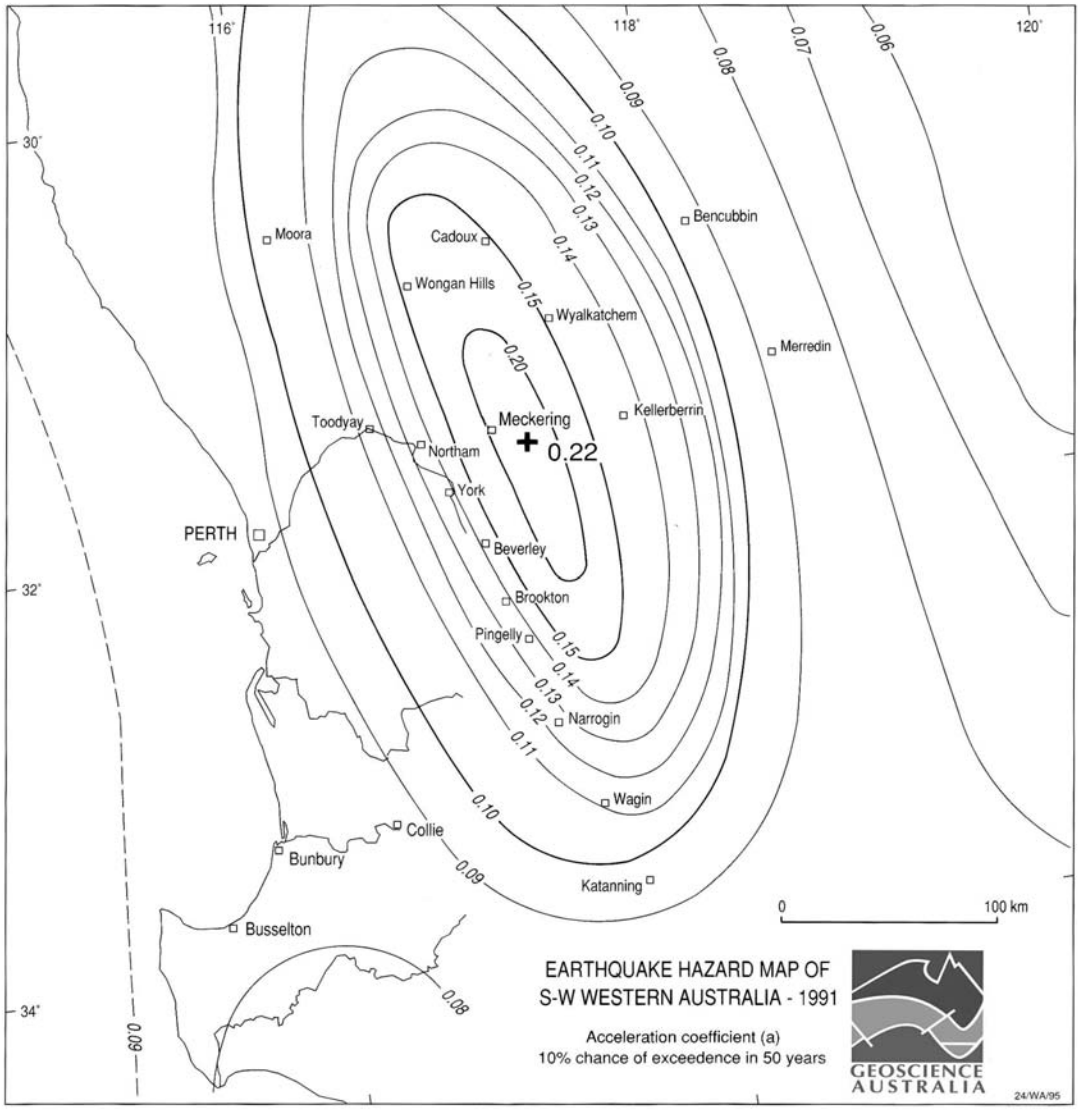

Figure 5.14: Earthquake loadings standard (Standards Australia, 1993) hazard map of WA

While hazard definition often centres on the PGA, building damage is influenced by the spectral period that corresponds with its natural period of vibration. For example, low to medium-rise structures are typically more vulnerable to ground shaking that has a period of vibration of approximately 0.3 *s*. Medium to high-rise structures are typically more vulnerable to ground shaking that has a period of vibration of approximately 1 s. The importance of spectral values as opposed to PGA is of particular note given that the high PGA values used for Perth in this study have little structural significance. Spectral acceleration values at 0.3 s and 1.0 s have been included in the hazard results presented below.

Whilst the Australian earthquake loadings code describes hazard in terms of the level of ground shaking that has a 10% chance of being exceeded in 50 years (i.e. for events with a return period of 475 years), it is often important to consider the possible effect of less likely but more damaging events. Consequently, this study has also determined the earthquake hazard that has a 2% chance of being exceeded in 50 years. This probability of being exceeded corresponds to events with a return period of approximately 2,500 years.

Perth study region hazard

There is currently no quantitative evidence to support the preferential use of either of the CENA attenuation models. Consequently the hazard was predicted using both, combining them with equal weighting. The hazard was calculated using the same simulated catalogue of earthquake events in conjunction with either Atkinson and Boore or Toro *et al.* relationship. The approach is illustrated in Figure 5.15, which presents the separate and combined PGA bedrock hazard for a 475-year return period. All maps have the same trend of increasing hazard towards the northeast of the study region due to the defined seismic activity in Zone 1. The two attenuation model results have notable differences in the hazard range predicted across the study region, mainly because of differences in the rate of RSA decay with distance. The PGA calculated within the majority of the Perth metropolitan area is typically double the hazard presented in the Australian earthquake loadings standard. The significance of this will be discussed later.

The hazard calculation process was repeated for all three spectral periods and the two return periods of interest. The plots are presented together in Figure 5.16 for comparative purposes. The hazard for all three parameters increased by a factor of approximately 2.2 in moving from a 475-year return period hazard to a 2,475 year. This factor is similar to, though slightly larger than, the 1.8 probability adjustment factor proposed in the draft standard (Standards Australia, 2004). The values of the hazard parameters for a 475-year return period at three key locations in the Perth metropolitan area are also presented in Table 5.2.

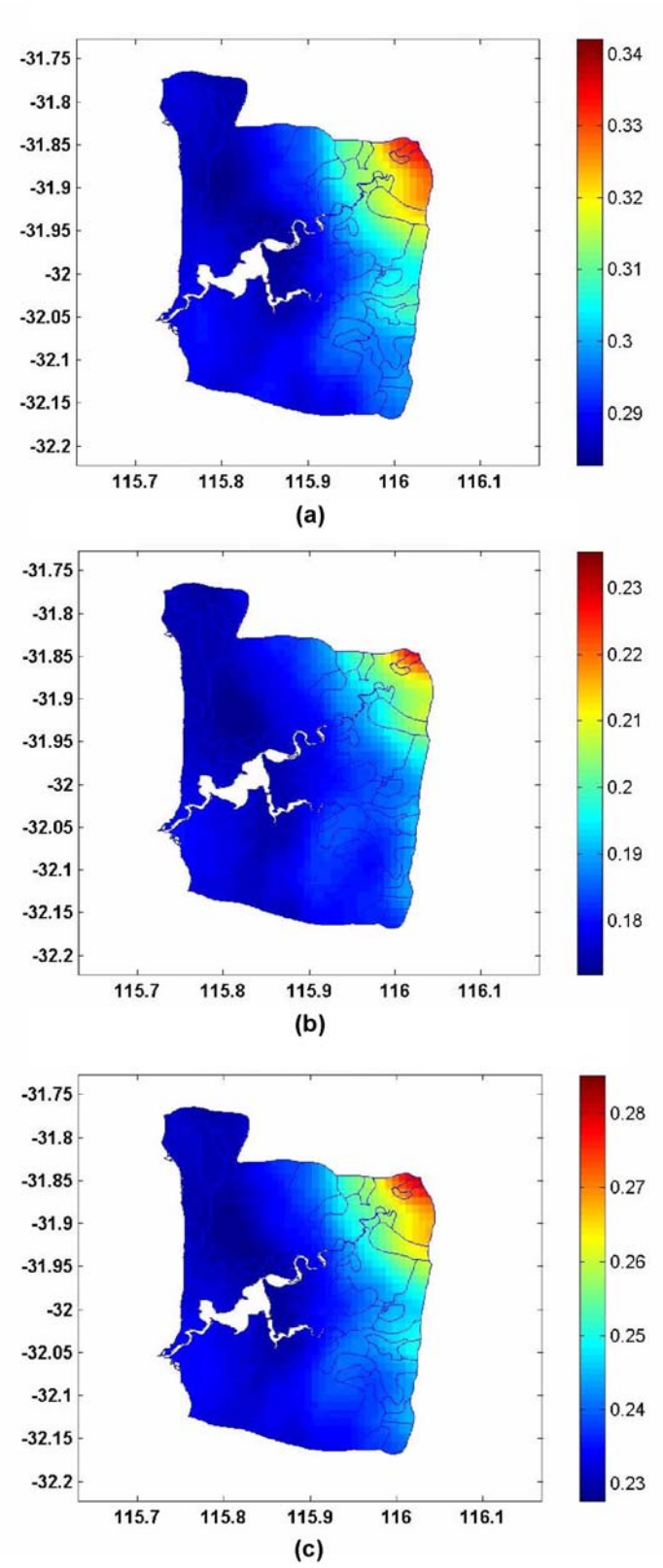

Figure 5.15: Earthquake hazard on rock in Perth with 10% probability of exceedence in 50 years, PGA(*g*). **a**) Atkinson and Boore attenuation model results. **b**) Toro *et al.* attenuation model results. **c**) Combined with 50/50 weighting to the Atkinson and Boore model and Toro *et al*. model

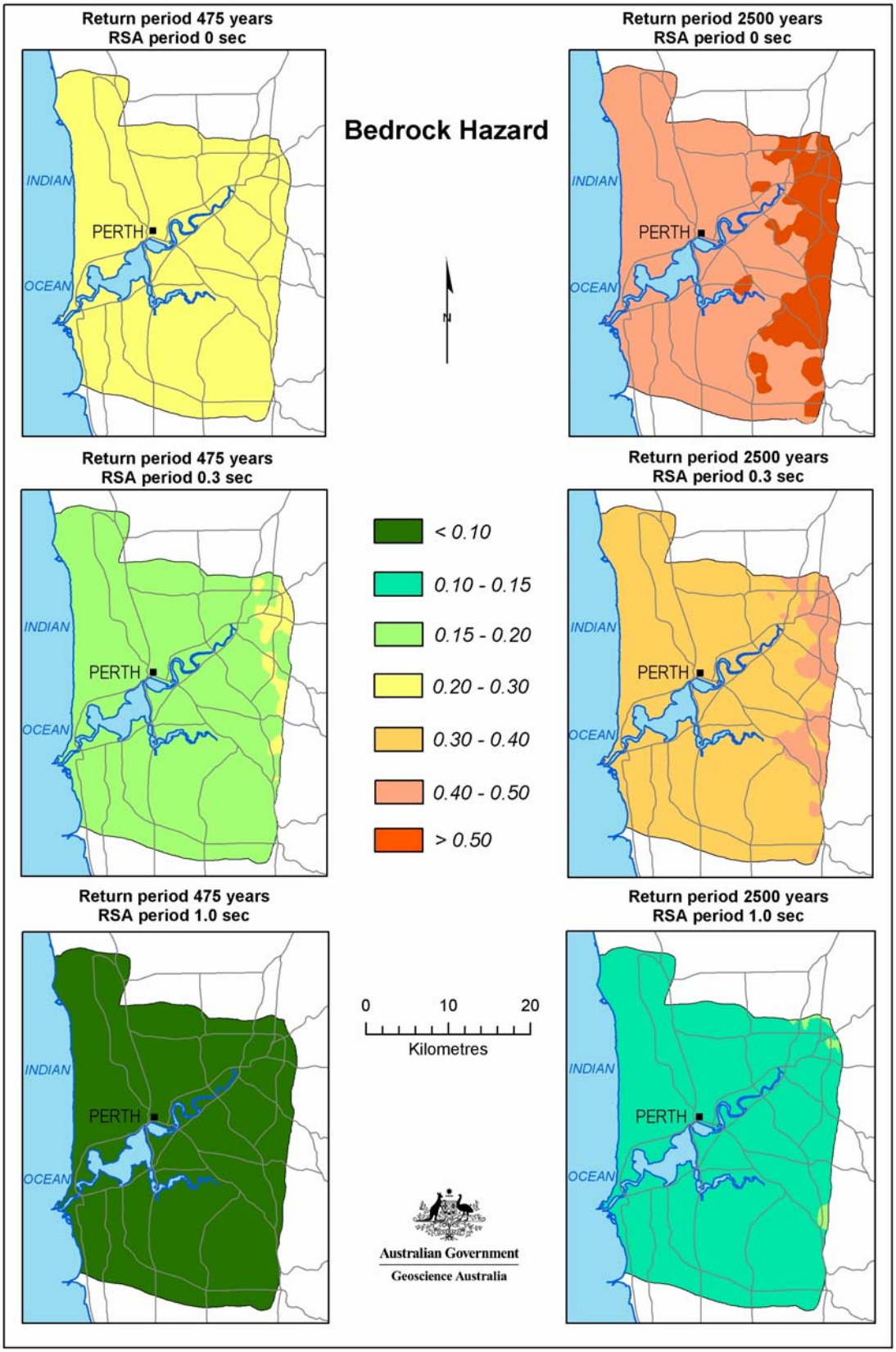

Figure 5.16: Perth metropolitan study region earthquake hazard on bedrock. All accelerations are presented as a fraction of the acceleration due to gravity (g).

Table 5.2: Perth region bedrock hazard for a 475-year return period of exceedence

Location	Both standards[1]	AS 1170.4 - 1993		DR 04303 - 2004	
	PGA(*g*)	S_A at 0.3 s(*g*)	S_A at 1.0 s(*g*)	S_A at 0.3 s(*g*)	S_A at 1.0 s(*g*)
Perth metro.					
Midland	0.093[2] [0.261][3]	0.233 [0.226]	0.116 [0.070]	0.273 [0.226]	0.082 [0.070]
Perth CBD	0.089 [0.232]	0.223 [0.205]	0.111 [0.065]	0.262 [0.205]	0.078 [0.065]
Fremantle	0.088 [0.229]	0.220 [0.202]	0.110 [0.064]	0.259 [0.202]	0.077 [0.064]
Perth region					
Moora	0.103 [0.401]	0.258 [0.321]	0.129 [0.090]	0.303 [0.321]	0.091 [0.090]
Cadoux	0.160 [0.620]	0.400 [0.474]	0.200 [0.123]	0.470 [0.474]	0.141 [0.123]
Meckering	0.200 [0.615]	0.500 [0.484]	0.250 [0.130]	0.588 [0.484]	0.176 [0.130]
Northam	0.136 [0.536]	0.340 [0.422]	0.170 [0.116]	0.400 [0.422]	0.120 [0.116]
Brookton	0.138 [0.593]	0.345 [0.456]	0.173 [0.118]	0.406 [0.456]	0.121 [0.118]
Pinjarra	0.088 [0.218]	0.220 [0.188]	0.110 [0.058]	0.259 [0.188]	0.077 [0.058]

Notes: (1) Bedrock peak ground acceleration (PGA) unchanged from AS 1170.4 (1993) in DR 04303.
(2) Hazard values have been interpolated from hazard maps in standards to capture variation across the study region.
(3) Values derived from this study are shown in square brackets.

Perth regional bedrock hazard

The bedrock hazard for the larger Perth region was determined using the same methodology to that described above. The 475-year return period hazard results are presented in Figures 5.17–5.19 and the hazard values at several key Western Australian towns are summarised in Table 5.2. The elevated hazard in the Wheatbelt region is clearly evident with the common trend of reducing hazard in a westerly direction towards the Perth metropolitan area.

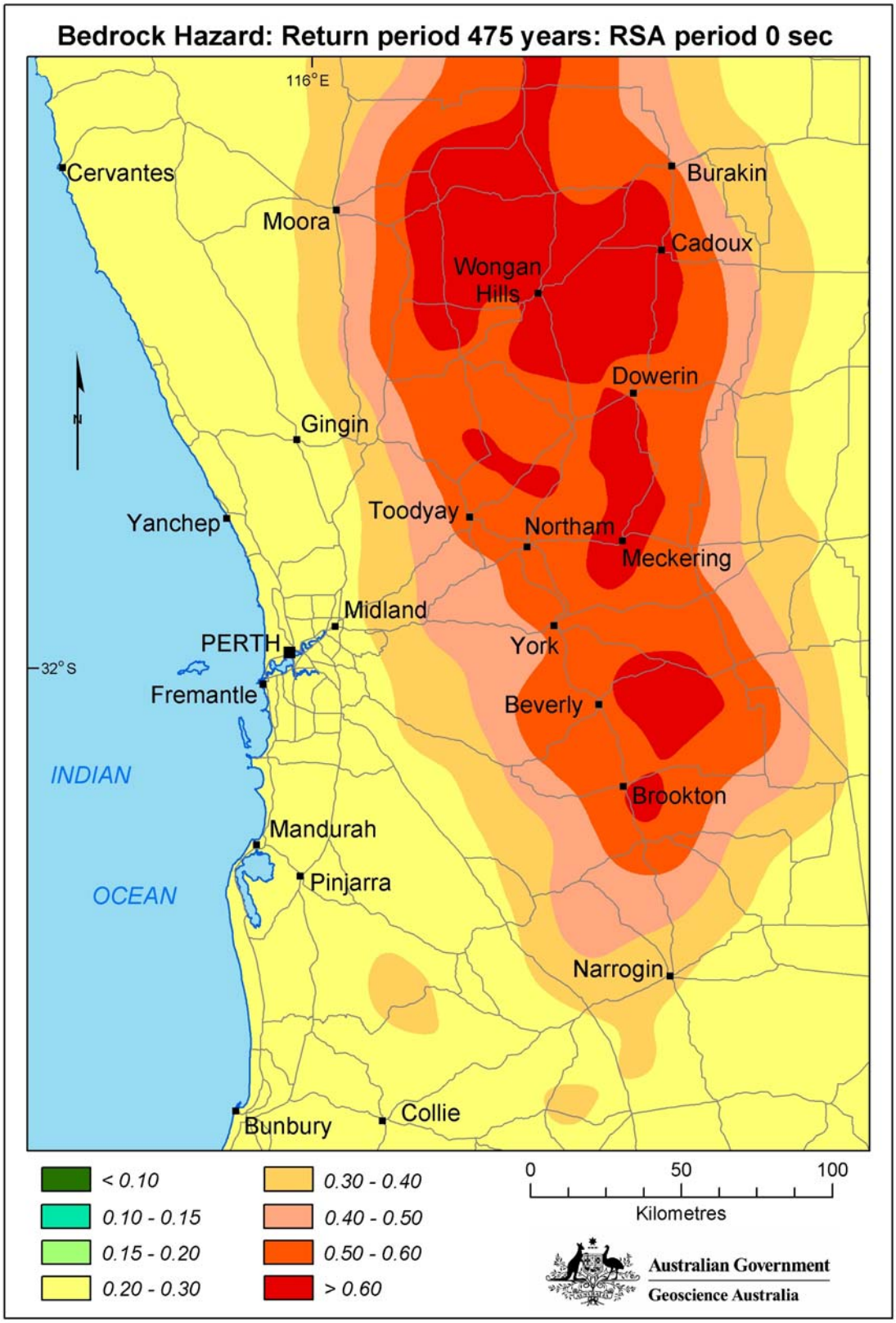

Figure 5.17: Perth region PGA on bedrock for 475-year return period

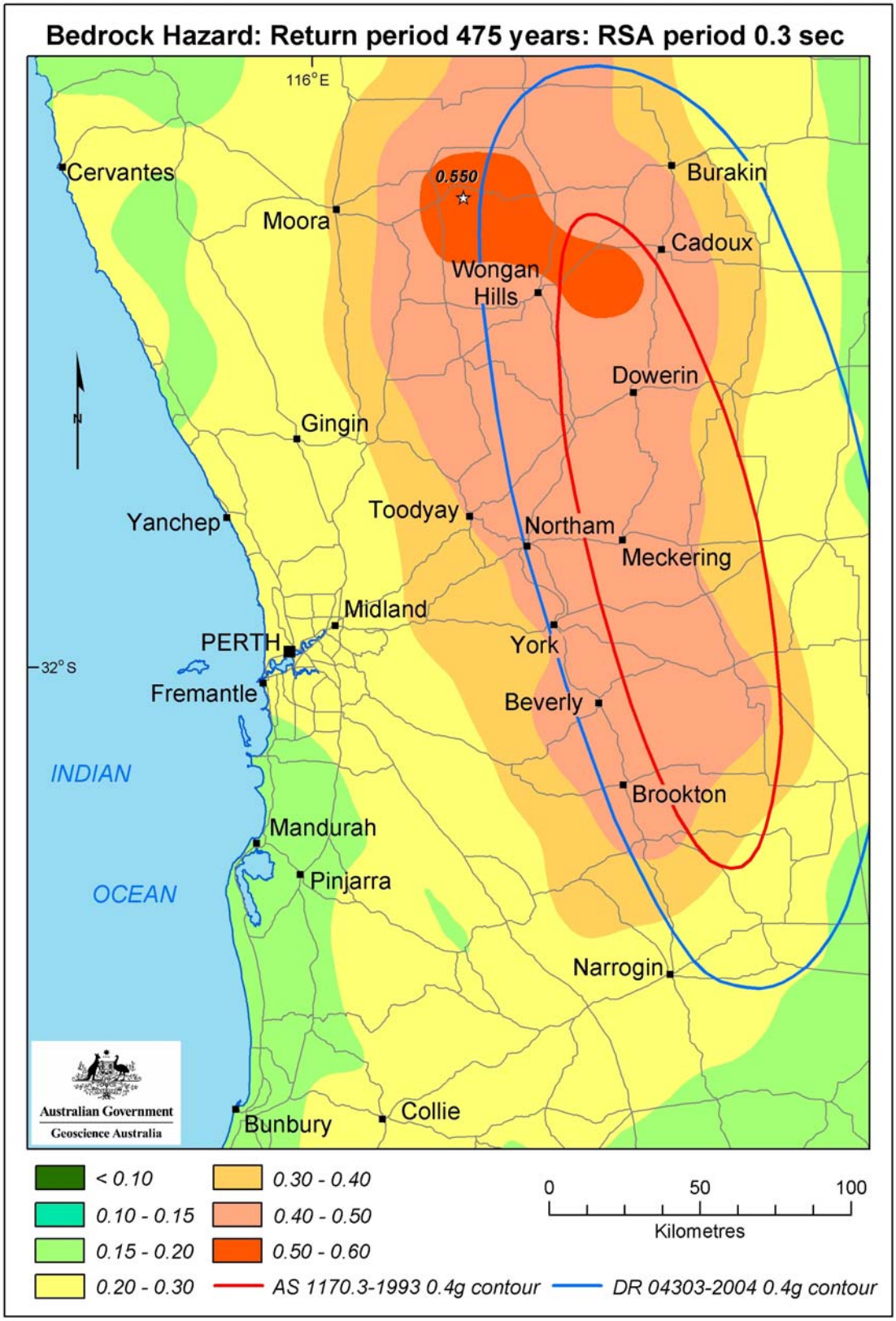

Figure 5.18: Perth region 0.3 s spectral acceleration on bedrock for 475-year return period

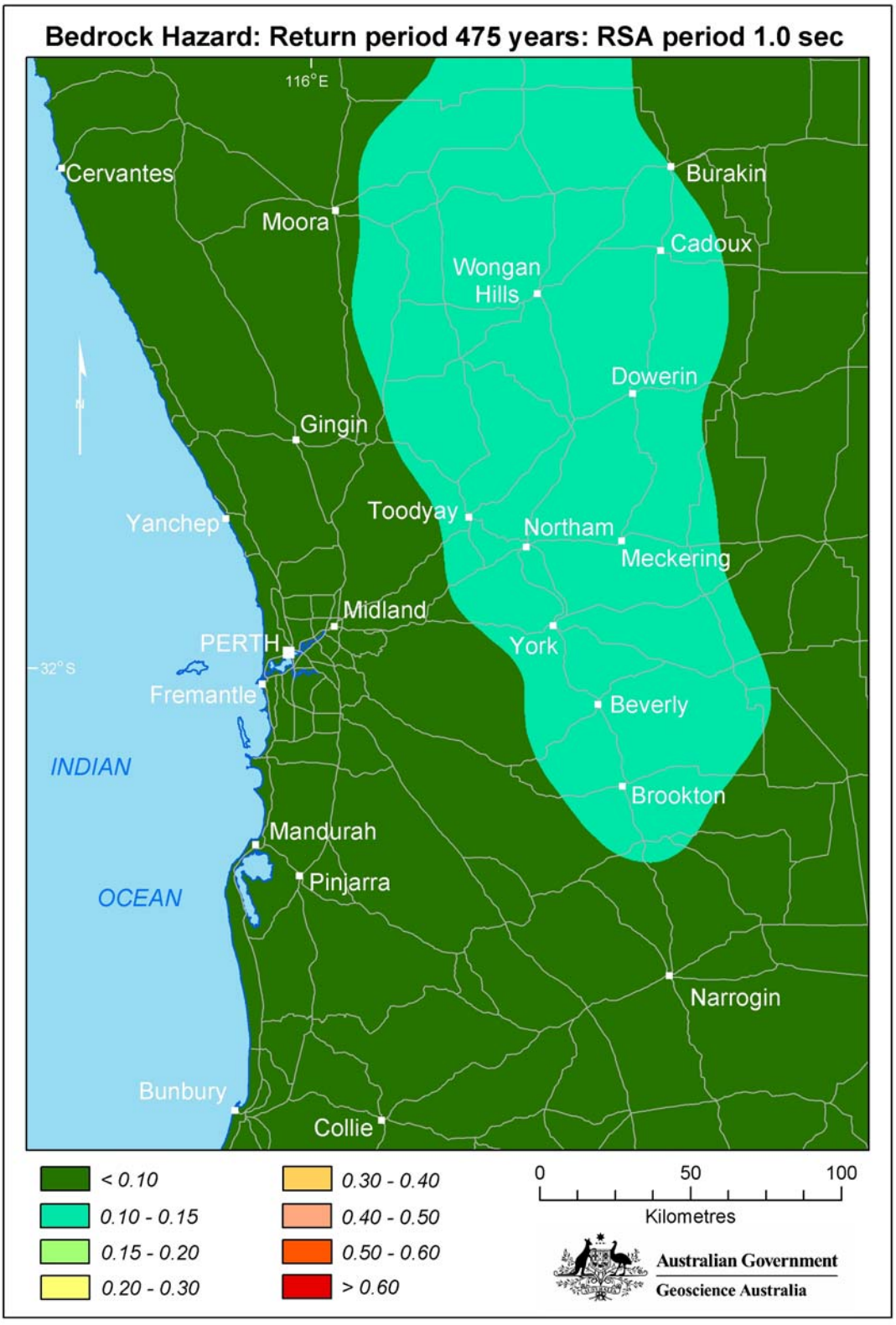

Figure 5.19: Perth region 1.0 s spectral acceleration on bedrock for 475-year return period

Comparison with current loadings standard definition of bedrock hazard

The hazard in Perth is significantly influenced by the Cadoux–Meckering zone which is located, at its closest, approximately 100 km northeast of the study region. The estimated hazard decreases with distance towards the southwest. This suggests that the PGA with a 10% probability of being exceeded in 50 years is probably being driven by small-to-moderate sized earthquakes at distances of around 100 km or more.

The averaged hazard results tend to be higher than the level prescribed by the Atkinson and Boore (1995) model. They explicitly stated that their model 'grossly over-predicted… amplitudes of small-to-moderate earthquakes at distances greater than 30 km'. This was a deliberate compromise of their model to ensure that their simple functional form adequately described spectral shapes that displayed complicated magnitude dependence. Similarly, Toro *et al.* (1997) focused on accurately describing larger earthquakes that were seen to be important to the earthquake hazard in CENA. Their model does not claim to grossly over-predict small-to-moderate earthquakes and predicts notably lower hazard than that predicted by Atkinson and Boore (1995).

Table 5.2 permits a comparison between the currently used definition of Perth hazard as presented in the earthquake loadings standard (Standards Australia, 1993), how that hazard definition is expected to change by the substitution of the draft standard (Standards Australia, 2004) and that determined by this study. A number of observations can be made from the table.

- The PGA predicted by this study greatly exceeds the PGA values in the standards but has little structural significance. These elevated values do not mean that the Perth regional hazard needs to be increased and should not be substituted for the 'a' or 'Z' values in the design standards.
- The spectral values at a 0.3 s period are very similar to the current and draft code values. The re-assessed hazard for the study tends to be slightly lower, particularly when compared to the draft standard (20% lower). This drop is less evident for the Perth region where the hazard shows some increase from that in the current standard and is comparable to that in the draft. The larger earthquake catalogue used for this study that includes the Burakin swarm events is, in part, responsible for the upward shift.
- The spectral values at a 1.0 s period are significantly lower than those derived from the current standard but are similar, though slightly lower, than those proposed in the draft.
- The bedrock hazard values for the Perth study region are expected to be generally conservative as they do not capture the attenuating effect of the Perth sedimentary basin. This effect has been later captured in the predictions of earthquake hazard on regolith.

The spatial extent of the elevated hazard in the Wheatbelt can be seen in Figure 5.18. The area of highest hazard has moved from the Meckering area to the vicinity of Cadoux and Wongan Hills. The S_A = 0.4g contour as determined from the current and draft standards have been superimposed on Figure 5.18. Significantly, the area of elevated hazard is more extensive than previously identified being wider in an east–west direction, extending further northwards and located closer to Perth. While the draft standard will define the area of elevated hazard slightly better than the current, neither will capture the full spatial extent of the elevated hazard determined by this study.

Assumptions and uncertainties of the earthquake hazard models

The earthquake hazard results in this work are based on numerous assumptions and idealisations ranging from the empirical relationships used to determine rupture dimension through to the use of an equivalent-linear methodology for modelling site response. The majority of these are thought to have minimal impact on the results presented in this chapter. However, there are some assumptions and uncertainties that are thought to strongly influence the presented results and these are discussed below.

Earthquake source model

There are two key issues relating to the earthquake source zones that have had a significant impact on the earthquake hazard results, specifically:

- The GR relationships defined for the southwest WA zones are based on datasets that have some uncertainty associated with the consistency of the catalogue of earthquakes and their magnitude computation. Variations in the GR relationships for the closest zones could affect the hazard estimates.
- The definition of the source zones in the region has been based on the expert opinion of the participants in the workshop of 2002 and represent GA's current knowledge of the complex structures and processes in the area. Nevertheless, a discovery of some active fault system may influence the seismic parameters defined in the region and consequently could change the present hazard calculations.

Attenuation model

The attenuation model used in this study is one of the most important inputs to the earthquake hazard analysis. Every estimate of earthquake ground shaking is based on this model's prediction of earthquake attenuation. Consequently, a change in the attenuation model could potentially cause a significant change in the estimated hazard. As mentioned previously, the attenuation model of Toro *et al.* (1997) is based on the tectonic and geological conditions of central and eastern North America. To date there has been only one detailed analysis of the applicability of this model to Australian conditions – in Newcastle (Dhu *et al.*, 2002), and consequently questions exist as to the appropriateness of this attenuation model. The Atkinson and Boore (1995) attenuation model has not been tested as to its applicability to Australian conditions. Preliminary work on strong-motion data recorded from the 2001–02 Burakin, WA earthquake swarm suggests that the Fourier spectral amplitude models (eg, Atkinson, 2004a, 2004b) that form the basis for this attenuation model may underestimate ground shaking at hypocentral distances less than approximately 70 km (Allen *et al.*, accepted). This is particularly apparent for periods between 0.3 s and 1.0 s.

5.4 Localised Ground Motion Model

The Perth study region is located on the sediments of the Perth Basin. This basin consists of some 10–15 km of sedimentary material ranging in age from ~430 Ma to <500,000 years, overlying Proterozoic basement rock. The upper sedimentary sequences in the study region are characterised by 30–80 m of Quaternary sands, muds and limestone. Appendix D describes the regional geology in more detail, however two key points are summarised below.

- The Perth Basin has poorly constrained shear-wave velocities, however the limited available data suggests that the top 5 km of the crust has shear-wave velocities significantly slower than the central and eastern North American (CENA) crust assumed by Toro *et al.* (1997) and Atkinson and Boore (1997).
- The regions regolith tends to have shear-wave velocities on the order of 100–300 ms^{-1}, however the material thickness and spatial distribution is extremely variable.

This geological environment (i.e., a deep sedimentary basin overlain by significant regolith material) is distinctly different from the environment assumed by Toro *et al.* (1997) and Atkinson and Boore (1997). These two attenuation models both predict ground motions at the surface of what is effectively hard, crystalline basement. Consequently, a modification was required to account for the effect of the slow crust and regolith material.

Ground motions recorded during a sequence of earthquakes that occurred near Burakin in 2000–2002 (Leonard, in prep.) have been used to create an empirical correction for the two CENA attenuation models used in this risk assessment. Specifically, two ground motions recorded from the magnitude M_w 4.4 Burakin earthquake, located approximately 200 km northeast of the Perth CBD (Figure 5.20), have been used. The recording at PIG4 is located within the Yilgarn Craton, and hence is assumed to be unaffected by the crust and regolith that will modify the ground shaking in the study region. In contrast, the recording at EPS is located in the centre of the study region and is assumed to incorporate the effects of the region's geology.

The process for creating an empirical correction factor for Perth is detailed below.

1. The two recorded response spectra were smoothed using an 11-point Savitsky–Golay smoothing filter (Press *et al.*, 1992) (Figure 5.21a).
2. The EPS recording was corrected for its 34 km offset from the PIG4 recording. This was done by simulating response spectra at 168 km and 204 km using various attenuation models and determining a distance correction from these models (Figure 5.21b).
3. Each of the distance corrected EPS recordings were divided by the PIG4 recording in order to generate three different empirical corrections.
4. The mean and standard deviation of the three empirical corrections were derived as a function of period (Figure 5.21c).

The final correction factor has significant de-amplification of ground shaking for all periods less than 0.1 s. This is at least an intuitive result, as it suggests the slow crustal materials within the Perth Basin are de-amplifying ground motions when compared with the faster crustal materials of the Yilgarn Craton. There is a small amount of amplification for periods of motion greater than 0.1 s. The peak amplification of 1.5 occurs at a period of 0.5 s. This amplification is most likely caused by the surficial regolith material.

There are some obvious problems with the creation of an empirical correction in this fashion. In particular, the derivation of a correction factor from only two recordings is a point of concern. An alternative would be to use detailed numerical modelling to try to better model how the region's geology would affect ground shaking. However, the lack of quantitative geological and geotechnical data from the Perth Basin currently makes this alternative less reliable than an empirical model.

Another issue is that the correction factor has been derived from a small magnitude event, but will be applied to ground motions from significantly larger events. One possible issue from this is that larger ground motions may induce non-linear effects in the region's regolith and hence reduce the amount of amplification seen at higher periods. However, this work has taken the conservative approach of adopting the one correction factor for all earthquakes. This is again due to the lack of quantitative data available for modelling the change in amplification for larger earthquakes.

The appropriateness of these models has been checked to some degree by the validation of the EQRM against historical events, as described at the end of Section 1.2, 'Earthquake Risk Methodology'. This validation is described later in this report; however, it is important to note that the validation is for the model as a whole and does not guarantee the accuracy of any individual component.

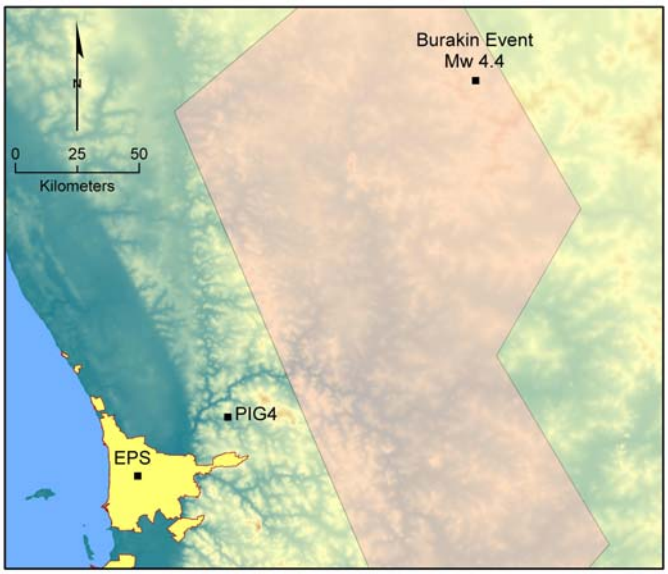

Figure 5.20: Location of the Burakin earthquake and ground-motion recorders used to derive the geological correction factor for Perth.

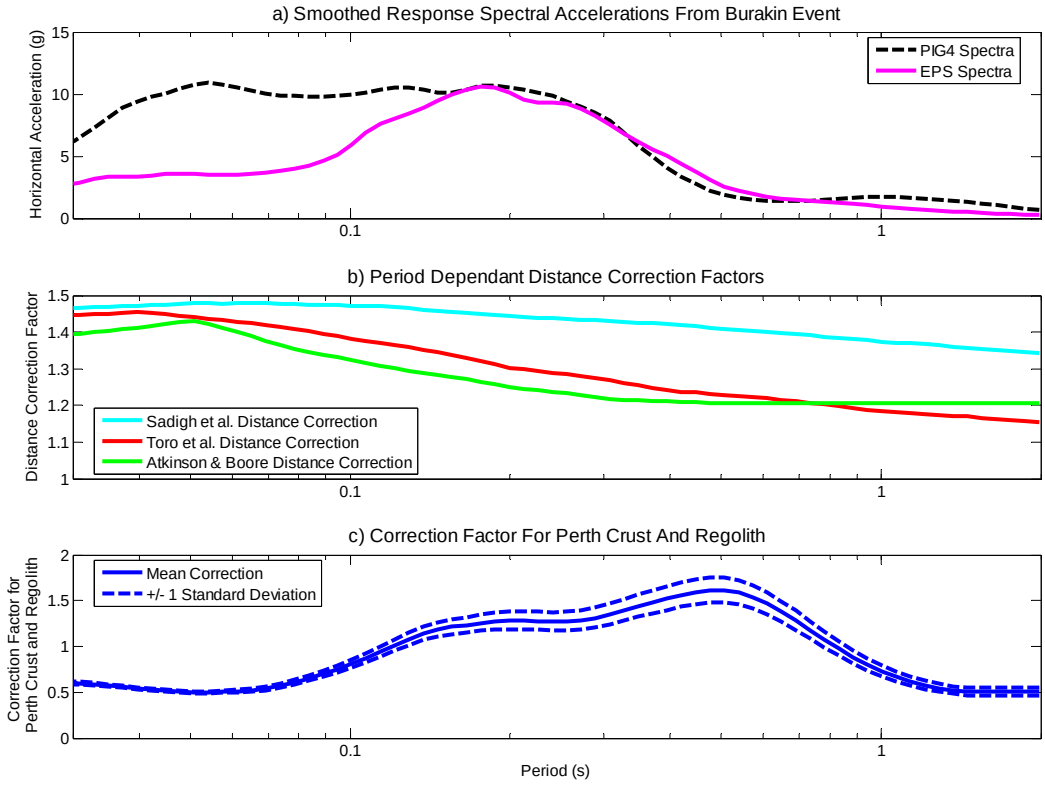

Figure 5.21: Data used for the development of a geological correction factor to account for the crust and regolith in the Perth study region. **a**) Response spectra recorded from the Burakin event. **b**) Period dependant distance corrections derived from Sadigh *et al.* (1997), Toro *et al.* (1997) and Atkinson and Boore (1997). **c**) Final correction including variability

5.5 Earthquake Regolith Hazard

As described earlier, the Perth study region is situated on significant regolith and crustal geology that is markedly different from the hard-rock models used to produce the previous bedrock hazard. The regolith hazard was determined for two exceedence return periods and at three spectral periods of interest. The two return period results have been presented alongside each other in Figure 5.22 for comparative purposes. In most plots the westerly reducing hazard characteristic of the bedrock hazard can be observed on the regolith. The variable influences of changes in regolith across the study region which could not be captured in this hazard assessment would add further localised features to the plots in the Figure. The 475-year exceedence return period hazard values at a number of key study region locations are also presented in Table 5.3.

The presence of regolith tends to decrease the bedrock earthquake hazard at very short spectral periods such as PGA (compare Figures 5.16 and 5.22, and Tables 5.2 and 5.3). This reduction in PGA hazard will have little effect on the potential for structural damage in Perth as essentially all structures have longer natural periods of vibration.

The ground shaking at a period of 0.3 s will tend to affect the medium to low-rise structures that are prevalent in the Perth study region. A comparison between Tables 5.2 and 5.3 demonstrates that the Perth Basin and regolith tends to slightly increase (approx. 20%) the bedrock hazard at this structural period. Clearly, the regolith in Perth will tend to increase the risk to the residential structures in the study region.

Longer periods of motion tend to have marginally lower hazard than on bedrock (compare Table 5.2 and 5.3). This is predominantly due to the effect of the crustal geology in the Perth Basin which tends to de-amplify most periods of ground shaking. This suggests that medium to high-rise structures will be offered some measure of protection from earthquake damage due to the attenuation of ground motions in the Perth Basin.

Table 5.3: Perth study region regolith hazard for a 475-year return period of exceedance

Perth metropolitan location	**Both standards**[1]	**AS 1170.4 - 1993**		**DR 04303 - 2004**	
	PGA(*g*)	S_A at 0.3 s(*g*)	S_A at 1.0 s(*g*)	S_A at 0.3 s(*g*)	S_A at 1.0 s(*g*)
Midland	0.093[2] [0.159][3]	0.233 [0.277]	0.145 [0.047]	0.342 [0.277]	0.116 [0.047]
Perth CBD	0.089 [0.139]	0.223 [0.248]	0.139 [0.043]	0.328 [0.248]	0.111 [0.043]
Fremantle	0.088 [0.132]	0.220 [0.243]	0.138 [0.042]	0.324 [0.243]	0.110 [0.042]

Notes: [1] Bedrock peak ground acceleration (PGA) unchanged from AS 1170.4 (1993) in DR 04303.
[2] Hazard values have been interpolated from hazard maps in standards to capture variation across the study region.
[3] Values derived from this study are shown in square brackets.

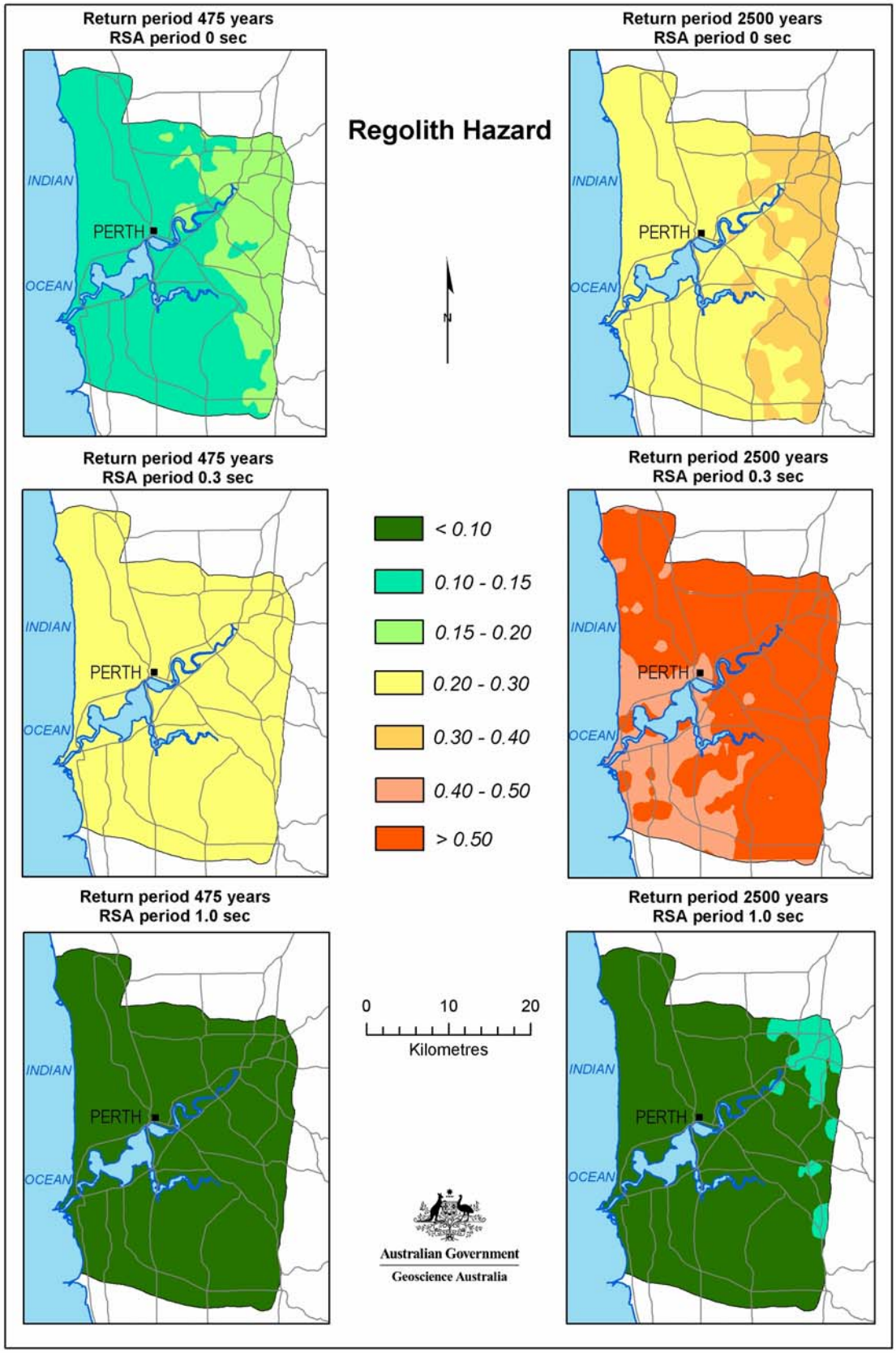

Figure 5.22: Perth study region earthquake hazard on regolith. All accelerations are presented as a fraction of the acceleration due to gravity (g).

5.6 Elements at Risk

The assessment of seismic risk requires a definition of both the hazard and the infrastructure exposed to it. For this Perth study the exposure is limited to the building stock (and contents) in the study region that has been defined as to its distribution, individual building size and construction type. The methodology used to do this is described under separate headings below.

Distribution of building stock in study area

Perth's beginnings date back to Captain James Stirling, who arrived in 1829 with a handful of settlers to establish a new colony on the banks of the Swan River. The development of the city to its present sprawl has comprised periods of rapid growth interspersed with more gradual development. The residential component of Perth's development over time within the study region is presented in Figure 5.23 and is based on spatial data supplied by the WA State Government (Department of Planning and Infrastructure, 2004). It can be seen that construction was initially centred on Fremantle and Cottesloe/Claremont at the mouth of the Swan River and both north and south of the Swan in the proximity of the current CBD. Consequently the older building stock in these areas of early development is expected to be more vulnerable as a result of the less regulated standards of construction in earlier years and the building deterioration that takes place with time, particularly near the coast. Subsequently this initial development has in-filled along with a radial spread from the river. More recently residential development has extended in a northerly/southerly coastal spread confined by the Indian Ocean to the west and the Darling Scarp to the east. Ribbon development has also taken place along the Great Western Highway, reaching almost as far as Northam with the suburbs exposed to incrementally increased seismic hazard. This later easterly development into the Wheatbelt region is outside the study region.

Perth metropolitan building data were obtained from the Perth Valuer-General's Office (VGO, 2002, 2003) for the years 2002 and 2003. Complementary footprint data were used to provide the area of each building (see Appendix B for details of databases). The building stock included in the Perth study and its usage types are depicted in Figure 5.24. There are about 350,000 built structures in the study area and approximately 50% of them are in the LGAs of Stirling, Joondalup, Melville, Cockburn, and Canning (see Table 5.4). For outer LGAs – Wanneroo, Swan, Northam, Mundaring, Kalamunda, Armadale, and Cockburn – only a portion of the total building stock is incorporated. The building database is not comprehensive, as the base VGO data does not include all non-rateable public buildings. Notwithstanding this limitation, the database does represent the most complete exposure data that could be assembled using available resources.

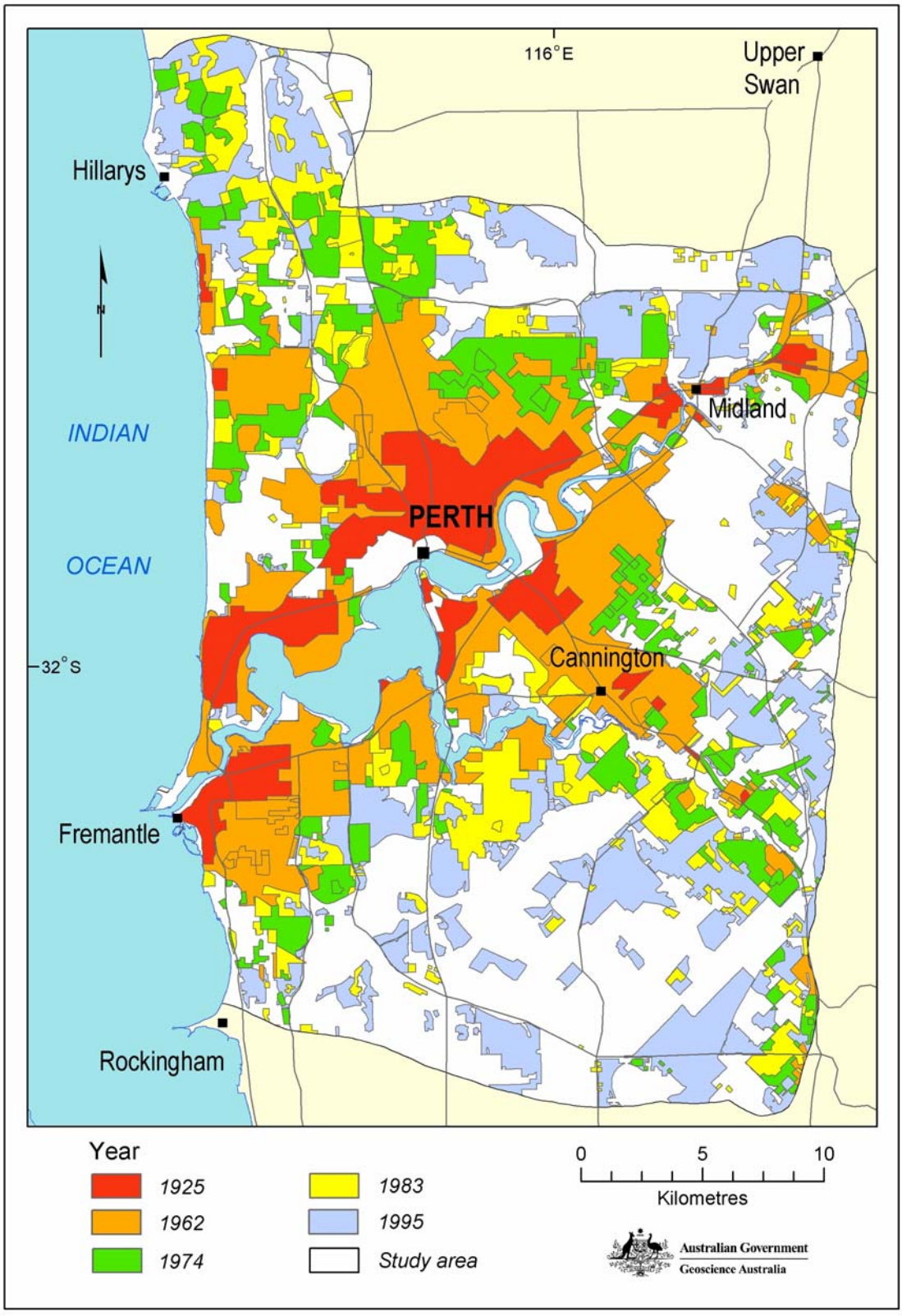

Figure 5.23: Extents of Perth residential development with time within the study region

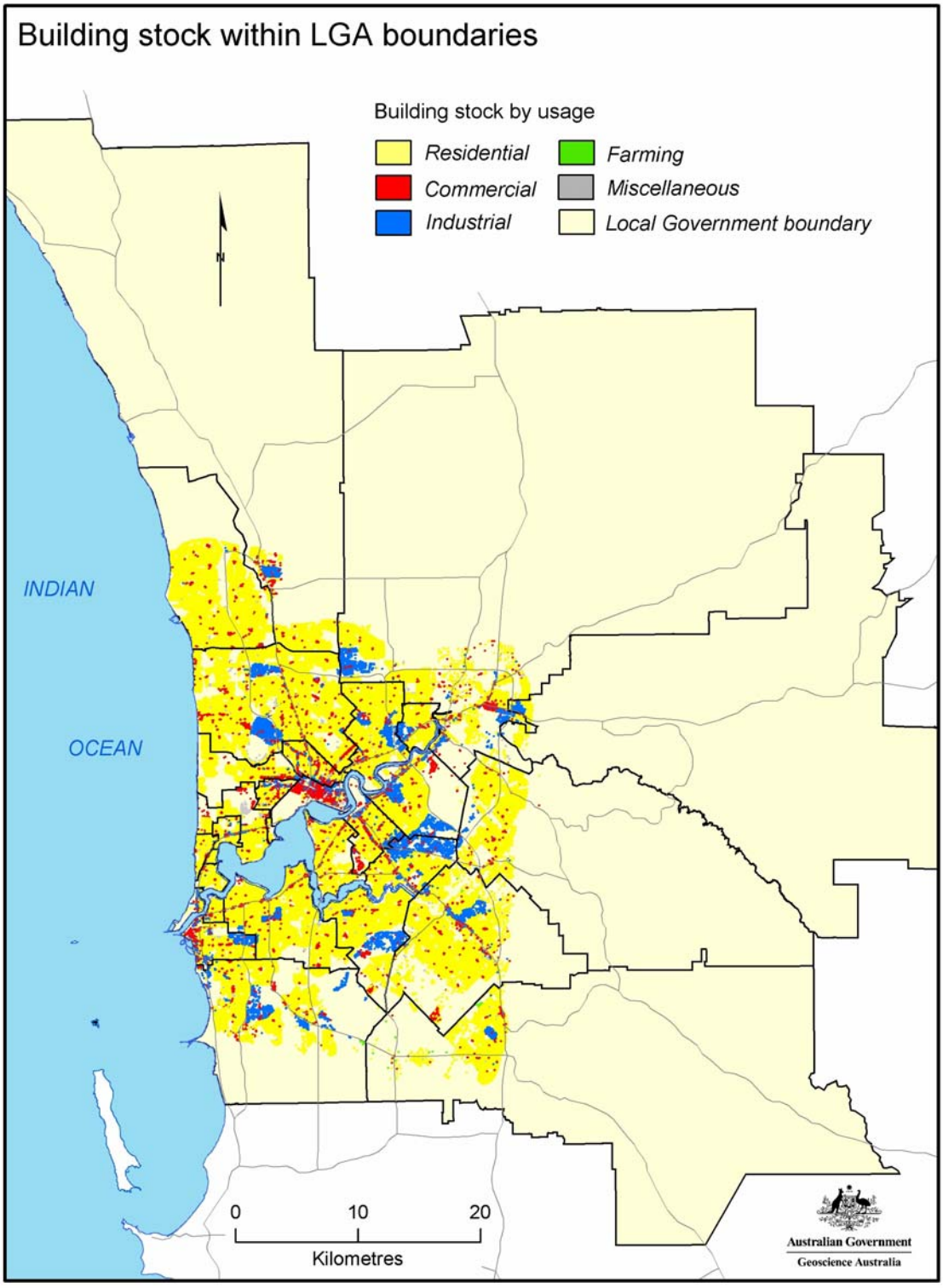

Figure 5.24: Building stock within LGA boundaries

Table 5.4: Building count by LGA

LGA	Number of buildings	% Study area
Stirling	56 016	15.82
Joondalup	36 410	10.28
Melville	32 928	9.30
Cockburn	28 868	8.15
Canning	28 320	8.00
Gosnells	26 452	7.47
Bayswater	16 323	4.61
Fremantle	12 088	3.41
Belmont	12 064	3.41
Swan	11 525	3.25
Armadale	10 658	3.01
Kalamunda	9 907	2.80
South Perth	9 328	2.63
Cambridge	8 483	2.40
Wanneroo	7 972	2.25
Nedlands	7 611	2.15
Victoria Park	7 544	2.13
Vincent	6 895	1.95
Perth City Council	4 483	1.27
Subiaco	4 122	1.16
Cottesloe	2 386	0.67
Mundaring	2 331	0.66
Mosman Park	2 282	0.64
East Fremantle	2 199	0.62
Claremont	2 133	0.60
Bassendean	1 746	0.49
Peppermint Grove	477	0.13
TOTAL	354112	100

The building stock is broadly classified by usage type – residential, commercial, industrial and government – and structural type. The usage types have been further sub-divided according to the Functional Classification of Buildings (FCB), developed by the Australian Bureau of Statistics (ABS) (see Table 5.5).

Residential buildings make up over 95% of the total building stock of the Perth study area, 90% of which are detached houses (see Table 5.6). Industrial and commercial building stock represents less than 5% of the total building stock in the study area. Of the commercial buildings, 53% are offices and 36% are retail outlets. Factories make up about 75% of the industrial building stock.

Table 5.5: Functional classification of buildings

FCB	Building usage
	Residential buildings
111	Separate house
113	Transportable house
121	Semi-detached – 1 storey
122	Semi-detached – 2 or more storeys
131	Flat – 1or 2 storeys
132	Flat – 3 storeys
133	Flat – 4 or more storeys
134	Building attached to a house
	Commercial buildings
211	Retail/wholesale trade
221	Passenger transport
223	Car parks
224	Transport buildings (not elsewhere classified)
231	Offices
291	Commercial (not elsewhere classified)
	Industrial buildings
311	Factories and other secondary production
321	Warehouses
391	Industrial buildings (not elsewhere classified)
	Other non-residential buildings
411	Education
421	Religion
431	Aged-care facilities
441	Hospitals
442	Health
451	Entertainment and recreation
461	Self contained short-term apartments
462	Hotels, motels, boarding houses, hostels or lodges
463	Other short-term accommodation (not elsewhere classified)
491	Non-residential (not elsewhere classified)

Source: Australian Bureau of Statistics, 2001a

Table 5.6: Perth metropolitan building stock by usage type

FCB	Building usage	No. of buildings	
	Residential buildings	**95.5%**	***% Residential buildings***
111	Separate house	301 187	90
121/122	Semi detached – 1 to 2 storeys	26 034	7.7
131-134	Flats	7 890	2.3
	Commercial buildings	**3.4%**	***% Commercial buildings***
231	Office	6 228	53
211	Retail/wholesale trade	4 298	36
291	Other	777	6.5
223	Car park	330	3
221/224	Passenger transport	178	1.5
	Industrial buildings	**1.3%**	***% Industrial buildings***
311	Factories and other secondary production	3 466	75.5
321	Warehouses	1 085	23.5
391	Other	40	1
	Other non-residential	**0.8%**	***% Non-Residential buildings***
442	Health	633	24
451	Entertainment and recreation	619	23.5
431	Aged care facilities	334	13
491	Other	331	13
462/463	Hotels, motels, boarding houses, short term accommodation	304	12
411	Education	288	11
441	Hospitals	48	2
421	Religion	25	1
461	Self contained short term apartments	14	0.5

Source: VGO, 2002

Definition of the size of building structures

Building vulnerability models furnish the damage loss as a percentage of the full replacement cost of the structure concerned. Consequently the replacement value for each exposed building is required and was determined using an estimated total floor area for each building and the cost models described in Section 5.7. The floor area estimation methods adopted for the range of building usages are described below.

Discrete residential homes

Free-standing discrete residential homes represent 86% of the total building stock (Table 5.6). Several data sources were utilised to determine their floor areas with a source accuracy hierarchy established. These are described below.

Building footprints

In total 525,000 Perth roof-plan footprints were available with 320,000 falling within the study region. Most were supplied by the WA Department of Land Information (DLI) through the Western

Australian Land Information System (WALIS), though the set was supplemented with additional footprints created by GA. These polygons represent a direct measure of the house size but include attached garage, eaves areas and other peripheral roof areas such as verandas. These were considered the most accurate measure of building floor area after correction for the non-enclosed areas.

VGO room number data

The VGO database includes equivalent floor areas for 490,000 building occupancies, some of which were part of multi-occupancy dwellings such as blocks of flats and apartments. The area is expressed as a room number that is related to the rateable floor area. Each room has a notional area of 18.5 m^2, incorporating secondary floor areas such as hallways and bathrooms. The area does not include garages and non-enclosed roof areas. With corrections this was considered to be the second most reliable indicator of house size.

ABS building permit data

The ABS processes building permit data and publishes the average annual size of newly constructed homes (ABS, 2004). The floor area given is that enclosed by walls and so includes attached garages. The area does not include eaves areas or peripheral roof areas. This was considered the default floor area when the preceding area measures were unavailable but building age could be assigned.

Area adjustment factors

Correction factors for all three sources of building area were derived using data obtained from two surveys of Perth buildings and one from Victoria. The first was a Perth survey (August/September 2003) of 2,600 buildings located in three Perth suburbs (Clarkson, Winthrop and Duncraig). The survey utilised aerial photography and recorded roof areas and building plan shapes, matching these to the corresponding VGO data. The second was a Perth floodplain foot survey (December 2003) of 2,080 buildings that provided a measure of the variation of eaves width with age. Finally, a peripheral roof area survey of 188 Bendigo, Victoria, homes (Edwards *et al.*, 2004a) was used as an indicator of typical peripheral roof areas for Perth homes. The application of this data is summarised in Figure 5.25. Firstly, the 2,600 aerially surveyed Perth roof areas are reduced for eaves width using the eaves width size data but with no adjustment made for other non-enclosed roof areas. The areas obtained are plotted as construction year averages in the figure. Secondly, the linear regression of this area data is adjusted using the Bendigo data for the other non-enclosed roof areas to obtain the enclosed roof area also shown. The resultant line compares very closely with the mean ABS permit data floor areas (shown as triangles in the Figure 5.25), even though the approach did not consider the proportion of two-storey homes with living areas on the ground floor. Finally, the adjusted areas are factored up on the basis of construction cost data to obtain an area that would give a reconstruction cost for the entire house, including verandas and carports. The corresponding VGO data areas are also shown in Figure 5.25 and correction factors are also derived for adjustment to the target area shown. The suite of adjustment factors obtained was sequentially applied to the full residential building database.

The steps in deriving the representative floor areas for each house, which reflect the accuracy hierarchy discussed above, were:

1. Where the building footprint area is known, correct to target costing area.
2. Where the VGO area based on room number is known, correct to the target costing area.
3. Where only the construction year is known, use the ABS floor area for that year and correct for non-enclosed roof areas.
4. Where nothing is known about the house, take the mean of the known house ages in suburb and use the ABS floor area for that year, correcting it for non-enclosed roof areas.

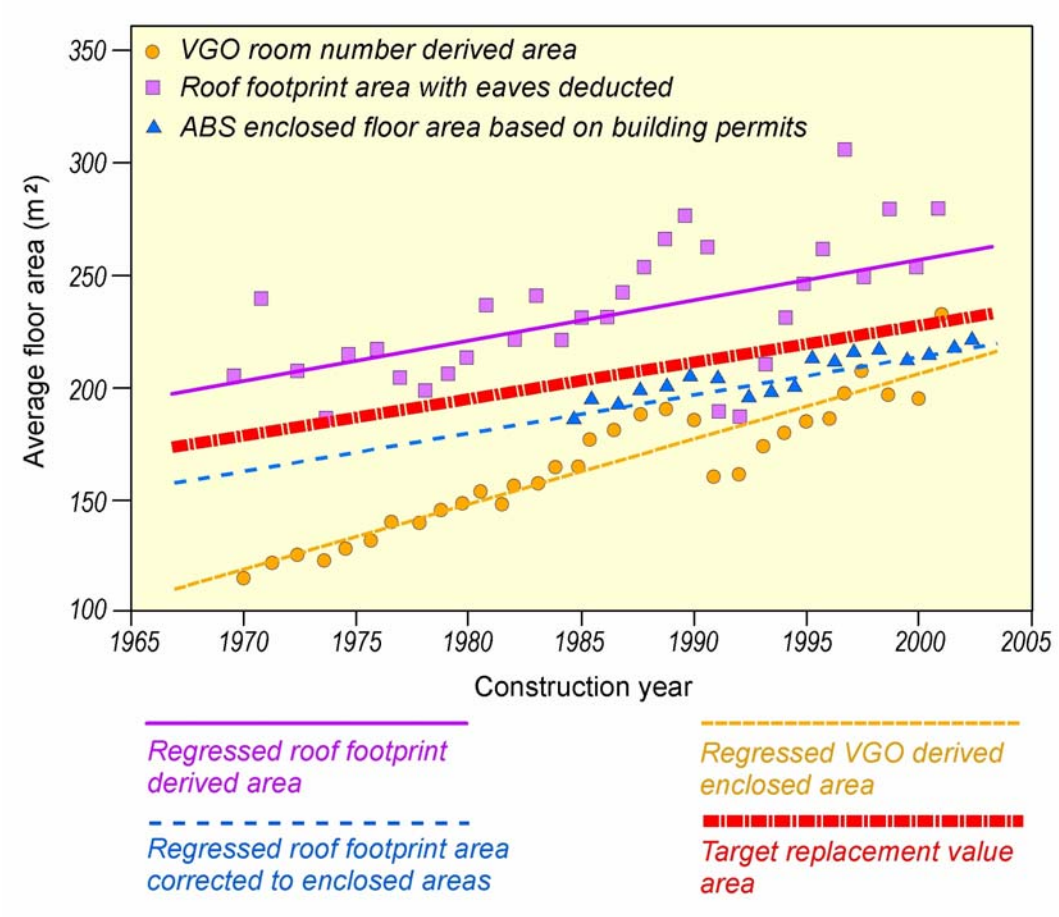

Figure 5.25: Verification of residential home floor area determination

Multi-dwelling residential buildings

Multi-dwelling residential structures represent a further 9.6% of the total building stock (Table 5.6). These were identified in the VGO database where several leaseable occupancies were assigned to a single land parcel. The separate occupancies were aggregated into a single multi-level residential building using the footprint area, the total VGO derived occupancy areas, and the assumption that the residential occupancies are equally distributed on all floors. Eaves areas and peripheral structures were assumed to be negligibly small.

Commercial

The storey number and the total building area were determined using a similar methodology to that used for multi-dwelling residential structures.

Industrial and other non-residential

Where the VGO database included a floor area for the building this was adopted. Where no floor area was available the building was assumed to be single story with limited eaves width and the building footprint area used.

Construction types

For the risk-simulation modelling the 350,000 buildings that comprise the building data base were classified into sub-groups of building construction types. The assignment influences both the level of building response to each simulated earthquake event (accelerations and displacements) and the damage degree probabilities associated with the response. The classifications used follow those of the methodology used by HAZUS (National Institute of Building Sciences, 1999) with the inclusion of

several additional building types developed to better represent the vulnerability of Australian structures. The VGO base data included fields for roof material type and wall material type. It was found that only a small proportion of fields were unpopulated (12,000 wall types and 32,000 roof types of 500,000 study region occupancies) and defaults were nominated for the small 'unknown' percentage. The construction type was assigned using a combination of the FCB and the roof and wall types with mappings provided to cover a minimum of 95% percent of the building stock in each building usage category. The mappings of structural models for residential structures are presented in Table C4 in Appendix C.

The construction types used in the Perth database are listed in Table 5.7 below. Not all 36 HAZUS types were present in Perth and so are not presented below. Some of the types were subdivided into sub-classes based on wall and roof type to better reflect the building stock vulnerability. For a full list of the HAZUS construction types see the *HAZUS99 Technical Manual* (National Institute of Building Sciences 1999, Chapter 5). Table 5.7 shows the percentages of each construction type in the Perth building database. The most common are unreinforced masonry followed by timber frame. The primary types are described further below.

Table 5.7: Building types, codes and percentages for Perth

Construction types	HAZUS/EQRM type codes	Total buildings (%)
Steel framed buildings	S1L	0.05
	S2L	0.59
	S3	0.04
	S5L	1.85
Timber framed	W1BVTILE	2.54
	W1BVMETAL	0.44
	W1TIMBERTILE	3.19
	W1TIMBERMETAL	2.22
Reinforced and pre-cast concrete buildings	C1LMEAN	0.05
	C1LNOSOFT	0.006
	C1MMEAN	0.007
	PC1	0.19
Unreinforced masonry	URMLTILE	87.83
	URMLMETAL	1.00

Unreinforced masonry buildings

This type of buildings is very common in Perth and is the most common construction form for new residential structures. A wide range of buildings (including houses, terraced houses, shops, schools, churches and hospitals) are constructed of unreinforced masonry. Infill walls in reinforced concrete framed buildings are also commonly constructed of unreinforced masonry.

Unreinforced masonry buildings have historically performed poorly in earthquakes, as demonstrated by the 1989 Newcastle earthquake (Melchers, 1990). While these types of structures can perform satisfactorily if designed and constructed according to current building standards, buildings which are old, decayed, of poor design or construction may perform poorly during an earthquake.

A common deficiency in this type of construction is a lack of ties between the two leaves of double-brick cavity wall construction. This deficiency may be the result of corrosion or either the lack of ties or their incorrect placement. Soft and eroded lime mortar joints also contributed to structural weakness and to widespread corner failures in the Newcastle 1989 earthquake (Melchers, 1990). These deficiencies commonly manifest themselves in the failure of parapets, gable roof ends, corners, chimneys and the transverse failure of walls. Cracking due to racking is another common type of damage, although this result is less dependent on construction quality.

Continuity of the structure and ductile behaviour are keys to good seismic performance. The latest Australian standard for masonry structures, the 3rd edition of AS3700 (Standards Australia, 2001b), gives recommendations for design, including requirements to take seismic effects into consideration to achieve adequate performance levels. This standard replaced the second edition issued in 1998. In general, Australian Standards for buildings are enacted by federal parliament into the Building Code of Australia. The latest version of AS3700 is referenced by BCA Amendment 3 and was published in November 2001.

Timber frame buildings

In Perth timber frame housing is often identified by brick veneer, timber and sometimes fibreboard cladding. Brick veneers, which can easily be confused with unreinforced masonry buildings, are becoming more popular in Perth, though they still represent a smaller portion of new construction due to economies in double brick construction. Timber frames are largely limited to smaller buildings such as houses.

Timber frame buildings generally perform very well in earthquakes, although non-structural and contents damage can be significant. Brick veneer cladding, brick chimneys, plasterboard linings and cornices are commonly damaged by earthquake shaking. However, serious structural damage is perhaps most likely in the subfloor and foundations, particularly where there is a lack of subfloor bracing or if there is a lack of continuity.

Timber frame housing must be designed according to AS1720.1 (Standards Australia, 2002) or AS1684.1–4 (Standards Australia, 1999a, 1999b, 1999c, 1999d), though consideration of lateral loading is dominated by discussion of wind loading in these documents. The consideration of seismic effects has had practically no effect on the construction practices for this category of structure. Despite non-structural and contents components of these building types being more vulnerable than the structural components, little attention has been paid to improving their performance, and this is reflected by a lack of requirements in Australian Standards.

Reinforced and pre-stressed concrete buildings

Concrete buildings form a significant percentage of the large buildings in Perth. These buildings are used for a wide range of purposes, including commercial, car parking, industrial, residential, educational and government purposes. These concrete buildings may be normally reinforced and/or prestressed, cast *in situ* and/or precast, consisting of slabs, moment frames and/or shear walls.

Concrete construction performs well when detailed to ensure continuity and ductility and if structural irregularities are avoided. A vertical structural irregularity, often called a ‘soft’ or ‘weak’ storey is particularly susceptible to collapse. These soft/weak storeys are common where car parking or large open spaces are located on the ground floor of a multi-storey building. Irregularities in building plan are equally undesirable since torsional effects can amplify the response for torsionally eccentric components. Soft storey construction can also be an issue for types of construction other than concrete.

The presence of unreinforced masonry infill walls in multi-storey frame buildings can inadvertently cause structural irregularities. Also, the failure or cracking of such walls in racking or out-of-plane response can be costly in terms of repair and also in terms of the hazard they present as falling debris. Falling debris from other failed non-structural components, such as glass windows, can be equally hazardous.

'Tilt-up' forms of pre-cast concrete construction have become more popular in recent decades. However, this construction method has not been well tested by real earthquake events in Australia.

The current Australian Standard for concrete structures, AS3600, issued in 2001 (Standards Australia, 2001a), requires special seismic design and detailing only in special cases and has not been modified from the 1994 version. Previous versions had no such requirements. In general, however, requirements for seismic effects have had practically no influence on construction practice. Non-structural and contents components are expected to be more vulnerable, although, as previously mentioned, few requirements exist in Australian Standards for these components.

Steel framed buildings

Steel framed buildings make up a significant proportion of large light commercial and industrial buildings in Perth. These buildings are mainly in the form of large shed-type structures and include buildings used for recreational purposes.

Although steel is a ductile material, the connections between steel members can have limited ductility, particularly when poorly designed and/or constructed welds are used. Structural irregularities, and non-structural elements and contents are the sources for the greatest concern, as they are for concrete buildings.

Both editions of the Australian Standard for steel structures, AS4100, first published in 1990 and revised in 1998 (Standards Australia, 1998), contain requirements for seismic effects, whereas previous versions lacked them. As with concrete structures, generally the requirements for seismic effects have had practically no influence on construction practice.

5.7 Direct Economic Loss Models

Estimations of economic losses from natural hazards can be used for a number of purposes, including risk assessments, appraisals of community vulnerability, evaluation of mitigation options, and the determination of levels of disaster assistance. In this chapter, a risk assessment approach for estimating direct damage losses from earthquakes is described. The method used is based on the HAZUS economic loss framework (National Institute of Building Sciences, 1999).

Definition of economic losses

Economic losses resulting from natural hazards are typically classified into tangible losses (items and services that can be costed using existing market prices) and intangible losses (items and services that are not traded directly in markets and so require proxy prices for estimation: eg, environmental damage). Tangibles and intangibles can be further sub-divided into direct and indirect losses (see Figure 5.26). For the Perth risk assessment tangible losses only have been considered.

Direct losses

In general, direct losses, or more specifically, direct damage losses, refer to losses resulting from the physical impact of a hazard event. Direct tangible losses include physical damage to capital stocks such as buildings, contents, infrastructure, and vehicles. In most loss assessments, tangible direct damage losses are measured in terms of the replacement value of the damaged property at a single point in time. It is worth noting that in an economic analysis, the losses would usually be calculated in terms of the changes in *flows* of goods and services over time rather than at a single point in time.

Buildings, inventories and public facilities are treated as capital investments that produce income, and the value (or loss) of the building and inventory would be the capitalised value (or loss) of the income produced by the investment that created the building or inventory.

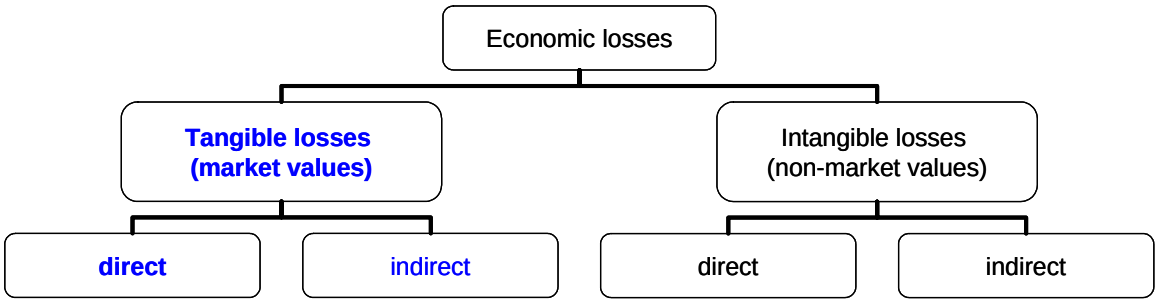

Figure 5.26: Classification of economic loss

Some loss assessments classify the cost of disruption to businesses directly affected by the hazard event as direct tangible losses (National Institute of Building Sciences, 1999). Here, a distinction needs to be made between financial losses (i.e., losses to individual entities) and economic losses (losses to society). Financial losses may be incurred by entities where the normal functioning of businesses is not possible due to the hazard event. However, if other producers in the region can provide the goods and services at no additional cost to the consumer, then there will be no disruption to the flows of goods and services and hence no economic loss is incurred. By including the losses to all affected entities in an economic loss assessment, economic losses would be overestimated.

Indirect losses

Natural hazard events not only disrupt households and businesses directly impacted by the event but may also produce dislocations in economic sectors 'downstream'. The extent of these indirect losses depends on the availability of alternative suppliers and customers for the goods and services as well as the length of the production disturbance. Indirect losses have not been calculated for this study but will be available for the Perth region in the future.

Availability of post-disaster data for economic loss assessments

In Australia, economic loss data are not systematically and consistently collected following a natural hazard event. Under the five-year Disaster Mitigation Australia Package (DMAP), administered by the Department of Transport and Regional Services (DOTARS), efforts are being made to collect more consistent and comprehensive data for damage and recovery post-disaster economic loss. These data would allow a broader assessment of economic losses over time, particularly with the inclusion of household and business disruption and recovery data. For the Perth study, no attempt was made to capture losses that occur after the immediate impact of the event. Estimates of the injury or death tolls due to earthquakes are also not included.

Direct loss model for Perth

The direct loss model for metropolitan Perth is a first step in developing an economic loss model for the impacts of natural hazard events on Australian communities. Given the complexity of the problem and the present lack of post-disaster data, the direct losses are only measured in terms of the tangible losses derived from direct building and contents damage. Losses from infrastructural damage – such as road, water and electricity networks – are not included. The direct economic loss model essentially converts the structural and non-structural damage state information, derived from the engineering vulnerability models, into repair and replacement costs of the building stock and contents. Direct costs are therefore measured in terms of the current value of resources required to rebuild and repair the damaged stock. In using building replacement costs to value building damage, a number of simplifying assumptions have been made. It is assumed that damaged buildings will be repaired and rebuilt in accordance with the current building codes and to the identical size and structural type of their pre-disaster state. In addition, it is assumed, irrespective of the hazard event, that damaged buildings were not due for demolition, and hence will be rebuilt after the event.

Building cost models

Initial estimates of replacement costs of buildings were developed by Reed Construction Data (2003) and provided in 2003 dollars. For the Perth metropolitan area, 86 building cost models were developed to capture at least 95% of the building stock of the metropolitan area. In Appendix C the replacement costs per square metre of representative buildings are tabulated for each usage type (Tables C.1–C.4). Since the residential cost models were developed for different sized buildings, the costs per square metre estimates were regressed to provide a continuum of cost estimates for the full range of house sizes.

In costing residential buildings, the age of the building was also considered and closely aligned to the structural type. For all other usage types, contemporary replacement cost models were assumed. The age classifications for residential buildings are as follows:

- Victorian: 1840–1890;
- Federation: 1891–1913;
- War period: 1914–1945;
- Post-war: 1946–1959; and
- Contemporary: 1960 to present.

Given the significant cost variations for each building type, the cost estimates are only indicative of the potential building losses and considered most useful for larger rather than smaller spatial analysis.

Calculation of building losses

To calculate the cost of replacing a building damaged by an earthquake, the building value is divided into three components: structural, non-structural (acceleration-sensitive) and non-structural (drift-sensitive). Acceleration-sensitive components include hung ceilings, mechanical and electrical equipment, and elevators. Drift-sensitive components include partitions, exterior wall panels, and glazing. The percentage component breakdown is based on US figures and is estimated for each building usage classification (Jackson, 1994) (Table 5.8).

Damage costs are expressed as a percentage of the complete damage state. However, it is recognised that once a certain level of damage is reached, it is usually more cost-effective to demolish the building and rebuild the entire structure rather than replace the damaged components. This is often the case with older houses, especially where buildings may not be built to the current building codes. In terms of the model, once the upper limits of ‘extensive damage levels’ are reached for older structures it is classified as ‘complete damage’. The relationship between damage states and repair/replacement

costs for both structural and non-structural components are presented in Table 5.9 and is consistent with those used in HAZUS.

Table 5.8: Percentage breakdown of building replacement costs by FCB and structural and non-structural components

FCB	Structural (%)	Non-structural, drift-sensitive (%)	Non-structural, acceleration-sensitive (%)
111	23.44	50.00	26.56
112	23.44	50.00	26.56
113	0.00	50.00	50.00
121	23.44	50.00	26.56
122	23.44	50.00	26.56
131	13.75	42.50	43.75
132	13.75	42.50	43.75
133	13.75	42.50	43.75
134	23.44	50.00	26.56
191	23.44	50.00	26.56
211	29.41	27.45	43.14
221	16.18	33.82	50.00
222	16.18	33.82	50.00
223	60.87	17.39	21.74
224	16.18	33.82	50.00
231	19.18	32.88	47.95
291	16.18	33.82	50.00
311	15.69	11.76	72.55
321	32.35	26.47	41.18
331	46.15	7.69	46.15
391	15.69	11.76	72.55
411	18.92	48.65	32.43
421	19.77	32.56	47.67
431	18.42	40.79	40.79
441	14.05	34.71	51.24
442	14.44	34.44	51.11
451	9.90	35.64	54.46
461	23.44	50.00	26.56
462	13.58	43.21	43.21
463	13.58	43.21	43.21
491	15.32	34.23	50.45

Source: National Institute of Building Science, 1999.

The repair cost (loss) for each building is the weighted sum of the probable damage costs to each of the three building components. For a given usage type and each of the defined damage states, building repair and replacement costs are estimated as the product of the floor area of each building within the given usage type, the probability of the building structural type being in the given damage state, and repair costs of the building type per square metre for the given damage state, summed over all building structural types within the usage class (National Institute of Building Sciences, 1999).

Contents losses

Estimated contents damage from earthquake events has been calculated based on the building acceleration, structure and usage. In costing the contents damage, it is assumed that the losses increase

as the level of damage to the building increases. It is also assumed that some of the contents will be salvaged even where 'complete damage' of the structure is assumed (see Table 5.10).

Table 5.9: Percentage building losses by damage states (percentage of complete replacement cost)

Damage state	Structural	Non-structural drift	Non-structural acceleration
No damage	0	0	0
Slight damage	2	2	2
Moderate damage	10	10	10
Extensive damage	50	50	30
Complete damage	100	100	100

Table 5.10: Percentage contents losses by damage state

Damage state	% Replacement cost
Slight damage	1
Moderate damage	5
Extensive damage	25
Complete damage	50

Residential contents losses

For metropolitan Perth, estimated contents values were only available for residential buildings. They differ according to the location and size of the residence. The contents category (average, quality or prestige) was assigned to an LGA based on average weekly income (ABS, 2001b) (see Table 5.11). For a contents value classification of each LGA in the study area, see Appendix C, Table C.5. The residential contents values were also assigned to each building according to the size of the structure (see Table 5.12).

Table 5.11: Value of contents by average household income

Average weekly household income ($)	Contents classification
500–899	Average
900–1,350	Quality
Over 1,350	Prestige

Table 5.12: Estimated residential contents costs by house size

Area of building (m^2)	Average ($)	Quality ($)	Prestige ($)
120	44 000	97 000	249 000
200	54 000	118 000	285 000
275	73 000	161 000	392 000
350	85 000	190 000	468 000
Unit (low rise)	54 000	120 000	289 000
Apartment (high rise)	25 060	55 690	134 220

Source: RCD 2003

Contents losses for non-residential buildings

For commercial contents values, estimates were only available for a select number of usage types (see Table 5.13). For the remaining commercial usage types in the study area, the value of contents was assumed to be the equivalent of the building replacement cost, consistent with the assumption made in HAZUS (National Institute of Building Sciences, 1999). With respect to industrial buildings, where contents values were not available, the value of contents was assumed to be 1.5 times greater than the cost of replacing the building (National Institute of Building Sciences, 1999). This assumption was also made for religious, entertainment, short term accommodation, education and hospital buildings.

Table 5.13: Contents costs by usage type

FCB	Sub-category	Average cost of contents per m^2 ($)
211	Supermarket	430
211	Shopping centre	290
211	Arcade	390
211	Restaurant	1 055
211	Take-away outlet	1 135
231	Commercial office – low rise	710
231	Commercial office – mid rise	1 770
231	Commercial office – high rise	1 765
291	Garage/workshop	260
291	Service station	530
321	Depot/yard	80
442	Health buildings	119
461	Hotel	630
461	Club (RSL type)	345
462	Hotel – small	780

5.8 Risk Model Verification Against Historical Earthquake Losses

There is a paucity of documented Australian earthquake damage data that can be drawn upon to verify earthquake risk models. However, it has been possible to make use of two damaging WA earthquakes to test the realism of GA's combined ground motion, exposure and damage models that comprise the risk model used. The events selected were the M_w 6.6 Meckering 1968 event and the M_w 6.1 Cadoux event of 1979. Both events were simulated 1,050 times using the EQRM software (Robinson and Fulford, 2003) in order to capture the variability in ground motion and damage models. The results and the assumptions made to obtain comparable study region losses (structure and contents combined) are presented below.

Meckering

The Meckering scenario simulation predicted a mean study region loss of 0.27 % with a standard deviation of 0.06 % (Figure 5.27). Peele (1993) claims that the Meckering event caused approximately $700,000 (1968 dollars) of insured residential loss in the Perth metropolitan region. This number must be converted into the percentage loss to both uninsured and insured structures in order to be comparable with GA's simulated results. However, there is no published information on the 1968 Perth ratio of insured to uninsured structures, nor on the total number of structures in the region.

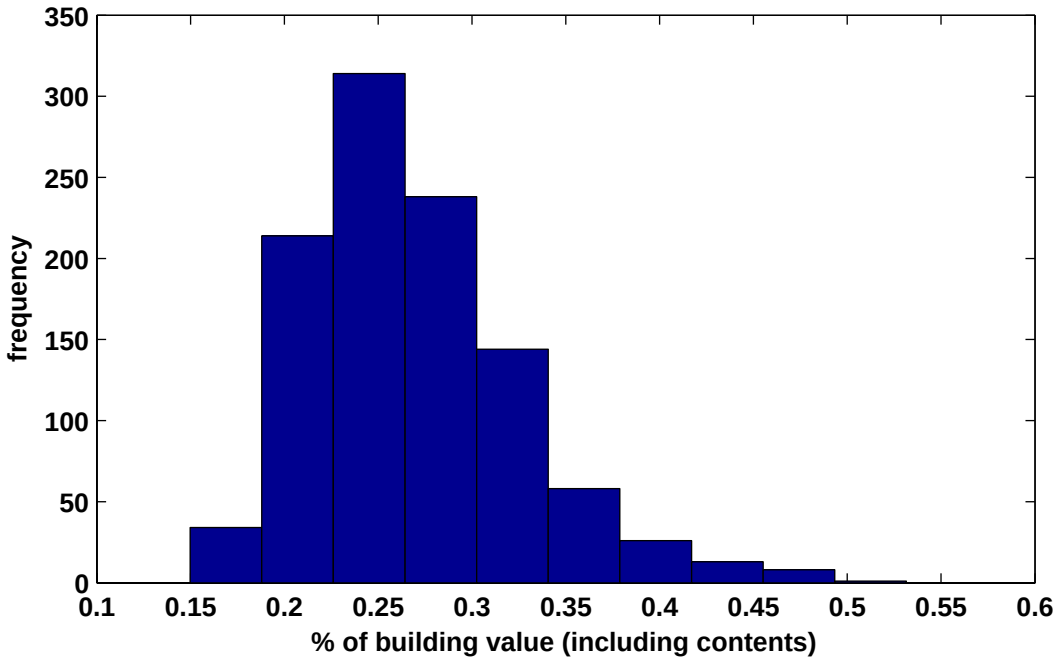

Figure 5.27: Estimated study region loss from the Meckering 1968 earthquake

Consequently, the comparison with GA's simulated event required a number of assumptions, specifically that:

- 40 % of structures in Perth were insured in 1968;
- the number of structures in Perth in 1968 was 52 % of the number of structures present in 2001, and;
- the replacement value of insured structures in Perth in 1968 can be derived from 2003 cost models discounted using the consumer price index.

Based on these assumptions the Meckering event is thought to have caused less than 0.1 % damage with a best estimate of 0.05 % of the total value of buildings and contents in the Perth region in 1968. The estimate is only an indicative value due to uncertainties in the ratio of insured to uninsured structures and the total number of structures in Perth in 1968. However, this estimate is similar to the insured loss of 0.05–0.075 % estimated by Dr George Walker of Aon Re (pers. comms 2004).

Cadoux

The Cadoux simulation gave a mean estimated loss of 0.0046% for the event (Figure 5.28). The extremely small loss predicted for Cadoux is considered to be at the threshold of damage and is consistent with observations that no damage was reported in Perth due to that event.

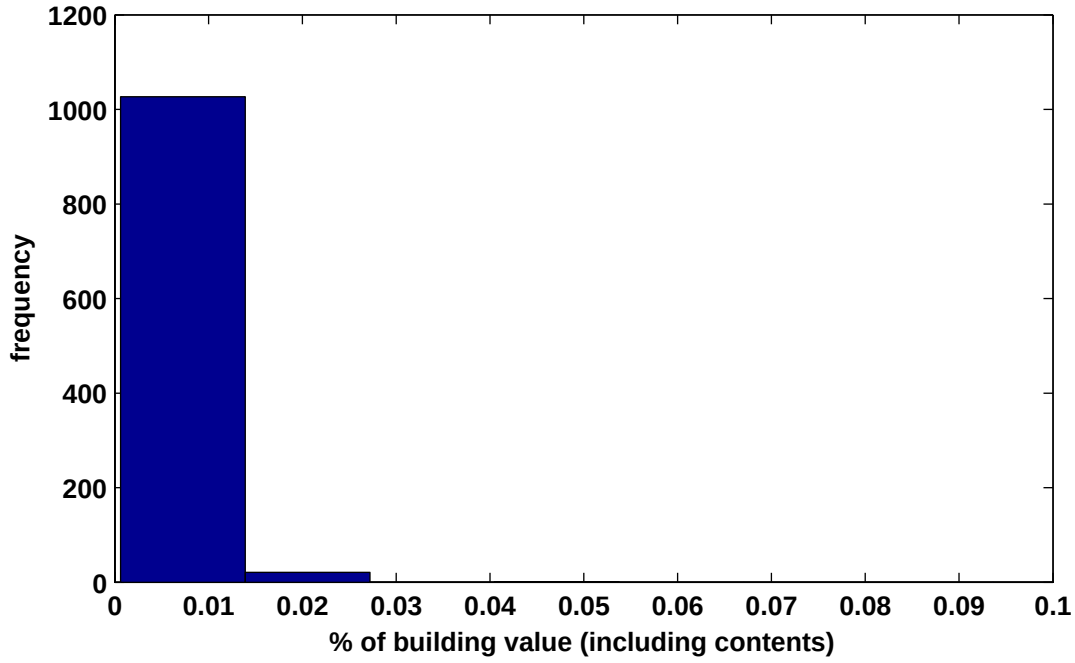

Figure 5.28: Estimated loss from the Cadoux 1979 earthquake

Discussion

Despite the uncertainties associated with this process, the EQRM simulated losses for the two historical events are of similar magnitude to the best estimate of the loss associated with the Meckering event and the negligible reported loss levels for the Cadoux earthquake. It is noted that the damage levels for both events are at the very threshold of damage making a precise prediction of a very small damage level challenging. Despite this the comparisons have provided some, albeit limited, verification of the composite risk model used by GA to assess the earthquake risk in Perth.

5.9 Financial Vulnerability

The financial vulnerability of households and businesses needs to be considered in order to assess the ability of a household or business to rebuild and replace damaged property post-event. The level of household insurance, together with tenure type and income level, are generally fair indicators of this ability after a major hazard event. An uninsured household would usually be considered financially vulnerable if exposed to a natural hazard event as they would have to use up existing savings, borrow needed funds (with additional interest payments) or require longer to save the required amount. If the affected households are also in a lower income bracket, they will tend to have limited disposable income to spend on replacing damaged property and hence are more likely to have to borrow funds or have to wait longer to replace damaged property. Uninsured households in the lower income brackets are also more likely to require government relief, both in terms of payments for replacing damaged items and temporary accommodation and services.

According to the Insurance Council of Australia (ICA, 2002), lower income households who are renting are more likely to be uninsured whilst high-income earning homeowners with a mortgage are most likely to be insured. Dwyer *et al.* (2004) also highlight the significance of tenure type and house insurance in determining the time required for an individual to recover from a natural hazard event.

In metropolitan Perth, about 65% of the households are purchasing or own a property and approximately 30% of households live in rented places (ABS, 2001b). According to the ICA (2002), almost three-quarters of uninsured households rent property (Table 5.14).

In terms of contents insurance, approximately 70% of rental tenants in WA do not insure their household contents. In contrast, over 90% of homeowners with or without a mortgage have either or both building and contents insurance policies (see Table 5.15).

Table 5.14: Tenure type of Perth metropolitan area, 2001

Tenure type	Households by tenure type (%)	Uninsured households by tenure type (%)
Rent	26	74
Rent free	3	6
Ownership without mortgage	37	11
Ownership with mortgage	28	8
Not stated	7	

Source: ABS, 2001b and ICA, 2002

Table 5.15: Insured and uninsured households by tenure type, WA

Tenure type	Percentage insured contents	Percentage uninsured contents	Number of uninsured households
Rent	32	68	14 7840
Rent free	40	60	12 840
Ownership without mortgage	92	8	21 555
Ownership with mortgage	92	8	16 855

Source: ICA, 2002

Table 5.16: Percentage uninsured Australian households by tenure type and income

Tenure type	Quintile 1 (%)	Quintile 2 (%)	Quintile 3 (%)	Quintile 4 (%)	Quintile 5 (%)
Rent	82	74	72	52	50
Ownership with mortgage	6.5	6.6	7	4.3	1.2
Ownership- no mortgage	13	8	6.7	5.8	4

Source: ICA, 2002

In dividing all households across Australia into quintiles1 it is evident that the number of uninsured households decreases with increasing levels of income across all tenure types (Table 5.16).

Using tenure type and household income as indicators of financial vulnerability to a natural hazard event, Census data were used to identify Perth LGAs with high numbers of government tenants (equal to or greater than 5% of households), other rental (equal to or greater than 20% of households in the LGA) and low income households (average household income less than $900/week) (see Table 5.17).

1 Each quintile contains approximately 20% of the population, ranked according to average household income, where 1 is the lowest income group and 5 is the highest income group.

Table 5.17: LGAs and financial vulnerability indicators

LGA	No. of house-holds	High % govt. tenants (>= 5% of households)	High rental other (>= 20% of households)	High no. of household renting (>1900 households)	Low household average weekly income (<$900/week)
Armadale	18,064				
Bassendean	5,493				
Bayswater	23,127				
Belmont	12,446				
Cambridge	8,936				
Canning	27,441				
Claremont	3,638				
Cockburn	24,058				
Cottesloe	3,006				
East Fremantle	2,626				
Fremantle	10,901				
Gosnells	28,644				
Joondalup	50,889				
Kalamunda	16,481				
Melville	34,915				
Mosman Park	3,391				
Mundaring	11,869				
Nedlands	7,314				
Peppermint Grove	514				
Perth	4,105				
South Perth	16,221				
Stirling	72,839				
Subiaco	7,101				
Swan	28,449				
Victoria Park	12,392				
Vincent	11,600				
Wanneroo	27,366				

Source: ABS, 2001b

From Table 5.17 it can be observed that Bayswater, Belmont and Victoria Park have a high percentage and number of households renting and a high percentage of households on low average weekly incomes. It can also be seen that Armadale has a large number of households on low income and renting. Due to the confidentiality limitations on household census data, it was not possible to calculate the number of households who are both on low incomes and renting.

Given that low income households and those who live in rented places are more likely to be uninsured, households with either or both of these characteristics are also more likely to require relief payments to assist in their recovery such as personal hardship and distress (PHD) payments under the Natural Disaster Relief Arrangements. Under the PHD arrangements, individuals are eligible for immediate assistance, temporary living expenses, essential household contents and building repairs and structural damage payments. The arrangements in Western Australia are currently under review in order to

establish eligibility criteria and approved formal limits. Historically, no means or assets test has been applied to PHD payments.

5.10 Results and Discussion

In this section the results of both the earthquake hazard and risk calculations are discussed. These are reviewed in the context of the currently applied hazard definitions found in the building design standards and the earthquake risk determined elsewhere in Australia. The hazard and risk is also examined at both suburb and LGA level with reference made to the financial vulnerability of population sub-groups that may struggle to recover following a major earthquake impact on Perth.

Bedrock and regolith hazard

The assessment of bedrock hazard has been undertaken with all efforts made to produce the most reliable results possible. Notwithstanding this there have been several uncertainties in the model components. Achieving consistency in the earthquake catalogue is difficult and the definition of source zone boundaries has required considerable judgement. The Perth hazard was found to be influenced to a significant extent by the local earthquakes in the background source zone. Very few historical earthquakes beneath Perth exist in the catalogue making the definition of recurrence parameters for this zone difficult. Finally, the hazard and downstream risk assessment is very dependent on the choice of attenuation relationships. The need for models developed for Australian crustal zones that can accommodate the significant effects of sedimentary basins is clear.

The bedrock hazard assessment reported in this study has a wider scope than the immediate metropolitan study region. The results have provided an opportunity to compare the re-assessed seismic hazard to that defined in the current earthquake loadings standard (Standards Australia, 1993) that furnishes the design loadings for structures. It has also been possible to review the hazard definition in the draft standard (Standards Australia, 2004) that will soon replace AS 1170.4 1993. The peak ground accelerations for both the 500-year and 2,500-year return periods significantly exceed those published in both standards. This result has little structural significance as the spectral values of 0.3 s and 1.0 s better reflect the earthquake demands placed on buildings. It was found that the 0.3 s spectral values compared favourably with the current standards with a 20% reduction in hazard suggested for the Perth metropolitan area. The 1.0 s spectral values from the study also compared favourably with the draft standard values. Limited strong motion data has shown that the basin does de-amplify ground motion suggesting that the bedrock hazard assessed is conservative. Future research may substantiate a further reduction of the Perth Basin bedrock hazard by incorporating the basin attenuation effects that could not be captured in this study.

The effects of regolith and the Perth sedimentary basin were combined into a localised ground motion model. This approach required a generalisation of the four Perth study region site classes into a single class, thereby losing a definition of the localised effects of regolith that can influence damage to certain structure types and, hence, local risk. The model was also based on very limited strong motion data from a relatively low magnitude event. Despite this, the model did contribute centrally to the achievement of a measure of correspondency between the overall risk model predictions and historical earthquake damage. The predicted regolith accelerations for a spectral period of 0.3 s compared favourably with the hazard defined in the new draft standard, though moderately lower. The spectral accelerations at a period of 1.0 s were considerably lower. The effect of the combined basin and regolith model is to increase the bedrock hazard for low-rise structures and de-amplify the earthquake demands on taller structures that have a longer natural period of response.

The significance of the findings of this study is that design earthquake loads presently being applied to structures outside the Perth Basin are largely compatible with the local hazard. One opportunity for refinement is in the extent of the elevated hazard for low rise structures (S_A at 0.3 s) in the Wheatbelt region where the region of elevated hazard was found to be more extensive both in a northerly and westerly direction. The portion of the Wheatbelt with the greatest hazard has also shifted from the

proximity of Meckering to north of Wongan Hills. The new draft standard (Standards Australia, 2004) gives a more extensive coverage of the region of elevated hazard by moderately increasing the spectral accelerations. However, a north-westerly shift of the hazard contours will achieve an improved coverage of the revised hazards determined by the study (refer Figure 5.18).

Study region risk

Each of the 9,400 earthquakes simulated in the risk calculations was assigned a magnitude, location and probability. The epicentral locations were randomly distributed within each source zone and the magnitude and probability taken from the corresponding GR distribution. For each earthquake scenario, the economic damage loss values were determined for a suite of 6,000 reference structures which were then expanded to represent every building in the building database. Each scenario was simulated twice to obtain a loss result from each of the two earthquake attenuation relationships used. The process involved over 110 million individual predictions of building earthquake response and attendant damage.

By considering the impact of all earthquake events on any one or group of buildings an annual probability of exceedance loss curve can be generated. The probability of a loss level being exceeded and the associated annualised loss are of particular interest for risk management decision-making. They can provide guidance on how much should be spent annually on mitigation efforts such as building improvement, emergency response facilities, insurance premiums, etc. Annualised economic loss can also be determined for building sub-populations, depending on the interests of the stakeholder. For example, federal and state governments may be interested in the whole study area, local governments in their own local area, emergency management agencies in their own districts, and insurance companies may be interested in their portfolio exposure to loss. The approach is applicable to populations of structures distributed over a region of interest rather than to discrete structures. Consequently, property owners interested in the risk posed to their buildings would best seek risk advice from experienced professionals. Annualised economic loss values are also useful for making comparisons to other hazards, particularly if rankings of impact intensity are dependent on the return period selected. The earthquake risk results have been evaluated for both the study region as a whole and for the individual suburbs that comprise the study region, each of which are presented separately below.

Aggregated study region risk

The economic loss curve estimated for the entire study region is presented in Figure 5.29. This curve describes the probability of the study region incurring various minimum levels of building plus contents damage loss within a single year. Economic loss is expressed as a percentage of the total value of all buildings and their contents in the study region. The integration of the area under the annual probability of exceedance-economic damage loss curve gives the annual expected economic damage loss (or annualised economic loss). The annualised economic loss for the whole study region, varying according to the rarity (return period) of events considered, is shown in Figure 5.30.

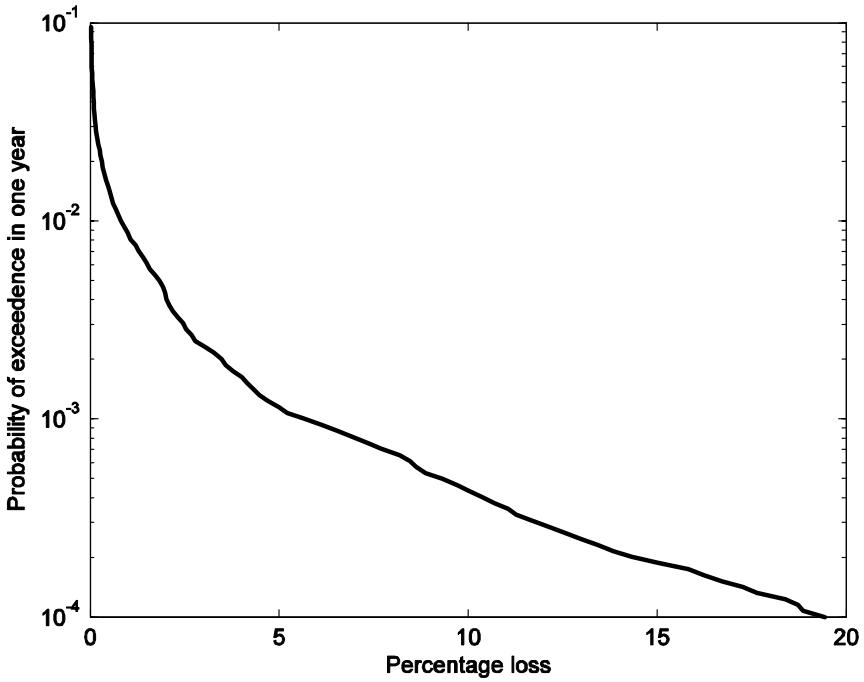

Figure 5.29: Probable maximum loss curve for Perth study region

The results of this study suggest that, on average, the Perth metropolitan region will suffer an estimated economic loss of around 0.040% per year. This corresponds to an annualised loss of the order of $69 million per year. This value has been calculated on the basis of the total value of buildings in the study region, which is estimated by our models to be approximately $171 billion. This compares with a value of 0.022% for the Newcastle/Lake Macquarie region (Robinson *et al.*, 2004), showing that Perth has a significantly greater risk.

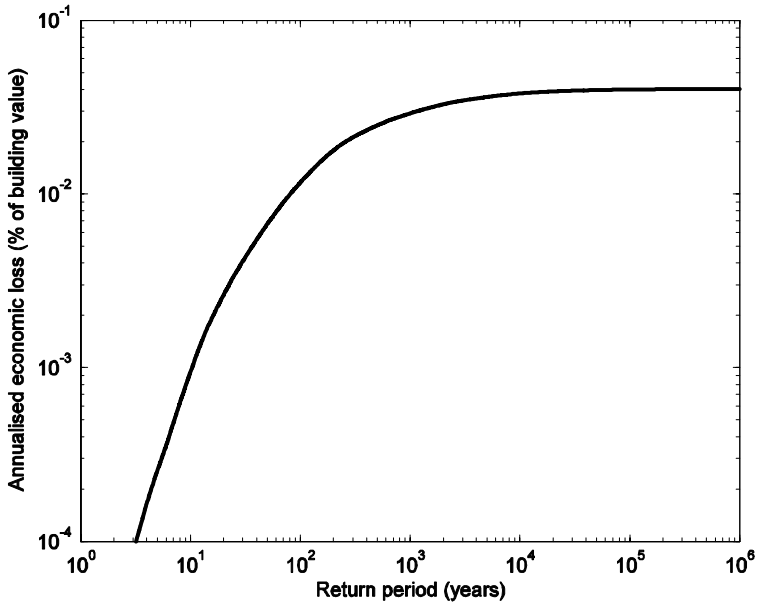

Figure 5.30: Annualised economic loss versus maximum return period considered, for the Perth study region

A prima facie comparison of the average annualised loss to those from historical Perth earthquake losses suggests a poor correspondency. For the period 1967–1999, the actual average annual losses were $3 million, which differs greatly from those assessed. However, the majority of the earthquake risk in the study region is from events that have annual probabilities of occurrence of 0.004 or less (return periods of 250 years or more). This indicates that the risk to the region is primarily from relatively infrequent events having moderate to high impacts. In contrast, very frequent events will have low impacts, and, in the case of Perth, represent a smaller part of the overall risk. Very high impact events could also occur in the region. These extremely rare events contribute little to the annualised risk but present a serious challenge to emergency management due to their sometimes catastrophic consequences.

It is possible to determine the relative contributions to annualised risk of earthquakes from the suite simulated that comprise a range of magnitudes and distances from each building location. The distance used is the Joyner–Boore distance, which is the closest horizontal distance from the building of interest to the rupture plane of the earthquake. In Figure 5.31, a histogram is given for the contribution of overall annual risk for a number of moment magnitude and distance combinations.

The plot shows some interesting features. Most of the earthquake risk in the study region is due to earthquakes with moment magnitudes around 5 at distances of less than 30 km. This result further suggests that the majority of the risk in the region is from moderate-impact, relatively infrequent events rather than high-impact but extremely rare events. The contribution of the SWSZ can also be discerned with large events at the Perth edge of this region (80 km distance) of higher activity making a significant contribution. The Newcastle/Lake Macquarie region lacked this feature as the primary region of seismic activity was directly located under the study region.

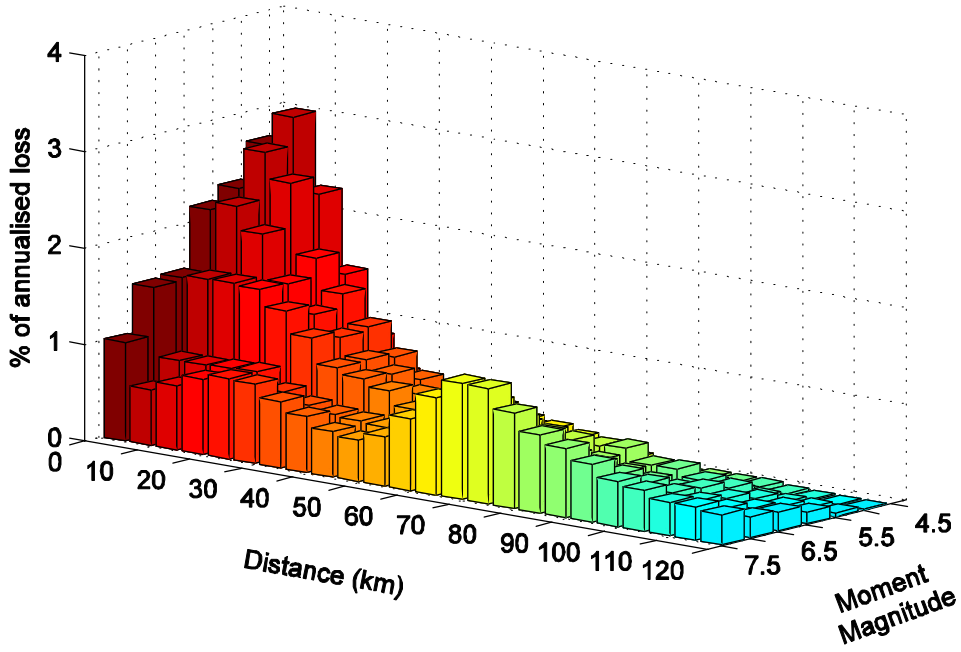

Figure 5.31: Contributions to the earthquake risk in Perth from earthquakes of different magnitudes at varying distances to the building stock

The unique capital city profile of Perth has greatly influenced the risk results. In total 89% of the total building stock and 91% of the residential building subset are of unreinforced masonry construction. The performance of residential construction of this construction type in historical Australian earthquakes has shown it to be a significantly more vulnerable than timber framed construction (Edwards *et al.*, 2004b). Consequently, buildings constructed from unreinforced masonry (cavity brick construction) were found to have a higher annualised loss than any other building type in the study region. The variation of annualised loss across all the building construction types is shown in Figure 5.32 with masonry construction significantly higher. The more engineered steel and concrete structures were found to have much lower annualised losses within their building populations.

The construction type contribution to regional annualised loss is also a function of the relative predominance of the building types. In Table 5.18 annualised risk results are given for the sub-divided building construction types for the four common classes of Perth buildings. Unreinforced masonry (URMLTILE and URMLMETAL) contributes 93% of the total annualised loss. If the population of residential structures were predominantly timber framed the regional risk would be approximately halved. The Perth building profile has 8% timber framed buildings which represent a further 2.7% of the risk. Steel structures were the next largest contributor after masonry to risk (3.2%) by virtue of the greater value of these typically larger structures (13% of the total building stock value) offset by their reduced vulnerability.

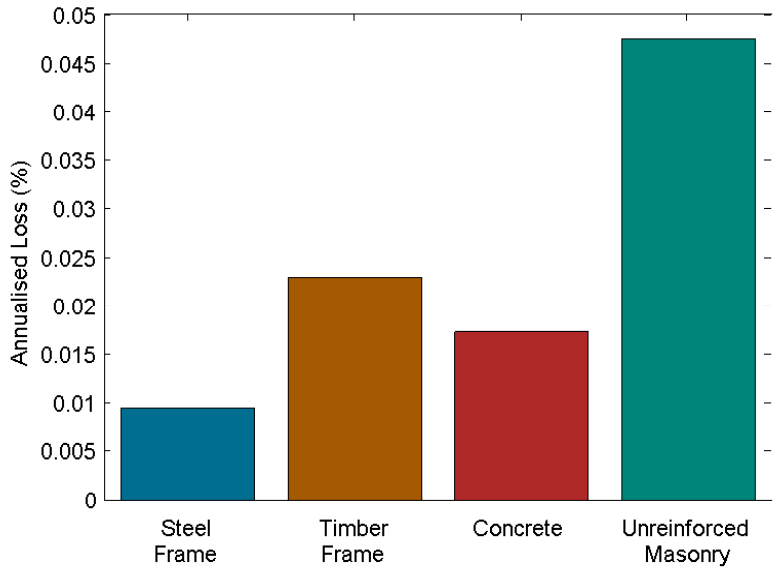

Figure 5.32: Annualised risk for a selection of building types in the study region. The annualised loss for a specific building type is described as a percentage of the total value of that building type in the study region.

Localised impact and risk

Of key interest to this study is the spatial variation of risk and a determination of which suburbs are most at risk. The risk value is a function of the local hazard and the composition of its building stock. By calculating the annualised risk for each suburb in the study region as a percentage of the total annualised risk for the entire study region it appears that some locations are more at risk (on average) than others. A map of the annualised economic loss due to building and contents damage has been determined and aggregated up to the suburb level in Figure 5.33 to help assess the proportion of risk carried by each local authority. Indicated also on the figure are the four LGAs identified in Section 5.9 to be more financially vulnerable. The respective risks of the twenty highest Perth suburbs are also

presented in Table 5.19 along with the corresponding LGAs. Finally, the earthquake risk faced by the LGAs (the aggregation of the risk of all suburbs in each LGA) with more vulnerable sub-populations is summarised in Table 5.20. It can be seen that all four LGAs face close to the mean study region annualised loss of 0.04% or greater. The highest annualised loss of 0.048% was for Armadale.

Table 5.18: Annualised risk for building construction types

Building construction type	Structural model	Estimated number of buildings (% of total)	Estimated total value of buildings of that type (% of total)	Annualised risk (% of total annualised risk)	Annualised risk (% of building value)
Steel framed buildings	S1L	0.052	0.30	0.048	0.006
	S2L	0.59	4.47	0.98	0.009
	S3	0.044	0.55	0.16	0.012
	S5L	1.85	8.04	1.97	0.010
Timber framed buildings	W1BVTILE	2.54	1.28	0.67	0.021
	W1BVMETAL	0.44	0.21	0.12	0.023
	W1TIMBERTILE	3.19	1.54	0.83	0.022
	W1TIMBERMETAL	2.22	1.73	1.09	0.025
Reinforced and pre-cast concrete buildings	C1LMEAN	0.045	1.40	0.61	0.018
	C1LNOSOFT	0.006	0.066	0.021	0.013
	C1MMEAN	0.007	0.32	0.020	0.003
	PC1	0.19	1.29	0.66	0.021
Unreinforced masonry	URMLTILE	87.8	75.6	89.8	0.048
	URMLMETAL	1.00	3.23	3.04	0.038

Figure 5.33 clearly demonstrates that risk varies spatially across the study region. The variation in annualised risk can be partially attributed to differences in building stock across the study region. Some suburbs may have a greater proportion of less vulnerable building types that another. Significantly the impact of building age on vulnerability has not been captured in Figure 5.33 as the vulnerability models available for this study were independent of age. The older residential areas of the city were identified in Figure 5.23 in which the building stock is expected to be, on average, of poorer construction that has been more affected by corrosion, decay and poor building maintenance. The underlying regolith also affects the annualised losses, and areas that are built on substantial thicknesses of regolith typically have an accentuated risk. In this instance the regolith effects have not been captured due to the generalised regolith treatment in which the Perth Basin attenuation and the average regolith amplification have been combined into a single generally applied relationship. What can be seen from the figure is the gradual reduction in risk across the region in a south westerly direction as distance from the SWSZ increases. Changes to the building parameters used could change this spatial distribution. For example, changes to unreinforced masonry parameters to account for degradation and age may well increase the annualised risk in suburbs containing older buildings.

The implications of these results and recommendations for future work that could improve the models that are the basis of these results are discussed in Section 5.11 ‘Recommendations and Future Research’.

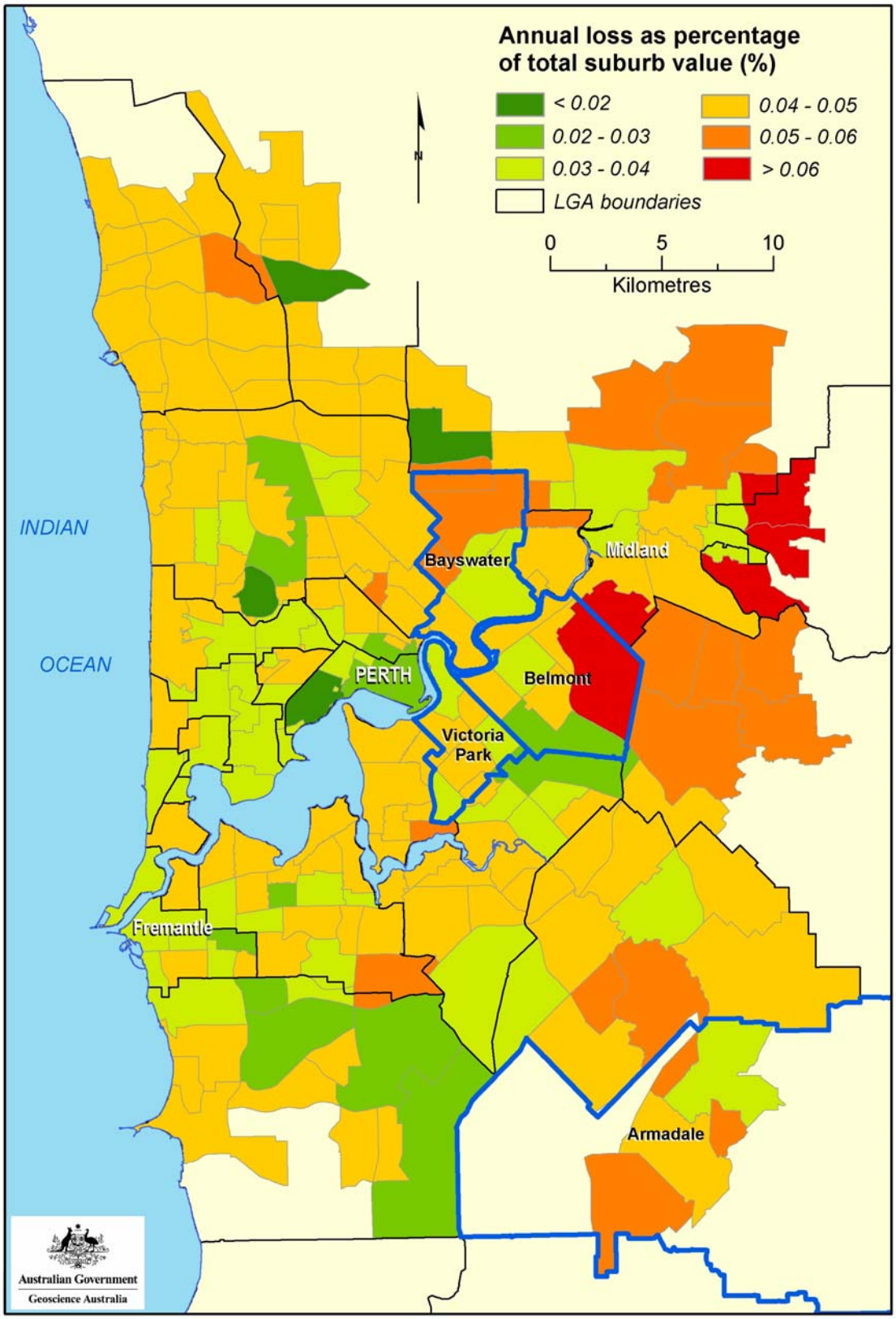

Figure 5.33: Annualised risk by suburb. Note that some suburbs have not been classified due to the relatively low number of buildings surveyed. Suburbs identified as financially vulnerable are indicated

Table 5.19: Annualised risk for the 20 worst impacted Perth suburbs

Suburb	LGA	Building stock value ($)	Annualised loss ($)	Annualised loss (%)
Perth airport	Belmont	1.07m	691	0.064
Swan view	Mundaring	261.7m	165,231	0.063
Helena valley	Mundaring	170.6m	105,992	0.062
Greenmount	Mundaring	73.3m	44,604	0.061
Gooseberry hill	Kalamunda	82.9m	49,932	0.060
Stratton	Swan	89.2m	53,172	0.060
Westfield	Armadale	429.0m	249,052	0.058
Forrestfield	Kalamunda	1,568m	878,323	0.056
Viveash	Swan	105.4m	59,327	0.056
West swan	Swan	58.9m	32,274	0.055
Brookdale	Armadale	112.9m	60,552	0.054
Morley	Bayswater	2,244m	1,203,646	0.054
Herne hill	Swan	2.19m	1,186	0.054
Mount Nasura	Armadale	14.7m	7,837	0.053
Noranda	Bayswater	778.7m	415,193	0.053
Gosnells	Gosnells	2,027m	1,081,116	0.053
High Wycombe	Kalamunda	999.4m	533,054	0.053
Kalamunda	Kalamunda	50.6m	27,054	0.053
Leeming	Melville	1,438m	756,409	0.053
Bedford	Bayswater	390.9m	203,969	0.052

Table 5.20: Annualised risk for LGAs with vulnerable sub-populations

LGA	Building stock value ($)	Annualised loss ($)	Annualised loss (%)
Bayswater	7.25b	3.23m	0.045
Belmont	7.04b	2.52m	0.036
Victoria Park	4.34b	1.77m	0.041
Armadale	2.71b	1.29m	0.048

5.11 Recommendations and Future Research

From the earthquake assessment of this study the following recommendations are made:-

- that the updated earthquake hazard maps for Perth and the Perth region are used to review, improve and complement the design and construction guidelines for earthquakes set by state and local governments. The inclusion of the wider region of hazard identified in the Wheatbelt area into building regulations is one specific application of the research that should be considered;
- that state and local authorities enforce the compliance of all new structures with current earthquake loadings standards;

- that post-disaster essential facilities such as police, SES, fire and ambulance stations and hospitals, be structurally retrofitted to ensure operability immediately following a major earthquake. These facilities should be examined by suitably qualified engineers on a site-by-site basis to assess their expected performance under earthquake loadings. This recommendation is pertinent for SWSZ communities;
- that the importance of adequate insurance against earthquakes be promoted with householders, small business operators and corporations, and;
- that the fields captured in the VGO database be slightly enlarged to include other features besides roof and wall type to enable the more accurate assignment of structural response, vulnerability and replacement cost models. The database could be further improved by the inclusion of additional non-rateable buildings, thereby developing a more comprehensive assessment of the building stock exposed to hazard.

The following areas for future research in the Perth region have also been identified:-

- Research to develop a better understanding of the sedimentary basin attenuation. The seismic hazard and risk assessment of the Perth region has been heavily influenced by the selection of attenuation functions to capture the energy dissipation of the full wave path through the bedrock. Geoscience Australia has recognized the importance of developing a robust spectral attenuation model for Australian conditions in order to reduce the uncertainties in its risk assessments.
- The development of improved regolith modelling to capture the localised amplification of regolith.
- The development of building vulnerability models that can differentiate between building age and proximity to a marine environment.
- The inclusion of critical infrastructure (e.g. utilities, energy production assets and transportation facilities) in the range of vulnerable infrastructure considered in regional earthquake risk assessments. Historical Australian earthquakes have shown that the direct damage to assets of this type can be expensive and the service disruption can have wide reaching economic and community impacts.
- Research into a wider range of economic losses including indirect tangible losses and intangible losses that all contribute to a holistic assessment of risk.

5.12 References

Allen, T.I., Dhu, T., Cummins, P.R. and Schneider, J. (accepted) 'Empirical attenuation of ground-motion spectral amplitudes in southwestern Western Australia', *Bulletin of the Seismological Society of America.*

Atkinson, G.M. (2004a) 'Empirical attenuation of ground-motion spectral amplitudes in southeastern Canada and the northeastern United States', *Bulletin of the Seismological Society of America*, 94:1079–95.

Atkinson, G.M. (2004b) 'Erratum to "Empirical attenuation of ground-motion spectral amplitudes in southeastern Canada and the northeastern United States"', *Bulletin of the Seismological Society of America*, 94:2419–23.

Atkinson, G.M. and Boore, D.M., (1995) 'Ground-motion relations for eastern North America', *Bulletin of the Seismological Society of America*, 85(1):17–30.

Atkinson, G.M. and Boore, D.M. (1997) 'Some comparison between recent ground-motion relations', *Seismological Research Letters*, 68(1):24-40.

Australian Bureau of Statistics (2001a) *Building Approvals, Australia.* ABS Cat. No 8731.0, ABS, Canberra.

Australian Bureau of Statistics (2001b) *CDATA 2001 Your Census at Work*, ABS, Canberra.

Australian Bureau of Statistics (2004) *Australia Now*. ABS Cat. No 1301.0, ABS, Canberra.

Bureau of Transport Economics (2001) *Economic Costs of Natural Disasters in Australia*, Report 103, BTE, Canberra.

Denham, D. (1976) Earthquake hazard in Australia. Australian Academy of Science 7, pp. 94–118.

Department for Planning and Infrastructure (2004) Residential development GIS files showing extent of Perth residential development with year, supplied by Government of Western Australia – Department for Planning and Infrastructure

Dhu, T., Allen, T., Cummins, P., Leonard, M., Robinson, D. and Schneider, J. (2004) 'A comparison of response spectra from Australian earthquakes and North American attenuation models', *Proceedings of the Annual Conference for the New Zealand Society for Earthquake Engineering*, Rotorua, New Zealand. March 2004.

Dhu, T., Robinson, D., Sinadinovski, C., Jones, T., Corby, N., Jones T. and Schneider, J. (2002) 'Earthquake risk in Newcastle and Lake Macquarie', *Geoscience Australia Record 2002/15*. Geoscience Australia, Canberra, pp. 43–76.

Dwyer, A., Zoppou, C., Nielsen, O., Day, S. and Roberts, S. (2004) *Quantifying social vulnerability: A methodology for identifying those at risk to natural hazards*, Geoscience Australia, Canberra.

Edwards, M. R., Lin, X. G. and Corby, N. (2004a) 'Observations on tornado damage to residential structures in Bendigo', *Proceedings of 12th Australasian Wind Engineering Society Workshop*, Darwin, Australia, June 2004

Edwards, M. R., Robinson, D., McEneney, K.J. and Schneider, J. (2004b) 'Vulnerability of residential structures in Australia', *Proceedings of 13th World Conference on Earthquake Engineering*, Vancouver, Canada, 1–6 August 2004.

Electric Power Research Institute (1993) *Guidelines for Determining Design Basis Ground Motions*, Vol. 5: 'Quantification of Seismic Source Effects'.

Electric Power Research Institute (1994) *The Earthquakes of Stable Continental Regions*, Vol. 1: 'Assessment of Large Earthquake Potential'.

Everingham, I.B. (1968) Seismicity of Western Australia. Bureau of Mineral Resources, Australia, Report 132.

Everingham, I.B. and Gregson, P.J. (1970) *Meckering earthquake intensities and notes on earthquake risk for Western Australia*, BMR Record 1970/97, Bureau of Mineral Resources, Australia.

Gaull, B.A. and Michael-Leiba, M.O. (1987) 'Probabilistic earthquake risk maps of southwest Western Australia', *BMR Journal of Australian Geology and Geophysics*, 10:145–51.

Gaull, B.A., Michael-Leiba, M.O. and Rynn, J.M.W. (1990) 'Probabilistic earthquake risk maps of Australia', *Australian Journal of Earth Sciences*, 37:169–87.

Gee, R.D., Baxter, J.L., Wilde, S.A. and Williams, I.R. (1981) 'Crustal development in the Archaean Yilgarn Block, Western Australia', *Special Publications*, Geological Society of Australia No. 7, pp. 43–56.

Gutenberg, B. and Richter, C.F. (1949) *Seismicity of the Earth and Associated Phenomena*, Princeton University Press, New Jersey, USA.

Insurance Council of Australia (2002) *Report on non-insurance/under-insurance in the home and small business portfolio*, ICA.

Jackson, P.L. (Editor) (1994) *Means Square Foot Costs*, R.S. Means Company, Inc., Kingston, MA.

Kárník, V. (1971) *Seismicity of European Area*, Part 2, D. Reidel Publishing Company, Dordrecht, Holland.

Kircher, C.A., Aladdin, A.A.., Kusto, O. and Holmes, W.T. (1997) 'Development of building damage functions for earthquake loss estimation', *Earthquake Spectra*, 13(4):663-682.

Kramer, S.L. (1996) *Geotechnical Earthquake Engineering*, Prentice Hall, NJ.

Leonard M. (in preparation) 'One hundred years of earthquake recording in Australia', *Bulletin of the Seismological Society of America.*

Mathur, S.P. (1976) 'Relation of Bouguer anomalies to crustal structure in southwestern and central Australia', *BMR Journal of Australian Geology and Geophysics*, 1:277–86.

McCue, K.F. (1973) *On the seismicity of Western Australia*, Report to the Western Australia Public Works Department and the Commonwealth Department of Works, Parts I and II, PWD, Perth.

McEwin, A.J., Underwood, R. and Denham, D. (1976) 'Earthquake risk in Australia', *BMR Journal of Australian Geology and Geophysics*, 1:15–21.

Melchers, R.E. (1990) Newcastle Earthquake Study, The Institution of Engineers, Australia

Myers, J.S., and Hocking, R.M. (compilers) (1998) *Geological Map of Western Australia*, Geological Survey of Western Australia.

National Institute of Building Sciences (1999) *HAZUS99 Technical Manual*, Federal Emergency Management Agency, Washington DC.

Peele, B. (1993) 'Earthquake insurance', *Proceedings of Australian Earthquake Engineering Society Conference*, Melbourne, Australia, October 1993.

Press, W.H., Teukolsky, S.A., Vetterling, W.T. and Flannery, B.P. (1992) *Numerical recipes in FORTRAN*, 2nd ed., Cambridge University Press.

Reed Construction Data (2003) *Replacement Cost Models for Metropolitan Perth*, Consultancy Report for Geoscience Australia, RCD, Sydney.

Robinson, D., Dhu, T. and Schneider, J. (2004) 'The effect of different attenuation models on earthquake hazard in the Newcastle and Lake Macquarie region, Australia', *Proceedings of ASEG 17th Geophysical Conference and Exhibition*, Sydney 2004.

Robinson, D. and Fulford, G. (2003) *EQRM : Earthquake Risk Modelling Software: Technical Manual, Version 2.0*, Geoscience Australia.

Sadigh, K., Chang, C.Y., Egan, J.A., Makdisi, F. and Youngs, R.R. (1997) Attenuation relationships for shallow crustal earthquakes based on California strong motion data. *Seismological Research Letters*. Vol.68(1), pp180-189.

Sinadinovski, C. (2000) Computation of recurrence relation for Australian earthquakes, AEES Conference, Hobart, Paper No. 22, pp1-5.

Standards Australia (1993) AS 1170.4-1993: Minimum design loads on structures – Part 4: Earthquake Loads, Standards Australia, Homebush, Sydney.

Standards Australia (1998) AS 4100 : Steel Structures, Standards Australia, Homebush, Sydney

Standards Australia (1999a) AS 1684.1 : Residential timber framed construction – Part 1 : Design criteria, Standards Australia, Homebush, Sydney

Standards Australia (1999b) AS 1684.2 : Residential timber framed construction – Part 2 : Non-cyclonic areas, Standards Australia, Homebush, Sydney

Standards Australia (1999c) AS 1684.3 : Residential timber framed construction – Part 3 : Cyclonic areas, Standards Australia, Homebush, Sydney

Standards Australia (1999d) AS 1684.4 : Residential timber framed construction – Part 4 : Simplified-non-cyclonic areas, Standards Australia, Homebush, Sydney

Standards Australia (1999e) *Risk Management, AS/NZS4360*, Standards Association of Australia, Sydney, Australia

Standards Australia (2001a) AS 3600 : Concrete Structures, Standards Australia, Homebush, Sydney

Standards Australia (2001b) AS 3700 : Masonry Structures, Standards Australia, Homebush, Sydney

Standards Australia (2002) AS 1720.1 : Timber structures – Part 1, Design Methods, Standards Australia, Homebush, Sydney

Standards Australia (2004) *DR 04303 : Structural design actions – Part 4 : Earthquake actions in Australia*, Standards Australia, Homebush, Sydney

Toro, G.R., Abrahamson, N.A. and Schneider, J.F. (1997) 'Model of strong ground motions from earthquakes in central and eastern North America: Best estimates and uncertainties', *Seismological Research Letters*, 68(1):41–57.

Utsu, T. (1999) 'Representation and analysis of the earthquake size distribution: A historical review and some new approaches, *Pure and Applied Geophysics*, 155:503-535.

Valuer Generals' Office (2002) Microsoft Access database, supplied by Government of Western Australia - Department of Land Information.

Valuer Generals' Office (2003) Microsoft Access database, supplied by Government of Western Australia - Department of Land Information.

Weichert, D.H. (1980) 'Estimation of the earthquake recurrence parameters for unequal observation periods for different magnitudes', *Bulletin of the Seismological Society of America*, 70:1337-1346.

Whitaker, A.J. (1992) 'Integrated geological and geophysical mapping of southwestern Western Australia', *AGSO Journal of Australian Geology and Geophysics*, 15:313–28.

Whitaker, A.J., and Bastrakova, I.V. (2002) *Yilgarn Craton Aeromagnetic Interpretation* (1:1 500 000 scale map) Geoscience Australia, Canberra.

Wilde, S.A., Middleton, M.F., and Evans, B.J. (1996) 'Terrane accretion in the southwest Yilgarn Craton: evidence from a deep seismic crustal profile', *Precambrian Research*, 78:179–96.

Chapter 6: COMMUNITY RECOVERY

Anita Dwyer
Geoscience Australia

6.1 Introduction

Risk assessments

Beyond the damage estimates from the earthquake modelling results outlined in Chapter 5, any measurement of the impact of natural hazards must also consider social factors. Technical risk assessments have often neglected community recovery and how people cope after a natural hazard has affected their community. The factors influencing recovery are complex, however, key aspects of recovery are recognised by researchers, practitioners and the recent Council of Australian Governments (COAG) Review into Natural Disasters, and these can be incorporated into a natural hazard risk assessment for a community (COAG, 2004). They include environmental, financial and economic, physical, community, psychosocial and emotional factors (COAG, 2004; Emergency Management Australia (EMA), 2004a; Ministry of Civil Defence and Emergency Management, 2004).

This chapter discusses three factors it is suggested underpin community recovery:

- household financial capacity,
- social networks (an element of community capacity) and
- distance to services.

There are many more factors that influence the recovery process, as the anecdotes of recovery managers and sociologists studying natural disasters make clear. Other integral factors influence recovery, such as local economic activity, business interruption, environmental impacts and infrastructure effects. These are not explored in this chapter because no adequate data sets are available at the national level. Characteristics of available data are discussed in Dwyer *et al*., 2004).

Geoscience Australia is developing a national risk assessment framework to assist the whole of government to better manage the risk from natural disasters. Any such framework must incorporate factors influencing community recovery from a natural disaster. However, for any risk to a specific community, such as the Perth metropolitan area, local knowledge and local data are essential in contributing to measures of recovery.

The research outlined in this chapter emphasises that community recovery issues should be included with any geological, engineering and economic assessment of natural hazards in Perth.

Floods, earthquakes, severe storm and bushfire are some of the more frequent hazards that affect people in the Perth community, disrupting the lives of anywhere from one to more than ten thousand households. The early chapters in this report have outlined the scientific methods defining the magnitude and probability of hazards in Perth. This chapter will focus on some of the social factors that may be relevant to the Perth community's capacity to recover when any of these hazards affects the Perth metropolitan region.

Perth recovery services

The West Australian government has numerous mechanisms in place to assist people who have experienced a natural disaster or trauma. The Department for Community Development has a

website dedicated to information on coping and recovery, a telephone helpline, referral services and a list of assistance available. The website makes an integral link between emergency management and community development, stating that 'This website can help you with recovery, coping, healing and starting to make sense of it all…' It is essential reading for all involved with the development of a risk assessment for the Perth community. The website can be found at: http://www.emergency.communitydevelopment.wa.gov.au/.

Factors influencing community recovery

Recovery can have different meanings, describing both a process and an outcome and with different measures. This chapter aims to highlight that recovery 'is more than simply the replacement of what has been destroyed and the rehabilitation of those affected. It is a complex social and developmental process.' (EMA, 2004).

The framework

Enduring a natural hazard can have a significant, if not devastating, effect on people, their households and their communities. The extent of the impact is reflected in people's recovery, a complex process involving many factors. The January 1997 bushfires at Wooroloo, the 1979 Cadoux earthquake, the 1961 Dwellingup bushfires and the 1983 flood on the Canning River are just some of the natural hazards that have affected people living in the Perth region (EMA, 2004b; Insurance Council of Australia, 2002). How each person, household and broader community has recovered from these events has related to a range of factors, including physical, social, emotional, psychological, economic and financial circumstances (EMA, 2004a).

Emotional and psychological recovery is complex. Some people's psychological recovery may be strongly linked to financial stressors, while some may be more linked to feelings of safety. Each person will have an individual path to recovery, but there are some common themes or factors that will influence it. A framework has been developed to capture some of these factors in a simple but useful manner. It draws on some of the factors reported to contribute to recovery, using national data sets so that a picture of recovery factors can eventually be developed for all of Australia. The framework does not provide a holistic measure, but rather a guide to better understanding some significant factors. Three factors explore different aspects of recovery; household financial capacity, social networks and access to services (Figure 6.1). Four aspects of each factor will be discussed: concept, measures, Perth assessment and interpretation. The intention is to provide decision-makers with an insight into some of the issues facing communities during the recovery process.

Figure 6.1: A simple framework of factors influencing recovery from natural hazard events. Only three of many factors influencing community recovery are explored here

6.2 Household Financial Capacity

Concept

The financial situation of a household is important to both how fast and effectively people recover from a natural hazard. The capacity to buy house insurance, access temporary accommodation, build a new house, purchase new clothes and household goods, access on-going medical treatment and take time off work clearly contributes to the recovery of a person or a household from a natural hazard. Research has demonstrated that people's vulnerability to natural hazards is strongly affected by the relationship between their income level, tenure type and house insurance level (Dwyer *et al.*, 2004). Limited financial options can contribute to stress that, in turn, can adversely affect personal relationships. It is, therefore, important to know which households may require financial assistance in both the medium to long term.

Table 6.1: The Perth LGAs divided into quartiles for the Index of Economic Resources ranked for all of Australia (no LGAs are in the first quartile)

Quartile	LGA Name	Population	Rank
2nd	Kwinana	19452	934.1
3rd	Belmont	28999	951.2
	Armadale	50108	967.0
	Bassendean	13322	971.1
	Rockingham	69163	980.6
	Gosnells	80049	983.9
	Wanneroo	79959	985.3
	Bayswater	54390	986.5
4th	Swan	82201	989.2
	Victoria Park	25716	989.3
	Fremantle	24315	995.4
	Cockburn	66108	1000.2
	Stirling	168747	1004.0
	Serpentine-Jarrahdale	10855	1010.5
	Mundaring	32582	1011.6
	Kalamunda	46245	1017.6
	Canning	73727	1017.8
	Vincent	25618	1038.5
	Perth	9831	1055.4
	Joondalup	148268	1066.2
	Melville	91385	1068.1
	South Perth	36108	1075.6
	Mosman Park	7824	1090.2
	East Fremantle	6345	1091.0
	Subiaco	15673	1115.0
	Claremont	8733	1137.1
	Cambridge	22451	1144.3
	Nedlands	19274	1166.6
	Cottesloe	6987	1181.7
	Peppermint Grove	1540	1210.2

Source: ABS 2001 SEIFA, 2004a

Measures

Some financial attributes of a household that may contribute to a quicker or longer recovery include appropriate house insurance, tenure type, income, disposable income and savings. These data are captured by the SEIFA Index of Economic Resources (ABS, 2004a), developed from the Australian Bureau of Statistics (ABS) 2001 Census. The variables for this index relate to income, expenditure and assets – for example, family income, rent, mortgage and dwelling size – and

capture the financial situation of individuals within a household. The SEIFA Index ranks each administrative area on a relative scale according to the proportion of households with high and low economic resources (ABS, 2004a). The index is not designed to specifically measure vulnerability to natural hazard, such a detailed national index does not yet exist. It does provide a very thorough insight into the differing financial capacities of Perth households.

Perth assessment: local government areas

There are 30 local government areas (LGAs) in the Perth metropolitan area. Each has a relative rank in the SEIFA Index of Economic Resources (ABS, 2004a). The Perth LGAs are listed in Table 6.1 from lowest to greatest proportion of household financial capacity. As the index is relative, it is important to compare the areas against the Australian total. As such, the index can be divided into quartiles. No Perth LGA is in the lowest quartile and only Kwinana is in the second quartile (Table 6.1). Of the other 29 LGAs in the top 50% of all LGAs in Australia, 22 are in the top 25% of Australian LGAs. When compared with the Australian average (1000.0), the Perth metropolitan area has a high proportion of households with high financial resources, and a low proportion of households with very low financial resources.

The distribution of the LGAs, ranked by SEIFA quartiles, is shown in Figure 6.2. All the LGAs in central Perth are in the top 25% of all LGAs in Australia, indicating that these areas have a high proportion of households with high financial capacity. The areas with a lower proportion of households with high financial capacity are located in the very north (Wanneroo), the very south (Rockingham and Kwinana) and the central-east (Belmont, Armadale, Bassendean, Gosnells and Bayswater). If a natural disaster affected the households of Perth, recovery could be more difficult in these areas because a higher proportion of households have reduced financial capacity.

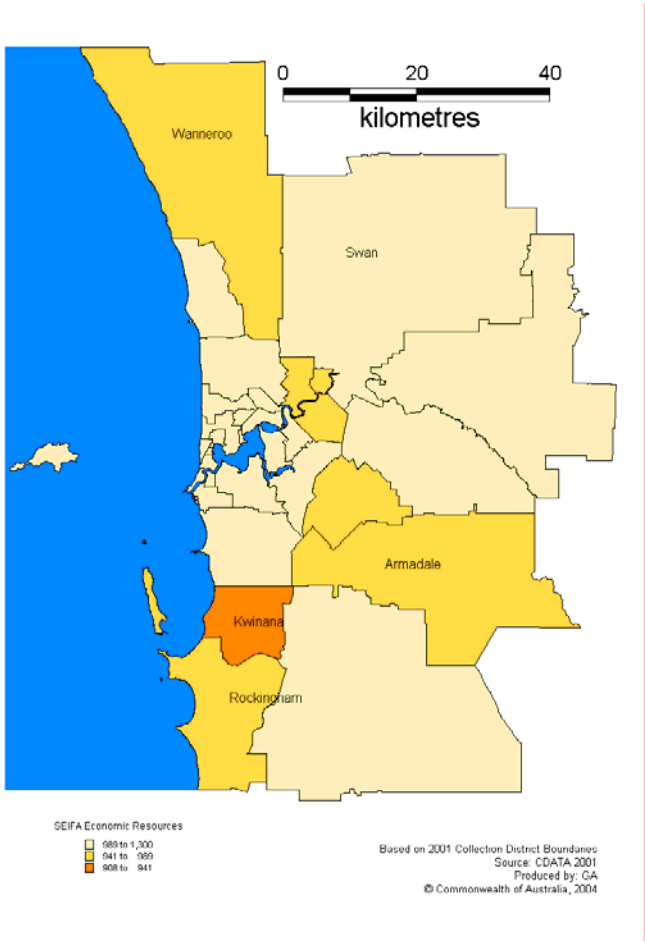

Figure 6.2: The SEIFA ranks for the 30 LGAs in the Perth metropolitan area

Perth assessment: Census Districts

One benefit of using the SEIFA Index is its capacity to analyse small areas, such as census districts. While Census District (CD) analysis can look like an unhelpful patchwork quilt over very large areas, it can be useful in observing trends in small areas, giving us more insight than the LGA rankings. There are 2,772 CDs in the Perth metropolitan area, ranging from 80 to 280 households, with an average of approximately 220 households (ABS, 2004a). Figure 6.3 shows the CDs for the Perth area, with some trends observable in the metropolitan fringe areas.

Unlike the LGA SEIFA ranking, which did not have any Perth areas in the first quartile of LGAs, the CDs of metropolitan Perth span all four quartiles when ranked against all Australian CDs. It is important to note that the difference between the top ranks of some quartiles and the bottom ranks of adjacent quartiles can be very small, so the quartile classification should be viewed in context with the values of all areas, remembering that the Australian average is 1000.0. There are CDs in the first quartile scattered across the Perth area, but there are four distinct clusters of CDs in the first and second quartiles, indicating a high proportion of households with reduced financial capacity and a low proportion of households with high financial capacity. These clusters are highlighted in Figure 6.4 and shown in more detail in Figures 6.4 and 6.5. The districts that might suffer financial difficulties following a natural disaster are:

- *Inner-north*: suburbs just east of the Wanneroo Road and south of Marangaroo Road, including Girrawheen, Koondoola, Mirrabooka, Balga, Westminster, Nollarma.
- *North-east Perth*: the suburbs at the junctions of the Great Northern, Great Eastern and Roe Highways, including Midland, Midvale and Bellevue.
- *South Fremantle to Rockingham*: suburbs along Rockingham Road, including Medina, Orelia, Parmelia, Calista, Hillman, East Rockingham, Rockingham, Hamilton Hill Coolbellup, Cooloongup.
- *South-east Perth*: suburbs along the Albany Highway from the junction with the Great Eastern Highway down to the junction with Armadale Road, including Belmont, Bentley, Cannington, Kenwick, Thornlie, Kelmscott, Gosnells, Armadale, Langford.

Interpretation

The clusters of households with low financial capacity, as shown in Figure 6.3, tend to be along major highways or freeways in Perth, or at major intersections, with the exclusion of the Rockingham area in the south of cluster 4. While it is beyond the scope or expertise of this report to discuss why households with low financial capacities are located in these areas of Perth, it is possible to suggest a relationship with the lower real estate values associated with houses along major road networks. Houses with lower real estate values provide an opportunity for people with lower financial capacity to access housing. However, the important point to note is that households in these four clusters may take longer to repair or rebuild their house, or replace damaged items, due to a lower household financial capacity.

6.3 Social Networks

Concept

Other factors than financial strength contribute to the recovery of a household, including our social networks. These include interactions with our neighbours, friends, family and the wider community. Social networks, support in times of crisis and our feelings about our community will influence aspects of our recovery. People and communities who have a greater degree of self-determination are better placed to recover (EMA, 2004a). Having an input into re-planning or contributing to community development, being able to access services or people for support, volunteering in your community or participating in activities may assist in the recovery process.

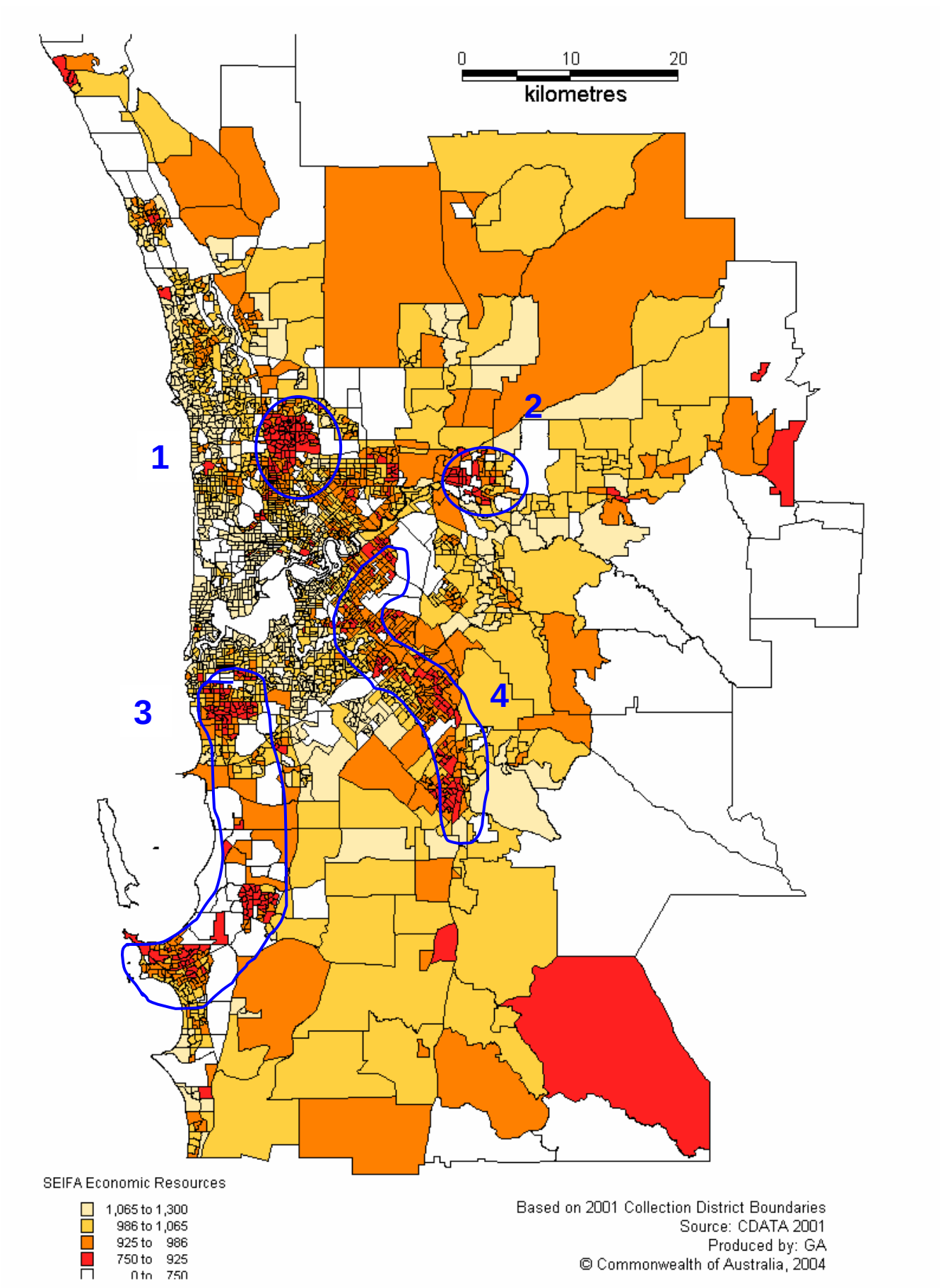

Figure 6.3 The four clusters of areas with a high proportion of households with low financial capacity in the Perth metropolitan area.

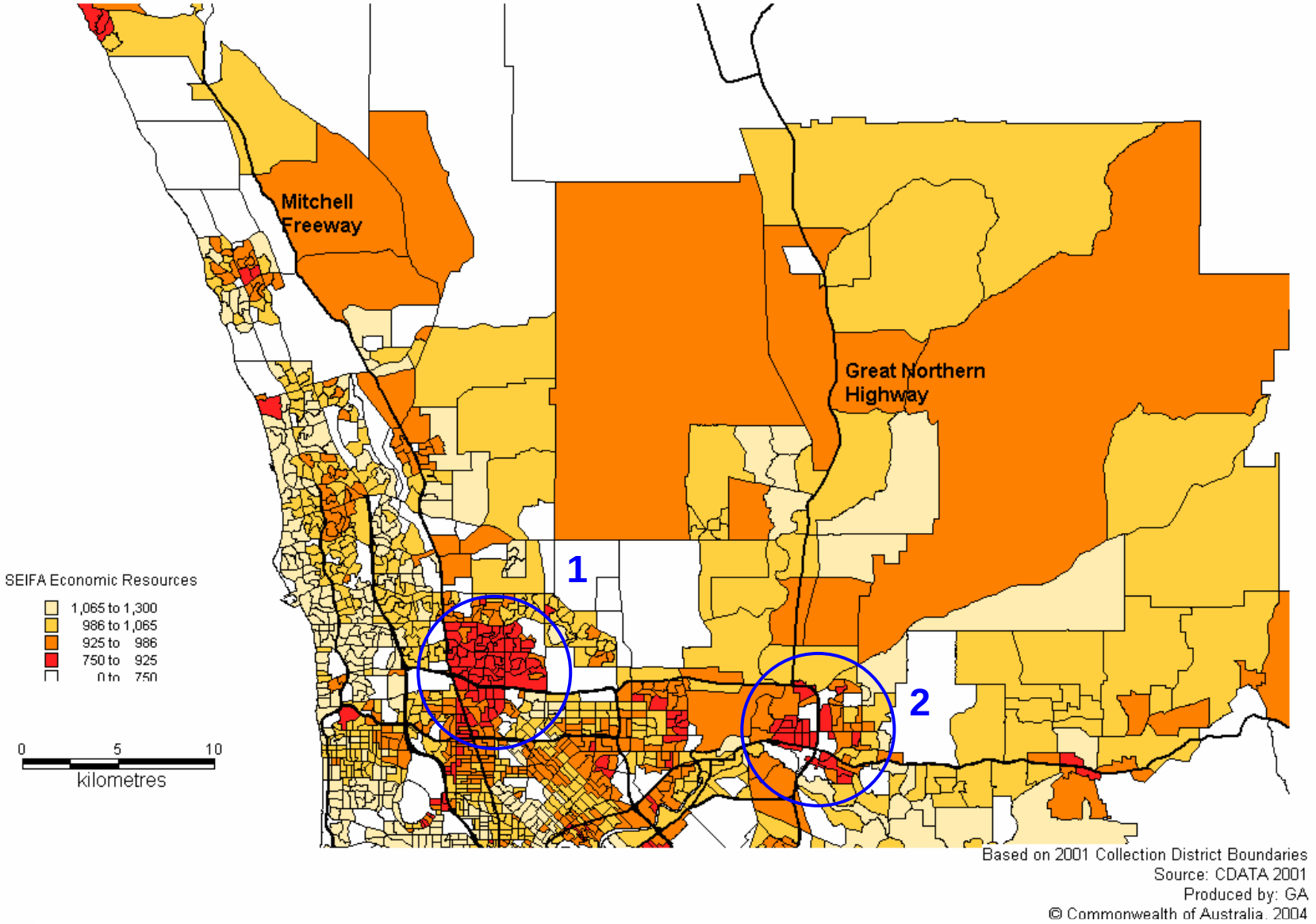

Figure 6.4 Two of the clusters of areas with a high proportion of households with low financial capacity: Inner-north and North-east Perth.

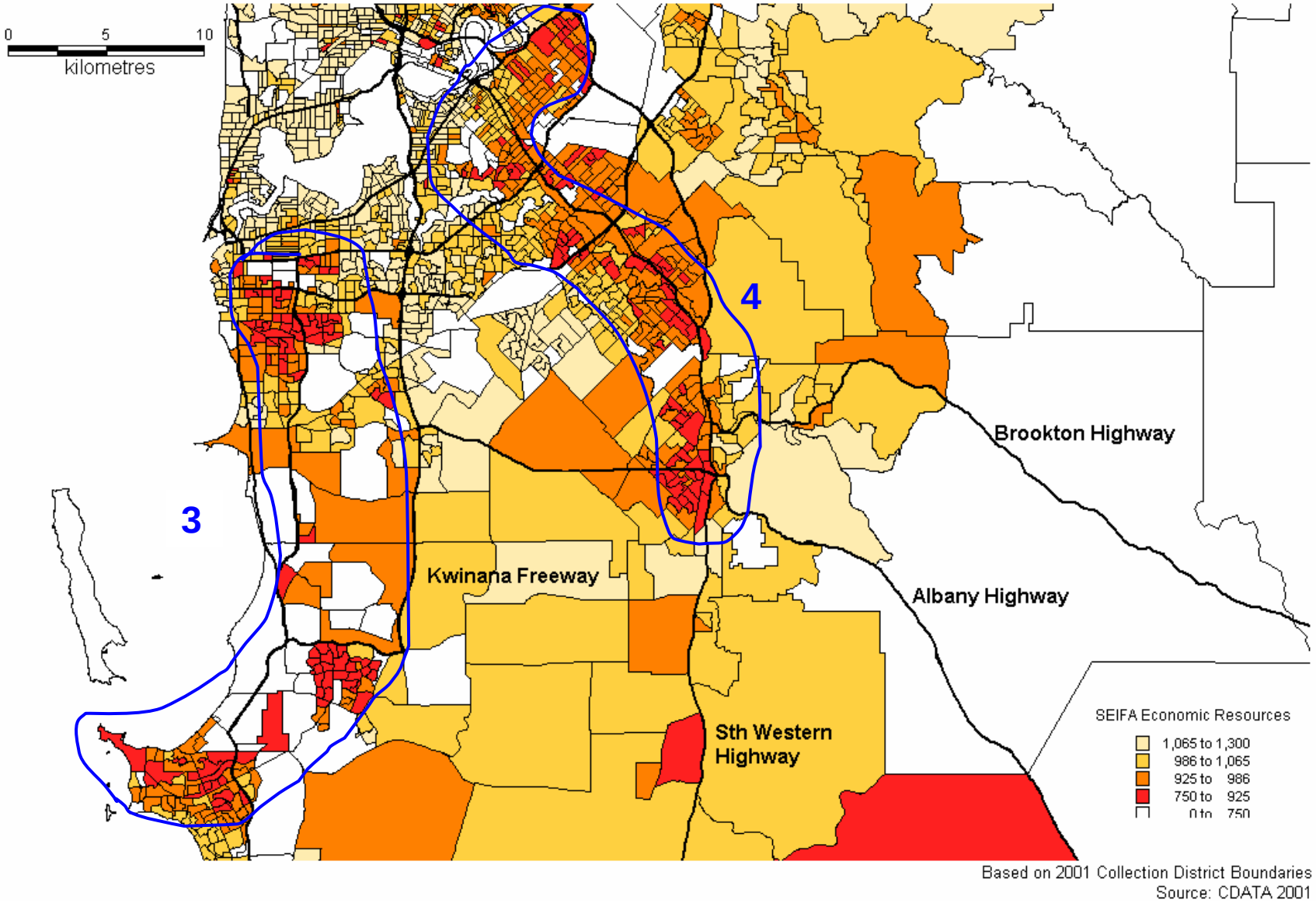

Figure 6.5 Two of the clusters of areas with a high proportion of households with low financial capacity: South Fremantle - Rockingham, Southeast Perth

Methods of communication are also very important in the recovery process, as different people and communities access information through different means. To ensure that information about recovery services, community meetings, and building and financial services reach those who have been affected, the characteristics of the affected community need to be taken into consideration. For example, some communities may rely on town meetings to disseminate information, other communities may have a high home internet use rate and some, especially rural and remote communities, may rely on local radio networks. Methods of communication are an aspect of social capital, a concept which aims to define and sometimes measure characteristics in communities often considered difficult to capture (Productivity Commission, 2003). Knowing what social attributes, including methods of communication, are specific to communities affected by natural hazard events allows planners to better assist in the recovery process.

Measures

General Social Survey (GSS) data provides an insight into the community characteristics across Australia at state level, and also for cities, inner regional areas and other localities (ABS, 2004b). The data collected in the first GSS, conducted in 2002 by the ABS, measure aspects of social capital and other socio-economic issues that are generally considered 'unmeasurable'. The World Bank (World Bank, 2004), the United Nations, the ABS (ABS, 2004c) and numerous other socio-economic research agencies are attempting to develop and refine measures of social capital – an individual and community concept that relates to social networks, trust, support and social cohesion. These agencies view social capital as an important aspect of community resilience, but acknowledge that it is very difficult to measure. Nonetheless, there have been common data items collected by various agencies, some of which include questions about membership in organisations, community groups and volunteerism. Other questions relate to contact with family and friends, and feelings of safety and trust in the community (World Bank, 2004; ABS, 2004c).

As well as collecting general measures of social capital, the GSS asks specific questions about safety and support in times of crisis, the use of government and charity services, frequency of contact with friends and families, attendance at social/sporting events and purpose and frequency of internet usage. Seven data items from the GSS have been used to assess community recovery issues in the Perth Cities Project. This data can provide insight into some of the unique social needs of a city or region, which is important when assisting the recovery.

Perth assessment

A comparison of the Western Australia results for each of the seven data items provides an insight into some of the unique attributes of the West Australian population compared with the rest of Australia. Perhaps even more importantly, the data provides a discussion point for how and why some of these items are important in understanding the many complex factors that may influence long-term community recovery.

1. Ability to raise emergency money

The GSS defines an ability to raise emergency money as being able to access $2,000 in one week. Possible sources of the money include personal savings, loans from financial institutions or from family and friends, providing insight into both financial capacity and relationships with friends and family. In the event of a natural disaster, government relief arrangements assist people in the immediate relief and response period, but access to emergency money is an important indicator of longer-term financial resilience.

The results across Australia were fairly uniform, with an average of 82.4% of all respondents indicating that their households could raise emergency money. The ACT had the highest capacity, with 90.5% of respondents able to raise emergency money: Western Australia had the next highest rate at 83.4%. While the difference between the states is negligible, it is

worth noting that West Australians have a greater capacity to raise emergency money than the rest of Australia, excluding the ACT.

2. Ability to ask for small favours

Natural hazard impacts can greatly interrupt the routine of a household and require people to ask for help. It is important to know people's capacity to ask for assistance, as those who don't ask may need pro-active assistance from government during times of disaster. It also gives an insight into the strength and reliability of informal networks, which are an important factor in the recovery of households and their communities. Respondents in the GSS were asked if they could ask someone who does not live with them for a small favour.

The GSS found that between 92.5% and 95.7% of Australians can ask someone for a small favour when help is needed (Figure 6.6). West Australia has the highest percentage (95.8%) of respondents who could ask someone outside their home for a small favour. However, like the previous data item, the difference between the states is relatively negligible.

3. Frequency of face-to-face contact with family or friends

Contact with people is at the foundation of social capital. How often we have contact with family and friends provides an insight into the strength of our social networks, which is an important aspect of support during the recovery from a natural hazard. According to the GSS results, between 80–90% of Australians have face-to-face contact with family or friends outside their household, on a weekly basis. At only one per cent lower than the ACT, 89% of WA residents indicated that they have face-to-face contact with friends or family outside their household at least once a week.

4. Feelings of safety at home alone after dark

Perception of safety at home provides an insight into how people feel about the community they live in, as well as previous experiences that may influence their judgement. Feelings of safety after dark also suggest the level of trust that people may have in unannounced visitors at night. If a natural hazard were to occur after dark, people who feel very unsafe may be less willing to open their doors to listen to emergency services or police. Approximately 8.5% of West Australian respondents feel neither safe nor unsafe at home alone after dark, which is the lowest proportion across all states and territories. The Australian average is 40 and 41% respectively (Figure 6.7).

5. Sources of support in times of crisis

Knowing who people turn to in times of crisis is essential information for risk managers involved in community recovery after a natural hazard impact. The GSS asked respondents whether or not they turned to seven different areas of support (Figure 6.8). While the trends across Australia are relatively similar, there are some unique state identifiers. Western Australians are more likely to turn to a health, legal or financial professional than residents of other states, or to a community, charity or religious organization. However, they are most likely to turn to a family member/friend, neighbour/colleague. This indicates that informal networks are the strongest in times of crisis, and also that in WA people are more likely to use some formal sources of support.

6. Participation in organised and non-organised activities

Activities that are associated with leisure time are an important part of recovery. Participation indicates either that people have spare time and money to attend such events, indicating a relatively good lifestyle, or that such events are important enough to warrant financial sacrifice to take part. More West Australian respondents are likely to participate in non-organised activities (36%) than any other state except the ACT. They are also more likely than the residents of other states to attend both organised and non-organised activities,

indicating a strong informal network in conjunction with more formally organised activities (Figure 6.9).

7. Type of unpaid voluntary work

Volunteerism is thought to contribute directly to the Australian economy (in 1997, it was estimated to be worth between $24 billion and $31 billion) and also indirectly. Indirect benefits include increased levels of trust, greater engagement in public affairs and increases in personal satisfaction and worth (Mayer, 2003). Between 35% and 41% of Australians responding to the GSS undertook unpaid voluntary work in the past 12 months. Voluntary work done by West Australians was more likely to involve a sport, recreation or hobby, or welfare/community activity (Figure 6.10).

Interpretation

The GSS is an encouraging first step in obtaining national-level data on complex social capital issues. However, due to privacy and confidentiality restrictions, the data are unsuited to analysis of regions or smaller communities. The few questions presented in this report show that West Australians have a slightly higher capacity than is average for social networking and community involvement. It would be useful to be able to separate the results for various communities within West Australia, and this could be a research priority for the future.

It is beyond the capacity or expertise of this report to analyse why people have provided the answers they did to the questions asked in the GSS. Complex social capital and perception of community issues affect recovery from natural hazards. State and local government community development agencies and staff are best placed to capture the relevant data, as well as interpret and mitigate these issues in order to assist the recovery process. These agencies need to be consulted in all stages of risk management to ensure that the recovery process, as well as other social factors contributing to mitigation, is a priority for emergency management planning and action.

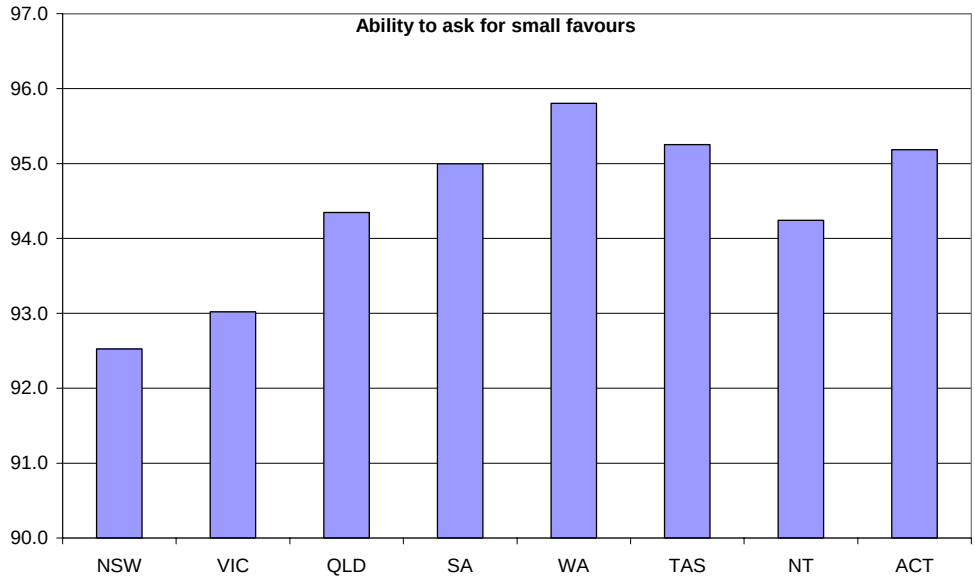

Figure 6.6: Ability to ask for small favours by state. WA respondents indicated the highest ability

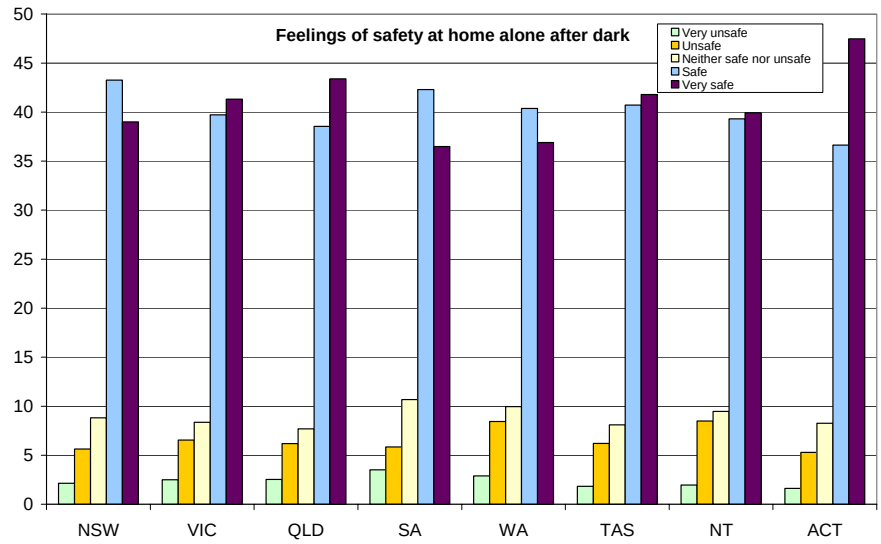

Figure 6.7: Feelings of safety at home alone after dark

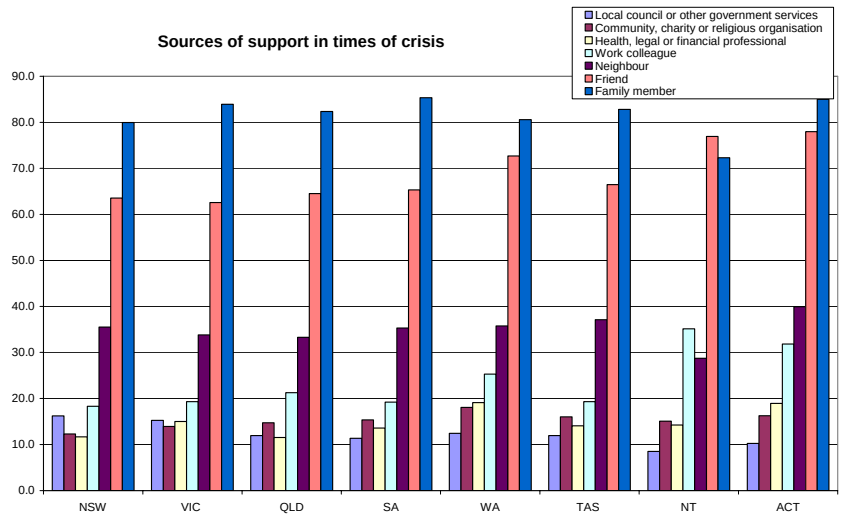

Figure 6.8: Various sources of support used in times of crisis

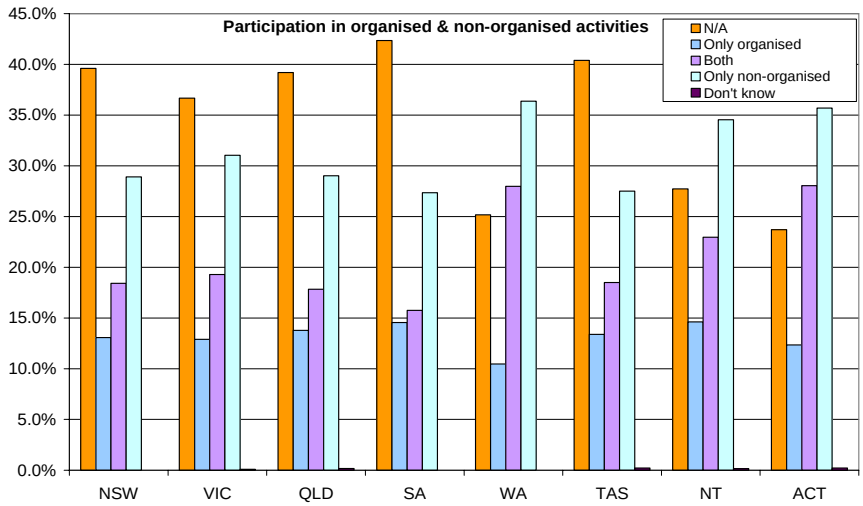

Figure 6.9: Participation in organised and non-organised activities

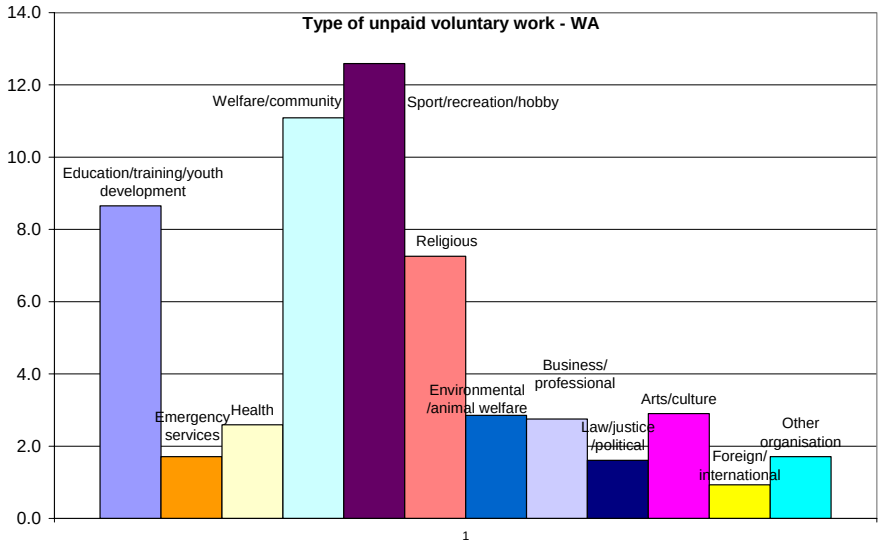

Figure 6.10: Type of unpaid voluntary work undertaken by West Australian respondents

6.4 Access to Services

Concept

Distance is still an important factor in the recovery of many communities, particularly outside major cities. Following a natural disaster, people may need regular visits to medical and welfare services, so the ability to access these is an important factor in recovery. Reconstructing houses, rebuilding local playgrounds and reconnecting water, electricity and gas depends, among other factors, on the distance between the disaster and the available materials and workforce. Other obstacles to service access – cultural, psychological and other barriers are just as significant as distance – are difficult to measure and an index including them does not yet exist for Australia.

Measure

The ABS Remoteness Classification aims to capture some of these issues by measuring the distance of an area or town to a centre with major services. The Remoteness Classification takes into account the types of services that different sized centres provide. For example, while some medical services may be found in the classifications ‘Inner Regional’, ‘Outer Regional’ and ‘Remote’, specialised medical services, such as obstetrics or burns care, may only be found in a ‘Major City’ (ABS, 2001b). The classification is therefore weighted according to the level of services provided and provides a valuable insight into the distance issues that may affect the recovery of some households and communities. It is important to note that some regional areas have some significant services, such as the large regional hospitals found in both Armadale and Kalamunda, two LGAs that the ABS classification identifies as partially outside the ‘Major City’ classification.

Perth assessment

The Perth metropolitan area falls into two remoteness classifications; Major City and Inner Regional (ABS, 2003). Of the 30 LGAs in the Perth metropolitan area, 23 are Major City areas, only one (Serpentine–Jarrahdale) falls into the Inner Regional classification and 6 LGAs straddle both Major City and Inner Regional areas. Table 6.3 lists the remoteness classification for each LGA in metropolitan Perth. This information allows us to consider where disaster recovery might be affected by distance from a major service centre. The areas are Serpentine–Jarrahdale, northern Wanneroo, northern Swan, southern Rockingham, southeastern Kwinana, eastern Kalamunda and eastern Armadale.

Table 6.2: The remoteness classification of the LGAs in metropolitan Perth

LGA Name	ABS Remoteness Classification
Armadale, Kalamunda	City/Inner Regional
Kwinana, Rockingham	City/Inner Regional
Swan, Wanneroo	City/Inner Regional
Serpentine–Jarrahdale	Inner Regional
Bassendean, Bayswater	Major City
Belmont, Cambridge	Major City
Canning, Claremont, Cockburn	Major City
Cottesloe, East Fremantle	Major City
Fremantle, Gosnells, Joondalup	Major City
Melville, Mosman Park	Major City
Mundaring, Nedlands	Major City
Peppermint Grove, Perth	Major City
South Perth. Stirling, Subiaco	Major City
Victoria Park, Vincent	Major City

Source: ABS 2001 Census Data, 2003

Interpretation

West Australia has some of the most remote communities in Australia, so distance to services is a particularly important factor in the recovery process for many communities. Perth communities are generally close to the major services that would be needed in the recovery process. Residents of the outer communities of Armadale, Kalamunda, Kwinana, Rockingham, Swan and Wanneroo have greater distances to travel to major services. If transport routes are affected by a natural disaster, people in these communities will be more physically isolated than central areas.

6.5 Findings

Most households in the Perth metropolitan area do not have very low economic resources. In the event of a natural disaster that damages residences, many households can draw on their own economic resources to assist their recovery. However, it must be noted that there are some areas, or clusters, of households that may experience difficulties in the recovery process due to limited financial capacity.

The strong informal network that is indicated by the results from the GSS suggests that for many in Perth, recovery may involve a strong utilisation of friends, family, neighbours and informal organizations. The strong community network in WA is also evident. Almost all residents indicated that they can ask someone outside of their home, including a health, legal or financial professional, a charity or religious organization, for assistance in an emergency, which is much needed during recovery from natural disaster. Recovery managers should consider this when tailoring programs and services for people in the Perth community. People in some outer suburban areas may have much further to travel to major services. Access to services, whether medical, welfare, social, physical or cultural, may be an important factor influencing the recovery of outer communities. This information may assist recovery managers in understanding some access/transport issues for people living in this part of the Perth metropolitan community.

The three factors explored in this chapter show that the Perth community has many characteristics that will influence the recovery process following a natural hazard event.

While the 'household financial capacity', 'community and social networks' and 'distance to services' only skim the surface of the many factors influencing recovery, the framework presented in this chapter shows Perth to have attributes that will influence and assist the recovery process of many households.

6.6 Recommendations and Future Research

We need to know more about the social processes of disaster recovery and how better risk assessments can be developed. The following points highlight some key recommendations:

- Local community development agencies and state recovery managers have an invaluable role and ***must*** be involved in risk assessment development and strategic risk management decisions. Only then can government begin to more effectively reduce the impact that natural disasters have on Australian communities.
- We need to better understand the emotional and psychological factors associated with accessing services during recovery.
- The effect of environmental factors on recovery should be studied.
- The role local economies play a community's recovery needs to be better understood.
- Finally, we need to involve people who are familiar with technical and social aspects of risk management in the development of risk assessments, so that they provide a more accurate picture of the issues involved in natural disasters.

6.7 References

Anderson-Berry, L. (2002) *Community Hazard and Risk Information and Education Needs*, Report prepared for Geoscience Australia, July 2002, James Cook University, Cairns.

Australian Bureau of Statistics (2001a) *Socio-Economic Indexes for Areas*, Information Paper 2039.0, ABS, Canberra.

Australian Bureau of Statistics (2001b) *ABS Views on Remoteness*, Information Paper 1244.0, ABS, Canberra.

Australian Bureau of Statistics (2003) *2001 Census of Population and Housing (CD-ROM)*, ABS, Canberra.

Australian Bureau of Statistics (2004a) *SEIFA 2001 Standalone (CD-ROM)*, Release 2 2004, ABS, Canberra.

Australian Bureau of Statistics (2004b) *2002 General Social Survey (CD-ROM)*, ABS, Canberra.

Australian Bureau of Statistics (2004c) *Measuring Social Capital: An Australian framework and indicators*, Information Paper 1378.0, ABS, Canberra.

Council of Australian Governments (2004) *Natural Disasters in Australia: Reforming mitigation, relief and recovery arrangements*, COAG, Canberra.

Dwyer, A., Zoppou, C., Day, S., Nielsen, O. and Roberts, S. (2004) *Quantifying Social Vulnerability: A methodology for identifying those at risk to natural hazards*, Geoscience Australia Technical Record 2004/14, GA, Canberra.

Emergency Management Australia (2004a) *Recovery*, Australian Emergency Manuals Series 10, EMA, Canberra.

Emergency Management Australia (2004b), *Disasters Database* [http://www.ema.gov.au/ema/emaDisasters.nsf] accessed 18 September 2004.

Insurance Council of Australia (2002) Report on Non-Insurance and Under-Insurance in the Home and Small Business Portfolio, Insurance Council of Australia. Reports on the website at [http://www.ica.com.au/reports]

Insurance Disaster Response Organisation (2004), *Disaster List* [http://www.idro.com.au/disaster_list/default.asp] accessed 18 September 2004.

Mayer, P. (2003) *The Wider Economic Value of Social Capital and Volunteering in South Australia*, Office for Volunteers, Government of South Australia.

Mileti, D.S. (1999) *Disasters by Design: A reassessment of natural hazards in the United States*, Joseph Henry Press, Washington DC.

Mileti, D.S. and J.H. Sorensen (1990) *Communication of Emergency Public Warnings: A social science perspective and state-of-the-art assessment*, Federal Emergency Management Agency, New York.

Ministry of Civil Defence and Emergency Management (2004) *Proceedings of the New Zealand Recovery Symposium*, 12–13 July 2004, Ministry of Civil Defence and Emergency Management, Wellington.

Productivity Commission (2003), *Social Capital: Reviewing the concept and its policy implications*, Commission Research Paper, Department of Communications, IT and the Arts, Melbourne.

World Bank (2004) *Measuring Social Capital: An integrated questionnaire*, The World Bank, Washington.

Chapter 7: POTENTIAL COASTAL EROSION OF THE SWAN COASTAL PLAIN DUE TO LONG-TERM SEA LEVEL RISE

Andrew Jones
Geoscience Australia

7.1 Summary

It is highly likely that coastal erosion due to long-term sea level rise associated with global warming will have a significant impact on Australia's coastal systems, and any associated infrastructure, over the next century. Long-term coastal erosion is thought to occur largely through sudden-onset storm events. Therefore, attempting to quantify this natural hazard is critical to future development and management of these localities. The potential impact of coastal erosion on the Western Australian built environment between Cape Naturaliste and Yanchep is assessed in this report.

Intergovernmental Panel on Climate Change (IPCC, 1996; 2001) sea level rise figures are the most widely accepted and used in coastal erosion studies. An increase in global temperatures will result in a sea level rise of 0.09 to 0.88 m between 1990 and 2100, with a central value of 0.48 m. Over the next 50 years the projected global sea level rise is 0.05 to 0.32 m, with a central value of 0.18 m (IPCC, 2001).

The nearshore bathymetry and onshore geomorphology of the Swan Coastal Plain is dominated by a series of shore-parallel submarine to emergent Pleistocene carbonate aeolianite ridges. Locally generated wind waves are the dominant mechanism controlling net northward littoral sand transport and determining the nearshore morphology of sandy beaches. The subsurface distribution of the erosion-resistant limestone has been determined in order to assess the erosion potential of the coastline. This reconstruction shows that the upper surface of the limestone is generally above sea level, suggesting the majority of the Perth coastal region is not at risk of significant erosion. At three localities (Port/South Beach, Swanbourne Beach, Pinaroo Point), however, the contact between the limestone and the overlying sand is below sea level. These areas are prone to erosion from storms and sea level rise, resulting in significant risk to urban development.

A Bruun Rule analysis reveals potential erosion rates at Swanbourne Beach over the next century may be approximately 1 m per year. The impact of this modelled recession is not significant due to a lack of overlying infrastructure. Similar erosion at the other vulnerable localities would have a much greater impact.

The majority of the Mandurah to Fremantle sector does not appear to be susceptible to coastal erosion over the next century, despite the fact that the Tamala Limestone is preserved below sea level across the majority of the area. This is due to the fact that this sector has been the primary depositional province for the Swan coast over the last 8,000 years. The Bunbury to Mandurah sector appears to be most susceptible to coastal erosion over the next century. This is because the Tamala Limestone is preserved below sea level, this sector is not well sheltered from offshore swell, and this location is at the southern end of the net northward littoral conveyor that operates along the Swan coast. The Hillarys to Yanchep sector does not appear to be susceptible to erosion over the next century as Tamala Limestone is preserved above sea level along the majority of the coast, and the beaches are well sheltered by three lines of offshore reefs. The Cape Naturaliste to Bunbury sector may be impacted by coastal erosion associated with long-term sea level rise.

A Bruun Rule calculation should be undertaken as a preliminary methodology in planning for coastal recession due to sea level rise. Future research should be focussed on the Bunbury to Mandurah sector, the Cape Naturaliste to Bunbury sector, and the Port/South beach area of Fremantle. The two significant problems that must be overcome before more modelling can be undertaken in the region are a lack of data (particularly sector specific wave data and more detailed subsurface data) and a lack of sophistication in current models that do not allow calculation in areas where the nearshore/offshore includes competent substrate.

7.2 Introduction

The latest IPCC report states that an increase in the concentration of greenhouse gases will cause global sea levels to rise over the next 100 years (IPCC, 2001). This sea level rise will cause extensive coastal erosion of many sandy beaches; more than two-thirds of the world's sandy coastlines have retreated in the past few decades (Bird, 1996). For example, it is estimated that over the next 60 years erosion may claim one out of four houses within 150 m of the US shoreline (H. John Heinz III Centre for Science Economics and the Environment, 2000).

With eight out of nine major Australian cities located on the coast, and the potential impact of this natural hazard still essentially unassessed, detailed risk assessments are critical to future planning. In this context, the Institution of Engineers (2000) identified marine climate change and its effect on the coastal zone as the most important research priority for coastal and ocean engineering in Australia. With extensive deposits of coastal sand, some of which host significant urban developments, Perth is an excellent example of a major city that may be at risk from sea level rise.

This report identifies areas of the Swan Coastal Plain between Cape Naturaliste in the south and Yanchep in the north, which may be susceptible to coastal erosion over the next century due to long-term sea level rise associated with global warming (Figure 7.1). The analysis is based on an integrated investigation of the Swan coastal system, comprising an examination of the geomorphology of the region in the context of coastal dynamics and sediment budgets. The key stage in this process involves a number of regional geographic information system (GIS) datasets that are used to reconstruct the three-dimensional architecture of the shoreline geology, to comment on the potential erosivity of the substrate and shoreline.

In order to present meaningful results along this 300 km section of coast, the study area is divided into sectors (Figure 7.2). The sectors are defined primarily by the data available for analysis, from a potential field of: bathymetry; LandSat; significant wave height; 1:50,000 scale environmental geology; microtremor; Seismic Cone Penetrometer Test (SCPT); geotechnical borehole; and Digital Elevation Model (DEM). The sectors are described in the following order, based upon the relative abundance of data (sectors are listed in order from that which contains the most data to that which contains the least):

- Fremantle to Hillarys (equivalent to the northern part of Searle and Semeniuk's (1985) Cape Bouvard – Trigg Island sector);
- Mandurah to Fremantle (equivalent to the southern part of Searle and Semeniuk's (1985) Cape Bouvard – Trigg Island sector);
- Hillarys to Yanchep (equivalent to the southern part of Searle and Semeniuk's (1985) Whitfords – Lancelin sector);
- Bunbury to Mandurah (equivalent to Searle and Semeniuk's (1985) Leschenault – Preston sector);
- Cape Nauraliste to Bunbury (equivalent to Searle and Semeniuk's (1985) Geographe Bay sector).

It should be noted that the accuracy of susceptibility interpretations varies between the sectors, in correspondence with the data that were available for analysis. Interpretations made in regards to the Fremantle to Hillarys sector are of a confidence level higher than the remaining sectors. Furthermore,

interpretations in the Mandurah to Fremantle are of moderate confidence, whereas confidence in the other sectors is relatively low (primarily due to the lack of onshore subsurface data (Figure 7.1).

Given the overlap with the sectors of Searle and Semeniuk (1985), their comprehensive descriptions of morphology and sedimentation/erosion are utilised in outlining the geomorphology and sediment budgets of the sectors within this report.

A quantitative evaluation of potential erosion rates over the next century using a conventional two-dimensional coastal behaviour model is presented for one site within the Fremantle to Hillarys sector. Similar quantitative evaluations within the remainder of this sector, and throughout the other sectors, were precluded by a lack of data and/or more sophisticated models. This will be discussed in more detail in each of the sections describing the coastal sectors.

Sea level rise

Based on tide gauge data, the rate of global mean sea level rise during the 20th century is in the range 1.0 to 2.0 mm/yr (IPCC, 2001). This rate of sea-level rise is consistent with recent satellite altimeter data (Nerem *et al*., 1997), which directly measures eustatic variations in sea level. IPCC (1996; 2001) future sea level rise figures are the most widely accepted and used in coastal erosion studies, as they are compiled by an international panel of climate change experts using what is considered the most reliable data and modelling techniques (Atmospheric and Oceanic Global Circulation Models (AOGCM's)). The IPCC (2001) climate models indicate the globally averaged surfaced temperature will increase by 1.4 to 5.8°C over the period 1990 to 2100. This increase in global temperatures will result in a sea level rise of 0.09 to 0.88 m between 1990 and 2100, with a central value of 0.48 m. Over the next 50 years the projected global sea level rise is 0.05 to 0.32 m, with a central value of 0.18m (IPCC, 2001).

The local rate of relative sea level change may diverge from the global change due to a number of processes, including coastline subsidence or uplift. Tectonic movements, isostatic subsidence, compaction of sediments, or extraction of groundwater, oil, and/or gas can cause subsidence. Uplift, as a result of postglacial isostatic rebound or tectonic processes, reduces or reverses relative sea level rise. This is very significant in coastal erosion studies as the validity of using global estimates to determine erosion rate is dependent on establishing the fact that the relative sea level change at any given locality is similar to the global baseline. Where this has the potential to impact on recession estimates in this study, this concept is explained in more detail.

Regional geomorphic setting and oceanographic conditions

The Rottnest Shelf encompasses the continental shelf between the Abrolhos Islands and Cape Leeuwin (Clarke, 1926; Carrigy and Fairbridge, 1954). However, this study is focussed only on the Rottnest Shelf adjoining the Swan Coastal Plain, from Yanchep in the north to Cape Naturaliste in the south. The 50 m isobath is over 50 km from sections of the coast along this part of the shelf (Figure 7.2); hence the slope of the inner shelf is gentle (Masselink and Pattariatchi, 2001).

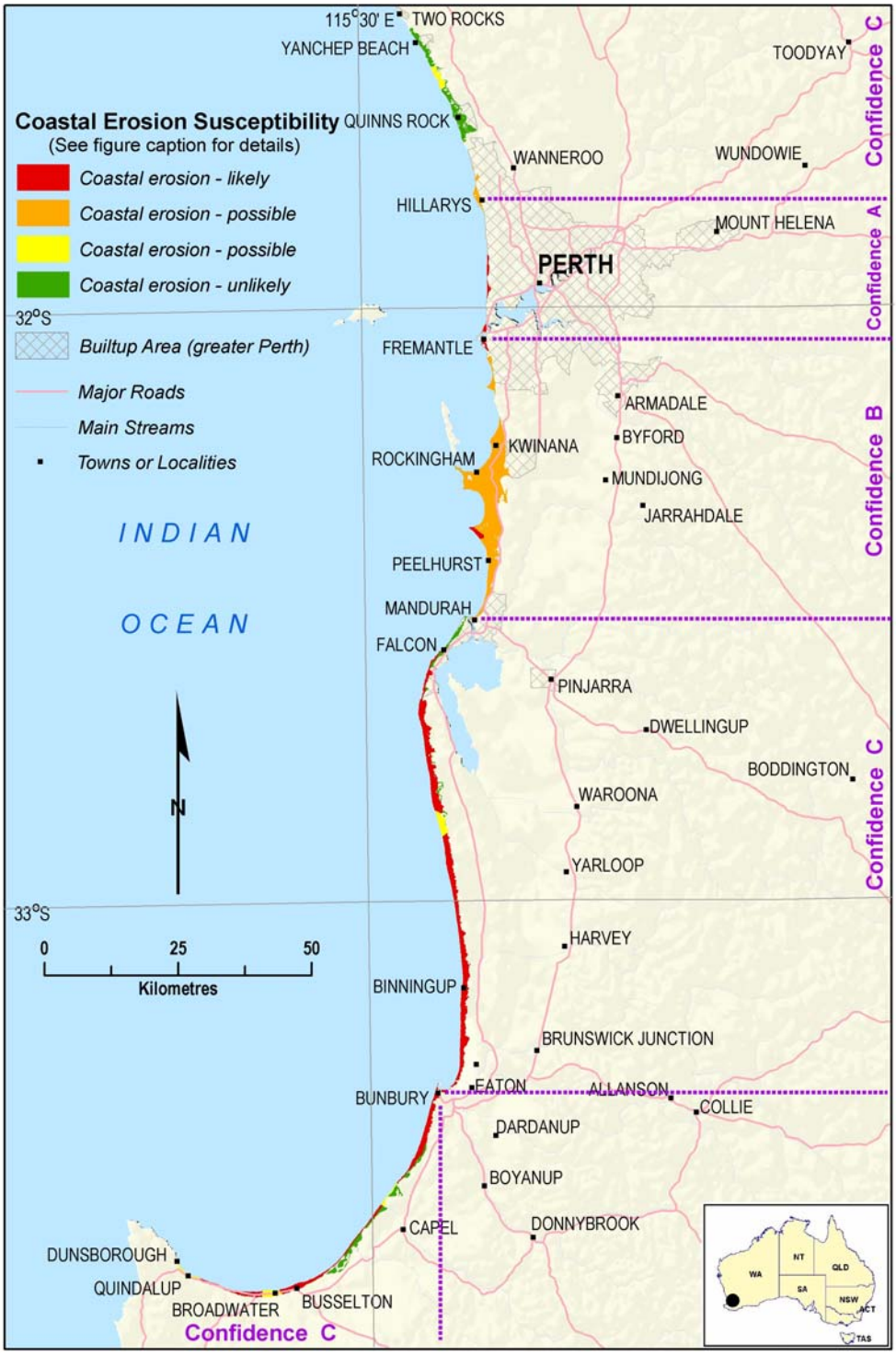

Figure 7.1: Potential coastal erosion due to long-term sea level rise for the greater Perth region. Details for colour key: Red – Coastal erosion likely as competent lithologies are preserved below sea level and external sediment input is minimal; Orange – Coastal erosion possible as competent lithologies are preserved below sea level, but external sediment input appears sufficient to fill any accommodation space created by sea level rise; Yellow – Coastal erosion possible as competent lithologies are preserved close to sea level, more detailed subsurface data necessary to more accurately delineate this surface in these areas; Green – Coastal erosion unlikely as competent lithologies are preserved above sea level.

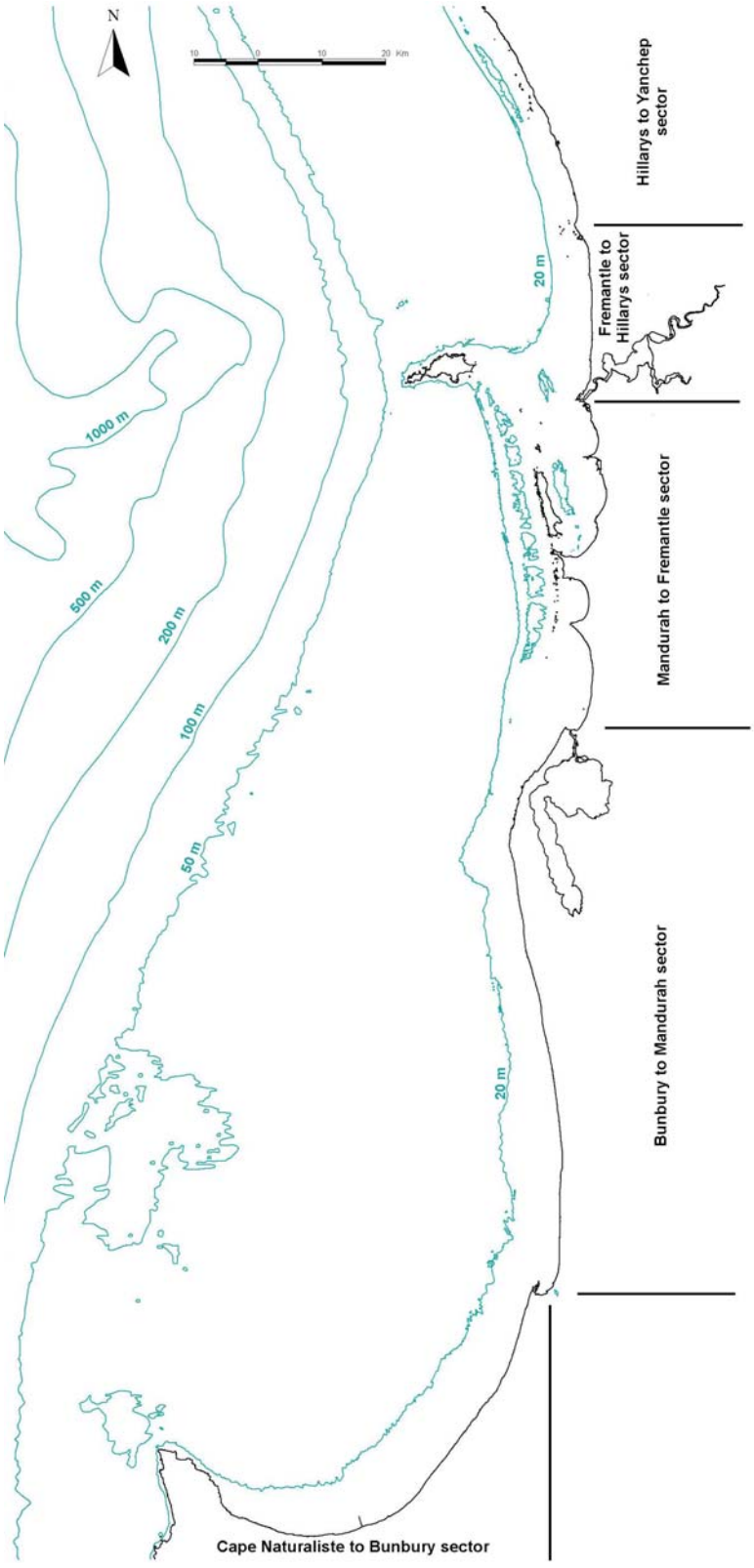

Figure 7.2: Map showing the location of the sectors within the study area. Note the relative width of the continental shelf, and the simple bathymetry of the southernmost two sectors relative to the remaining three

The coastline of the Swan Coastal Plain is dominated by a series of shore-parallel submarine to emergent Pleistocene carbonate aeolianite ridges and associated depressions. Onshore, this aeolianite comprises the Tamala Limestone (Playford *et al*., 1976). The Tamala Limestone also forms the core of nearshore and offshore islands, and dominantly underlies the extensive continental shelf in this region (Collins, 1983; Searle, 1984; Searle and Semeniuk, 1985). The coastal dune and beach sediments of the Swan Coastal Plain are termed the Safety Bay Sand (Passmore, 1967; Playford and Low, 1972; Playford *et al*., 1976). This formation extends discontinuously along the coast and is best developed in embayments, sheltered bays and tombolo settings where it forms prograded sediment bodies (Searle and Semeniuk, 1985).

Throughout the year offshore oceanographic conditions are dominated by oceanic swell with average significant wave height of 1.5 m and period between 10 and 20 seconds (Sanderson and Eliot, 1999). This swell is attenuated both as it crosses the continental shelf, and as it passes across any offshore reefs. On average, 39% of the offshore incident wave energy is filtered or dampened (Steedman, 1977), with local topography potentially attenuating up to 90% of the swell (Hegge, 1994; Lemm, 1996). Therefore, the inshore wave regime is relatively quiet, with an average significant wave height of less than 1 m and a period of approximately 10 seconds (Data courtesy of the Western Australian Department of Planning and Infrastructure (DPI)).

In contrast to the subdued wave regime, the Swan coast is exposed to one of the most energetic sea-breeze systems in the world (Masselink and Pattiaratchi, 2001). A significant feature of the sea breeze along the west coast of Australia is that it blows parallel to the shoreline (i.e. from the south-southwest; Pattiaratchi *et al*., 1997; Masselink and Pattiaratchi, 1998). This is in contrast to a ‘typical’ sea-breeze system, which blows perpendicular to the shoreline (Hsu, 1988; Abbs and Physick, 1992; Simpson, 1994). In the summer months, the sea breeze is present more than 60% of the time (Hounam, 1945) and the mean sea breeze velocity at the coastline is about 8 m/s (Masselink and Pattiaratchi, 2001). In winter, low pressure cells impinge on the Perth coastline, and disrupt the sea-breeze system (Bureau of Meteorology (BOM), 1969; Gentilli, 1971). The winds associated with the approach of a depression are initially from north and increase in strength while shifting to the northwest (Masselink and Pattiaratchi, 2001).

Sediment dynamics

Due to the subdued wave regime and the energetic sea breeze activity that exists along the Swan Coastal Plain, the locally generated wind waves are the dominant mechanism controlling littoral sand transport and determining the nearshore morphology of sandy beaches (Pattiaratchi *et al*., 1997; Masselink and Pattiaratchi, 1998).

The southerly sea-breeze system induces a northward sediment transport, whereas sand is moving south during winter as a result of southward flowing currents generated by the northwesterly storms. This oscillatory north–south motion of sand occurs on an annual cycle along the Swan coast with a resultant northerly bias (Silvester, 1961; Masselink and Pattiaratchi, 2001). Therefore, the northward longshore sediment transport induced by the sea breeze accounts for the net littoral drift that occurs along this part of the coast (Masselink and Pattiaratchi, 1998).

7.3 Methods

Assessing the erosivity of the Swan coastline requires differentiation between the ‘erosion-prone’ sand and ‘erosion-resistant’ limestone, which dominate the shoreline geology of the Perth coastal system. Environmental geology maps (eg, Gozzard, 1986) provide a spatial distribution of shoreline geology at the surface, but accurately assessing erosivity requires understanding of lithology distribution at depth. In order to reconstruct the three-dimensional distribution of the limestone in each of the sectors, environmental geology maps were combined with geophysical (microtremor) and geotechnical (borehole descriptions and SCPTs) data. The availability of this data varies between sectors, therefore the datasets and methods utilised for each sector are described in the relevant sections. The remainder

of this section outlines the way in which the limestone architecture is reconstructed using each of these datasets.

Geotechnical boreholes

The location of approximately 28,000 boreholes was supplied to Geoscience Australia (GA) by the Western Australian Department of the Environment (DOE). In addition to the locations, DOE supplied a spreadsheet of lithological descriptions for some of the boreholes (comprising over 80,000 rows of data). The boreholes were drilled primarily with the aim of exploring for aquifers across the Swan Coastal Plain. The coverage of these boreholes in the region is excellent, and as such is the only onshore data available in a number of the sectors, but the lithological descriptions are highly variable in terms of their detail. In most cases broad descriptions of grain size were documented for relatively coarse intervals, disregarding any differences between consolidated and unconsolidated sections. For example, shales and siltstones are often described as mud or clay. Therefore in many cases it was necessary to interpret the lithological strata in the context of published descriptions of the Quaternary stratigraphy. Another limiting factor of this dataset is due to the fact that the holes were drilled with the aim of delineating aquifers. In many places along the coast it was therefore unnecessary to drill to the top of the limestone, given that the overlying Safety Bay Sand comprises the primary superficial aquifer. Consequently many of the logs that have an associated description do not penetrate sufficiently deep to assist in the reconstruction of the upper limestone surface.

Where geotechnical boreholes with sufficiently detailed lithological descriptions were available, the height at which the ground surface lies at that point was determined by relating the borehole position to a DEM. The depth at which the top of the limestone was penetrated was then taken away from the ground height relative to the Australian Height Datum (AHD) to determine whether or not that limestone surface lies above or below sea level.

Seismic Cone Penetrometer Tests

In seismic cone penetrometer tests (SCPTs), a conical penetrometer tip is pushed slowly into the ground and monitored. The device contains electrical transducers to measure both tip (Qc) and side (Fs) resistances as the instrument is advanced. A friction ratio is calculated by relating the sleeve friction to the tip resistance ($^{Fs}/_{Qc}$). Coarse-grained sediments such as sands and gravels tend to resist penetration at the tip, whereas finer grained sediments such as clays and silts resist penetration along the sleeve, therefore there is a direct relationship between the friction ratio and lithology. The higher the friction ratio, the finer the sediment grain size. In addition to providing an estimation of lithology, SCPTs measure the seismic velocity of the sediments.

GA has undertaken 58 SCPTs around Greater Metropolitan Perth as part of a study of earthquake hazard in the region (Figure 7.3). The usefulness of these SCPTs for reconstructing the upper surface of the limestone is limited due to both their sparse coverage across the Swan Coastal Plain, and because the test terminates for a number of reasons (including encountering a competent substrate). The first point is highlighted by the fact that only three tests were undertaken in Safety Bay Sand directly adjacent to the coast. The second point, that SCPTs cannot penetrate limestone, means the logs produced from these tests are only useful if the test went below sea level. If the test terminated above sea level then it is impossible to determine if termination was due to encountering limestone, as opposed to hitting a buried boulder or a very coarse sand layer.

The most useful aspect of SCPTs in this study is seen in the fact that they provide a measurement of the seismic velocity of sediments. This seismic velocity is used in association with the microtremor data to estimate the limestone architecture (see below).

Microtremor data

One of the most useful tools in reconstructing the three-dimensional architecture of the sand and limestone is a microtremor dataset collected during an extensive GA field survey (Figure 7.4). The survey involved using a ground seismometer and measuring the resonant vibration of unconsolidated regolith (T), as created by phenomena such as wind, waves and anthropogenic influences (eg, traffic).

Where the unconsolidated Holocene sediments of the Safety Bay Sand overlie 'competent' rock (Tamala Limestone), resonant vibration in the sediments occurs for shear waves with a wavelength of four times the sediment thickness. In this case:

$$V_s = 4\frac{H}{T}$$

Equation 7.1

where V_s is seismic shear wave velocity in metres per second, T is resonant period of the fundamental mode of vibration in seconds and H is sediment thickness in metres. Therefore to estimate the thickness of the sand, and correspondingly determine the position of the upper surface of the limestone, it is necessary to have measurements of V_s and T.

Shear wave velocities measured in the Safety Bay Sand (V_s) during the SCPT's were averaged and related to natural period of ground vibration (*T*) at each point in the microtremor survey, to yield an estimate of regolith thickness (*H*). This theory was utilised to reconstruct the position of contact between the limestone and the overlying sand.

7.4 Fremantle to Hillarys

Geomorphology and sediment dynamics

The nearshore bathymetry and onshore geomorphology of the Fremantle to Hillarys sector is dominated by Spearwood Ridge of Tamala Limestone, which forms the north–south trending shoreline in the lower part of the sector and 330° trending nearshore reefs in the upper part of the sector (Figure 7.5). Holocene coastal sedimentation in this region has formed minor stable dunes and pocket beaches flanking the seaward side of the Spearwood Ridge (Searle and Semeniuk, 1985).

Much of the coastline of this sector is sheltered from the direct impact of swell and storm-wave activity by the extensive chain of reefs formed by the Five Fathom Bank and Garden Island Ridges. As a result of wave refraction and attenuation, wave energy at the shoreline tends to be low (Pattiaratchi *et al.*, 1997).

In the context of sedimentation in this sector the Garden Island Ridge, up to and including Rottnest Island, acts as a barrier to the northward littoral drift (see Mandurah to Fremantle section). The discrete nature of the depositional loci south and west of Swan River outlet suggest that very little sediment derived from the longshore drift reaches the northern Perth coastline. This is supported by observed beach recession/accretion trends, which show that beaches in the southern part of the sector (Port Beach to City Beach; Figure 7.6) experience average erosion rates of c. 1 m/yr, whereas those north of City Beach are characterised average accretion rates of c. 1 m/yr (Silvester, 1961). Long-term beach width measurements on Scarborough Beach (Figure 7.6) demonstrate an accretion rate of 3 m/yr (Clarke and Eliot, 1983). This suggests that sediment taken from the southern part of the sector by northward drift is not being renewed from south of Fremantle. Given that very little sediment is introduced into the sector from longshore drift, Safety Bay Sand along the northern Perth sector has been primarily derived from local benthic assemblages (principally the seagrass assemblage) and from erosion of the Tamala Limestone within the sector (Searle and Semeniuk, 1985). One exception is the sand bank directly adjacent to the eastern point of Rottnest Island, which was likely deposited by the penetration of the longshore drift through the Garden Island Ridge at this point.

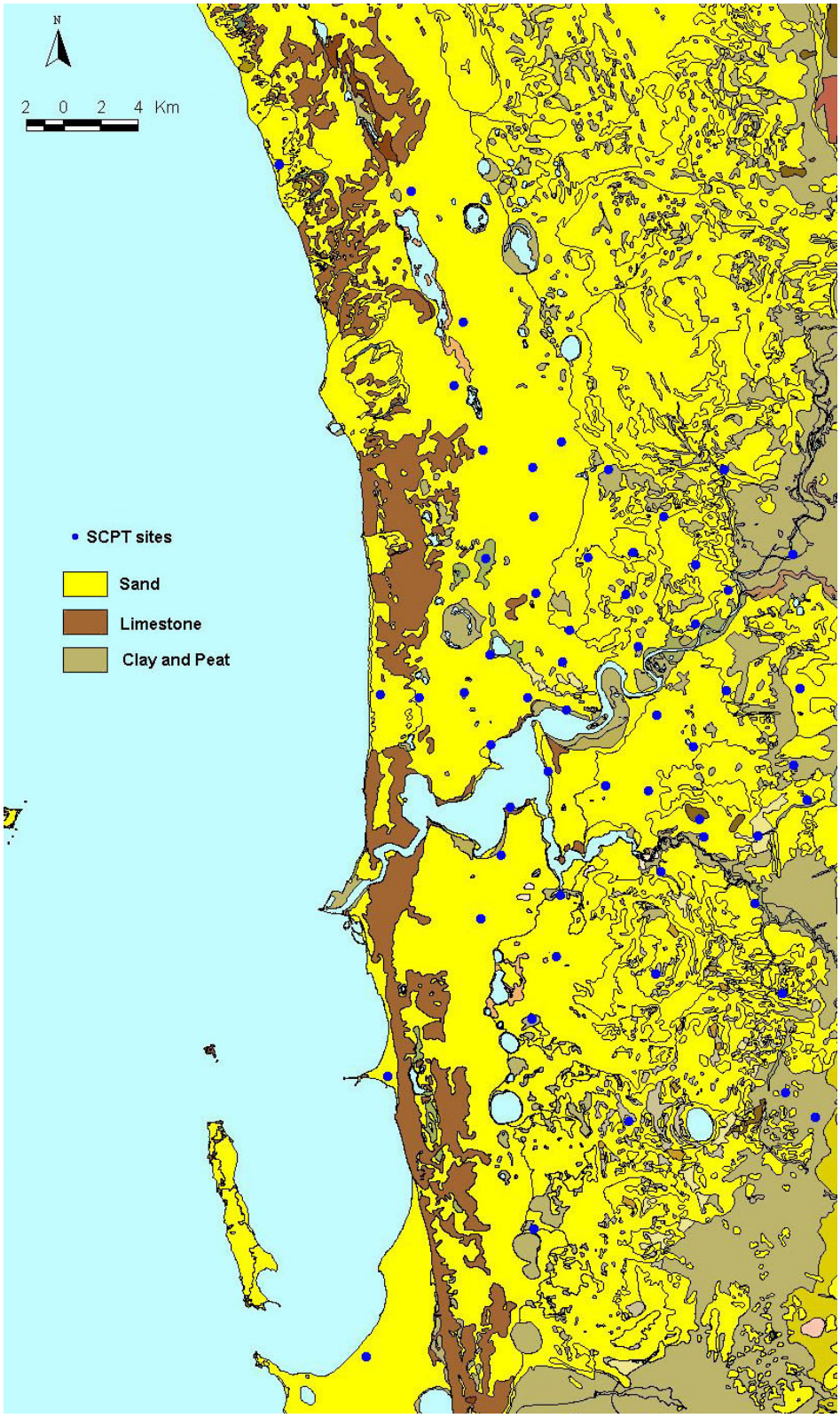

Figure 7.3: Location of SCPTs undertaken by GA as part of its earthquake risk assessment in the Perth region. Depth data from a number of these tests were utilised to reconstruct the three-dimensional architecture of the limestone. Measured seismic velocities were also used, in association with microtremor tests

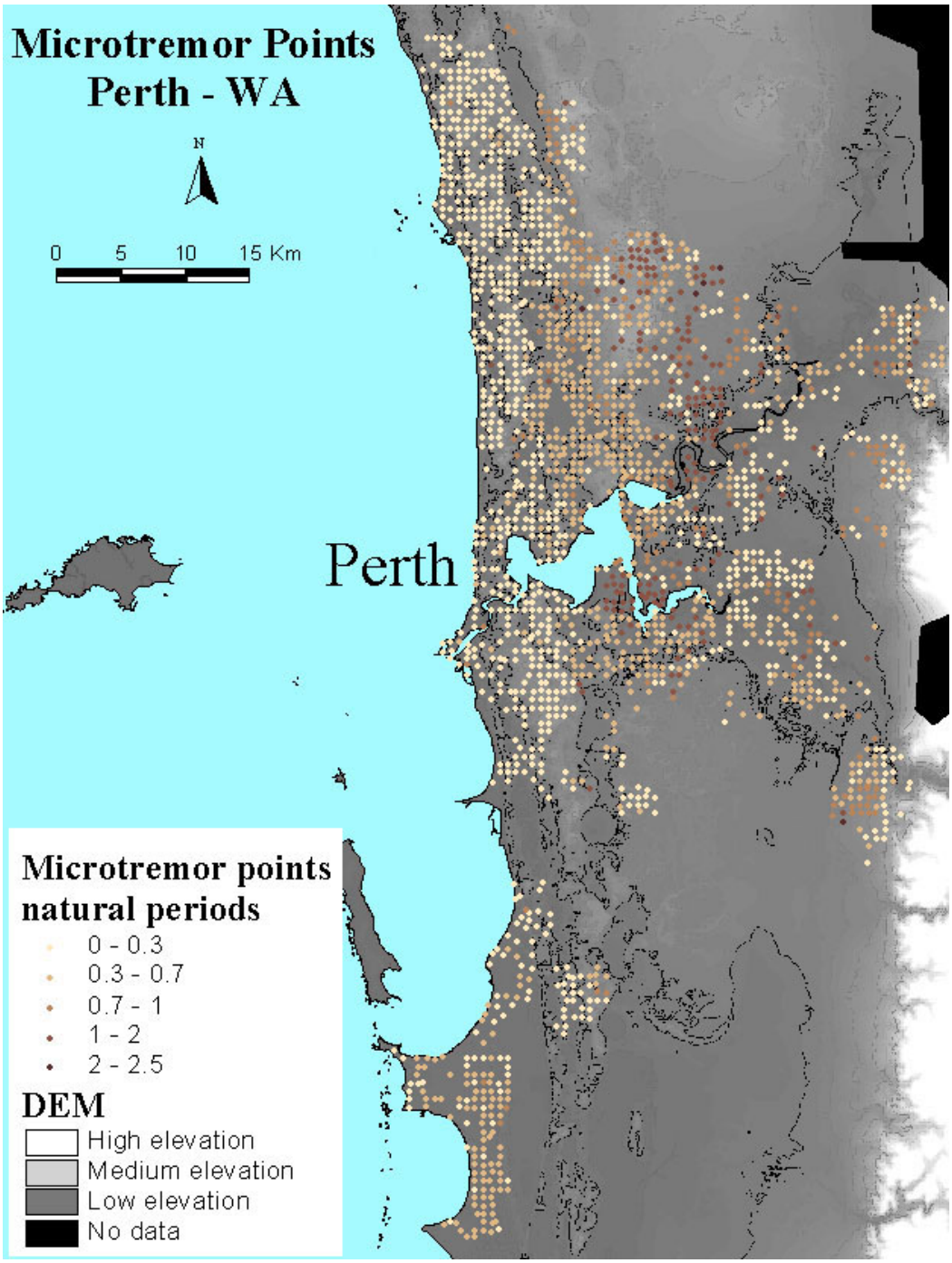

Figure 7.4: Location of microtremor tests undertaken by GA as part of its earthquake risk assessment in the Perth region. Measured natural periods at these sites were used in association with seismic velocities from SCPTs to estimate depth to limestone

The source of the sediment lobe adjacent to the coast 5 km north of the Swan River outlet is ambiguous (Figure 7.5). The lobate morphology suggests the sediments are allochthonous and the position of the lobe (with the flat edge adjacent to the coast) suggests the depositional mechanism was not longshore drift. The preservation of shore perpendicular channel features across the top of the lobe suggests this sediment lobe was likely deposited as a delta (Jones and Hayne, 2003). The delta was probably deposited during a relative sea level highstand approximately 6,000 years ago (Semeniuk and Semeniuk, 1991). Alternatively, it may have formed during a Pleistocene highstand, although if this is

the case it is difficult to reconcile the preservation of the lobe and associated channel features with the length of time that it has existed in a relatively high-energy environment.

Erosivity of the coastline

The microtremor dataset was utilised in reconstructing the upper limestone surface within this sector due to the excellent coverage of this part of metropolitan Perth. This reconstruction, displayed in Figure 7.7, shows that the upper surface of the limestone is generally above sea level, therefore the majority of the Fremantle to Hillarys coastal sector is not at risk of erosion. At a number of localities, however, the top of the limestone is below sea level, suggesting that overlying sediments and infrastructure is vulnerable, as storm events have the capacity to erode sand into the offshore. Three regions in particular may be at risk (Figure 7.8): the Pinaroo Point region; the Swanbourne to Floreat Beach region; and the Port/South Beach region at the Swan River outlet (Jones and Hayne, 2003).

Borehole data from the region adjacent to the coast (Figure 7.6) provide information on the accuracy of this reconstruction. Recorded heights of the upper limestone surface from 35 boreholes within 2 km of the coast were compared with values estimated from the contours shown in Figure 7.6. Significantly, the reconstruction gave only two localities where a value above sea level and the borehole value below sea level failed to correlate. At all other localities values corresponded, being either both above or both below sea level, suggesting the method is suitable for broad scale mapping of sediment interfaces.

Qualitative assessment of erosion hazard in susceptible areas

The majority of the coastline in this sector (Leighton to Cottesloe Beach and Brighton to Sorrento Beach), and the associated infrastructure, appears to be at little risk in terms of major recession due to erosive events and long-term sea level rise over the next century (Figure 7.1; Figure 7.7). It is possible that any narrow beaches backed or underlain by limestone may disappear, leading to coastal cliffs dominating the coastline geomorphology. While this erosion is unlikely to have a major impact in terms of land-loss and infrastructure damage, it may have some consequences in the context of recreational activity use. Due to net northward littoral drift through the sector the impact is likely to be more evident in the short term in areas such as Leighton Beach, as opposed to areas such as Trigg Beach.

The three localities in the northern Perth region that display some potential for erosion in the future can be ranked in order of relative hazard by examining their spatial distribution in the context of sediment dynamics for the region (Jones and Hayne, 2003). The Port/South Beach area is likely to be most vulnerable, as it is in the most southerly position (Figure 7.1). The net northward longshore drift is stripping sand from this part of the coast; therefore there is less of an erosional buffer. This hazard may be offset somewhat by the fact that the majority of storms influencing this part of the coast do so in winter (BOM, 1969; Gentilli, 1971). During this season there is a reversal in the longshore drift direction, and consequently the beaches are at their widest (Masselink and Pattiaratchi, 2001).

The Swanbourne to Floreat Beach region is likely to be the second-most vulnerable locality (Figure 7.1), although the relative hazard is somewhat ambiguous for two reasons: first, the area is in a quasi-steady state in the context of longshore drift as it is close to the boundary point between accreting and eroding beaches (Silvester, 1961); and second, the microtremor coverage in the Swanbourne region is relatively poor (Figure 7.7) due to restricted access to that part of the coast. It is possible that the Tamala Limestone is actually at, or above, sea level at this location, and that the vulnerability is considerably less than suggested by Figure 7.8. There is some evidence of this in that modern beach-rock is periodically exposed along Swanbourne Beach (I. Eliot, University of Western Australia, pers. comm., 2002), but the thickness and continuity of this unit is unknown.

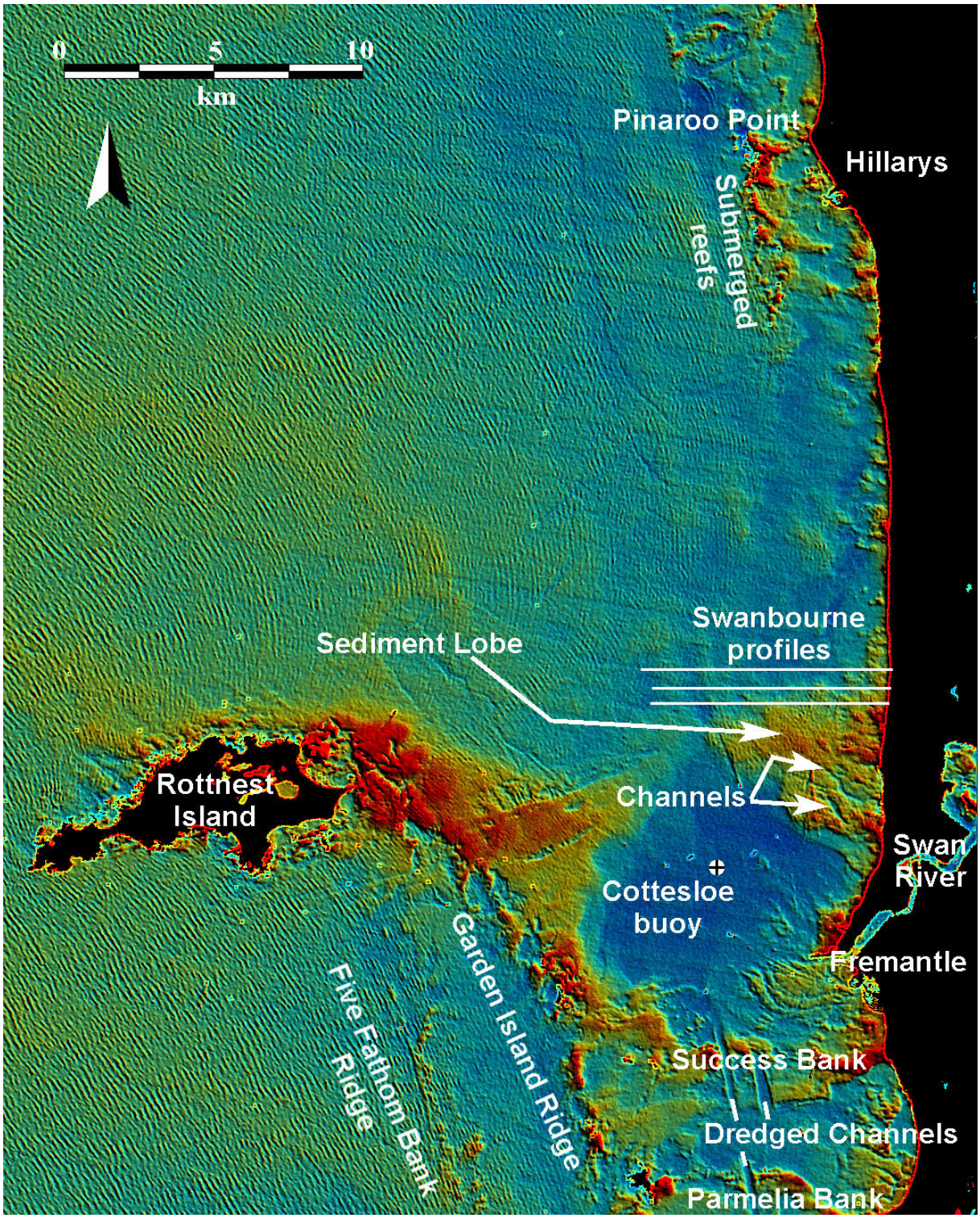

Figure 7.5: A Landsat image of the Fremantle to Cottesloe sector, processed with the GA Shallow Water Image Mapping (SWIM) method to display bathymetry. The 'hot' and 'cool' colours indicate shallow and deep water respectively. The level of precision displayed in this image is evident in the dredged shipping channels southwest of the Swan River outlet

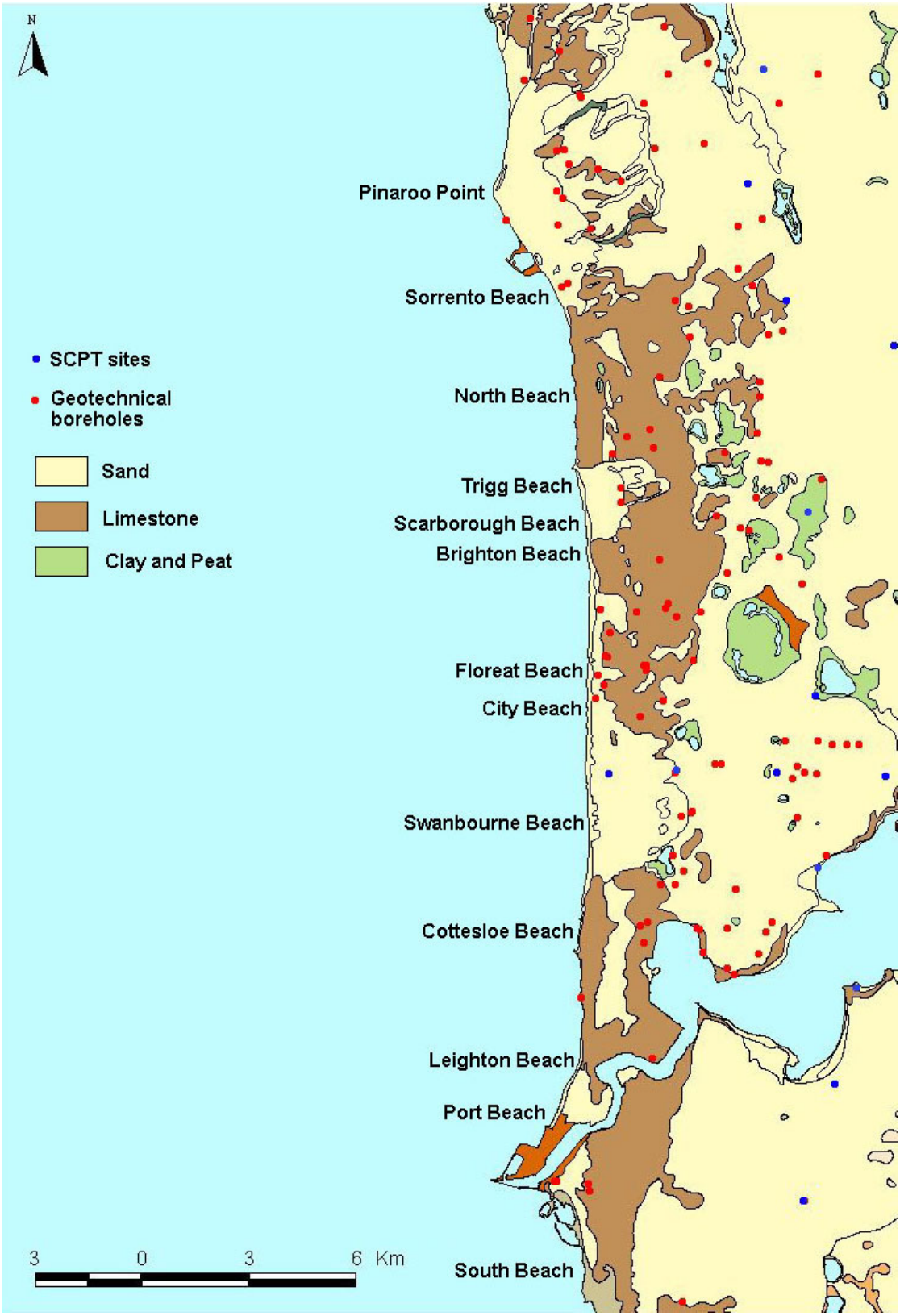

Figure 7.6: Spatial distribution of seismic cone penetrometer tests (SCPTs) and geotechnical boreholes in the Perth region, overlain on the environmental geology of the area from Gozzard (1986)

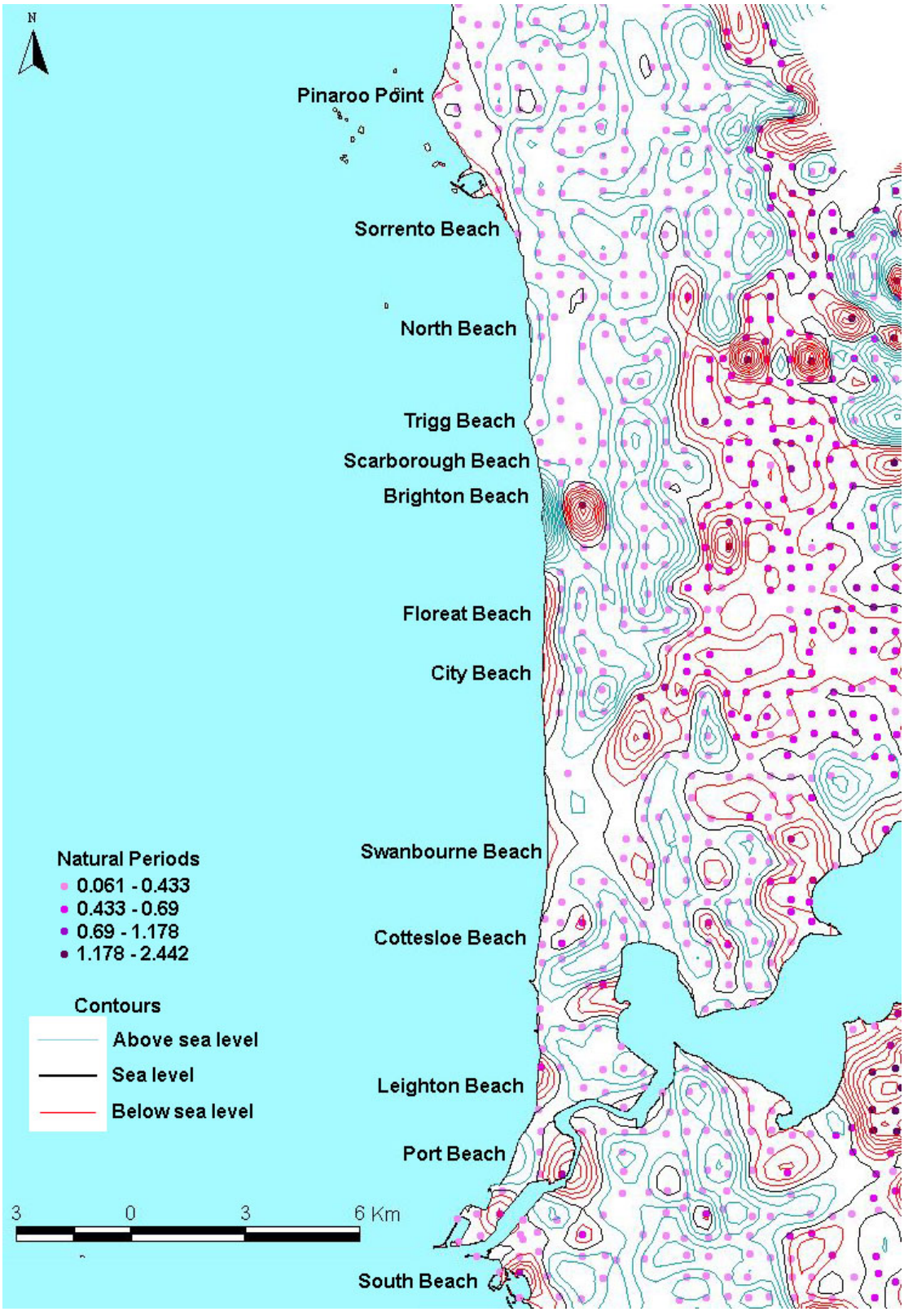

Figure 7.7: Spatial distribution of microtremor tests in the Perth region, and the reconstructed estimate of the upper surface of the Tamala Limestone relative to sea level. The reconstruction is based on the natural period measured at each microtremor test and the seismic velocity of the sand measured in the SCPTs

Figure 7.8: Zones potentially prone to coastal erosion along the northern Perth coastline. The interpretation is based on an intersection of sandy areas in the environmental geology maps (Figure 7.6) with areas in which the upper limestone surface are below sea level (Figure 7.7)

The Pinaroo Point area (Figure 7.8) is likely to be the least vulnerable of the three regions (Figure 7.1), as it is at the northern end of the sector and is supplied with sediment over the course of the year by

net northward longshore drift. The Safety Bay Sand in this area is relatively wide and as such there is a considerable buffer to sudden-impact erosional events. Additionally, any accommodation space created in the offshore by long-term sea level rise is likely to be infilled by longshore drift sediments, and will not require sediment to be eroded from the shoreline.

Potential erosion at Swanbourne following the Bruun Rule

The Swanbourne Beach section of the northern Perth coast was selected as a test case for quantitative assessment of potential erosion rates over the next 50 and 100 years. It was selected for a number of reasons.

- It is one of the areas identified as being susceptible to erosion in the analysis presented above.
- There is no significant input or output of sediment due to longshore drift.
- There is no evidence of a submerged limestone ridge forming a reef adjacent to that part of the coast (Figure 7.5).
- All data necessary for modelling was available.

The bathymetry and topography along three profiles in this area, taken from spot depth bathymetry and a DEM respectively, are utilised in a Bruun Rule analysis to calculate the potential erosion at Swanbourne Beach due to long term sea level rise (Figure 7.5).

The first and best-known model relating shoreline retreat to an increase in local sea level is that proposed by Bruun (1962; 1988). The analysis by Bruun assumes that with a rise in sea level, the equilibrium profile of the beach and shallow offshore moves upward and landward (Figure 7.9). Bruun derived the basic relationship for the extent of shoreline recession, R, due to an increase in sea level, S:

$$R=\left(\frac{L}{B+h}\right)S$$

Equation 7.2

where L is the cross-shore distance to the water depth h, taken by Bruun as the depth to which nearshore sediments exist (depth of closure), and B is the height of the dune. The analysis is two-dimensional and assumes (Scientific Committee on Ocean Research (SCOR), 1991):

- The upper beach is eroded due to the landward translation of the profile;
- The material eroded from the upper beach is transported immediately into the offshore and deposited, such that the volume eroded is equal to the volume deposited; and
- The rise in the nearshore bottom as a result of deposition is equal to the rise in sea level, thus maintaining a constant water depth in the offshore.

Despite its simplicity and numerous assumptions, which have in some instances led to criticism (eg, Pilkey *et al*., 1993), the Bruun Rule works remarkably well in many settings (Morang and Parson, 2002). The use of the Bruun Rule may still be the valid step forward in the short term, as it gives an estimate of future recession values without requiring long-term monitoring of shoreline trends (cf. Stive and de Vriend, 1995).
In studying coastal erosion at Swanbourne Beach, the validity of assumption one (erosion of the upper beach due to profile translation) is relatively critical, as there is some evidence of beach-rock along this part of the coastline (I. Eliot, University of Western Australia, pers. comm., 2002). If this is the case then the calculations presented below are invalidated. However, in the absence of distribution data for the beach-rock a Bruun Rule analysis provides a useful measure of potential erosion.

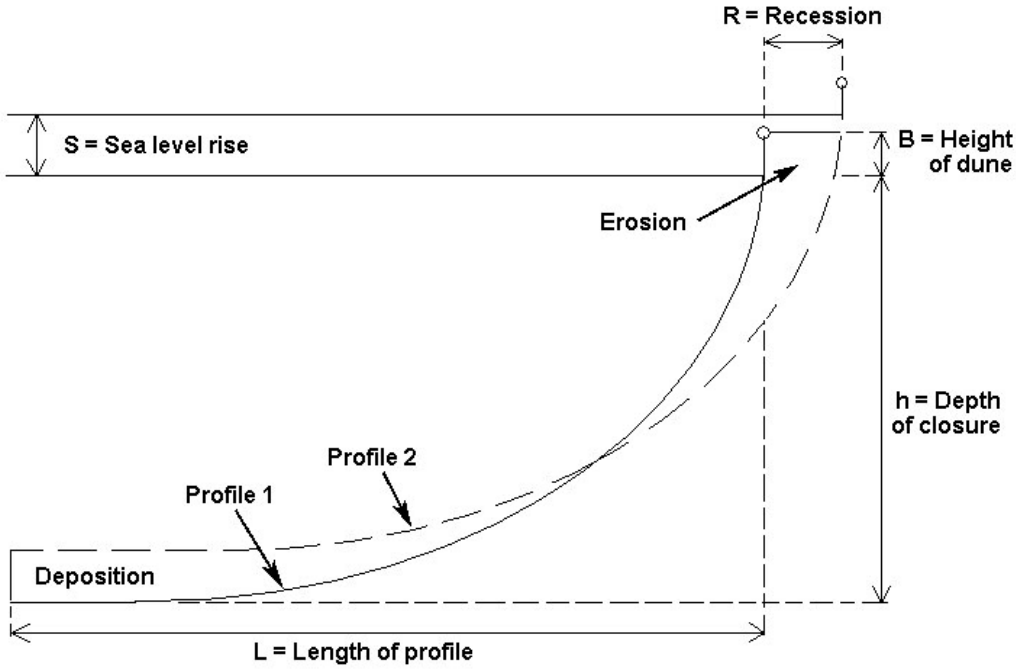

Figure 7.9: The net change in beach-profile position due to a rise in sea level, S, according to the Bruun model, resulting in a zone of offshore deposition and erosion of the upper beach, with an overall recession rate, R

Input variables

Sea level rise

Based on tide gauge data, the rate of global mean sea level rise during the 20th century is in the range 1.0 to 2.0 mm/yr (IPCC, 2001). As previously discussed, the local rate of relative sea level change may diverge from the global change due to a number of processes, including coastline subsidence or uplift. The tide record from Fremantle Harbour over the last 90 years shows an increasing sea level with a rate of approximately 1.1 mm/yr (Figure 7.10), which falls within the range of rates presented as global baseline over the past century (IPCC, 2001). Therefore, the sea level rise scenarios presented by the IPCC (2001) are considered to be appropriate for studying coastal erosion in the Perth region. These figures are 18 cm and 48 cm respectively.

Dune height

The heights of the dunes in the study area were measured directly from a digital elevation model (DEM) of the Perth region. The dune heights measured from three profiles in the Swanbourne area are 12.9 m, 15.4 m and 19.7 m for the north, central and southern profile, respectively.

Depth of closure

The depth of closure is the discontinuity in the offshore limit of a beach profile considered in coastal erosion studies. Bruun (1962) originally explained this discontinuity as the transition between nearshore sediments and deep-water sediments. Inherent in this division is the relative importance of sediment transport processes and how they change with depth and offshore distance (SCOR, 1991).

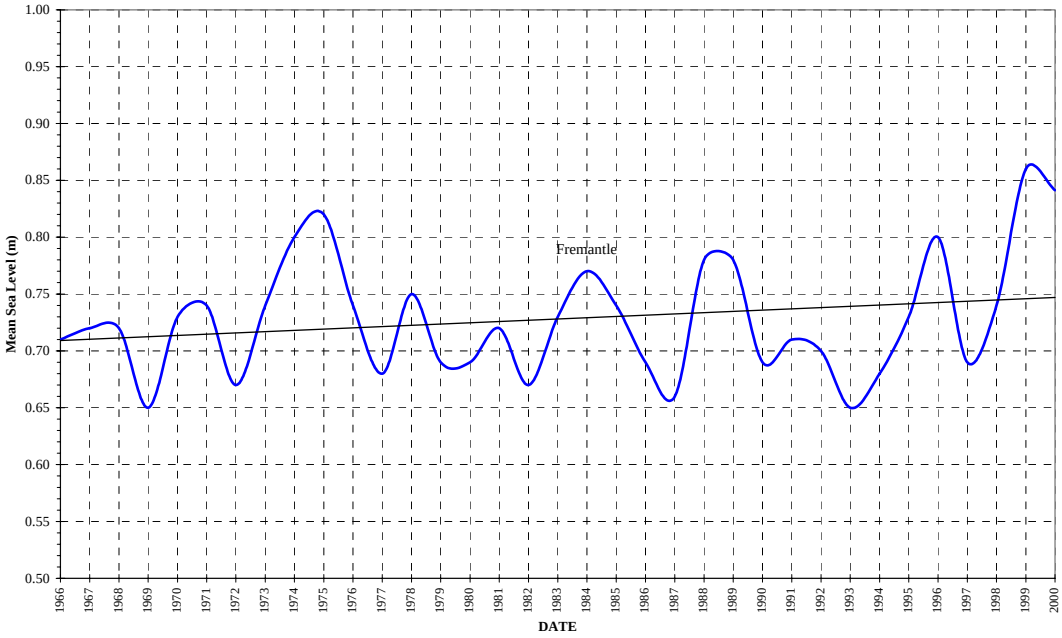

Figure 7.10: Long-term tide gauge record from Fremantle Harbour courtesy of the DPI. The average increase of 1.1 mm/year falls within the range of rates presented as global baseline over the past century (IPCC, 2001). Therefore, the sea level rise scenarios presented by the IPCC (2001) are considered to be appropriate for studying coastal erosion in the Perth region

The analysis procedures developed by Hallermeier (1981) relating wave and sediment conditions to profile zonation provide a satisfactory methodology for selecting the closure depth. Hallermeier (1981) defined the depth as being the maximum water depth for sand motion initiation by the annual median wave condition. The formula for calculating depth of closure (d) is:

$$d=(H-0.3\sigma)T\left(\frac{g}{5000D}\right)^{0.5}$$ **Equation 7.3**

where H is the significant wave height, σ the standard deviation of significant height, T is the mean significant wave period, g is gravity, and D is the mean grain size.
The significant wave height and period utilised in closure depth calculation are shown in Table 7.1. The figures, provided by the Western Australia Department of Planning and Infrastructure, are averaged monthly measurements from the Cottesloe wave buoy (Figure 7.5), for the period between 1994 and 2001.

The grain size of the sediments that comprise the shoreface in the Perth area varies between gravel and coarse to fine sand (Semeniuk and Searle, 1985; Sanderson, 1992). Predominantly sands were moderately well sorted, with some material being well sorted or moderately sorted (Sanderson and Eliot, 1999); therefore for this purpose an average grain size of 0.35 mm (medium-grained sand) was used.

Following these estimates of wave climate and sediment size, the depth of closure for the Perth area is:

$$d = (0.921 - 0.3 \times 0.44) \times 10.997 \times (9.8/(5000 \times 0.00035))^{0.5}$$

$$d = 20.5\text{m}$$ **Equation 7.4**

Table 7.1: Wave data measured at Cottesloe wave buoy

1994–2001 wave data for Cottesloe buoy	Significant wave height (m)	Significant wave period (sec)
Mean	0.921	10.997
Standard deviation	0.44	3.881

Length of profile

Once the depth of closure was determined it became possible to define beach profiles used for the calculation of potential coastal erosion scenarios. Three profiles from the Swanbourne beach area northwest of Perth CBD are shown in Figure 7.12. The profiles were constructed by combining elevation data from detailed bathymetry and a DEM. Figure 7.12 displays the lengths of the three profiles, which are 8.09 km, 8.96 km and 9.07 km.

Calculated erosion according to the Bruun Rule

In this study, the Bruun Rule is applied to three profiles in the Swanbourne area, north of the Perth CBD (Figures 7.5 and 7.12). As discussed previously, the depth of closure for the area is 20.5 m. The sea level rise scenarios upon which potential erosion is modelled are those of the IPCC (2001; 50 years: 18 cm, 100 years: 48 cm). The input variables determined from the three profiles are shown in Table 7.2. The potential coastal erosion at Swanbourne Beach over the next 50 and 100 years, as calculated using the Bruun Rule, is shown in Table 7.3. Figure 7.11 shows the approximate position of the coastline following the 100-year sea level rise scenario in Table 7.3.

Table 7.2: Input variables determined from the three profiles at Swanbourne beach

Variable	South profile	Central profile	North profile
B – Dune height	12.85 m	19.71 m	15.38 m
L – Profile length	9070 m	8960 m	8085 m

Table 7.3: Calculated potential coastal erosion for the Swanbourne area of Perth using the Bruun Rule

Scenario	South profile	Central profile	North profile
50 year	48.95 m	40.10 m	40.56 m
100 year	130.53 m	106.94 m	108.15 m

Impact on infrastructure

The zones within the Fremantle to Hillarys sector that are potentially prone to coastal erosion contain approximately 1,600 buildings and 70 km of roads. Of those buildings, approximately 700 are located in the ‘red’ zone, in which coastal erosion due to long-term sea level rise over the next century is considered likely (Figure 7.1). The quantitative modelling in the Swanbourne Beach area allows for an estimation of the number of these buildings and the length of road that is likely to be impacted by this erosion.

The total number of buildings within the Swanbourne Beach to Floreat Beach ‘red’ zones is 18, and there is 11 km of roads. This is relatively low compared to the majority of the study area, because these zones primarily cover the Campbell Barracks and parkland. Of that infrastructure, 3 buildings and 110 m of road is located within 110 m of the coastline, which is the amount that the coastline is likely to recede over the next century (see above). These buildings are beach facilities, designed to be close to the beach, and the roads are primarily access roads for these facilities. Consequently, these figures cannot be used as proportion estimates for the other zones; that is, 17% of the buildings within this area are likely to be affected by coastal erosion due to long-term sea level rise, but this is not going to be the case for the other zones that contain hundreds of buildings.

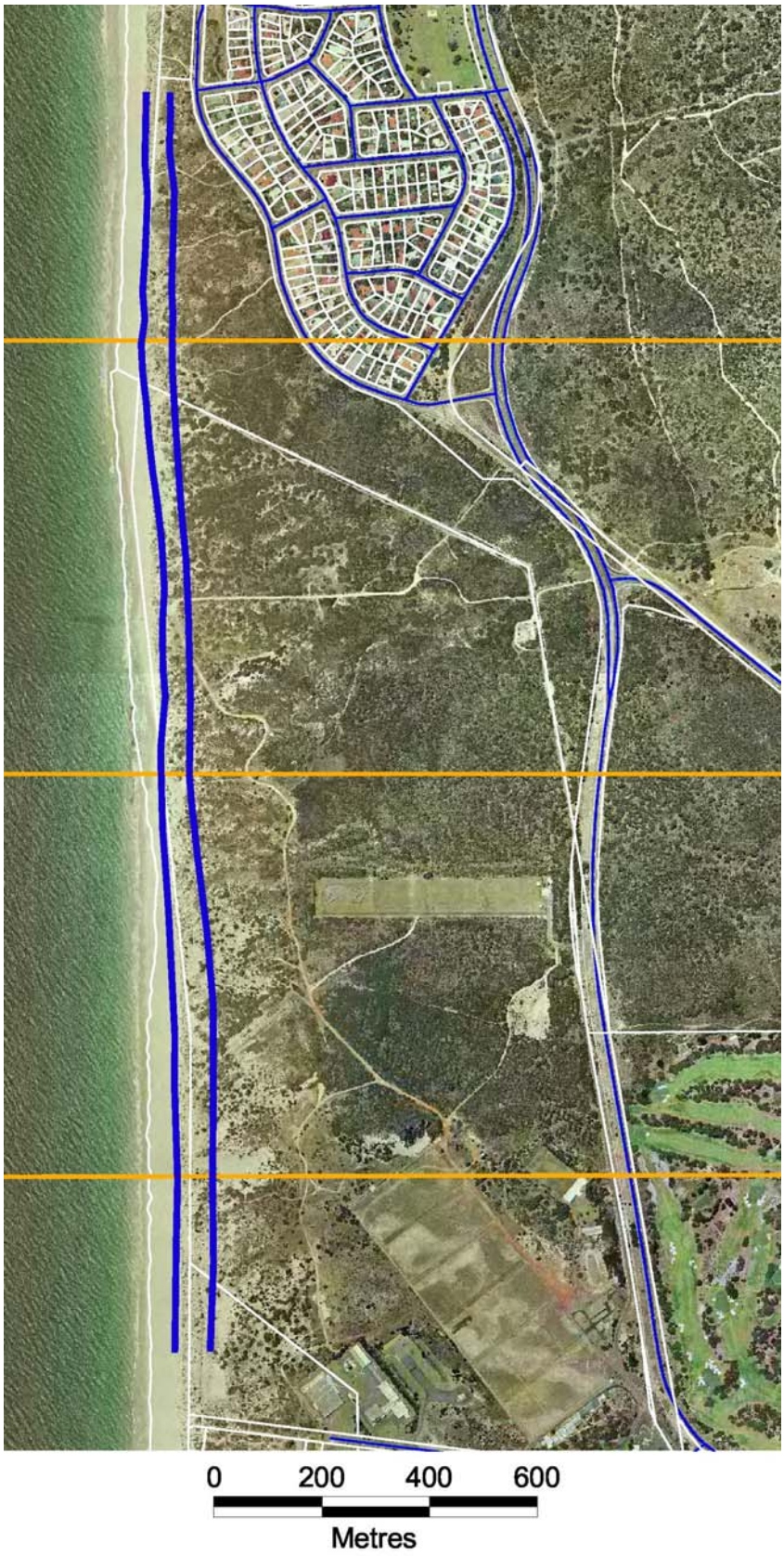

Figure 7.11: Swanbourne Beach, southwestern Western Australia, showing the current position of the coastline and the potential coastline position given the recession calculated with the Bruun Rule

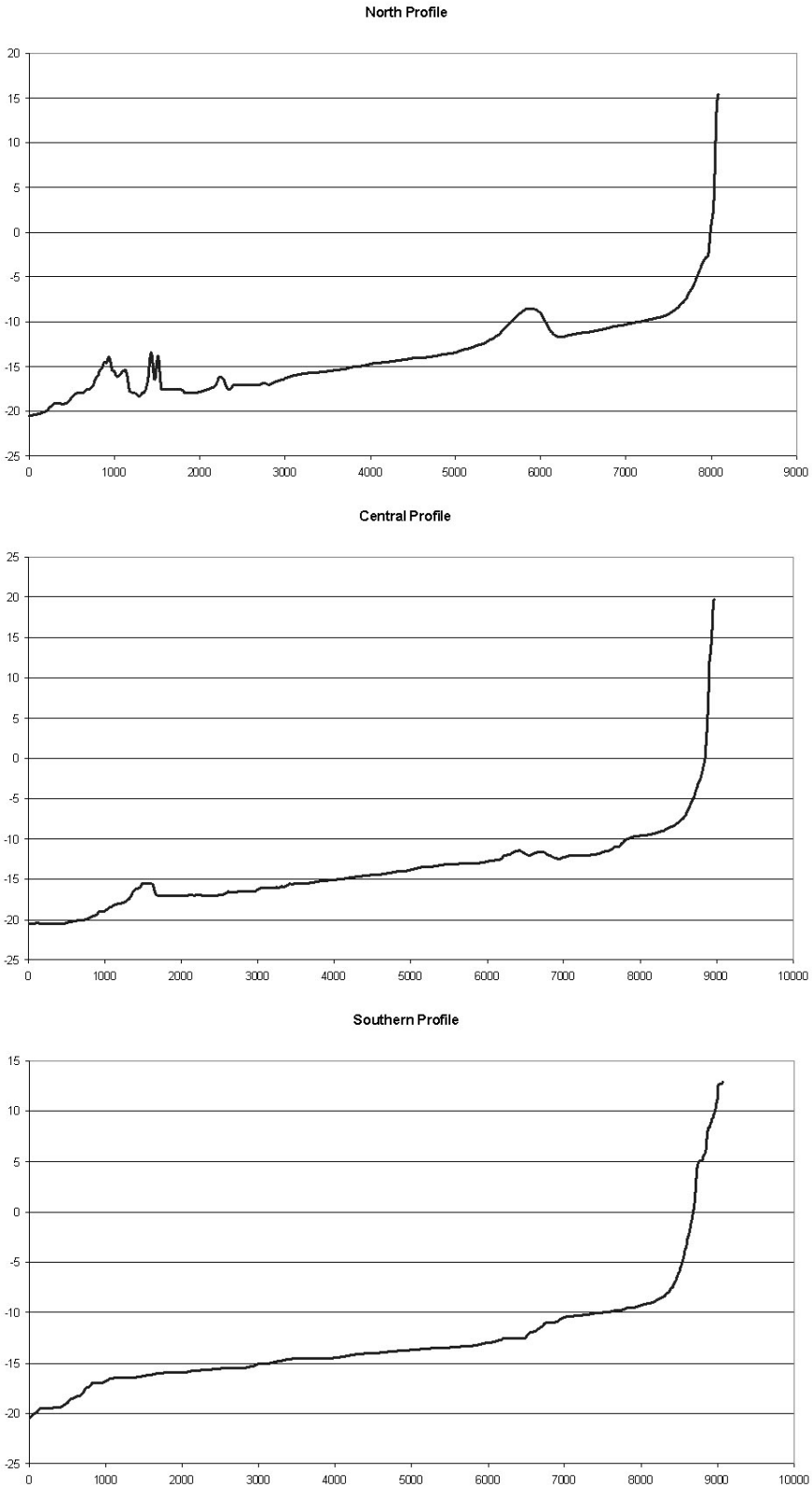

Figure 7.12: Beach profiles for Swanbourne beach, constructed by stitching together detailed bathymetry and a DEM. Vertical and horizontal axes in metres. Mean Sea Level and depth of closure are at approximately 0 m and 20.5 m, respectively

7.5 Mandurah to Fremantle

Geomorphology and sediment dynamics

This sector is characterised by a complex nearshore bathymetry and extensive but discrete cells of Holocene sediment accumulation. The nearshore/onshore geomorphology and bathymetry is dominated by a series of 330° trending Pleistocene ridges. These are termed, from west to east: the Five Fathom Bank Ridge, the Garden Island Ridge, and the Spearwood Ridge (Figure 7.13).

Holocene sediment accretion in this region has primarily been controlled by the interaction of the shelf wave climate and the complex ridge-and-depression bathymetry (Searle, 1984). Under the influence of the net northward littoral drift, there has been northward sediment transport along the exposed seaward face of the Garden Island Ridge (Figure 7.13). The Garden Island Ridge has therefore acted, and continues to function, as a perforate barrier, allowing a portion of the incident waves through gaps and passages into otherwise sheltered depressions. Waves passing through breaches in the ridge divert sediment from the transport pathway on the seaward side of the ridge, transporting it eastward into the adjacent depression to form lobate submarine banks (Searle *et al*., 1988).

Discrete and significant bodies of Holocene sediment have developed across the submarine depression between the coastal mainland Spearwood Ridge and the offshore Garden Island Ridge, dividing it into a series of marine basins (including Cockburn Sound). This process has led to the shoreline progradation of the Rockingham/Becher cuspate foreland (located 30 km south of Fremantle), and the deposition of the Success and Parmelia Banks (Figure 7.13; Kempin, 1953). In contrast, accretion in the depression between the Garden Island and Five Fathom Bank Ridges has been minimal (Searle and Semeniuk, 1985). It is interesting to note the depth of Madora Bay relative to Cockburn Sound in Figure 7.13. It is clear that Madora Bay is considerably shallower, which is likely to be a result of the net northward littoral drift depositing relatively more sediment in the more southerly basin.

Erosivity of the coastline

The environmental geology maps of this sector (Gozzard, 1983a; 1983b) show that the areas comprising Safety Bay Sand are the Rockingham/Becher Plain and Woodman Point (Figure 7.14; The Port/South Beach area was discussed in the Fremantle to Hillarys section). Erosion resistant limestone is preserved adjacent to the landward side of these sediment complexes, and comprises the remainder of the coast.

The upper surface of the limestone in the Rockingham/Becher Plain is reconstructed with microtremor data, as the coverage in this area is adequate (Figure 7.14). The coverage is not extensive enough to allow for a full reconstruction in a GIS environment, as with the Fremantle to Hillarys sector, but the results are sufficiently clear to allow for an assessment of erosivity without this step. There is a clear distinction between the estimates of top limestone on the Rockingham/Becher Plain, which are almost without exception below sea level, relative to the estimates directly to the east, in the vicinity of the Kwinana Town Centre, which are predominantly above sea level.

The SCPT that was undertaken in this area (Figure 7.14) also suggests the top of the limestone is well below sea level. The SCPT penetrated 33.05 m before terminating, and the height of the ground surface at this point is approximately 5 m, as estimated from a DEM. Therefore the top of the limestone is at or below approximately 28 m below sea level at this point. The estimate of top limestone at the nearest microtremor point (to the east) is -26.6 m AHD, which is further evidence of the robustness of reconstructing the upper limestone surface with microtremor measurements.

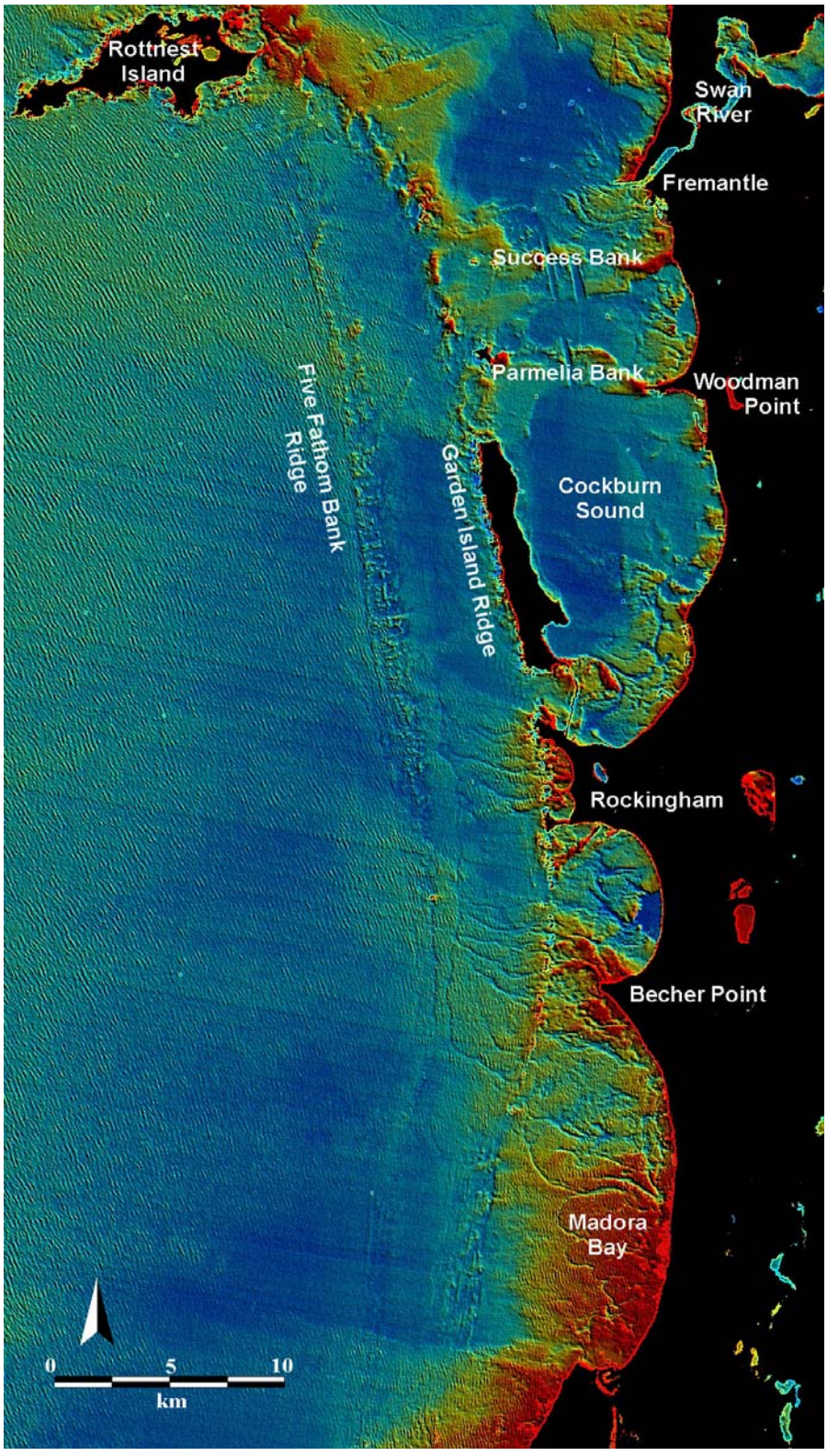

Figure 7.13: A Landsat image of the Mandurah to Fremantle sector, processed with the Geoscience Australia Shallow Water Image Mapping (SWIM) method to display bathymetry. The 'hot' and 'cool' colours indicate shallow and deep water respectively. Note the shallow (red) Madora Bay relative to the deep (blue) Cockburn Sound

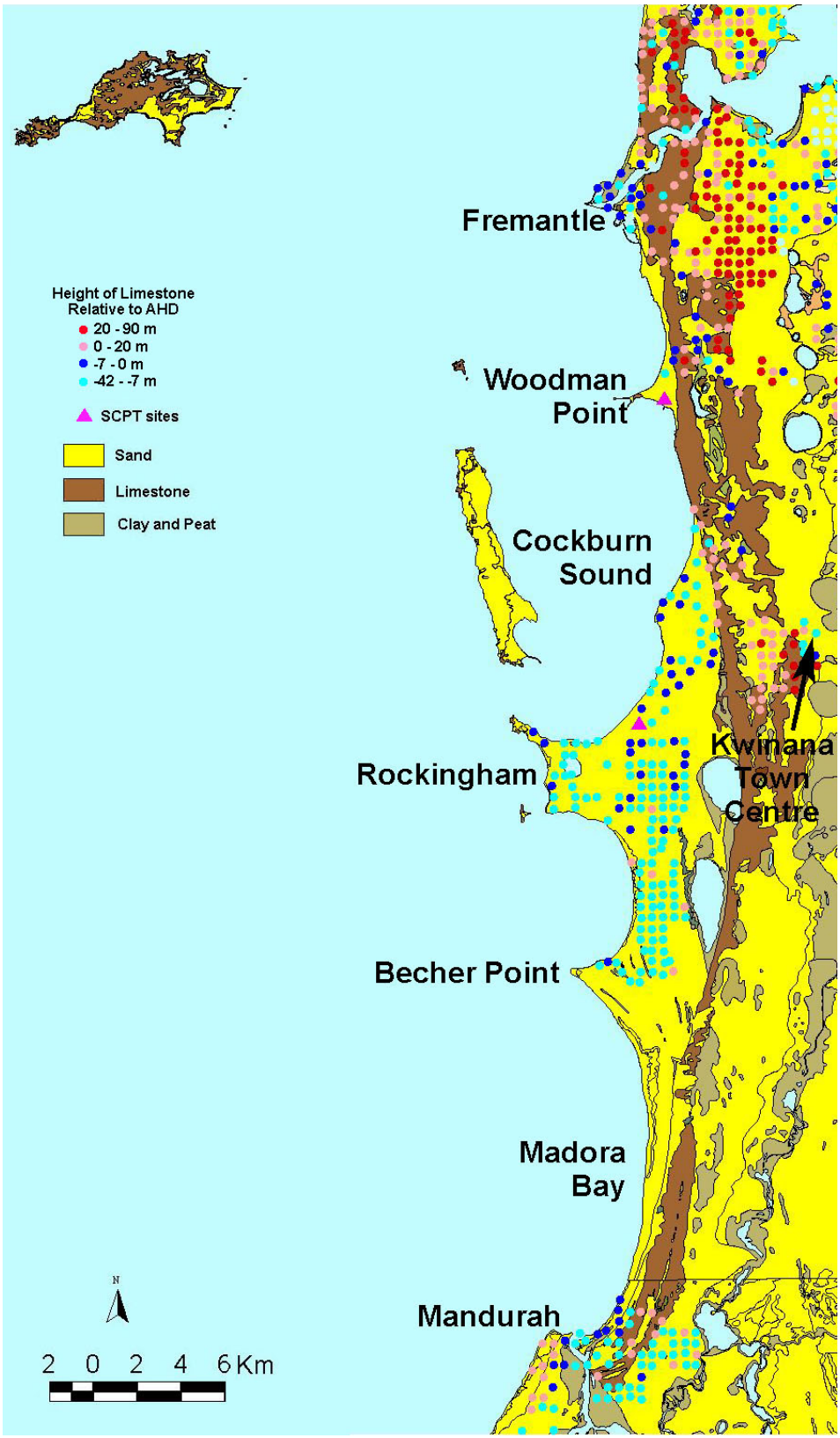

Figure 7.14: Height of top Tamala Limestone relative to Australian height datum, as estimated through microtremor tests, and spatial distribution of SCPTs in the Mandurah to Fremantle sector, overlain on the environmental geology of the area from Gozzard (1983a; 1983b)

There is a distinct lack of data with which the upper limestone can be reconstructed in the Woodman Point area. One SCPT was undertaken here (Figure 7.14), the results of which suggest the top of the limestone is below sea level. The SCPT penetrated 16.3 m before terminating, and height of the ground at this point is approximately 7.75 m, therefore the upper limestone surface is approximately 8.5 m below sea level.

Qualitative assessment of erosion hazard in susceptible areas

The Rockingham/Becher Plain comprises the majority of the Mandurah to Fremantle coast (Figure 7.13), and given the fact that the upper surface of the limestone under this plain appears to be below sea level it could be suggested that this area is susceptible to erosion over the next century. For the most part this is unlikely as this area has been the primary depositional province for the entire Swan Coastal Plain over the last 8,000 years (Figure 7.1). The most erosive province of the Swan coast is directly to the south (the Bunbury to Mandurah sector), therefore the net northward littoral drift will provide ample sediment to infill any accommodation space created by future sea level rise.

It is possible that there will be localised erosion of Becher Point in the foreseeable future (Figure 7.1). The fetch across Madora Bay is relatively significant, and will only be increased in the future due to the continued erosion of the Garden Island Ridge. A consequential increase in incident wave energy may result in minor erosion at Becher Point. This is supported by the palaeogeographic maps of Searle *et al*. (1988), which show some erosion occurring at the point in the present. However, any erosion should theoretically be replenished by sediment introduced by the net northward longshore drift, which has led to the rapid outbuilding of this part of the plain relative to the more northerly portion over the last 4,000 years (Searle *et al*., 1988).

The upper surface of the limestone is also below sea level at Woodman Point but, as with the Rockingham/Becher Plain, the area is not likely to be susceptible to erosion over the next century. The area is sheltered by Garden Island and the Rockingham/Becher Plain, and therefore not exposed to significant incident wave energy. As with Becher Point, there is potential for localised erosion due to the fetch across Cockburn Sound, which is relatively deeper than Madora Bay and as such would allow for the development of larger waves (Figure 7.13). However, the Parmelia Bank/Woodman Point complex appears to be the primary loci of deposition after the Rockingham/Becher Plain and as such replenishment through longshore drift should be rapid.

Calculating erosion

Despite having detailed bathymetry in this sector, and the potential to use Cottesloe wave data, it is impossible to undertake a Bruun Rule analysis of this part of the coast for two reasons.

- The nearshore in this part of the sector is complicated by the presence of limestone ridges and reefs (Figure 7.13). The nearshore sediment–water interface cannot be remoulded by wave energy, and as such is unlikely to rise by an amount equal to the rise in sea level. Consequently, the third assumption outlined above is invalidated and the Bruun Rule cannot be used.
- A significant amount of sediment is introduced into this sector as a result of the net northward longshore drift. Therefore any accommodation space created by a rise in sea level may be infilled with sand from somewhere other than the upper beach. As such the volume eroded from the beach at any given profile is unlikely equal to the volume deposited, and the second assumption outlined above is invalidated.

Calculating the amount of potential erosion in this sector due to global warming related sea level rise over the next century should not be a priority, as erosion is not likely to be significant and there are no coastal behaviour models that can accommodate the complications outlined in the two points above.

Impact on infrastructure

The zones within this sector that are potentially prone to coastal erosion contain approximately 28,000 buildings and 641 km of roads. This is the largest amount of infrastructure in any of the sectors when

all zone types are considered. This is primarily due to the very large geographical extent of the Rockingham/Becher Plain, which is comprised of unconsolidated sand but hosts an extensive built environment. Of these buildings it is unlikely that any will be directly impacted by coastal erosion over the next century, due to this being a predominantly depositional environment and also because none is located within close proximity of the shoreline.

7.6 Bunbury to Mandurah

Geomorphology and sediment dynamics

Unlike the previously described sectors, the Bunbury to Mandurah sector is characterised by a simple offshore bathymetry, and a barrier dune system with associated lagoon onshore (Figure 7.15). This sector is also unique amongst those outlined in this report as it is oriented approximately north–south, but there are no well-developed offshore limestone ridges. Thus the west-facing shores are fully exposed to the wind, wave, and current regime of the Rottnest Shelf.

Seaward of the shore, the sand-mantled shoreface slopes seaward to merge with the inner shelf plain about 1–2 km offshore in water depths of 12–15 m. Low-lying limestone pavement surfaces and discontinuous limestone ridges (1–2 m high) and beachrock slabs are exposed on the inner shelf, but they are not sufficiently prominent or continuous to influence sedimentation in this sector (Searle and Semeniuk, 1985).

The onshore area in this sector is dominated by a series of Tamala Limestone and Safety Bay Sand dune ridges trending approximately north–south, which form a topographic barrier between the main low-lying Swan Coastal Plain and the continental shelf. In depressions between the dune ridges there are elongate, shallow (usually less than 2 m deep) water bodies.

Harvey estuary, Peel Inlet and Lake Clifton occur in depressions between ridges of Tamala Limestone (Figure 7.15). Lake Preston and Leschenault Inlet occur between a dune ridge of Safety Bay Sand and the adjacent Tamala Limestone ridge (Figure 7.15; Searle and Semeniuk, 1985).

The sea level history for this sector (and the southernmost part of the Mandurah to Fremantle sector) is at variance with studies of accretionary sequences elsewhere along the Swan coast (Figure 7.16). Along the majority of the coast the sea level rose to a level approximately 2–2.5 m above the present level at the termination of the most recent glaciation, following which it gradually fell to the current level over the last 7,000 years. In contrast, sea level in this sector stayed approximately 2 m below the present level between 7,000 and 6,000 years ago, following which it rose dramatically by approximately 5 m. It stayed more than 3 m above the present sea level for over 1,000 years before dramatically dropping to the current level, at which it has stayed for the last 2,500 years (Semeniuk, 1985; Semeniuk and Semeniuk, 1991). This is likely to be a function of local tectonic forces (Semeniuk and Searle, 1986).

The combination of relatively simple geomorphology and relatively complex sea level curve for this sector has led to an interesting sediment budget history. The first stage involved deposition of lagoonal/estuarine sediment behind a coastal barrier approximately 2–3 km further offshore than present, when the sea level rose subsequent to the termination of the last glaciation. With still-stand conditions 2–3 m below present sea level, the dunes of Safety Bay Sand encroached eastward until their eastern edge reached approximately the position the eastern margin of the peninsula occupies today. The sea level rise over the following 500 years resulted in dramatic erosion of the seaward face of the barrier. The next phase of deposition took place with a still-stand approximately 3–4 m above the present level, when the coast prograded through deposition of beach and dune sediments on the western face of the barrier. The barrier system is currently migrating eastward, in association with the present marine incursion. Erosion and net northward sediment mobilisation are the major processes along the seaward edge of the barrier dune system today (Semeniuk, 1983; Semeniuk, 1985).

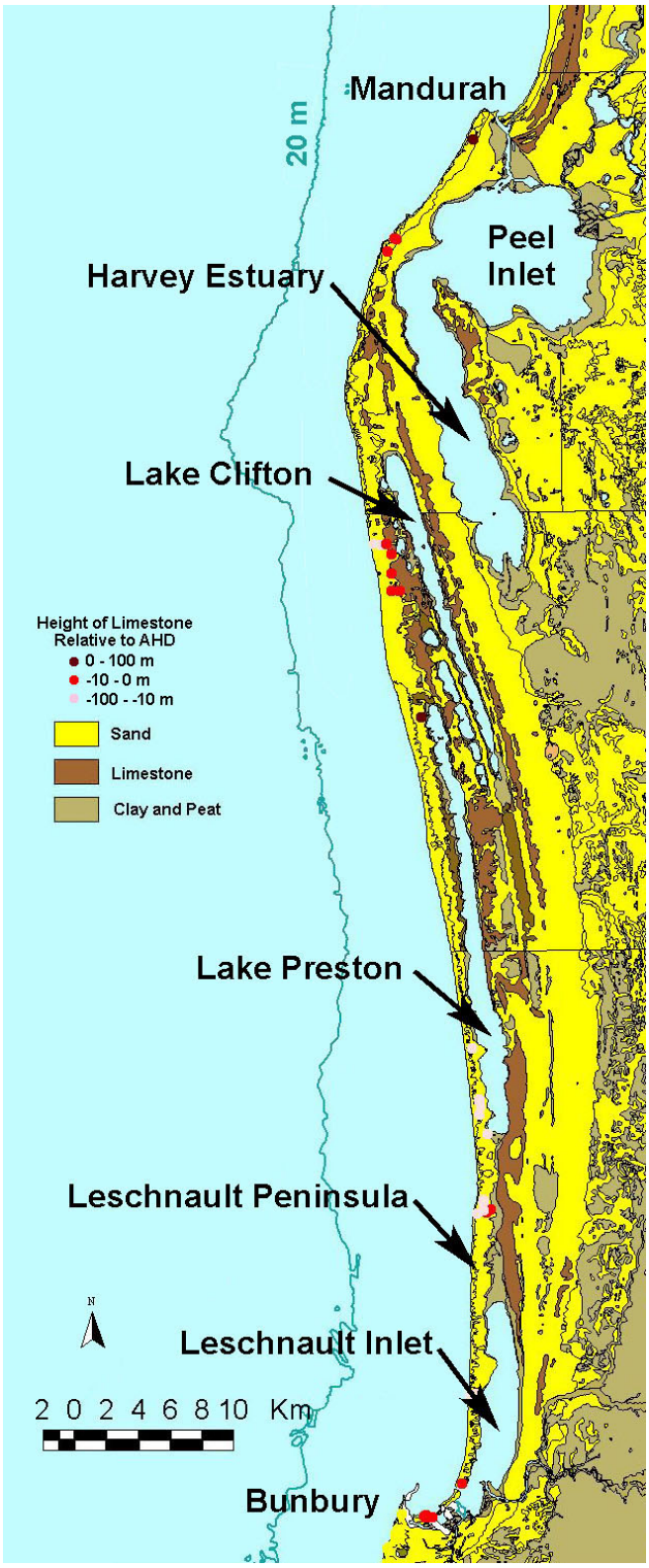

Figure 7.15: Height of top Tamala Limestone relative to Australian height datum, as measured in geotechnical boreholes in the Bunbury to Mandurah sector, overlain on the environmental geology of the area from Gozzard (1987)

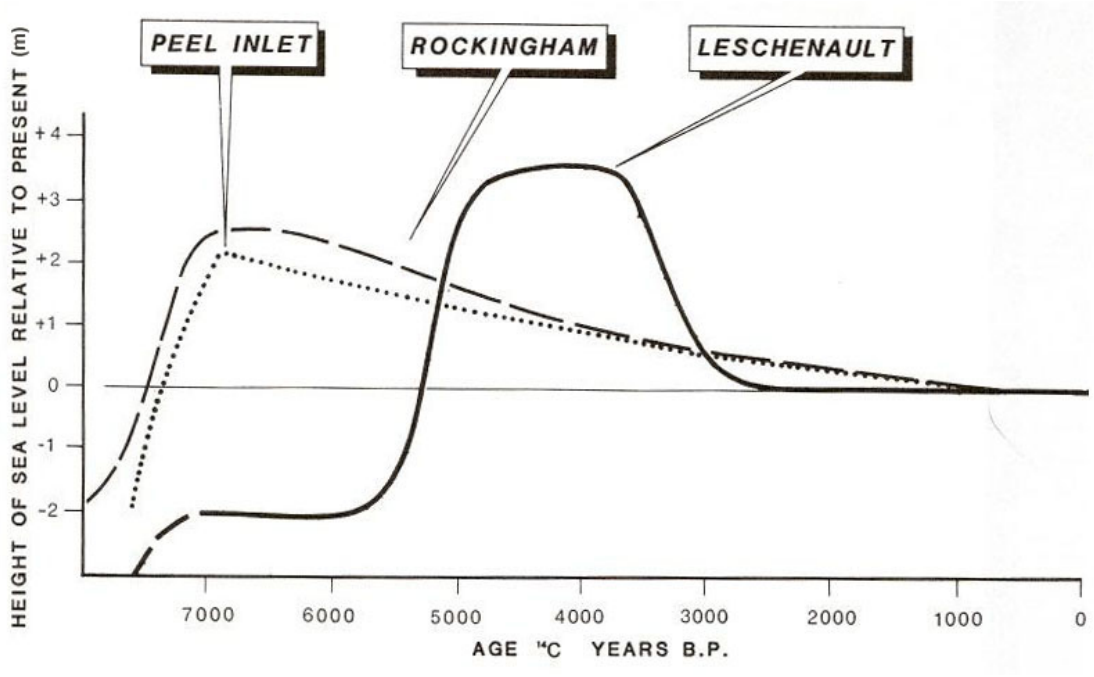

Figure 7.16: Sea level history curve for the Peel–Harvey estuary, the Rockingham–Becher area, and the Leschenault Peninsula (Semeniuk and Semeniuk, 1991)

Erosivity of the coastline

The environmental geology maps of this sector (Gozzard, 1987) show that Safety Bay Sand comprises a continuous strip adjacent to the coastline. Erosion-resistant limestone is predominantly preserved adjacent to the landward side of this unit, and only forms part of the coastline in the very northernmost part of the sector.

There is no SCPT data along this section of the Swan Coastal Plain, and microtremor data is confined to the region of the coast formed by, and on the landward side of, Tamala Limestone (Figure 7.17). The microtremor survey in this area shows the limestone is above sea level adjacent to the coast, but given this can be seen on the environmental geology map for the region, this data does not increase our understanding of erosion susceptibility for the area. Therefore geotechnical borehole descriptions from the DOE dataset were utilised in delineating the upper surface of the limestone throughout the majority of the sector. Of the boreholes drilled in the coastal units of this sector, 46 were found to give useful descriptions of lithology. The heights of lithological horizons relative to sea level were estimated by relating the drilled depth to DEM height at that point.

In the northern half of the sector the top limestone surface was encountered above sea level in only two of 13 holes (Figure 7.17). The northern of the two holes was drilled into an area of limestone, thus the upper surface is obviously above sea level. The height of the limestone in the southern of the two holes, according to the relationship between the DEM and drilling log, is approximately 30 cm above sea level. The average height of the upper limestone surface for all 13 holes in the northern part of the sector is approximately 4.8 m below sea level.

In the southern half of the sector the top limestone surface was not encountered above sea level in any of the holes (Figure 7.18). In 20 of the holes, the limestone is preserved more than 10 m below sea level. The average height of the upper limestone surface for all 33 holes in the southern part of the sector is approximately 13.3 m below sea level.

Qualitative assessment of erosion hazard in susceptible areas

Of the five sectors outlined in this report, the Bunbury to Mandurah sector is the most susceptible to coastal erosion over the next century (Figure 7.1). Almost the entire sector, with the exception of the northernmost component in which the shoreline is formed of Tamala Limestone, is likely to experience a degree of erosion before 2100. This erosion is primarily a function of this sector being towards the southern end of the net northward littoral transport path, the greater exposure to the incident wave and wind regime relative to the other sectors, and the preservation of limestone below sea level.

It is the northward longshore sediment transport induced by the sea breeze that accounts for the net littoral drift that occurs along this part of the coast (Masselink and Pattiaratchi, 1998). The Cape Naturaliste to Bunbury sector is a north-facing embayment. This orientation, perpendicular to the southerly sea breeze, means that a northward current cannot be established any further south than Bunbury. Therefore, very little sediment is introduced into this sector from the south. This sector is the southern part of the south to north littoral conveyor that operates along Swan coast, therefore it is a source area from which sediment that accumulates in other sectors is derived.

Previous research has suggested that the erosion currently occurring along this part of the coast is related to a marine incursion (Semeniuk, 1985). An accelerated sea level rise over the next century in association with global warming may increase the rate at which the coast is eroding. The environmental geology maps and boreholes drilled in this sector show that the upper surface of the Tamala Limestone is only above sea level on the eastern side of the northern Leschnault Peninsula (Figures 7.16–7.18). Safety Bay Sand comprises the majority of the peninsula; therefore the majority of the peninsula has the potential to be eroded. The outcome of continued erosion of the barrier system may be either that:

- the barrier is completely eroded, transforming Leschnault Inlet into an open embayment and Lake Preston into a semi-enclosed inlet; or,
- the barrier steps back through overwashing, infilling Leschnault Inlet and Lake Preston.

Calculating erosion

Calculating the erosion rate for this sector over the next century due to long-term sea level rise would be a valuable exercise but it is dependent on assembling a considerable amount of data that is not readily available. Correspondingly, the data to be collected are dependent on the model utilised.

If a Bruun-type model were to be used in calculating potential erosion then there are a number of considerations that must be taken into account. Firstly, and perhaps most importantly, wave data for this sector would have to be collected. The DPI currently manages four wave buoys that measure wave heights and periods. These are located offshore from Cape Naturaliste, Rottnest Island, Cottesloe, and Jurien (Figure 7.19). Cape Naturaliste is the closest of the buoys, and as such it might be expected that wave measurements from this station could be used. Unfortunately this buoy measures the offshore incident wave heights and periods. The energy in these incident waves will be attenuated as they cross the continental shelf, especially in this sector, as the shelf is over 50 km wide (Figure 7.1). Therefore this wave data could not be used in a Bruun Rule analysis in this sector, as it would give anomalously high estimates of closure depth, which would consequently produce overestimates of recession. A second consideration is the need for detailed bathymetry data from which profiles could be constructed. It is possible that this data exists but it was not available to the author at the time of analysis.

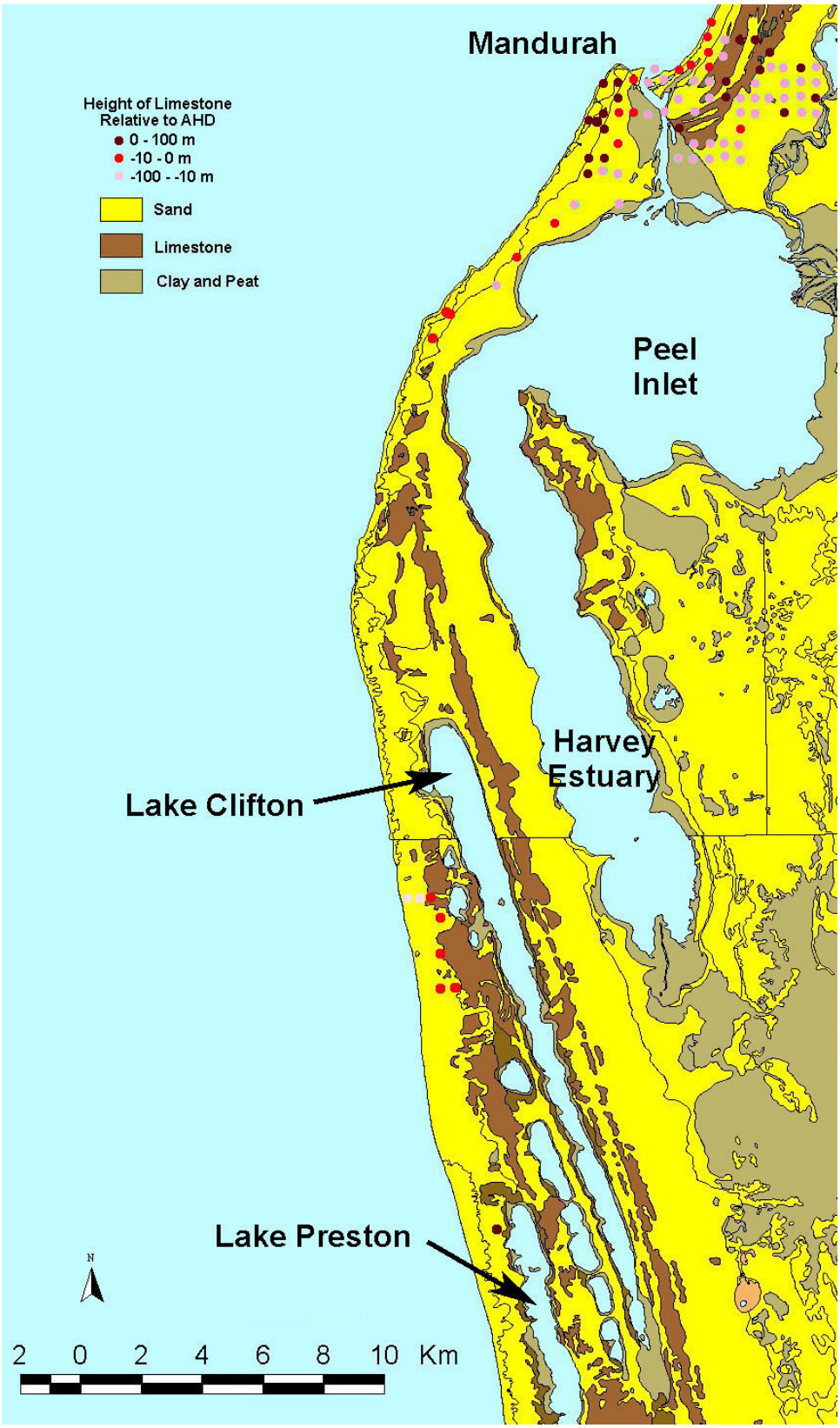

Figure 7.17: Height of top Tamala Limestone relative to Australian height datum, as measured in geotechnical boreholes and estimated through microtremor tests in the northern Bunbury to Mandurah sector, overlain on the environmental geology of the area from Gozzard (1987). Note the limestone is above sea level to the immediate south of Mandurah, and in a borehole near the northern end of Lake Preston

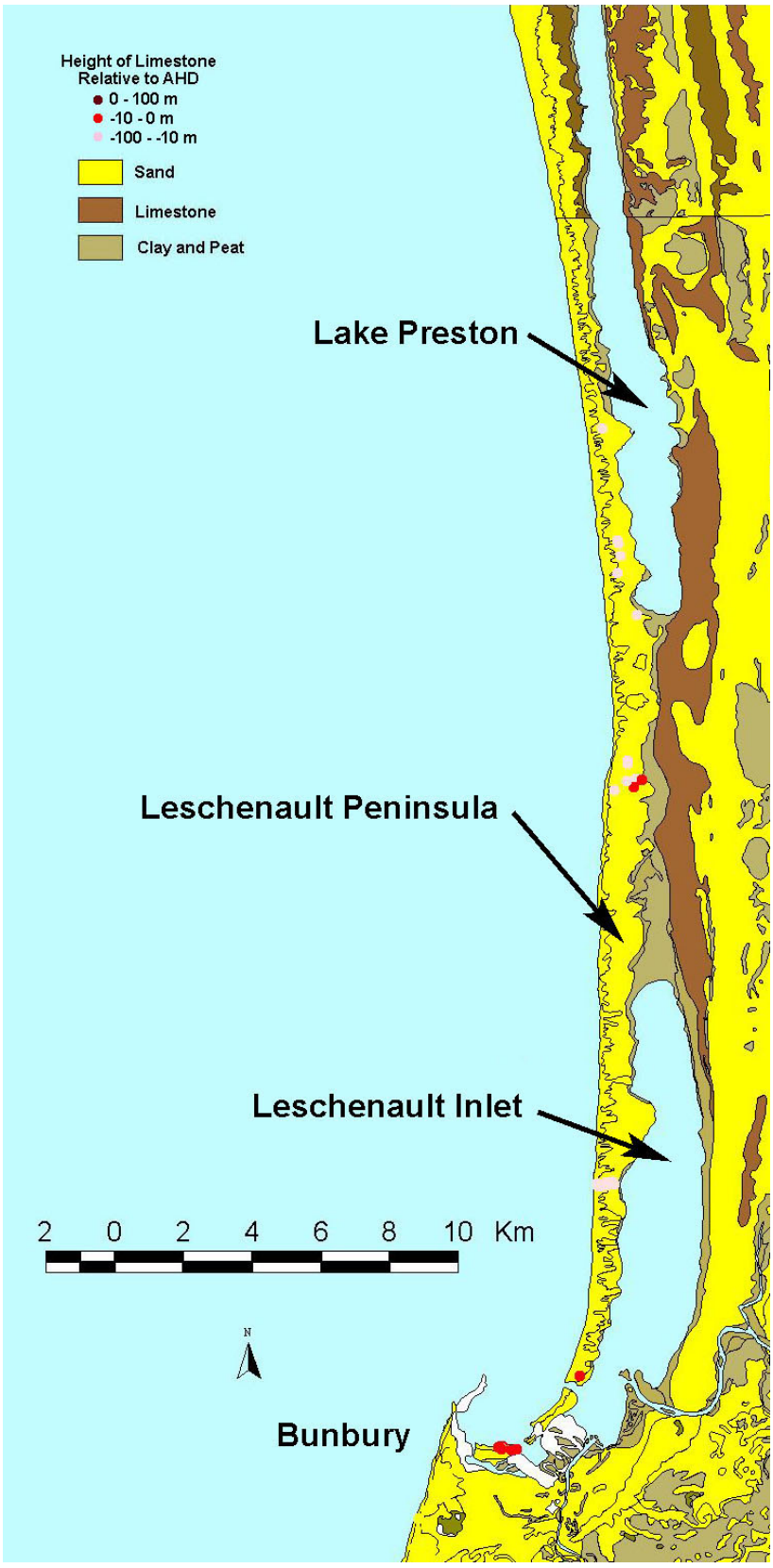

Figure 7.18: Height of top Tamala Limestone relative to Australian height datum, as measured in geotechnical boreholes in the southern Bunbury to Mandurah sector, overlain on the environmental geology of the area from Gozzard (1987). Note that the limestone is below sea level in all of the holes

Another consideration that would have to be taken into account in any Bruun-type analysis would be the volume of sediment that is transported out of the system by the net northward longshore drift. An inherent assumption of the Bruun Rule is that the material eroded from the upper beach is transported immediately into the offshore and deposited, such that the volume eroded is equal to the volume deposited (see above). This is clearly not the case for the Bunbury to Mandurah sector, as a considerable volume of sediment is taken out of the system and deposited further north, particularly in the Mandurah to Fremantle sector. This net volume loss would have to be taken into account, possibly through utilising the sediment budget equation of SCOR (1991). It should be noted that before applying this equation, which is simply an adaptation of the Bruun Rule, it is necessary to know the volume of sediment that is leaving or entering the system. This could be undertaken by following the example of Masselink and Pattariatchi (2001) in their study of sediment movements along Perth metropolitan beaches.

An alternative to using the Bruun Rule would be to apply the coastal behaviour model of Stive and de Vriend (1995). The complicating factor with this model is that it requires long-term measurements of shoreface morphology.

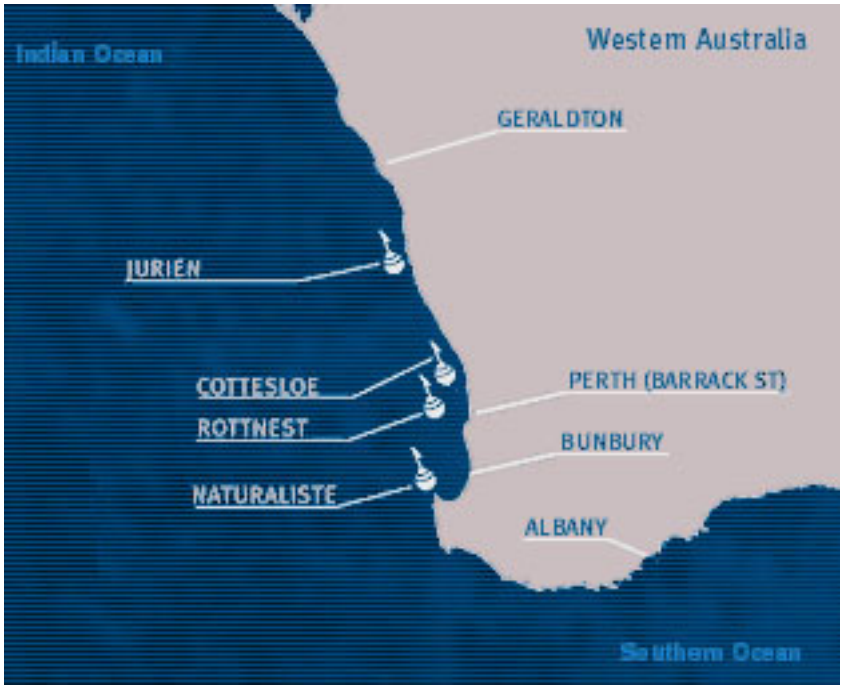

Figure 7.19: Location of wave buoys managed by the Western Australian Department for Planning and Infrastructure (http://www.coastaldata.transport.wa.gov.au/tides/real_time.html)

Impact on infrastructure

The zones within this sector that are potentially prone to coastal erosion contain approximately 400 buildings and 268 km of roads. This is relatively low, as much of the region has not been settled. Coastal erosion is likely to be high in this sector over the next century, therefore detailed quantitative modelling should be undertaken to determine the potential extent, which will allow for comment on the number of buildings and roads likely to be affected.

7.7 Hillarys to Yanchep

Geomorphology and sediment dynamics

The coast in this sector is characterised by a variety of features. The nearshore bathymetry has four well-defined largely submarine, 330° trending shore parallel Pleistocene limestone ridges (Figure

7.20). An unnamed ridge forms the architecture of the shore, and the other three ridges, termed Spearwood Ridge, Marmion Reef Ridge, and Staggie Reef Ridge, are located c. 2, 4 and 6 km from the shore respectively. In several locations subridges extend obliquely (trending 0–010°) across the main ridges. The subridges form discontinuous chains of submarine rock pinnacles and reefs commonly less prominent than the main ridges. The unnamed main ridge forms diffuse rocky coasts and pocket beaches interspersed with straight beached coasts backed by dune systems (Searle and Semeniuk, 1985).

Since the Pleistocene limestone ridge-and-depression topography first began to be inundated by rising post-glacial sea levels, it has been subjected to extensive but selective erosional modification. This has resulted in non-uniform retreat of the shoreline. As in the Mandurah to Fremantle sector, accretion has occurred in loci of wave-energy convergence in the comparatively sheltered inter-ridge depression between the shoreline ridge and the adjacent offshore ridge. The accretionary sites, however, are not prominent and have prograded only relatively small distances seaward. Sediment in these loci has again been derived from local benthic assemblages (principally the seagrass assemblage) and from the erosion of the Pleistocene ridges (Searle and Semeniuk, 1985).

Erosivity of the coastline

The environmental geology maps of this sector (Gozzard, 1982) show that Safety Bay Sand comprises the majority of the coastline (Figure 7.21). Erosion-resistant limestone is predominantly preserved adjacent to the landward side of this unit, and comprises very little of the coastline.

There is no microtremor or SCPT data along this section of the Swan Coastal Plain, therefore geotechnical borehole descriptions from the DOE dataset were utilised in delineating the upper surface of the limestone. Of the boreholes drilled in the coastal units of this sector, 34 were found to give useful descriptions of lithology. The heights of lithological horizons relative to sea level were estimated by relating the drilled depth to DEM height at that point. The top limestone surface was encountered below sea level in only two of the 34 holes. Limestone was encountered less than 2 m below sea level in these two holes. The average height of the upper limestone surface for all 34 holes is approximately 23.5 m above sea level.

Qualitative assessment of erosion hazard in susceptible areas

With the exception of the discrete region in the Alkimos area, marked by the two holes in which limestone appears to be below sea level, there does not appear to be any potential for erosion in the Hillarys to Yanchep sector (Figure 7.1). It is not considered worthwhile assessing the potential for erosion at this locality for two reasons:

- Heights of -1.8 m and -1.1 m for the top limestone in the two holes is well within the range of the uncertainty in the DEM, therefore it is possible the limestone actually exists above sea level at these localities.
- There is no infrastructure within 4 km of the coast at this locality.

Calculating erosion

Despite having detailed bathymetry in this sector, and the potential to use Cottesloe wave data, it is impossible to undertake a Bruun Rule analysis of this part of the coast for two reasons.

- The nearshore in this part of the sector is complicated by the presence of limestone ridges and reefs (Figure 7.20). The nearshore sediment-water interface cannot be remoulded by wave energy, and as such is unlikely to rise by an amount equal to the rise in sea level. Consequently, the third assumption of the Bruun Rule is invalidated and it cannot be used.
- The upper surface of the limestone is above sea level for the most part. Thus the upper beach cannot be eroded due to the landward translation of the profile and the first Bruun Rule assumption is invalidated.

Calculating the amount of potential erosion in this sector due to global warming related sea level rise over the next century should not be a priority, as the coastline does not appear to be susceptible to erosion, there is no infrastructure along this part of the coast, and there are no coastal behaviour models that can accommodate the complications outlined in the two points above.

Impact on infrastructure

As previously stated, there is no infrastructure at risk from coastal erosion due to long-term sea level rise in this sector.

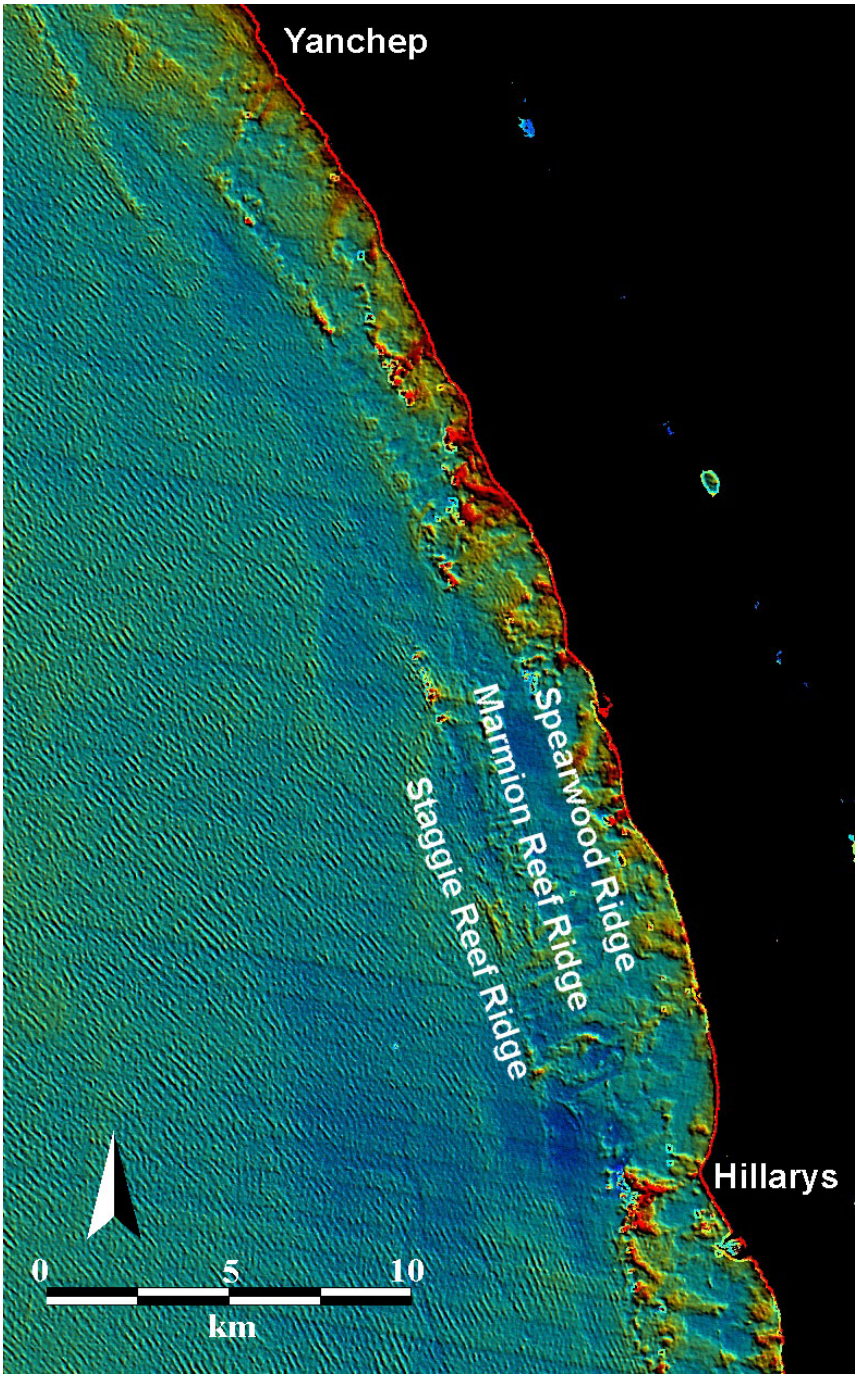

Figure 7.20: A Landsat image of the Hillarys to Yanchep sector, processed with the GA Shallow Water Image Mapping (SWIM) method to display bathymetry. The 'hot' and 'cool' colours indicate shallow and deep water respectively

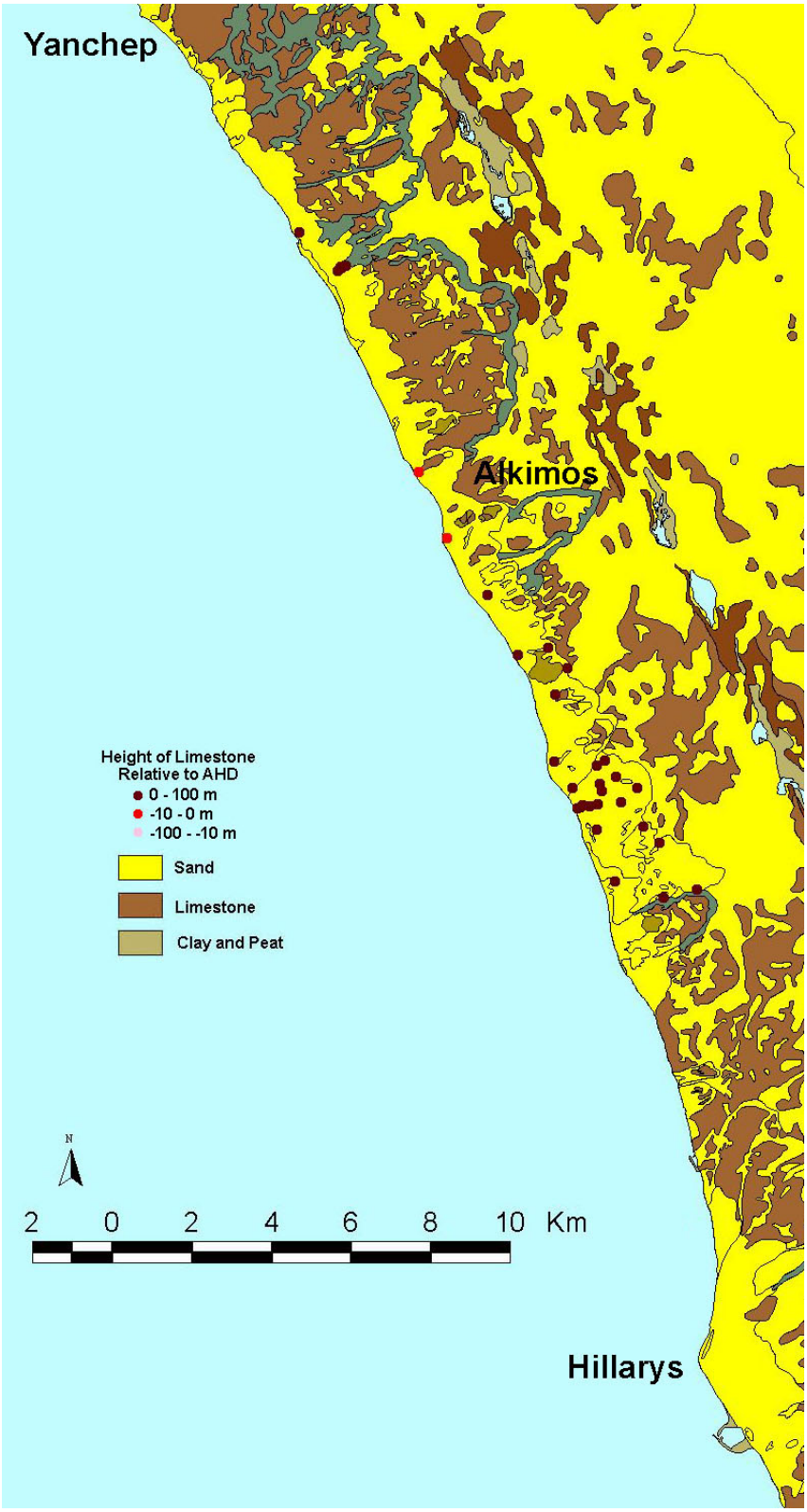

Figure 7.21: Height of top Tamala Limestone relative to Australian height datum, as measured in geotechnical boreholes in the Hillarys to Yanchep sector, overlain on the environmental geology of the area from Gozzard (1982). Note that the limestone is preserved below sea level in only two boreholes, in the Alkimos area

7.8 Cape Naturaliste to Bunbury

Geomorphology and sediment dynamics

Geographe Bay, which comprises the Cape Naturaliste to Bunbury sector, is a broad, 100 km wide, north-facing embayment at the southern end of the Rottnest Shelf. This sector is characterised by a simple offshore bathymetry, a lowland onshore, and Holocene sedimentation confined to an onshore beachridge/strandplain to nearshore sand sheet deposits (Figure 7.22). The coastal hinterland and seafloor of this sector slope gently northward to depths of 12–15 m where the embayment floor opens out onto the inner Rottnest Shelf. A narrow band (average 500 m wide) of Holocene beachridges that young towards the present shore is developed behind the contemporary coastline. Offshore the gently sloping shore of the bay is a sand sheet, vegetated by dense sea grass meadows (Searle and Semeniuk, 1985).

In the long-term (past 5,000 years) sediment accretion in this sector has resulted in this sector has resulted in an average progradation of approximately 500 m. The accumulated sediment is derived from the erosion of Pleistocene coastal deposits and *in situ* accumulation of carbonates from benthic communities, both the seagrass community and organisms inhabiting adjacent bare sand (Searle and Semeniuk, 1985). Under prevailing conditions, refracted westerly swell and longer period wind waves impinge on the entire shoreline of this sector. Sediment tends to be transported shoreward from scours and bars. The refracted westerly waves induce a slight littoral movement eastward, which is reversed by winter storms (Searle and Semeniuk, 1985).

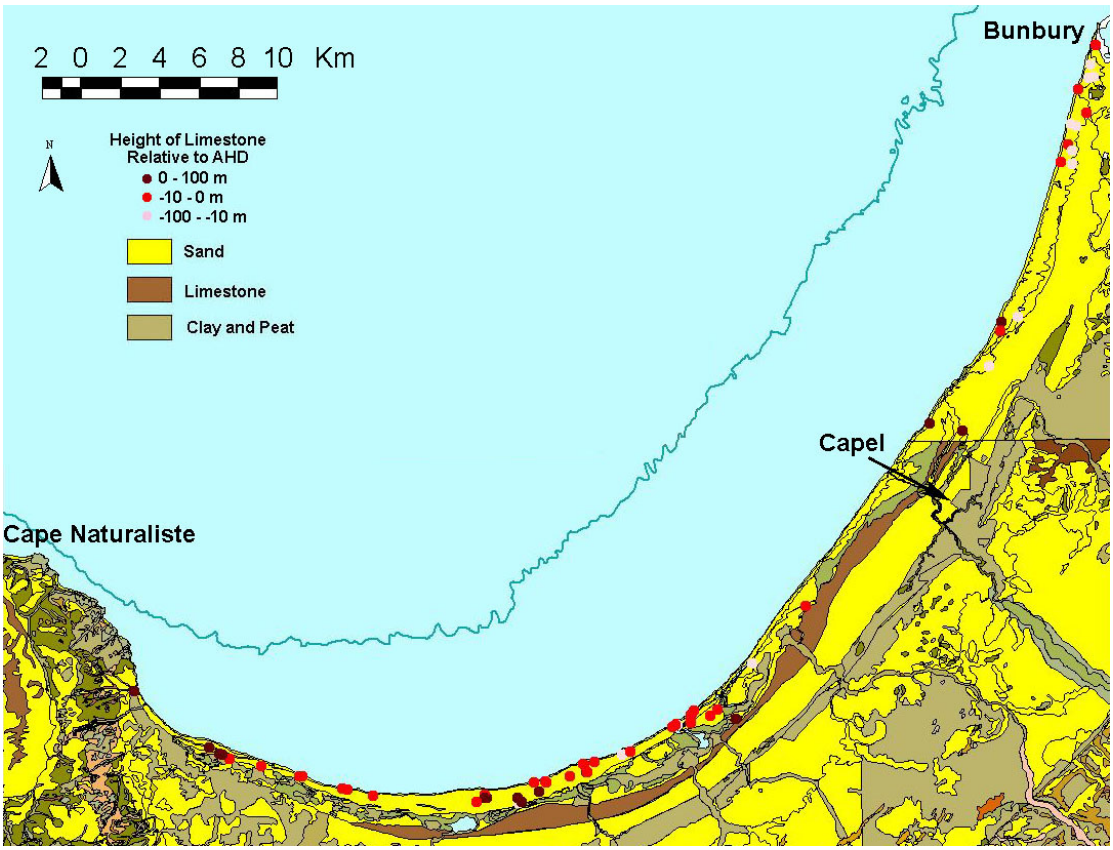

Figure 7.22: Height of top Tamala Limestone relative to Australian height datum, as measured in geotechnical boreholes in the Cape Naturaliste to Bunbury sector, overlain on the environmental geology of the area

Erosivity of the coastline

The Safety Bay Sand comprises the entirety of the coastline in this sector (Figure 7.22; Searle and Semeniuk, 1985). This sand is flanked on the landward side by either Tamala Limestone or muds of the Guilford Formation.

There is no microtremor or SCPT data along this section of the Swan Coastal Plain, therefore geotechnical borehole descriptions from the DOE dataset were utilised in delineating the upper surface of the limestone. Of the boreholes drilled in the coastal units of this sector, 69 were found to give useful descriptions of lithology (Figure 7.22). The heights of lithological horizons relative to sea level were estimated by relating the drilled depth to DEM height at that point.

The top limestone surface was encountered above sea level in approximately 20% of the holes. This suggests that the majority of the coastline in this sector is likely to be susceptible to erosion over the next century due to long-term sea level rise. The average height of the upper limestone surface for all 69 holes is approximately 5.5 m below sea level.

Qualitative assessment of erosion hazard in susceptible areas

The coastline appears to be susceptible to erosion along almost the entire length of this sector (Figure 7.1). A lack of differentiation between those areas that are prone to erosion and those areas that are not makes qualitative assessment unnecessary for the most part. Two holes in the vicinity of the township of Capel record the top limestone as above sea level, therefore it may be suggested that this section of coast is somewhat less susceptible to erosion (Figure 7.22). However, the heights recorded by these holes are 1.4 m and 12 cm above sea level, which is not significant enough to differentiate this stretch of coast as disparate from the remainder of the sector.

Calculating erosion

The coastline of the Cape Naturaliste to Bunbury sector appears to satisfy the three primary conditions upon which the Bruun Rule is dependent:

- Any erosion resistant lithologies in the onshore are below sea level so the upper beach can be eroded due to the landward translation of the profile.
- There is no significant littoral drift in this sector so the material eroded from the upper beach is likely to be equally to the amount deposited in the offshore.
- There are no reefs in the nearshore so the sediment–water interface can be remoulded by wave processes, maintaining a constant water depth in the offshore.

Along with the Swanbourne Beach area, the beaches in this sector comprise the best opportunity to estimate erosion rates using the simple but effective Bruun Rule. Unfortunately, the lack of wave data for the sector prevents this analysis being undertaken. As with the Bunbury to Mandurah sector, Cape Naturaliste is the closest of the wave buoys (Figure 7.19). This buoy measures the offshore incident wave heights and periods. The energy in these incident waves is attenuated as they are refracted around Cape Naturaliste and they cross the continental shelf. Therefore this wave data could not be used in a Bruun Rule analysis in this sector, as it would give anomalously high estimates of closure depth, which would consequently produce overestimates of recession. A second consideration is the need for detailed bathymetry data from which profiles could be constructed. It is possible that this data exists but it was not available to the author at the time of analysis.

Impact on infrastructure

The zones within this sector that are potentially prone to coastal erosion contain approximately 2,900 buildings and 213 km of roads. Of those buildings, approximately 2,000 are located in the ‘red’ zone, in which coastal erosion due to long-term sea level rise over the next century is considered likely (Figure 7.1). As a consequence of this relatively significant volume of infrastructure, this sector should be the primary focus in detailed quantitative coastal erosion modelling in southern Western Australia.

At the very least, Bruun Rule estimates should be undertaken to determine the potential extent of erosion, which will allow for comment on the number of buildings and roads that may be affected.

7.9 Impact of Coastal Erosion Due to Long-term Sea Level Rise

Although the adoption of statutory planning schemes in a number of states over the last 5–10 years indicates a change in the local planning environment to one in which sea level rise is taken into account, the current process for assessing potential erosion is still inconsistent between the states. The coastal management strategies of Queensland, New South Wales and South Australia require a Bruun Rule calculation to be incorporated into coastal planning, whereas Tasmania has no planning requirements. Victoria is in the process of undertaking more focussed regional studies (Walsh *et al*., 2004). The Western Australian Coastal Statement of Planning Policy (Coastal SPP) includes a schedule on the calculation of setbacks, which takes into account sea level rise. The sea level rise component has been derived from IPCC (2001) and is taken to be 38 cm, translating into a setback of 38 m by the Bruun Rule (Walsh *et al*. 2004).

The figures presented in the Bruun Rule analysis in the Fremantle to Hillarys section (approximately 1 m per year over the next 100 years) indicate that the use of 38 m as a guide for planning setbacks due to sea level rise may be a gross underestimation for the Swanbourne Beach area. Assuming the figure of 38 m relates to the potential recession over the next century, the calculations presented in this study indicate that erosion may be 2.5 times that currently used in planning (Jones and Hayne, 2002). Despite this underestimation, the potential impact on the Swanbourne Beach area is likely to be minimal, as very little infrastructure is located within 100 m of the shoreline at this locality (Figure 7.11). Given the Port/South Beach area appears to be most vulnerable of the hazardous regions in this sector presented in Figure 7.8, it is likely that erosion rates would be similar to, or greater than, rates at Swanbourne Beach. If this were the case, then the impact would be much greater than experienced at Swanbourne Beach, as there is considerably more infrastructure at the southerly location (Figure 7.8).

Response to coastal erosion

Modelling of potential recession within the susceptible zones outlined in this report will allow for the relevant planning agencies to respond to future coastal erosion. These agencies have two primary options in responding to potential erosion, they may choose to do nothing or do something. If they choose to act, then there are three generic responses:

- planned retreat (eg, building setbacks);
- accommodation (of sea level rise, by means such as raising buildings on pilings above the increased flood elevations); and
- protection (Nicholls *et al*., 1995). Protection of coastal land is traditionally achieved through either building seawalls or placement of sand to increase the size of the beach (usually by pumping from offshore) and so counteracting erosion, commonly described as ‘beach nourishment’.

Decisions regarding the appropriate mitigation measures for the Perth coast are beyond the scope of this report, as such judgments should be made by coastal engineers with knowledge of the local conditions and relevant resource structures that will fund the measures.

Consideration of increased storminess

A potential issue that relates to climate change, but is beyond the scope of this report, is that long-term sea level rise is not the only driving factor of shoreline change. Sources of potential hazard to the coast other than sea level rise, such as changes in the wave climate or an increase in storminess, are not considered in detail here. It is suggested that global warming and the associated higher sea surface temperatures may lead to a more ‘stormy’ climate (Henderson-Sellers *et al.*, 1998; IPCC, 2001). While increased ‘storminess’ will also affect levels of coastal erosion such influences are not considered in this study. The estimates of future erosion rates presented in this study, therefore, may be considered an underestimate of potential shoreline change through their absence.

Attempting to quantify erosion resulting from storms requires storm-surge modelling, using software packages such as SBEACH (developed by the US Army Corps of Engineers). The application of storm-surge models in association with long-term coastal erosion estimates is invaluable. For example, storm-surge models may indicate that *X* number of buildings in the Swanbourne Beach area will be inundated by a 100-year storm. If the same modelling is undertaken with a shoreline that has receded approximately 110 m and a sea level that is 48 cm higher than it is presently, particularly in a stormier climate, then the impact of the storm will be much greater. This suggests that detailed modelling of coastal erosion due to long-term sea level rise should be undertaken as a primary step in understanding coastal behaviour over the next century, subsequent to which storm-surge modelling will reveal a more accurate picture of effects on infrastructure within that timeframe.

Further research

An advance on the Bruun Rule that may be applied to sections of the Swan coast is the vector-based Bruun–GIS model, which is based on work undertaken by Bruun and describes the full implementation of the Bruun Rule in a GIS (Hennecke and Cowell, 2000). The Bruun–GIS model may be applied to areas such as Swanbourne Beach, although it is likely that this will give similar results to the conventional Bruun analysis presented above, which suggested erosion rates may be approximately 1 m per year over the next century due to sea level rise.

Attempting to quantify the amount of potential erosion over the next century at many localities along the Swan coast is problematic due to inadequacies inherent in available models, complications in the local geomorphology, and the influence of engineering works. Of the areas identified as being susceptible to coastal erosion in the Fremantle to Hillarys sector, estimating future recession rates would be complicated in the Port/South Beach and Pinaroo Point areas relative to the Swanbourne area. The southern locality is heavily influenced by the engineering works at Fremantle Harbour and the Swan River outlet, and the northern locality is bordered by extensive submerged reefs that would invalidate any modelling (Figure 7.1). A more detailed investigation of these areas is required in the future, to more accurately delineate the areas and infrastructure at risk.

Of the remaining sectors, future research into potential coastal erosion should be focussed on the Cape Naturaliste to Bunbury sector and the Bunbury to Mandurah sector. Undertaking recession estimate calculations in the former are more feasible given the current state of coastal behaviour models and any future erosion due to sea level rise will likely affect relatively more infrastructure in this area. In contrast, the latter sector is more likely to be heavily damaged by erosion over the next century, but modelling potential rates is complicated by a lack of data in the context of current models.

The difference between the figure presented in the Western Australian Coastal SPP and the calculations presented above highlights the need for site-specific investigations for determining potential coastal erosion. This approach has been adopted in Queensland, New South Wales and Victoria, but Tasmania and Western Australia are still to factor it into statutory planning schemes. A first-order assessment in any planning process should involve a Bruun Rule analysis at the very least. Given the resources (eg, time, money, expertise), it is also recommended that a more process-oriented analysis of sediment budgets be undertaken, as this will incorporate local factors, which can greatly influence the potential extent of erosion.

7.10 Conclusions

- It is highly likely that coastal erosion will have a significant impact on coasts around the globe, including Australian coasts, over the next century.
- Three sections of the Fremantle to Hillarys sector appear to be susceptible to coastal erosion: Port/South Beach; Swanbourne to Floreat Beach; and the Pinaroo Point area. The hazard decreases from south to north, primarily due to the northward net longshore drift.

- Given a sea level rise of 18 cm over the next 50 years, and 48 cm over the next 100 years, Swanbourne beach is likely to erode approximately 40–50 m and 100–130 m respectively. These figures are approximately 2.5 times the value currently used in planning in WA.
- The impact of modelled recession at Swanbourne Beach is not significant due to a lack of overlying infrastructure. Similar erosion at the other vulnerable localities would have a much greater impact.
- The majority of the Mandurah to Fremantle sector does not appear to be susceptible to coastal erosion over the next century, despite the fact that the Tamala Limestone is preserved below sea level across the majority of the area. This is due to the fact that this sector has been the primary depositional province for the Swan coast over the last 8,000 years.
- The Bunbury to Mandurah sector is the section of Swan coast that appears to be most susceptible to coastal erosion over the next century. This is because the Tamala Limestone is preserved below sea level, this sector is not well sheltered from offshore swell, and this location is at the southern end of the net northward littoral conveyor that operates along the Swan coast.
- The Hillarys to Yanchep sector does not appear to be susceptible to erosion over the next century as Tamala Limestone is preserved above sea level along the majority of the coast, and the beaches are well sheltered by three lines of offshore reefs.
- The Cape Naturaliste to Bunbury sector may be affected by coastal erosion associated with long-term sea level rise.
- A Bruun Rule calculation should be undertaken as a preliminary methodology in planning for coastal recession due to sea level rise. Future research should be focussed on the Bunbury to Mandurah sector, the Cape Naturaliste to Bunbury sector, and the Port/South beach area of Fremantle.
- The two significant problems that must be overcome before more modelling can be undertaken in the region are: a lack of data (particularly sector-specific wave data and more detailed subsurface data); and a lack of sophistication in current models that do not allow for calculation in areas where the nearshore/offshore includes competent substrate.

7.11 References

Abbs, D.J. and Physick, W.L. (1992) ‘Sea-breeze observations and modelling: A review’, *Australian Meteorological Magazine*, 41:9–19.

Bird, E.F.C. (1996) ‘Coastal erosion and sea-level rise’, in Milliman, J.D. and Haq, B.U. (editors) *Sea-level Rise and Coastal Subsidence*, Kluwer Academic Publishers, Dordrecht, The Netherlands, pp. 84–104.

Bruun, P. (1988) ‘The Bruun Rule of erosion by sea-level rise’, *Journal of Coastal Research*, 4:627–48.

Bruun, P. (1962) ‘Sea-level rise as a cause of shore erosion’, *Journal of the Waterways and Harbours Division, American Society Civil Engineers*, 88:117–30.

Bureau of Meteorology (1969) *The Climate of Perth, Western Australia*, Australian Government Printing, Tasmania.

Carrigy, M.A. and Fairbridge, R.W. (1954) ‘Recent sedimentation, physiography and structure of the continental shelves of Western Australia’, *Journal of the Royal Society of Western Australia*, 38:65–95.

Clarke, D.J. and Eliot, I.G. (1983) ‘Mean sea-level and beach-width variation at Scarborough, Western Australia’, *Marine Geology*, 51:251–67.

Clarke, E.deC. (1926) ‘The geology and physiography of the neighbourhood of Perth Western Australia’, *Handbook of the Australian Association for the Advancement of Science*, Perth, pp. 23–30.

Collins, L.B. (1983) ‘Post-glacial sediments and history, southern Rottnest Shelf, Western Australia’, PhD Thesis, Department of Geology, The University of Western Australia.

Gentilli, J. (1971) 'Climate of Australia and New Zealand', in Landsberg, H.E. (editor) *World Survey of Climatology*, Volume 13, pp. 108–114, Elsevier, Amsterdam.

Gozzard, J.R. (1987) *Lake Clifton–Hamel Sheet 2032 II and part 2032 III*, Environmental Geology Series, Geological Survey of Western Australia.

Gozzard, J.R. (1986) *Perth, Sheet 2034 II and part 2034 III and 2134 III*, Perth Metropolitan Region Environmental Geology Series, Geological Survey of Western Australia.

Gozzard, J.R. (1983a) *Fremantle Part Sheets 2033 I and 2034 IV*, Perth Metropolitan Region Environmental Geology Series, Geological Survey of Western Australia.

Gozzard, J.R. (1983b) *Rockingham Part Sheets 2033 III and 2033 II*, Perth Metropolitan Region Environmental Geology Series, Geological Survey of Western Australia.

Gozzard, J.R. (1982) *Yanchep Sheet 2034 IV*, Perth Metropolitan Region Environmental Geology Series, Geological Survey of Western Australia.

Hallermeier, R.J. (1981) 'A profile zonation for seasonal sand beaches from wave climate', *Coastal Engineering*, 4:253–77.

Hegge, B. (1994) 'Low-energy sandy beaches of southwestern Australia: two-dimensional morphology, sediments and dynamics', PhD Thesis, Department of Geography, The University of Western Australia.

Henderson-Sellers, A., Zhang, H., Berz, G., Emanuel, K., Gray, W., Landsea, C., Holland, G., Lighthill, J., Shieh, S-L., Webster, P., and McGuffie, K. (1998) 'Tropical cyclones and global climate change: a post-IPCC assessment', *Bulletin of the American Meteorological Society*, 79(1):19–38.

Hennecke, W. and Cowell, P.J. (2000) 'GIS modelling of impacts of an accelerated rate of sea-level rise on coastal inlets and deeply embayed shorelines', *Environmental Geosciences*, 7:137–48.

H. John Heinz III Centre for Science Economics and the Environment (2000) *Evaluation of Erosion Hazards – Contract EMW-97-CO-0375*, Federal Emergency Management Agency (FEMA), USA.

Hounam, C.E. (1945) 'The sea breeze in Perth', *Weather Developments and Research Bulletin*, 3:20–55.

Hsu, S.A. (1988) *Coastal Meteorology*, Academic Press, New York.

Institution of Engineers (2000) *Research Priorities for Coastal and Ocean Engineering*, National Committee on Coastal and Ocean Engineering, Canberra, Australia.

Intergovernmental Panel on Climate Change (IPCC) (2001) *Climate Change 2001: Impacts, Adaptions and Vulnerability: Contribution of Working Group II to the Third Assessment Report of the Intergovernmental Panel on Climate Change*, Cambridge University Press, Cambridge and New York.

Intergovernmental Panel on Climate Change (1996) *Climate Change 1995, The Science of Climate Change*, Cambridge University Press, Cambridge.

Jones, A.T. and Hayne, M. (2002) 'Modelling coastal erosion at Perth due to long-term sea level rise', *Proceedings of Australia's National Coastal Conference (Coast to Coast) – Source to Sea*, Tweed Heads, pp. 225–28.

Jones, A.T. and Hayne, M. (2003) 'Assessing the vulnerability of the Perth Coastal System to coastal erosion through GIS' in Woodroffe, C.D and Furness, F.A. (editors.) *Coastal GIS 2003: an integrated approach to Australian coastal issues*, University of Wollongong, Wollongong Papers on Maritime Policy, 14:303–316.

Kempin, E.T. (1953) 'Beach sand movements at Cottesloe, Western Australia', *Journal of the Royal Society of Western Australia*, 37:35–58.

Lemm, A. (1996) 'Offshore wave climate, Perth, Western Australia', BEng (Hons) Thesis, Centre for Water Research, The University of Western Australia.

Masselink, G. and Pattiaratchi, C.B. (2001) 'Seasonal changes in beach morphology along the sheltered coastline of Perth', Western Australia, *Marine Geology*, 172:243–63.

Masselink, G. and Pattiaratchi, C.B. (1998) 'The effect of sea breeze on beach morphology, surf zone hydrodynamics and sediment resuspension', *Marine Geology*, 146:115–35.

Morang, A. and Parson, L. (2002) 'Coastal morphodynamics', in Morang, A. (editor) *Part IV, Coastal Geology, Chapter IV-3. Engineer Manual 1110-2-1100*, US Army Corps of Engineers, Washington, DC.

Nerem, R.S., Haines, B.J., Hendricks, H., Minster, J.F., Mitchum, G.T., and White, W.B. (1997) 'Improved determination of global mean sea level variations using TOPEX/POSEIDON altimeter data', *Geophysical Research Letters*, 24:1331–34.

Nicholls, R.J., Leatherman, S.P., Dennis, K.C. and Volonté, C.R. (1995) 'Impacts and responses to sea-level rise: qualitative and quantitative assessments', *Journal of Coastal Research*, SI 14:26-43.

Passmore, J.R. (1967) 'The geology, hydrology, and contamination of shallow water aquifers in the Rockingham district, Western Australia', PhD Thesis, The University of Western Australia.

Pattiaratchi, C., Hegge, B., Gould, J. and Eliot, I. (1997) 'Impact of sea breeze activity on nearshore and foreshore processes in south-western Australia', *Continental Shelf Research*, 17:1539–60.

Pilkey, O.H., Young, R.S., Riggs, S.R., Smith, A.W.S., Wu, H., and Pilkey, W.D. (1993) 'The concept of shoreface profile of equilibrium: a critical review', *Journal of Coastal Research*, 9(1):255–78.

Playford, P.E., Cockbain, A.E. and Low, G.H. (1976) 'Geology of the Perth Basin, Western Australia', *Geological Society of Western Australia Bulletin*, 124.

Playford, P.E. and Low, G.H. (1972) 'Definitions of some new and revised rock units in the Perth Basin', *Western Australia Geological Survey Annual Report*, 1971:44–46.

Sanderson, P.G. (1992) 'A longshore compartmentalisation and distribution of beach sediments on the central coast of Western Australia', BSc (Hons) Thesis, Department of Geography, The University of Western Australia.

Sanderson, P.G. and Eliot, I. (1999) 'Compartmentalisation of beachface sediments along the southwestern coast of Australia', *Marine Geology*, 162:145–64.

Scientific Committee on Ocean Research (SCOR) Working Group 89 (1991) 'The response of beaches to sea-level changes: a review of predictive models', *Journal of Coastal Research*, 7:895–921.

Searle, D.J. (1984) 'A sedimentation model of the Cape Bouvard to Trigg Island sector of the Rottnest Shelf, Western Australia', PhD Thesis, The University of Western Australia.

Searle, D.J. and Semeniuk, V. (1985) 'The natural sectors of the inner Rottnest Shelf coast adjoining the Swan Coastal Plain', *Journal of the Royal Society of Western Australia*, 67:116–36.

Searle, D.J., Semeniuk, V. and Woods, P.J. (1988) 'Geomorphology, stratigraphy and Holocene history of the Rockingham-Becher Plain, South-western Australia', *Journal of the Royal Society of Western Australia*, 70(4):89–109.

Semeniuk, V. (1985) 'The age structure of a Holocene barrier dune system and its implications for sea level history reconstructions in southwestern Australia', *Marine Geology*, 67:197–212.

Semeniuk, V. (1983) 'The Quaternary stratigraphy and geological history of the Australind–Leschenault Inlet area', *Journal of the Royal Society of Western Australia*, 66:71–83.

Semeniuk, V. and Searle, D.J. (1986) 'Variability of Holocene sealevel history along the southwestern coast of Australia – evidence for the effect of significant local tectonism', *Marine Geology*, 72:47–58.

Semeniuk, V. and Searle, D.J. (1985) 'The Becher Sand, a new stratigraphic unit for the Holocene of the Perth Basin', *Journal of the Royal Society of Western Australia*, 67:109–15.

Semeniuk, V. and Semeniuk, C.A. (1991) 'Radiocarbon ages of some coastal landforms in the Peel–Harvey estuary, south-western Australia', *Journal of the Royal Society of Western Australia*, 73(3):61–71.

Silvester, R. (1961) 'Beach erosion at Cottesloe, Western Australia', *Civil Engineering Transactions*, 3:27–33.

Simpson, J.E. (1994) *Sea Breeze and Local Wind*, Cambridge University Press, Cambridge.

Steedman, R.K. (1977) *Mullaloo Marine: a report on oceanography and marine environment*, Shire of Waneroo, Western Australia.

Stive, M.J.F. and de Vriend, H.J. (1995) 'Modelling shoreface profile evolution', *Marine Geology*, 126:235–48.

Walsh, K.J.E., Betts, H., Church, J., Pittock, A.B., McInnes, K.L., Jackett, D.R. and McDougall, T.J. (2004) 'Using sea level rise projections for urban planning in Australia', *Journal of Coastal Research*, 20:586–98.

Chapter 8: CONCLUSIONS

Trevor Jones

Geoscience Australia

8.1 Key Results

In the Introduction to this report, we posed a series of Key Questions that the essential research in Cities Project Perth aimed to answer. This chapter summarises the main results of Cities Project Perth. Most of these results are integrated from the individual chapters in the report.

One overriding feature of Cities Project Perth is its use of predictive computational models to provide information on rare events with high impacts, not seen in the historic record, that could occur in the future.

The model results show that Perth could experience an extremely rare earthquake with high socio-economic losses. Similarly, the analysis of severe winds indicates that a damaging cool season storm could impact broadly on exposed areas of Perth with an intensity never before recorded. The flood modelling also indicates higher water levels for scenarios much rarer than the 1% AEP scenarios that have been experienced in the past and that are used in planning guidelines. In this way, Cities Project Perth has provided important new information for emergency risk management.

We emphasise that this report should be regarded as the best and most recent hazard and risk assessment for the natural hazards covered in this report for metropolitan Perth. However, we acknowledge that there are limitations in the models and data we have used, and that we have an incomplete understanding of the natural variability inherent in atmospheric, marine and terrestrial systems, building response and human behaviour. The results, interpretations and conclusions could change with the incorporation of new data and with different model assumptions. Therefore, the reader should not take action based on information in this report alone.

Severe wind hazard

The key results from Chapter 3 follow.

- The severe wind hazard calculated in this report for Perth Airport is in close agreement with the wind hazard described for Perth in the Australian wind loadings standard (Standards Australia, 2002). The Standard places Perth in Region A, the lowest hazard region of four in Australia. However, the historical record from the weather station at Perth Airport was the sole dataset used in calculations for the wind loadings standard. This airport is some 20 km inland and winds from the western quadrant, the strongest in Perth, are reduced in intensity in their path from the coast inland. Return period wind speeds in the standard are most applicable to Perth sites some kilometres inland. This study has produced a richness of wind hazard estimates extending across metropolitan Perth.
- Across metropolitan Perth, severe wind hazard varies considerably. Localised areas of Perth with measurably higher hazard than the wind loadings standard lie:
    - in a band several kilometres wide along the coastline, with a nearshore coastal strip a few hundred metres wide having the greatest hazard;

  - in a north–south band several kilometres wide running along the top of the Darling Scarp; and
  - on exposed shores of the lower reaches of the Swan River, extending inland approximately as far as the Kwinana Freeway.

- The reader needs to be aware that variability in wind speed, wind turbulence, incoming wind direction, and the ability of the models themselves to describe accurately the physical characteristics of the wind, all add variability to the wind hazard at any place and for any particular wind event. The variability in the behaviour of buildings and other structures, due to variability in construction strength and orientation to the wind, will also add variability to damage for any specific event.

Flood hazard

Chapter 4 incorporated hydrologic estimates and previously surveyed cross-sections into a single study and modelled the interactions of the tributaries with the Swan River. The geometry of the model was significantly enhanced by the addition of many cross-sections derived using a detailed DEM that was developed specifically for the modelling of flood flows.

- There are six major catchments in the study area that contribute flow to the Swan River, of which the Avon catchment is by far the largest. Not surprisingly, the hydrologic estimation of flows showed that the Avon River was the dominant flow contributor to the Swan River. Simulations showed that another significant source of flow is from the tributaries, particularly the Canning and Southern Rivers.
- The season of the tidal cycle was found to influence flood flows marginally, with water levels slightly higher in winter. As expected, the variation in water levels decreased with distance upstream from the Port of Fremantle.
- Perth has experienced a lengthy dry period in the past 40 years. Only two major flows have occurred, in 1983 and 1987, since all the streamflow gauging stations at the outer boundaries of the model became operational. The new model better models the hydraulic system and, being an unsteady flow model, is capable of reproducing non-linear behaviour such as tidal influence better than the earlier DOE model. Therefore when more data become available, the unsteady flow model should be recalibrated as far as possible.
- Water levels in this study were found to be lower than those modelled previously for the 1% AEP flood event. The variation in water levels can be explained by the differing methodology of this model and the earlier model. The model differences are best explained by the inclusion of the tributaries, followed by the use of an unsteady flow model rather than a steady flow model, in the Cities Project Perth model. The current lack of data has resulted in the model results being inconclusive and, therefore, the availability of the new model, on its own, does not warrant a complete replacement of current procedures on 1% floodplain mapping. This report provides recommendations that will help reconcile the two models and reduce uncertainties in flood hazard estimates.
- Eight flood scenarios were modelled for the Swan River and its tributaries ranging from AEPs of 10% to 0.05%. Previously, only the 1% AEP scenario had been mapped using a less complex steady flow model. The new model provides emergency managers and planners with important new hazard information for scenarios with a large range of return periods. The unsteady flow model and the stream levels predicted by the modelled events are now held by government agencies in WA, including DOE and BOM.

Earthquake risk

The earthquake risk to Perth discussed in Chapter 5 can be summarised by the following results.

- Overall, the estimates of earthquake hazard on rock foundation in Perth and in southwest WA are similar to those in the current and draft Australian earthquake loading standards. These results have come from a comprehensive update of the earthquake hazard in Perth and in

southwest WA. The reader is referred to Chapter 5 for a comparison of the earthquake hazard calculated in this report and the hazard described in the current and draft earthquake loadings standards.

- The earthquake risk to Perth has been aggregated across the metropolitan area and illustrated by a risk curve or probable maximum loss (PML) curve in Chapter 5. Loss is expressed as a percentage of the total value of all buildings and their contents in the study region.
- The results of this study suggest that, on average, greater metropolitan Perth will suffer an estimated economic loss of around 0.04% per year.
- About three-quarters of the earthquake risk in the study region is from events that have annual probabilities of occurrence of 0.004 or less (return periods of 250 years or more). This suggests that about three-quarters of the risk to metropolitan Perth is from rare events with major or, in extreme cases, catastrophic impacts. The long-term nature of earthquake risk to Perth and regional communities to the east indicates that the risk is likely to be realised very rarely. These earthquake events will have relatively high consequences. This provides a motivational challenge for emergency managers to remain vigilant and for appropriate risk treatments, such as adequate insurance, to remain in place.
- Impact events with annual probabilities of occurrence up to 0.004 (return periods up to 250 years) contribute an additional one-quarter of the risk. While these relatively frequent events will have low impacts, total losses could be significant when individual losses are aggregated.
- The earthquake risk to Perth varies spatially across the study region. A gradual reduction in risk occurs across metropolitan Perth in a southwesterly direction as distance from the southwest seismic zone (SWSZ) increases. The effect of the higher earthquake hazard in the Wheatbelt region can thereby be discerned.
- Most of the annualised risk for building usage type is for residential types (almost 90%) with the next most common being commercial. This is mainly because residential buildings make up the overwhelming majority of buildings in the study area, and comprise the majority of the total estimated value of all buildings in the study area.
- The unique capital city profile of Perth has also influenced the results in that the residential building stock is predominantly unreinforced double brick construction, with a much smaller proportion of framed timber construction. Unreinforced masonry is significantly more vulnerable than framed timber construction.
- The locations of earthquakes that create most of the risk to metropolitan Perth show a split distribution. About half of the earthquake risk in metropolitan Perth is due to moderate to strong earthquakes (magnitudes in the range about 5 to 6.5) that could occur with epicentres at distances of less than 30 km from Perth. Estimates of earthquake risk in Perth are sensitive to model assumptions of the rate of occurrence of earthquakes for these close-in earthquakes, because historic seismicity has been low in and around Perth.

  The second significant contribution to earthquake risk in Perth comes from large earthquakes that could occur at the western margin of the SWSZ (60–90 km from Perth), where the earthquake activity is higher than it is in Perth.
- The area of elevated hazard in the Wheatbelt is considerably more extensive than identified in the current earthquake loadings standard. This area is wider in an east-west direction, extends further northward and is generally located closer to Perth.

Indicators of social resilience for recovery

The indicators ‘household financial capacity’, ‘community and social networks’ and ‘distance to services’, explored in Chapter 6, show that Perth households and the broader community have many characteristics that will favourably influence the recovery process following a natural hazard event. However, these indicators are only three of many influencing recovery.

- The majority of households in metropolitan Perth have good economic resources, relative to the rest of Australia. Twenty-nine of 30 LGAs in the Perth Statistical Division rank in the top 50% of Australian LGAs in the ABS Index for Economic Resources (ABS, 2004a). Of these 29 LGAs, 22 rank in the top 25% nationally. Therefore, in the event of any natural disaster that has direct and widespread effects on residences, the community has many households that can draw on their economic resources to assist their recovery. However, it must be noted that there are some areas, or clusters, of households within suburbs that may experience difficulties in the recovery process due to limited financial capacity.
- The strong community network in WA is indicated by results from the General Social Survey (ABS, 2004b). This strong network suggests that, for many in Perth, recovery may involve a strong utilisation of friends, family, neighbours and informal organisations, such as community groups or sporting clubs. Almost all WA participants in the GSS indicated that they could ask someone outside of their home for assistance in times of need, including a health, legal or financial professional, charity or religious organisation. This information may assist recovery managers in tailoring programs and services for people in the Perth community.
- People in some outer suburban areas may have further to travel to access major services than those living more centrally. These major services, whether they are medical, welfare, social or cultural, can be important factors in influencing the recovery of the outer communities. This information may assist recovery managers in understanding some access/transport issues for people living in this part of the Perth metropolitan community.

Potential impact on the southwest WA coast from sea level rise due to climate change

Key findings from Chapter 7 follow.

- It is highly likely that coastal erosion will have a significant impact on coasts around the globe, including Australian coasts, over the next century.
- Three sections of the Fremantle to Hillarys coastline appear to be susceptible to coastal erosion: Port/South Beach; Swanbourne to Floreat Beach; and the Pinaroo Point area. The hazard decreases from south to north, primarily due to the northward net longshore drift.
- Given a sea level rise of 18 cm over the next 50 years, and 48 cm over the next 100 years, Swanbourne beach is likely to erode approximately 40–50 m and 100–130 m respectively.
- The impact of modelled coastal recession at Swanbourne Beach is not significant due to a lack of overlying infrastructure. Similar erosion at the other vulnerable localities would have a much greater impact.
- The Bunbury to Mandurah coastline is the section of Swan coast that appears to be most susceptible to coastal erosion over the next century. This is because (1) the Tamala Limestone is preserved below sea level, (2) this sector is poorly sheltered from offshore swell, and (3) this location is at the southern end of the net northward littoral conveyor that operates along the Swan Coast.
- The majority of the Mandurah to Fremantle coastline does not appear to be susceptible to coastal erosion over the next century, despite the fact that the Tamala Limestone is preserved below sea level across the major part of the area. This is due to the fact that this sector has been the primary depositional province for the Swan coast over the last 8,000 years.
- The Hillarys to Yanchep coastline does not appear to be susceptible to erosion over the next century as Tamala Limestone is preserved above sea level along the majority of the coast, and the beaches are well sheltered by three lines of offshore reefs.
- The Cape Naturaliste to Bunbury area may be impacted by coastal erosion associated with long-term sea level rise. With an increasing development of coastal urban infrastructure, this sector is an important focus for quantitative coastal erosion modelling in southern Western Australia.

A great deal of variability was included in the models used to generate these results. To some degree this variability was incorporated to account for our lack of knowledge about the various models used in the study. The effect of high levels of variability is to increase the estimates of risk. Future studies could focus on improving the models that have been used. This will allow for the variability in the models to be decreased, which will most probably result in a decrease in the estimates of risk.

8.2 Risk Management Recommendations

The broad-ranging information developed in this study presents new opportunities to improve risk assessment and risk management in Perth and the surrounding region. The suggested risk management options are largely focussed toward State and Local Government action that will reach many other public and private sector users of the information.

The risk management options include the following.

Severe wind hazard

Use the wind hazard maps:
- **to review, improve and complement the design and construction guidelines for severe winds set by state and local governments;**
- **as a source of information for response planning and response;**
- **as a basis for further research on severe wind risk in Perth; and**
- **as an aid to bushfire risk assessment at the Perth urban/rural interface.**

This report shows that the severe wind hazard values in the Australian wind loadings standard for Perth are most applicable to sites some kilometres inland, and that the wind hazard in exposed localities in Perth is measurably higher than the hazard in the standard. The wind hazard maps for return periods of 50, 100, 500 and 1,000 years for metropolitan Perth provide a rich new source of information on localised wind hazard to complement the wind loadings standard.

Use the wind hazard multipliers for topography, terrain roughness and shielding:
- **to review, improve and complement the design and construction guidelines for severe winds set by state and local governments;**
- **as a reference for design engineers and the construction industry;**
- **as a basis for further research on severe wind risk in Perth; and**
- **as an aid to bushfire risk assessment at the Perth urban/rural interface.**

Values of multipliers that modify the free field wind speeds for the effects of localised topography, terrain roughness, and shielding of buildings by other structures have been prepared across much of the metropolitan area. These values have been calculated on a grid with spacing of 25 m intervals for eight directions of the compass.

Note: the wind hazard values and the multipliers have been calculated for a grid across metropolitan Perth. The values provide a guide for low rise structures such as residential buildings in local areas. They are not suitable for application to individual properties and they should not be used for site-specific design purposes.

Flood hazard

The flood hazard model developed in this study is the most recent, rigorous and comprehensive model prepared for the Swan River and its tributaries. It estimates time-dependent inundation depths and lateral extents of flooding for AEPs as rare as 0.05%.

However, Perth has experienced a 40-year dry period, and only two major flows have occurred since all the streamflow gauging stations became operational at the outer boundaries of this model. These two factors have made validation of the model difficult.

Therefore, the following recommendations apply.

With regard to the flood model developed for the Swan and Canning Rivers:

- **acquire and apply further data to refine, revise and recalibrate the model;**
- **collect systematic data during future major flood events;**
- **review the model for river flooding in the Swan and Canning Rivers after each major event; and**
- **until adequate data are available to further refine and calibrate the new flow model, continue to use the Department of Environment's 1% AEP floodplain mapping as the basis for ensuring that future development has adequate flood protection.**

Earthquake risk

The earthquake risk assessment in this report included a comprehensive review of earthquake hazard, not only in Perth, but in a region extending approximately 200 km from Perth. This hazard assessment is currently the best available for southwest WA.

The earthquake hazard maps (on rock foundation) for the Wheatbelt within 200 km of Perth are especially valuable. They indicate that the region associated with the seismically-active SWSZ has significantly higher earthquake hazard than metropolitan Perth. This result was previously known, and a zone of elevated hazard is shown in the current Australian earthquake loadings standard. However, the newly-mapped zone of elevated earthquake hazard has a much greater geographic extent, and is located closer to Perth, than the zone mapped in the earthquake loadings standard (Standards Australia, 1993). The new results place more Wheatbelt communities at higher risk than the earthquake loading standard may indicate.

The following recommendations are made to reduce earthquake risk.

Use the earthquake hazard maps for metropolitan Perth and the Perth region:

- **to review, improve and complement the design and construction guidelines for earthquakes set by state and local governments;**
- **as a source of information for response planning and response.**

Enforce the compliance of all new structures with current earthquake loadings standards.

Promote the importance of adequate insurance against earthquakes for householders, small business operators and corporations.

Structurally retrofit where necessary facilities such as police, SES, fire and ambulance stations and hospitals, which provide essential services following any earthquake event. These facilities could be examined by suitably qualified engineers on a site-by-site basis to assess their expected performance under earthquake loadings. This recommendation is pertinent for Wheatbelt communities in or near the SWSZ.

The earthquake risk results are sensitive to the models used and to the data that were incorporated in the models. The sources of uncertainty are many. Two of the most important sources of uncertainty are the attenuation models, used to describe the decay of earthquake energy with distance from the

earthquake source, and the magnitude–recurrence relationships that describe the rate of earthquake occurrence in the various earthquake source zones. The most effective way to improve our understanding of these critical parts of the earthquake risk models is to collect instrumental data in the field.

Therefore, it is recommended that state and local government:

Support long-term earthquake monitoring, and recording of earthquake strong ground motion, in Perth and its surrounding region.

This support could take the form of direct financial support, provision of staff to assist station operations, use of government sites for establishing monitoring stations, and/or logistic support of field activities such as aftershock recording surveys.

Socioeconomic factors in community recovery

There is considerable scope to develop the social vulnerability model framework based around the elements of household financial resilience, community relationships and access to services. Application of this framework will improve risk assessments by broadening the concepts of risk. An understanding of how the framework applies to metropolitan Perth can also improve community recovery through focussed preparation by government agencies.

To improve understanding of the socio-economic cost of natural hazards to the community, relevant WA Government agencies and Local Governments should participate in national research in social vulnerability models as they apply to all sudden-onset hazards.

We further recommend that government agencies collect, integrate and analyse socioeconomic data that will improve their understanding of community vulnerability to natural hazards.

There are more factors that influence recovery not explored in this report that need to be researched and addressed in order to gain a better understanding of recovery. There are also many structural issues that need to be addressed on how socio-economic and environmental models and impacts can be incorporated into risk assessments. The following points highlight some of the key recommendations for the improved development of comprehensive risk assessments:

- Local community development agencies and state recovery managers have a valuable role and must be involved in risk assessment development and strategic risk management decisions. Only then can government begin to better reduce the impact that natural disasters have on Australian communities;
- We need to further understand emotional and psychological factors associated with accessing services during recovery.

Potential impact on the southwest WA coast from sea level rise due to climate change

Two recommendations related to future research and data collection that will assist coastal planning are taken from Chapter 7.

To improve decision making and reduce uncertainties about the potential for future coastal erosion due to sea level rise:

- **Undertake a Bruun Rule calculation as a preliminary methodology in planning for coastal recession due to sea level rise.**
- **Focus future research on the Bunbury to Mandurah coastline, the Cape Naturaliste to Bunbury coastline, and the Port/South beach area of Fremantle.**
- **Improve data availability, particularly sector specific wave data and more detailed subsurface data.**

- **Improve the sophistication of current models to allow for calculation in areas where the nearshore/offshore includes competent substrate.**

Spatial databases and risk assessment models

More than a dozen major spatial databases and risk assessment models, including the flood hazard model and comprehensive building and building footprint databases, digital elevation models and GIS hazard maps, were developed for use in Cities Project Perth.

WALIS and DLI have played leading coordination roles in ensuring that the Cities Project Perth databases will be added to, maintained and made available by the appropriate WA government agencies. These databases will be reviewed for possible inclusion in the WA Shared Land Information Platform (SLIP).

Risk assessment for floods and severe winds

The hazard assessments for severe wind and flood in this report provide an excellent basis for extension of the hazard assessments to risk assessments that estimate physical impacts on the built environment and socio-economic losses. Comprehensive data for exposure and vulnerability are available to extend the hazard assessments in this way. Building databases are available through the WA Valuer-General's Office, and GA researchers have acquired additional important information such as building and contents cost models, building floor area, and building floor height for structures in the Swan floodplain. Demographic and household financial and socioeconomic information for metropolitan Perth that can be used for socio-economic vulnerability and loss analysis is available from ABS, for example through the census.

Undertake probabilistic risk assessments for flood and severe wind in metropolitan Perth using the hazard assessments from this report as a basis.

The development of a flood risk assessment for Perth, and/or a severe wind risk assessment, provides an excellent opportunity to compare and contrast risks from important sudden-onset natural hazards in Perth. Other risk assessment studies already developed or under development include the WA government initiative on bushfire threat analysis for the Perth urban/rural interface and the probabilistic earthquake risk assessment in Cities Project Perth. GA has also commissioned a study by Risk Frontiers on average annualised damage for metropolitan Perth as a single entity. The annualised losses from these risk assessments could be compared against the annualised historic losses estimated by BTE (2001) for WA as a whole, in order to obtain information on the costs of forecast rare events, the likes of which have not occurred in the historic record.

Bushfire risk assessment

The historic record (see Chapters 1 and 2) indicates that bushfires have caused major damage in southwest WA. Climate change may modify the frequency and intensity of these events in future decades. The work of government agencies such as FESA and the WA Department of Conservation and Land Management (DCLM) in bushfire threat analysis would benefit from aligning their methods of research with that of Cities Project Perth, so that bushfire hazard and risk can be compared more systematically with other natural hazard risks. Therefore, it is recommended that the department's bushfire threat analysis methodology and the methodologies in Cities Project Perth are drawn together.

Align the bushfire threat analysis currently being undertaken by WA government agencies with the hazard, exposure, vulnerability and loss assessment methodologies and databases of Cities Project Perth in order to develop a systematic and consistent set of information on the risks from the major sudden-onset natural hazards in Perth.

Cost of disasters

Chapter 1 mentioned the difficulties in obtaining accurate and complete information on the costs of natural disasters. Improved information on the total costs, and the breakdown of costs into who pays and who benefits, will improve risk assessment models and decisions on cost effective mitigation, as recognised in the report to COAG (High Level Group, 2002). Recommendation 11 from that report is repeated here.

> *that jurisdictions jointly and progressively develop processes and systems that capture costs for all areas of disaster management, so that the cost of natural disasters, government expenditures, and costs and benefits of disaster mitigation are increasingly accurate and understood.*

In the case of future natural hazard events that cause significant losses, efforts should be made to capture systematic loss information. This action is necessary to obtain a full understanding of the event with the aim of introducing measures to mitigate similar future events. Also, the loss information, combined with information on the physical intensity of the event itself, provides extremely valuable 'calibration' data to improve risk models, and therefore our understanding of future risk from natural hazards. Recommendation 40 in the report to COAG is repeated here (High Level Group, 2002).

> *'that post-disaster assessments be undertaken routinely after every event of significance and the findings incorporated into improved disaster management processes to deal with future events.'*

8.3 Where to from here?

In this chapter we have suggested mitigation options that could reduce natural hazard risks in Perth based on the results of the research in Cities Project Perth. Most of the suggested options are aimed at the key public and private sector agencies who are responsible for emergency management, land use planning and information management in WA. Some of these mitigation options include recommendations for additional research and additional data gathering to make the risk management more effective again.

It is now largely the task of the WA partners in Cities Project Perth, and the people and organisations with whom they work, to implement decisions based on the new information herein made available.

8.4 References

Australian Bureau of Statistics (2004a) *SEIFA 2001 Standalone (CD-ROM)*, Release 2 2004, Australian Bureau of Statistics, Canberra.

Australian Bureau of Statistics (2004b) *2002 General Social Survey (CD-ROM)*, Australian Bureau of Statistics, Canberra.

Bureau of Transport Economics (2001) *Economic Costs of Natural Disasters in Australia*, Report 103, Bureau of Transport Economics, Canberra.

Bureau of Transport Economics (2000) *Road Crashes in Australia*, Report 102, Bureau of Transport Economics, Canberra.

High Level Group (2002) *Natural Disasters in Australia: Reforming mitigation, relief and recovery arrangements, a report to the Council of Australian Governments*, Australian Department of Transport and Regional Services, Canberra.

Standards Australia (2004) *DR 04303 : Structural design actions – Part 4 : Earthquake actions in Australia*, Standards Australia, Homebush, Sydney.

Standards Australia (2002) *Structural Design Actions, Part 2: Wind actions*, AS/NZS 1170.2:2002.

Standards Australia (1993) *Minimum Design Loads on Structures, Part 4: Earthquake loads*, AS 1170.4-1993.

Appendix A: WIND HAZARD METHODOLOGY

Xun Guo Lin

CSIRO Mathematical and Information Sciences

Generalized Extreme Value Distribution (GEV)

The general functions of GEV are given here.

Fitting the dataset to a GEV

Data fitting methods used were based on maximum likelihood and probability-weighted moments. Statistical hypothesis tests such as Gumbel tests have also been performed on all datasets with a 95% significance level. If a null hypothesis of a Gumbel Distribution (ie, zero shape parameter) could not be rejected, then the dataset was fitted to a Gumbel Distribution. If a Gumbel Distribution has been rejected in favour of a positive shape parameter, a Weibull Distribution fitting was then performed. Finally, the maximum value of these estimates (different fitting methods and different datasets, yearly and monthly) has been chosen as the estimate for the return period speed. Note that when an estimate from the yearly maxima differed by more than 5% from the estimate derived by the monthly maxima, only the estimate from the monthly maxima has been used. This is because we rank the results from monthly data (ie, a larger sample) as more reliable than the corresponding results from the yearly data (ie, a smaller sample), especially when the data period is short.

The cumulative distribution function (CDF) of GEV

The GEV has a CDF of

$$H(x;\xi,\sigma,\mu)=\begin{cases} e^{-\left(1-\xi\frac{x-\mu}{\sigma}\right)^{1/\xi}} & \xi\neq 0 \\ e^{-e^{-(x-\mu)/\sigma}} & \xi=0 \end{cases} \qquad \textbf{Equation A.1}$$

where ξ, σ and μ are the shape, scale and location parameters, respectively, and x is the maximum for an epoch.

When $\xi = 0$, the distribution is a Type I GEV or Gumbel Distribution. When $\xi < 0$, the GEV has a long right tail. It is called the Type II (or Frechet) Distribution. When $\xi > 0$, it has a short tail. It is sometimes called the Type III GEV (which is a form of the Weibull Distribution). The Type III GEV has a theoretical upper bound ($\mu+\sigma/\xi$) that may be useful for estimates of extreme values (such as largest possible wind gusts). Many scientists believe that due to physical and meteorological limitations, there is an upper bound to the maximum wind gust.

Return periods

When a threshold of the magnitude of an event is chosen to be sufficiently large, the number of exceedances N_u (where u is the threshold) has an approximate Poisson distribution with parameter λ (the rate of exceedances per year, also called the crossing rate). Hence λT is the number of exceedances in T years. Let λ_U be the number of events exceeding a very high level U. That is,

$$\lambda_U = \lambda T \cdot \Pr\{X > U\} = \lambda T(1-F(U)). \qquad \textbf{Equation A.2}$$

Assume U_T is the event with the largest value in T years, and by definition $\lambda_{U_T} = 1$ (i.e. it only happens once in T years). Now

$$\lambda_{U_T} = \lambda T(1 - F(U_T)) = 1 \qquad \textbf{Equation A.3}$$

so

$$F(U_T) = 1 - \frac{1}{\lambda T} \qquad \textbf{Equation A.4}$$

or

$$U_T = F^{-1}\left(1 - \frac{1}{\lambda T}\right) \qquad \textbf{Equation A.5}$$

where $F^{-1}(\cdot)$ is the inverse of the CDF of the GEV. The crossing rate λ has the value 1 if yearly maximum data are used in the extreme value analysis, or 12 if the monthly maxima are used.

Quantile estimation

Once its parameters have been estimated, quantile estimates for the GEV can be obtained by inverting Equation A.1 and using Equation A.6:

$$U_T = \begin{cases} \mu + \dfrac{\sigma}{\xi}\left\{1 - \left[-\ln\left(1 - \dfrac{1}{\lambda T}\right)\right]^{\xi}\right\} & \xi \neq 0 \\ \mu - \sigma \ln\left[-\ln\left(1 - \dfrac{1}{\lambda T}\right)\right] & \xi = 0. \end{cases} \qquad \textbf{Equation A.6}$$

Appendix B: PERTH SPATIAL DATABASE METADATA

build_db; footprints; ft_bld_join; flood_srv; cbd_srv

Neil Corby
Geoscience Australia

Spatial Database: BUILD_DB.SHP

Keywords

Theme: building, database, points, VGO, GA
Place: Perth

Description

Abstract

This point database was created from the Valuer-General's Office (VGO) Microsoft Access database 2002. Geoscience Australia (GA) has value added to this database by generating additional attribute fields, and creating a spatial context using the X/Y columns and the functionality of ESRI software.

Purpose

This dataset was used as a base dataset for earthquake, wind and flood modelling. The attributes from this shapefile were extracted and saved as another shapefile called export8, extra fields such as lat/long values were added. Only the dbf file from this shapefile was used for the earthquake risk modelling (EQRM) MapLab program.

Supplementary information

Some errors are inherent from the original data and difficult to rectify such as street address information. This dataset was joined with the building footprints dataset using the PIN attribute data field.

Links to graphics describing the data

Extent of shapefile (JPEG): build_db.jpg

Status of the data

Complete
Data update frequency: As needed

Time period for which the data is relevant

Date and time: 2002 – base data
Description: Ground condition

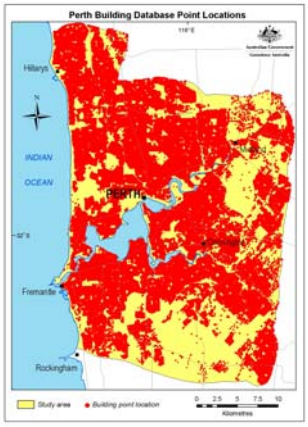

Publication information

Who created the data: Geoscience Australia
Date and time: from unpublished material

Data storage and access information

File name: build_db
Type of data: vector digital data
Location of the data: dvd\build_db.shp
Data processing environment: Microsoft Windows 2000 Version 5.0 (Build 2195) Service Pack 4; ESRI ArcCatalog 9.0.0.535

Accessing the data

Size of the data: 9.487 MB
Data transfer size: 9.487 MB

Constraints on accessing and using the data

Access constraints: Contact GA/VGO/DLI
Use constraints: Some fields are VGO owned

Details about this document

Contents last updated: 20050221 at time 15423300

Who completed this document

Neil Corby, Geoscience Australia
Mailing address:

P.O. BOX 378
Canberra, ACT 2601
Australia
02 62499 9176 (voice)
02 62499 986 (fax)
neil.corby@ga.gov.au

Hours of service: 7am–7pm

Contact instructions: First contact via email

Spatial description

Horizontal coordinate system

Projected coordinate system name: GDA_1994_MGA_Zone_50
Geographic coordinate system name: GCS_GDA_1994

Details

Map projection

Name: Transverse Mercator
Scale Factor at Central Meridian: 0.999600
Longitude of Central Meridian: 117.000000
Latitude of Projection Origin: 0.000000
False Easting: 500000.000000
False Northing: 10000000.000000

Planar Coordinate Information

Planar Distance Units: meters
Coordinate Encoding Method: coordinate pair

Coordinate Representation

Abscissa Resolution: 0.000064
Ordinate Resolution: 0.000064

Geodetic Model

Horizontal Datum Name: D_GDA_1994
Ellipsoid Name: Geodetic Reference System 80
Semi-major Axis: 6378137.000000
Denominator of Flattening Ratio: 298.257222

Bounding Coordinates

In decimal degrees
West: 115.727196
East: 116.057747
North*:* -31.764400
South*:* -32.168344

In projected or local coordinates
Left: 379989.000000
Right: 410773.250000
Top: 6484979.500000
Bottom: 6440512.000000

Lineage

FGDC lineage
Process step 1
Process description: Please see FLOWCHART.jpg for lineage.
Process software and version: ArcGIS

ESRI description

build_db
ESRI feature type: Simple
Geometry type: Point
Topology: FALSE
Feature count: 355265
Spatial Index: TRUE
Linear referencing: FALSE

Attributes details for build_db

Type of object: Feature Class
Number of records: 355265

Attributes

FID
Alias: FID
Data type: OID
Width: 4
Precision: 0
Scale: 0
Definition: Internal feature number
Definition source: ESRI

Shape
Alias: Shape
Data type: Geometry
Width: 0
Precision: 0
Scale: 0
Definition: Feature geometry
Definition Source: ESRI

AREA
Alias: AREA
Data type: Number
Width: 9
Number of decimals: 3
Definition: Feature geometry (Sourced from Footprints coverage)
Definition Source: ESRI

PERIMETER
Alias: PERIMETER
Data type: Number
Width: 9
Number of decimals: 3
Definition: Feature geometry (Sourced from Footprints coverage)
Definition Source: ESRI

*BUILD_DB_*
Alias: BUILD_DB_
Data type: Number
Width: 9
Definition: UFI
Definition Source: ESRI

FT_AREA
Alias: FT_AREA
Data type: Number
Width: 19
Number of decimals: 3
Definition: Footprint area

Definition Source: Geoscience Australia

FT_PERIM
Alias: FT_PERIM
Data type: Number
Width: 19
Number of decimals: 3
Definition**:** Footprint Perimeter
Definition Source: Geoscience Australia

PIN
Alias: PIN
Data type: Number
Width: 19
Number of decimals: 3
Definition: Property/Cadastre number UFI
Definition Source: Valuer-General's Office

PROPERTY_N
Alias: PROPERTY_N
Data type: String
Width: 10
Definition: Property number
Definition Source: Geoscience Australia

CLASSIFICA
Alias: CLASSIFICA
Data type: String
Width: 50
Definition: Building Classification
Definition Source: Valuer-General's Office

PROPERTY_U
Alias: PROPERTY_U
Data type: String
Width: 50
Definition: Property usage
Definition Source: Geoscience Australia

PRIMARY_LA
Alias: PRIMARY_LA
Data type: String
Width: 20
Definition: Primary (unknown)
Definition Source: Valuer-General's Office

UNIT_NO
Alias: UNIT_NO
Data type: String
Width: 9
Definition: Unit Number
Definition Source: Valuer-General's Office

HOUSE_NO
Alias: HOUSE_NO
Data type: String
Width: 9
Definition: House number
Definition Source: Valuer-General's Office

HSE_NO_SUF
Alias: HSE_NO_SUF
Data type: String
Width: 1
Definition: House number suffix
Definition Source: Valuer-General's Office

STREET
Alias: STREET
Data type: String
Width: 40
Definition: Street number
Definition Source: Valuer-General's Office

ST_SUFFIX
Alias: ST_SUFFIX
Data type: String
Width: 4
Definition: Street suffix
Definition Source: Valuer-General's Office

SUBURB
Alias: SUBURB
Data type: String
Width: 40
Definition: Suburb name
Definition Source: Valuer-General's Office

LOCAL_GOVE
Alias: LOCAL_GOVE
Data type: String
Width: 50
Definition: Local Government Area
Definition Source: Valuer-General's Office

YEAR_BUILT
Alias: YEAR_BUILT
Data type: String
Width: 4
Definition: Year built
Definition Source: Valuer-General's Office

WALLS
Alias: WALLS
Data type: String
Width: 6
Definition: Wall type
Definition Source: Valuer-General's Office

ROOF
Alias: ROOF
Data type: String
Width: 6
Definition: Roof type
Definition Source: Valuer-General's Office

DERIVED_AR
Alias: DERIVED_AR
Data type: Number
Width: 19
Number of decimals: 3
Definition: Derived area
Definition Source: Geoscience Australia/VGO

ROOM_COUNT
Alias: ROOM_COUNT
Data type: Number
Width: 19
Number of decimals: 3
Definition: Number of rooms
Definition Source: Valuer-General's Office

BEDROOMS
Alias: BEDROOMS
Data type: Number
Width: 19
Number of decimals: 3
Definition: Number of bedrooms
Definition Source: Valuer-General's Office

FCB
Alias: FCB
Data type: Number
Width: 19
Number of decimals: 3
Definition: Functional classification of buildings
Definition Source: Geoscience Australia

HAZ_STRUC
Alias: HAZ_STRUC
Data type: String
Width: 20
Definition: HAZUS structural building classification
Definition Source: Geoscience Australia

AREA_VGO
Alias: AREA_VGO
Data type: Number
Width: 19
Number of decimals: 3
Definition: Area by VGO
Definition Source: Geoscience Australia

WEALTH_CAT
Alias: WEALTH_CAT
Data type: String
Width: 12
Definition: Wealth category
Definition Source: Geoscience Australia/Australian Bureau Statistics (ABS)

REPLACE
Alias: REPLACE
Data type: Number
Width: 19
Number of decimals: 3
Definition: Replacement cost
Definition Source: Geoscience Australia

PIN_OLD
Alias: PIN_OLD
Data type: Number
Width: 19
Number of decimals: 3
Definition: QA/QC purposes
Definition Source: Geoscience Australia

FREQUENCY
Alias: FREQUENCY
Data type: Number
Width: 19
Number of decimals: 3
Definition: QA/QC purposes
Definition Source: Geoscience Australia

CONTENTS
Alias: CONTENTS
Data type: Number
Width: 19
Number of decimals: 3
Definition: Estimated contents replacement
Definition Source: Geoscience Australia

EQRM_AREA
Alias: EQRM_AREA
Data type: Number
Width: 19
Number of decimals: 3
Definition: Earthquake modelling building area (EQRM)
Definition Source: Geoscience Australia

YEAR
Alias: YEAR
Data type: Number
Width: 9
Definition: Estimated year built
Definition Source: Geoscience Australia

STOREYS
Alias: STOREYS
Data type: Number
Width: 9
Definition:
Number of stories
Definition Source:
Geoscience Australia

Spatial Database: FOOTPRINTS.SHP

Keywords

Theme: Building, Footprints, polygons

Description

Abstract

This database was created from 1600 CAD–MicroStation data files supplied by the WA Department of Land Information (DLI). These files were merged, cleaned and exported into an ESRI shapefile, using FME Universal Translator and other GIS software.

Purpose

To create a clean polygon shapefile so the building footprints could be spatially intersected with the Valuer General's data, and to populate attribute fields such as area and perimeter. This dataset has proven to be a valuable resource for the Reed Construction Data contract in defining replacement cost models for metropolitan Perth.

Supplementary information

The original CAD files of the building footprints primary error was topology associated. The arcs associated with the building outlines were not 'closed' to form a true polygon, approximately 10% to 15% had this data error.

The shapefile now represents approximately 600,000 building footprints that cover 280 suburbs for metropolitan Perth. The closed building footprints have been spatially intersected with the Valuer-General's Office data (VGO).

Links to graphics describing the data

Extent of shapefile (JPEG): footprints.jpg

Status of the data

Complete
Data update frequency: As needed

Time period for which the data is relevant

Beginning date and time: 1989
Ending date and time: 1999
Description: Ground condition

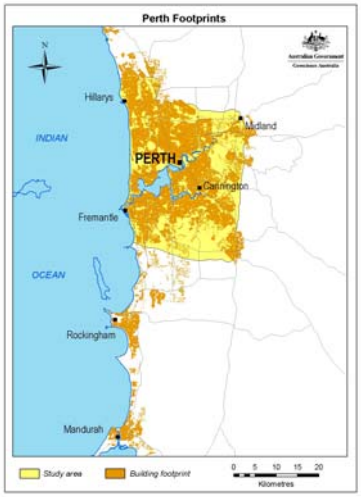

Publication information

Who created the data: GA/DLI
Date and time: from unpublished material

Data storage and access information

File name: footprints
Type of data: vector digital data
Data processing environment: Microsoft Windows 2000 Version 5.0 (Build 2195) Service Pack 4; ESRI ArcCatalog 9.0.0.535

Accessing the data

Size of the data: 116.555 MB
Data transfer size: 116.555 MB

Constraints on accessing and using the data

Access constraints: Contact DLI
Use constraints: Contact DLI

Details about this document

Contents last updated: 20050221 at time 17545000

Who completed this document

Neil Corby, Geoscience Australia

Mailing address:

P.O. Box 378
Canberra, ACT 2601
Australia
02 6249 9176 (voice)
02 6249 9986 (fax)
neil.corby@ga.gov.au

Hours of service: 7am–7pm

Contact instructions: First contact via email

Spatial description

Horizontal coordinate system

Projected coordinate system name: GDA_1994_MGA_Zone_50
Geographic coordinate system name: GCS_GDA_1994

Details

Map projection

Name: Transverse Mercator
Scale Factor at Central Meridian: 0.999600
Longitude of Central Meridian: 117.000000
Latitude of Projection Origin: 0.000000
False Easting: 500000.000000
False Northing: 10000000.000000

Planar Coordinate Information

Planar Distance Units: meters
Coordinate Encoding Method: coordinate pair

Coordinate Representation

Abscissa Resolution: 0.000256
Ordinate Resolution: 0.000256

Geodetic Model

Horizontal Datum Name: D_GDA_1994
Ellipsoid Name: Geodetic Reference System 80
Semi-major Axis: 6378137.000000
Denominator of Flattening Ratio: 298.257222

Bounding coordinates

In decimal degrees
West: 115.677391
East: 116.072916
North: -31.656055
South: -32.583995

In projected or local coordinates
Left: 375861.375000
Right: 412108.031250
Top: 6496942.500000
Bottom: 6394443.000000

Lineage

FGDC lineage
Process step 1
Process description: FME Universal Translator was used to convert the dgn files into ESRI shape files and a number of AMLs have been created to produce the closed linework. Please see FLOWCHART.jpg for lineage.
Process software and version: ArcGIS

ESRI description

footprints
ESRI feature type: Simple
Geometry type: Polygon
Topology: FALSE
Feature count: 524598
Spatial Index: FALSE
Linear referencing: FALSE

Attributes details for Footprints

Type of object: Feature Class
Number of records: 524598

Attributes

FID
Alias: FID
Data type: OID
Width: 4
Precision: 0
Scale: 0
Definition: Internal feature number.
Definition Source: ESRI

Shape
Alias: Shape
Data type: Geometry
Width: 0
Precision: 0
Scale: 0
Definition: Feature geometry
Definition Source: ESRI

AREA
Alias: AREA
Data type: Number
Width: 19
Number of decimals: 3
Definition: Feature geometry
Definition Source: ESRI

PERIMETER
Alias: PERIMETER
Data type: Number
Width: 19
Number of decimals: 3
Definition: Feature geometry
Definition Source: ESRI

BUILD_DCDB
Alias: BUILD_DCDB
Data type: Number
Width: 9
Definition: UFI
Definition Source: ESRI

FT_AREA
Alias: FT_AREA
Data type: Number
Width: 9

Number of decimals: 3

Definition: Footprint area (sourced from Arc coverage)
Definition Source: GA

FT_PERIM
Alias: FT_PERIM
Data type: Number
Width: 9
Number of decimals: 3
Definition: Footprint perimeter (sourced from Arc coverage)
Definition Source: GA

PIN
Alias: PIN
Data type: Number
Width: 19
Number of decimals: 3
Definition: VGO, Cadastre/Property number
Definition Source: VGO

Spatial Database: FT_BLD_JOIN.SHP

Keywords

Theme: Building, Footprints, Join, database, polygon

Description

Abstract

This database was created by joining the GA BUILD_DB (VGO) point database to the FOOTPRINTS (DLI) polygon shapefile using the PIN field as the unique identifying attribute for the join. Any polygons that don't join with a PIN from the point shapefile will be removed automatically – see lineage for more detail.

Purpose

This dataset is a combination of a point shapefile database which was used for earthquake modelling purposes and a polygon shapefile which was used for wind and flood vulnerability modelling.

Supplementary information

For the complete polygon shapefile of the DLI building footprints see FOOTPRINTS shapefile.
For the complete point shapefile of the GA building (VGO) database see BUILD_DB shapefile.

Links to graphics describing the data

extent of ft_bld_join shapefile (JPEG): ft_bld_join.jpg

Status of the data

Complete
Data update frequency: As needed

Time period for which the data is relevant

Beginning date and time: 1989 – 1999 DLI CAD files
Ending date and time: 2002 – VGO data
Description: Ground condition

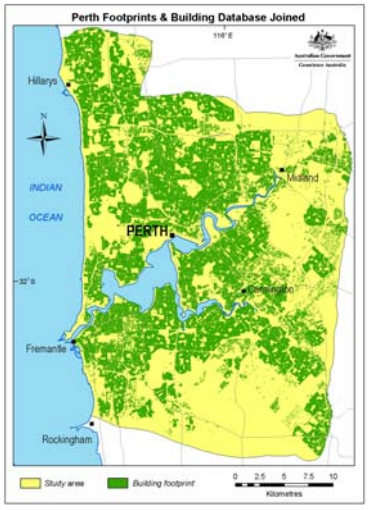

Publication information

Who created the data: GA, DLI
Date and time: from unpublished material

Data storage and access information

File name: ft_bld_join
Type of data: vector digital data
Location of the data: dvd\ft_bld_join.shp
Data processing environment: Microsoft Windows 2000 Version 5.0 (Build 2195) Service Pack 4; ESRI ArcCatalog 9.0.0.535

Accessing the data

Size of the data: 87.647 MB
Data transfer size: 87.647 MB

Constraints on accessing and using the data

Access constraints: Contact DLI/GA
Use constraints: Contact DLI/GA

Details about this document

Contents last updated: 20050221 at time 18302000

Who completed this document

Neil Corby, Geoscience Australia

Mailing address:

P.O. BOX 378
Canberra, ACT 2601
Australia
02 62499 9176 (voice)
02 62499 986 (fax)
neil.corby@ga.gov.au

Hours of service: 7am–7pm

Contact instructions: First contact via email

Spatial description

Horizontal coordinate system

Projected coordinate system name:
GDA_1994_MGA_Zone_50
Geographic coordinate system name:
GCS_GDA_1994

Details

Map projection

Name: Transverse Mercator
Scale Factor at Central Meridian: 0.999600
Longitude of Central Meridian: 117.000000
Latitude of Projection Origin: 0.000000
False Easting: 500000.000000
False Northing: 10000000.000000

Planar Coordinate Information

Planar Distance Units: meters
Coordinate Encoding Method: coordinate pair

Coordinate Representation

Abscissa Resolution: 0.000064
Ordinate Resolution: 0.000064

Geodetic Model

Horizontal Datum Name: D_GDA_1994
Ellipsoid Name: Geodetic Reference System 80
Semi-major Axis: 6378137.000000
Denominator of Flattening Ratio: 298.257222

Bounding Coordinates

Horizontal

In decimal degrees
West: 115.728199
East: 116.063865
North: -31.764324
South: -32.165607

In projected or local coordinates
Left: 380079.968750
Right: 411352.593750
Top: 6484989.000000
Bottom: 6440820.500000

Lineage

FGDC lineage
Process step 1
Process description: A join was created using the footprints dataset as the main dataset. The build_db shapefile was joined by the attribute called PIN. Any polygon which didn't join was assigned a null value and removed to produce a complete database, this is an automatic process within ArcGIS.
Process software and version: ArcGIS 9

Who did this process

Neil Corby
Geoscience Australia
mailing address:
GPO Box 378
Canberra, ACT 2601
Australia

02 6249 9176 (voice)
02 6249 9986 (fax)
neil.corby@ga.gov.au
Hours of service: 7am - 7pm
Contact Instructions:
First contact via email

ESRI description

ft_bld_join
ESRI feature type: Simple
Geometry type: Polygon
Topology: FALSE
Feature count: 384133
Spatial Index: FALSE
Linear referencing: FALSE

Attributes details for ft_bld_join

Type of object: Feature Class
Number of records: 384133

Attributes

FID
Alias: FID
Data type: OID
Width: 4
Precision: 0
Scale: 0
Definition: Internal feature number
Definition Source: ESRI

Shape
Alias: Shape
Data type: Geometry
Width: 0
Precision: 0
Scale: 0
Definition: Feature geometry
Definition Source: ESRI

AREA
Alias: AREA
Data type: Number
Width: 19
Number of decimals: 3
Definition: Area of polygon
Definition Source: ESRI

PERIMETER
Alias: PERIMETER
Data type: Number

Width: 19
Number of decimals: 3
Definition: Perimeter of polygon
Definition Source: ESRI

BUILD_DCDB
Alias: BUILD_DCDB
Data type: Number
Width: 9
Definition: UFI
Definition Source: Cadastre

PIN
Alias: PIN
Data type: Number
Width: 19
Number of decimals: 3
Definition: Property/Cadastre number
Definition Source: Valuer-General's Office

FID_1
Alias: FID_1
Data type: Number
Width: 9
Definition: Unique field identifier
Definition Source:

PROPERTY_N
Alias: PROPERTY_N
Data type: String
Width: 10
Definition: Property number
Definition Source: Geoscience Australia

CLASSIFICA
Alias: CLASSIFICA
Data type: String
Width: 50
Definition: Building classification
Definition Source: Valuer-General's Office

PROPERTY_U
Alias: PROPERTY_U
Data type: String
Width: 50
Definition: Property Usage
Definition Source: Geoscience Australia

PRIMARY_LA
Alias: PRIMARY_LA
Data type: String
Width: 20
Definition: Primary (unknown)
Definition Source: Valuer-General's Office

UNIT_NO
Alias: UNIT_NO
Data type: String
Width: 9
Definition: Unit number
Definition Source: Valuer-General's Office

HOUSE_NO
Alias: HOUSE_NO
Data type: String
Width: 9
Definition: House number
Definition Source: Valuer-General's Office

HSE_NO_SUF
Alias: HSE_NO_SUF
Data type: String
Width: 1
Definition: House number suffix
Definition Source: Valuer-General's Office

STREET
Alias: STREET
Data type: String
Width: 40
Definition: Street number
Definition Source: Valuer-General's Office

ST_SUFFIX
Alias: ST_SUFFIX
Data type: String
Width: 4
Definition: Street suffix
Definition Source: Valuer-General's Office

SUBURB
Alias: SUBURB
Data type: String
Width: 40
Definition: Suburb name
Definition Source: Valuer-General's Office

LOCAL_GOVE
Alias: LOCAL_GOVE
Data type: String
Width: 50
Definition: Local Government Area
Definition Source: Valuer-General's Office

YEAR_BUILT
Alias: YEAR_BUILT
Data type: String
Width: 4
Definition: Year built
Definition Source: Valuer-General's Office

WALLS
Alias: WALLS
Data type: String
Width: 6
Definition: Wall type
Definition Source: Valuer-General's Office

ROOF
Alias: ROOF
Data type: String
Width: 6
Definition: Roof type
Definition Source: Valuer-General's Office

DERIVED_AR
Alias: DERIVED_AR
Data type: Number
Width: 19
Number of decimals: 3
Definition: Derived area
Definition Source: Geoscience Australia/VGO

ROOM_COUNT
Alias: ROOM_COUNT
Data type: Number
Width: 19
Number of decimals: 3
Definition: Number of rooms
Definition Source: Valuer-General's Office

BEDROOMS
Alias: BEDROOMS
Data type: Number
Width: 19
Number of decimals: 3
Definition: Number of bedrooms
Definition Source: Valuer-General's Office

FCB
Alias: FCB
Data type: Number
Width: 19
Number of decimals: 3
Definition: Functional classification of buildings
Definition Source: Geoscience Australia

HAZ_STRUC
Alias: HAZ_STRUC
Data type: String
Width: 20
Definition: HAZUS structural building classification
Definition Source: Geoscience Australia

AREA_VGO
Alias: AREA_VGO
Data type: Number
Width: 19
Number of decimals: 3
Definition: Area by VGO
Definition Source: Geoscience Australia

WEALTH_CAT
Alias: WEALTH_CAT
Data type: String
Width: 12
Definition: Wealth category
Definition Source: Geoscience Australia (ABS)

REPLACE
Alias: REPLACE
Data type: Number
Width: 19
Number of decimals: 3
Definition: Replacement cost
Definition Source: Geoscience Australia

PIN_OLD
Alias: PIN_OLD
Data type: Number
Width: 19
Number of decimals: 3
Definition: QA/QC purposes
Definition Source: Geoscience Australia

FREQUENCY
Alias: FREQUENCY
Data type: Number
Width: 19
Number of decimals: 3
Definition: QA/QC purposes
Definition Source: Geoscience Australia

CONTENTS
Alias: CONTENTS
Data type: Number
Width: 19
Number of decimals: 3
Definition: Estimated contents replacement
Definition Source: Geoscience Australia

EQRM_AREA
Alias: EQRM_AREA
Data type: Number
Width: 19
Number of decimals: 3
Definition: Earthquake modelling building area
Definition Source: Geoscience Australia

YEAR
Alias: YEAR
Data type: Number
Width: 9
Definition: Estimated year built
Definition Source: Geoscience Australia

STOREYS
Alias: STOREYS
Data type: Number
Width: 9
Definition: Number of stories
Definition Source: Geoscience Australia

Spatial Database: FLOOD_SRV.SHP

Keywords

Theme: Survey, Flood, Building
Place: Perth

Description

Abstract

This dataset contains the Perth fieldwork survey completed 1–10 December 2003 for a 1 in 500 year flood zone. Building attributes were collected using PDA units, Global Positioning Systems and digital cameras.

Purpose

To capture building attributes to enter into GA's flood modelling database.

Links to graphics describing the data

Landsat image with flooding polygon with flow strength (JPEG): flood_srv.jpg

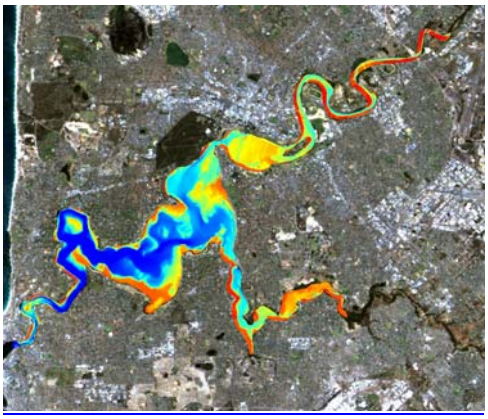

Status of the data

Complete
Data update frequency: As needed

Time period for which the data is relevant

Beginning date and time: 01/12/2003 at time 7:30am
Ending date and time: 10/12/2003 at time 4:30pm
Description: Ground condition

Publication information

Who created the data: Geoscience Australia
Date and time: from unpublished material

Data storage and access information

File name: flood_srv
Type of data: vector digital data
Location of the data: dvd\fieldwork\flood_srv.shp
Data processing environment: Microsoft Windows 2000 Version 5.0 (Build 2195) Service Pack 4; ESRI ArcCatalog 9.0.0.535

Accessing the data

Size of the data: 0.056 MB
Data transfer size: 0.056 MB

Constraints on accessing and using the data

Access constraints: Contact GA
Use constraints: Contact GA

Details about this document

Contents last updated: 20050222 at time 12263500

Who completed this document

Neil Corby, Geoscience Australia

Mailing address:

P.O. BOX 378
Canberra, ACT 2601
Australia
02 62499 9176 (voice)
02 62499 986 (fax)
neil.corby@ga.gov.au

Hours of service: 7am–7pm

Contact instructions: First contact via email

Spatial description

Horizontal coordinate system

Projected coordinate system name: WGS_1984_UTM_Zone_50S
Geographic coordinate system name: GCS_WGS_1984

Details

Grid Coordinate System Name: Universal Transverse Mercator
UTM Zone Number: -50

Transverse Mercator Projection
Scale Factor at Central Meridian: 0.999600
Longitude of Central Meridian: 117.000000
Latitude of Projection Origin: 0.000000

False Easting: 500000.000000
False Northing: 10000000.000000

Planar Coordinate Information

Planar Distance Units: meters
Coordinate Encoding Method: coordinate pair

Coordinate Representation

Abscissa Resolution: 0.000032
Ordinate Resolution: 0.000032

Geodetic Model

Horizontal Datum Name: D_WGS_1984
Ellipsoid Name: WGS_1984
Semi-major Axis: 6378137.000000
Denominator of Flattening Ratio: 298.257224

Bounding coordinates

Horizontal

In decimal degrees
West: 115.876936
East: 116.003628
North: -31.895418
South: -32.036597

In projected or local coordinates
Left: 393958.553216
Right: 405779.657371
Top: 6470607.962976
Bottom: 6455072.569810

Lineage

FGDC lineage
Process step 1
Process description: Capture building attributes with PDA units, GPS and digital camera. 3 field data capture units were used and the data combined to make this dataset. Photos renamed using photo.aml to match unit number.
Process software and version: ArcPad Version 6.0.1 and ArcGIS 8.3
Process date: 10/12/2004 at 5:00pm

Spatial data quality

Horizontal positional accuracy
All point locations were placed within the cadastre boundary. GPS position is accurate to +/- 10m
Estimated accuracy: +/- 10m
How this value was determined: More likely to be +/- 5m due to GPS readings

Vertical positional accuracy
Was not captured

Spatial data description

Vector data information

ESRI description

flood_srv
ESRI feature type: Simple
Geometry type: Point
Feature description: Building site attributes
Topology: FALSE
Feature count: 2092
Spatial Index: FALSE
Linear referencing: FALSE

Attributes details for flood_srv

Type of object: Feature Class
Number of records: 2092

Attributes

FID
Alias: FID
Data type: OID
Width: 4
Precision: 0
Scale: 0
Definition: Internal feature number
Definition Source: ESRI

Shape
Alias: Shape
Data type: Geometry
Width: 0
Precision: 0
Scale: 0
Definition: Feature geometry
Definition Source: ESRI

ID
Alias: ID
Data type: Number
Width: 6
Definition: UFI
Definition Source: ESRI

CONSTR
Alias: CONSTR
Data type: Number
Width: 4
Definition: Construction site if equal to 1
Definition Source: Geoscience Australia

HOUSE_TXT
Alias: HOUSE_TXT
Data type: String
Width: 10
Definition:
Housing number
Definition Source:
Geoscience Australia

STREET
Alias: STREET
Data type: String

Width: 35
Definition: Street address
Definition Source: Geoscience Australia

SUBURB
Alias: SUBURB
Data type: String
Width: 20
Definition: Suburb
Definition Source: Geoscience Australia

DATETIME
Alias: DATETIME
Data type: Date
Width: 8
Definition: Date collected
Definition Source: Geoscience Australia

CAM_JPG
Alias: CAM_JPG
Data type: String
Width: 20
Definition: Camera filename for a photo
Definition Source: Geoscience Australia

CAM_MOV
Alias: CAM_MOV
Data type: String
Width: 20
Definition: Camera filename for a movie
Definition Source: Geoscience Australia

AGE
Alias: AGE
Data type: String
Width: 15
Definition: Estimated age of building
Definition Source: Geoscience Australia

LIV_UNIT
Alias: LIV_UNIT
Data type: Number
Width: 9
Definition: Number of living units in complex
Definition Source: Geoscience Australia

BASEMENT
Alias: BASEMENT
Data type: String
Width: 10
Definition: Number of basements levels
Definition Source: Geoscience Australia

STOREYS
Alias: STOREYS
Data type: String
Width: 30
Definition: Number of storeys
Definition Source: Geoscience Australia

FLOOR_H
Alias: FLOOR_H
Data type: String
Width: 10
Definition: Floor height
Definition Source: Geoscience Australia

EAVE_H
Alias: EAVE_H
Data type: String
Width: 10
Definition: Eaves height
Definition Source: Geoscience Australia

WIDTH
Alias: WIDTH
Data type: String
Width: 10
Definition: Width of building
Definition Source: Geoscience Australia

DEPTH
Alias: DEPTH
Data type: String
Width: 10
Definition: Depth of building
Definition Source: Geoscience Australia

ROOF_TYPE
Alias: ROOF_TYPE
Data type: String
Width: 20
Definition: Roof material
Definition Source: Geoscience Australia

ROOF_SHAPE
Alias: ROOF_SHAPE
Data type: String
Width: 25
Definition: Roof shape
Definition Source: Geoscience Australia

ROOF_PITCH
Alias: ROOF_PITCH
Data type: String
Width: 10
Definition: Roof pitch
Definition Source: Geoscience Australia

ROOF_EAVES
Alias: ROOF_EAVES
Data type: String
Width: 10
Definition: Width of eaves
Definition Source: Geoscience Australia

SOFFIT
Alias: SOFFIT
Data type: Number
Width: 4
Definition: Under eaves covering
Definition Source: Geoscience Australia

SKYLIGHT
Alias: SKYLIGHT
Data type: String
Width: 15
Definition: Skylight exists
Definition Source: Geoscience Australia

ROOF_SPAN
Alias: ROOF_SPAN
Data type: String

Width: 10
Definition: Roof span
Definition Source: Geoscience Australia

STRUCTURE
Alias: STRUCTURE
Data type: String
Width: 35
Definition: Structural type
Definition Source: Geoscience Australia

FOUNDATION
Alias: FOUNDATION
Data type: String
Width: 25
Definition: Foundation type
Definition Source: Geoscience Australia

WALLS
Alias: WALLS
Data type: String
Width: 25
Definition: Wall type
Definition Source: Geoscience Australia

GABLE
Alias: GABLE
Data type: String
Width: 15
Definition: How many gables
Definition Source: Geoscience Australia

PARAPET
Alias: PARAPET
Data type: String
Width: 10
Definition: Parapet percentage of width
Definition Source: Geoscience Australia

PARA_HGT
Alias: PARA_HGT
Data type: String
Width: 10
Definition: Parapet height
Definition Source: Geoscience Australia

ROOF_VENT
Alias: ROOF_VENT
Data type: Number
Width: 4
Definition: Roof ventalation
Definition Source: Geoscience Australia

WALL_VENT
Alias: WALL_VENT
Data type: Number
Width: 4
Definition: Wall ventalation
Definition Source: Geoscience Australia

CHIMNEY
Alias: CHIMNEY
Data type: String
Width: 20
Definition: Chimney exists + height
Definition Source: Geoscience Australia

VERANDA
Alias: VERANDA
Data type: String
Width: 20
Definition: Verandah
Definition Source: Geoscience Australia

WIN_PROT
Alias: WIN_PROT
Data type: Number
Width: 4
Definition: Window protectors
Definition Source: Geoscience Australia

WIN_SIZE
Alias: WIN_SIZE
Data type: String
Width: 15
Definition: Window size
Definition Source: Geoscience Australia

WIN_PERC
Alias: WIN_PERC
Data type: String
Width: 15
Definition: Window percentage cover
Definition Source: Geoscience Australia

SILL_HGT
Alias: SILL_HGT
Data type: String
Width: 15
Definition: Sill height
Definition Source: Geoscience Australia

TREE
Alias: TREE
Data type: Number
Width: 4
Definition: Tree danger
Definition Source: Geoscience Australia

NEAREST
Alias: NEAREST
Data type: String
Width: 10
Definition: Nearest building
Definition Source: Geoscience Australia

PLAN_REGUL
Alias: PLAN_REGUL
Data type: String
Width: 25
Definition: Plan regularity
Definition Source: Geoscience Australia

VERT_REGUL
Alias: VERT_REGUL
Data type: String
Width: 25
Definition: Vertical regularity
Definition Source: Geoscience Australia

PARKING
Alias: PARKING
Data type: String

Width: 25
Definition: Parking
Definition Source: Geoscience Australia

P_SPACE
Alias: P_SPACE
Data type: String
Width: 10
Definition: Number of parking spaces
Definition Source: Geoscience Australia

P_MATERIAL
Alias: P_MATERIAL
Data type: String
Width: 25
Definition: Garage material
Definition Source: Geoscience Australia

P_DOOR
Alias: P_DOOR
Data type: String
Width: 15
Definition: Garage door
Definition Source: Geoscience Australia

STRUC_COM
Alias: STRUC_COM
Data type: String
Width: 60
Definition: Other structures
Definition Source: Geoscience Australia

CONFID
Alias: CONFID
Data type: String
Width: 10
Definition: Confidence in data collected
Definition Source: Geoscience Australia

INDUSTRY
Alias: INDUSTRY
Data type: String
Width: 15
Definition: Industry type
Definition Source: Geoscience Australia

CATEGORY
Alias: CATEGORY
Data type: String
Width: 20
Definition: Category type
Definition Source: Geoscience Australia

TYPE
Alias: TYPE
Data type: String
Width: 15
Definition: Usage type
Definition Source: Geoscience Australia

COMMENT
Alias: COMMENT
Data type: String
Width: 60
Definition: Comment field
Definition Source: Geoscience Australia

SPARE1
Alias: SPARE1
Data type: String
Width: 30
Definition: Spare field
Definition Source: Geoscience Australia

SPARE2
Alias: SPARE2
Data type: String
Width: 30
Definition: spare field
Definition Source: Geoscience Australia

UFI
Alias: UFI
Data type: Number
Width: 8
Definition: Unique field number
Definition Source: Geoscience Australia

PICTURE
Alias: PICTURE
Data type: String
Width: 75
Definition: picture jpg filename
Definition Source: Geoscience Australia

MOVIE
Alias: MOVIE
Data type: String
Width: 75
Definition: movie filename
Definition Source: Geoscience Australia

Spatial Database: CBD_SRV.SHP

Keywords

Theme: Buildings, points, database, GA
Place: Perth CBD

Description

Abstract

Fieldwork completed in the Perth CBD area using PDA units, GPS and digital cameras. Photos were taken of individual buildings and can be connected using attribute field photo_l.

Purpose

This database was used for the Perth Counter Terrorism exercise and 3D modelling.

Links to graphics describing the data

Screen snap of ArcGIS (JPEG): cbd_srv.jpg

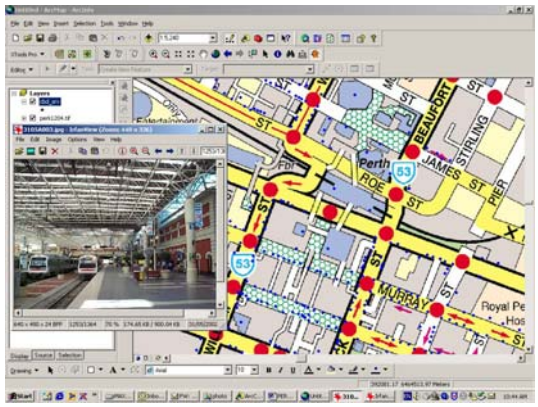

Status of the data

Complete
Data update frequency: As needed

Time period for which the data is relevant

Date and time: May 2002
Description: Ground condition

Publication information

Who created the data: Geoscience Australia
Date and time: from unpublished material

Data storage and access information

File name: cbd_srv
Type of data: vector digital data
Location of the data:
dvd\fieldwork2\cbd_srv.shp
Data processing environment: Microsoft Windows 2000 Version 5.0 (Build 2195) Service Pack 4; ESRI ArcCatalog 9.0.0.535

Accessing the data

Size of the data: 0.028 MB
Data transfer size: 0.028 MB

Constraints on accessing and using the data

Access constraints: Contact GA
Use constraints: Contact GA

Details about this document

Contents last updated: 20050223 at time 10272800

Who completed this document

Neil Corby, Geoscience Australia

Mailing address:

P.O. BOX 378
Canberra, ACT 2601
Australia
02 62499 9176 (voice)
02 62499 986 (fax)
neil.corby@ga.gov.au

Hours of service: 7am–7pm

Contact instructions: First contact via email

Spatial description

Horizontal coordinate system

Projected coordinate system name:
GDA_1994_MGA_Zone_50
Geographic coordinate system name:
GCS_GDA_1994

Details

Map Projection

Name: Transverse Mercator
Scale Factor at Central Meridian: 0.999600
Longitude of Central Meridian: 117.000000
Latitude of Projection Origin: 0.000000
False Easting: 500000.000000
False Northing: 10000000.000000

Planar Coordinate Information

Planar Distance Units: meters
Coordinate Encoding Method: coordinate pair

Coordinate Representation

Abscissa Resolution: 0.000128
Ordinate Resolution: 0.000128

Geodetic Model

Horizontal Datum Name: D_GDA_1994
Ellipsoid Name: Geodetic Reference System 80
Semi-major Axis: 6378137.000000
Denominator of Flattening Ratio: 298.257222

Bounding coordinates

Horizontal

In decimal degrees
West: 115.737191
East: 116.067647
North: -31.717430
South: -32.246440

In projected or local coordinates
Left: 381033.247246
Right: 411666.179387
Top: 6490199.000000
Bottom: 6431862.036641

Lineage

FGDC lineage
Process step 1
Process description: Data collected using PDA, GPS and digital cameras
Process software and version: ArcPAD 5.0.1
Process date: 2002

Who did this process

Don Gordon, Geoscience Australia
Mailing address as above
donald.gordon@ga.gov.au

Hours of service: 7am–7pm

Contact instructions: First contact via email

Spatial data quality

Horizontal positional accuracy

GPS units used were accurate to +/- 10m, building footprints and cadastre were used in the field to place points into polygons when GPS units could not find satellites.

ESRI description

cbd_srv
ESRI feature type: Simple
Geometry type: Point
Topology: FALSE
Feature count: 1038
Spatial Index: FALSE
Linear referencing: FALSE

Attributes details for cbd_srv

Type of object: Feature Class
Number of records: 1038

Attributes

FID
Alias: FID
Data type: OID
Width: 4
Precision: 0
Scale: 0
Definition: Internal feature number
Definition Source: ESRI

Shape
Alias: Shape
Data type: Geometry
Width: 0
Precision: 0
Scale: 0
Definition: Feature geometry
Definition Source: ESRI

STUD_PT_ID
Alias: STUD_PT_ID
Data type: Number
Width: 9
Definition: UFI
Definition Source: ESRI

CONSTR
Alias: CONSTR
Data type: Number
Width: 4
Definition: Construction site if equal to 1
Definition Source: Geoscience Australia

QUALITY
Alias: QUALITY
Data type: Number
Width: 4
Definition: QA/QC
Definition Source: Geoscience Australia

UNIT
Alias: UNIT
Data type: String
Width: 6
Definition: PDA unit used
Definition Source: Geoscience Australia

DATETIME
Alias: DATETIME
Data type: Date
Width: 8
Definition: Date of collection
Definition Source: Geoscience Australia

HOUSE_NUM
Alias: HOUSE_NUM
Data type: String
Width: 5
Definition: House number
Definition Source: Geoscience Australia

HOUSE_TXT
Alias: HOUSE_TXT
Data type: String
Width: 10

Definition: House letter
Definition Source: Geoscience Australia

STREET
Alias: STREET
Data type: String
Width: 20
Definition: Street address
Definition Source: Geoscience Australia

SUBURB
Alias: SUBURB
Data type: String
Width: 20
Definition: Suburb
Definition Source: Geoscience Australia

AGE
Alias: AGE
Data type: String
Width: 20
Definition: Estimated age of building
Definition Source: Geoscience Australia

CAM_INDEX1
Alias: CAM_INDEX1
Data type: String
Width: 3
Definition: Camera index
Definition Source: Geoscience Australia

CAM_INDEX2
Alias: CAM_INDEX2
Data type: String
Width: 3
Definition: Camera index
Definition Source: Geoscience Australia

LIV_UNIT
Alias: LIV_UNIT
Data type: String
Width: 8
Definition: Number of living units in complex
Definition Source: Geoscience Australia

BASEM
Alias: BASEM
Data type: String
Width: 8
Definition: Number of basements levels
Definition Source: Geoscience Australia

STOREYS
Alias: STOREYS
Data type: String
Width: 8
Definition: Number of storeys (times by 3.5 to get building height)
Definition Source: Geoscience Australia

HEIGHT1
Alias: HEIGHT1
Data type: String
Width: 8
Definition: Floor height
Definition Source: Geoscience Australia

HEIGHT2
Alias: HEIGHT2
Data type: String
Width: 8
Definition: Eaves height
Definition Source: Geoscience Australia

FLOOR_WID
Alias: FLOOR_WID
Data type: String
Width: 8
Definition: Width of building
Definition Source: Geoscience Australia

FLOOR_DEP
Alias: FLOOR_DEP
Data type: String
Width: 8
Definition: Depth of building
Definition Source:
Geoscience Australia

NEAREST
Alias: NEAREST
Data type: String
Width: 8
Definition: Nearest building
Definition Source: Geoscience Australia

PLAN_REGUL
Alias: PLAN_REGUL
Data type: String
Width: 15
Definition: Plan regularity
Definition Source: Geoscience Australia

VERT_REGUL
Alias: VERT_REGUL
Data type: String
Width: 15
Definition: Vertical regularity (soft storey e.g. car park under)
Definition Source: Geoscience Australia

FOUNDATION
Alias: FOUNDATION
Data type: String
Width: 20
Definition: Foundation type
Definition Source: Geoscience Australia

WALLS
Alias: WALLS
Data type: String
Width: 35
Definition: Wall type
Definition Source: Geoscience Australia

ROOF_MAT
Alias: ROOF_MAT
Data type: String
Width: 10
Definition: Roof material
Definition Source: Geoscience Australia

WINDOWS
Alias: WINDOWS
Data type: String
Width: 8
Definition: Window size
Definition Source: Geoscience Australia

WIN_PROT
Alias: WIN_PROT
Data type: Number
Width: 4
Definition: Window protectors fitted
Definition Source: Geoscience Australia

VERAN
Alias: VERAN
Data type: String
Width: 10
Definition: Veranda attached
Definition Source: Geoscience Australia

BRI_CHIM
Alias: BRI_CHIM
Data type: String
Width: 4
Definition: Brick chimney height
Definition Source: Geoscience Australia

BRI_PARA
Alias: BRI_PARA
Data type: String
Width: 4
Definition: Brick parapet height
Definition Source: Geoscience Australia

BRI_FENC
Alias: BRI_FENC
Data type: String
Width: 4
Definition: Brick fence
Definition Source: Geoscience Australia

GABLE
Alias: GABLE
Data type: Number
Width: 4
Definition: Gable end
Definition Source: Geoscience Australia

SOFFIT
Alias: SOFFIT
Data type: Number
Width: 4
Definition: Soffit (Eaves exists)
Definition Source: Geoscience Australia

WAT_TANK
Alias: WAT_TANK
Data type: Number
Width: 4
Definition: Water tank
Definition Source: Geoscience Australia

VENT
Alias: VENT
Data type: Number
Width: 4
Definition: Roof ventilation
Definition Source: Geoscience Australia

PARK_STR
Alias: PARK_STR
Data type: String
Width: 20
Definition: Park structure
Definition Source: Geoscience Australia

PARK_SPA
Alias: PARK_SPA
Data type: String
Width: 20
Definition: Number of parking spaces
Definition Source: Geoscience Australia

PARK_MAT
Alias: PARK_MAT
Data type: String
Width: 20
Definition: Parking material
Definition Source: Geoscience Australia

STR1_NUM
Alias: STR1_NUM
Data type: String
Width: 8
Definition: Other structures
Definition Source: Geoscience Australia

STR1_SIZ
Alias: STR1_SIZ
Data type: String
Width: 8
Definition: Other structures size
Definition Source: Geoscience Australia

STR1_MAT
Alias: STR1_MAT
Data type: String
Width: 20
Definition: Other structures material
Definition Source: Geoscience Australia

STR2_NUM
Alias: STR2_NUM
Data type: String
Width: 8
Definition: Other structures2
Definition Source: Geoscience Australia

STR2_SIZ
Alias: STR2_SIZ
Data type: String
Width: 8
Definition: Other structures2 size
Definition Source: Geoscience Australia

STR2_MAT
Alias: STR2_MAT
Data type: String
Width: 20
Definition: Other structures2 material
Definition Source: Geoscience Australia

CONFID
Alias: CONFID
Data type: String
Width: 10
Definition: Confidence in collection
Definition Source: Geoscience Australia

BUILD_TYPE
Alias: BUILD_TYPE
Data type: String
Width: 40
Definition: Building structure
Definition Source: Geoscience Australia

FEAT_IND
Alias: FEAT_IND
Data type: String
Width: 20
Definition: Industry type
Definition Source: Geoscience Australia

FEAT_CAT
Alias: FEAT_CAT
Data type: String
Width: 20
Definition: Category type
Definition Source: Geoscience Australia

FEAT_TYPE
Alias: FEAT_TYPE
Data type: String
Width: 20
Definition: Usage type
Definition Source: Geoscience Australia

UFI
Alias: UFI
Data type: Number
Width: 8
Definition: UFI
Definition Source: Geoscience Australia

PHOTO_L
Alias: PHOTO_L
Data type: String
Width: 12
Definition: Photo link attribute
Definition Source: Geoscience Australia

Standards used to create this document and preceding metadata

Standard name: FGDC Content Standards for Digital Geospatial Metadata
Standard version: FGDC-STD-001-1998
Time convention used in this document: local time

Metadata profiles defining additional information
ESRI Metadata Profile:
http://www.esri.com/metadata/esriprof80.html

Perth Spatial Database Metadata on PROCESSES

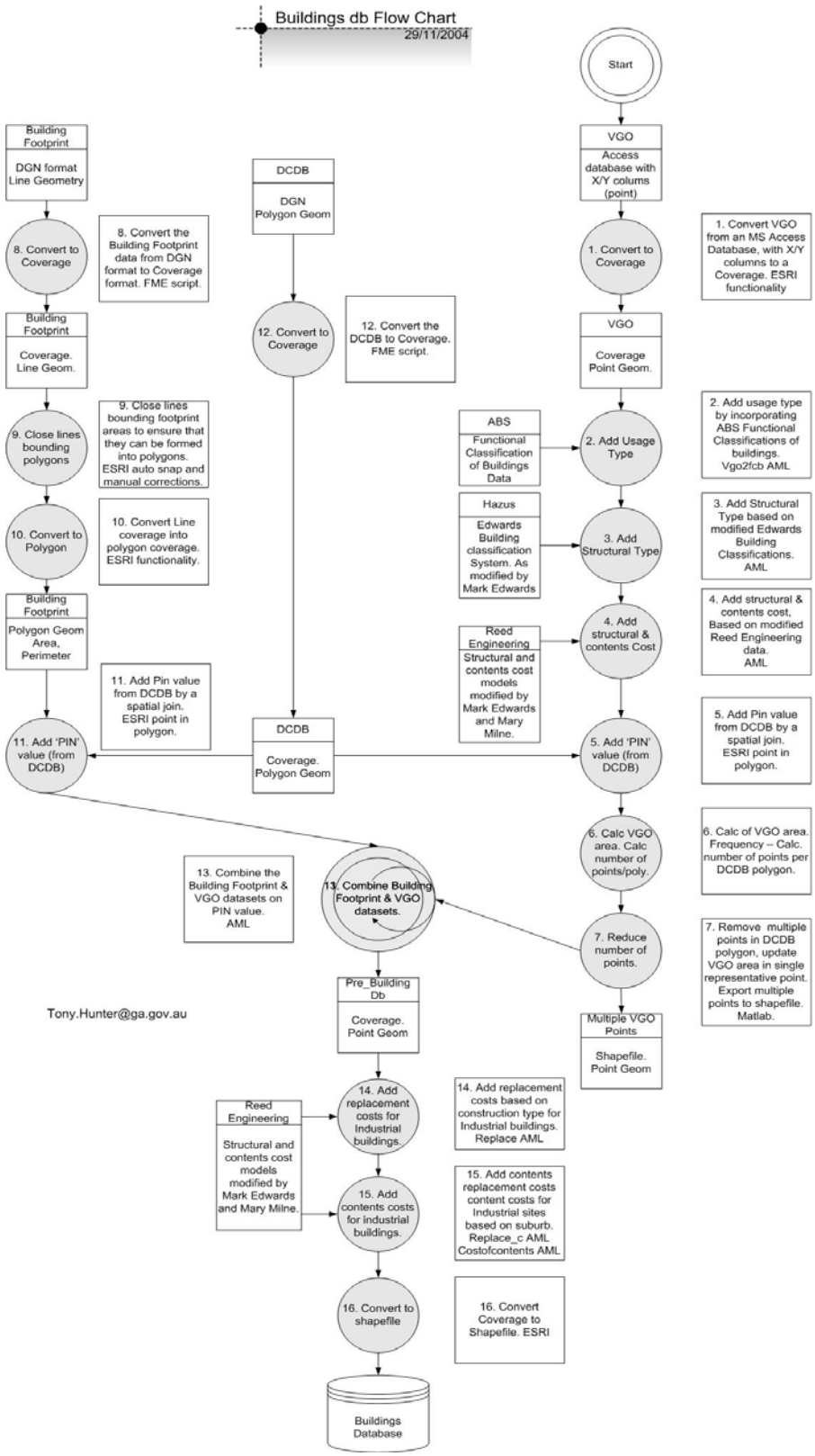

ESRI: Arc Marco Language (AMLs) created

Location: dvd/processes
AML
CONTENTS.AML
COSTOFCONTENTS.AML
REPLACE_C.AML
SUB_POST.AML
STRUC_MAP.AML
BUILD_MARK.AML
BUILD_PTH.AML
BUILD_PTH1.AML
BUILD1.AML
BUILD2.AML
BUILD3.AML
BUILD4.AML

VGO2FCB.AML

Creator: JUSTIN WHITE
Date: 04/02/04
This AML is the one used to map the VGO 2002 input file to the FCB classification system.

Files required: VGO (coverage)

CONTENTS.AML

Creator: JUSTIN WHITE
Date: 04/11/03
Modified: 09/08/04
This AML sets the contents value per square metre, based on Reed construction data and Mary Milne (GA) modifications and interpretations.

Files required: VGO (coverage)

COSTOFCONTENTS.AML

Creator: JUSTIN WHITE
Date: 04/11/03
Modified: 25/05/04
This AML is the one used to classify suburbs regarding their contents quality. Information was derived by Reed Construction and modified by Mary Milne using Census 2001 data.

Files required: VGO (coverage)

REPLACE_C.AML

Creator: JUSTIN WHITE
Date: 04/11/03
Modified: 09/08/04
This AML sets the replacement cost per square metre. Based on Reed construction data and Mark Edwards' modifications.

Files required: VGO (coverage)

SUB_POST.AML

Creator: JUSTIN WHITE
Date: 04/11/03
Modified: 09/08/04
This AML sets the postcode for each suburb.

Files required: VGO (coverage)

STRUC_MAP.AML

Creator: JUSTIN WHITE
Date: 04/11/03
Modified: 25/05/04
This AML maps the Edwards structural classification (based on HAZUS) to the building use, wall and roof. Information from Mark Edwards with reference to HAZUS.

Files required: VGO (coverage)

BUILD_MARK.AML

BUILD_PTH1.AML

BUILD_PTH.AML

Creator: KANE ORR and JUSTIN WHITE
Date: 05/05/03
Modified: 25/11/03
These AML's join Perth VGO residential data to building footprints through a series of steps that involve intersecting the Perth cadastre (1 only may need to be run).

Files required:
1. DCDB coverage
2. postcode_clips_shp (folder contains shapefiles)
3. VGO
4. info

Final output file not to be deleted, all redundant coverages will be deleted automatically, selected VGO attributes will be deleted in the final coverage

Each time the AML is run it will put the VGO data into the building footprints coverage.. Each time a new file is to run through this AML you need to change (name_of_shape) and (suburb_clip_zone) with the building footprint shapefile and suburb clip shapefile respectively.

BUILD1.AML

BUILD2.AML

BUILD3.AML

BUILD4.AML

Creator: JUSTIN WHITE
Date: 05/05/03
Modified: 17/11/03
These AMLs join Perth building footprints through a series of steps that takes lines and combines them into a polygon coverage.

Files required:
1. DCDB
2. postcode_clips_shp (folder contains shapefiles)
3. info

Final output file not to be deleted, all redundant coverages will be deleted automatically, selected VGO attributes will be deleted in the final coverage

Each time the AML is run it will put the VGO data into the building footprints coverage. Each time a new file is to run through this AML you need to change (name_of_shape) and (suburb_clip_zone) with the building footprint shapefile and suburb clip shapefile respectively.

Perth Spatial Database Metadata on VALIDATION CHECKS

Geoscience Australia

Attribute Checks

- Range checks on all individual attribute columns.
- Comparison of FCB and Classification pairs.
- Comparison of Haz-struc, Walls and Roof triplets.

Feature Count Checks

- Detection of mismatch between numbers of buildings per parcel from VGO database and Building Footprint database.

Building Area Checks

- Comparison of building areas from VGO database and Building Footprint database.
- Comparison of aggregated areas of building(s) per parcel from VGO database and Building Footprint database taking into consideration multiple buildings on a single parcel.

Perth Microtremor Survey DATA LINEAGE

Perth Microtremor Survey

- Field data-collection was carried out from 23rd October 2001 to 23rd November 2001
- Team of 5 persons (one being a GIS specialist) form Geoscience Australia - Geohazards – Cities Project Perth
- Each with a standard set field equipment:
  - Pentium Laptop > 166MhZ
  - Windows 98
  - PCMCIA type 1 slot
  - LabView Microtremor application software
  - 48 Meg PCMCIA data card
  - PAR4CH 24 bit 4 Channel Analog to Digital Converter
  - Calibration pulse box
  - 12v to 240 volt inverter
  - 12v SLA battery and charger
  - Garmin 12 GPS
  - Various cables
  - Mark Products L4C3D seismometer
  - Safety cones and triangle, safety vest and mobile phone.
  - Street directory and colour copy of individual pages (with borehole and geology data overlaid).
- High end Dell Laptop with ESRI GIS software was used as BASE PC & used for download of data from field units each evening, as well as data processing & backup
- In excess of 3000 sites recorded
- On a 500m rectangular grid across the Perth Metropolitan area (minor relocation for OH&S or proximity to borehole sites permitted)

- Total area covered approx. 800 km^2

GPS calibration site

All GPS units were calibrated on a State Survey Mark at the beginning and end of the survey. A single reading taken by each GPS (at the same time), using WGS 84 Datum which was the closest available to GDA 94.

  - SSM APPLECROSS 26
  - Datum GDA 94
  - Easting 393272.874
  - Northing 6458358.989
  - AHD 11.112M

- However the UBD (edition 44) directories used AGD 66 Datum , so the GPS units were reset to **AGD 66** for this data collection exercise.

Field Recording Guidelines

1) Wait for the GPS to give a position and check the Eastings and Northings are close to the desired position on the UBD, and or near bore site
2) Run *setup.exe* on the laptop and check the settings are correct
3) Run *microtremor.exe*. Wait for 10 positions on the GPS to be averaged
4) Add comments in site information box in the order site material/ landuse/ weather/ other
5) Check all channels from the seismometer are working and the accumulating spectra look realistic
6) Check that the calibration looks OK. An unlevelled seismometer would be apparent here
7) Acquire the data and check the sample spectra look realistic and note the site number
8) After about 400 secs save and exit.
9) Check the file size is around 1.3 MB
10) Pack up and move to the next site.

All recording sets, recorded the same site for comparison and accuracy (at the same time) at the beginning, middle and end of the survey. This site was on the southern side of the Swan River opposite the city.

Microtremor Recording Procedure in the field

Each operator given mapped area of the PMA. The sites pre-selected on a rectangular grid of 500 metres. However, minor adjustments to the actual recording site was made by the operator using the following guidelines:

1) The site chosen should be as close as possible, within reason, to the grid reference
2) If a registered borehole is marked near to the site, then it is advantageous to bias the observation site so that it is nearest as possible to it.
3) Stable compacted ground is preferred. Road base or bitumen is normally used, otherwise dig a hole down to solid ground. Concrete (especially drains) may have a cavity underneath and hence should be avoided. Also large or tall objects like trees and power transformers, excessive wind or rain, pedestrians will introduce noise.
4) Safety of personnel and equipment is most important, so do not put yourself at risk. Use safety cones and/or triangles at a safe distance around the equipment.
5) Run out the seismometer keeping it clear of the car.
6) The seismometer should be oriented to the north and levelled.

The microtremor interpretation at base (field office)

- Nightly download of the day's data from each field laptop, onto the Base GIS Laptop,
- Scaling the fundamental period for each of the days recordings using this Base Computer for interpreting the plots generated by *MatLab software.*
- Two parameters scaled from each of the spectral plots
  - Natural period of vibration of the ground and quality factor (A,B,C).
  - The quality factor was an expression of how sharp and pronounced the resonance was observed
  - All data files were lodged into the Microtremor sub-directory on the PC

Saving the interpreted data created a text file. The natural period and quality, along with site ID and location, are stored in a ".txt" file and were ultimately transferred into another software environment known as *ArcView* by the designated GIS officer in the field party.

GIS component

- All .txt files were then converted to Event themes in ESRI ArcView & combined into one daily file and backed up by date of collection.
- Event theme converted to shape file as Lat / long file in AGD66

- Shape file reprojected to WGS84 (closest available to GDA94) using the ESRI Projection Utility Wizard extension.
- Daily shape file added to previous day's combination shape file, to produce a daily hard copy & digital map of survey progress & suspect site recordings requiring a revisit.
- Once the point data was spatially located in ArcView GIS, the natural period values were used for giving a visual impression of natural period using contouring over the study area. The contouring process was of little value, until adequate areas had been covered by the field party.

Once back at head office all field data was re-scrutinised & values refined.

Ultimately only sites that were considered to the highest confidence of quality factor (A & B) were to be used for site class mapping.

Name and location of microtremor coverage, as at 11/11/04

Data Type: Point Feature Class
Coverage: V:\5\cit\perth\hazards\earthquake\microtremor\mt_18-01_a-b.shp
Feature Class: point
Coordinate System: Transverse_Mercator
False_Easting: 500000.000000
False_Northing: 10000000.000000
Central_Meridian: 117.000000
Scale_Factor: 0.999600
Latitude_Of_Origin: 0.000000
GCS_GDA_1994
Datum: D_GDA_1994
Prime Meridian: 0

Items/Attributes imported from field units

Field	Value
FID	153
Shape	Point
AREA	0
PERIMETER	0
MT_22-12_A-B#	153
MT_22-12_A-B-ID	204
ID	1204
LONG	115.8348
LAT	-32.0671
NATURAL_FR	1.9878
NATURAL_PE	0.50307
QUALITY	B
UTC_DATE	4/11/2001
UTC_TIME	31/12/1899
PROJECT_NA	Perth 200
GROUP_ID	1
OPERATOR	Brian
GEOPHONE_I	608
SITE_INFO	bit uni carpark some breeze rel traffic free near grid out of order
SAMPLE_RAT	100
$POLYGONID	153
$SCALE	1
$ANGLE	1

Perth Seismic Cone Penetrometer SURVEY DATA

Contractor

Probedrill Pty Ltd, 17 Wichmann Road, Attadale, W.A., 6156

Survey information

Survey No.	Survey Dates	No. of Sites	Data File ID Numbers
1	Jan-May 2002	16	GSA001-GSA016
2	31 Mar 2003 - 30 Apr 2003	24	GSA017-GSA039 (site 14 - no data file)
3	May 2003	18	GSA040-GSA057

Equipment:
24 tonne truck-mounted electric friction-cone penetrometer with seismic testing.

Cone Information:
Serial Numbers - 667TC and 823TC
Seismic geophone 250 mm from cone tip.
Marker, Delay and Velocity selected by Hogentogler & Co., Inc. Seismic Program C.P.T. Seismic Version 1.07A and Probedrill Pty Ltd.

Testing interval - 1.5m

Measurement Units:
Metric, Absolute (SI)

Testing standard:
AS 1289.6.5.1 – 1999

Data Formats and Storage

Data were provided to GA in hardcopy (paper) and digital form, the latter as ASCII files (.CPD extension). These files were converted to text files (see figure below) using Coneplot software supplied by Probedrill Pty Ltd (Coneplot, version 2.30 Beta, April 2002 - Hogentogler & Co., Inc.).

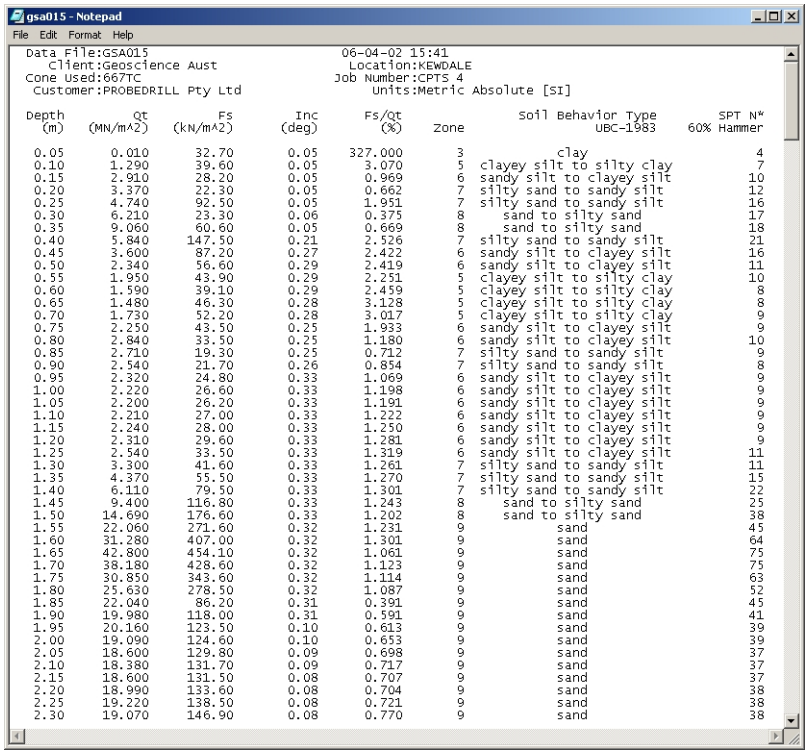

gsa015 - Notepad

File Edit Format Help

Data File:GSA015 06-04-02 15:41
Client:Geoscience Aust Location:KEWDALE
Cone Used:667TC Job Number:CPTS 4
Customer:PROBEDRILL Pty Ltd Units:Metric Absolute [SI]

Depth (m)	Qt (MN/m^2)	Fs (kN/m^2)	Inc (deg)	Fs/Qt (%)	Zone	Soil Behavior Type UBC-1983	SPT N^ 60% Hammer
0.05	0.010	32.70	0.05	327.000	3	clay	4
0.10	1.290	39.60	0.05	3.070	5	clayey silt to silty clay	7
0.15	2.910	28.20	0.05	0.969	6	sandy silt to clayey silt	10
0.20	3.370	22.30	0.05	0.662	7	silty sand to sandy silt	12
0.25	4.740	92.50	0.05	1.951	7	silty sand to sandy silt	16
0.30	6.210	23.30	0.06	0.375	8	sand to silty sand	17
0.35	9.060	60.60	0.05	0.669	8	sand to silty sand	18
0.40	5.840	147.50	0.21	2.526	7	silty sand to sandy silt	21
0.45	3.600	87.20	0.27	2.422	6	sandy silt to clayey silt	16
0.50	2.340	56.60	0.29	2.419	6	sandy silt to clayey silt	11
0.55	1.950	43.90	0.29	2.251	5	clayey silt to silty clay	10
0.60	1.590	39.10	0.29	2.459	5	clayey silt to silty clay	8
0.65	1.480	46.30	0.28	3.128	5	clayey silt to silty clay	8
0.70	1.730	52.20	0.28	3.017	5	clayey silt to silty clay	9
0.75	2.250	43.50	0.25	1.933	6	sandy silt to clayey silt	9
0.80	2.840	33.50	0.25	1.180	6	sandy silt to clayey silt	10
0.85	2.710	19.30	0.25	0.712	7	silty sand to sandy silt	9
0.90	2.540	21.70	0.26	0.854	7	silty sand to sandy silt	8
0.95	2.320	24.80	0.33	1.069	6	sandy silt to clayey silt	9
1.00	2.220	26.60	0.33	1.198	6	sandy silt to clayey silt	9
1.05	2.200	26.20	0.33	1.191	6	sandy silt to clayey silt	9
1.10	2.210	27.00	0.33	1.222	6	sandy silt to clayey silt	9
1.15	2.240	28.00	0.33	1.250	6	sandy silt to clayey silt	9
1.20	2.310	29.60	0.33	1.281	6	sandy silt to clayey silt	9
1.25	2.540	33.50	0.33	1.319	6	sandy silt to clayey silt	11
1.30	3.300	41.60	0.33	1.261	7	silty sand to sandy silt	11
1.35	4.370	55.50	0.33	1.270	7	silty sand to sandy silt	15
1.40	6.110	79.50	0.33	1.301	7	silty sand to sandy silt	22
1.45	9.400	116.80	0.33	1.243	8	sand to silty sand	25
1.50	14.690	176.60	0.33	1.202	8	sand to silty sand	38
1.55	22.060	271.60	0.32	1.231	9	sand	45
1.60	31.280	407.00	0.32	1.301	9	sand	64
1.65	42.800	454.10	0.32	1.061	9	sand	75
1.70	38.180	428.60	0.32	1.123	9	sand	75
1.75	30.850	343.60	0.32	1.114	9	sand	63
1.80	25.630	278.50	0.32	1.087	9	sand	52
1.85	22.040	86.20	0.31	0.391	9	sand	45
1.90	19.980	118.00	0.31	0.591	9	sand	41
1.95	20.160	123.50	0.10	0.613	9	sand	39
2.00	19.090	124.60	0.10	0.653	9	sand	39
2.05	18.600	129.80	0.09	0.698	9	sand	37
2.10	18.380	131.70	0.09	0.717	9	sand	37
2.15	18.600	131.50	0.08	0.707	9	sand	37
2.20	18.990	133.60	0.08	0.704	9	sand	38
2.25	19.220	138.50	0.08	0.721	9	sand	38
2.30	19.070	146.90	0.08	0.770	9	sand	38

Due to issues with importing non-delimited header rows, text file data were manually transferred into Microsoft Excel spreadsheets, which were in turn imported into a Microsoft Access database:

Perlite\cit\5\cit\perth\hazards\earthquake\SCPT_Vs\Perth_Study_SCPT_database_full.mdb

Seismic data were provided separately, and were combined into a single Microsoft Excel file (Perlite\cit\5\cit\perth\hazards\earthquake\SCPT_Vs\AllperthVsData.xls) prior to transfer into the Access database

Spatial Information

Sites were located predominantly in parks and reserves, and were spatially referenced visually using orthophoto imagery and a Perth Street Directory based on an AGD66 datum. As such, site location co-ordinates derived using these methods can be expected to incorporate significant error.

GIS Component:

Text files from Microsoft Excel spreadsheets were combined and exported as .dbf (IV) files.

Fields pertaining to site and survey identification, and spatial location were included. These data were imported into ESRI ArcMap and converted into an Event theme. The theme was converted to a shapefile as map grid coordinates in AGD66, and reprojected to GDA94 using ESRI Projection Utility Wizard Extension.

Properties of Seismic Cone Penetrometer Test survey coverage, as at 16/11/2004

Location:
Perlite\5\cit\perth\hazards\earthquake\GIS\SCPT\allSCPTsites_XY.shp
Data Type: Point feature Class
Feature Class: Point
Coordinate System:
Transverse_Mercator
False_Easting: 500000.000000
False_Northing: 10000000.000000
Central_Meridian: 117.000000
Scale_Factor: 0.999600
Latitude_Of_Origin: 0.000000
GCS_GDA_1994
Datum: D_GDA_1994
Prime Meridian: 0

Perth Cities Project SOFTWARE and HARDWARE

Geographic Information Systems

Spanning the life of the Perth Cities project many programs were created to run inside purchased software. These programs are too numerous to list, but the major software and hardware used in the project are listed below.

Software

ESRI ArcInfo 8.3 (unix and PC)
ESRI ArcInfo 9.0 (PC)
ESRI ArcPAD 6.0.1 (PDA)
MapInfo 7.5
MapLab 7.0.1
ERDAS Imagine
ER Mapper
Exceed 6.2
Windows NT/2000/CE
Microsoft Office – Access/Excel/Word

Hardware

PC – DELL Precision 350/360
UNIX Storage Disk – 120 Gigabytes
iPAQ 5550 PDA units (field survey)
Bluetooth Global Positioning System (GPS – field survey)
3.2 Mega-pixel Kodak Digital Cameras (field survey)
Colour Design Jet Printers
Maxtor External Hard Drive 160 Gigabytes

Appendix C: COST MODELS

Mary Milne
Geoscience Australia

A building database was constructed using Perth's Valuer Generals Office (VGO) 2002 access database combined with Geoscience Australia's (GA) value added attribute fields. These value added attribute fields include floor area, functional classification, HAZUS structural classification and estimated year built.

A decision was made to use only the 2002 VGO access database due to the incompleteness of the 2003 VGO data. Some data attributes in the 2002 VGO fields also required further work, including intersecting the Perth footprint database with the building database to attain a derived area for all residential buildings. (See Chapter 5, 'Earthquake Risk' for more information on derived area.)

Building entries in the VGO database were mapped to the functional classification of buildings (FCB) usage types and to the structural models developed by Edwards and the National Institute of Building Science. The combinations of usage and structural type were then mapped to building replacement cost models. The cost estimates for the total replacement of buildings were developed by Reed Construction Data, ('Replacement cost models for metropolitan Perth', report for Geoscience Australia), 2003, and were provided in 2003 dollars. Where specific models were not available, default cost models were used.

The building cost estimates are based on a pyramid structure (RCD, 2003). Component costs (such as the cost per hour of labour or of a bag of cement) are built into unit rates, which calculate the inputs required for particular activities. In turn these unit rates are then built into elements (a complete brick veneer wall). Building cost models are constructed from elements and are expressed in square metres.

For the Perth metropolitan area, 86 building cost models were developed to capture at least 95% of the building stock of the metropolitan area. The cost models used in the risk model are listed below by usage type: industrial, commercial, non-residential and residential. For residential buildings, more data were available on the age and size of buildings. As a result, regression equations are used to capture the costs according to size of structure.

In Table C.5, the LGAs within the Perth study are listed according to the assigned level of contents. The level of contents was determined by the average income of the LGA.

Table C.1: Industrial building cost models

FCB	Sub-category	Exterior walls	Interior walls	Floor type	Roof type	Rate (m^2)
321	Showroom/shop–warehouse	Cavity brick	Plasterboard	Concrete	Metal	$587
321	Warehouse (small)	Cavity brick	Plasterboard	Concrete	Metal	$522
391	Service station/workshop	Cavity brick	Brick	Timber	Tile	$997

Table C.2: Commercial building cost models

FCB	Reed's cost model	Exterior walls	Interior walls	Floor type	Roof type	Rate (m^2)
211	Shop	Cavity brick	Brick	Concrete slab, timber upper	Metal	$640-
211	Supermarket	Cavity brick	Brick	Concrete	Metal	$919
211	Shopping centre	Concrete/glazed curtain	Concrete block	Concrete	Metal	$1,354
211	Café/pharmacy/hairdresser	Cavity brick	Brick	Concrete	Tile	$783
211	Restaurant	Cavity brick	Brick	Concrete	Tile	$1,066
211	Take-away outlet	Cavity brick	Brick	Concrete	Metal	$993
211	Food hall	Cavity brick	Brick	Concrete	Tile	$1,085
211	Sale yard	Iron	NA	Aggregate	Metal	$290
221	Airport	Concrete block	Concrete block	Concrete	Concrete membrane	$2,084
223	Car park	Cavity brick	Plasterboard	Concrete	Metal	$522
224	Garage/workshop	Cavity brick	Plasterboard	Concrete	Metal	$587
231	Office-low rise	Cavity brick	Brick	Concrete slab, timber upper	Metal	$640
231	Office-low rise	Cavity brick	Brick	Concrete	Tile	$783
231	Office - mid rise	Concrete block	Concrete block	Concrete	Concrete membrane	$1,571
231	Office - high rise	Concrete/glazed curtain	Concrete block	Concrete	Concrete membrane	$1,636
231	Office-showroom	Cavity brick	Brick	Concrete	Metal	$919
291	Depot/yard	Cavity brick	Brick	Concrete	Metal	$94
291	Service station	Cavity brick	Brick	Concrete	Metal	$997

Table C.3: Government building cost models

FCB	Sub-category	Exterior wall	Interior wall	Floor type	Roof type	Rate (m^2)
411	School	Cavity brick	Brick	Concrete	Tile	$1,172
411	Child care facility	Cavity brick	Brick	Concrete	Metal	$858
421	Church	Cavity brick	Brick	Concrete	Tile	$1,085
431	Nursing and aged home	Cavity brick	Concrete block	Concrete	Concrete membrane	$1,537
441	Hospitals	Cavity brick	Concrete block	Concrete	Concrete membrane	$1,537
442	Day surgery/ clinic	Cavity brick	Brick	Concrete	Tile	$775
442	Medical centre	Cavity brick	Concrete block	Concrete	Tile	$1,412
451	Museum/Art gallery	Cavity brick	Brick	Concrete	Tile	$1,442
451	Night club/RSL club	Concrete block	Concrete block	Concrete	Concrete membrane	$2,084
451	Amusement centre/TAB agency	Cavity brick	Brick	Concrete	Tile	$783
451	Cinema	Concrete/glazed curtain	Concrete block	Concrete	Metal	$1,354
462	Hotel motel	Cavity brick	Brick	Concrete	Tile	$1,630
461	Hotel – high rise/ tavern	Concrete block	Concrete block	Concrete	Concrete membrane	$1,925
491	Police Station	Cavity brick	Brick	Concrete	Metal	$700
491	Ambulance Station	Cavity brick	Plasterboard	Concrete	Tile	$708
491	Fire Station	Cavity brick	Plasterboard	Concrete	Tile	$715
491	Vet Surgery	Cavity brick	Brick	Concrete	Tile	$775

Table C.4: Residential building cost models

FCB	Usage type	Wall type	Roof type	Structural model	Contemporary 1960–2004	Post-war 1946–1959	War period 1914–1945	Before 1914
111	Detached house	Brick	Tile	URMLTILE	-0.772*X + 989.7 (A)	-0.691*X + 1037.3 (E)		
		Brick veneer	Tile	W1BVTILE	(A)			
		Brick	Iron	URMLMETAL	-0.725*X + 964.9 (B)	-0.606*X + 1002.2 (F)		
		Brick	Asbestos	URMLMETAL	(B)	(F)		-0.525*X +1277.0
		Brick	Asbestos	URMLMETAL	(B)	(F)		-0.525*X +1277.1
		Concrete	Iron	PC1	(B)			
		Brick veneer	Asbestos	W1BVMETAL	(B)			
		WB/asbestos	Iron	W1TIMBERMETAL	-0.665*X + 865.4 (C)	(G)	-0.663*X + 900.5 (I)	-0.300*X + 856.0 (J)
		Asb/WB/iron	Iron/asb	W1TIMBERMETAL	(C)	-0.700*X + 916.0 (G)		
		Steel frame	Iron	W1BVMETAL	(C)			
		Default		**Other**	**(A)**	**(E)**	**(I)**	**(J)**
113	Transportable home	All	All	W1TIMBERMETAL	-0.665*X + 865.4 (C)			
		Asbestos/WB	Tile	W1TIMBERTILE	-0.715*X + 890.8 (D)	-0.763*X + 949.5 (H)		
121	Semi-detached	Brick	Tile	URMLTILE	-0.499*X + 885.7 (K)			
		Brick veneer	Tile	W1BVTILE	(K)			
		Concrete	Iron	PC1	(K)			
		Asbestos/WB	Tile	W1TIMBERTILE	-0.555*X + 828.8 (L)			
		Brick	Asbestos	URMLMETAL	-0.447*X + 861.4 (M)			
		Brick veneer	Asbestos	W1BVMETAL	(M)			
		Steel frame	Iron	W1BVMETAL	(M)			
		Iron	Iron	W1TIMBERMETAL	(M)			
		WB	Iron/Asb	W1TIMBERMETAL	-0.510*X + 805.8 (N)			
		Asbestos	Iron	W1TIMBERMETAL	(N)			
131	1 or 2 storeys	All	All		854/m^2			
132	3 storeys	All	All		854/m^2			
133	>=4 storeys	All	All		854/m^2			
134	Attached to a house				854/m^2			

Table C.5: Level of contents by LGA

Level of contents	Perth LGAs
Prestige (over $1350 pw)	Cambridge, Cottesloe, Nedlands, Peppermint Grove
Quality ($901–$1350 pw)	Canning, Claremont, Cockburn, East Fremantle, Fremantle, Gosnells, Joondalup, Kalamunda, Melville, Mosman Park, Mundaring, Perth, South Perth, Stirling, Subiaco, Swan, Wanneroo, Vincent
Average ($500–$900 pw)	Armadale, Bassendean, Bayswater, Belmont, Victoria Park

Appendix D: PERTH BASIN GEOLOGY REVIEW and SITE CLASS ASSESSMENT

Andrew McPherson and Andrew Jones
Geoscience Australia

Introduction

The presence of soils, sediments and weathered rock, which are collectively referred to as regolith, can affect earthquake ground shaking, and so influence local earthquake hazard in a region. In order to quantify localised changes in earthquake hazard due to variations in the regolith, the Perth metropolitan area was divided into a series of site classes. The site classes encompass regions that are considered to have a similar response to earthquake ground shaking.

This appendix details the background information, datasets, and procedures utilised in developing these site classes. The first section briefly reviews the regional geologic and geomorphic setting. The geology of this part of the Perth Basin is then described in more detail, in particular the Late Tertiary and Quaternary units, as it is these parts of the basin succession that comprises the majority of the regolith. These sections of the report are almost exclusively taken from the literature, particularly the studies of Playford *et al*. (1976) and Davidson (1995). The subsequent section details the development of site classes for the region and describes the geotechnical properties of each class. The final section discusses the site classes in the light of previous geotechnical investigations for the area.

Included within this report is a brief summary of the site conditions at Northam, one of Western Australia's largest inland towns, which is located 98 km northeast of Perth on the Avon River (see Chapter 1, Figure 1.2). The information on Northam is provided as a basis for comparison of potential earthquake hazard between 'rock' sites of the Yilgarn Block and 'soil' sites in the Perth Basin.

Regional Setting – Perth Basin

The following Basin summary, unless otherwise indicated, is taken from the study of Playford *et al*. (1976).

The Perth Basin is a deep trough nearly 1,000 km long that averages about 65 km in width, filled with sedimentary rocks. The total thickness of the Phanerozoic succession may exceed 15,000 m. The eastern margin of the basin is defined throughout most of its length by the Darling Fault, which generally marks the contact between the Perth Basin and the Archaean Yilgarn Block. The northern part of the basin is bordered by a ridge of relatively shallow basement rocks (The Northampton Complex – Iasky and Mory, 1993) that extend from the north. The western and southern offshore margins of the Perth Basin have not been precisely defined. The southwestern corner of the basin is bounded by a narrow belt of Proterozoic granulite and gneiss in the Leeuwin Block.

Structure

The Perth Basin is a faulted trough filled with sediments, the dominant structural feature being the Darling Fault. The fault itself is obscured by sediments, and is presently located approximately 1–3 km west of the fault's surface expression – the Darling Scarp (Janssen *et al*., 2003). The Darling Fault is nearly 1,000 km long, and its maximum throw may exceed 15,000 m. The Perth Basin is generally intensely faulted, with most faults having north to northwest trends and throwing both to the east and west. There are a number of moderately large cross-faults trending approximately east–west.

A number of structurally controlled sub-divisions are recognised in the Perth Basin, but the Perth metropolitan region under investigation lies exclusively over the Dandaragan Trough (Figure D.1).

Stratigraphy

Pre-Mesozoic stratigraphy includes Proterozoic siliciclastic sedimentary rocks, the Silurian Tumblagooda Sandstone, and a well-developed Permian succession that comprises nine formations over at least 2,600 m. Within the Mesozoic, the Triassic succession varies between continental and marine, and is of a similar thickness to the Permian sequence. The mainly continental Jurassic sediments are widespread throughout the basin, and are believed to be at least 4,200 m thick. The Perth Basin Cretaceous succession, which may be as thick as 12,000 m, comprises a lower continental unit, a mixed continental, paralic and marine unit, and a lower marine unit, which are separated by unconformities. A well-marked unconformity occurs within the continental to paralic sequence of the Lower Cretaceous. Tertiary marine sediments up to 600 m thick occur beneath the Perth area and over much of the continental shelf. Quaternary deposits blanket much of the Perth Basin (Playford *et al*., 1976), and these are outlined in detail in the following section. Thicknesses of Tertiary/Quaternary deposits in the region generally increase to the west and north.

Geomorphology

An excellent summary of the geomorphology of the Swan Coastal Plain in the vicinity of Perth is provided by Davidson (1995), and reproduced below. Wyrwoll (2003) presents a succinct account of the Perth region geomorphology.

In the Perth region, the Swan Coastal Plain is about 34 km wide in the north, 23 km in the south, and is bounded to the east by the Gingin and Darling Fault Scarps, which rise to over 200 m above sea level. The scarps represent the eastern boundary of Tertiary and Quaternary marine erosion. The Swan Coastal Plain consists of a series of distinct landforms (McArthur and Bettenay 1960), roughly parallel to the coast (Figure D.2). The most easterly landform comprises the colluvial slopes which form the foothills of the Darling and Dandaragan Plateaus and which represent dissected remnants of a sand-covered, wave-cut platform known as the Ridge Hill Shelf. To the west of the colluvial slopes lies the Pinjarra Plain, a piedmont and valley-flat alluvial plain consisting predominantly of clayey alluvium that has been transported by rivers and streams from the Darling and Dandaragan Plateaus. The plain is generally about 5 km wide west of the colluvial slopes, but along the Serpentine River it is about 15 km wide in an east–west direction.

To the west of the Pinjarra Plain, the Bassendean Dune System forms a gently undulating aeolian sand plain about 20 km wide with the dunes to the north of Perth generally having greater topographic relief than those to the south. The dunes probably accumulated as shoreline deposits and coastal dunes during interglacial periods of high sea level and originally consisted of mostly lime (calcareous) sand with quartz sand and minor fine-grained, black, heavy-mineral concentrations. Apart from a small local area to the south of Perth, the carbonate material has been completely leached leaving dunes consisting entirely of quartz sand.

West of the Bassendean Dune System are two systems of dunes which fringe the coastline. The most easterly of these is the Spearwood Dune System, which consists of slightly calcareous aeolian sand remnant from leaching of the underlying Pleistocene Tamala limestone. The most westerly dune system, which flanks the ocean, is the Quindalup Dune System, consisting of wind-blown lime and quartz beach sand forming dunes or ridges that are generally oriented parallel to the present coast, but which may also occupy blowouts within the Spearwood Dune System.
The rivers crossing the coastal plain are flanked by clayey floodplains and river terraces of recent origin. Other wetlands, consisting of swamps and lakes, have formed in the inter-dunal swales of the Bassendean Dune System, in the inter-barrier depressions between the Spearwood and Bassendean Dune Systems, and within the Spearwood Dune System.

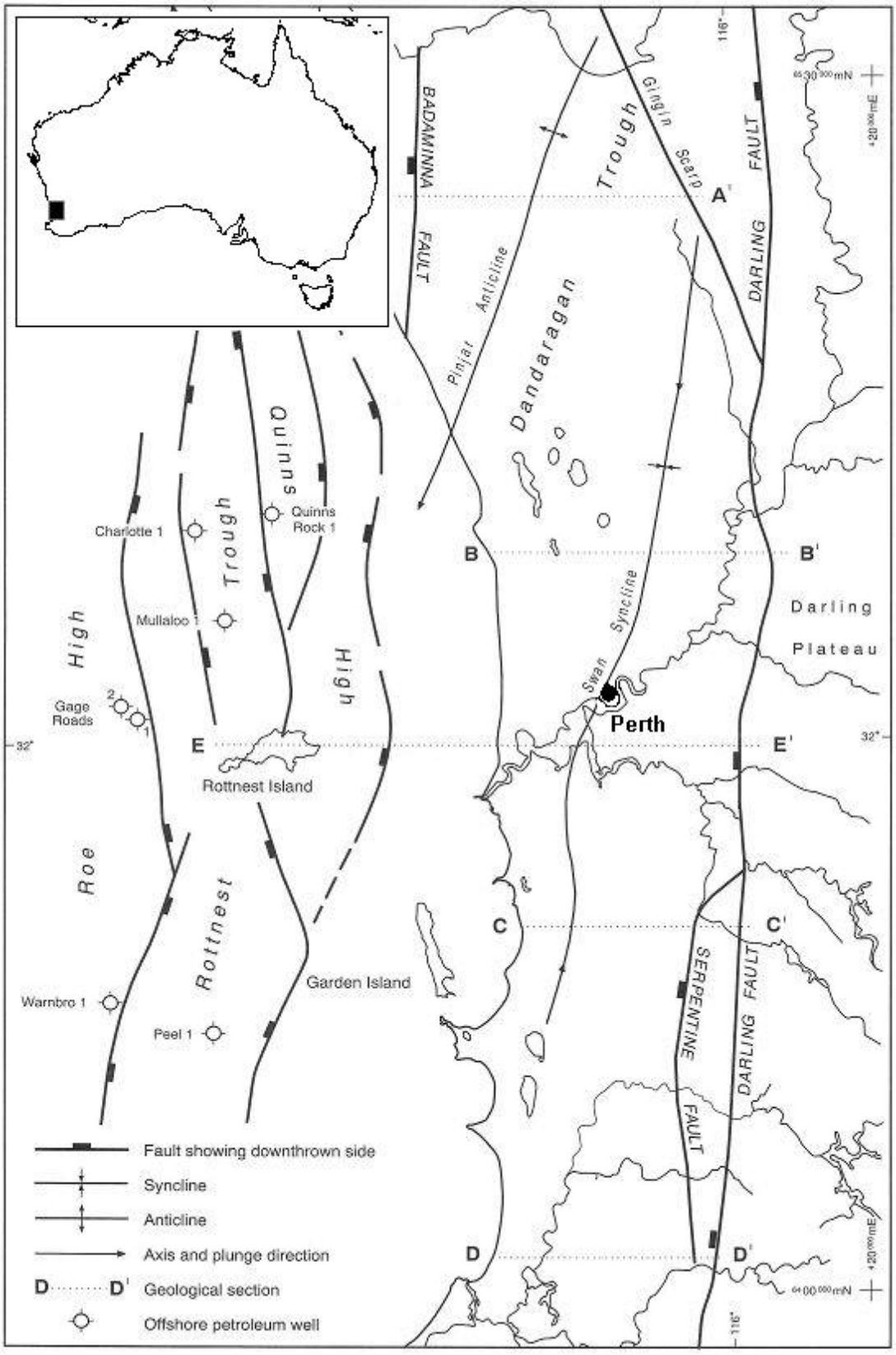

Figure D.1: Structural geology of the Perth region (from Davidson, 1995)

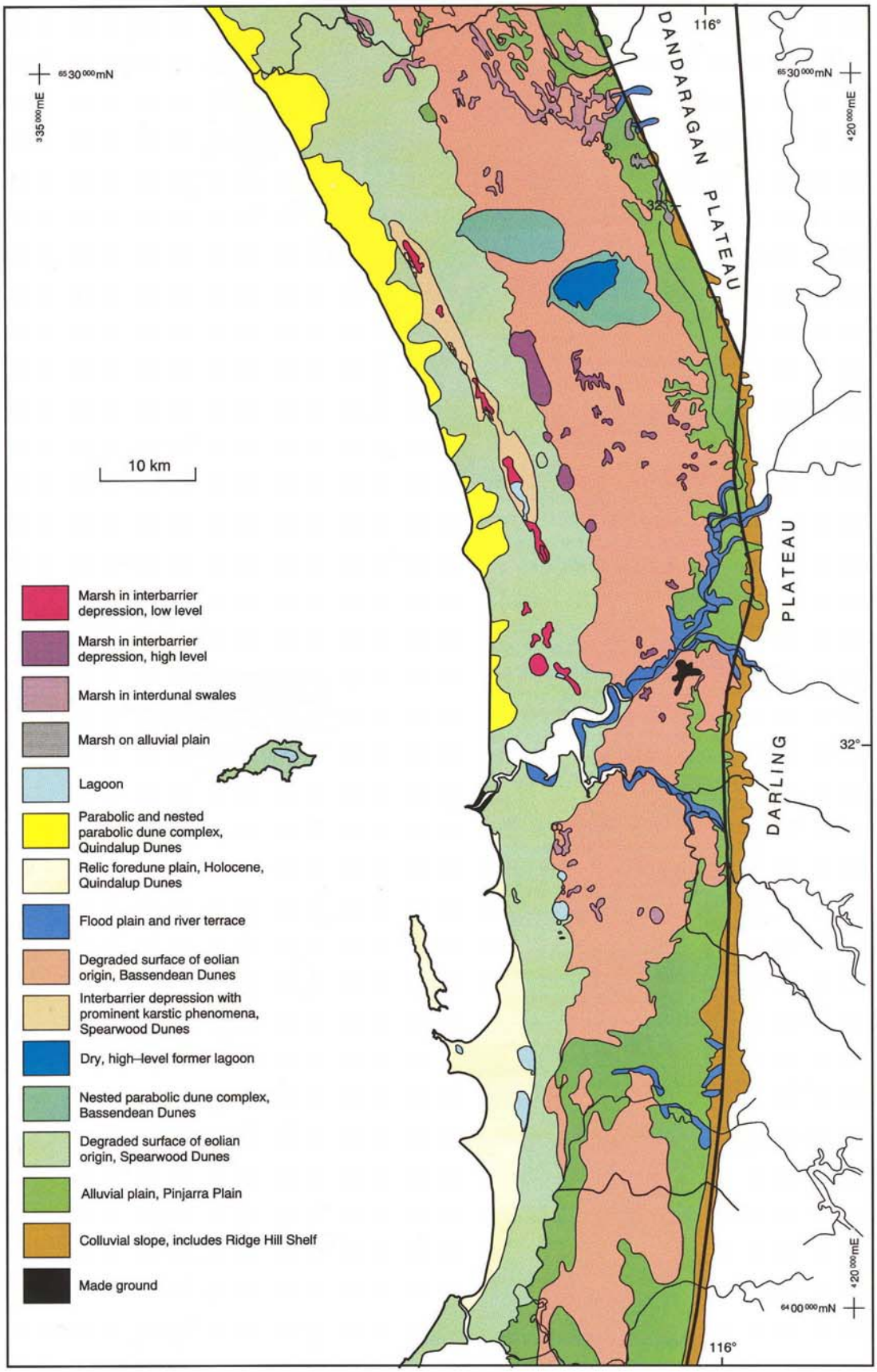

Figure D.2: Geomorphology of the Perth region (from Davidson 1995)

Geology

The character, distribution and depositional history of the geological units outlined in this section have previously been described by Playford *et al.* (1976), and are summarised by Davidson (1995). A succinct outline of the Perth region geology is given by Commander (2003). The sequence stratigraphy for the major Mesozoic and Cainozoic units are presented in Figure D.3. Unless otherwise indicated, the following summaries are taken from Davidson (1995).

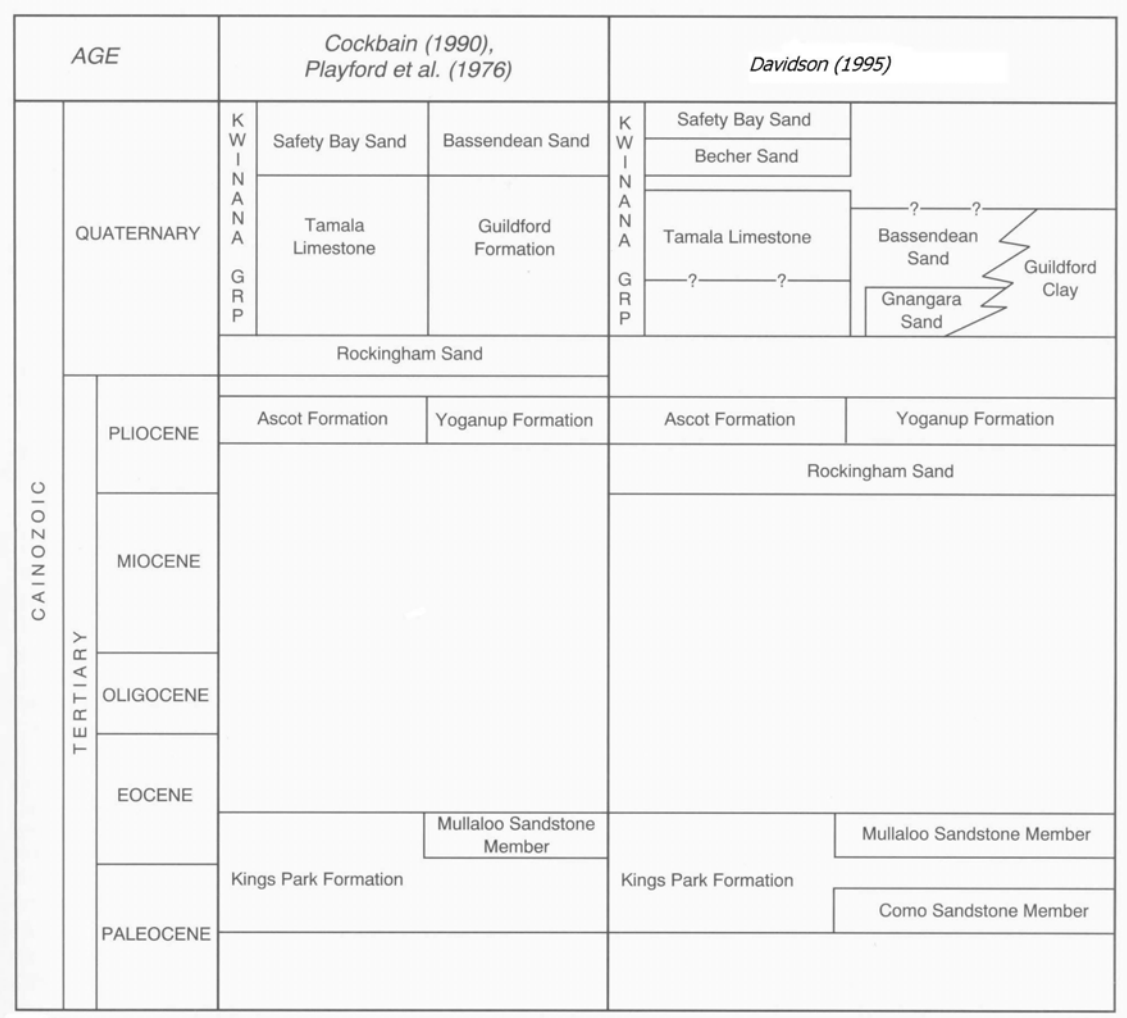

Figure D.3: Stratigraphic column of Perth Basin sediments in the Perth region (from Davidson 1995) [continues over]

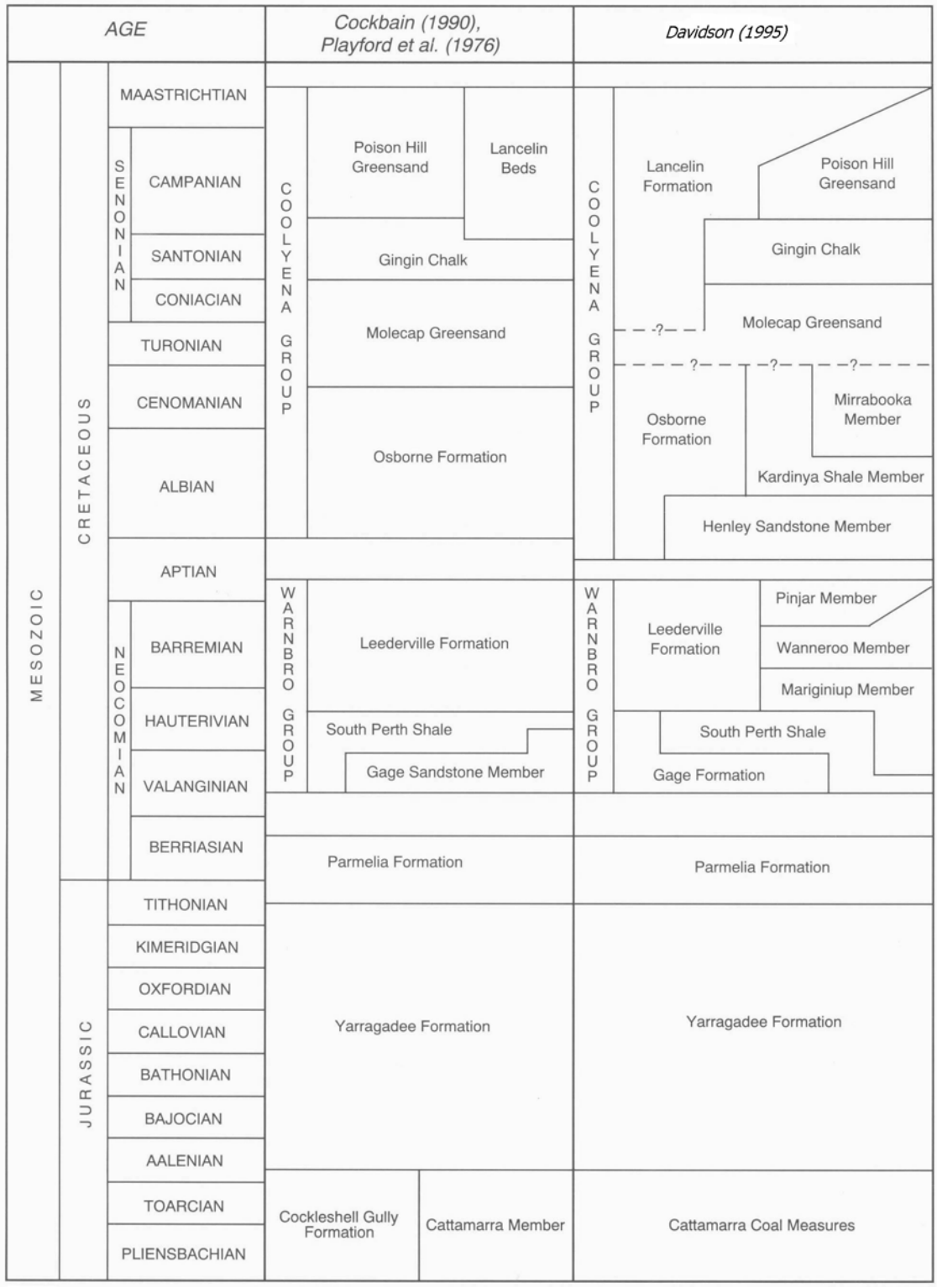

Figure D.3: Stratigraphic column of Perth Basin sediments in the Perth region (from Davidson 1995)

Underlying Cretaceous–Tertiary formations

The Late Tertiary–Quaternary formations that cover the area under investigation predominantly overlie one or more Cretaceous–Tertiary units, namely the Osborne Formation, the Molecap and Poison Hill Greensands, and the Kings Park Formation (see Figure D.3). Henceforth these underlying units are collectively referred to as 'basement', as it is the overlying regolith that is of most relevance to this site class study.

Osborne Formation

The Osborne Formation (McWhae *et al*., 1958) comprises a basal sandstone unit (Henley Sandstone Member), a middle shale unit (Kardinya Shale Member), and an upper, interbedded sandstone and shale succession (Mirrabooka Member). The majority of the southern part of the study area is underlain by the Mirrabooka Member. The Osborne Formation is of shallow marine origin, has a maximum thickness of about 180 m, and is Early Cretaceous (~114 Ma) in age.

Molecap Greensand

The Molecap Greensand (Fairbridge, 1953) consists of fine to medium-grained, yellowish-brown to greenish-grey, glauconitic, silty and locally clayey sandstone. It underlies the superficial formations in sections of the northern study area. The Molecap Greensand is of shallow marine origin, has a maximum thickness of about 80 m, and is Late Cretaceous (98 Ma) in age.

Poison Hill Greensand

The Poison Hill Greensand (Fairbridge, 1953) consists of unconsolidated pale yellow to dark green, fine to very coarse-grained, richly glauconitic, silty and locally clayey sand. It underlies the superficial formations in the north of the study area. The Poison Hill Greensand was deposited locally through erosion of the Osborne Formation. This unit was originally thought to be a channel infill deposit of Quaternary age (Morgan, 1964; Allen, 1977; Barnes, 1977), but extensive palynological investigation has been unable to confirm this. It is currently considered to be Cretaceous–Tertiary (~80 Ma) in age. The unit has a maximum thickness of about 90 m).

Kings Park Formation

The Kings Park Formation (Quilty, 1974) occupies a deep channel incised through the Cretaceous sedimentary succession. The valley in which it is preserved may once have been connected with the Perth canyon, which cuts the continental slope west of Rottnest Island (Playford *et al*., 1976). The formation predominantly comprises grey, calcareous, glauconitic siltstone and shale of shallow marine to estuarine origin. It has a maximum onshore thickness of about 530 m and is Early to Mid-Tertiary (~54 Ma) in age (Playford *et al*., 1976).

Superficial formations

A thin veneer of Late Tertiary and (primarily) Quaternary regolith comprise the surficial cover over much of the Perth Basin (Playford *et al*., 1976) (Figure D.4, see also D.3). These 'superficial' formations (a collective term coined by Allen, 1976) consist mainly of sand, silt, clay and limestone in varying proportions. Along the eastern margin of the Swan Coastal Plain materials are dominated by silts and clays (muds), while those in the central area of the Plain are predominantly sandy. To the west, the sandy materials pass laterally into limestone, which borders the coastal strip. Formal stratigraphic names have not been given to many Quaternary units (Playford *et al*., 1976): where they are formally named, the distribution of the units has not been clearly defined.

This section outlines the material characteristics of the superficial units that comprise the majority of the Swan Coastal Plain, which were utilised in reconstructing the three-dimensional regolith architecture of the Perth region.

Ascot Formation

Originally defined as the Ascots Beds by Playford *et al*. (1976), the Ascot Formation (Cockbain and Hocking, 1989) consists of hard to friable, grey to fawn calcarenite with thinly interbedded sand commonly containing shell fragments, glauconite and phosphatic nodules near the base of the formation. The fine to coarse sand is very poorly sorted, angular to rounded, and contains a rich assemblage of bivalves and gastropods. Where present, the Ascot Formation lies unconformably on the Leederville Formation, Osborne Formation, Molecap Greensand, or Poison Hill Greensand. The formation was deposited as a prograding shoreline (Kendrick *et al*., 1991). It has a maximum thickness of 25 m in the southern and northern Perth areas, and is widespread as a basal unit of the superficial formations.

Yoganup Formation

The Yoganup Formation, defined by Low (1971), comprises white to yellowish-brown, unconsolidated, poorly sorted sand, gravel and pebbles, with local subordinate clay, ferruginised grains and heavy minerals. It occurs sporadically along the eastern margin of the Perth region and westwards (as sub-crop) about 5 km from the foothills of the Darling Scarp, and is generally about 10 m thick. The Yoganup Formation unconformably overlies the Osborne Formation and/or the Leederville Formation, and is unconformably overlain by the Guildford Formation. It may inter-finger with the Ascot Formation at the base of the superficial formations. The unit is a buried pro-graded shoreline deposit, with dunes, beach ridge, and deltaic facies (Baxter, 1982). In the Perth region, it has a maximum known thickness of about 10 m and has been extensively eroded prior to deposition of the Guildford Formation.

Guildford Formation

The Guildford Formation, raised to formation status by Low (1971) from the Guildford Clay (Aurousseau and Budge, 1921), consists of pale-grey, blue, but predominantly brown silty and slightly sandy clay. The unit is up to 35 m thick and commonly contains lenses of fine to coarse-grained, very poorly sorted, conglomeratic and (in places) shelly sand at its base, particularly in the type area of the Swan Valley. The Guildford formation outcrops over much of the eastern Perth region, unconformably overlies Jurassic and Cretaceous rocks, Kings Park Formation, Ascot Formation or Yoganup Formation. It is essentially a fluvial mud deposit.

Bassendean Sand

The Bassendean Sand, defined by Playford and Low (1972) from the type area in the Perth suburb of Bassendean, is present over much of the central Perth region, with a maximum thickness of about 80 m (Davidson, 1995). It is pale grey to white and includes fine to coarse, but is predominantly medium-grained. It comprises moderately sorted, sub-rounded to rounded quartz sand, and commonly exhibits fining upward textures. A layer of friable, limonite-cemented sand, colloquially called ‘coffee rock’, occurs throughout most of the area near the watertable. The Bassendean Sand unconformably overlies the Cretaceous and Tertiary strata, and inter-fingers to the east with the Guildford Formation. To the west, it is unconformably overlain by the Tamala Limestone. The depositional mechanism for this unit is unclear; it was likely deposited in a variety of fluvial, estuarine, and shallow-marine environments.

Tamala Limestone

The Tamala Limestone, defined by Playford *et al*. (1976), extends along the coastal strip of the Perth region. It consists of a creamy-white to yellow, or light-grey, calcareous aeolianite, which by definition suggests deposition as coastal dunes (Nidagal and Davidson, 1991). The Tamala Limestone contains various proportions of quartz sand, fine- to medium-grained shell fragments, and minor clayey lenses. The quartz sand varies from fine to coarse-grained, but is predominantly medium-grained, moderately sorted, sub-angular to rounded, frosted, and commonly stained with limonite. The limestone contains numerous solution channels and cavities, particularly in the zone of watertable fluctuation, and in some areas exhibits karst structures. Its upper surface is exposed and leached to the extent that the upper part of the unit comprises unconsolidated sand. Depending on the location, this unit unconformably overlies the Leederville Formation, Osborne Formation or the Bassendean Sand, and has a maximum known thickness of 110 m in the Perth area, but may be up to 150 m thick outside

the Perth area (eg, Hutt River). Along the coastal margin it is unconformably overlain by the Becher Sand or the Safety Bay Sand.

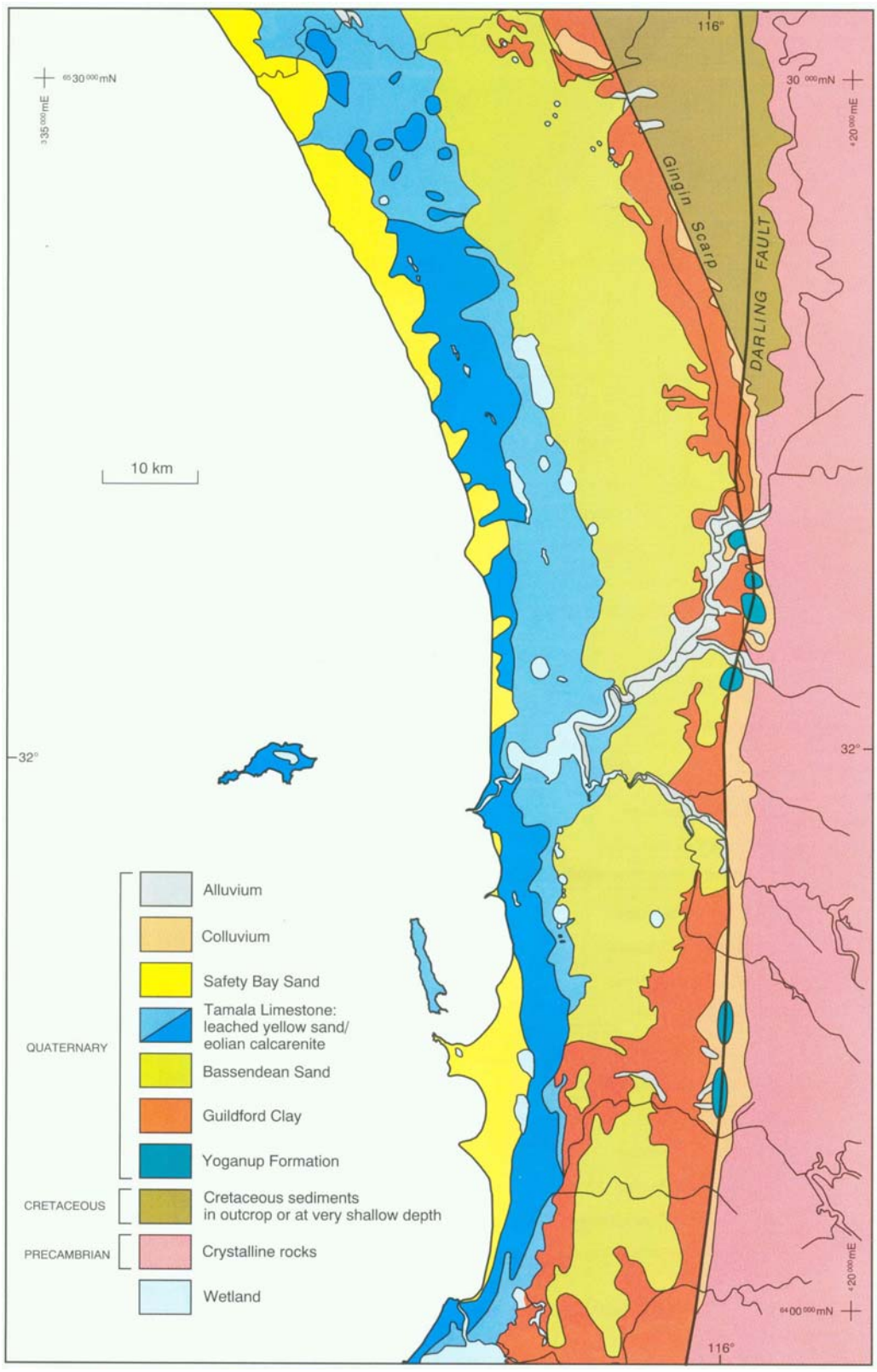

Figure D.4: Generalised surface geology of the Perth region (from Davidson 1995)

Becher Sand

The Becher Sand, defined by Semeniuk and Searle (1985), extends along the coastal margin of the Perth region, and consists of fine to medium-grained quartz and skeletal sand that is mostly structureless and bioturbated. Although it has not been extensively studied, the Becher Sand is typically 10–15 m thick (Semeniuk and Searle, 1985) with a maximum thickness of 20 m in the Rockingham area. It unconformably overlies the Tamala Limestone and is unconformably overlain by the Safety Bay Sand. The Becher Sand was previously referred to as the Safety Bay Sand but, because it is of nearshore marine origin and not aeolian, it is genetically distinct from the Safety Bay Sand.

Safety Bay Sand

The Safety Bay Sand, defined by Passmore (1967, 1970) and Playford and Low (1972), comprises white, unlithified, calcareous fine to medium-grained quartz sand and shell fragments with traces of fine-grained, black, heavy minerals. It occurs along the coastal margin as stable and mobile aeolian dunes, which overlie the Tamala Limestone and Becher Sand (Davidson, 1995). The type section at Rockingham is 24 m thick, but may be upwards of 100 m in other parts of the Perth Basin (Playford *et al*., 1976).

Northam

Northam is located in the western Yilgarn Craton, adjacent to the Perth Basin (see Chapter 1, Figure 1.2). The western margin of the craton is defined by the Darling Fault (Figure D.1). The Yilgarn Craton is dominated by ancient granitic rocks of the Precambrian Western Shield. This block is comprised of Archaean rocks that have essentially remained tectonically stable since the Late Carboniferous–Early Permian glaciation (BMR Palaeogeographical Group, 1990), an event considered responsible for removing much of the pre-existing regolith (Ollier, 1978). The oldest dated sediments are Late Tertiary (early to mid-Eocene, 55–40 Ma) marine sediments found primarily as palaeo-drainage channel fill (Ollier, 1988).

The Atlas of Australian Soils (Northcote *et al*., 1967) shows the Northam area as being dominated by rolling to hilly or river terrace type geomorphology. The primary soil types are red clayey subsoils, which may set hard during the dry season. The Western Australian Department of Agriculture's catchment hydrogeologist in Northam states the regolith in the area comprises 6–10 m of silt/clay alluvium, overlying approximately 30 m of weathered granite bedrock (Shahzad Ghauri, pers. comm., 2003). The absence of any significant sand component in these sediments is interesting given the presence of granitic bedrock. One excavation within the town intersected bedrock at less than 3 m, which was likely a basement high. This is consistent with the findings of Anand and Paine (2002), who, despite reporting regolith thicknesses of up to 150 m on the Yilgarn Craton, consider average values to be closer to 30–50 m, including 5–10 m of transported overburden. Johnston and McArthur (1981) report similar results for regolith profiles north of Narrogin, some 100 km southeast of Northam.

D.3 Key Datasets

This section outlines a number of the datasets that were critical to the development of site classes for the Perth region. A number of other secondary datasets used (e.g. digital elevation models) are not outlined in this section.

Water and Rivers Commision boreholes

The Water and Rivers Commision (WRC), an agency of the Western Australian State Government, provided Perth Cities Project with the locations of approximately 28,000 boreholes distributed throughout the Perth study area. In addition to the locations, WRC supplied a spreadsheet of accompanying drillers/geologists records (ie, geological and regolith information) for a proportion of the boreholes (over 80,000 records). A subset of 2,717 bores with their associated descriptive records

(12,199 records in total) were extracted from the larger WRC dataset on the basis of spatial location within or in proximity to the Perth study area (Figure D.5).

The descriptions of the boreholes are highly variable in terms of their detail and the context in which they were logged. However, it is reasonable to assume that the majority were drilled with the aim of exploring for aquifers across the Swan Coastal Plain. In most cases broad descriptions of grain size are documented for relatively coarse intervals, and there is poor differentiation between consolidated and unconsolidated sections: for example, weathered shales and siltstones are often described as mud or clay. The borehole records are rarely described in terms of Perth Basin stratigraphy and where they are, the Cainozoic section is usually described as a single unit. Another limiting factor of this dataset is that the holes were drilled with the primary aim of delineating aquifers. In many places along the coast it was only necessary to drill to the top of the Tamala Limestone, given that the overlying Safety Bay Sand comprises the primary superficial aquifer. Consequently many of the logs that have an associated description do not penetrate to sufficient depths to assist in the reconstruction of the complete regolith architecture (therefore in the majority of cases regolith thicknesses can only be considered as *minimums*).

Seismic Cone Penetrometer Test data

Seismic Cone Penetrometer Test (SCPT) survey involves monitoring a conical penetrometer tip that is pushed slowly into the ground. The device contains electrical transducers to measure both tip (Q_c) and side (F_s) resistances as the instrument is advanced. A friction ratio is calculated by relating the sleeve friction to the tip resistance ($^{Fs}/_{Qc}$). Coarse-grained sediments such as sands and gravels tend to resist penetration at the tip, whereas finer-grained sediments such as clays and silts resist penetration along the sleeve, therefore a direct relationship between the friction ratio and regolith material can be inferred (in general, the higher the friction ratio the finer the grain size). In addition to providing an estimate of regolith material type, the seismic velocity of the sediment was measured every 1.5 m during the SCPT.

The maximum depth to which a SCPT can penetrate is approximately 30 m, and discontinuation of a SCPT (the completion of a successful test) can be due to a combination of circumstances, primarily:

- excessive pressure at the probe tip due to coarse sand, rock or highly consolidated material;
- excessive friction along the probe sleeve due to fine-grained sediments;
- over-inclination of the probe due to skewing of the bore path.

This is significant as an SCPT does not necessarily provide an accurate measurement of the thickness and character of regolith at a site. If the regolith within the region is thicker than 30 m, or has a thin competent layer such as a limestone lens at a relatively shallow depth, the results will not reflect the true nature of the regolith.

For the Perth study, three SCPT surveys were completed, constituting a total of 57 sites. The distribution of SCPT sites in the Perth study area is shown in Figure D.6.

Microtremor data

One of the primary datasets collected to assist in the assessment of Perth's vulnerability to earthquake hazard was a series of natural period estimates calculated from microtremor measurements. An extensive microtremor field survey was undertaken in October and November of 2001 by Geoscience Australia in the Perth metropolitan area (and Northam). Readings were taken at over 3,000 locations in the Perth metropolitan area at a nominal grid spacing of 500 m (Figure D.7). The survey involved using a ground seismometer and measuring the resonant vibration of unconsolidated regolith (T), as generated by phenomena such as wind, waves and anthropogenic influences (eg, traffic). The method used for the analysis was the Nakamura Method (Nakamura, 1989), which is used to identify the fundamental natural period of vibration of the upper layer of sediments.

The results of the microtremor survey were utilised by Brian Gaull of Guria Consulting in the development of shear wave velocity estimates for the region (Gaull, 2003). He utilised the measured natural periods in conjunction with regolith thickness determined from the WRC boreholes to calculate estimates of seismic shear wave velocity for isolated regions within the Perth metropolitan area. Comparison of the Gaull shear wave velocity measurements and the shear wave velocities in the context of the site classes produced as part of this study is outlined in the discussion.

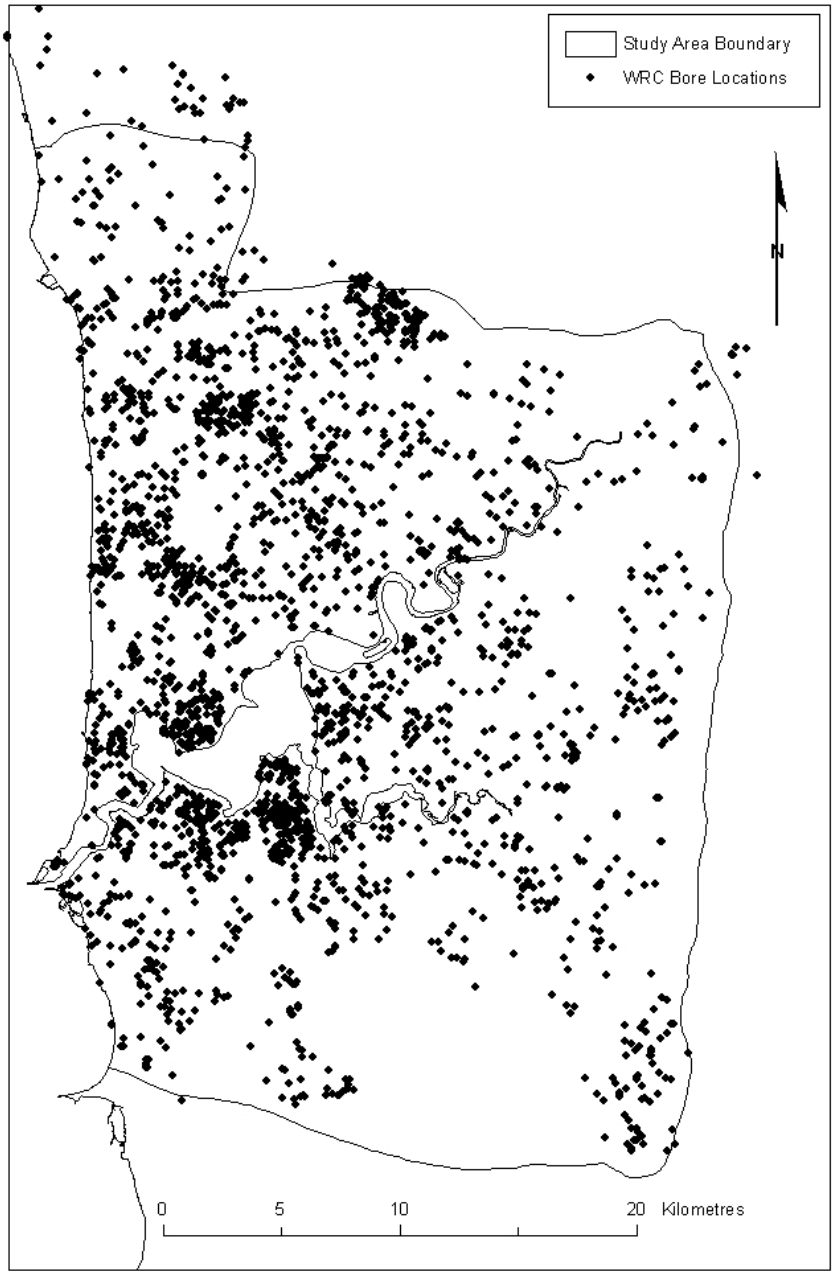

Figure D.5: Borehole locations for the Perth study area

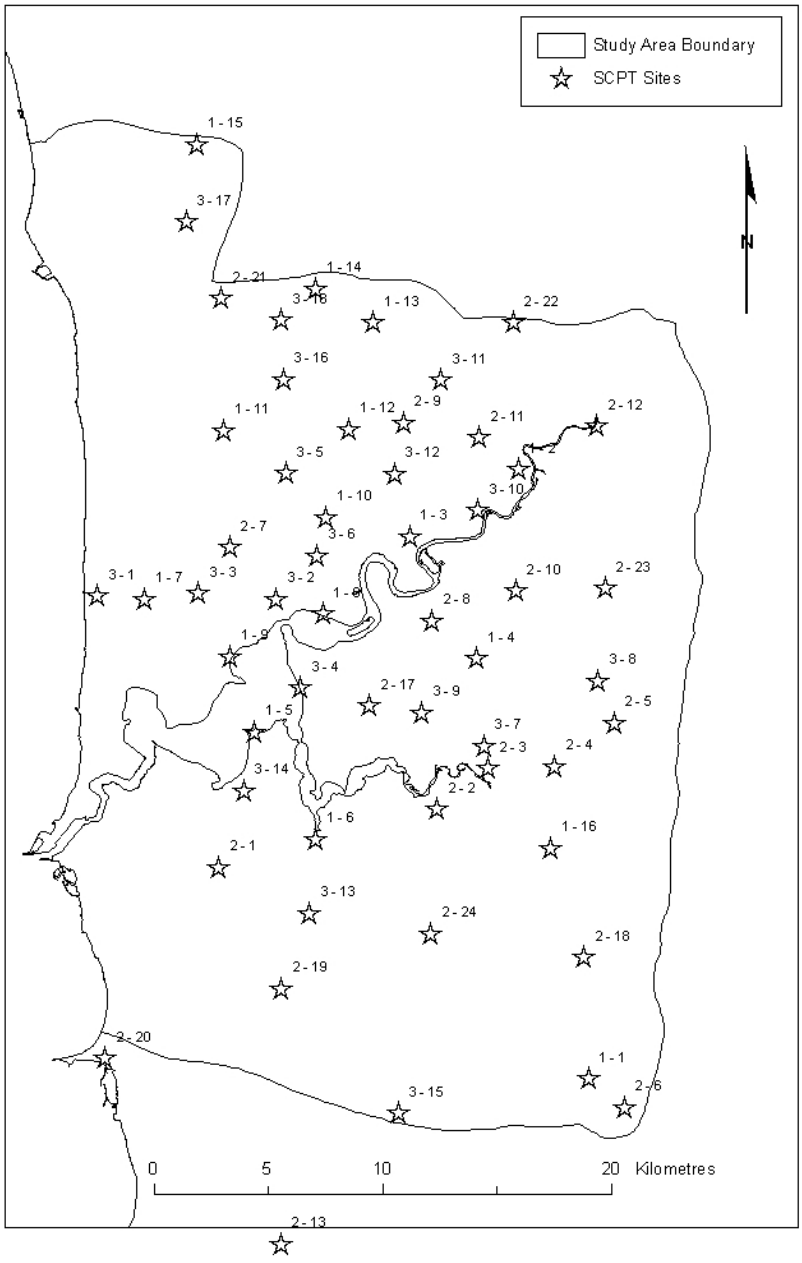

Figure D.6: SCPT site locations for the Perth study area

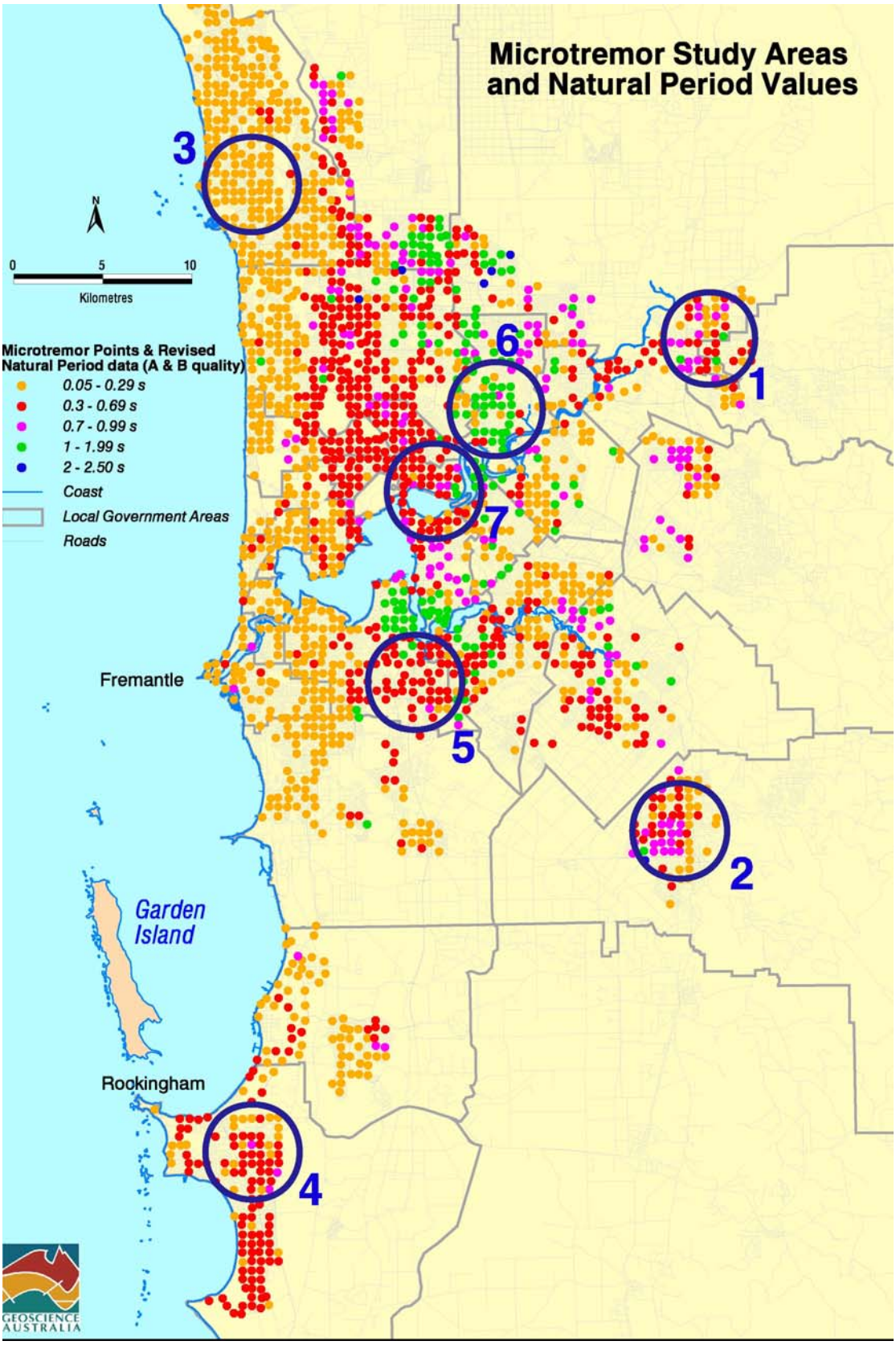

Figure D.7: Microtremor measurement locations for the Perth study area. Gaull's measurement zones are shown as blue circles

D.4 site class Development

The environmental geology maps produced by the Geological Survey of Western Australia (Gozzard, 1982a–b, 1983a–b, 1985, 1986; Jordan, 1986a–c, Smurthwaite, 1989) provide a valuable starting point for site class studies as they show the spatial distribution of Quaternary units at the surface. However, to accurately characterise site classes it is necessary to describe the distribution of the regolith in three dimensions. This process has primarily involved analysis of the geotechnical borehole data provided by the Western Australian Water and Rivers Commission.

In developing site classes for the Perth study area, it was necessary to consider the dominant regolith factors that influence the attenuation and amplification of earthquake ground motion, namely regolith thickness and regolith material type.

Regolith thickness plays a major role in determining the shear wave velocity of an earthquake energy wave as demonstrated by the quarter wavelength theory equation:

$V_s = 4H / T$ **Equation D.1**

where V_s = shear wave velocity (m/s), H = thickness of material or layer (m) and T = period (s). Hence, for a given period in a given material, as the value of H decreases (ie, the regolith gets shallower) the shear wave velocity is reduced, and the damping of the energy is increased.

Regolith material type also exerts a major control on the degree of amplification or attenuation experienced by travelling waves. The properties of regolith materials are represented by cyclic stress–strain curves, which describe the shear modulus and damping effects on energy applied to a material under strain. These relationships are a key component of modelling earthquake site response. In most instances, for a given period and magnitude, coarse-grained regolith materials (eg, sand or gravel) tend to amplify ground motion by virtue of low internal friction and particle movement which dissipates earthquake energy and increases the energy wave amplitude. Finer-grained, denser regolith materials (such as silt or clay) will have a slightly weaker amplification effect due to a higher internal friction and lower shear modulus which permit more effective energy transfer. Consolidated or cemented regolith materials tend to behave more like bedrock, attenuating earthquake energy and generally causing little or no amplification.

Regolith thickness assessment

The first step in analysing the WRC borehole data was to assess which holes were useful in characterising the three-dimensional architecture of the regolith, as many holes only penetrated the uppermost layers. Preliminary assessment in this context was achieved through comparison of borehole depth and published isopach maps of regolith thickness (Davidson, 1995) in a GIS environment. Holes that penetrated to depths greater than that indicated by the regolith isopachs were included in the preliminary investigation. Unfortunately, at the majority of localities, the depths to basement in the selected boreholes were significantly different to the depths indicated at those localities by the isopach map. The primary implication of this was that the only known isopach map of regolith thickness in the Perth region (that by Davidson 1995) was not sufficiently accurate to be included in any site class analysis.

Automatic selection of basement depths was attempted for each hole using keywords in a Microsoft Excel querying procedure. This was largely unsuccessful as depths to basement may be either:

- Underestimated due to boulders, rock/limestone floaters, indurated (cemented) or gravel layers that cause drill refusal; or
- Overestimated as there is no clear differentiation between consolidated and unconsolidated sediments, as mentioned previously.

As such, it became necessary to manually check through the borehole database and interpret the lithological strata and thickness of the superficial formations in the context of published descriptions of the Cainozoic stratigraphy (outlined previously). This stage of the analysis was very labour-intensive and time-consuming due to the size of the database. It was further complicated as the critical step in this process, identifying the basement, was very difficult for the most part due to the lack of distinction between consolidated and unconsolidated sediments.

Of the 2,717 boreholes selected, 604 are interpreted as having intercepted the basement/superficial boundary, with some or all of their regolith materials belonging to defined superficial formations. The most common basement formations encountered throughout the region (where identifiable) are the grey to black clays or shales of the Kings Park Formation, and the Kardinya Shale Member of the Osborne Formation. The isopach map of regolith thickness produced through this borehole interpretation and analysis is presented in Figure D.8. It should be noted that these regolith isopachs include both the Tamala Limestone (despite the fact that it is predominantly consolidated regolith) and the Poison Hill Greensand (as this unit is unconsolidated and consequently will have an impact on earthquake energy amplification). The inclusion of the Poison Hill Greensand is the main reason for the deeper regolith contours in the north of the study area (Figure D.8), and by way of example, the borehole at this anomalously deep locality penetrated 57 m of Poison Hill Greensand.

Statistics for the 604 manually interpreted bore logs show an average thickness for the superficial regolith of 29 m, with a distribution indicating that the majority of profiles are <50 m deep (Figure D.9). Statistics for borehole depths (as opposed to interpreted regolith thicknesses) in all 2,717 bores across the region show an average of 26 m, and present a similar distribution (Figure D.10). These average thickness values are in good agreement with each other, although they are slightly at odds with Playford *et al.*'s (1976, p. 206) assertion that the majority of the Quaternary deposits overlying the Swan Coastal Plain are <20 m thick. However, as mentioned previously, the inability to readily differentiate the base of the Quaternary deposits from the underlying basement materials means that several metres of weathered basement could potentially have been included in the borehole depth values. The inclusion of this 'extra' material in the averaged thickness estimates is considered justifiable, particularly given that their physical weathering state is likely to be similar to those of materials in the superficial formations above, and that the materials behaviour in response to an earthquake ground motion will also be similar.

Regolith data reclassification

Recognising the massive task involved in manually interpreting the remaining 2,100 bore logs with respect to discriminating the basement/superficial boundary and formation type, the decision was taken to develop a simplified material classification for all of the Perth study area WRC bore data (Table D.1). Given the degree of variability and inconsistency in the borehole database records, it was considered that a simplified classification would:

- capture the majority of regolith material information at a level of detail suitable for use in site class assessment, and;
- provide a 'cleaner', more consistent dataset for interpreting regolith material distribution across the Perth study area.

This re-classified data was produced and analysed to provide a broader spatial assessment of dominant regolith material distribution, and was used to develop the final site classes in conjunction with the previous detailed interpretation undertaken on regolith information from 604 bores.

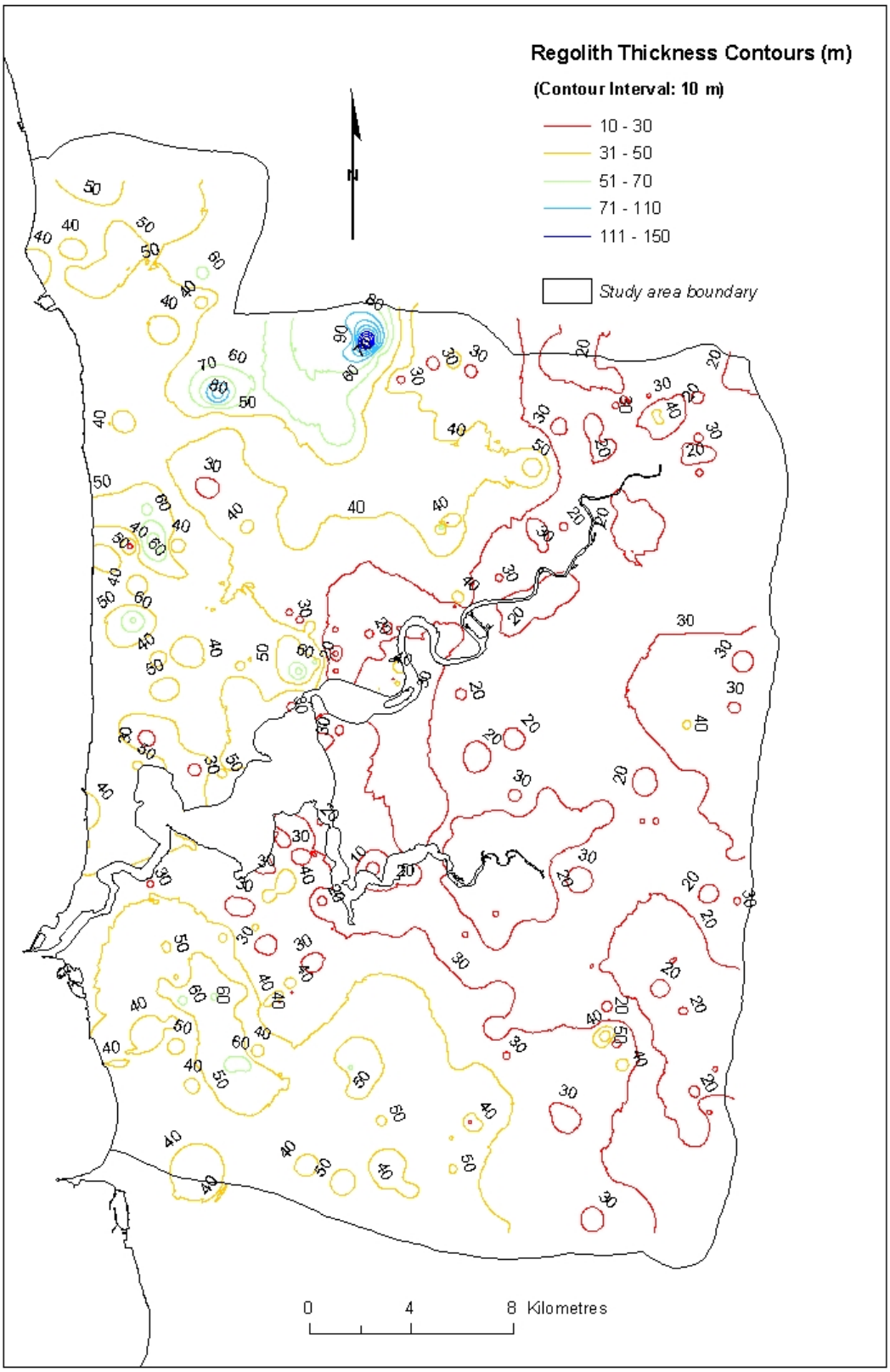

Figure D.8: Perth study area regolith thickness contours. Thicknesses include the (consolidated) Tamala Limestone and the Cretaceous (unconsolidated) Poison Hill Greensand

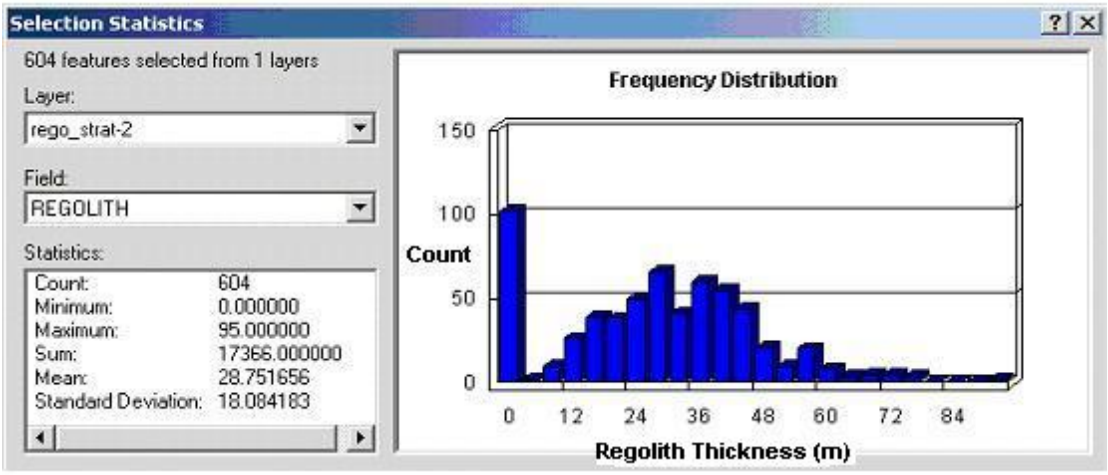

Figure D.9. Regolith thickness statistics for the 604 reinterpreted Water and Rivers Commission bores in the Perth study area.

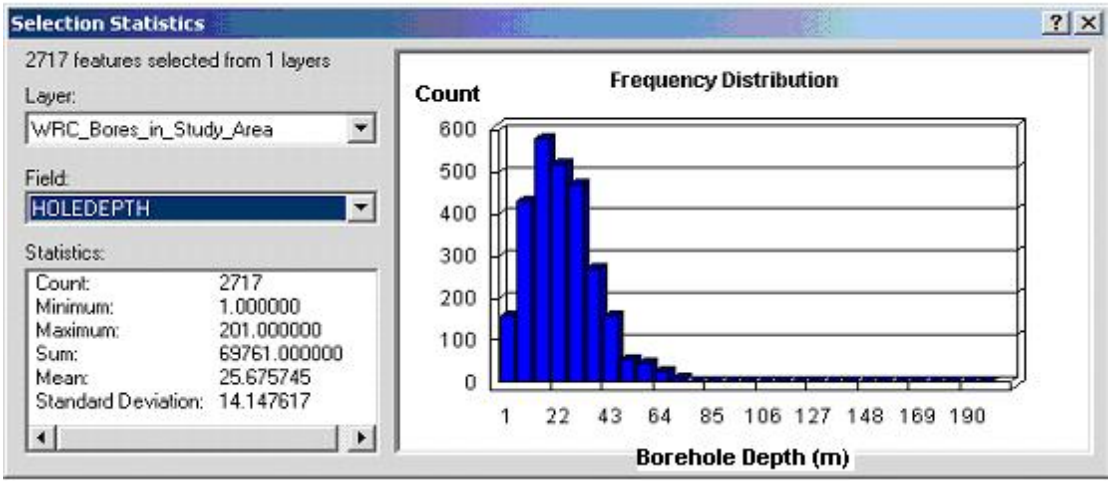

Figure D.10: Borehole depth statistics for the 2,717 Water and Rivers Commission bores across the Perth study area

Regolith material type

Having already developed a regolith thickness map for the Perth study area based on the initial 604 interpreted bores, the reclassified regolith data was used to cross-check the thicknesses and assess the spatial distribution of the dominant regolith material types.

The regolith materials of the Swan Coastal Plain are dominated by sands and calcareous deposits (limestone and secondarily cemented calcareous sands), with areas in the east closer to the Darling Range characterised by significant deposits of mud (silts and clays) (Figure D.11; Table D.2a–b). Given the general dominance of these broad regolith material types across the Perth study area, classification of bore records on the basis of material dominance within each profile was undertaken to refine this distribution. Of the logged bores (2,717) in the study area, the total thickness of material in any given profile is classified as containing >50% sand, mud or limestone for 97% (2,622) of profiles (Table D.2a). Seventy percent of profiles (1,891) are classified as containing >75% of one or other of these materials (Figure D.11; Table D.2b).

Table D.1: Summary of simplified regolith classes, dominant materials and number of records attributable to each class from the Perth study dataset

Material class	Identifier	Description	No. of records	% of records
Not logged	0	No record for the materials in the specified depth range.	54	0.5
Sand	1	Sand; silty sand; gravel; other coarse unconsolidated materials.	7 692	63.1
Mud	2	Silt; sandy silt; clay; sandy clay; mud.	1 611	13.2
Limestone	3	Limestone and any materials indurated by calcareous cements, including secondarily cemented calcareous sands.	2 030	16.6
Consolidated	4	Materials indurated by non-calcareous cements such as secondarily silicified sands; iron-oxide indurated materials (ferricrete); bedrock.	554	4.5
Coffee rock	5	Generally sands (occasionally muds) partly or completely indurated by organic complexes and iron-oxides.	203	1.6
Other	6	Rubble, fill and construction materials; refuse; organic matter (e.g. peat); other 'items' from the drillers logs not readily attributable to any other material class (e.g. slime, soup, seaweed).	55	0.5

Table D.2: Regolith materials (**a**) >50% and (**b**) >75% of total hole depth for the 2,717 logged profiles in the Perth study area

(a)

Dominant material	Profiles of >50% of material	% of profiles	Material thickness (m)		
			Minimum	Maximum	Average
Limestone	464	53	5	87	35
Mud	227	30	1	45	18
Sand	1 931	73	1	201	24
TOTAL	**2 622**	**96.5**			

(b)

Dominant material	Profiles of >75% of material	% of profiles	Material thickness (m)		
			Minimum	Maximum	Average
Limestone	230	26	5	87	36
Mud	81	11	4	45	19
Sand	1 580	60	1	78	23
TOTAL	**1 891**	**69.6**			

5. Perth Site Classes

The classification of regolith materials on the basis of the methods presented above permits distinct spatial groupings to be identified, both in terms of material type and thickness. Using this information four separate site classes have been established for the Perth study area (Figure D.12).

For areas where a given regolith material comprises >75% of the profile in a majority of profiles, the site class is represented by a single geotechnical profile for that regolith material. However, there is overlap between areas in the distribution of materials (eg, there are appreciable numbers of sand-dominated profiles within the limestone area in the west – see Figure D.11). Furthermore, the use of a single geotechnical profile accounting for only one material type can not always be considered representative across all areas. For example, in the west the limestone is commonly covered with a layer of sand. Given this heterogeneity, any one site class is modelled as one or more geotechnical profiles for a representative regolith profile overlying 15 m of weathered basement (an averaged figure for the Perth study area) which in turn is overlying 'bedrock'. Where more than one profile (or material within a profile) is necessary, a proportional weighting is applied to the quantity of each material within the geotechnical profile, and also to the proportion of the site class represented by that particular geotechnical profile.

The incorporation of information on multiple regolith material types within a site class accounts for the variation in spatial distribution of these materials. As it is potentially misleading to represent all of the regolith within a defined area on the basis of one standard geotechnical profile, multiple profiles for the dominant regolith materials were incorporated into the regolith amplification model, where applicable. By applying a weighting to account for the proportion of each geotechnical profile type within the site class, the variability in amplification due to differences in regolith material type and thickness is captured.

In the following section each of the four site classes outlined above (Figure D.12) is described in terms of its lithology, regolith thickness, geotechnical profiles and natural period. Each class is then classified into some of the widely used generic site classification schemes:

- current Australian Loading Standard (Standards Australia, 1993);
- draft Australia/NZ Loading Standard (in prep.);
- NEHRP (Building Seismic Safety Council, 2000a; 2000b); and
- International Building Code (International Code Council, 2003).

Classification into the current Australian Loading Standard was based on thickness and lithology, classification into the new draft Australia/NZ standard was based on natural period, and classification into the NEHRP and International Building Codes was based on shear wave velocity.

Shallow Sand site class

Lithology

This class is dominated by fine to very coarse, but predominantly medium-grained, moderately sorted, sub-angular to rounded quartz sand, yellow to pale grey and white in colour. Shell fragments, heavy minerals, and clay and rare limestone lenses and horizons are found throughout the section.

Regolith thickness

The 145 boreholes within this site class have an interpreted regolith thickness varying from 4–61 m, with an average thickness of 20 m (standard deviation = 13 m).

Geotechnical profiles

The entire Shallow Sand site class is represented by a sand profile 10–40 m thick. Profile averaged shear wave velocities for the 14 SCPTs undertaken within this site class ranged from 237 m/s to

382 m/s, with an average profile value of 294 m/s (standard deviation = 43 m/s). Figure D.13 shows the distribution of shear wave velocity profiles for the Shallow Sand site class.

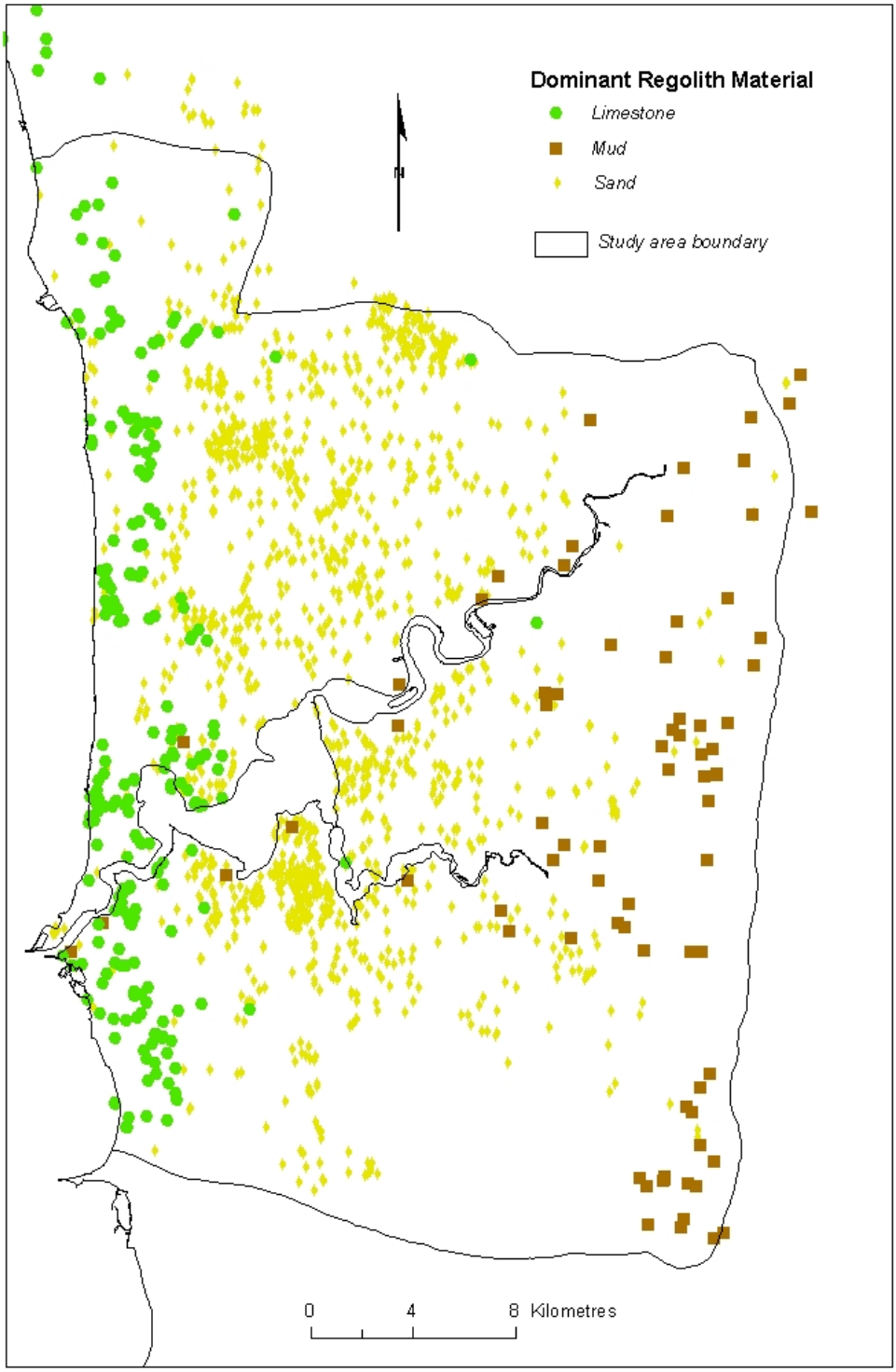

Figure D.11: Distribution of dominant regolith materials (>75% of total hole depth) across the Perth study area

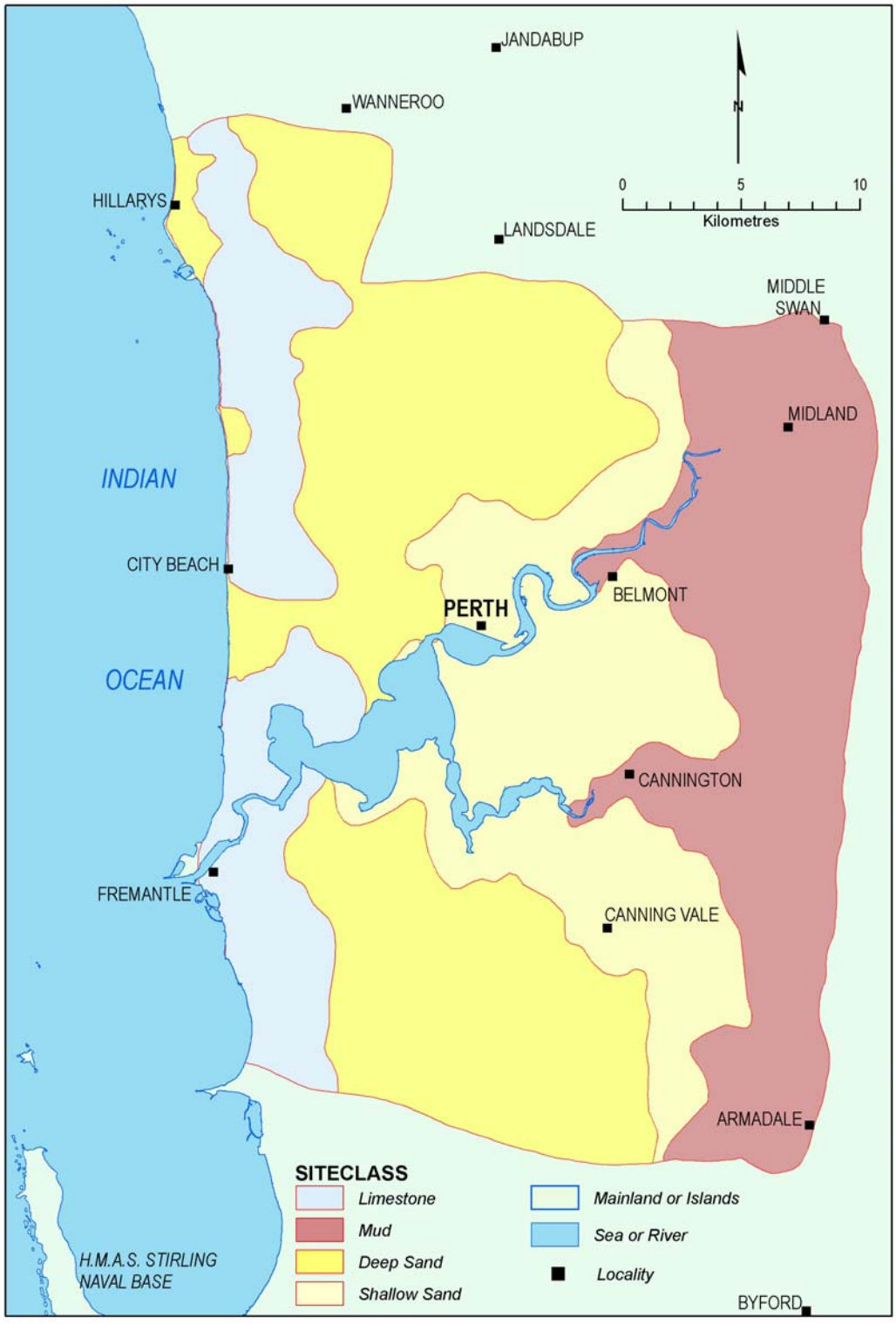

Figure D.12: Site classes defined for the Perth study area

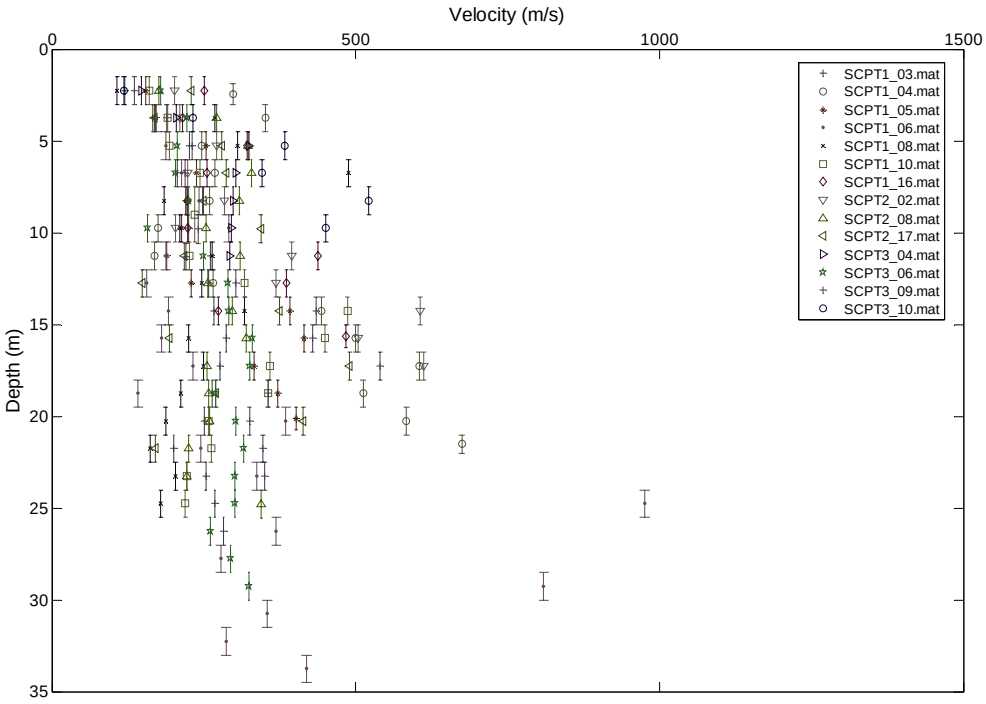

Figure D.13: Shear wave velocity data for the Shallow Sand site class

Natural period

Microtremor survey measurements across this class comprise 687 sites, with an average natural period of 0.65 seconds and a standard deviation of 0.46.

Classification in generic site class schemes

- Australian Loading Standard: *Soil profile with more than 12 m of very loose or loose sands*, as this class comprises an average of 20 m of sand.
- New Australia/NZ Loading Standard: *Class D – Deep or Soft Soil Sites*, as the average natural period for the class is greater than 0.6 s. However, the standard deviation for the microtremor measurements may force values below 0.6 and hence shift the site class into *Class C – Shallow Soil Sites*.
- NEHRP: *Class D – Stiff Soil*, as the majority of measured shear wave velocities are greater than 180 m/s and less than 360 m/s.
- International Building Code: *Class D – Stiff Soil Profile*, as the shear wave velocity of this class is between 200 m/s and 400 m/s (600-1,200 ft/s).

Deep Sand site class

Lithology

The materials in this class are essentially identical to those of the Shallow Sand class.

Regolith thickness

The 193 boreholes within this site class have an interpreted regolith thickness varying from 0–95 m, with an average thickness of 42 m (standard deviation = 14 m).

Geotechnical profiles

The entire Deep Sand site class is represented by a sand profile 30–60 m thick. Profile averaged shear wave velocities for the 26 SCPTs undertaken within this site class ranged from 129 m/s to 539 m/s, with an average profile value of 300 m/s (standard deviation = 82 m/s). Figure D.14 shows the distribution of shear wave velocity profiles for the Deep Sand site class.

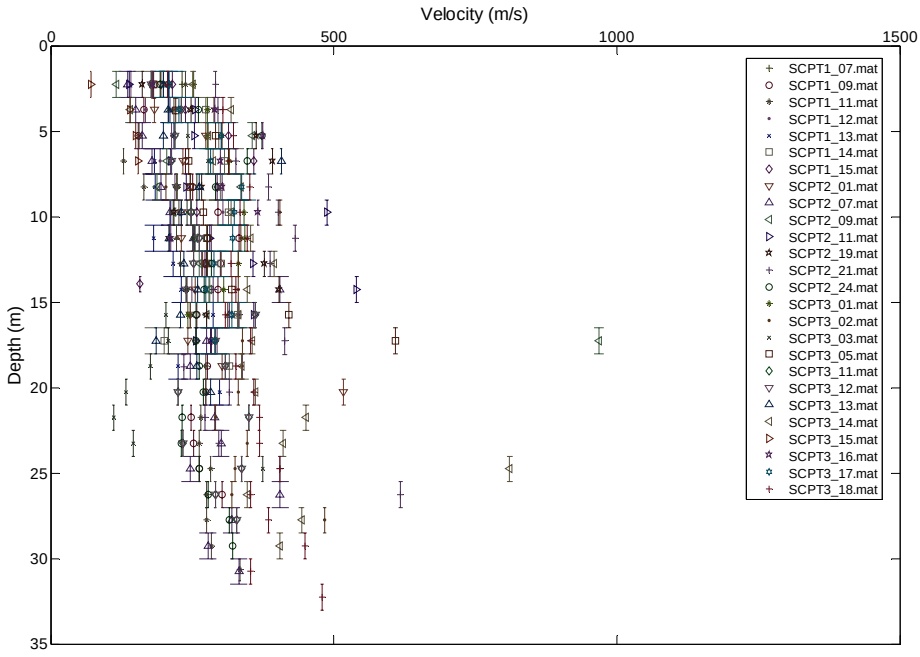

Figure D.14: Shear wave velocity data for the Deep Sand site class

Natural period

Microtremor survey measurements across this class comprise 928 sites, with an average natural period of 0.5 s and a standard deviation of 0.50.

Classification in generic site class schemes

- Australian Loading Standard: *Soil profile with a total depth of 20 m or more, and containing 6–12 m of very loose or loose sands*, as this class comprises an average of 42 m of sand.
- New Australia/NZ Loading *Standard: Class D – Deep or Soft Soil Sites*, as the average natural period for the class is greater than 0.6 seconds. The large standard deviation for the microtremor measurements gives potential values below 0.6, suggesting a shift into Class C – Shallow Soil Sites, although the significant regolith thickness values should preclude this.
- NEHRP: *Class D – Stiff Soil*, as the majority of measured shear wave velocities are greater than 180 m/s and less than 360 m/s, although spread on the distribution may move some sites into *Class C – Very Dense Soil/Soft Rock.*
- International Building Code: *Class D – Stiff Soil Profile*, as the shear wave velocity of this class is between 200 m/s and 400 m/s (600-1,200 ft/s).

Mud-dominated site class

Lithology

This class is characterised by mud-dominated regolith profiles containing variegated, but predominantly brown clays, silts, silty clays, and less commonly sandy clays and silts. Sandy lenses and horizons, occasionally shell-bearing towards the lower part of the succession, are distributed throughout. The class also contains some sand-dominated regolith profiles with materials similar to those of Shallow Sand class.

Regolith thickness

The 191 boreholes within this site class have an interpreted regolith thickness varying from 0–4 m, with an average thickness of 18 m (standard deviation = 13 m).

Geotechnical profiles

Approximately 80% of the mud-dominated site class is represented by a mud profile 10–30 m thick, while the remaining 20% is represented by a shallow sand profile (10–30 m thick) as per the Shallow Sand class. Profile averaged shear wave velocities for the 13 SCPTs undertaken within this site class ranged from 178 m/s to 895 m/s, with an average profile value of 330 m/s (standard deviation = 179 m/s). If the anomalous maximum value of 895 m/s (associated with Site 2-23, which intercepts a consolidated conglomeratic layer) is removed, the 12 remaining profiles give an average of 283 m/s (standard deviation = 60 m/s). Figure D.15 shows the distribution of shear wave velocity profiles for the Mud-dominated site class.

Natural period

Microtremor survey measurements across this class comprise 410 sites, with an average natural period of 0.5 s and a standard deviation of 0.35.

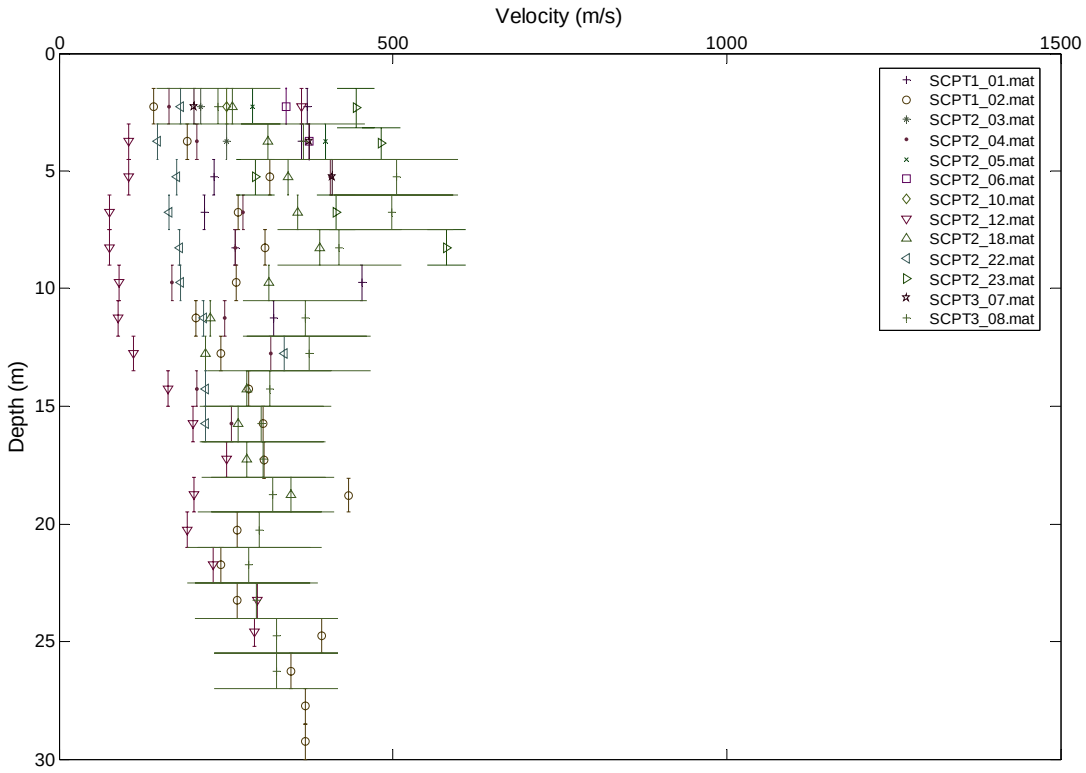

Figure D.15: Shear wave velocity data for the Mud-dominated site class.

Classification in generic site class schemes

- Australian Loading Standard: *Soil profile with more than 12 m of silts*, as this class comprises an average of 18 m of mud. However, it should be noted that this site class is not characterised by shear wave velocities less than 150 m/s, as suggested by the code, and therefore it may be more appropriate to identify this class in a S*oil profile with not more than 30 m of firm, stiff or hard clays*.
- New Australia/NZ Loading Standard: *Class C – Shallow Soil*, as the average natural period for the class is less than 0.6 s. However, the standard deviation for the microtremor measurements may force values above 0.6 and hence shift the site class into *Class D – Deep or Soft Soil*.
- NEHRP: *Class D – Stiff Soil*, as the majority of measured shear wave velocities (minus the anomalous value) are greater than 180 m/s and less than 360 m/s.
- International Building Code: *Class D – Stiff Soil Profile*, as the shear wave velocity of this class is between 200 m/s and 400 m/s (600–1,200 ft/s).

Limestone-dominated site class

Lithology

The sands within this class are identical to those in the Shallow Sand class. The limestone is composed of hard to friable calcareous aeolianite, commonly containing shells and shell fragments. Thin sand interbeds are preserved throughout the succession. It is creamy-white to yellow, or more commonly light-grey to fawn coloured at depth. The limestone contains numerous solution cavities.

Regolith thickness

The 74 boreholes within this site class have an interpreted regolith thickness varying from 0-79 m, with an average thickness of 40 m (standard deviation = 18 m).

Geotechnical profiles

Approximately 80% of the Limestone-dominated site class is represented by a geotechnical profile 15–60 m thick, composed of 10 m of sand overlying 30 m of limestone. The remaining 20% of the class is represented by a deep sand profile (30–60 m thick) as per the Deep Sand site class. Profile averaged shear wave velocities are unavailable for the limestone in this class, as SCPTs failed to penetrate the substrate. Wilkens *et al*. (1992) suggest shear wave velocities for limestone in the range 700–1,100 m/s, with an average of about 900 m/s. In the absence of real data for limestone in the Perth study area, this average figure has been adopted. Shear wave velocities for the sand profiles are as per the Deep Sand class.

Natural period

Microtremor survey measurements across this class comprise 504 sites, with an average natural period of 0.22 s and a standard deviation of 0.38.

Classification in generic site class schemes

- Australian Loading Standard: *Soil profile with a total depth of 20 m or more, and containing 6–12 m of very loose or loose sands*, as this class comprises an average of 42 m of sand.
- New Australia/NZ Loading Standard: *Class C – Shallow Soil Sites*, as the average natural period for the class is less than 0.6 s. The low average value for the microtremor measurements suggests that *Class B – Rock* may be more appropriate for this site class, however, the Standard specifies a 3 m maximum thickness of the overlying soil, and as such precludes this classification.
- NEHRP: *Class B – Rock*, as the shear wave velocity range of Wilkens *et al.* (1992) suggests a range between 760 m/s and 1,500 m/s.
- International Building Code: *Class B – Roc*k, as the suggested shear wave velocity of this class is between 800 m/s and 1,300 m/s (2,500–5,000 ft/s).

Site classification in Northam

The regolith in the Northam area comprises 6–10 m of silt/clay alluvium, so based purely on regolith material type and thickness, its most appropriate classification is into the Mud-dominated class. Microtremor survey data from the area show an average natural period of 0.39 s across 20 sites. This figure is quite low when compared to the average figures for all defined sites classes in the Perth Basin. However, given the large standard deviations associated with these figures, the average for Northam is within the range of one standard deviation for the Mud-dominated site class.

D.6. Discussion

Site class distribution

The distribution of site classes defined for the Perth study area (see Fig. D.12) strongly reflects the occurrence and distribution of regolith materials, whose type and thickness influence the potential

amplification of earthquake ground motion. Despite the complex geomorphic history of the Swan Coastal Plain, the regolith materials of the superficial formations (and hence the defined site classes) can be generalised and effectively separated into three spatially distinct zones.

Eastern Zone
Mud-dominated materials found in association with the Pinjarra Alluvial Plain and colluvial slopes of the Ridge Hill Shelf (Davidson, 1995). Materials consist of fluvial mud deposits of the Guildford Formation and more recent alluvial and colluvial materials, with minor contributions of sand, gravel and minor clays from palaeo-shoreline deposits of the Yoganup Formation. Regolith thicknesses are <50 m, and average ~20 m. The distribution of regolith materials in Figure D.8 highlights the fact that small areas of mud-dominated materials can be expected to be found in association with present drainage (for example, along the Swan River) outside the mapped site class boundary.

Central Zone
Shallow and deep sand-dominated profiles related to multiple generations of prograding shoreline deposits and aeolian reworking. Materials are primarily associated with the degraded surfaces of the Bassendean and Spearwood Dune Systems (McArthur and Bettenay, 1960). Regolith thicknesses average ~20 m in the shallower areas in the east, while generally increasing to the west where averages are closer to 40 m. Local variability is encountered, particularly where underlying unconsolidated Cretaceous–Tertiary units such as the Poison Hill and Molecap Greensands are present.

Western Zone
Limestone-dominated materials underlying the degraded surface of the western Spearwood Dune System, and foredune plains/dune complexes of the Quindalup Dune System (McArthur and Bettenay, 1960). The limestone has formed primarily as a result of solution of calcareous dune sands and re-precipitation of carbonate material further down the sequence. The occurrence of quartz sand deposits overlying (and interspersed with) the limestone can be attributed partly to this solution process, which has chemically 'winnowed' the quartz sands. However, the primary mechanisms for the occurrence of the sand deposits are near-shore marine sand deposition of the Becher Sand, and more recent aeolian deposition of the Safety Bay Sand unit (coincident with the Quindalup Dune System – McArthur and Bettenay 1960). Regolith thicknesses tend to be <80 m, with an average of approximately 40 m for both Limestone-dominated and interspersed Deep Sand profiles.

Liquefaction potential

Liquefaction is a phenomenon in which the strength and stiffness of a soil is reduced by earthquake shaking or other rapid loading. Liquefaction and related phenomena have been responsible for tremendous amounts of damage in historical earthquakes around the world (Yanagisawa, 1983; Borchardt, 1991; Morales *et al*., 1995). Liquefaction occurs in saturated soils, that is, soils in which the space between individual particles is completely filled with water. This water exerts a pressure on the soil particles, thereby influencing how tightly the particles themselves are pressed together. Prior to an earthquake, the water pressure is generally relatively low. However, earthquake shaking can cause the water pressure to increase to the point where the soil particles can readily move with respect to each other. Because liquefaction only occurs in saturated soil, its effects are most commonly observed in low-lying areas near bodies of water such as rivers, lakes, bays, and oceans (University of Washington 2005).

There are a number of different ways to evaluate the liquefaction susceptibility of a soil deposit (Kramer, 1996).

1. Historical Criteria: Soils that have liquefied in the past can liquefy again in future earthquakes.
2. Geological Criteria: Saturated soil deposits that have been created by sedimentation in rivers and lakes, deposition of debris or eroded material, or deposits formed by wind action can be very liquefaction susceptible.

3. Compositional Criteria: Liquefaction susceptibility depends on the soil type. Soils composed of particles that are all about the same size are more susceptible to liquefaction than soils with a wide range of particle sizes.
4. State Criteria: At a given effective stress level, looser soils are more susceptible to liquefaction than dense soils. For a given density, soils at high effective stresses are generally more susceptible to liquefaction than soils at low effective stresses.

Andrus and Stokoe (2000) compiled 225 liquefaction case histories from the United States, Taiwan, Japan and China. Of these case history sites 90% of the liquefied horizons had a critical layer thickness of less than 7 m, an average depth below land surface of less than 8 m, and a standing water level (water table) less than 4 m.

There does not appear to be any record of liquefaction in the Perth area, therefore there are no soils that fulfil Kramer's (1996) criteria 1. Sediments deposited by rivers or lakes (criteria 2) and well-sorted sand layers (criteria 3) are widely distributed throughout the study area. However, the water table is generally close to the surface only in close proximity to the Swan and Canning Rivers, therefore potentially liquefiable saturated sediments are likely to be confined to this region. To test which, if any, of these layers have the potential to liquefy, the shear wave velocities from five SCPT sites were modelled.

Of the five SCPT sites assessed, three sites (1-5, 1-6 and 2-12, see Figure D.5) were considered to have some potential for liquefaction. Site 1-6 contains a single thin (~1 m) sand horizon at approximately 14 m depth, capped by mud layers. Site 2-12 has two potentially liquefiable layers, which consist of sand to silty-sand horizons approximately 2 m thick at depths of about 15 m and 18 m. The water table depths at these two sites are about 5 m and 8 m respectively (Davidson, 1995). In light of the case history database presented by Andrus and Stokoe (2000), it is unlikely that these layers will liquefy as each of these horizons is considerably deeper than 8 m, and the water table is deeper than 4 m.

Site 1-5 contains a sand and gravel sequence approximately 15 m thick extending from a depth of 5 m down to nearly 20 m, with a 5 m overlying (confining) layer of silt and a water table at approximately 1 m (Davidson, 1995). Despite having the correct material type under a confining layer coupled with a shallow water table, the significant thickness of the sand/gravel sequence and the occurrence of the majority of the sequence at a depth of greater than 8 m below the land surface make it unlikely that this sequence will liquefy.

On the basis of these test cases there is a very low liquefaction potential in the Perth region, a conclusion similar to that reached by Cocks *et al*. (2003).

Guria Consulting Report

The results presented by Brian Gaull in his report on the 2001 microzonation study of the Perth region (Gaull, 2002; 2003) are based on a series of shear wave velocities for seven zones in the greater Perth metropolitan region (Figure D.6). Shear wave velocities were estimated by relating the natural period and thickness of the regolith in each zone. A mean depth and mean natural period, and the gradient of depth-natural period plots were used to calculate shear wave velocities for each zone. As outlined above, one of the datasets collected during the site class study was a series of seismic cone penetrometer tests. These tests were undertaken within or very close to Gaull's seven zones, allowing for direct comparison between measured shear wave velocities and Gaull's (2002) velocity estimates derived from microtremor data. This comparison is presented below by site (or 'target' – Gaull, 2003).

Site 1: Midland

Estimated shear wave velocity for this zone of approximately 235 m/s based on the total depth and natural period data, and 200 m/s based on a mean depth and mean period.

SCPT site 2-12 is located within this zone. The test pushed to a depth of 25.2 m, the upper 12 m of which was predominantly organic clays with lesser clay to clayey silt, while the lower 13 m was predominantly sandy silt to sand. The shear wave velocity of the upper 12 m varies around 100 m/s. The shear wave velocity of the lower sandier section increases down-hole from approximately 200 m/s to 250 m/s.

Site 2: Kelmscott

Estimated shear wave velocity for this zone is approximately 220 m/s based on the total depth and natural period data, and 190 m/s based on a mean depth and mean period.

SCPT site 1-1 is located within this zone. The test pushed through to 12.0 m, the upper 6.5 m of which was a fining down sequence of sand to clay, while the lower 5.5 m was predominantly gravelly sand. The shear wave velocity of the upper section decreases down-hole from approximately 350 m/s to 225 m/s. The shear wave velocity of the lower sandy section varies significantly around 275 m/s.

Site 3: Hillarys

Estimated shear wave velocity for this zone is approximately 450 m/s based on the total depth and natural period data, and 285 m/s based on a mean depth and mean period.

SCPT site 3-17 is located within this zone. The test pushed through 19.85 m of silty sand to sand. The velocity plots show the shear wave velocity varies slightly around a value of approximately 300 m/s.

Site 4: Rockingham

Estimated shear wave velocity for this zone is approximately 190 m/s based on the total depth and natural period data, and 200 m/s based on a mean depth and mean period.

SCPT site 3-14 is located within this zone. The test pushed through 33.05 m of predominantly silty sand to sand. The velocity plots show the shear wave velocity varies slightly around a value of approximately 350 m/s for the majority of the profile.

Site 5: Bateman

Estimated shear wave velocity for this zone is approximately 250 m/s based on the total depth and natural period data, and 180 m/s based on a mean depth and mean period.

SCPT site 1-6 is located within this zone. The test pushed through 34.5 m of predominantly silty sand to sand, with lesser clay and clayey silt layers. The velocity plots show the shear wave velocity in the upper half of the test varies slightly around a value of approximately 200 m/s. The shear wave velocity in the lower half of the test varies slightly around a value of approximately 300 m/s, with the exception of two distinct layers with shear wave velocities between 900 m/s and 1,000 m/s.

Site 6: Bayswater

Estimated shear wave velocity for this zone is approximately 220 m/s based on the total depth and natural period data, and at least 185 m/s based on a mean depth and mean period.

SCPT site 3-12 is located within this zone. This test penetrated 29.25 m of regolith, the upper 20 m of which was predominantly sand, while the lower 10 m was dominated by clayey silt to silty sand. The shear wave velocity of the upper sandy section increases down-test from 220 m/s to 250 m/s. The shear wave velocity of the lower sandy section varies around a value of approximately 300 m/s.

Site 7: Perth

Estimated shear wave velocity for this zone is approximately 265 m/s based on the total depth and natural period data, and 230 m/s based on a mean depth and mean period.

SCPT site 1-8 is located within this zone. The test penetrated 25.5 m, the upper half of which was predominantly clay with silty bands, while the lower half is dominated by sandy silt to clayey silt. The shear wave velocity in the test decreases down-hole from approximately 250 m/s to 200 m/s.

Discussion

Overall the shear wave velocity estimates presented by Gaull (2002) do not compare favourably with the measured shear wave velocities. At most sites the calculated shear wave velocity values based on either the total or mean natural period and depth data can only be considered comparable to the measured SCPT value in a small percentage (generally <50%) of the profile. For example, the estimate of 220 m/s (based on the total data) for Site 6 agrees with the measured shear wave velocity values near the top of the profile for SCPT site 3-12. However, the SCPT data demonstrate an increase in shear wave velocity with depth, with values in the lower profile averaging 300 m/s – significantly higher than either of the calculated values. Overall, the calculated shear wave velocity data tend to either underestimate (eg, Sites, 2, 4 and 6) or overestimate (eg, Site 3) the actual (measured) shear wave velocities in almost the entire profile.

There does not appear to be any trend in the reliability of the estimates calculated from the total data as opposed to the mean data. That is, in some cases the total data estimate was closer to the measured shear wave velocity value, while in others it was the average data estimate that was more accurate. For example, the total data estimate for Site 2 (220 m/s) is closer to the measured shear wave velocity, but at Site 3 the average data estimate (285 m/s) is more accurate.

Estimated shear wave velocity values presented by Gaull also do not appear to account for the presence of very high or low velocity layers, as we would expect from an assessment of the capabilities of the methods available to Gaull. A good example of this is seen at Site 5, where estimated values are 3–4 times lower than measured values for high velocity layers.

Overall, the method applied and results presented by Gaull (2002) should be used with caution in relation to earthquake studies. Conversion of microtremor-derived natural periods into shear wave velocities through depth relations should be confined to areas in which the regolith comprises a low variability (preferably homogeneous) sequence of material with well constrained thickness information. As the Quaternary geology of the Perth Basin fulfils neither of these criteria, the results of Gaull's (2002) report should be appraised carefully.

D.7 References

Allen, A.D. (1976) 'Outline of the hydrogeology of the superficial formations of the Swan Coastal Plain', *Western Australia Geological Survey, Annual Report 1975*, 31-42.

Allen, A.D. (1977) 'The hydrogeology of the Mirrabooka East area, Perth', *Western Australia Geological Survey, Annual Report* 1976, 14-21.

Anand, R.R. and Paine, M. (2002) 'Regolith geology of the Yilgarn Craton', *Australian Journal of Earth Sciences*, 49(1):1–162.

Andrus, R.D. and Stokoe, K.H. (2000) 'Liquefaction resistance of soils from shear wave velocity', *Journal of Geotechnical and Geoenvironmental Engineering*, 126(11): 1015–25.

Aurousseau, M. and Budge, E.A. (1921) 'The terraces of the Swan and Helena Rivers and their bearing on recent displacement of the strand line', *Journal of the Royal Society of Western Australia*, 7:24–43.

Barnes, R.G. (1977) 'Hydrogeological report on the Pacminex alumina refinery site, Upper Swan', *Western Australia Geological Survey, Hydrogeology Report 879*.

Baxter, J.L. (1982) 'History of mineral sand mining in Western Australia', in *Reference Papers, Exploitation of Mineral Sands*. Western Australian School of Mines, WAIT AID Ltd., Perth.

BMR Palaeogeographic Group. (1990) '*Australia: Evolution of a Continent*', Bureau of Mineral Resources, Canberra.

Borchardt, G. (1991) 'Liquefaction and shaking damage in the Watsonville and Oakland areas and its implications for earthquake planning scenarios (in Loma Prieta earthquake; engineering geologic perspectives)', *Special Publication – Association of Engineering Geologists* 1:83–103.

Building Seismic Safety Council. (2000a) *National Earthquake Hazards Reduction Program (NEHRP) recommended provisions for seismic regulations for new buildings and other structures*. *Part 1: Provisions (FEMA 368)*, Building Seismic Safety Council, Washington DC.

Building Seismic Safety Council. (2000b) *National Earthquake Hazards Reduction Program (NEHRP) recommended provisions for seismic regulations for new buildings and other structures*. *Part 2: Commentary (FEMA 369)*, Building Seismic Safety Council, Washington DC.

Cockbain, A.E. and Hocking, R.M. (1989) 'Revised stratigraphic nomenclature in Western Australian Phanerozoic basins', *Western Australia Geological Survey, Record* 1989/5.

Cockbain, A.E. (1990) 'Perth Basin', in 'Geology and mineral resources of Western Australia', *Western Australia Geological Survey, Memoir* 3, pp. 495–524.

Cocks, G., Hillman, M. and Simpson, K. (2003) 'Liquefaction and settlement assessment for the Mortimer Road Bridge, Perth, Western Australia', *Australian Geomechanics*, 38(4):148–56.

Commander, P. (2003) 'The geomorphology of the Perth region, Western Australia', *Australian* Geomechanics, 38(3):7–16.

Davidson, W.A. (1995) 'Hydrogeology and groundwater resources of the Perth region, Western Australia', *Western Australia Geological Survey, Bulletin 142*.

Fairbridge, K.R.W. (1953) *Australian stratigraphy: Perth*, University of Western Australia Text Books Board.

Gaull, B.A. (2002) Microzonation of the Perth Basin in the region of Perth, Western Australia, Consulting report written for Geoscience Australia by Guria Consulting.

Gaull, B.A. (2003) 'Seismic characteristics of the sediments of the Perth basin', *Australian Geomechanics*, 38(3):111–22.

Gozzard, J.R. (1982a) *Muchea, Sheet 2034 I and part 2134 IV*, Perth Metropolitan Region 1:50,000 Environmental Geology Series, Geological Survey of Western Australia.

Gozzard, J.R. (1982b) *Yanchep, Sheet 2034 IV*, Perth Metropolitan Region 1:50,000 Environmental Geology Series, Geological Survey of Western Australia.

Gozzard, J.R. (1983a) *Fremantle, Part Sheet 2033 I and 2033 IV*, Perth Metropolitan Region 1:50,000 Environmental Geology Series, Geological Survey of Western Australia.

Gozzard, J.R. (1983b) *Rockingham, Part Sheet 2033 I and 2033 III*, Perth Metropolitan Region 1:50,000 Environmental Geology Series, Geological Survey of Western Australia.

Gozzard, J.R. (1985) 'Medium-scale engineering- and environmental-geology mapping of the Perth metropolitan region, Western Australia', *Engineering Geology*, 22(1):97–107.

Gozzard, J.R. (1986) *Perth, Sheet 2034 II and part 2034 III and 2134 III*, Perth Metropolitan Region 1:50,000 Environmental Geology Series, Geological Survey of Western Australia.

Iasky, R. P. and Mory, A. J. (1993) 'Structural and tectonic framework of the onshore northern Perth Basin', *Exploration Geophysics*, 24(3–4):585–92.

International Code Council. (2003) *International Building Code*, Delmar Publishers, New York.

Janssen, D.P., Collins, A.S. and Fitzsimons, I.C.W. (2003) 'Structure and tectonics of the Leeuwin Complex and Darling Fault Zone, southern Pinjarra Orogen, Western Australia – a field guide', *Western Australia Geological Survey, Record 2003/15*.

Johnston, C.D. and McArthur, W.M. (1981) *Subsurface salinity in relation to weathering depth and landform in the eastern part of the Murray River catchment area, Western Australia*, Land Resources Management Technical Paper No. 10, CSIRO, Melbourne.

Jordan, J.E. (1986a) *Armadale, Part Sheet 2033 I and 2133 IV*, Perth Metropolitan Region 1:50,000 Environmental Geology Series, Geological Survey of Western Australia.

Jordan, J.E. (1986b) *Mundaring, Part Sheet 2134 II and 2134 III*. Perth Metropolitan Region 1:50,000 Environmental Geology Series, Geological Survey of Western Australia.

Jordan, J.E. (1986c) *Serpentine, Part Sheet 2033 II and 2133 III*, Perth Metropolitan Region 1:50,000 Environmental Geology Series, Geological Survey of Western Australia.

Kendrick, G.W., Wyrwoll, K-H. and Szabo, B.J. (1991) 'Pliocene–Pleistocene coastal events and history along the western margin of Australia', *Quaternary Science Reviews* 10, pp. 419–39.

Kramer, S.L. (1996) *Geotechnical Earthquake Engineering*, Civil Engineering and Engineering Mechanics Series, Prentice Hall, NJ.

Low, G.H. (1971) 'Definition of two new Quaternary formations in the Perth Basin', *Western Australia Geological Survey, Annual Report 1970*, pp. 33–34.

McArthur, W.M. and Bettenay, E. (1960) *The Development and Distribution of the Soils of the Swan Coastal Plain, Western Australia*, CSIRO Soil Publication No. 16. CSIRO, Melbourne.

McWhae, J.R.H., Playford, P.E., Lindner, A.W., Glenister, B.F., and Balme, B.E. (1958) 'The stratigraphy of Western Australia', *Geological Society of Australia, Journal*, 4(2):161.

Morales, E.M., Tokimatsu, K., Kojima, H., Kuwayama, S., Abe, A. and Midorikawa, S. (1995) 'Liquefaction-induced damage to buildings in 1990 Luzon earthquake; discussion and closure', *Journal of Geotechnical Engineering*, 121(5):453–54.

Morgan, K.H. (1964) 'Hydrogeology of the southern part of the Gnangara Lake area, South-West Division, Western Australia', *Western Australia Geological Survey, Record 1964/17*.

Nakamura, Y. (1989) 'A method for dynamic characteristics estimation of subsurface using microtremor on the ground surface', *Quarterly Report of the Railway Technical Research Institute (RTRI)*, 30(1):25–33.

Nidagal, V. and Davidson, W.A. (1991) 'North coastal groundwater investigation (Burns Beach–Pipidinny)', *Western Australia Geological Survey, Hydrogeology Report 1991/17*.

Northcote, K.H., Bettenay, E., Churchward, H.M., and McArthur, W.M. (1967) *Atlas of Australian Soils, Explanatory Data for Sheet 5 – Perth-Albany-Esperance Area*, CSIRO, Melbourne.

Ollier, C.D. (1978) 'Early landform evolution' in Jeans, J.N. (editor) *Australia, a Geography*, pp. 85–98. University Press, Sydney.

Ollier, C.D. (1988) 'Deep weathering, groundwater and climate', *Geografiska Annaler* 70:285–89.

Passmore, J.R. (1967) *The geology, hydrology, and contamination of shallow water aquifers in the Rockingham district, Western Australia*, Ph.D. Thesis, University of Western Australia, Perth.

Passmore, J.R. (1970) 'Shallow coastal aquifers in the Rockingham District, Western Australia', *Water Research Foundation of Australia, Bulletin 18*, p. 83.

Playford, P.E., Cockbain, A.E. and Low, G.H. (1976) 'Geology of the Perth Basin Western Australia', *Geological Society of Western Australia, Bulletin 124*.

Playford, P.E. and Low, G.H. (1972) 'Definitions of some new and revised rock units in the Perth Basin', *Western Australia Geological Survey, Annual Report 1971*, pp. 44–46.

Quilty, P.G. (1974) 'Cainozoic stratigraphy in the Perth area', *Journal of the Royal Society of Western Australia 57*, pp. 16–31.

Semeniuk, V. and Searle, D.J. (1985) 'The Becher Sand, a new stratigraphic unit for the Holocene of the Perth Basin', *Journal of the Royal Society of Western Australia 67*, pp. 109–15.

Smurthwaite, A.J. (1989) *Gleneagle, Part Sheet 2133 II and 2133 III*, Perth Metropolitan Region 1:50,000 Environmental Geology Series, Geological Survey of Western Australia.

Standards Australia. (1993) *AS 1170.4-1993 – Minimum design loads on structures (SAA Loading Code). Part 4: Earthquake loads*, Standards Australia, Homebush, Sydney.

University of Washington. (2005) Soil Liquefaction website. Available at http://www.ce.washington.edu/~liquefaction/html/main.html. Last accessed March 3 2005.

Wilkens, R.H., Cheng, C.H. and Meredith, J.A. (1992) 'Evaluation and prediction of shear wave velocities in calcareous marine sediments and rocks', *Journal of Geophysical Research*, 97(B69):9297–305.

Wyrwoll, K.-H. (2003) 'The geomorphology of the Perth region, Western Australia, *Australian Geomechanics*, 38(3):17–32.

Yanagisawa, E. (1983) 'Damage to structures due to liquefaction in the Japan Sea earthquake of 1983', *Disasters*, 7(4):259–65.

Appendix E: On TSUNAMI HAZARD IN WESTERN AUSTRALIA

The recent occurrence of two massive earthquakes off the coast of Sumatra in December 2004 and March 2005 has greatly heightened the awareness of the tsunami hazard among the Australian public, especially in Western Australia. The following is a brief summary of tsunami hazard for the Perth region, which emphasizes the hazard due to subduction zone earthquakes off Sumatra.

Tsunami Source Zones and Tsunami Hazard for Perth

Tsunami are usually generated by earthquakes in subduction zones, where one of the rigid, tectonic plates which comprise the earth's surface dives beneath another. The subduction zone which lies offshore Indonesia to the northwest of Australia, where the Australian plate subducts beneath the Eurasian plate, is the one which presents the most direct tsunami hazard to Australia. In the recent past earthquakes off Java have caused large tsunami which have reached heights of 4 to 6 metres on Australia's northwest coast (due to the 1994 Java and 1977 Sumbawa earthquakes, respectively). Although these events have hitherto caused little damage and taken no lives, the rapid increase in population of northwest Australia suggests that these tsunami are potentially an important hazard that merit further consideration. This is especially true when the substantial investment in oil and gas infrastructure along the Northwest Shelf is considered. Since this infrastructure supports much of Western Australia's economy, a tsunami affecting production facilities on the Northwest Shelf may have a severe economic impact. These tsunami appear capable of having a significant impact on the northwest coast, but do not typically generate significant wave heights in the Perth area.

The occurrence of the 26 December, 2004 Sumatra-Andaman earthquake, however, established that the tsunami source zone which poses a greater hazard for the Perth area lies off the coast of Sumatra, to the west of Java. It is now widely recognized that this subduction zone can produce some of the largest earthquakes in the world and the associated tsunami are massive enough to affect the entire Indian Ocean Basin. These tsunami have the potential to affect the coastline near Perth.

Historical Earthquakes and Tsunami Off Sumatra

As pointed out in the Sept. 2004 edition of Geoscience Australia's AusGeo News (Cummins and Burbidge, 2004), great thrust earthquakes have occurred off Sumatra in historic times, prior to the events of 26 December 2004 and 28 March 2005. Newcomb and McCann (1987) document the occurrence of these earthquakes in 1833 (Mw=8.7-8.8) and 1861 (Mw= 8.3-8.5), which occurred before widespread European settlement in WA. Zachariasen et al (1999) have recently used the growth ring record of coral microatolls to estimate the uplift associated with the 1833 earthquake, and estimate that its moment magnitude may have been as high as 9.2, a truly massive earthquake which may affect the entire Indian Ocean basin, including the Perth area. However, until archival evidence of the 1833 tsunami was discovered in the Seychelles by a Canadian team during a post-tsunami survey of the Boxing Day Tsunami, no known historical evidence existed to suggest that the tsunami associated with the 1833 earthquake affected the Indian Ocean beyond Sumatra. In particular, no observations of tsunami were made in WA, but there was only sparse European settlement in 1833 (the first settlement on the Swan River was established in 1829).

Results of modelling of the open-ocean propagation of the tsunami associated with the 1833 Sumatra earthquake are illustrated in Figure 2 (Cummins and Burbidge, 2004). This modelling is accurate only for tsunami propagation in deep water, and does not account for actual run-up of the tsunami onto the shoreline, where its amplitude will usually increase several fold. What the numerical simulation shows is that, although the waves are large enough to affect the entire Indian Ocean basin, the pattern of radiated tsunami energy is highly directional (Fig. 2c), with most of the energy concentrated in the

southwest direction, away from Sumatra and into the open Indian Ocean. This pattern is determined by the strike of the Sumatra subduction thrust fault. Unlike tsunami generated off Java, which direct most of their energy towards a limited section of Australia's northwest coast, tsunami from massive earthquakes off Sumatra spread considerable energy throughout the Indian Ocean. Such tsunami can affect a much wider stretch of Australia's coastline, extending from the northwest coast to the Perth area and even as far south as Tasmania. In the numerical simulation of the 1833 tsunami, open-ocean tsunami wave heights all along the WA coast are 15-25 cm, and the run-up from these may be as high as 1 metre or more. Thus, these tsunami events are a concern for the entire western coast of Australia, including the Perth area.

The Great 26 December 2004 Sumatra-Andaman Earthquake and Tsunami

The Great Sumatra-Andaman Islands earthquake of 26 December 2004, which initial was ascribed a magnitude of 9.0, was the largest earthquake since the 1964 Alaskan earthquake (M9.2) and is among the five largest earthquakes in the past century. Subsequent analysis has shown that a more accurate estimate of the magnitude is 9.3, making it the 2nd largest earthquake ever recorded (after the 1960 Chile earthquake, magnitude 9.6). The 'Boxing Day Tsunami' generated by this earthquake caused over 290,000 deaths and widespread destruction, mainly in Indonesia, but also in Sri Lanka, India, Thailand, and even on the east coast of Africa.

Like the 1833 earthquake, the effects of the tsunami in Sumatra were catastrophic. Tsunami run-up exceeding 30 m has been measured in Sumatra, where people had little time to escape, and whole villages have been razed. Unlike the 1833 event, fault rupture extended well north of Sumatra into the Nicobar and Andaman Islands, which resulted in waves of 5-10 m in height hitting Thailand and Sri Lanka approximately 1½-2 hours after the earthquake occurred. As is typical for a subduction zone earthquake, the seafloor was uplifted near the plate boundary and subsided 100-200 km landward of the plate boundary. In the case of the Boxing Day Tsunami, this resulted in a wave travelling to the east whose leading edge was receding, corresponding to withdrawal of the sea, while to the west the leading edge resulted in inundation. Thus, people who first encountered the wave in Thailand were given some warning by the sudden withdrawal of the sea, and in some cases lives were saved when this warning was recognized and acted upon. In many cases, however, this natural warning was not understood and the subsequent sudden inundation claimed many lives. In Sri Lanka the first effect of the wave was inundation, and people had little or no warning. This would also have been the case in most areas impacted by the 1833 tsunami.

The Great 28 March 2005 Sumatra Earthquake: No Indian Ocean-wide Tsunami

On 28 March 2005, another great subduction zone earthquake occurred off Sumatra. Although this earthquake was not as large as the 26 December 2004 event, at a magnitude of 8.7 it was still the 7th largest earthquake to have occurred worldwide since 1900, a massive earthquake by any standard. Like almost all other earthquakes of similar size, and in particular like the 26 December event, it had a shallow thrust faulting mechanism and would therefore normally be expected to generate a tsunami. In the hours following the occurrence of this event, most seismologists worldwide expected another large tsunami to be generated, and were surprised when only a minor tsunami was subsequently observed in the Indian Ocean. Although eventually reports were received of a 3-metre wave causing considerable damage on the island of Simeulue, the tsunami caused by the 28 March earthquake was in general not as large as had been expected. How could an earthquake which was in many respects similar to the 26 December earthquake behave so differently in its ability to generate a tsunami?

While the 28 March earthquake was considerably smaller than the 26 December one (magnitudes 8.7 and 9.3, respectively), the main reason the former failed to cause a large Indian Ocean-wide tsunami is likely related to the different way in which the fault slip for each earthquake was distributed over the fault surface. The epicentre is generally associated with the point at which the fault slip that causes an

earthquake first occurs, but this initial slip subsequently spreads over some finite area of the fault surface. For great subduction zone earthquakes such as the Sumatra events of 26 December 2004 and 28 March 2005, this area can extend for up to 500-1000 km along the strike of the subduction zone, and 100-200 km down dip. The usual pattern is for rupture to initiate near the deepest part of the fault plane, and then spread along strike and to more shallow depths. It is fault slip at shallow depth that is most effective in displacing the large mass of water required to generate a tsunami, because it occurs closer to the sea floor and therefore displaces it more than slip at greater depth, resulting in greater displacement of water above the sea floor.

The effectiveness of fault slip at shallow depth in exciting a tsunami is important when considering different tsunami excitation associated with the 26 December 2004 and 28 March 2005 earthquakes. While the slip distribution, estimated from observed seismic waveforms, for the former earthquake features a localized concentration of slip near about 15 km depth, much of the slip is distributed over the fault plane, with a large zone of 5-8 m slip occurring at shallow depth near the trench axis. As discussed in (a) above, it is this latter slip which dominates the vertical seafloor displacement, and this occurs near the trench access where it displaces a deep column of water, resulting in a large tsunami. The slip for the 28 March 2005 earthquake, on the other hand, was highly concentrated near the epicentre at 30 km depth. In this case only two small patches of seafloor were vertically displaced 2 m in the deep water near the trough axis, while the largest vertical displacement of 3 m occurred about 100 km landward of the trough axis near the island of Nias, where the water is less than 1 km deep. Therefore, we can tentatively conclude that the 28 March 2005 earthquake was not effective in displacing the large mass of water required to generate a large, Indian Ocean-wide tsunami due to the unusual character of its fault slip, although evidently a sufficient mass of water was displaced to produce a 3 m local tsunami on the island of Simeulue.

Stress Triggering and the Potential for Further Earthquakes and Tsunami along the Sunda Arc

The occurrence of two great earthquakes rupturing adjacent segments of the Sumatra subduction zone within 3 months strongly suggests a causal connection between the two events. The most plausible candidate for this connection was elucidated in a paper by McClosky et al. (2005) a few weeks prior to the occurrence of the 28 March earthquake. Subduction zone earthquakes occur in response to stress which accumulates due to the frictional contact between the tectonic plates as one slides beneath the other (in this case the Indian/Australian plate sliding beneath Sumatra). When the fault slips during an earthquake, this accumulated stress on the plate boundary in the area of rupture will be wholly or partially relieved. The fault slip will also change the stress field in the region surrounding the rupture area, and this stress change almost always adds to the stress accumulating on the adjacent segments of the fault as a result of relative plate motion. If these adjacent segments have not experienced a major earthquake for a time long enough for stress to have increased to a level close to the frictional strength of the interplate contact, the additional stress due to a nearby large earthquake may be enough to initiate a new earthquake in the adjacent segment. This mechanism is called 'stress triggering', and has been inferred to be responsible for earthquake sequences in Turkey, Japan, and California.

The Great 28 March 2005 Sumatra earthquake ruptured the segment of the Sumatra subduction zone immediately to the southeast of the rupture area of the 26 December 2004 earthquake, with the epicentres of the two earthquakes separated by only 200 km. Since the rupture of the 26 December 2004 earthquake spread to the northwest of its epicentre, this event relieved stress on the plate boundary only off northern Sumatra and in the Nicobar and Andaman Islands region, but added to the stress accumulating on the plate boundary southeast of its epicentre, off central and southern Sumatra. As described above, we know that the most recent large earthquakes occurred on these segments of the subduction zone in 1861 and 1833 respectively, so that stress has been accumulating on this section of the plate boundary for over 100 years, and it seems likely that the level of stress is approaching the strength of the interplate contact in this area. It thus seems reasonable to conclude that the additional

stress caused by the 26 December 2004 earthquake on the plate boundary to the southeast of its epicentre was sufficient to trigger the 28 March 2005 earthquake, which occurred in roughly the same area as the 1861 earthquake and had similar magnitude (8.7 for the 2005 vs. 8.3-8.5 for the 1861 earthquake).

Will this stress-triggering mechanism be effective in triggering further earthquakes along the Sumatra subduction zone, and if so what will be the impact on the West Australian coast and the Perth area? The next segment along the Sumatran subduction zone, immediately to the southeast of the 1861 and 28 March 2005 rupture areas, corresponds to the rupture area of the Great 1833 Sumatra Earthquake. Newcomb and McCann (1987) estimated a magnitude for this earthquake of 8.8 based on historical accounts, but more recent estimates based on evidence from coral microatolls on the Sumatran coast (Zachariasen et al., 2000) suggest a magnitude of 9.2. This latter estimate would mean that the size of the 1833 earthquake rivals that of the 26 December 2004 earthquake (magnitude 9.3, Stein et al., 2005). Although there are at present still no well-documented historical accounts of an Indian Ocean-wide tsunami following the occurrence of the 1833 earthquake, reports from a Canadian team conducting a post-event survey of the 26 December 2004 tsunami in the Seychelles indicate that there is archival evidence that a tsunami occurred there in 1833 of similar size to the 2004 event. Thus, a recurrence of the 1833 earthquake would seem likely to produce another Indian Ocean-wide tsunami. Since this segment of the subduction zone has been accumulating stress for over 180 years, it is likely close to failure and therefore seems a possible candidate for stress triggering.

Because the amount of stress involved in earthquake stress triggering is typically only a very small fraction of that required to cause an earthquake, and because the failure strength of the interplate contact and variations thereof are poorly understood, it is unfortunately impossible to predict just when and where the next earthquake on the Sumatra subduction zone will occur. A recurrence of the 1833 Great Sumatra Earthquake seems likely within the next 50 years based simply on the accumulation of stress in this part of the subduction zone, but a consideration of stress triggering due to the recent large earthquakes in the Sumatra subduction zone suggests there is heightened possibility of another large earthquake within the next few years. A tsunami caused by such an earthquake would direct more energy southward towards Australia than was the case for the 26 December 2004 event, but preliminary modelling suggests that, while the impact would be larger, it would not be dramatically so. Further work is required to quantify just how large the tsunami impact in the Perth area would from a recurrence of the 1833 event.

Other Tsunami Sources that May Affect the Perth Area

As described above, while large earthquakes off Java can generate large tsunami that may affect Australia's northwest coast, these events typically do not generate the type of Indian Ocean-wide tsunami that may be a threat to the Perth area. Other large earthquakes have occurred in the Indian Ocean in historic times, but with the exception of Sumatra there are no other sources of massive subduction zone earthquakes that could pose a serious threat to Perth. Sources of tsunami other than subduction zone earthquakes off Indonesia are both rare and difficult to quantify.

Another type of tsunamigenic event which might threaten the Perth area are volcanic eruptions in Indonesia. Active volcanoes are numerous and include two catastrophic eruptions in the 1800's, Tambora in 1815 and Krakatoa in 1833. The Krakatoa eruption produced a devastating tsunami, whose runup on the coast of WA was in the range 0.5-2 m (Allport & Blong, 1995). This tsunami was even observed on the coast of New South Wales, where its height was typically about 10 cm. While generally regarded as rare, Indonesia is one of the most volcanically active regions in the world, and the hazard from such events cannot be discounted but is difficult to assess.

The remaining two types of tsunamigenic events are asteroid impacts and submarine landslides. The former are exceedingly rare, and the only well-studied but still controversial example of a large tsunami generated from an asteroid impact is that if the Chixulub impact which is thought to have

resulted in the extinction of the dinosaurs 65 million years ago (Stinnesbeck et al., l993). Compared to asteroid impacts, the hazard from submarine landslides, including the possibility of massive flank collapses of volcanoes such as Heard Island, are more likely but, like volcanic eruptions, difficult to assess. Finally, the hazard from local tsunami generated by landslides off the West Australian coast, possibly associated with unstable accumulations of sediments, is unknown.

Conclusion

Thus, although the tsunami hazard for Australia is probably highest along the northwest coast, the tsunami hazard along the WA coast near Perth may be higher than recent historical experience suggests. Massive events such as the 1833 Sumatra earthquake and the 1883 eruption of Krakatoa may not be well represented in the historical record because of the historical differences in population trends on the west vs. east coast of Australia. The potential for such tsunami to cause harm is compounded by the lack of a formal tsunami warning system in place for the Indian Ocean. Currently, preparations are under way to establish such a system, which is proposed to be operated jointly by the Bureau of Meteorology, Geoscience Australia and Emergency Management Australia.

In any case, further research into tsunami hazard for the West Australian coast seems warranted. One important step forward would be a systematic study of tsunami deposits along the western coast. A first step towards this has been made by Nott and Bryant (2003), but a more systematic approach would require a reliable method for distinguishing between tsunami and storm deposits. Another important area of research is to search for and collate historical accounts of the tsunami associated with the 1833 earthquake; although there may be no Australian accounts, there are many Indonesian ones, and there should also be evidence in historical documents from elsewhere in the Indian Ocean. More accurate tsunami run-up calculations are also needed, to identify the particular hot spots along the coast where tsunami energy may be focused (this would also be useful to narrow down the search for tsunami deposits). Finally, some effort should be made to establish an operational warning capability by using tide gauges on Cocos and Christmas Islands, which can provide several hours advance warning for a tsunami generated off Sumatra.

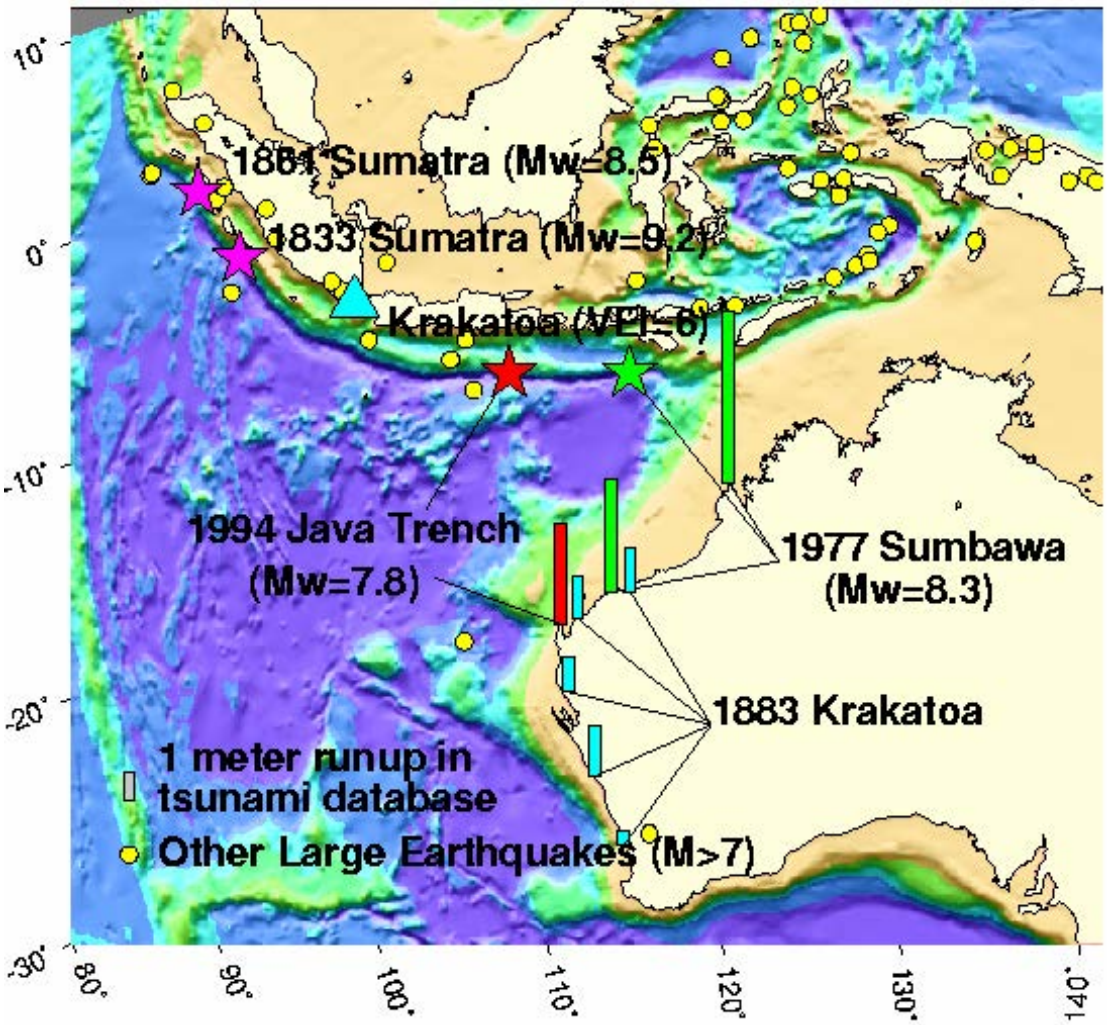

Figure 1. WA Tsunami run-up observations and the corresponding tsunamigenic events, with events color-coded to match the runup observations. Mw is a logarithmic measure of earthquake size, similar to the Richter scale but better suited to very large events, while VEI is the Volcanic Explosivity Index, with 6 for Krakatoa being one of the largest in recorded history. There are no recorded observations in Australia of the tsunami events of 1833 and 1861.

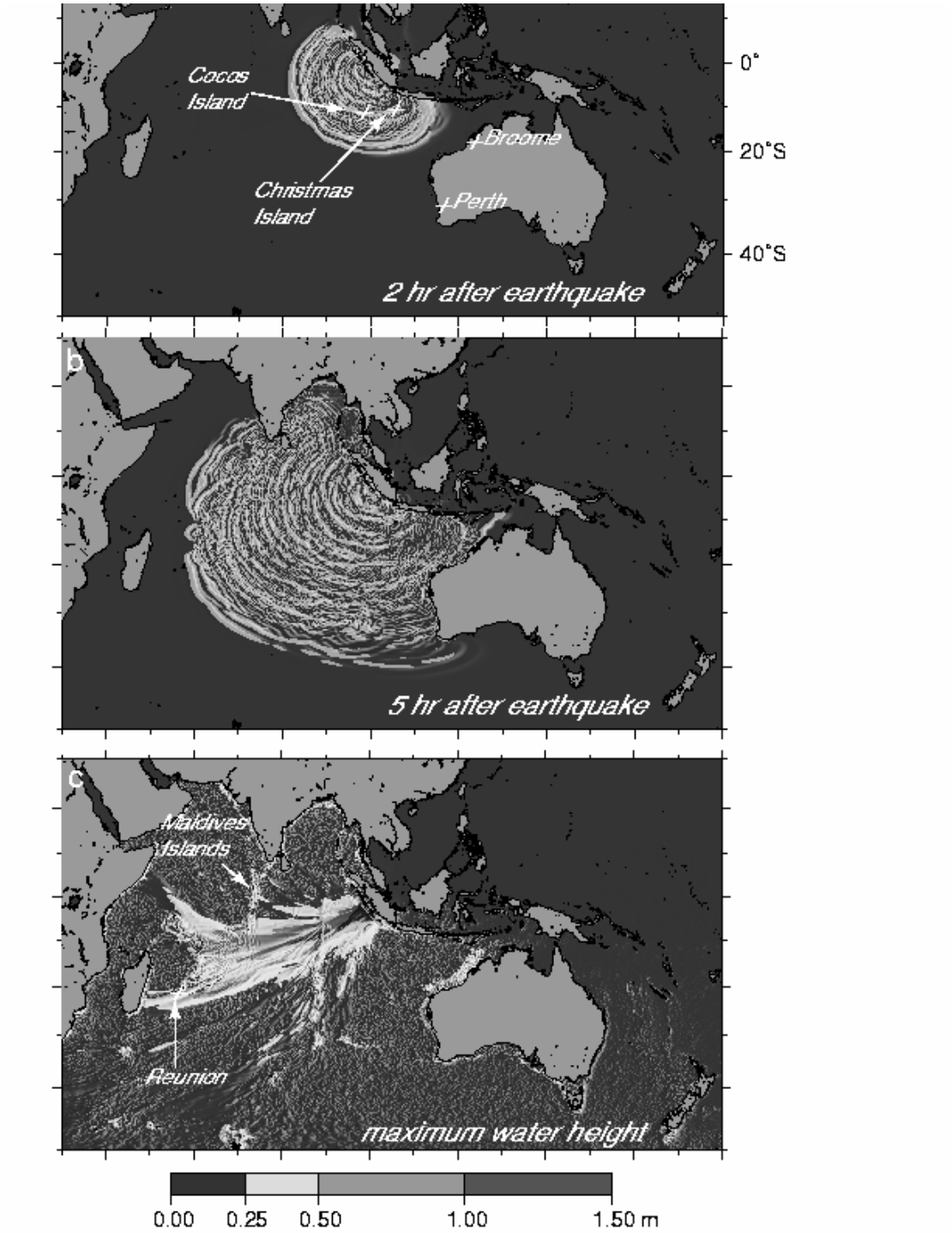

Figure 2. Numerical modelling results of the propagation of the tsunami associated with the 1833 Sumatra earthquake throughout the Indian Ocean. Note that the tsunami's early arrival at Cocos and Christmas Islands may provide a basis for warning more distant affected areas.

References

Abercrombie, R. E., Antolik, M., Flezer, K. and Ekstrom G., (2001). The 1994 Java tsunami earthquake: Slip over a subducting seamount, *J. Geophys. Res. , No. B4 , p. 6595.*

Allport, J.K. and Blong, R., 1995. The Australian Tsunami Database.

Cummins, P., and Burbidge, D., (2004). Small threat, but warning sounded for tsunami research, AusGeo News, 75, p.4-7, http://www.ga.gov.au/image_cache/GA5018.pdf

McCloskey J., Nalbant S. S. & Steacy S, (2005). Earthquake risk from co-seismic stress Nature, 434. 291.

Newcomb, K.R. and McCann, W. R., (1987). Seismic history and seismotectonics of the Sunda Arc, *1987. Jou. Geophys. Res.*, 92, 421-439.

Nott, J. and E. Bryant, Extreme Marine Inundations (Tsunamis?) of Coastal Western Australia, *Jou. Geology*, 11, 691-706.

Stein, S., and Okal, E. A., (2005). Speed and size of the Sumatra earthquake, *Nature*, 434, 581-582. Stinnesbeck W. et al. l993. Deposition of near K/T boundary clastic sediments in NE Mexico: Impact or turbidite deposits? Geology 21: 797-800.

Yoshida, Y., Satake, K. and Abe, K., (1992). The large normal-faulting earthquake of April 5, 1990 in uncoupled subduction zone, *Geophys. Res. Lett*., 19, 297-300.

Zachariasen, M., Sieh, K., Taylor, F. W., Edwards, R. L. & Hantoro, W. S. (1999). Submergence and uplift associated with the giant 1833 Sumatran subduction earthquake: evidence from coral microatolls. *J. Geophys. Res.*, 104, 895-919.